



# Use of UV and Fluorescence Spectra as Surrogate Measures for Contaminant Oxidation and Disinfection in the Ozone/H<sub>2</sub>O<sub>2</sub> Advanced Oxidation Process



Use of UV and Fluorescence Spectra as  
Surrogate Measures for Contaminant Oxidation  
and Disinfection in the Ozone/H<sub>2</sub>O<sub>2</sub> Advanced  
Oxidation Process

## About the WateReuse Research Foundation

The mission of the WateReuse Research Foundation is to conduct and promote applied research on the reclamation, recycling, reuse, and desalination of water. The Foundation's research advances the science of water reuse and supports communities across the United States and abroad in their efforts to create new sources of high quality water through reclamation, recycling, reuse, and desalination while protecting public health and the environment.

The Foundation sponsors research on all aspects of water reuse, including emerging chemical contaminants, microbiological agents, treatment technologies, salinity management and desalination, public perception and acceptance, economics, and marketing. The Foundation's research informs the public of the safety of reclaimed water and provides water professionals with the tools and knowledge to meet their commitment of increasing reliability and quality.

The Foundation's funding partners include the Bureau of Reclamation, the California State Water Resources Control Board, the California Energy Commission, and the California Department of Water Resources. Funding is also provided by the Foundation's subscribers, water and wastewater agencies, and other interested organizations.

# Use of UV and Fluorescence Spectra as Surrogate Measures for Contaminant Oxidation and Disinfection in the Ozone/H<sub>2</sub>O<sub>2</sub> Advanced Oxidation Process

Shane A. Snyder, Ph.D.  
*University of Arizona*

Gregory Korshin, Ph.D.  
*University of Washington*

Daniel Gerrity, Ph.D.  
*University of Nevada, Las Vegas*  
*Trussell Technologies, Inc.*  
*Southern Nevada Water Authority*

Eric Wert, P.E.  
*Southern Nevada Water Authority*

## **Cosponsors**

Bureau of Reclamation  
APTwater, Inc.



WaterReuse Research Foundation  
Alexandria, VA



## **Disclaimer**

This report was sponsored by the WateReuse Research Foundation and cosponsored by the Bureau of Reclamation and APTwater, Inc. The Foundation and its Board Members assume no responsibility for the content reported in this publication or for the opinions or statements of facts expressed in the report. The mention of trade names of commercial products does not represent or imply the approval or endorsement of the WateReuse Research Foundation. This report is published solely for informational purposes.

### **For more information, contact:**

WateReuse Research Foundation  
1199 North Fairfax Street, Suite 410  
Alexandria, VA 22314  
703-548-0880  
703-548-5085 (fax)  
[www.WateReuse.org/Foundation](http://www.WateReuse.org/Foundation)

© Copyright 2013 by the WateReuse Research Foundation. All rights reserved. Permission to copy must be obtained from the WateReuse Research Foundation.

WateReuse Research Foundation Project Number: WRF-09-010  
WateReuse Research Foundation Product Number: 09-010-1

ISBN: 978-1-934183-91-5  
Library of Congress Control Number: 2013950013

Printed in the United States of America

# Contents

---

List of Figures .....	viii
List of Tables .....	xii
List of Abbreviations and Acronyms .....	xv
Foreword .....	xvii
Acknowledgments .....	xviii
Executive Summary .....	xxi
<b>Chapter 1. Literature Review .....</b>	<b>1</b>
1.1 Introduction .....	1
1.1.1 Toxicological Implications for Aquatic Environments and Human Health.....	3
1.1.2 Current Water Reuse Guidelines and Regulations.....	6
1.2 Efficacy of Ozone for Contaminant Oxidation .....	10
1.3 Efficacy of Ozone for Wastewater Disinfection .....	12
1.4 Correlations between Bulk Organic Parameters and Process Efficacy .....	16
1.5 Pilot- and Full-Scale Ozonation for Trace Organic Contaminant Reduction.....	18
1.5.1 Pilot-Scale Ozone Applications .....	18
1.5.2 Full-Scale Ozone Applications for TOxC Oxidation and Removal .....	21
1.5.3 Full-Scale Ozone Applications and Toxicological Implications .....	23
1.6 Summary .....	24
<b>Chapter 2. Technical Approach and Methods .....</b>	<b>25</b>
2.1 Bench-Scale Oxidation Experiments.....	25
2.1.1 Wastewater Collection and Processing.....	25
2.1.2 Bench-Scale Ozone Testing.....	26
2.1.3 Bench-Scale UV Experiments .....	28
2.1.4 Quenching and Preservation .....	29
2.2 Target Compounds .....	29
2.2.1 Online SPE followed by LC-MS/MS .....	33
2.3 Organic Characterization.....	35
2.3.1 Excitation Emission Matrices .....	35
2.4 Target Microbes and Methods.....	37
2.4.1 Coliform Bacteria .....	37
2.4.2 MS2 Bacteriophage.....	38
2.4.3 <i>Bacillus subtilis</i> Spores .....	39
2.5 pCBA.....	39
2.6 Yeast Estrogen Screen (YES) Assay for Total Estrogenicity.....	40
2.7 NDMA.....	42
2.8 1,4-Dioxane .....	42

<b>Chapter 3. Bench-Scale Evaluation of Ozone for Water Reclamation.....</b>	<b>43</b>
3.1 Clark County Water Reclamation District, Las Vegas, Nevada .....	43
3.1.1 Ozone Demand/Decay.....	46
3.1.2 Bromate Formation .....	46
3.1.3 Hydroxyl Radical Exposure .....	47
3.1.4 Title 22 Contaminants .....	49
3.1.5 Trace Organic Contaminants.....	51
3.1.6 Disinfection .....	56
3.1.7 Organic Characterization.....	68
3.2 Metropolitan Water Reclamation District of Greater Chicago, IL .....	77
3.2.1 Ozone Demand/Decay.....	80
3.2.2 Bromate Formation .....	80
3.2.3 Hydroxyl Radical Exposure .....	81
3.2.4 Title 22 Contaminants .....	83
3.2.5 Trace Organic Contaminants.....	85
3.2.6 Disinfection .....	90
3.2.7 Organic Characterization.....	96
3.3 West Basin Municipal Water District, Los Angeles, CA .....	105
3.3.1 Ozone Demand/Decay.....	108
3.3.2 Bromate Formation .....	108
3.3.3 Hydroxyl Radical Exposure .....	109
3.3.4 Title 22 Contaminants .....	111
3.3.5 Trace Organic Contaminants.....	112
3.3.6 Disinfection .....	116
3.3.7 Organic Characterization.....	122
3.4 Pinellas County Utilities, St Petersburg, FL .....	131
3.4.1 Ozone Demand/Decay.....	133
3.4.2 Bromate Formation .....	133
3.4.3 Hydroxyl Radical Exposure .....	134
3.4.4 Title 22 Contaminants .....	135
3.4.5 Trace Organic Contaminants.....	136
3.4.6 Disinfection .....	142
3.4.7 Organic Characterization.....	147
3.5 Gwinnett County, Atlanta, GA .....	156
3.5.1 Ozone Demand/Decay.....	158
3.5.2 Bromate Formation .....	158
3.5.3 Hydroxyl Radical Exposure .....	159
3.5.4 Title 22 Contaminants .....	159
3.5.5 Trace Organic Contaminants.....	161
3.5.6 Disinfection .....	165
3.5.7 Organic Characterization.....	172
3.6 Summary of Bench-Scale Experiments .....	181
3.6.1 Ozone Versus Ozone/H <sub>2</sub> O <sub>2</sub> .....	181
3.6.2 Comparison of Filtered Secondary Effluents .....	183

<b>Chapter 4. Development of Organic Correlations .....</b>	<b>197</b>
4.1 Characterization of Surrogate Parameters .....	197
4.1.1 Absorbance Spectroscopy .....	197
4.1.2 Fluorescence Spectra .....	203
4.1.3 High Performance Size Exclusion Chromatography .....	208
4.1.4 Optimization of Surrogate Parameters.....	214
4.2 Empirical Organic Correlations.....	216
4.2.1 Relevance to November 2011 CDPH Regulations .....	222
4.3 Mechanistic Organic Correlations.....	224
4.4 Future Research.....	228
<b>Chapter 5. Pilot-Scale Evaluation of Oxidation Technologies for Water Reclamation.....</b>	<b>231</b>
5.1 Reno-Stead Water Reclamation Facility Pilot System .....	231
5.1.1 TOrC Mitigation in the RSWRF Pilot Treatment Train .....	234
5.1.2 Microbial Inactivation and Removal at RSWRF .....	237
5.1.3 Organic Characterization .....	239
5.2 Validation of Correlation Models.....	243
5.2.1 Wert et al. (2009b).....	243
5.2.2 Rosario-Ortiz et al. (2010).....	243
5.2.3 City of Las Vegas Water Pollution Control Facility.....	243
5.2.4 Reno-Stead Water Reclamation Facility.....	245
5.2.5 Green Valley Water Reclamation Facility .....	245
5.2.6 Comparison of Studies.....	245
5.3 Online Absorbance Analyzer .....	246
<b>Chapter 6. Conclusions.....</b>	<b>253</b>
<b>References.....</b>	<b>255</b>
<b>Appendices</b>	
1. Organic Characterization of Target Compounds .....	261
2. Comparison of Secondary Effluents—Ozone and Ozone/H <sub>2</sub> O <sub>2</sub> Correlations.....	267
3. Comparison of Filtered and Unfiltered Secondary Effluents—Ozone and Ozone/H <sub>2</sub> O <sub>2</sub> .....	278
4. Comparison of H <sub>2</sub> O <sub>2</sub> Doses—Ozone and Ozone/H <sub>2</sub> O <sub>2</sub> .....	289
5. Comparison of Secondary Effluents—UV/H <sub>2</sub> O <sub>2</sub> .....	300
6. Comparison of H <sub>2</sub> O <sub>2</sub> Doses—UV/H <sub>2</sub> O <sub>2</sub> .....	311
7. Validation of Empirical Correlations—Ozone and Ozone/H <sub>2</sub> O <sub>2</sub> .....	322
8. Validation of Empirical Correlations—UV/H <sub>2</sub> O <sub>2</sub> .....	333
9. Mechanistic Modeling—Ozone and Ozone/H <sub>2</sub> O <sub>2</sub> Correlations .....	342
10. CLV Pilot—Variable Dosing Experiment—s::can—Ozone Correlations .....	353

# Figures

---

1.1	Bulk organic correlations for ozone oxidation .....	17
1.2	Bulk organic correlations for UV/H <sub>2</sub> O <sub>2</sub> oxidation.....	17
1.3	Bulk organic correlations for nonthermal plasma.....	18
2.1	Wastewater collection containers and laboratory filtration apparatus .....	25
2.2	Collimated beam apparatuses for bench-scale UV experiments.....	29
2.3	Excitation emission matrix for secondary effluent .....	36
2.4	Absorbance and fluorescence fingerprints for sulfamethoxazole (10 mg/L).....	37
2.5	Colilert method for total and fecal coliforms.....	38
2.6	Double agar layer method for MS2 .....	39
2.7	Pour plate and membrane filtration methods for <i>Bacillus</i> spores .....	40
2.8	YES model corrections for low-dose and acute-toxicity conditions .....	42
3.1	Simplified treatment schematic for CCWRD .....	44
3.2	Ozone demand/decay curves for the CCWRD secondary effluent.....	46
3.3	Bromate formation during ozonation of CCWRD secondary effluent .....	48
3.4	Destruction of NDMA in the filtered CCWRD secondary effluent .....	50
3.5	Destruction of 1,4-dioxane in the filtered CCWRD secondary effluent.....	51
3.6	Reduction in total estrogenicity in the filtered CCWRD secondary effluent .....	53
3.7	Inactivation of spiked <i>E. coli</i> in the CCWRD secondary effluent.....	59
3.8	Inactivation of spiked MS2 in the CCWRD secondary effluent .....	60
3.9	Inactivation of spiked <i>Bacillus</i> spores in the CCWRD secondary effluent .....	61
3.10	Significance of CT for disinfection in the CCWRD secondary effluent .....	62
3.11	Excitation emission matrices during the reaction time experiment.....	63
3.12	Excitation emission matrices for the TSS coliform experiments.....	67
3.13	CCWRD absorbance spectra after ozonation .....	69
3.14	CCWRD absorbance spectra after UV and UV/H <sub>2</sub> O <sub>2</sub> .....	70
3.15	Differential UV <sub>254</sub> absorbance in the CCWRD secondary effluent.....	71
3.16	3D EEMs for ambient samples from CCWRD.....	72
3.17	3D EEMs after treatment for the filtered CCWRD secondary effluent.....	72
3.18	CCWRD fluorescence profiles (Ex <sub>254</sub> ) after ozonation .....	74
3.19	CCWRD fluorescence profiles (Ex <sub>254</sub> ) after UV/H <sub>2</sub> O <sub>2</sub> .....	74
3.20	CCWRD fluorescence profiles (Ex <sub>370</sub> ) after ozonation .....	76
3.21	Changes in fluorescence intensity after ozonation for CCWRD .....	76
3.22	Changes in fluorescence intensity after UV/H <sub>2</sub> O <sub>2</sub> for CCWRD.....	77
3.23	Simplified treatment schematic for MWRDGC facility .....	78
3.24	Ozone demand/decay curves for MWRDGC .....	80
3.25	Bromate formation during ozonation of MWRDGC secondary effluent .....	82
3.26	Destruction of NDMA in the filtered MWRDGC secondary effluent.....	84
3.27	Destruction of 1,4-dioxane in the filtered MWRDGC secondary effluent.....	85
3.28	Reduction in total estrogenicity in the filtered MWRDGC secondary effluent.....	86

3.29	Inactivation of spiked <i>E. coli</i> in the MWRDGC secondary effluent.....	92
3.30	Inactivation of spiked MS2 in the MWRDGC secondary effluent .....	93
3.31	Inactivation of spiked <i>Bacillus</i> spores in the MWRDGC secondary effluent.....	94
3.32	Significance of CT for disinfection in the MWRDGC secondary effluent .....	95
3.33	MWRDGC absorbance spectra after ozonation (unfiltered).....	97
3.34	MWRDGC absorbance spectra after ozonation (filtered).....	98
3.35	MWRDGC absorbance spectra after UV and UV/H <sub>2</sub> O <sub>2</sub> .....	99
3.36	Differential UV <sub>254</sub> absorbance in the MWRDGC secondary effluent.....	100
3.37	3D EEMs for ambient samples from MWRDGC .....	101
3.38	3D EEMs after treatment for the filtered MWRDGC secondary effluent.....	101
3.39	MWRDGC fluorescence profiles (Ex <sub>254</sub> ) after ozonation .....	102
3.40	MWRDGC fluorescence profiles (Ex <sub>254</sub> ) after UV/H <sub>2</sub> O <sub>2</sub> .....	102
3.41	MWRDGC fluorescence profiles (Ex <sub>370</sub> ) after ozonation .....	104
3.42	Changes in fluorescence intensity after ozonation for MWRDGC.....	104
3.43	Changes in fluorescence intensity after UV/H <sub>2</sub> O <sub>2</sub> for MWRDGC .....	105
3.44	Simplified treatment schematic for WBMWD.....	106
3.45	Ozone demand/decay curves for WBMWD (filtered) .....	109
3.46	Bromate formation during ozonation of WBMWD secondary effluent.....	110
3.47	Destruction of NDMA in the filtered WBMWD secondary effluent .....	111
3.48	Destruction of 1,4-dioxane in the filtered WBMWD secondary effluent .....	112
3.49	Reduction in total estrogenicity in the WBMWD secondary effluent .....	114
3.50	Inactivation of spiked <i>E. coli</i> in the WBMWD secondary effluent .....	118
3.51	Inactivation of spiked MS2 in the WBMWD secondary effluent .....	119
3.52	Inactivation of spiked <i>Bacillus</i> spores in the WBMWD secondary effluent.....	120
3.53	Significance of CT for disinfection in the WBMWD secondary effluent.....	121
3.54	WBMWD absorbance spectra after ozonation.....	124
3.55	WBMWD absorbance spectra after UV and UV/H <sub>2</sub> O <sub>2</sub> .....	125
3.56	Differential UV <sub>254</sub> absorbance in the filtered WBMWD secondary effluent.....	126
3.57	3D EEMs for ambient samples from WBMWD .....	127
3.58	3D EEMs after treatment for the filtered WBMWD secondary effluent .....	127
3.59	WBMWD fluorescence profiles (Ex <sub>254</sub> ) after ozonation.....	128
3.60	WBMWD fluorescence profiles (Ex <sub>254</sub> ) after UV/H <sub>2</sub> O <sub>2</sub> .....	128
3.61	WBMWD fluorescence profiles (Ex <sub>370</sub> ) after ozonation.....	129
3.62	Changes in fluorescence intensity after ozonation for WBMWD.....	130
3.63	Changes in fluorescence intensity after UV/H <sub>2</sub> O <sub>2</sub> for WBMWD .....	131
3.64	Simplified treatment schematic for PCU .....	132
3.65	Ozone demand/decay curves for PCU (filtered) .....	134
3.66	Bromate formation during ozonation of PCU secondary effluent .....	134
3.67	Destruction of NDMA in the filtered PCU secondary effluent.....	136
3.68	Destruction of 1,4-dioxane in the filtered PCU secondary effluent .....	137
3.69	Reduction in total estrogenicity in the filtered PCU secondary effluent.....	139
3.70	Inactivation of spiked <i>E. coli</i> in the PCU secondary effluent .....	143
3.71	Inactivation of spiked MS2 in the PCU secondary effluent.....	144
3.72	Inactivation of spiked <i>Bacillus</i> spores in the PCU secondary effluent .....	145

3.73	Significance of CT for disinfection in the PCU secondary effluent.....	146
3.74	PCU absorbance spectra after ozonation .....	148
3.75	PCU absorbance spectra after UV and UV/H <sub>2</sub> O <sub>2</sub> .....	149
3.76	Differential UV <sub>254</sub> absorbance in the PCU secondary effluent.....	150
3.77	3D EEMs for ambient samples from PCU .....	151
3.78	3D EEMs after treatment for the filtered PCU secondary effluent.....	151
3.79	PCU fluorescence profiles (Ex <sub>254</sub> ) after ozonation .....	152
3.80	PCU fluorescence profiles (Ex <sub>254</sub> ) after UV/H <sub>2</sub> O <sub>2</sub> .....	152
3.81	PCU fluorescence profiles (Ex <sub>370</sub> ) after ozonation .....	154
3.82	Changes in fluorescence intensity after ozonation for PCU .....	155
3.83	Changes in fluorescence intensity after UV/H <sub>2</sub> O <sub>2</sub> for PCU.....	155
3.84	Simplified treatment schematic for the GCGA facility .....	156
3.85	Ozone demand/decay curves for GCGA (filtered) .....	158
3.86	Bromate formation during ozonation of GCGA secondary effluent .....	159
3.87	Destruction of NDMA in the filtered GCGA secondary effluent.....	160
3.88	Destruction of 1,4-dioxane in the filtered GCGA secondary effluent.....	161
3.89	Reduction in total estrogenicity in the filtered GCGA secondary effluent.....	163
3.90	Inactivation of spiked <i>E. coli</i> in the GCGA secondary effluent .....	168
3.91	Inactivation of spiked MS2 in the GCGA secondary effluent.....	169
3.92	Inactivation of spiked <i>Bacillus</i> spores in the GCGA secondary effluent .....	170
3.93	Significance of CT for disinfection in the GCGA secondary effluent.....	171
3.94	GCGA absorbance spectra after ozonation.....	173
3.95	GCGA absorbance spectra after UV and UV/H <sub>2</sub> O <sub>2</sub> .....	174
3.96	Differential UV <sub>254</sub> absorbance in the GCGA secondary effluent .....	175
3.97	3D EEMs for ambient samples from GCGA .....	176
3.98	3D EEMs after treatment for the filtered GCGA secondary effluent .....	176
3.99	GCGA fluorescence profiles (Ex <sub>254</sub> ) after ozonation.....	177
3.100	GCGA fluorescence profiles (Ex <sub>254</sub> ) after UV/H <sub>2</sub> O <sub>2</sub> .....	177
3.101	GCGA fluorescence profiles (Ex <sub>370</sub> ) after ozonation.....	179
3.102	Changes in fluorescence intensity after ozonation for GCGA .....	180
3.103	Changes in fluorescence intensity after UV/H <sub>2</sub> O <sub>2</sub> for GCGA .....	180
3.104	Summary of differential UV <sub>254</sub> absorbance .....	195
3.105	Summary of total fluorescence .....	195
4.1	Differential absorbance spectra for CCWRD (H <sub>2</sub> O <sub>2</sub> :O <sub>3</sub> =0).....	198
4.2	Differential absorbance spectra for CCWRD (H <sub>2</sub> O <sub>2</sub> :O <sub>3</sub> =1.0).....	198
4.3	Normalized differential absorbance spectra for CCWRD (H <sub>2</sub> O <sub>2</sub> :O <sub>3</sub> =0).....	199
4.4	Normalized differential absorbance spectra for CCWRD (H <sub>2</sub> O <sub>2</sub> :O <sub>3</sub> =1.0).....	200
4.5	Relative changes in absorbance spectra for CCWRD (H <sub>2</sub> O <sub>2</sub> :O <sub>3</sub> =0).....	201
4.6	Relative changes in absorbance spectra for CCWRD (H <sub>2</sub> O <sub>2</sub> :O <sub>3</sub> =1.0).....	201
4.7	Differential absorbance spectra for CCWRD (H <sub>2</sub> O <sub>2</sub> =10 mg/L) .....	202
4.8	Normalized differential absorbance spectra for CCWRD (H <sub>2</sub> O <sub>2</sub> =10 mg/L) .....	202
4.9	Relative changes in absorbance spectra for CCWRD (H <sub>2</sub> O <sub>2</sub> =10 mg/L).....	202
4.10	Differential 3D EEMs for CCWRD (H <sub>2</sub> O <sub>2</sub> :O <sub>3</sub> =0).....	205

4.11	Differential 3D EEMs for CCWRD (H <sub>2</sub> O <sub>2</sub> :O <sub>3</sub> =1.0)	205
4.12	Normalized differential 3D EEM for CCWRD (H <sub>2</sub> O <sub>2</sub> :O <sub>3</sub> =0)	206
4.13	Normalized differential 3D EEM for CCWRD (H <sub>2</sub> O <sub>2</sub> :O <sub>3</sub> =1.0)	206
4.14	Relative changes in fluorescence intensity for CCWRD (H <sub>2</sub> O <sub>2</sub> :O <sub>3</sub> =0)	207
4.15	Relative changes in fluorescence intensity for CCWRD (H <sub>2</sub> O <sub>2</sub> :O <sub>3</sub> =1.0)	207
4.16	SEC chromatograms for CCWRD (H <sub>2</sub> O <sub>2</sub> :O <sub>3</sub> =0)	209
4.17	SEC chromatograms for CCWRD (H <sub>2</sub> O <sub>2</sub> :O <sub>3</sub> =1.0)	209
4.18	Differential SEC chromatograms for CCWRD (H <sub>2</sub> O <sub>2</sub> :O <sub>3</sub> =0)	211
4.19	Differential SEC chromatograms for CCWRD (H <sub>2</sub> O <sub>2</sub> :O <sub>3</sub> =1.0)	211
4.20	Normalized SEC chromatograms for CCWRD (H <sub>2</sub> O <sub>2</sub> :O <sub>3</sub> =0)	212
4.21	Normalized SEC chromatograms for CCWRD (H <sub>2</sub> O <sub>2</sub> :O <sub>3</sub> =1.0)	212
4.22	Comparison of total and regional fluorescence correlation models for DEET	215
4.23	Application of surrogate framework	216
4.24	Correlation between experimental r <sub>C/S2</sub> values and ozone rate constants	228
5.1	Pilot-scale treatment trains at RSWRF	232
5.2	Ozone demand/decay comparison for RSWRF	233
5.3	Differential UV <sub>254</sub> absorbance for RSWRF after ozonation	233
5.4	Summary of YES data for RSWRF	235
5.5	Coliform and spore removal/inactivation at RSWRF	238
5.6	MS2 and coliform inactivation during spiking study	239
5.7	EEMs after treatment for RSWRF	241
5.8	Regional fluorescence intensities for RSWRF	242
5.9	Absorbance spectra for Sample Event 1 at RSWRF	242
5.10	CLV pilot-scale MBR-O <sub>3</sub> -RO treatment train	244
5.11	Green Valley Water Reclamation Facility pilot	245
5.12	Online absorbance analyzer (s::can spectro::lyser)	247
5.13	Influent UV <sub>254</sub> absorbance monitoring with s::can spectro::lyser	249
5.14	Effluent UV <sub>254</sub> absorbance monitoring with s::can spectro::lyser	249
5.15	UV <sub>254</sub> absorbance monitoring with routine grab samples	250
5.16	UV <sub>254</sub> absorbance monitoring during variable dosing experiment	251

# Tables

---

1.1	Summary of Acute and Chronic Toxicity in Aquatic Environments.....	4
1.2	Summary of Toxicological Relevance of TOrcs in Water Supplies.....	5
1.3	Water Reuse Standards for Florida, Washington, and California.....	8
1.4	TOrc Oxidation During Ozonation ( $O_3$ :TOC=0.4).....	11
1.5	Second-Order Ozonation Rate Constants.....	12
1.6	Prevalence of Indicators and Pathogens in Secondary Effluent.....	13
1.7	Recommended Applied Ozone Doses for Total Coliform Inactivation.....	13
1.8	Summary of Experimental Conditions in Xu et al. (2002).....	14
1.9	Water Quality Data for Wert et al. (2009a) Pilot Study.....	19
1.10	Ozone Residuals in Reno-Stead Pilot System.....	19
1.11	Water Quality Data for the Regensdorf Wastewater Treatment Plant.....	22
2.1	Evaluation of Organic Leaching (TOC in mg/L) During Laboratory Filtration.....	26
2.2	Experimental Volumes for the 1-L Filtered CCWRD Samples.....	28
2.3	Target Compound List.....	30
2.4	Treatability of Target Compounds.....	33
2.5	Online SPE-LC-MS/MS Method Reporting Limits.....	34
2.6	FI and FRI Data for Secondary Effluent EEM.....	37
3.1	Initial Water Quality Data for CCWRD.....	44
3.2	Ozone Dosing Conditions for 1-L CCWRD Secondary Effluent Samples.....	45
3.3	•OH Exposure in the CCWRD Secondary Effluent.....	49
3.4	Direct NDMA Formation in the Filtered CCWRD Secondary Effluent.....	50
3.5	Ambient TOrc Concentrations at CCWRD.....	52
3.6	CCWRD TOrc Mitigation by Ozone (Unfiltered).....	54
3.7	CCWRD TOrc Mitigation by Ozone (Filtered).....	55
3.8	CCWRD TOrc Mitigation by UV (Filtered).....	56
3.9	Ambient Microbial Water Quality Data for CCWRD.....	56
3.10	Microbial Spiking Levels for CCWRD Bench-Scale Experiments.....	57
3.11	Summary of UV Inactivation in the CCWRD Secondary Effluent.....	59
3.12	Summary of <i>E. coli</i> Inactivation in the CCWRD Secondary Effluent.....	59
3.13	Summary of MS2 Inactivation in the CCWRD Secondary Effluent.....	60
3.14	Summary of <i>Bacillus</i> Spore Inactivation in the CCWRD Secondary Effluent.....	61
3.15	Summary of Reaction Time Experiment.....	64
3.16	Average Log Inactivation During TSS Experiment.....	64
3.17	TSS Experiment for Indigenous Total and Fecal Coliforms (MPN/100 mL).....	66
3.18	TSS Experiment for Spiked MS2 (PFU/mL).....	67
3.19	FI and TI Values for the CCWRD Secondary Effluent.....	75
3.20	Initial Water Quality Data for MWRDGC.....	78
3.21	Ozone Dosing Conditions for 1-L MWRDGC Secondary Effluent Samples.....	79
3.22	•OH Exposure in the MWRDGC Secondary Effluent.....	83

3.23	Direct NDMA Formation in the Filtered MWRDGC Secondary Effluent .....	84
3.24	Ambient TO <sub>r</sub> C Concentrations at MWRDGC .....	85
3.25	MWRDGC TO <sub>r</sub> C Mitigation by Ozone (Unfiltered).....	87
3.26	MWRDGC TO <sub>r</sub> C Mitigation by Ozone (Filtered).....	88
3.27	MWRDGC TO <sub>r</sub> C Mitigation by UV (Filtered) .....	89
3.28	Ambient Microbial Water Quality Data for MWRDGC.....	90
3.29	Microbial Spiking Levels for MWRDGC Bench-Scale Experiments.....	90
3.30	Summary of <i>E. coli</i> Inactivation in the MWRDGC Secondary Effluent .....	92
3.31	Summary of MS2 Inactivation in the MWRDGC Secondary Effluent.....	93
3.32	Summary of <i>Bacillus</i> Spore Inactivation in the MWRDGC Secondary Effluent .....	94
3.33	Summary of UV Inactivation in the MWRDGC Secondary Effluent.....	96
3.34	FI and TI Values for the MWRDGC Secondary Effluent.....	103
3.35	Initial Water Quality Data for WBMWD.....	107
3.36	Ozone Dosing Conditions for 1-L Filtered WBMWD Samples .....	108
3.37	•OH Exposure in the WBMWD Secondary Effluent.....	110
3.38	Direct NDMA Formation in the Filtered WBMWD Secondary Effluent .....	112
3.39	Ambient TO <sub>r</sub> C Concentrations at WBMWD.....	113
3.40	WBMWD TO <sub>r</sub> C Mitigation by Ozone (Filtered) .....	115
3.41	WBMWD TO <sub>r</sub> C Mitigation by UV (Filtered) .....	116
3.42	Ambient Microbial Water Quality Data for WBMWD .....	117
3.43	Microbial Spiking Levels for WBMWD Bench-Scale Experiments .....	117
3.44	Summary of <i>E. coli</i> Inactivation in the WBMWD Secondary Effluent.....	118
3.45	Summary of MS2 Inactivation in the WBMWD Secondary Effluent.....	119
3.46	Summary of <i>Bacillus</i> Spore Inactivation in the WBMWD Secondary Effluent .....	120
3.47	Summary of UV Inactivation in the WBMWD Secondary Effluent.....	122
3.48	FI and TI Values for the WBMWD Secondary Effluent .....	129
3.49	Initial Water Quality Data for PCU .....	132
3.50	Ozone Dosing Conditions for 1-L Filtered PCU Samples .....	133
3.51	•OH Exposure in the PCU Secondary Effluent.....	135
3.52	Direct NDMA Formation in the PCU Secondary Effluent .....	137
3.53	Ambient TO <sub>r</sub> C Concentrations at PCU.....	138
3.54	PCU TO <sub>r</sub> C Mitigation by Ozone (Filtered) .....	140
3.55	PCU TO <sub>r</sub> C Mitigation by UV (Filtered).....	141
3.56	Ambient Microbial Water Quality Data for PCU .....	141
3.57	Microbial Spiking Levels for PCU Bench-Scale Experiments .....	141
3.58	Summary of <i>E. coli</i> Inactivation in the PCU Secondary Effluent.....	143
3.59	Summary of MS2 Inactivation in the PCU Secondary Effluent .....	144
3.60	Summary of <i>Bacillus</i> Spore Inactivation in the PCU Secondary Effluent.....	145
3.61	Summary of UV Inactivation in the PCU Secondary Effluent .....	147
3.62	FI and TI Values for the PCU Secondary Effluent .....	153
3.63	Initial Water Quality Data for GCGA.....	157
3.64	Ozone Dosing Conditions for 1-L Filtered GCGA Samples.....	157
3.65	•OH Exposure in the GCGA Secondary Effluent .....	160
3.66	Direct NDMA Formation in the Filtered GCGA Secondary Effluent .....	161

3.67	Ambient TOrC Concentrations at GCGA.....	162
3.68	GCGA TOrC Mitigation by Ozone (Filtered) .....	164
3.69	GCGA TOrC Mitigation by UV (Filtered).....	165
3.70	Ambient Microbial Water Quality Data for GCGA .....	166
3.71	Microbial Spiking Levels for GCGA Bench-Scale Experiments .....	166
3.72	Summary of <i>E. coli</i> Inactivation in the GCGA Secondary Effluent.....	168
3.73	Summary of MS2 Inactivation in the GCGA Secondary Effluent .....	169
3.74	Summary of <i>Bacillus</i> Spore Inactivation in the GCGA Secondary Effluent.....	170
3.75	Summary of UV Inactivation in the GCGA Secondary Effluent .....	172
3.76	FI and TI Values for the GCGA Secondary Effluent .....	179
3.77	Water Quality Summary for Filtered Secondary Effluent .....	184
3.78	Comparison of Ozone CT (mg/min/L) for Filtered Secondary Effluent .....	184
3.79	Bromate Formation Summary for Filtered Secondary Effluent .....	185
3.80	Average •OH Exposures ( $10^{-11}$ M-s) for Filtered Secondary Effluent.....	185
3.81	UV Dose ( $\text{mJ}/\text{cm}^2$ ) Required for 1.2-log NDMA Destruction .....	186
3.82	Summary of Direct NDMA Formation During Ozonation.....	187
3.83	O <sub>3</sub> :TOC Ratio Required for 0.5-log Destruction of 1,4-dioxane.....	187
3.84	Summary of Secondary Effluent TOrC Concentrations (ng/L).....	188
3.85	Summary of Finished Effluent TOrC Concentrations .....	189
3.86	Average TOrC Mitigation (%) During Ozonation.....	191
3.87	Average TOrC Mitigation (%) for UV and UV/H <sub>2</sub> O <sub>2</sub> .....	192
3.88	Average Log Inactivation for <i>E. coli</i> During Ozonation .....	193
3.89	Average Log Inactivation for MS2 During Ozonation .....	193
3.90	Average Log Inactivation for <i>B. subtilis</i> Spores During Ozonation.....	193
3.91	Average Inactivation During UV and UV/H <sub>2</sub> O <sub>2</sub> .....	193
4.1	Notable Features of the 3D EEMs for the Five Secondary Effluents .....	204
4.2	Locations and Magnitudes of SEC Peaks .....	208
4.3	Molecular Weight Distributions by Group .....	213
4.4	Summary of Regression Parameters for UV/H <sub>2</sub> O <sub>2</sub> Correlations .....	219
4.5	Summary of Regression Parameters for Ozone Correlations .....	220
4.6	Summary of pCBA Surrogate Model .....	221
4.7	Classification of Target Compounds in Relation to CDPH Requirements.....	223
4.8	Dimensionless $r_{C/S2}$ Ratios for the Mechanistic Modeling Approach.....	227
5.1	TOrC Summary Data for the Six Sample Events at RSWRF.....	235
5.2	Estrogenicity of RSWRF Secondary Effluent .....	236
5.3	TOC Values (mg/L) for RSWRF.....	240
5.4	UV <sub>254</sub> Values ( $\text{cm}^{-1}$ ) for RSWRF.....	240
5.5	Summary of Treatment and Fluorescence Indices for RSWRF.....	241
5.6	Ozone Dosing Conditions During Variable Dosing Experiment.....	250

# Abbreviations and Acronyms

---

ADI	acceptable daily intake
AOC	assimilable organic carbon
AOP	advanced oxidation process
BAC	biological activated carbon
BAF	biologically active filtration
BDF	buffered demand-free
BHA	butylated hydroxyanisole
BOD	biochemical oxygen demand
BQ	benchmark quotient
CCL3	Contaminant Candidate List 3
CCWRD	Clark County Water Reclamation District
CDPH	California Department of Public Health
CFU	colony-forming unit
CLV	City of Las Vegas Water Pollution Control Facility
COD	chemical oxygen demand
CT	concentration x time (as used for disinfection)
DALY	disability adjusted life year
DBP	disinfection byproduct
DEET	<i>N,N</i> -diethyl- <i>meta</i> -toluamide
DOC	dissolved organic carbon
DWEL	drinking water equivalent level
EBCT	empty bed contact time
EDC	endocrine-disrupting compound
EEM	excitation emission matrix
EEq	estradiol equivalents
EfOM	effluent organic matter
EPA	Environmental Protection Agency
EU	European Union
FAT	full advanced treatment
FI	fluorescence index
FRI	fluorescence regional integration
GCGA	Gwinnett County, Georgia
HMW	high molecular weight
HPSEC	high-performance size exclusion chromatography
IMW	intermediate molecular weight
IOD	instantaneous ozone demand
IPR	indirect potable reuse
LC-MS/MS	liquid chromatography tandem mass spectrometry
LMW	low molecular weight
LT2ESWTR	Long Term 2 Enhanced Surface Water Treatment Rule
MBR	membrane bioreactor
MCL	maximum contaminant level
MF	microfiltration
MPN	most probable number
MRL	method reporting limit
MWRDGC	Metropolitan Water Reclamation District of Greater Chicago
NDMA	<i>N</i> -nitrosodimethylamine
NL	notification level

•OH	hydroxyl radical
pCBA	para-chlorobenzoic acid
PCU	Pinellas County Utilities
PFU	plaque-forming unit
PPCPs	pharmaceuticals and personal care products
QSAR	quantitative structural activity relationship
RO	reverse osmosis
RSWRF	Reno-Stead Water Reclamation Facility
SDWA	Safe Drinking Water Act
SEC	size exclusion chromatography
SPE	solid phase extraction
SRT	solids retention time
SUVA	specific UV absorbance
TCEP	tris-(2-chloroethyl)-phosphate
TCPP	tris-(2-chloroisopropyl)-phosphate
TF	total fluorescence
TI	treatment index
TKN	total Kjeldahl nitrogen
TN	total nitrogen
TOC	total organic carbon
TON	total organic nitrogen
TOrC	trace organic contaminant
TOX	total organic halides
TP	total phosphorus
TSA	tryptic soy agar
TSB	tryptic soy broth
TSS	total suspended solids
UF	ultrafiltration
UV	ultraviolet
WBMWD	West Basin Municipal Water District
YES	yeast estrogen screen

# Foreword

---

The WateReuse Research Foundation, a nonprofit corporation, sponsors research that advances the science of water reclamation, recycling, reuse, and desalination. The Foundation funds projects that meet the water reuse and desalination research needs of water and wastewater agencies and the public. The goal of the Foundation's research is to ensure that water reuse and desalination projects provide high-quality water, protect public health, and improve the environment.

An Operating Plan guides the Foundation's research program. Under the plan, a research agenda of high-priority topics is maintained. The agenda is developed in cooperation with the water reuse and desalination communities including water professionals, academics, and Foundation subscribers. The Foundation's research focuses on a broad range of water reuse research topics including:

- Definition of and addressing emerging contaminants
- Public perceptions of the benefits and risks of water reuse
- Management practices related to indirect potable reuse
- Groundwater recharge and aquifer storage and recovery
- Evaluation and methods for managing salinity and desalination
- Economics and marketing of water reuse

The Operating Plan outlines the role of the Foundation's Research Advisory Committee (RAC), Project Advisory Committees (PACs), and Foundation staff. The RAC sets priorities, recommends projects for funding, and provides advice and recommendations on the Foundation's research agenda and other related efforts. PACs are convened for each project and provide technical review and oversight. The Foundation's RAC and PACs consist of experts in their fields and provide the Foundation with an independent review, which ensures the credibility of the Foundation's research results. The Foundation's Project Managers facilitate the efforts of the RAC and PACs and provide overall management of projects.

The performance of advanced oxidation processes depends largely on water quality and the ability to form hydroxyl radicals to meet disinfection or contaminant destruction objectives. However, there are no direct methods to measure •OH exposure, and frequent monitoring for trace organic contaminants and pathogenic microorganisms is a costly and difficult proposition. This project addresses these issues by developing differential UV absorbance and fluorescence models to estimate •OH exposure, contaminant oxidation, and disinfection efficacy with ozone, ozone/H<sub>2</sub>O<sub>2</sub>, and UV/H<sub>2</sub>O<sub>2</sub>. Equipping utilities and operators with quick and simple proxies for oxidation efficacy reduces the need for continuous monitoring of trace organic contaminants, allows for rapid adjustments to operational conditions to account for variable water quality, and provides a basis for awarding credits for contaminant oxidation and disinfection.

**Richard Nagel**  
*Chair*  
WateReuse Research Foundation

**G. Wade Miller**  
*Executive Director*  
WateReuse Research Foundation

# Acknowledgments

---

This project was funded by the WateReuse Research Foundation, the Bureau of Reclamation, and APTwater, Inc.

This study would not have been possible without the insights, efforts, and dedication of many individuals and organizations. These include the members of the research team and Project Advisory Committee members (as identified herein); the WateReuse Research Foundation Project Manager, Caroline Sherony; and many key individuals at the participating utilities and related organizations.

The research team would like to thank the WateReuse Research Foundation for funding this applied research project, as well as the following organizations for their contributions: APTwater, Inc., Clark County Water Reclamation District, Green Valley Water Reclamation Facility, Gwinnett County, ITT/Wedeco, City of Las Vegas Water Pollution Control Facility, Metropolitan Water Reclamation District of Greater Chicago, Pima County, Pinellas County Utilities, City of Reno Public Works Department, Reno-Stead Water Reclamation Facility, s::can Messtechnik, Stantec (formerly ECO:LOGIC Engineering), Trojan Technologies, United Water, West Basin Municipal Water District, and WesTech Engineering.

## **Principal Investigators**

Shane A. Snyder, Ph.D., *University of Arizona*

Gregory Korshin, Ph.D., *University of Washington*

Daniel Gerrity, Ph.D., *Southern Nevada Water Authority and Trussell Technologies, Inc.*

Eric Wert, P.E., *Southern Nevada Water Authority*

## **Research Project Team**

Susanna Blunt, *Southern Nevada Water Authority*

Josephine Chu, *Southern Nevada Water Authority*

Shannon Ferguson, *Southern Nevada Water Authority*

Sujanie Gamage, *Southern Nevada Water Authority*

Janie Holady, *Southern Nevada Water Authority*

Darryl Jones, *University of Arizona*

Archana Kasinathan, *University of Washington*

Jasmine Koster, *Southern Nevada Water Authority*

Jing Lin, *Southern Nevada Water Authority*

Douglas Mawhinney, *Southern Nevada Water Authority*

Roxanne Phillips, *Southern Nevada Water Authority*

Aleksey Pisarenko, *Southern Nevada Water Authority*

Oscar Quiñones, *Southern Nevada Water Authority*

Rebecca Trenholm, *Southern Nevada Water Authority*

Brett Vanderford, *Southern Nevada Water Authority*

Dongxu Yan, *Southern Nevada Water Authority*

## **Participating Agencies**

APTwater, Inc. (CA)

City of Las Vegas Water Pollution Control Facility (NV)

Clark County Water Reclamation District (NV)

Green Valley Water Reclamation Facility (AZ)  
Gwinnett County (GA)  
Metropolitan Water Reclamation District of Greater Chicago (IL)  
Pinellas County Utilities (FL)  
Reno-Stead Water Reclamation Facility (NV)  
s::can Messtechnik (Austria)  
Southern Nevada Water Authority (NV)  
Trojan Technologies (Canada)  
University of Washington (WA)  
West Basin Municipal Water District (CA)

**Project Advisory Committee**

Saied Delagah, *Bureau of Reclamation*  
Kerwin Rakness, *Process Applications, Inc.*  
Andrew Salveson, *Carollo Engineers*  
Stanley Shumaker, *City of Reno Public Works Department (retired)*



# Executive Summary

---

## Project Background and Objectives

Researchers have known for decades that some trace organic contaminants (TOrcs) persist through conventional wastewater treatment processes; however, the more recent connection between effluent discharge and adverse ecological effects has driven some scientists and regulators to call for more effective forms of wastewater treatment. The environmental discharge concerns are compounded by the increased prevalence of indirect potable reuse (IPR), which increases the risk of human exposure to various TOrcs. As a result, advanced treatment processes such as high-pressure membrane filtration (e.g., reverse osmosis) and advanced oxidation (e.g., ozone/H<sub>2</sub>O<sub>2</sub>) are becoming increasingly common in wastewater treatment, particularly in water reuse applications. These unit processes are particularly effective for TOrc mitigation, and recent technological advances are improving efficiencies and reducing costs associated with advanced treatment.

The performance of advanced oxidation processes (AOPs) depends largely on water quality and the ability to form •OH to meet disinfection or contaminant destruction objectives. In wastewater, ozone reacts rapidly with effluent organic matter (EfOM) and decomposes naturally into •OH. The addition of hydrogen peroxide (H<sub>2</sub>O<sub>2</sub>) expedites these reactions, significantly reduces the structural footprints required for ozone-based oxidation processes, and also provides some degree of bromate mitigation. Unfortunately, there are no direct methods to measure •OH exposure, so it is currently impractical to monitor the performance of these processes with simple, inexpensive methods. Furthermore, frequent monitoring for TOrcs and pathogenic microorganisms is a costly and difficult proposition. The concentration x time (CT) concept is commonly used as a surrogate measure of disinfection efficacy, but, particularly with respect to ozone/H<sub>2</sub>O<sub>2</sub>, there is no oxidant residual that can be measured to warrant a CT credit.

To address this need, this project developed empirical correlations between changes in the bulk organic matter in five different secondary effluents with the oxidation of a suite of target compounds and surrogate microorganisms. The project evaluated ozone, ozone/H<sub>2</sub>O<sub>2</sub>, and ultraviolet (UV)/H<sub>2</sub>O<sub>2</sub>, and the bulk organic matter was characterized based on absorbance and fluorescence spectra at various wavelengths. The empirical relationships were also described in the context of quantitative structural activity relationships in that the compounds and resulting correlations were grouped based on ozone and •OH rate constants. The project also validated the bench-scale models with data from multiple, independent, pilot-scale oxidation processes and existing data in the literature. An online absorbance analyzer from Messtechnik was also installed on one of the pilot-scale systems to validate online monitoring of bulk organic matter and process performance.

Ultimately, the goal of this project was to better integrate AOPs into wastewater treatment by developing tools that were amenable to the current regulatory framework (e.g., California Department of Public Health Title 22 requirements for water recycling). Equipping utilities and operators with quick and simple proxies for AOP efficacy will reduce the analytical demand related to continuous TOrc monitoring, allow for rapid adjustments to operational variables (e.g., ozone or H<sub>2</sub>O<sub>2</sub> dose or both), and provide a basis for awarding credits for contaminant oxidation and disinfection. This project provides a greater understanding of AOP

processes and an additional safeguard against human exposure to pathogenic microorganisms and chemical contaminants in reuse applications.

## Project Summary

The initial phase of the project consisted of a comprehensive literature review to identify the state of knowledge regarding the public health implications, regulatory framework, and efficacy of AOPs in relation to a suite of TOrcs and microbes. Although several regulatory agencies have developed preliminary guidance, TOrc regulations and enforcement are extremely limited in water and wastewater treatment applications. One of the primary issues hindering the development of public health criteria is whether these organic compounds, generally present at trace concentration, pose any risk at all. Despite this uncertainty, some agencies are taking a proactive approach to TOrc mitigation by developing regulations that mandate certain percent removals based on their relative resistance or susceptibility to treatment (i.e., an indicator framework).

In order to facilitate this effort, this project included a series of bench-scale experiments on five secondary effluents with varying water quality. The bench-scale experiments consisted of spiking samples with approximately 20 different trace organic and microbial contaminants prior to advanced oxidation with ozone, ozone/H<sub>2</sub>O<sub>2</sub>, or UV/H<sub>2</sub>O<sub>2</sub>. The samples were then analyzed for the surrogate microbes and target compounds, including a number of pharmaceuticals and potential endocrine disrupting compounds (EDCs); several disinfection byproducts (DBPs), including N-nitrosodimethylamine (NDMA) and bromate; and a variety of bulk organic parameters, including UV absorbance and total fluorescence (TF). Advanced oxidation experiments were also performed with multiple pilot-scale reactors to validate the data collected during the bench-scale phase. The pilot-scale reactors consisted of two ozone H<sub>2</sub>O<sub>2</sub> units (HiPOx, APTwater, Inc.) that were part of larger water reuse treatment trains and an independently operated ozone/UV/H<sub>2</sub>O<sub>2</sub> unit (ITT/Wedeco).

The project report summarizes the data from these experiments in three sections: (1) bench-scale experiments, (2) development of organic correlations, and (3) pilot-scale validation. The bench-scale experiment section describes the general efficacy of each of the AOPs regarding TOrc oxidation, DBP formation, microbial inactivation, and transformation of bulk organic matter. The TOrc oxidation data are presented with an indicator/grouping framework using percent reductions. The transformation of bulk organic matter is described with UV absorption spectra, differential UV<sub>254</sub> absorbance, excitation emission matrices, and differential fluorescence. Organic characterization of the target compounds is also summarized in Appendix 1. Combined with microbial inactivation, these data serve as the foundation of the correlation models developed in the following section. The first section concludes with a more practical summary of the bench-scale experiments and a discussion of the advantages and disadvantages of H<sub>2</sub>O<sub>2</sub> addition during ozonation. Despite diverse water qualities, the data from the five secondary effluents proved to be highly consistent for the major water quality parameters, excluding DBP formation, as a result of the use of ozone: total organic compound (O<sub>3</sub>:TOC) ratios for ozone dosing.

The next section presents the bench-scale correlation models. The empirical correlation models use linear regression parameters to describe the relationship between changes in bulk organic matter, specifically UV<sub>254</sub> absorbance and TF; TOrc oxidation; and microbial inactivation. Because the relative removals proved to be highly consistent across the various secondary effluents, the data from the five sets of bench-scale experiments were combined

when developing the models. However, the relative removals of the individual target compounds varied considerably because of their respective ozone and  $\bullet\text{OH}$  rate constants. Therefore, separate regression models were developed for each contaminant. The indicator framework was then incorporated once again by developing a separate regression model representing each of the compound groupings. These models are illustrated in Appendices 2–6, and they are also validated using data from multiple pilot-scale AOP reactors and independent data from the literature (Appendices 7 and 8). Despite the differences in treatment scale and water quality, a range of pretreatment processes, and independent experimental protocols, the correlations proved to be highly consistent for all of the target compounds.

In addition to the empirical models, this study provides a framework for developing more mechanistic models based on theoretical chromophore and fluorophore reaction rates. The corresponding section outlines the derivation of these relationships and provides a set of general equations for subsequent numerical integration. Appendix 9 provides a series of figures that validates this alternative modeling approach.

The last section describes an additional validation step in which an online absorbance analyzer (the spectro::lyser from s::can Messtechnik) was used to continuously monitor one of the pilot-scale reactors. The correlation models were then integrated into the online monitoring data to further validate the underlying bench-scale data (Appendix 10).

## **Project Conclusions**

This project addresses the need to develop alternative monitoring strategies for AOPs in IPR applications. Specifically, the project indicates that the correlation models for differential absorbance or fluorescence, contaminant oxidation, and microbial inactivation were consistent regardless of secondary effluent water quality and scale of the oxidation process. Separate regression models were required for the various contaminants because of their respective oxidation rate constants, and separate models were also required for ozone- versus UV-based oxidation processes. Although the correlations were quite strong for the TOrCs, the microbial data were characterized by greater variability. The linear correlations between bulk organic matter and microbial inactivation were still evident, particularly for the bacteriophage MS2, despite the increased variability. Further study would be necessary to refine the microbial correlations and strengthen the argument to substitute the correlation concept for the CT framework. Regardless, this concept has tremendous promise for full-scale implementation, which will provide opportunities for process optimization, further redundancy in ensuring the integrity of unit process performance, and, most important, additional safeguards for public health.



## Chapter 1

# Literature Review

---

### 1.1 Introduction

Although pharmaceuticals and personal care products (PPCPs) and endocrine-disrupting compounds (EDCs) are often considered “emerging contaminants,” researchers have been aware of their ubiquity in water for decades. Demonstrated impacts on aquatic ecosystems, potential human health effects, and increased public awareness have stimulated recent interest in PPCPs and EDCs in water and wastewater (Snyder et al., 2003b). The development of extremely sensitive analytical methods has also allowed researchers to approach parts-per-quadrillion (sub-ng/L) detection limits for a variety of trace organic contaminants (TOrcs; Snyder et al., 2003a; Vanderford and Snyder, 2006). The use of online solid phase extraction (SPE) has reduced the material requirements and time associated with analyses (Trenholm et al., 2009), and state-of-the-art high-resolution equipment (e.g., quadrupole time-of-flight mass spectrometry) has even allowed for real-time detection and identification of oxidation byproducts (Vanderford et al., 2008). Each of these factors has increased the number and scope of scientific investigations into the presence, fate, and transport of TOrcs in natural and engineered systems.

Although there are a number of significant sources of PPCPs and EDCs in the environment, including industrial manufacturing processes and confined animal feeding operations (Snyder et al., 2008b), municipal wastewater is considered the primary source (Hollender et al., 2009). The occurrence of these compounds, associated byproducts, and transformation products in wastewater results from their release during manufacturing, excretion after personal use, and disposal of unused quantities (Daughton and Ternes, 1999). These researchers highlighted the ubiquity of pharmaceuticals, of which more than 3000 are now available by prescription (Benotti et al., 2009), due to their direct correlation to human presence: pharmaceuticals will be detected in any water supply in proximity to human populations. In a review of TOrc occurrence in municipal wastewater effluent, Snyder et al. (2008a) identified pharmaceutical residues, antibiotics, steroid hormones, and fragrances as the most frequently detected compound classes, and Ternes (1998) provided one of the first comprehensive evaluations of TOrc concentrations in municipal wastewater effluent and receiving waters. Fent et al. (2006) also provided a comprehensive review of TOrc concentrations in wastewater effluent in addition to the modes of action and toxicological implications of those contaminants.

With regard to wastewater treatment, compound removal and transformation are highly dependent on the unit processes (e.g., secondary treatment, filtration, disinfection) and operational variables (e.g., oxidant dose, solids retention time [SRT]) employed at a particular plant (Snyder et al., 2003b; Benotti et al., 2009). Even at a single wastewater treatment plant, effluent concentrations can be highly variable because they are influenced by temperature and dry versus wet weather flows (Ternes, 1998). After these contaminants are discharged, natural attenuation occurs through microbial degradation, dilution, adsorption to solids, photolysis, or other forms of abiotic transformation; however, these natural processes are generally insufficient to reduce TOrc concentrations to the limits of analytical methods. Furthermore, some receiving bodies can be composed of 50 to 90% wastewater effluent during dry weather conditions (Daughton and Ternes, 1999). This ultimately leads to TOrc detection in surface water, groundwater (i.e., after aquifer recharge or leaching from

landfilled solids), and even food supplies (i.e., after plant uptake from reclaimed irrigation water; Daughton and Ternes, 1999; Boxall et al., 2006). Kolpin et al. (2002) documented the occurrence of 95 TOrCs in 139 predominantly wastewater-impacted streams in the United States. Although identified as a conservative estimate because of method limitations (i.e., method reporting limits [MRLs]), at least one TOrC was detected in 80% of the sample sites, but the concentrations were generally less than 1 µg/L. To highlight immediate impacts on drinking water supplies, Benotti et al. (2009) monitored 51 TOrCs in the source water, finished drinking water, and distribution systems of 19 U.S. utilities. Although median concentrations of the target pharmaceuticals rarely exceeded 10 ng/L, some TOrCs were detected at maximum concentrations exceeding 100 ng/L. The herbicide atrazine was even detected in systems with no known agricultural applications. Therefore, recalcitrant compounds certainly have the potential to persist in drinking water supplies and contaminate finished drinking water.

Water and wastewater treatment trains are generally not designed for the removal of TOrCs; however, the interrelation of wastewater discharge and drinking water sources and potential effects on aquatic ecosystems now justify some consideration of TOrCs in the design process. In fact, expansion and optimization of wastewater treatment processes may be the most efficient strategy to mitigate the potential effects of these contaminants. Countless treatment processes have been evaluated for their ability to remove or destroy a variety of TOrCs. These evaluations span the continua of biological treatment (e.g., activated sludge), physicochemical treatment (e.g., media or membrane filtration), conventional oxidation (e.g., chlorine and ozone), and advanced oxidation processes (AOPs; e.g., ultraviolet [UV]/hydrogen peroxide [H<sub>2</sub>O<sub>2</sub>]) in drinking water and wastewater (Ternes et al., 2002; Huber et al., 2003; Westerhoff et al., 2005; Snyder et al., 2006; Kim et al., 2007; Snyder et al., 2007). Specifically, high-pressure membranes can be very effective for TOrC removal, but the concentrated brines pose disposal issues, particularly for inland applications. The UV AOP (e.g., UV/H<sub>2</sub>O<sub>2</sub>) is another viable alternative, but the relatively high consumption of H<sub>2</sub>O<sub>2</sub> and the general necessity of upstream pretreatment can result in a cost-prohibitive process.

Ozone is a unique option because its efficacy is generally similar to that of UV/H<sub>2</sub>O<sub>2</sub> but with significantly reduced energy and chemical requirements (Rosenfeldt et al., 2006). Ozone alone has the ability to generate •OH when applied to wastewater, which allows for the degradation of more recalcitrant compounds. The AOP can also be optimized with the addition of H<sub>2</sub>O<sub>2</sub> (Buffle et al., 2006a), which accelerates the overall treatment process, reduces structural footprints associated with ozone contactors, and allows for some degree of bromate mitigation. In addition, ozone is an effective disinfectant for wastewater applications, which is particularly important for regulatory compliance (e.g., the California Department of Public Health (CDPH) Title 22 requirements for recycled water).

Particularly in wastewater, ozone reacts rapidly with effluent organic matter (EfOM) and decomposes naturally into •OH; however, there are no direct methods to measure •OH exposure, so it is currently impractical to monitor the performance of most AOPs with simple, inexpensive methods. The concentration x time (CT) concept is commonly used as a surrogate measure of disinfection efficacy, but with regard to the ozone AOP and systems where the applied ozone dose is less than the instantaneous ozone demand (IOD), there is no oxidant residual that can be measured to warrant a CT credit. With the recent increase in the popularity of ozone-based technologies for water reuse applications, there is a need for inexpensive, online measures of process efficacy. Fortunately, recent studies indicate that bulk organic parameters, such as UV<sub>254</sub> absorbance and fluorescence spectra, are viable

surrogates for contaminant oxidation (Wert et al., 2009b), but a more comprehensive evaluation of these relationships is warranted prior to full-scale implementation.

The following review addresses the state of ozonation with respect to wastewater treatment and water reclamation, provides a brief overview of regulatory considerations and relevant toxicological issues, and summarizes the previous literature pertaining to correlations between bulk organic parameters and process efficacy.

### **1.1.1 Toxicological Implications for Aquatic Environments and Human Health**

Despite significant evidence of occurrence, scientists, regulators, and policy makers have not reached consensus regarding the actual toxicological implications of TOrCs in drinking water and aquatic ecosystems. One of the primary questions plaguing this issue is whether bioassays can be extrapolated to more complex organisms, populations, and ecosystems (Daughton and Ternes, 1999). Simple and complex organisms sometimes share similar organs and physiological traits, but there are other examples in which the pathways are dissimilar, which can lead to erroneous conclusions regarding toxicity (Fent et al., 2006). Despite its limitations, the current toolbox of toxicological assays provides valuable information in predicting health implications from exposure to waterborne TOrCs.

In the course of future regulatory discussions, scientists, regulators, and policy makers must first determine whether aquatic species or humans will be the critical population requiring protection from TOrCs in water. They may both need separate regulations in wastewater and water. Currently, there is little evidence to justify human-based regulations, as will be discussed later, but there is growing concern related to feminization and toxicity in aquatic species. Despite the low concentrations of EDCs in the environment, some fish prefer to live near wastewater outfalls because of the high availability of food in these nutrient-rich locations, thereby ensuring a constant exposure to these compounds (Snyder et al., 2008b). Of particular relevance—and this even applies to humans—is their exposure to trace concentrations of organic compounds during early life stages when they are particularly susceptible to the effects of environmental contamination (Snyder et al., 2008b).

Numerous studies have documented the effects of trace (i.e., low ng/L) steroid hormones, specifically estrone, 17 $\beta$ -estradiol, and 17 $\alpha$ -ethynylestradiol, on aquatic species. Degradation products of nonionic surfactants (e.g., octylphenol and nonylphenol) have also been shown to have estrogenic effects, albeit at concentrations orders of magnitude greater, and have been shown to accumulate in the tissues of fish (Snyder et al., 2008b). In one study on aquatic impacts, long-term exposure of fish to 17 $\alpha$ -ethynylestradiol at 4 ng/L resulted in complete feminization of entire populations within 2 years (Lange et al., 2009). Another study observed some degree of feminization in all male fish from wastewater-impacted rivers in England (Tyler and Jobling, 2008). The feminized fish had elevated vitellogenin levels, disrupted gonad development, low-quality sperm, and generally altered reproductive behavior. These controlled laboratory-scale fish studies have also been expanded to evaluate wastewater with varying levels of treatment. As will be discussed later, Stalter et al. (2010b) studied the toxicity and estrogenicity of ozonated effluent on rainbow trout.

In addition to studies on fish, numerous *in vitro* bioassays have been developed to evaluate a variety of toxicity and estrogenicity endpoints. As mentioned earlier, these assays (e.g., the yeast estrogen screen [YES] assay) are difficult to extrapolate to more complex organisms, but they provide useful information related to parameters such as baseline toxicity, neurotransmitter inhibition, photosynthesis inhibition, genotoxicity, and overall estrogenicity

(Escher et al., 2008; Escher et al., 2009; Macova et al., 2010; Reungoat et al., 2010; Stalter et al., 2010a). Escher et al. (2008) observed significant baseline toxicity, acetylcholinesterase inhibition (associated with insecticides), and estrogenicity in primary effluent, but all of these parameters decreased dramatically following conventional secondary treatment. Only slight decreases were observed after subsequent sand filtration. Macova et al. (2010) expanded the scope of the bioassay work to evaluate a variety of unit processes, and they identified coagulation/flocculation/dissolved air flotation, ozonation, and biological activated carbon (BAC) filtration as the most effective processes for reducing a variety of toxicity endpoints. As indicated by this list of unit processes, reductions in toxicity were highly correlated to reductions or transformations of EfOM. Fent et al. (2006) accumulated data for a variety of bioassays (e.g., based on phytoplankton, benthos, zooplankton, and fish) and TOrCs in order to summarize the acute (rapid onset) and chronic (long-term effects) toxicity levels for a variety of target contaminants. These data are summarized in Table 1.1. Lienert et al. (2007) presented an alternative ecotoxicology framework based on toxic potentials and relative risk. Although the environmental concentrations of most TOrCs are insufficient, the literature suggests that certain compounds, particularly steroid hormones, may be present at sufficient concentrations to induce changes in aquatic populations.

**Table 1.1. Summary of Acute and Chronic Toxicity in Aquatic Environments**

<b>Contaminant</b>	<b>Acute Toxicity Level<sup>a</sup> (mg/L)</b>	<b>Chronic Toxicity Level<sup>b</sup> (mg/L)</b>
Acetylsalicylic acid	100–10,000	1
Atenolol	100–1000	N/A
Betaxolol	100–1000	N/A
Bezafibrate	100–1000	N/A
Caffeine	100–10,000	N/A
Carbamazepine	10–100	0.01–100
Cimetidine	1000	N/A
Clofibrate	1–100	0.01
Clofibric acid	10–1000	0.1–100
Diazepam	1–10,000	N/A
Diclofenac	10–100	0.001–100
Fenofibrate	10–100	N/A
Fluoxetine	0.1–10	0.001–10
Gemfibrozil	100	N/A
Ibuprofen	1–1000	100–1000
Metformin	10–1000	N/A
Methotrexate	10–1000	N/A
Metoprolol	1–1000	N/A
Naproxen	10–1000	100–1000
Paracetamol	10–10,000	N/A
Propranolol	0.1–1000	0.0001–1000
Ranitidine	1000	N/A
Salicylic acid	10–10,000	10
Sotalol	100–1000	N/A

*Source:* Adapted from Fent et al., 2006

*Notes:* a=range based on different studies, bioassays, and exposure conditions; b=range based on different studies, bioassays, and endpoints; N/A=not applicable

In contrast to the observed effects on fish in wastewater-impacted receiving waters, scientists are still conflicted on the direct human health effects of TOrCs. As far as acute toxicity, it is unlikely that PPCPs will induce measurable effects on public health at observed concentrations (Snyder et al., 2003b); however, the effects of chronic exposure to mixtures of compounds are largely unknown. In the absence of concrete dose–response data, officials must rely on toxicological frameworks and screening models based on limited data (Australia, 2008; Snyder et al., 2008a; Schriks et al., 2010). As a result, studies may differ by orders of magnitude in their risk values. Using these various reference levels, conservative safety factors, and common risk assessment parameters (e.g., 70-kg person and water consumption of 2 L per day), drinking water equivalent levels (DWELs) can be developed and proposed as benchmarks for water quality. Depending on the study, the DWELs are often compared to observed concentrations in the environment or other exposure routes (e.g., beverages, foods; Snyder et al., 2008a) to develop benchmark quotients (BQs; Schriks et al., 2010), recommended MRLs (Snyder et al., 2008a), or other points of reference.

Subsets of the DWELs from two human risk assessment studies (Snyder et al., 2008a; Schriks et al., 2010) and the Australian Guidelines for Water Recycling (Australia, 2008) are provided in Table 1.2. Despite the uncertainty described previously, the general conclusions in these studies are consistent. In most cases, these values are only proposed as points of reference to communicate the relevance of TOrCs in water supplies, so they currently have little regulatory significance. In contrast to the ecotoxicological significance of some TOrCs, the observed concentrations of most contaminants are significantly lower than the human toxicological thresholds developed in the referenced studies. Despite this general disparity between observed concentrations and toxicological significance, there is strong pressure to regulate TOrCs in drinking water and wastewater effluent intended for indirect potable reuse (IPR).

**Table 1.2. Summary of Toxicological Relevance of TOrCs in Water Supplies**

Class/ Contaminant	Snyder et al.		Schriks et al.		Australia
	DWEL (µg/L)	Daily Consumption To Exceed ADI (L)	Guideline Value (µg/L)	BQ	Guideline Value (µg/L)
<b>Antianxiety</b>					
Diazepam	35	210,000	--	--	2.5
Meprobamate	260	12,000	--	--	--
<b>Antibacterial/antibiotic</b>					
Triclosan	2600	4,300,000	--	--	0.35
Sulfamethoxazole	18,000	12,000,000	440	0.00007	35
Trimethoprim	6700	>54,000,000	--	--	70
<b>Anticonvulsant</b>					
Carbamazepine	12	1300	1	0.03	100
Phenytoin	6.8	430	--	--	--
<b>Antidepressant</b>					
Fluoxetine	34	83,000	--	--	10
<b>Beta blocker</b>					
Atenolol	70	5400	--	--	--
<b>DBP</b>					
NDMA	--	--	0.1	0.02	0.01
<b>Flame retardant</b>					
	--	--	77	--	1

Class/ Contaminant	Snyder et al.		Schriks et al.		Australia
	DWEL (µg/L)	Daily Consumption To Exceed ADI (L)	Guideline Value (µg/L)	BQ	Guideline Value (µg/L)
TCEP					
<b>Fragrance</b>					
Musk ketone	--	--	--	--	350
<b>Herbicide/pesticide</b>					
Atrazine	3	6	--	--	40
DEET	--	--	6250	0.000005	2500
Diuron	--	--	7	0.01	30
Lindane	20	>4000	--	--	0.02
Methoxychlor	0.70	>140	--	--	--
<b>Industrial chemical</b>					
1,4-dioxane	--	--	30	0.02	--
Nonylphenol	1800	33,000	--	--	500
Octylphenol	5300	>430,000	--	--	50
PFOA	--	--	5.3	0.1	--
PFOS	--	--	0.5	0.04	--
<b>Lipid regulator</b>					
Atorvastatin	19	>150,000	--	--	5
Clofibric acid	--	--	30	0.005	750
Gemfibrozil	45	43,000	--	--	600
<b>NSAID</b>					
Diclofenac	2300	>18,000,000	--	--	1.8
Ibuprofen	--	--	--	--	400
Naproxen	20,000	>80,000,000	--	--	220
<b>Plasticizer</b>					
Bisphenol A	1800	140,000	--	--	200
<b>Steroid hormone</b>					
Estradiol	1.8	>7100	--	--	0.175
Estrone	0.46	>4500	--	--	0.03
Ethinylestradiol	0.0035	>7	--	--	0.015
<b>X-ray contrast</b>					
Iopromide	--	--	250,000	0.0000002	750

Sources: Snyder et al., 2008a; Schriks et al., 2010; Australia, 2008

Notes: ADI=acceptable daily intake, based on maximum observed concentration in drinking water;

BQ=benchmark quotient, maximum concentration in drinking water divided by guideline value; DBP=disinfection byproduct; DEET=*N,N*-diethyl-*meta*-toluamide; DWEL=drinking water equivalent level; NSAID=nonsteroidal anti-inflammatory drug; NDMA=N-nitrosodimethylamine; PFOA=perfluorooctanoic acid; PFOS= perfluorooctanesulfonic acid; TCEP=tris-(2-chloroethyl)-phosphate

### 1.1.2 Current Water Reuse Guidelines and Regulations

In contrast to drinking water standards, such as those established by the Safe Drinking Water Act (SDWA) in the United States, and nutrient levels mandated by wastewater discharge permits, there is a paucity of regulation related to TOxCs in wastewater effluents. The U.S. Food and Drug Administration requires companies to conduct an environmental impact assessment for any human pharmaceutical expected to be found in the environment at a concentration exceeding 1 µg/L (Fent et al., 2006); however, there is little regulatory guidance beyond that point. Although TOxCs may be the impetus for augmenting treatment

trains, it is unclear whether these contaminants will be a significant factor in establishing design criteria for advanced wastewater treatment processes. In many situations, design criteria may actually be based on disinfection requirements or DBP mitigation. One of the primary factors limiting ozone's widespread applicability to water and wastewater treatment is bromate formation. Although a drinking water maximum contaminant level (MCL) of 10 µg/L has been established in the United States, more relaxed targets (e.g., 3 mg/L) have been proposed for environmental discharge (Hollender et al., 2009), which would increase the applicability of ozone for wastewater treatment.

For water reuse in the United States, regulatory agencies can refer to the U.S. Environmental Protection Agency (EPA) *Guidelines for Water Reuse* (EPA, 2012), CDPH Title 22 requirements for water recycling (CDPH, 2009b; CDPH, 2011), or local standards for wastewater contaminants. Of course, water reuse regulations vary tremendously depending on the ultimate use of that resource (e.g., IPR vs. golf course irrigation). For unrestricted urban reuse, states generally specify an acceptable treatment train in addition to turbidity and disinfection requirements. Florida also requires periodic monitoring for *Giardia* and *Cryptosporidium*. Reuse requirements for Florida, Washington, and California are provided in Table 1.3 as an example.

In 2004, only four states (California, Florida, Hawaii, and Washington) had specific standards for IPR permits, and they generally addressed total suspended solids (TSS), total nitrogen (TN), total organic carbon (TOC), turbidity, total organic halides (TOX), and total coliforms. Wastewater intended for IPR is also expected to comply with primary and secondary drinking water standards. Washington specifically requires water intended for surface percolation or direct recharge to comply with established MCLs in accordance with the SDWA. For direct recharge applications, California and Washington specify the amount of time the water should be stored in an aquifer before it can be withdrawn for drinking water applications in addition to offset distances between recharge and withdrawal locations. Washington also requires reverse osmosis (RO) in all direct recharge applications (EPA, 2004). The permitting standards for Florida, Washington, and California are summarized in Table 1.3, and the California standards are described in greater detail in the following discussion of Title 22.

The CDPH Title 22 requirements discuss a number of parameters, including TN, TOC, turbidity, total coliforms, and viruses. In addition to specifying restrictions on proximity of use to municipal water wells and other high-risk areas, Title 22 defines three categories for reuse water: disinfected secondary-23 (e.g., inedible crops and freeway irrigation), disinfected secondary-2.2 (e.g., food crops with no contact between water and the edible portion of food), and disinfected tertiary recycled water (e.g., full-contact food crops and unrestricted golf course irrigation). For a disinfected secondary-23 designation, the median concentration of total coliforms over a 7-day period cannot exceed 23 most probable number (MPN)/100 mL, and no more than one sample can exceed 240 MPN/100 mL over a 30-day period. For a disinfected secondary-2.2 designation, the median concentration of total coliforms over a 7-day period cannot exceed 2.2 MPN/100 mL, and no more than one sample can exceed 23 MPN/100 mL over a 30-day period. Also, no sample can exceed a total coliform concentration of 240 MPN/100 mL. In addition to complying with the secondary-2.2 requirements, disinfected tertiary recycled water must satisfy specific turbidity requirements related to the mode of filtration. As a conservative guideline, the turbidity should not exceed 2 NTU for media-filtered water or 0.2 NTU for membrane-filtered water. The treatment must also satisfy one of the following disinfection requirements: (1) a free chlorine CT value of at least 450 mg/min/L or (2) an alternative treatment certified by the State of California to achieve at least 5-log inactivation of poliovirus or an acceptable

surrogate (e.g., MS2; CDPH, 2009b). Currently, the HiPOx<sup>®</sup> system by APTwater (Long Beach, CA) is the only ozone-based technology certified under Title 22.

For IPR in California, applications are now separated into three different categories according to the Draft Groundwater Replenishment Reuse Regulations published in November 2011: (1) groundwater replenishment via surface application without full advanced treatment (FAT), (2) groundwater replenishment via subsurface application with FAT, and (3) groundwater replenishment via surface application with FAT. With the exception of FAT, the requirements are relatively similar between the three categories. All systems are required to demonstrate wastewater source control; satisfy the definition of a disinfected tertiary effluent; provide a total of 12-, 10-, and 10-log removal/inactivation for viruses, *Giardia* cysts, and *Cryptosporidium* oocysts, respectively; achieve 10 mg N/L of TN; and achieve a maximum TOC concentration (TOC<sub>max</sub>) equal to 0.5 divided by the proposed recycled water contribution. For the pathogen reductions, no single treatment process can be credited with more than 6-log removal/inactivation, and each process used to demonstrate compliance must achieve at least 1-log removal/inactivation. Each month of underground storage also provides 1-log viral removal/inactivation, but the agency must calculate the retention time using specified methods. In combination with FAT, which will be described, six months of certified underground storage automatically qualifies for the 10-log parasite removal/inactivation requirements. In addition to satisfying the pathogen reduction requirements, the hydraulic residence time in the subsurface environment must allow for sufficient response time to address treatment failures and mitigate public health risks.

**Table 1.3. Water Reuse Standards for Florida, Washington, and California**

Application	Parameter	FL	WA	CA
<b>Unrestricted urban reuse</b>	TSS (mg/L)	5	30	N/A
	monthly average turbidity (NTU)	2–2.5	2	2
	maximum turbidity (NTU)	N/A	5	5
	indicator coliform	fecal	total	total
	average (MPN/100 mL)	ND <sup>a</sup>	2.2	2.2 <sup>a</sup>
	maximum (MPN/100 mL)	25	23	240 <sup>a</sup>
<b>Indirect potable reuse</b>	TSS (mg/L)	5	5	N/A
	monthly average turbidity (NTU)	N/A	0.1	2/0.2 <sup>d</sup>
	maximum turbidity (NTU)	N/A	0.5	10/0.5 <sup>d</sup>
	monthly average TOC (mg/L)	3	N/A	N/A
	maximum TOC (mg/L)	5	1	calculated
	total nitrogen (mg/N/L)	10	10	10
	monthly average TOX (mg/L)	0.2	N/A	N/A
	indicator coliform	total	total	Total
	median (MPN/100 mL)	N/A	1 <sup>b</sup>	2.2 <sup>b</sup>
	maximum (MPN/100 mL)	ND	5 <sup>b</sup>	240 <sup>c</sup>
storage time (months)	N/A	12	6	
minimum offset distance (feet)	500	2000	N/A	

Source: EPA, 2004

Notes: N/A=not applicable; ND=not detected at method limits; a=in 75% of samples over 30-day period; b=over a 7-day period; c=only one sample can exceed 23 MPN/100 mL over 30-day period; d=media filtration/membrane filtration; MPN=most probable number; TOC=total organic carbon; TOX=total organic halides; TSS=total suspended solids.

IPR systems must generally comply with primary and secondary MCLs for drinking water. The CDPH draft regulations specifically address a group of priority toxic pollutants, inorganic chemicals, radionuclide chemicals, organic chemicals, DBPs, lead, and copper. IPR systems must also achieve established notification levels (NLs) for organic contaminants. California has established a public health goal of 3 ng/L, an NL of 10 ng/L, and a response level of 300 ng/L for NDMA because of its demonstrated carcinogenicity. This is supplemented with NLs of 10 ng/L and response levels of 100 and 500 ng/L for *N*-nitrosodiethylamine and *N*-nitrosodi-n-propylamine; CDPH, 2009a). The NL concept differs from the original draft regulations, which mandated 1.2- and 0.5-log removal/destruction of NDMA and 1,4-dioxane, although the previous NDMA and 1,4-dioxane requirements can still be used as a general rule of thumb for treatment train design, as described herein.

The primary distinction between the three IPR categories involves the use of FAT, which is a combination of RO capable of achieving 99.5% sodium chloride rejection and a robust oxidation process. The oxidation process must achieve 0.5-log destruction of at least one indicator compound from each of the following seven compound classes: hydroxy aromatic, amino/acylamino aromatic, nonaromatic with carbon double bonds, deprotonated amine, alkoxy polyaromatic, alkoxy aromatic, and alkyl aromatic. The oxidation process must also achieve 0.3-log destruction of at least one indicator compound from each of the following two compound classes: saturated aliphatic and nitro aromatic. In order to ensure process integrity, a surrogate parameter (e.g., differential chloramine or UV<sub>254</sub> absorbance) must also be correlated to the destruction/removal of the indicator compounds and monitored continuously. These new regulations highlight the importance of compound groupings, which have been proposed in this study, and surrogate parameters suitable for real-time, online monitoring of process performance, which is the focus of other WateReuse Research Foundation projects (e.g., WRF-11-01).

Although federal regulations and guidelines pertaining to PPCPs, EDCs, and other TOxCs are extremely limited (e.g., atrazine MCL of 3 µg/L), several common compounds (e.g., 1,4-dioxane, erythromycin, steroid hormones, nitrosamines, pesticides) are listed in the most recent version of the U.S. EPA Contaminant Candidate List 3 (CCL3). The CCL3 is a list of unregulated contaminants that are known or have the potential to occur in public water supplies and may pose a threat to human health. Although these contaminants have been identified for priority research, target concentrations have not been identified, and these contaminants may never actually be regulated. Similarly, the European Union (EU) recently identified a list of 33 priority substances (e.g., atrazine, octylphenols) for which mitigation measures or environmental quality standards will be developed in the near future (EU, 2000). Australia has specifically identified a number of emerging contaminants in addition to identifying corresponding drinking water goals for their potable reuse and drinking water systems. In 2008, the Environment Protection Heritage Council, National Health and Medical Research Council and Natural Resource Management Ministerial Council published the Augmentation of Drinking Water Supplies module of the Australian Guidelines for Water Recycling. The authors emphasize that the information presented in the document is not legally binding and only serves as a summary of scientific evidence pertaining to water reuse paradigms (Australia, 2008).

The Augmentation of Drinking Water Supplies module is primarily based on the Australian Drinking Water Guidelines. Similar to frameworks used in other countries to establish regulations and goals, the treatment levels identified in the document balance the practicality and costs associated with water and wastewater treatment with the acceptable risk for a particular chemical or microbial contaminant. For microbial contaminants, Australia targets

pathogen levels corresponding to  $10^{-6}$  annual disability adjusted life years (DALYs) per person, and for most chemical contaminants, the treatment goals are based on no observed effect levels supplemented by safety factors or a cancer risk of  $10^{-6}$ . However, the treatment goals are slightly different for emerging contaminants: toxicity equivalents for dioxins and polychlorinated biphenyls, acceptable daily intakes (ADIs) for agricultural and veterinary pharmaceuticals, and therapeutic doses supplemented with safety factors ranging from 1000 to 10,000 for human pharmaceuticals (Australia, 2008). A plethora of compounds have been assigned treatment goals in the Australian document, but this review will only discuss several microbes and PPCPs/EDCs/TOrCs that have received considerable attention in recent years because of their ubiquity in wastewater effluent.

Based on their anticipated prevalence in wastewater coupled with the DALY risk framework, required log reductions for *Cryptosporidium*, enteric viruses, and *Campylobacter* are 8, 9.5, and 8.1, respectively. The Australian guidelines indicate that the typical IPR system comprising membrane filtration, RO, and advanced oxidation will be sufficient to achieve these microbial reductions. The document also provides a table of expected treatment efficacies for a variety of wastewater treatment processes, including ozonation: 2- to 6-log inactivation for vegetative bacteria and viruses, 2- to 4-log inactivation for *Giardia*, 1- to 2-log inactivation of *Cryptosporidium*, and 0 to 0.5-log inactivation of spore-forming bacteria. A similar table is provided for ozonation of emerging chemical contaminants, including antibiotics (>95% removal), carbamazepine (50–80% removal), ibuprofen (50–80% removal), steroid hormones (>95% removal), and other PPCPs/EDCs/TOrCs (Australia, 2008). The actual guidelines for a subset of these emerging contaminants are provided in Table 1.2.

Few emerging contaminants exceed the Australian guidelines for augmentation of drinking water supplies—even when considering the maximum concentrations observed in secondary effluents (Australia, 2008). For those compounds with higher concentrations than the recommended guidelines, optimized conventional wastewater treatment (e.g., biotransformation of caffeine) or disinfection processes (e.g., ozonation of steroid hormones) may be sufficient to achieve the specified goals. Implementation of advanced treatment processes, such as advanced oxidation or RO, would provide even greater safeguards for human and environmental health. A detailed discussion of ozone-related treatment parameters is provided in the following sections.

## 1.2 Efficacy of Ozone for Contaminant Oxidation

Regarding the oxidation of chemical contaminants, ozone reacts directly with organic molecules and indirectly through the formation of radical species (Langlais et al., 1991). For direct reactions, ozone reacts rapidly with amines, phenols, and double bonds in aliphatic compounds. In contrast to photolysis, many pharmaceuticals and EDCs are degraded rapidly (Snyder et al., 2006; Wert et al., 2009a) with ozone CTs commonly used for disinfection applications (less than 20 mg/min L<sup>-1</sup>). Because molecular ozone is very effective for TOrC mitigation, modifying the process with H<sub>2</sub>O<sub>2</sub> is not always necessary, although it may increase the reaction rate for some compounds, reduce the structural footprint associated with ozone contactors, and provide some degree of bromate mitigation (Snyder et al., 2007). In fact, the natural decomposition of molecular ozone during reactions with EfOM yields •OH exposure in wastewater applications similar to what would be achieved with ozone/H<sub>2</sub>O<sub>2</sub>.

Table 1.4 describes the relative removals of a suite of pharmaceuticals and potential EDCs in tertiary-treated wastewater with an applied ozone dose of 2.7 mg/L and a contact time of

24 minutes. It also highlights the potential use of QSARs to identify useful indicator compounds representative of larger compound classes rather than monitoring for the countless number of anthropogenic and natural contaminants found in water.

Huber et al. (2003) calculated second-order rate constants for the ozonation of pharmaceuticals and EDCs, and a summary is provided in Table 1.5 (additional rate constants are provided in Table 3.4). With respect to QSARs, the authors noted that the aromatic and tertiary amine moieties found in sulfonamide and macrolide antibiotics are reactive with ozone, and all compounds within these classes should have similar reaction rates. Furthermore, the authors indicated that ketone-containing steroid hormones are likely to have rate constants that are approximately one order of magnitude less than the phenolic steroid hormones. The compounds experiencing the least amount of degradation are generally characterized by extensive branching (e.g., meprobamate and iopromide) and are sometimes designed specifically to resist oxidation (e.g., the flame retardant tris-(2-chloroethyl)-phosphate [TCEP]). As with chlorine and other oxidation processes, complete mineralization with ozone is impractical given the energy requirement and the potential to form DBPs (e.g., bromate). Thus, the potential effects of ozone transformation products must be considered.

**Table 1.4. TOxC Oxidation During Ozonation (O<sub>3</sub>:TOC=0.4)**

<b>&lt;20% Degradation</b>	<b>20–50% Degradation</b>	<b>50–80% Degradation</b>	<b>&gt;80% Degradation</b>
TCEP	atrazine iopromide meprobamate	DEET diazepam dilantin ibuprofen	acetaminophen androstenedione caffeine carbamazepine diclofenac erythromycin estradiol estriol estrone ethinyl estradiol fluoxetine gemfibrozil hydrocodone naproxen oxybenzone pentoxifylline progesterone sulfamethoxazole testosterone triclosan trimethoprim

*Source:* Snyder et al., 2007

**Table 1.5. Second-Order Ozonation Rate Constants**

Contaminant	pK <sub>a</sub>	k <sub>ozone</sub> (M <sup>-1</sup> s <sup>-1</sup> )*	Reactive Species
Bezafibrate	3.6	6x10 <sup>2</sup>	dissociated
Carbamazepine	N/A	3x10 <sup>5</sup>	neutral
Diazepam	N/A	0.8	neutral
Diclofenac	4.2	1x10 <sup>6</sup>	dissociated
Ethinylestradiol	10.4	7x10 <sup>9</sup>	dissociated
Ibuprofen	4.9	10	dissociated
Iopromide	N/A	<0.8	neutral
Sulfamethoxazole	5.7	3x10 <sup>6</sup>	dissociated
Roxithromycin	8.8	5x10 <sup>6</sup>	neutral

Source: Adapted from Huber et al., 2003

Note: \*Reaction rates are specific to dominant species commonly found at pH 5–10.

### 1.3 Efficacy of Ozone for Wastewater Disinfection

Ozone inactivates microorganisms by disrupting membrane or protein capsid integrity, destroying vital enzymes, or denaturing genetic material (Maier et al., 2000). Although ozone does not provide a stable, long-term residual, which is necessary to prevent microbial regrowth in distribution systems, it is considered to be a stronger disinfectant than chlorine or chloramine. Some microbes (e.g., *Giardia* cysts and *Cryptosporidium* oocysts) demonstrate a small degree of resistance to ozone, but there are no significant outliers that limit its applicability to water or wastewater disinfection. In contrast, *Cryptosporidium* oocysts are considered highly resistant to free chlorine based on a CT of >7200 mg/min/L for 2-log inactivation (Maier et al., 2000). Because of its propensity for DNA repair after UV disinfection (Yates et al., 2006), 4-log inactivation of adenovirus may require anywhere from 100 to 225 mJ/cm<sup>2</sup> (Gerrity et al., 2008). In fact, this resistance is the basis for the viral UV disinfection requirements in the Long Term 2 Enhanced Surface Water Treatment Rule (LT2ESWTR; i.e., 186 mJ/cm<sup>2</sup> for 4-log inactivation credit; Yates et al., 2006). As a basis for comparison, ozone CT values for 2-log inactivation range from 0.006 to 0.02 mg/min/L for *E. coli*, 0.20 to 0.72 mg/min/L for poliovirus, and 0.53 to 7.0 mg/min/L for *Giardia* and *Cryptosporidium*, respectively (Maier et al., 2000). Contrary to these relative values, recent studies suggest that viral inactivation is more rapid than coliform inactivation (Xu et al., 2002; Gehr et al., 2003; Ishida et al., 2008).

Historically, water and wastewater utilities have relied on CT as a means to predict disinfection efficacy. Although the CT concept is adequate for conventional chlorine disinfection, it is not always appropriate for ozone processes, particularly for ozone/H<sub>2</sub>O<sub>2</sub> in which the ozone residual is quenched and •OH chemistry dominates. Similar situations arise with ozone in wastewater because it is short-lived and cannot be easily monitored as it is in drinking water treatment (Buffle et al., 2006b). Recent studies suggest that significant microbial inactivation is possible even when the applied ozone dose is less than the IOD, which corresponds to an apparent CT of 0 (Xu et al., 2002; Gehr et al., 2003; Ishida et al., 2008). Unfortunately, the current regulatory framework with its emphasis on CT values does not recognize these low-dose benefits. Furthermore, other studies have demonstrated oxidation of ozone-susceptible TORCs with doses less than the IOD (Wert et al., 2009a). Therefore, more research is necessary to fully characterize the efficacy and applicability of this low-dose strategy and increase regulatory acceptance.

Given the prevalence of pathogenic bacteria, viruses, and parasites in wastewater, effective disinfection is vital to human health, particularly in reclaimed water and IPR applications. In highly contaminated raw wastewater, studies report fecal coliform and *Salmonella* at levels of  $10^9$  MPN/100 mL, *Vibrio cholerae* at  $10^6$  MPN/100 mL, enterococci at  $10^2$ /100 mL, coliphages at  $10^3$  PFU/100 mL, *Cryptosporidium* at  $10^4$  oocysts/L, and a variety of amoebae and helminths (de Velasquez et al., 2008). For clarification, MPN is a statistical representation of the number of microbes in a sample, a plaque-forming unit (PFU) is assumed to represent a single virus in the original sample, and a colony-forming unit (CFU) is assumed to represent a single bacterium in the original sample. Although primary, secondary (refer to Table 1.6), and tertiary treatment provide slight reductions in pathogen loads, disinfection is always necessary to protect human health because of the low infectious doses for many pathogens.

**Table 1.6. Prevalence of Indicators and Pathogens in Secondary Effluent**

Microbe	Number/100 mL
Fecal coliform	104 to 106
Fecal streptococci	103 to 105
Human viruses	10-2 to 103
Salmonella	101 to 102
Total coliform	104 to 106

Source: EPA, 1986

Despite its use in municipal applications since the 1970s (Burns et al., 2007), the available literature related to ozone disinfection for wastewater is somewhat limited. In 1986, the U.S. EPA published its *Municipal Wastewater Disinfection* design manual describing recommended applied ozone doses for total coliform disinfection, which are provided in Table 1.7 (EPA, 1986; Burns et al., 2007). During these initial years, ozone was often considered cost-prohibitive and problematic in wastewater applications due to frequent operational issues (Xu et al., 2002; Burns et al., 2007; Ishida et al., 2008).

**Table 1.7. Recommended Applied Ozone Doses for Total Coliform Inactivation**

Water Matrix	2.2 CFU/100 mL	70 CFU/100 mL	200 CFU/100 mL
Tertiary treatment with partial nitrification	35–40 mg/L	15–20 mg/L	12–15 mg/L
Tertiary treatment with full nitrification	15–20 mg/L	5–10 mg/L	3–5 mg/L

Sources: EPA, 1986; Burns et al., 2007

More recent literature suggests that modern ozone systems are actually viable alternatives for wastewater disinfection. Xu et al. (2002) evaluated two different pilot-scale ozone systems to determine the most important factors affecting ozone efficacy in wastewater. Table 1.8 provides a summary of the experimental conditions for the three wastewaters in their study. Additional tests were performed on Wastewater B after microfiltration (10 µm) to determine the effect of TSS reduction on ozone efficacy.

**Table 1.8. Summary of Experimental Conditions in Xu et al. (2002)**

Parameter	Wastewater A	Wastewater B	Wastewater C
Location	Indiana, USA	Evry, France	Washington, UK
Flow rate (m <sup>3</sup> /day)	300,000	48,000	90,000
Matrix	tertiary effluent	secondary effluent	secondary effluent
<i>Clostridium</i> (log CFU/100 mL)	N/A	3.0–4.5	3.6–5.5
COD (mg/L)	30	36	71
Contact time (min)	3–15	2–10	2–10
<i>E. coli</i> (log CFU/100 mL)	2.7–4.3	N/A	N/A
Enterococci (log/100 mL)	N/A	N/A	4.5–4.9
Enterovirus (PFU/10 L)	N/A	N/A	544–775
F-specific coliphage (PFU/mL)	N/A	N/A	96–144
Fecal coliforms (log CFU/100 mL)	N/A	3.6–4.5	4.3–6.5
IOD (mg/L)	2.5–5.3	3.1–4.2	7.4–9.6
O <sub>3</sub> dose, applied (mg/L)	1–35	3–16	4–50
O <sub>3</sub> dose, transferred (mg/L)	0.5–12	2–13	4–30
pH	7.0	7.3	7.5
TOC (mg/L)	8	<10	26
TSS (mg/L)	2.3	5	18
UV <sub>254</sub> absorbance (cm <sup>-1</sup> )	0.155	0.222	0.349

Notes: COD=chemical oxygen demand; IOD=instantaneous ozone demand; TOC=total organic carbon; TSS=total suspended solids; UV=ultraviolet

With a transferred ozone dose of 7.5 mg/L (O<sub>3</sub>:TOC=0.94), the authors demonstrated consistent fecal coliform levels of <2.2 MPN/100 mL for Wastewater A. With similar ozone to TOC ratios in the more challenging wastewaters, the authors could only maintain fecal coliforms levels of <100 MPN/100 mL. It is interesting that the authors reported 1- to 3-log inactivation of fecal coliforms with transferred ozone doses less than the IOD (i.e., apparent ozone CT of 0). Compared to other pathogens and surrogates in Wastewater C, enterococci and *Salmonella* were highly susceptible to ozonation; >2.2- and 2.9-log inactivation of F-specific coliphages (e.g., MS2) and enteroviruses were achieved with transferred ozone doses of 8.6 (O<sub>3</sub>:TOC=0.33) and 4.8 mg/L (O<sub>3</sub>:TOC=0.18); and spore-forming *Clostridium* experienced less than 2-log inactivation with a transferred ozone dose of 33 mg/L (O<sub>3</sub>:TOC=1.27). Finally, in order to comply with World Health Organization guidelines for

irrigation (i.e., fecal coliforms  $<10^3$  CFU/100 mL), the authors indicated that transferred ozone doses of 2, 4, and 10 mg/L would be required for Wastewaters A, B, and C, respectively. These doses correspond to  $O_3$ :TOC ratios of 0.25,  $>0.40$ , and 0.38, respectively. CDPH Title 22 compliance (i.e.,  $<2.2$  MPN/100 mL) could only be achieved with practical doses in Wastewater A.

As indicated, wastewater quality and level of pretreatment significantly impact ozone efficacy for coliform disinfection. As further evidence, Gehr et al. (2003) performed bench-scale ozone disinfection experiments on a primary effluent from the City of Montreal Wastewater Treatment Plant. The treatment plant, which is designed to handle up to 7.6 million  $m^3$ /day (343 MGD), consists only of coarse screening, chemical addition (alum, ferric chloride, and polymer) to improve settling of suspended particles, and primary clarification. There is no disinfection prior to environmental discharge. Because of the limited pretreatment, the wastewater quality was highly variable during the experimental period: TOC of 90 to 110 mg/L (Gagnon et al., 2008), chemical oxygen demand (COD) of 123 to 240 mg/L, TSS of 16 to 45 mg/L, and turbidity of 16 to 31 NTU. Because of substantial reactivity with dissolved organic matter, the IOD of this wastewater was determined to be 25 mg/L ( $O_3$ :TOC $\approx$ 0.25). The authors were able to achieve approximately 3-log inactivation of fecal coliforms with a transferred ozone dose of 70 mg/L ( $O_3$ :TOC=0.70), but the residual fecal coliform level still exceeded  $10^3$  CFU/100 mL. As expected, *Clostridium* proved to be more resistant and only experienced 1-log inactivation at the same transferred ozone dose. In contrast, the authors achieved 4-log inactivation of MS2, which approached the detection limit of the assay (i.e., 1 PFU/mL), with a transferred ozone dose approximately equal to the IOD (i.e., 25 mg/L or  $O_3$ :TOC=0.25).

Mezzanotte et al. (2007) evaluated ozone disinfection in a 4.5  $m^3$ /h (20-gpm) pilot wastewater treatment plant in Italy. The pilot plant treated secondary effluent with the following average water quality characteristics: pH of 7.1, COD of  $<20$  mg/L, TOC of 5.1 mg/L, TSS of 2.3 mg/L, turbidity of 1.8 NTU, and  $UV_{254}$  transmittance of 75%. The total coliform, fecal coliform, and *E. coli* levels were  $2.0 \times 10^5$  CFU/100 mL,  $4.7 \times 10^4$  CFU/100 mL, and  $1.2 \times 10^4$  CFU/100 mL, respectively. The authors tested ozone doses ranging from 2.0 to 7.1 mg/L ( $O_3$ :TOC=0.39–1.39) with contact times ranging from 6 to 13 minutes. They determined that 4-log inactivation of total coliforms, fecal coliforms, and *E. coli* required ozone doses and contact times of 3.6 mg/L ( $O_3$ :TOC=0.71) and 12.8 minutes, 4.6 mg/L ( $O_3$ :TOC=0.90) and 12.8 minutes, and 5.3 mg/L ( $O_3$ :TOC=1.04) and 6.4 minutes, respectively.

Ishida et al. (2008) evaluated a pilot-scale ozone/ $H_2O_2$  system (HiPOx<sup>®</sup>) based on its ability to inactivate total coliforms in media-filtered effluent and MS2 in microfiltered effluent. With preliminary bench-scale experiments, the study first determined that 5-log poliovirus inactivation, which is the disinfection goal according to the CDPH Title 22 requirements, corresponded to a more conservative 6.5-log MS2 inactivation. Operating at a flow rate of 4.2  $m^3$ /h (18.4 gpm), the pilot system required minimum ozone CT values of 0.20 mg/min/L for 6.5-log reduction of MS2 and 1.0 mg/min/L to reach the  $<2.2$  MPN/100 mL threshold for CDPH. Similar to Xu et al. (2002), significant (i.e.,  $>4.5$ -log) inactivation of MS2 occurred with ozone doses less than the IOD, which corresponds to an apparent CT of 0. Although bromate mitigation was observed, the addition of  $H_2O_2$  did not have any significant impacts on microbial inactivation.

As demonstrated by these studies, one of the main issues affecting the efficacy of ozone disinfection is the level of pretreatment, particularly for EfOM and suspended solids. TSS can

contribute to decreased disinfection efficacy through particle shielding, which often necessitates “boil-water” advisories during high-turbidity events. Dietrich et al. (2007) identified 11  $\mu\text{m}$  as the threshold for significant particle shielding. In relation to ozone disinfection, Xu et al. (2002) compared the same wastewater before (TSS of 5 mg/L) and after (TSS of <2 mg/L) MF. The authors discovered that MF had no impact on ozone demand, but an additional 1-log inactivation of total coliforms was achieved in the low-TSS condition. Ishida et al. (2008) also observed increased MS2 inactivation with ozone in microfiltered versus media-filtered wastewater. Dietrich et al. (2007) evaluated the efficacy of ozone disinfection in three wastewaters with varying particle size distributions. The authors supported the claim that oxidant demand is generally dominated by EfOM, and they indicated that applied doses must exceed the organic demand before oxidants, particularly ozone, will diffuse into the particle pore space and overcome the shielding effect.

## 1.4 Correlations between Bulk Organic Parameters and Process Efficacy

Currently, there are few studies that describe the relationship between changes in bulk organic parameters and process efficacy. Studies using fluorescence as part of an analytical method to detect TOrCs are becoming more common (Camacho-Munoz et al., 2009), but the goal of these studies is inherently different than using changes in bulk organic parameters to estimate the extent of oxidation of a target compound or microbe. Wert et al. (2009b) performed one of the first studies to identify  $\text{UV}_{254}$  absorbance and color as viable surrogates for ozone oxidation efficacy. They indicated that ozone-susceptible target compounds (i.e.,  $k_{\text{ozone}} > 10^3 \text{ M}^{-1} \text{ s}^{-1}$ ) correlated well with 0 to 50% reductions in  $\text{UV}_{254}$  absorbance, whereas ozone-resistant compounds (i.e.,  $k_{\text{ozone}} < 10^3 \text{ M}^{-1} \text{ s}^{-1}$ ) correlated well with 15 to 65% reductions in  $\text{UV}_{254}$  absorbance. In addition to developing individual correlations for six pharmaceuticals, the study also indicated that the empirical correlations were consistent between different wastewater qualities, as shown in Figure 1.1. Rosario-Ortiz et al. (2010) extended this concept to the UV/ $\text{H}_2\text{O}_2$  AOP. The authors evaluated different UV and  $\text{H}_2\text{O}_2$  dosing conditions to determine the extent of oxidation for six pharmaceuticals. Similar to Wert et al. (2009b), each compound exhibited a different correlation with changes in  $\text{UV}_{254}$  absorbance, primarily because of their variable resistance to  $\bullet\text{OH}$ , but the authors concluded that the empirical correlations were consistent among several water qualities. Figure 1.2 provides examples of the UV/ $\text{H}_2\text{O}_2$  correlations developed during their study. Finally, Nanaboina and Korshin (2010) developed more mechanistic correlations equating changes in chromophore and contaminant concentrations.

Gerrity et al. (2010) illustrated how this concept can be applied to novel forms of advanced oxidation, specifically nonthermal plasma. Nonthermal plasma uses high voltage electrical pulses across a carbon fiber/stainless steel electrode to generate a corona discharge directly above the target water matrix. The corona discharge creates ozone,  $\bullet\text{OH}$ , and UV light that simultaneously oxidize and photolyze target contaminants in the water. Figure 1.3 illustrates the correlations developed during their study, but because the authors only focused on one wastewater quality, it is not possible to conclude whether the correlations would remain consistent between different wastewaters for this technology.

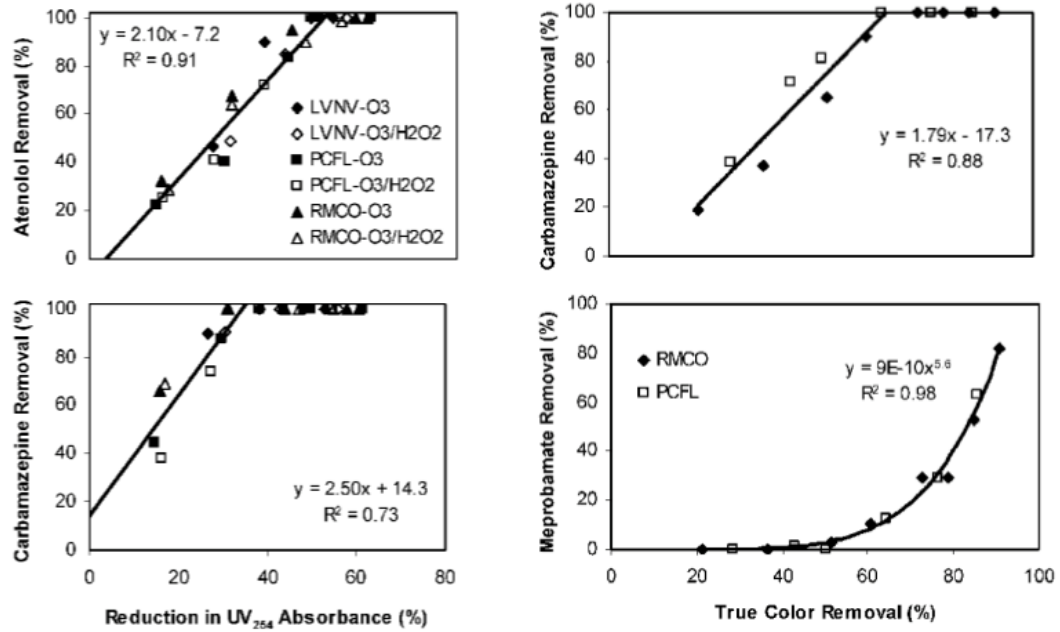


**Figure 1.1. Bulk organic correlations for ozone oxidation.**

Source: Wert et al., 2009b

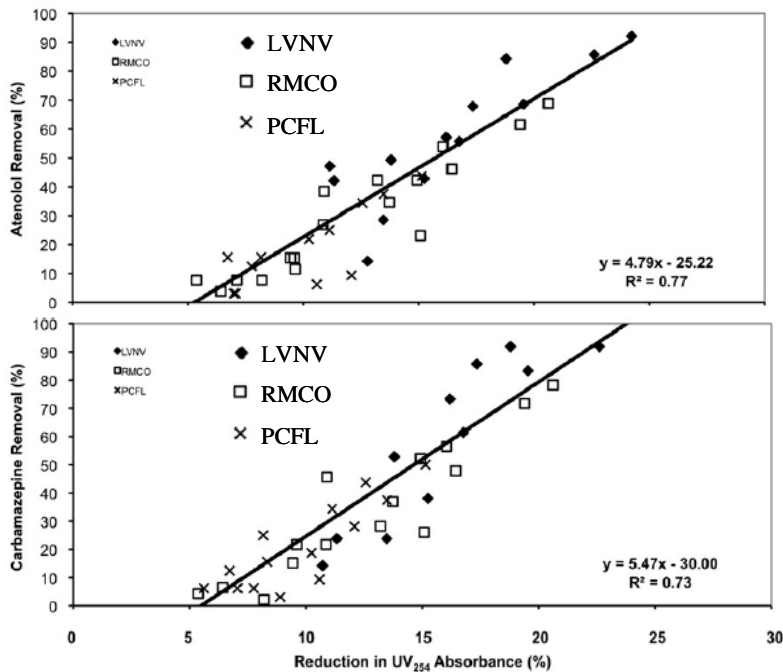


**Figure 1.2. Bulk organic correlations for UV/H<sub>2</sub>O<sub>2</sub> oxidation.**

Source: Rosario-Ortiz et al., 2010

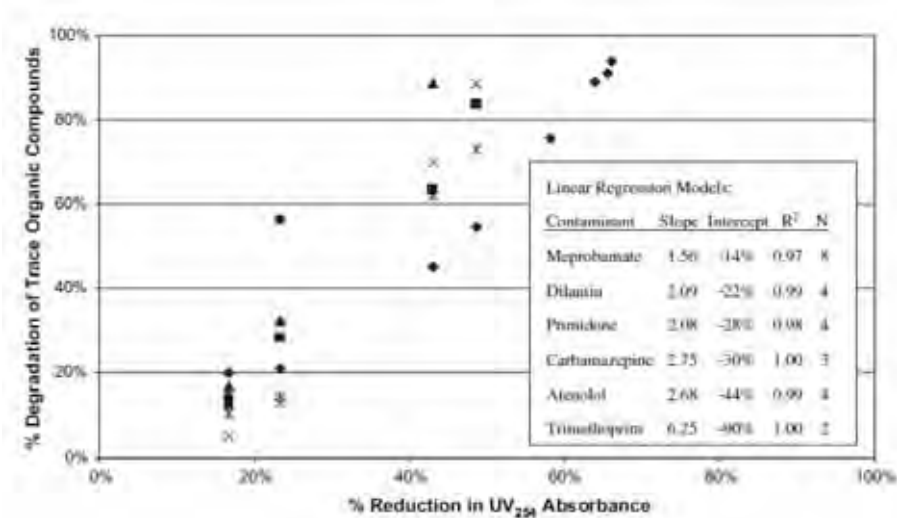


**Figure 1.3. Bulk organic correlations for nonthermal plasma.**

Source: Gerrity et al., 2010

On the basis of these studies, it is apparent that UV<sub>254</sub> absorbance is a viable surrogate for assessing contaminant oxidation. The current study evaluated this concept with additional wastewaters, target contaminants, microbial indicators, and organic surrogate parameters to determine whether it is sufficiently robust for full-scale implementation for a variety of locations, target contaminants, and treatment objectives.

## 1.5 Pilot- and Full-Scale Ozonation for Trace Organic Contaminant Reduction

Water and wastewater treatment technologies sometimes experience significant obstacles as the processes are scaled up from bench-scale evaluations to pilot- and full-scale demonstrations. Although bench-scale experiments provide an invaluable scientific foundation for a particular process, the value of a novel technology cannot be realized until it is implemented in the field. Pilot- and full-scale installations often expose the limitations of a particular technology, but they also provide a wealth of resources and information that cannot always be duplicated in a laboratory setting (e.g., large quantity of treated water, integration into a larger treatment train to evaluate synergistic or antagonistic relationships, discharge to the environment). The following sections describe evaluations of ozone technologies after field deployment and highlight the importance of scale to those particular studies.

### 1.5.1 Pilot-Scale Ozone Applications

Wert et al. (2009a) evaluated pilot-scale ozonation with three tertiary-treated U.S. wastewaters based on oxidation of a suite of ambient TOCs and spiked para-chlorobenzoic acid (pCBA). Based on the water quality data in Table 1.9, these experimental matrices offered a wide range of conditions related to competing organic matter and level of pretreatment (i.e., nitrification/denitrification). The pilot-scale ozone system was operated at a flow rate of 1 L/min (0.26 gpm); targeted O<sub>3</sub>:TOC ratios of 0.2, 0.6, and 1.0; and provided a contact time of 24 minutes. In each scenario, the ozone residual was entirely consumed during the 24-minute contact time.

**Table 1.9. Water Quality Data for Wert et al. (2009a) Pilot Study**

Parameter	A	B	C
Location	Nevada	Florida	Colorado
pH	8.2	7.6	7.1
Alkalinity (mg/L as CaCO <sub>3</sub> )	128	269	101
Bromide (mg/L)	0.18	0.17	0.19
k <sub>OH-EfOM</sub> (10 <sup>9</sup> M <sup>-1</sup> s <sup>-1</sup> )	0.68	2.72	1.12
NH <sub>4</sub> (mg/N/L)	<0.2	6.98	1.28
NO <sub>2</sub> (mg/N/L)	<0.05	0.77	0.40
NO <sub>3</sub> (mg/N/L)	12	0.074	9.7
SUVA (L/mg/m)	2.11	2.52	1.66
TOC (mg/L)	6.6	10.3	10.3
Total nitrogen (mg/N/L)	14.8	9.38	13.8
UV <sub>254</sub> absorbance (cm <sup>-1</sup> )	0.140	0.260	0.171

Notes: EfOM=effluent organic matter; SUVA=specific UV absorbance; TOC=total organic carbon; UV=ultraviolet

In all three wastewaters, an O<sub>3</sub>:TOC ratio of 0.2 was insufficient to generate a measurable ozone residual (i.e., CT≈0 mg/min/L), but the process still demonstrated significant concentration reductions for many ozone-susceptible contaminants, particularly for Wastewater A. An O<sub>3</sub>:TOC ratio of 0.6 achieved greater than 70% reductions in 15 of the 27 detected contaminants for all three wastewaters, and only TCEP, tris-(2-chloroisopropyl)-phosphate (TCPP), iopromide, atrazine, and meprobamate experienced reductions of less than 80% with an O<sub>3</sub>:TOC ratio of 1.0. For all three wastewaters, the authors indicated that a CT of less than 1 mg/min/L was sufficient to remove more than 95% of the ozone-susceptible compounds (i.e., carbamazepine, diclofenac, naproxen, sulfamethoxazole, and triclosan), and a CT of approximately 6 mg/min/L was sufficient to remove more than 50% of the ozone-resistant compounds (i.e., atrazine, iopromide, diazepam, ibuprofen, and pCBA). The study also included bench-scale experiments indicating that both the amount and type of EfOM contribute to a wastewater's ozone reactivity, as indicated by the k<sub>OH-EfOM</sub> values in Table 1.9.

Sundaram et al. (2009) described the efficacy of a pilot-scale HiPOx<sup>®</sup> reactor operated at the Reno-Stead Water Reclamation Facility (RSWRF) in Reno, NV. In their study, the HiPOx reactor was part of a 40-L/min (10.7-gpm) pilot-scale treatment train consisting of conventional secondary effluent (SRT of 25 days), ultrafiltration (UF), ozone (refer to Table 1.10), and BAC filtration with a bed depth of 4.5 feet and an empty bed contact time (EBCT) of 30 minutes. As for water quality, the UF effluent had a pH of 6.9, TOC of 6.4 mg/L, alkalinity of 92 mg/L as CaCO<sub>3</sub>, and nitrite less than 0.06 mg N/L.

**Table 1.10. Ozone Residuals in Reno-Stead Pilot System**

Applied Ozone Dose (mg/L)	3	5	7
O <sub>3</sub> :TOC	0.47	0.78	1.09
Duration of residual (min)	3.6	7.7	13.5

Source: Sundaram et al., 2009

During the initial ozone optimization phase, the initial concentrations of 13 monitored TOxCs (out of 30 total) were below the reporting limits for the analytical methods, presumably because of the preceding biological process and UF. With 3 mg/L of applied ozone, 12 compounds were removed by greater than 99%, and 5 compounds (*N,N*-diethyl-*meta*-toluamide [DEET], fluoxetine, phenytoin, sulfamethoxazole, and meprobamate) were removed by greater than 50%. With the exception of meprobamate (75%), all of the detected compounds were removed by greater than 95% with 5 mg/L of applied ozone, and even meprobamate was removed by greater than 90% with 7 mg/L of applied ozone. However, even with peroxide addition at a molar ratio ( $\text{H}_2\text{O}_2:\text{O}_3$ ) of 1.5, bromate formation exceeded 10  $\mu\text{g/L}$  with 7 mg/L of applied ozone. Therefore, continuous ozonation was limited to 3 mg/L of applied ozone or 5 mg/L of applied ozone supplemented with peroxide addition at a molar ratio ( $\text{H}_2\text{O}_2:\text{O}_3$ ) of 1.0.

Because advanced wastewater treatment and source protection are particularly common practices in Europe, there are many examples of ozone field deployment related to European utilities. Huber et al. (2005) monitored the concentrations of spiked antibiotics, EDCs, and antineoplastics (i.e., chemotherapy drugs) during pilot-scale ozonation. The pilot-scale reactor consisted of two contactors in series with a total hydraulic retention time of 8.4 minutes. The influent to the reactor consisted of conventional secondary effluent, secondary effluent spiked with 15 mg/L of TSS, and permeate from a pilot-scale membrane bioreactor (MBR). Secondary effluent samples were collected from a full-scale wastewater treatment plant in Kloten-Opfikon, Switzerland, that serves a population of 55,000 and includes grit removal, primary clarification, and nitrification/denitrification with an SRT of approximately 11 days. The membrane permeate was fed with the same primary clarified water, but the SRT for the MBR was greater than 70 days. The pH ranged from 7.0 to 7.5, the dissolved organic carbon (DOC) ranged from 7.7 to 6.6 mg/L, the COD ranged from 41 to 22 mg/L, the TSS ranged from 20 to 0 mg/L, and the alkalinity ranged from 310 to 540 mg/L for the secondary effluent and MBR. Target contaminants were spiked at levels ranging from 0.5 to 5  $\mu\text{g/L}$  to mimic common environmental conditions.

In this study, an applied ozone dose of 0.5 mg/L ( $\text{O}_3:\text{DOC}=0.06\text{--}0.08$ ) achieved less than 50% reductions for the ozone-susceptible compound classes (i.e., macrolide antibiotics, sulfonamide antibiotics, and estrogens) and less than 10% for the X-ray contrast media. However, an applied ozone dose of only 2 mg/L ( $\text{O}_3:\text{DOC}=0.26\text{--}0.30$ ) was sufficient to remove greater than 90% of the ozone-susceptible compounds. Ozone doses of 2 and 5 mg/L ( $\text{O}_3:\text{DOC}=0.65\text{--}0.76$ ) achieved 30 and 60% removals of the X-ray contrast media. In these experiments, an ozone residual was only present in the second contactor when the applied ozone dose exceeded 2 mg/L ( $\text{O}_3:\text{DOC}=0.25\text{--}0.30$ ). Regarding pretreatment, the authors indicated that suspended solids generally had limited effects on ozone efficacy. This was confirmed by a mathematical model suggesting that ozone consumption by sludge particles greater than 50  $\mu\text{m}$  in diameter can be considered insignificant, thereby emphasizing the interactions with dissolved organic matter and colloidal material. The authors attributed the few exceptions in which the MBR permeate actually experienced minor, yet significant, reductions in performance to the effect of elevated pH, which leads to more rapid ozone decomposition and reduced oxidant exposure. Although the oxidation of TOxCs was not significantly affected by pretreatment, disinfection was hindered—by as much as 1 log—by the presence of suspended solids.

The studies discussed here evaluated pilot-scale ozonation in relatively high-quality wastewater (i.e., secondary effluent or better). In contrast, Gagnon et al. (2008) evaluated pilot-scale ozonation in primary effluent at the City of Montreal Wastewater Treatment Plant,

which was described in relation to a separate disinfection study. The primary effluent in this study was characterized by a pH of 8.1 to 8.2, TSS of 5 mg/L, DOC ranging from 90 to 110 mg/L, and residual aluminum and iron concentrations of 0.6 to 0.9 and 0.3 to 0.4 mg/L. The pilot-scale ozone generator was capable of producing 15 to 30 mg/L of dissolved O<sub>3</sub>, and the contactor provided approximately 18 minutes of contact time. The authors monitored a suite of TOrCs (salicylic acid, clofibric acid, ibuprofen, 2-hydroxy-ibuprofen, naproxen, triclosan, carbamazepine, and diclofenac) with ambient concentrations ranging from 23 to 2556 ng/L for clofibric acid and salicylic acid. With an applied ozone dose of 15 mg/L (O<sub>3</sub>:DOC≈0.15), only 2-hydroxy-ibuprofen experienced less than a 50% reduction in concentration. As the ozone dose increased to 20 mg/L (O<sub>3</sub>:DOC≈0.20), only ibuprofen and 2-hydroxy-ibuprofen experienced less than 70% reductions in concentration. Furthermore, with the exception of 2-hydroxy-ibuprofen, there was little difference in treatment for the various contaminants when the applied ozone dose increased from 20 to 30 mg/L (O<sub>3</sub>:DOC≈0.30). Given the extremely high concentration of competing organic matter, the pilot-scale ozone system was quite effective in oxidizing the trace contaminants, but it is unclear whether this type of application is cost effective given the extremely high applied ozone dose required.

### 1.5.2 Full-Scale Ozone Applications for TOrC Oxidation and Removal

From 2003 to 2005, Nakada et al. (2007) analyzed four sets of samples from a full-scale wastewater treatment plant in Tokyo, Japan. Serving a population of approximately 460,000, the plant treats 0.17 million m<sup>3</sup>/day (45 MGD) with primary and secondary treatment (SRT not specified). Following the secondary clarifiers, a portion of the flow is diverted for advanced treatment consisting of upflow sand filtration at a velocity of 110 m/day followed by ozonation at an applied dose of 3 mg/L and contact time of 27 minutes. Additional water quality data (e.g., pH, DOC) were not provided. Regarding sand filtration, the authors reported limited removals for hydrophilic (log K<sub>ow</sub><3) pharmaceuticals and EDCs, but the more hydrophobic compounds (log K<sub>ow</sub>>3) experienced high, yet sporadic, removals. Following the overall treatment process, many of the compounds approached the limits of quantification after activated sludge, filtration, and ozonation; however, there were a few notable exceptions with relatively high effluent concentrations in one or more sample events, including nonylphenol, octylphenol, bisphenol A, diethyltoluamide, mefenamic acid, ketoprofen, and even carbamazepine. These outliers can be explained by their resistance to oxidation (e.g., ketoprofen), spikes in influent concentrations (e.g., bisphenol A), seemingly poor ozone performance (e.g., carbamazepine), or a combination of these factors.

Hollender et al. (2009) monitored the transformation and destruction of TOrCs by ozone at the Regensdorf (Wüeri) Wastewater Treatment Plant in Regensdorf, Switzerland. Although focused on the ecotoxicological effects of the ozone transformation products, Stalter et al. (2010b) also evaluated this particular full-scale system. The Regensdorf Wastewater Treatment Plant serves a population of approximately 25,000, which amounts to an average daily flow of 5550 m<sup>3</sup>/day (1.5 MGD). Regensdorf operates as a conventional wastewater treatment plant without disinfection (i.e., grit removal, primary clarification, conventional activated sludge with an SRT of 16 days, secondary clarification, and sand filtration with a depth of approximately 1 m and a velocity of 14.4 m/h). The plant also targets full nitrification, partial denitrification, and biological phosphorus removal. From August 2007 to October 2008, the plant was supplemented with a full-scale ozone system positioned between the secondary clarifiers and sand filters. The ozone system was originally commissioned in response to impending regulations on recalcitrant TOrCs (e.g., diclofenac, carbamazepine) in discharged wastewater. This is particularly important for the Regensdorf facility as its

receiving stream (Furtbach Creek) is dominated by wastewater ( $\approx 60\%$ ) during dry weather conditions. Table 1.11 provides the general water quality parameters for this plant.

**Table 1.11. Water Quality Data for the Regensdorf Wastewater Treatment Plant**

Parameter	Influent	Secondary Effluent	Ozonation + Sand Filtration
Alkalinity (mM HCO <sub>3</sub> <sup>-</sup> )	5	N/A	N/A
BOD (mg/L)	190	2.5	N/A
COD (mg/L)	380	17	15
DOC (mg/L)	N/A	4–7	N/A
NH <sub>4</sub> (mg N/L)	20–30	0.1	0.04
NO <sub>2</sub> (mg N/L)	N/A	0.05	N/A
NO <sub>3</sub> (mg N/L)	N/A	11.5	9.8
pH	7.0–8.3	7.0–8.3	7.0–8.3
Total phosphorus (mg P/L)	8	0.19	0.17
TSS (mg/L)	N/A	4.8	2

Sources: Hollender et al., 2009; Stalter et al., 2010b

Notes: BOD=biochemical oxygen demand; COD=chemical oxygen demand; DOC=dissolved organic carbon; TSS=total suspended solids

Hollender et al. (2009) monitored the concentrations of 220 TOrCs after full-scale ozonation with applied ozone doses of 1.6 to 5.3 mg/L (O<sub>3</sub>:DOC=0.36–1.16). Based on a hydraulic retention time ranging from 4 to 10 minutes, the ozone exposure varied from  $9.5 \times 10^{-4}$  to  $3.4 \times 10^{-2}$  M-s (0.76 to 27.2 mg/min/L), and the •OH exposure varied from  $5.0 \times 10^{-11}$  to  $6.9 \times 10^{-10}$  M-s. The suite of TOrCs included biocides, pharmaceuticals and their known transformation products, X-ray contrast media, nitrosamines, and corrosion inhibitors. As expected, the study indicated that many compounds were transformed or degraded during the activated sludge process, but there were also a number of biologically recalcitrant compounds capable of challenging the full-scale ozone system. For the biologically recalcitrant compounds, the authors indicated that the concentrations of nearly all of the monitored compounds, except those with second-order ozone rate constants  $< 10^4$  M<sup>-1</sup>s<sup>-1</sup>, were below the limit of quantification after ozonation. At the O<sub>3</sub>:DOC ratio of 0.6, the authors detected only 11 of the 220 compounds at concentrations exceeding 100 ng/L. Many of these compounds, which include atenolol, diatrizoate, iopromide, mecoprop, benzotriazole, 5-methylbenzotriazole, sucralose, DEET, diazinon, galaxolidone, and benzothiazole, require extended exposure to •OH to achieve significant concentration reductions. At the highest O<sub>3</sub>:DOC ratio, only two X-ray contrast media were detected at concentrations exceeding 100 ng/L.

Hollender et al. (2009) also monitored transformation products, DBPs, and the costs associated with the operation of the full-scale ozone plant. For example, assimilable organic carbon (AOC) concentrations increased because of ozonation, but a portion of the AOC was removed during the subsequent sand filtration. The use of ozone, particularly in drinking water treatment applications, is often hindered by the formation of bromate, which is regulated at 10 µg/L by the EPA. During full-scale ozonation, the bromate concentration never exceeded 7.5 µg/L even at the highest applied ozone dose, primarily because of low

influent bromide concentrations (<30 µg/L). Nitrosamine formation, however, proved to be problematic in that varying influent concentrations of NDMA, although partially removed during the activated sludge process, were compounded by NDMA formation during the ozonation process (up to 14 ng/L). The authors indicated that the variability in the secondary clarifier effluent (i.e., variable concentrations of NDMA and its precursors) was more significant than the ozone dose. NDMA destruction was limited (<25%) even at the highest ozone and •OH exposure, but the subsequent sand filtration achieved up to 50% reductions in NDMA concentrations through biological activity. Finally, the full-scale ozone system consumed approximately 0.012 kWh/g O<sub>3</sub>, which amounts to 0.035 kWh/m<sup>3</sup> of wastewater at an O<sub>3</sub>:DOC ratio of 0.6. According to the authors, this is slightly more than 10% of the total energy consumption (≈0.3 kWh/m<sup>3</sup>) of a typical wastewater treatment plant targeting nutrient removal.

### 1.5.3 Full-Scale Ozone Applications and Toxicological Implications

In Stalter et al. (2010b), secondary-clarified, ozonated, and post-ozone, sand-filtered wastewaters were compared with an artificial control water to determine their toxicity during an *in vivo* rainbow trout assay (fish early life stage toxicity test). In this study, the O<sub>3</sub>:DOC ratio ranged from 0.4 to 1.0. Using Organisation for Economic Cooperation and Development guideline 210 as an experimental template, three tests were performed on these waters: (1) extended exposure of fertilized eggs to each water without additional treatment, (2) extended exposure of fertilized eggs to each water after 0.4-µm MF, and (3) extended exposure of recently hatched fish to each water without additional treatment.

Toxicity was evaluated based on a combination of objective and subjective factors, including egg coagulation, hatching, swim up, mortality, malformation, abnormal behavior, and vitellogenin concentrations in whole-body homogenates. The first experiment was hindered by the development of fungal contamination in all of the wastewater exposures. After eliminating this contamination with MF pretreatment, the subsequent testing indicated that all of the wastewaters, and particularly the ozonated sample, negatively impacted egg coagulation, hatching, swim up, biomass, and survival in comparison to the control. Because no ozone residual was detected in any of the samples, the authors hypothesized that oxidation byproducts (e.g., aldehydes, carboxylic acids, ketones, or more specific compounds) were responsible for the increased toxicity of the ozone effluent, but the subsequent sand filtration was able to reduce this toxicity. In contrast, no developmental differences were observed in recently hatched fish that had not been previously exposed to wastewater. The secondary effluent was linked to increased feminization of the rainbow trout, but this effect was significantly reduced after ozone and post-ozone sand filtration, even below that of the control sample. Therefore, the authors suggest that ozone is extremely effective in reducing the potential estrogenic effects of wastewater that is discharged to the environment, but post-ozone biological filtration is necessary to reduce the toxicity of oxidation byproducts.

Reungoat et al. (2010) evaluated the concentrations and toxicity of ambient TOxCs at a full-scale water reclamation plant with ozonation. Macova et al. (2010) provided a more in-depth analysis of the toxicity data from this plant. The South Caboolture Water Reclamation Plant in Queensland, Australia, serves a population of approximately 40,000 and receives effluent from a nearby wastewater treatment plant operating a conventional activated sludge process at an SRT of 16 days. The influent DOC ranges from 15 to 20 mg/L, and the effluent DOC is less than 8 mg/L. Although the final product is considered nonpotable, the reclamation plant targets drinking water standards using an extensive treatment train that includes biological denitrification with methanol addition, pre-ozonation (O<sub>3</sub>:DOC=0.1, 2 mg/L O<sub>3</sub>),

coagulation/flocculation/dissolved air flotation, sand filtration, main ozonation ( $O_3$ :DOC=0.5, 5 mg/L  $O_3$ , 15 minutes of contact time), BAC filtration, and final ozonation ( $O_3$ :DOC=0.1, 2 mg/L  $O_3$ ). During the sampling period, the BAC had only been operating for four months since its last replacement, thereby suggesting that both adsorption and biological degradation contributed significantly to the observed removals.

The authors reported that all of the compounds detected in the influent were still present at reportable concentrations following pre-ozonation because of the high concentration of competing organic matter (DOC>20 mg/L). Only half of the original contaminants were detected at reportable concentrations following the main ozonation phase, and of the remaining contaminants, only the most recalcitrant compounds (e.g., iopromide and gabapentin) were removed by less than 70%. After the subsequent BAC and final ozonation processes, only gabapentin and roxithromycin were confidently detected at reportable concentrations. With few exceptions, each component of the treatment train generally demonstrated reductions in baseline toxicity, estrogenicity, Ah-receptor response, genotoxicity, neurotoxicity, and phytotoxicity, but the most significant reductions were associated with the dissolved air flotation and sand filtration, main ozonation, and BAC processes. Although Reungoat et al. (2010) suggest that the final ozonation process provided no significant benefits regarding TORCs and toxicity, there may still be significant disinfection benefits, particularly related to pathogen regrowth during the BAC process, thereby justifying its implementation. As will be discussed further in this report, UV disinfection may be more appropriate than ozonation as a final disinfection step.

## 1.6 Summary

Despite the recent research emphasis on pharmaceuticals and other TORCs in water supplies, there is limited guidance that utilities can rely on when developing, expanding, or optimizing treatment strategies. As municipalities increasingly turn to IPR to augment their water supplies, these systems often take a proactive approach to removing TORCs and oxidation byproducts. Although conventional water and wastewater technologies were not specifically designed to address these concerns, many of these treatment options are quite effective for TORC mitigation. In the event that recalcitrant compounds are detected, conventional treatment trains can be augmented with advanced treatment technologies, including RO, UV/ $H_2O_2$ , and ozone (with or without  $H_2O_2$ ). Unfortunately, the use of some of these technologies is limited by the regulatory structure that is currently in place. For example, the CT concept is commonly used to validate a treatment process and award disinfection credits, but AOPs that are dominated by  $\bullet OH$  reactions provide no residual with which a CT can be demonstrated. AOPs are extremely effective for TORC mitigation and disinfection, but their widespread use is hindered by the CT issue and the inability of operators to monitor process efficacy. Therefore, there is a need to develop alternative monitoring strategies for AOPs targeting TORC oxidation and microbial inactivation. Changes in bulk organic parameters, specifically UV and fluorescence spectra, provide a viable alternative to the monitoring of conventional oxidant residuals; however, this novel strategy must be examined in greater detail to determine its robustness and applicability to full-scale wastewater treatment. The experiments described in this report address the gap in the literature and describe how this strategy can be incorporated into wastewater treatment.

## Chapter 2

# Technical Approach and Methods

---

## 2.1 Bench-Scale Oxidation Experiments

### 2.1.1 Wastewater Collection and Processing

For the bench-scale oxidation experiments, unfiltered secondary effluent was collected from each participating utility in 75-L, high-density, polyethylene containers (Figure 2.1A). The water was then filtered in series through 10- $\mu\text{m}$  and 0.5- $\mu\text{m}$  polypropylene, spiral-wound, cartridge filters (MicroSentry™, Shelco Filters, Middletown, CT) in the laboratory (Figure 2.1B). After completing the first and second sets of bench-scale experiments, organic leaching from the cartridge filters became evident in the unfiltered versus filtered TOC values. In a separate experiment, deionized water was passed through different types of cartridge filters to evaluate organic leaching.

For all of the materials, significant leaching was evident with little preconditioning, as indicated in Table 2.1. For the third, fourth, and fifth sets of bench-scale experiments, approximately 200 L of deionized water was passed through the cartridges prior to filtering each wastewater. This reduced the amount of organic leaching, but a small level of contamination was still evident based on the TOC values in some of the bench-scale data sets. This leaching had a slight impact on some of the analyses during the second sample event, but there were no significant effects during any of the other experiments. Separate oxidation experiments were performed for each of the major tests (e.g., ozone demand/decay, TOrCs, disinfection) to provide sufficient sample volume for the analytical methods and reduce potential interferences caused by spiked contaminants. Samples were collected immediately for TOC and UV<sub>254</sub> absorbance to determine proper dosing conditions for the subsequent ozone and UV experiments.



**Figure 2.1. Wastewater collection containers and laboratory filtration apparatus.**

**Table 2.1. Evaluation of Organic Leaching (TOC in mg/L) During Laboratory Filtration**

Material	Preconditioning: Volume of DI Water (L)				
	0	25	75	150	225
Cotton	44	3.2	1.4	0.64	0.42
Glass fiber	530	1.6	0.29	<0.2	<0.2
Polypropylene A	29	0.92	0.73	<0.2	<0.2
Polypropylene B	72	0.84	0.21	<0.2	<0.2

### 2.1.2 Bench-Scale Ozone Testing

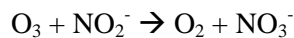
Bench-scale ozone tests were performed by spiking aliquots of ozone stock from a batch reactor. Nanopure water (Barnstead, Dubuque, IA) was placed inside a water-jacketed flask and cooled to 2 °C. Once cooled, 11% gaseous ozone was diffused into the water using an oxygen-fed generator (model CFS-1A, Ozonia North America, Inc., Elmwood Park, NJ). Ozone stock solution concentrations and dissolved ozone residuals were measured with the indigo trisulfonate colorimetric method according to Standard Method 4500-O3. The concentration of the stock solution remained relatively constant during each set of experiments, but day-to-day concentrations ranged from 80 to 110 mg/L over the course of the project. For the ozone/H<sub>2</sub>O<sub>2</sub> experiments, H<sub>2</sub>O<sub>2</sub> was added immediately before the addition of the ozone stock solution. In order to encompass a range of treatment conditions, O<sub>3</sub>:TOC ratios of 0.25, 0.50, 1.0, and 1.5 and molar H<sub>2</sub>O<sub>2</sub>:O<sub>3</sub> ratios of 0, 0.5, and 1.0 were selected for evaluation. The final ozone dose also accounted for nitrite at a 1:1 mass ratio as NO<sub>2</sub>. An example dose calculation is provided herein.

The Clark County Water Reclamation District (CCWRD) secondary effluent had the following water quality characteristics (after dilution):

$$\text{TOC}=6.8 \text{ mg/L}$$

$$\text{NO}_2 = (0.051 \text{ mg/L as N}) \times \left( \frac{46 \text{ mg/L as NO}_2}{14 \text{ mg/L as N}} \right) = 0.167 \text{ mg/L as NO}_2$$

Ozone reacts with nitrite as follows:



Because NO<sub>2</sub>=46 g/mole as NO<sub>2</sub> and O<sub>3</sub>=48 g/mole, the reaction requires an approximate 1:1 mass ratio in order to satisfy the ozone demand caused by nitrite. Therefore, assuming standard mass-based ratios for O<sub>3</sub>:TOC and O<sub>3</sub>:NO<sub>2</sub>, the following equation can be used to calculate the applied ozone dose:

$$\text{Applied O}_3 \text{ Dose (mg/L)} = \text{O}_3:\text{TOC} \times [\text{TOC}] \text{ (mg/L)} + [\text{NO}_2^-] \text{ (mg/L as NO}_2\text{)}$$

Assuming the CCWRD water quality characteristics described, an example dose for an O<sub>3</sub>:TOC ratio of 1.5 can be calculated as follows:

$$\text{Applied O}_3 \text{ Dose (mg/L)}=1.5 \times 6.8 \text{ mg/L} + 0.167 \text{ mg/L}=10.37 \text{ mg/L}$$

Although more complex models are now being developed to describe the reaction between ozone and hydrogen peroxide, the following simplified reaction can be used to describe this AOP:



Because the masses of H<sub>2</sub>O<sub>2</sub> (34 g/mole) and O<sub>3</sub> (48 g/mole) are not equivalent, H<sub>2</sub>O<sub>2</sub> addition is often described on a molar basis, as opposed to the mass-based ratios for O<sub>3</sub>:TOC and O<sub>3</sub>:NO<sub>2</sub>. On the basis of the simplified stoichiometry demonstrated here, molar H<sub>2</sub>O<sub>2</sub>:O<sub>3</sub> ratios of 0.5 and 1.0 are often used. The 0.5 ratio is based on balanced stoichiometry, whereas the 1.0 ratio is used to provide excess H<sub>2</sub>O<sub>2</sub> for competing reactions (e.g., background organic matter). The following equation can be used to calculate the H<sub>2</sub>O<sub>2</sub> dose.

$$\text{H}_2\text{O}_2 \text{ (mg/L)} = \text{Modified O}_3 \text{ (mg/L)} \times \frac{1 \text{ mmole O}_3}{48 \text{ mg O}_3} \times \text{molar H}_2\text{O}_2 : \text{O}_3 \times \frac{34 \text{ mg H}_2\text{O}_2}{1 \text{ mmole H}_2\text{O}_2}$$

$$\text{Modified O}_3 \text{ (mg/L)} = \text{O}_3 : \text{TOC} \times [\text{TOC}] \text{ (mg/L)}$$

The nitrite-associated ozone is theoretically not available for reaction with H<sub>2</sub>O<sub>2</sub>, so this portion of the applied ozone dose is not included in the calculation. Using the previous example, the H<sub>2</sub>O<sub>2</sub> dose for a mass-based O<sub>3</sub>:TOC ratio of 1.5 and a molar H<sub>2</sub>O<sub>2</sub>:O<sub>3</sub> ratio of 1.0 can be calculated as follows:

$$\text{H}_2\text{O}_2 \text{ (mg/L)} = 1.5 \times 6.8 \text{ mg/L} \times \frac{1 \text{ mmole O}_3}{48 \text{ mg O}_3} \times 1.0 \times \frac{34 \text{ mg H}_2\text{O}_2}{1 \text{ mmole H}_2\text{O}_2} = 7.23 \text{ mg/L}$$

The precise calculations and values described are nearly impossible to duplicate in practice as a result of various sources of experimental error, including variations in ozone stock concentrations and the actual water matrix over time; however, the project team attempted to duplicate the dosing calculations as closely as possible.

Ozone doses were administered by transferring an aliquot of the ozone stock solution into 250-mL or 1-L amber glass bottles containing a mixture of wastewater, nanopure water, and the appropriate spiked contaminant(s). An iterative approach was used to calculate the necessary aliquots of ozone based on the dilution effect of the spiked ozone. Particularly for wastewaters with high TOC values, the potentially large volume of ozone added to each sample will dilute the EfOM. In order to treat all samples similarly, the highest ozone spiking volume (i.e., for an O<sub>3</sub>:TOC ratio of 1.5) was calculated for each wastewater because this condition had the greatest dilution effect. Regardless of the O<sub>3</sub>:TOC value, the volume of wastewater in each sample was held constant based on the difference between the total sample volume (i.e., 250 mL or 1 L) and the volume of ozone stock for the O<sub>3</sub>:TOC ratio of 1.5. For the lower O<sub>3</sub>:TOC ratios, the samples were supplemented with nanopure water to target final volumes of 250 mL or 1 L. In order to account for background concentrations of the wastewater matrix, the spiking controls also contained the same volume of wastewater and a sufficient volume of nanopure water to reach the total sample volumes. The O<sub>3</sub>:TOC values, and inherently the ozone doses, were based on the final TOC value of each wastewater (plus nitrite) after accounting for the dilution effect. The volumes for each wastewater are provided in their corresponding sections of the report, but an example is provided in Table 2.2.

**Table 2.2. Experimental Volumes for the 1-L Filtered CCWRD Samples**

Concentration of O<sub>3</sub> stock solution=95 mg/L  
 Concentration of H<sub>2</sub>O<sub>2</sub> stock solution=10 g/L  
 Before dilution: TOC=7.6 mg/L | NO<sub>2</sub>=0.057 mg/L as N=0.187 mg/L as NO<sub>2</sub>  
 Dilution ratio=(892/1000)=0.892  
 After dilution: TOC=6.8 mg/L | NO<sub>2</sub>=0.051 mg/L as N=0.167 mg/L as NO<sub>2</sub>

O <sub>3</sub> :TOC/ H <sub>2</sub> O <sub>2</sub> :O <sub>3</sub>	Wastewater Volume (mL)	Nanopure Volume (mL)	O <sub>3</sub> Volume (mL)	O <sub>3</sub> Dose (mg/L)	H <sub>2</sub> O <sub>2</sub> Volume (μL)	H <sub>2</sub> O <sub>2</sub> Dose (mg/L)
Spike	892	108	0	0	0	0
0.25/0	892	88	20	1.9	0	0
0.25/0.5	892	88	20	1.9	61	0.6
0.25/1.0	892	88	20	1.9	122	1.2
0.5/0	892	70	38	3.6	0	0
0.5/0.5	892	70	38	3.6	123	1.2
0.5/1.0	892	70	38	3.6	246	2.5
1.0/0	892	35	73	7.0	0	0
1.0/0.5	892	35	73	7.0	242	2.4
1.0/1.0	892	35	73	7.0	483	4.8
1.5/0	892	0	108	10.3	0	0
1.5/0.5	892	0	108	10.3	363	3.6
1.5/1.0	892	0	108	10.3	725	7.3

*Note:* Some values are affected by rounding error and the precision of the ozone spike.

### 2.1.3 Bench-Scale UV Experiments

Based on the suggested protocols of Bolton and Linden (2003) and Kuo et al. (2003), bench-scale collimated beams containing one (Figure 2.2A) or two (Figure 2.2B) 46-cm, 15-watt, low-pressure, mercury arc bulbs (model G15T8, Ushio, Cypress, CA) were used for the UV irradiation experiments. Two collimated beams were used because of the large number of samples and the long exposure times required for UV doses characteristic of advanced oxidation (i.e., >250 mJ/cm<sup>2</sup>). The bulbs produced nearly monochromatic, germicidal light at a peak wavelength of 254 nm. The collimated beam apparatuses also included adjustable platforms and slow-speed stir plates to ensure proper mixing during the irradiation periods. Following a 5-minute warm-up period for the UV lamp, the intensity of the UV light was measured using an IL1700 research radiometer with sensor SUD240 (International Light, Newburyport, MA). A calibration on each component, traceable to National Institute of Standards and Technology standards, was performed by the manufacturer prior to the experiments. Prior to the irradiation experiments, the platform was adjusted to ensure that the surface of the radiometer detector and the wastewater sample were at the same level during the calibration and irradiation phases. The incident UV intensity for the collimated beam in Figure 2.2A was approximately 0.23 mW/cm<sup>2</sup>, and the incident UV intensity for the collimated beam in Figure 2.2B was approximately 0.58 mW/cm<sup>2</sup>.

UV doses were calculated as the product of the incident UV intensity (I<sub>0</sub>), a series of collimated beam correction factors, and the exposure times. The corrections accounted for the reflection factor (RF), Petri factor (PF), water factor (WF), and divergence factor (DF) associated with each collimated beam (Bolton and Linden, 2003; Kuo et al., 2003), which are described in Figure 2.2. The water factor is described as a range because it depends on the UV<sub>254</sub> absorbance of the sample matrix and is therefore sample dependent. The UV and

UV/H<sub>2</sub>O<sub>2</sub> experiments were repeated in 100 mL aliquots until a sufficient sample volume had been collected for the various analytical methods. In order to capture disinfection- and contaminant-specific effects related to UV photolysis and oxidation, a wide range of UV doses were evaluated. For the CCWRD experiments, UV doses of 23, 45, 225, and 680 mJ/cm<sup>2</sup> were used. After further evaluation of full-scale AOP conditions, UV doses of 50, 250, and 500 mJ/cm<sup>2</sup> were used for the remaining four sets of experiments. An H<sub>2</sub>O<sub>2</sub> concentration of 10 mg/L was selected for the CCWRD UV AOP experiments, and H<sub>2</sub>O<sub>2</sub> concentrations of 5 and 10 mg/L were selected for the other four sets of experiments.

### 2.1.4 Quenching and Preservation

Hydrogen peroxide controls (i.e., 10 mg/L of H<sub>2</sub>O<sub>2</sub> with no ozone or UV exposure) were also collected for each experiment. The duration of H<sub>2</sub>O<sub>2</sub> exposure, which generally ranged from 30 minutes to 1 hour, was selected to mimic the longest potential exposure time during each set of experiments. This always corresponded to UV irradiation with 500 or 680 mJ/cm<sup>2</sup>. At the end of the exposure time, the H<sub>2</sub>O<sub>2</sub> controls were quenched with 10 mg/L of sodium thiosulfate. For the ozone and ozone/H<sub>2</sub>O<sub>2</sub> samples, H<sub>2</sub>O<sub>2</sub> residuals were quenched with 10 mg/L of sodium thiosulfate after at least 30 minutes of reaction time, which was sufficient for complete ozone decay in all samples. For the UV/H<sub>2</sub>O<sub>2</sub> experiments, samples were quenched with 10 mg/L of sodium thiosulfate at the end of each UV exposure. Finally, TOxC and NDMA samples were preserved with 1 g/L of sodium azide to prevent biodegradation prior to analysis.

## 2.2 Target Compounds

Analytical methods for TOxCs are now approaching parts-per-quadrillion detection limits with high degrees of accuracy and precision. Coupled with state-of-the-art equipment, these methods have allowed researchers to detect and quantify a seemingly infinite number of TOxCs in countless matrices (e.g., air, soil, water, wastewater, food). These contaminants include PPCPs, pesticides, household chemicals, industrial chemicals, flame retardants, DBPs, and steroid hormones (Trenholm et al., 2009). Many of these contaminants are also suspected EDCs.

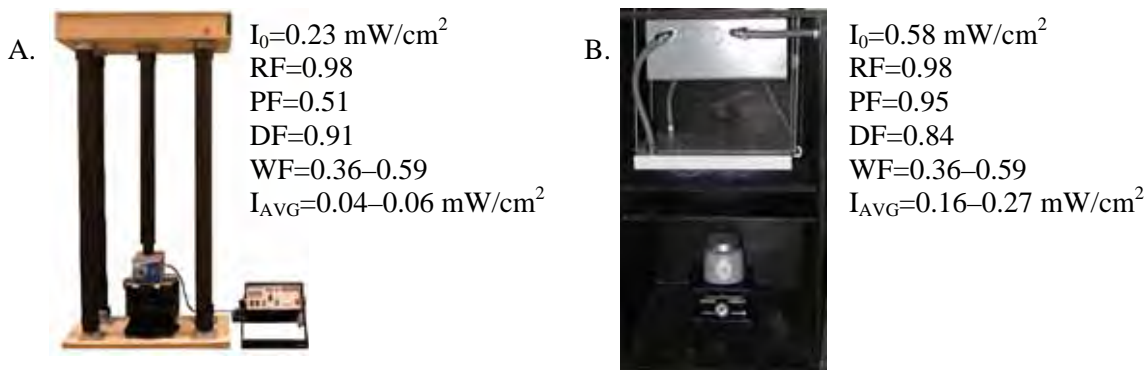
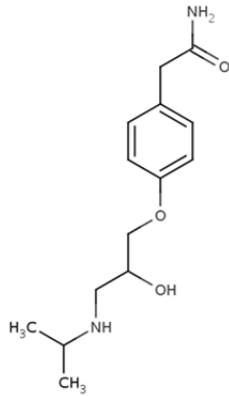
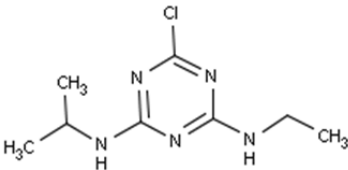
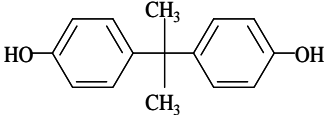
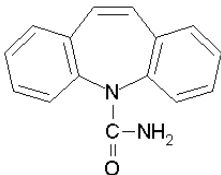
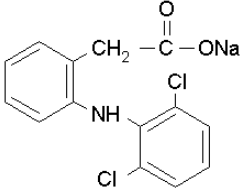
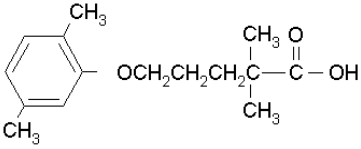
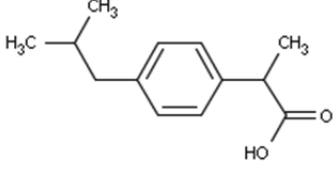
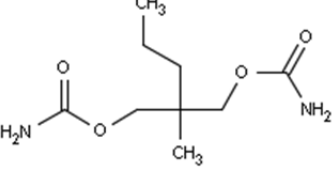
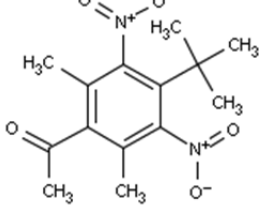
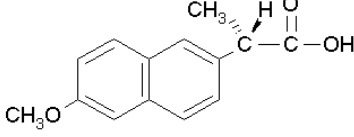
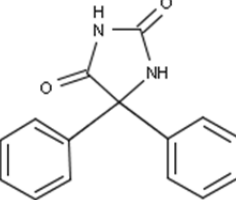


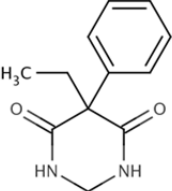
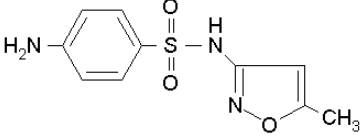
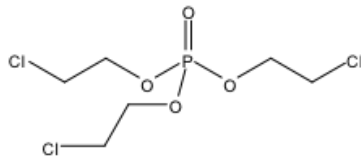
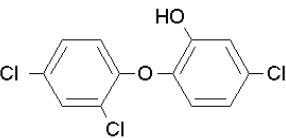
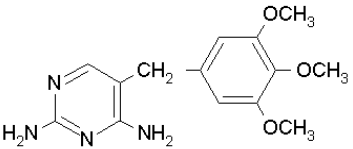
Figure 2.2. Collimated beam apparatuses for bench-scale UV experiments.

In order to focus the scope of the research, a representative subset of the TOrC universe was selected for evaluation. The indicator compounds were selected based on several factors, including structural and chemical properties (e.g., functional groups, polarity, aromaticity), use classes (e.g., antibiotic, fragrance, anticonvulsant), high frequency of environmental occurrence (Kolpin et al., 2002; Snyder et al., 2008a; Benotti et al., 2009), resistance to natural (e.g., biodegradation, photolysis) and engineered treatment processes (e.g., adsorption, oxidation; Ternes et al., 2002; Huber et al., 2003; Westerhoff et al., 2005), and amenability to existing analytical methods (Trenholm et al., 2009). The compounds selected for this study and their corresponding structures and guideline concentrations are listed in Table 2.3. Although these compounds have generated considerable interest in the research, treatment, and regulatory arenas, only atrazine is currently regulated by the EPA at an MCL of 3 µg/L.

**Table 2.3. Target Compound List**

Contaminant	Use Class	Structure	DWEL (µg/L)	AG (µg/L)
Atenolol	beta blocker		13,000	N/A
Atrazine	herbicide		3 <sup>a</sup>	40
Bisphenol A	plasticizer		1800	200
Carbamazepine	anticonvulsant		35,000	100

Contaminant	Use Class	Structure	DWEL (µg/L)	AG (µg/L)
DEET	pesticide		N/A	2.5
Diclofenac	NSAID		49,000	1.8
Gemfibrozil	lipid regulator		600,000	600
Ibuprofen	NSAID		N/A	400
Meprobamate	anti-anxiety		260	N/A
Musk ketone	fragrance		N/A	350
Naproxen	NSAID		140,000	220
Phenytoin	anticonvulsant		150,000	N/A

Contaminant	Use Class	Structure	DWEL (µg/L)	AG (µg/L)
Primidone	anticonvulsant		N/A	N/A
Sulfamethoxazole	antibiotic		18,000	35
TCEP	flame retardant		N/A	1
Triclosan	Antimicrobial		N/A	0.35
Trimethoprim	antibiotic		81,000	70

Notes: a=EPA MCL for atrazine; AG=Australian guidelines (Australia, 2008); DEET=*N,N*-diethyl-*meta*-toluamide; DWEL=drinking water equivalent level (Snyder et al., 2008a); NSAID=nonsteroidal anti-inflammatory drug; TCEP=tris-(2-chloroethyl)-phosphate

The chemical structures of organic compounds have a significant effect on their treatability (e.g., removal profiles after exposure to various oxidants). Although these structures make certain compounds highly useful for a particular purpose (e.g., TCEP as a flame retardant), this utility is sometimes offset by their recalcitrance after they are discharged into the environment and ultimately the water supply. The target compounds for this study were selected to represent a broad range of treatability for a variety of processes, thereby including compounds that are likely to be removed during conventional wastewater treatment and those that may persist into drinking water supplies. A general summary of the relative treatability of the target contaminants, whether by natural or engineered processes, is provided in Table 2.4.

As shown in Table 2.4, the target compounds were also classified based on their relative resistance to oxidation, which will become important in future discussions of the ozone oxidation data. The Group 1 compounds are characterized by relatively high ozone ( $>10^5 \text{ M}^{-1}\text{s}^{-1}$ ) and  $\bullet\text{OH}$  ( $>5 \times 10^9 \text{ M}^{-1}\text{s}^{-1}$ ) rate constants because of their electron-rich moieties, including phenols (triclosan and bisphenol A), anilines (diclofenac and sulfamethoxazole), olefins (carbamazepine), and activated aromatics (trimethoprim and naproxen). The Group 2 compounds are characterized by moderately high ozone ( $10 < k_{\text{ozone}} < 10^5 \text{ M}^{-1}\text{s}^{-1}$ ) and high  $\bullet\text{OH}$

rate constants ( $>5 \times 10^9 \text{ M}^{-1} \text{ s}^{-1}$ ); the Group 3 compounds are characterized by low ozone ( $<10 \text{ M}^{-1} \text{ s}^{-1}$ ) but high  $\bullet\text{OH}$  rate constants ( $>5 \times 10^9 \text{ M}^{-1} \text{ s}^{-1}$ ); the Group 4 compounds are characterized by low ozone ( $<10 \text{ M}^{-1} \text{ s}^{-1}$ ) and moderately low  $\bullet\text{OH}$  ( $10^9 < k_{\text{OH}} < 5 \times 10^9 \text{ M}^{-1} \text{ s}^{-1}$ ) rate constants; and the Group 5 compounds are very resistant to both ozone ( $<1 \text{ M}^{-1} \text{ s}^{-1}$ ) and  $\bullet\text{OH}$  ( $<10^9 \text{ M}^{-1} \text{ s}^{-1}$ ).

**Table 2.4. Treatability of Target Compounds**

Compound	Ozone <sup>a</sup>	$\bullet\text{OH}^b$	Photolysis	Biodegradation	Sorption
<b>Group 1</b>					
Bisphenol A	$7 \times 10^5$	$1 \times 10^{10}$			
Carbamazepine	$3 \times 10^5$	$9 \times 10^9$			
Diclofenac	$1 \times 10^6$	$8 \times 10^9$			
Naproxen	$2 \times 10^5$	$1 \times 10^{10}$			
Sulfamethoxazole	$3 \times 10^6$	$6 \times 10^9$			
Triclosan	$4 \times 10^7$	$1 \times 10^{10}$			
Trimethoprim	$3 \times 10^5$	$7 \times 10^9$			
<b>Group 2</b>					
Atenolol	$2 \times 10^3$	$8 \times 10^9$			
Gemfibrozil	$2 \times 10^4$	$1 \times 10^{10}$			
<b>Group 3</b>					
DEET	$<10$	$5 \times 10^9$			
Ibuprofen	10	$7 \times 10^9$			
Phenytoin	$<10$	$6 \times 10^9$			
Primidone	$<10$	$7 \times 10^9$			
<b>Group 4</b>					
Atrazine	6	$3 \times 10^9$			
Meprobamate	$<1$	$4 \times 10^9$			
<b>Group 5</b>					
Musk ketone	$<1$	$1 \times 10^9$			
TCEP	$<1$	$7 \times 10^8$			

High Treatability (e.g.,  $>80\%$  removal)  Low Treatability (e.g.,  $<20\%$  removal)

Sources: Huber et al., 2003; Packer et al., 2003; Deborde et al., 2005; Huber et al., 2005; Latch et al., 2005; Dodd et al., 2006; Rosenfeldt et al., 2006; Suarez et al., 2007; Benner et al., 2008; Razavi et al., 2009; Song et al., 2009; Watts and Linden, 2009

Notes: a=values in this column correspond to  $k_{\text{O}_3}$  ( $\text{M}^{-1} \text{ s}^{-1}$ ) at pH 7; b=values in this column correspond to  $k_{\text{OH}}$  ( $\text{M}^{-1} \text{ s}^{-1}$ ); DEET=*N,N*-diethyl-*meta*-toluamide; TCEP=tris-(2-chloroethyl)-phosphate

## 2.2.1 Online SPE Followed by LC-MS/MS

The target compounds were analyzed by online SPE followed by liquid chromatography tandem mass spectrometry (LC-MS/MS) with isotope dilution (Trenholm et al., 2009; Gerrity et al., 2010). This method was selected for its reduced sample volumes, solvent volumes, and total analysis time per sample ( $\approx 20$  minutes) compared to traditional offline SPE-LC-MS/MS methods. Therefore, it was able to shorten sample turnaround times and increase experimental throughput. Online SPE-LC-MS/MS was accomplished with a Symbiosis<sup>TM</sup> Pharma (Spark Holland, Emmen, Netherlands) system in XLC mode using Analyst<sup>®</sup> 1.4.2 (Applied Biosystems, Foster City, CA). Samples were collected in 40-mL amber glass vials

with quenching agents and preservatives as described previously. If analysis was not performed immediately following each experiment, samples were refrigerated at 4° C and extracted within 14 days of collection.

Prior to analysis, 10 mL of sample was measured in a volumetric flask and spiked with isotopically labeled standards at 100 ng/L. This provided sufficient sample volume for replicates, matrix spikes, and dilutions, if necessary. A 1.5-mL aliquot of each sample was transferred into a 2-mL autosampler vial, although only 1.0 mL was used for extractions. Extractions were performed using Waters Oasis HLB Prospekt cartridges (30 mm, 2.5 mg, 10 x 1 mm, 96 tray; Milford, MA). Prior to sample loading, each cartridge was sequentially conditioned with 1 mL of dichloromethane, methyl *tert*-butyl ether, methanol, and reagent water (Milli-Q). Samples were loaded onto the SPE cartridges at 1 mL/min, after which the cartridges were washed with 1 mL of reagent water. After sample loading, the analytes were eluted from the SPE cartridge to the LC column with 200 mL methanol, using the LC peak focusing mode. A 5-mM ammonium acetate solution and methanol gradient were used for LC mobile phases with a flow rate of 800 mL/min. Analytes were separated using a 150 x 4.6-mm Luna C18(2) column with a 5- $\mu$ m particle size (Phenomenex, Torrance, CA). MRLs were established at 3 to 5 times the method detection limits (MDLs). The MRLs for the target compounds are listed in Table 2.5. Although lower MRLs can be achieved with offline SPE-LC-MS/MS methods, the elevated concentrations in wastewater, particularly after spiking at 1  $\mu$ g/L, were sufficient to justify the use of the online alternative. Stringent quality assurance/quality control protocols (i.e., matrix spikes, duplicate samples, field blanks, and laboratory blanks) were followed throughout the duration of the project. Based on extensive method development and past studies, the concentrations of duplicate samples rarely varied by more than 5%. Additional details are provided in Trenholm et al. (2009).

**Table 2.5. Online SPE-LC-MS/MS Method Reporting Limits**

<b>Contaminant</b>	<b>MRL (ng/L)</b>
Atenolol	25
Atrazine	10
Bisphenol A	50
Carbamazepine	10
DEET	25
Diclofenac	25
Gemfibrozil	10
Ibuprofen	25
Meprobamate	10
Musk ketone	100
Naproxen	25
Phenytoin	10
Primidone	10
Sulfamethoxazole	25
TCEP	200
Triclosan	25
Trimethoprim	10

Notes: DEET=*N,N*-diethyl-*meta*-toluamide;  
TCEP=tris-(2-chloroethyl)-phosphate

## 2.3 Organic Characterization

### 2.3.1 Excitation Emission Matrices

The transformation of bulk organic matter can be evaluated with highly sensitive excitation emission matrices (EEMs), which qualitatively and quantitatively describe changes in fluorescence intensity. In order to develop an EEM, the organic matter in a water sample is excited by light of various wavelengths (e.g., 240–470 nm), and the corresponding fluorescent emissions are recorded over a similar range of wavelengths (e.g., 280–580 nm). These wavelength ranges are selected for their applicability to environmental matrices in addition to instrument limitations. After collecting the excitation emission intensities, the raw data set is then processed with mathematical software (e.g., MATLAB from MathWorks™, Natick, MA) to account for blank response, correct for instrument- and matrix-specific effects, and plot the final 3D image. In addition to developing 3D EEM images, this process also provides underlying fluorescence spectra (i.e., EEM cross-sections at a particular excitation wavelength) that can be correlated to contaminant oxidation and disinfection.

EEMs were created using a QuantaMaster UV-Vis QM4 Steady State Spectrofluorometer (Photon Technology International, Inc., Birmingham, NJ). The spectrofluorometer included a 75-watt, short-arc xenon lamp with an effective excitation range of 240 to 470 nm. Data processing included corrections for the spectral sensitivity of the lamp, and an inner filter correction was also applied using equations from the literature (MacDonald et al., 1997) and the UV absorbance spectra of the sample matrices. For the inner filter correction, the light was assumed to illuminate a small volume at the center of the cell, and the excitation and emission pathlengths were assumed to be 0.5 cm (Westerhoff et al., 2001). The width of the excitation beam was assumed to be 0.1 cm, and the width of the emission was assumed to be 1 cm. These assumptions are incorporated into the modification to Beer's Law, as described in the literature (MacDonald et al., 1997).

Figure 2.3 is an EEM characteristic of secondary wastewater effluent because it includes intense fluorescence in all three regions, particularly in those associated with soluble microbial products and fulvic acids. As shown in Figure 2.3, EEMs include an upper boundary resulting from “bleeding” when the excitation and emission wavelengths are approximately equal to each other. Molecules cannot emit light at energy levels greater than the excitation source, so emissions at wavelengths *less than* the excitation wavelength are not possible. Therefore, the region above the upper boundary is always blank. As shown in Figure 2.3, EEMs sometimes include a lower boundary characteristic of second-order light scattering, which occurs at emission wavelengths that are approximately twice the excitation wavelength. In contrast to the upper boundary, fluorescence data can be collected below the second-order scattering boundary. Figure 2.3 also provides delineations for the organic regions first described in Chen et al. (2003). The regions were modified by the project team to account for the limitations (e.g., effective excitation range) of the spectrofluorometer used in this study. The regions also account for 15-nm safety factors near the bleeding and second-order scatter boundaries. Fluorescence in each region indicates the presence of specific organic fractions, as follows: (I) aromatic proteins and soluble microbial products; (II) fulvic-like substances; and (III) humic-like substances. The relative reactivity of each region with ozone will be described in the discussion of the bench-scale experiments.

EEMs can be analyzed qualitatively by observing changes in fluorescence intensity (i.e., color), but there are also quantitative alternatives such as the fluorescence index (FI;

McKnight et al., 2001). The FI is the ratio of the fluorescence emission at 450 nm to that of 500 nm when excited by a wavelength of 370 nm (i.e.,  $Ex_{370}Em_{450}/Ex_{370}Em_{500}$ ). The FI has been used to differentiate terrestrially derived organic matter (e.g., surface water from a forested watershed) with lower FIs from microbially derived organic matter (e.g., wastewater) with higher FIs (McKnight et al., 2001). In the literature, the FI generally ranges from 1 to 3, so small changes can be significant.

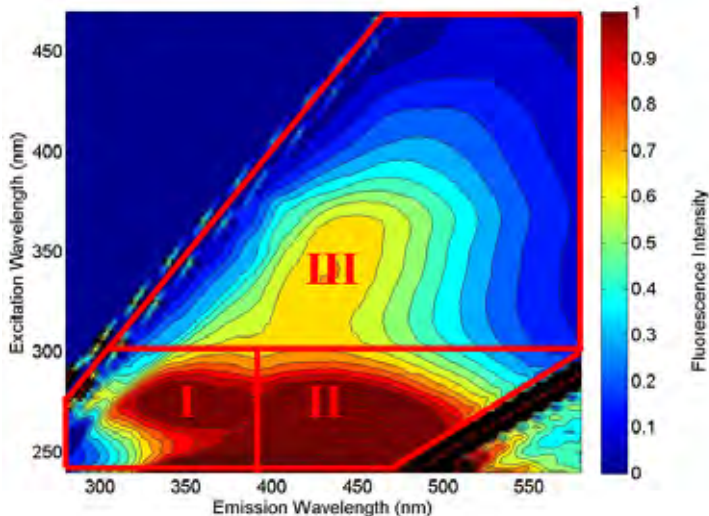


**Figure 2.3. Excitation emission matrix for secondary effluent.**

The maximum fluorescence intensity in secondary effluent EEMs often occurs near an excitation wavelength of 254 nm and an emission wavelength of 450 nm. Based on this observation, the treatment index (TI) was defined as the change in fluorescence intensity between ambient and treated samples at this particular point (i.e.,  $Ex_{254}Em_{450,T}/Ex_{254}Em_{450,A}$ ). The TI is useful for evaluating the efficacy of a particular treatment process, such as oxidation, on the transformation of bulk organic matter.

The fluorescence intensities can also be integrated within each zone using the fluorescence regional integration (FRI) method proposed by Chen et al. (2003). It is important to note that the FRI method provides normalized total fluorescence (TF) intensities to correct for the different projected areas associated with each region. Changes in the TF intensities in each region can then be observed after treatment to assess the rate of change for each organic fraction. This indicates which fractions are preferentially targeted by a particular treatment process. The FI and FRI data for the EEM in Figure 3.3 are provided in Table 2.6.

The project team also identified the absorbance and fluorescence fingerprints of the target compounds dissolved in nanopure water at concentrations of approximately 10 mg/L. Ultimately, these fingerprints could be used to determine the optimal wavelengths for the correlation models based on the peak responses for a particular compound. For example, sulfamethoxazole is characterized by a strong absorbance peak at approximately 254 nm and a strong fluorescence peak at an excitation emission pair of 260 nm/340 nm, as indicated in Figure 2.4 and Appendix 1. Therefore, this compound may demonstrate the strongest correlations with changes in the bulk organic matter associated with these wavelengths. This concept will be explored in greater detail later in the report. The full absorbance and fluorescence database for the target compounds is provided as Appendix 1.

**Table 2.6. FI and FRI Data for Secondary Effluent EEM**

Region 1		Region 2		Region 3	
Regional Fluorescence	Relative Contribution	Regional Fluorescence	Relative Contribution	Regional Fluorescence	Relative Contribution
14,697	38%	18,401	47%	5777	15%
Total fluorescence: 38,874 (arbitrary fluorescence units)					
Fluorescence index: 1.39					

Note: All total fluorescence values and relative contributions are normalized to the projected regional areas.

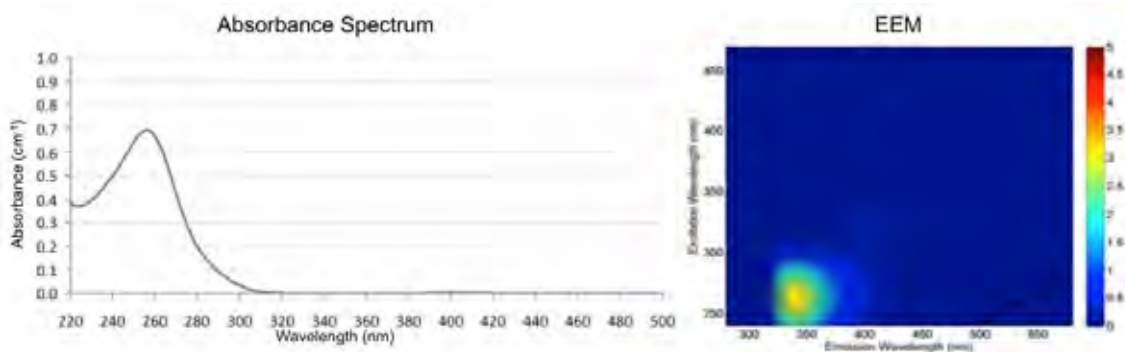


**Figure 2.4. Absorbance and fluorescence fingerprints for sulfamethoxazole (10 mg/L).**

## 2.4 Target Microbes and Methods

Disinfection was evaluated using indicator coliform bacteria, f-specific coliphages as a surrogate for human viruses (e.g., poliovirus, coxsackievirus, echovirus), and spore-forming bacteria as a surrogate for protozoan parasites (e.g., *Cryptosporidium* oocysts and *Giardia* cysts). Spiking experiments were performed with *Escherichia coli* 15597, MS2 bacteriophage, and *Bacillus subtilis* spores to represent the three groups described herein. In the bench-scale experiments, the wastewaters were spiked with sufficient target microbes to quantify a range of inactivation. A subset of the pilot-scale experiments was performed with spiked microbes particularly to address the 5-log/6.5-log viral inactivation requirements in Title 22. When possible, pilot-scale experiments were also performed with indigenous microbes to address other reuse guidelines and requirements, particularly the total coliform requirement of <2.2 MPN/100 mL in Title 22. The following sections describe the microbial assays and protocols used to prepare the spiking stocks for the bench- and pilot-scale experiments.

### 2.4.1 Coliform Bacteria

Because the current focus was on total and fecal coliforms for water reuse requirements, *E. coli* 15597 (ATCC 15597) was used in the spiking studies, and total and fecal coliforms were monitored in certain pilot-scale experiments. *E. coli* is a gram-negative, rod-shaped bacterium that is often used as an indicator of fecal contamination in water supplies. Total coliforms, fecal coliforms, and spiked *E. coli* were assayed with the 24-hour Colilert (Idexx, Westbrook, ME) method using the Quanti-Tray 2000 quantification protocol. The Colilert is an EPA-approved method for total and fecal coliform quantification in wastewater. Coliform bacteria

can be assayed with 100 mL of sample as described in Figure 2.5, and total and fecal coliforms can be differentiated based on fluorescence after 24 hours of incubation at 35 °C.

*E. coli* 15597 spiking stocks were propagated in log-phase in tryptic soy broth (TSB). The concentrated stocks were then centrifuged, washed, and resuspended in buffered demand-free (BDF) water (Thurston-Enriquez et al., 2003). The final stocks generally contained  $\approx 10^{10}$  CFU/100 mL.



**Figure 2.5. Colilert method for total and fecal coliforms.**

#### 2.4.2 MS2 Bacteriophage

MS2 is a single-stranded RNA bacteriophage (virus that infects bacteria) that is approximately 27 nm in diameter. MS2 is often used as a surrogate for human enteroviruses, such as poliovirus, coxsackievirus, and echovirus. MS2 (ATCC 15597-B1) was prepared and assayed with the double agar layer method (Adams, 1959) using antibiotic-resistant *E. coli* 700891 (ATCC 700891) as the bacterial host. All MS2 culture media (i.e., TSA, 0.7% tryptic soy agar [TSA] for the soft overlay, and 1.5% TSA as the solid substrate) were spiked with ampicillin and streptomycin at final concentrations of 15 mg/L to prevent growth of indigenous bacteria. Because *E. coli* 700891 can grow in media supplemented with antibiotics, this host is commonly used for MS2 assays in environmental samples. Plaques were counted after 18 hours of incubation at 35 °C. Figure 2.6 illustrates the double agar layer method for MS2.

MS2 stocks were purified with a polyethylene glycol precipitation and Vertrel extraction before being resuspended in BDF water (Thurston-Enriquez et al., 2003). This purification process was used to monodisperse the bacteriophages and remove a significant portion of the organic matter associated with the culture media, thereby reducing potential scavenging effects during the oxidation experiments (Mesquita et al., 2010). The final stocks generally contained  $\approx 10^{11}$  PFU/mL.

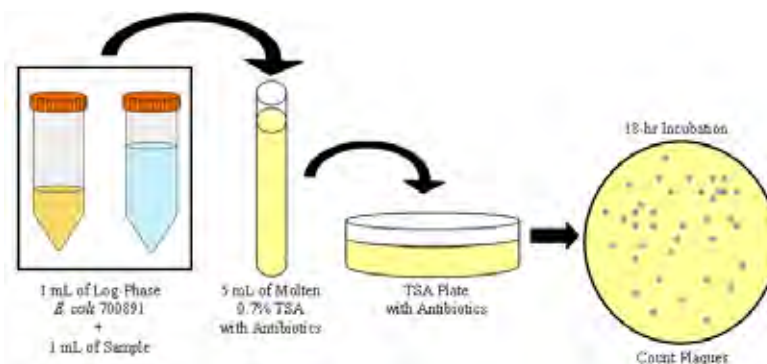


Figure 2.6. Double agar layer method for MS2.

### 2.4.3 *Bacillus subtilis* Spores

In its vegetative form, *B. subtilis* is a gram-positive, rod-shaped bacterium, but when it is exposed to adverse environmental conditions (i.e., desiccation, starvation), it can form 1- $\mu\text{m}$ -diameter endospores that are highly resistant to oxidation. This ability to form spores resistant to environmental and engineered treatment processes makes *B. subtilis* an excellent surrogate for *Cryptosporidium* oocysts and *Giardia* cysts.

*B. subtilis* (ATCC 23059) was propagated in TSB at 35 °C and 150 rpm for 24 hours, centrifuged and washed twice in BDF water to remove the nutrient-rich media, and sporulated in BDF water at 35 °C and 150 rpm for an additional 24 hours. The sporulated stock was heat-shocked at 80 °C and 50 rpm for 12 minutes to inactivate any remaining vegetative bacteria. The spore suspension was centrifuged and washed twice in BDF water in order to create the final spiking stock. The final stocks generally contained  $\approx 10^8$  CFU/100 mL in the sporulated form.

All spore samples were heat-shocked at 80 °C ( $\pm 5$  °C) and 50 rpm for 12 minutes prior to plating. Samples with higher anticipated concentrations of spores (i.e.,  $>1/\text{mL}$ ) were assayed with the pour plate method using molten nutrient agar (1%) supplemented with tryptan blue. Lower concentrations of spores were assayed with membrane filtration using 0.45- $\mu\text{m}$  filters and nutrient agar plates supplemented with tryptan blue. Plates were counted after 24 hours of incubation at 35 °C. Figure 2.7 illustrates the two spore assays.

## 2.5 pCBA

Because of its selectivity in reacting with  $\bullet\text{OH}$ , pCBA is often used to determine the  $\bullet\text{OH}$  exposure during AOPs. The rate of pCBA degradation during  $\bullet\text{OH}$  exposure can be modeled according to the following second-order reaction, where  $k_{\text{OH,pCBA}}$  has been previously determined to be  $5 \times 10^9 \text{ M}^{-1} \text{ s}^{-1}$ :

$$\frac{d[\text{pCBA}]}{dt} = -k[\bullet\text{OH}][\text{pCBA}]$$

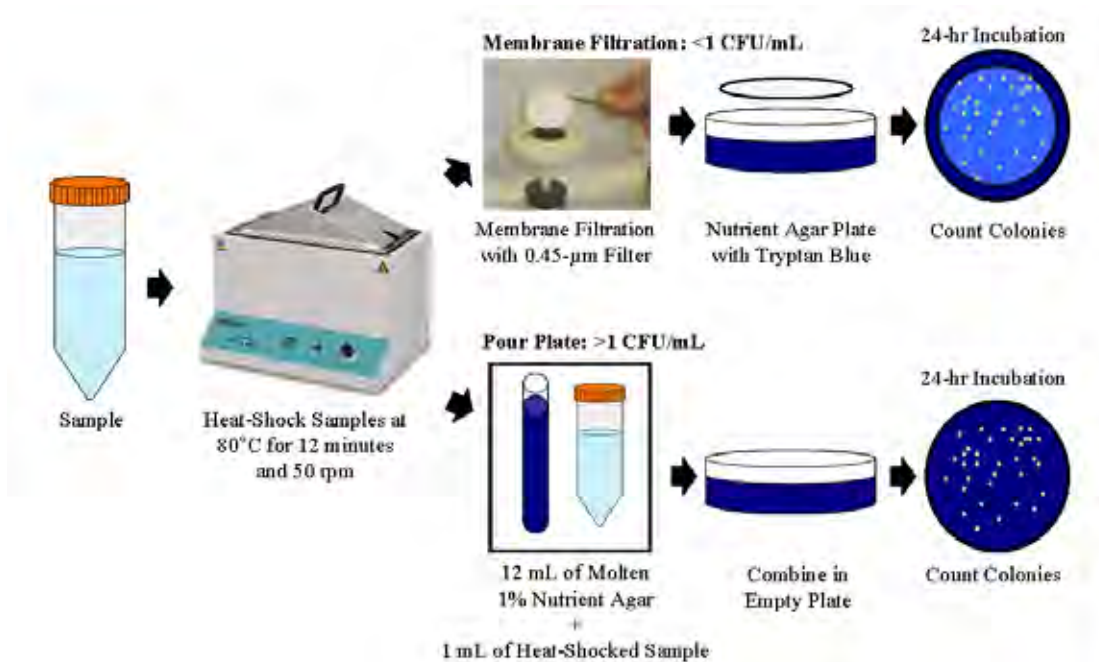


Figure 2.7. Pour plate and membrane filtration methods for *Bacillus* spores.

After rearrangement and solving, the following equation can be used to determine the overall  $\bullet\text{OH}$  exposure during AOPs.

$$\int [\bullet\text{OH}] dt = \left( \ln \left[ \frac{p\text{CBA}}{p\text{CBA}} \right]_t \right) \left( \frac{1}{-k} \right)$$

The pCBA samples in this study were analyzed by LC-MS/MS based on previously published methods (Vanderford et al., 2007).

## 2.6 Yeast Estrogen Screen (YES) Assay for Total Estrogenicity

A YES assay (Routledge and Sumpter, 1996) was used to analyze a subset of the samples for total estrogenic activity. A human estrogen receptor–transfected yeast strain was supplied by Duke University with the permission of John Sumpter of Brunel University (Middlesex, UK). Assay procedures followed those originally published (Routledge and Sumpter, 1996) with several modifications. Yeast colonies were propagated on sterile plates filled with a Difco Sabouraud dextrose agar (Becton, Dickinson, and Company, Sparks, MD) at 60 mg/L plus 3 mL of 2.5 mg/mL chloramphenicol (Alfa Aesar, Ward Hill, MA). A new plate was streaked every 30 to 60 days using a single colony from the previous plate. Stock plates were incubated in the dark for 3 days at 30 °C and then stored at 4 °C. Growth and assay media were prepared as originally described but were inoculated with a single colony from the most recent streak plate. All incubation was carried out at 30 °C in a dark, temperature-controlled incubator.

For sample analysis, microplates (96-well) were inoculated with aliquots of the sample, yeast, and chlorophenol red- $\beta$ -D-galactopyranoside (EMD Bioscience, La Jolla, CA). The wells

were allowed to develop for up to 5 days to reach adequate color development, which was measured using a PowerWave 340 Microplate Reader (BioTek, Winooski, VT) at 650 nm for turbidity correction and 570 nm for color change. The corrected absorbance was calculated as  $A_{570} - A_{650}$ , and data were analyzed using the open source software “R,” Version 2.4.0 (R\_Development\_Core\_Team, 2006) in conjunction with a dose–response curve add-on package (Ritz and Streibig, 2005). This software was used to calculate the concentration of estradiol, or relative concentration of the sample extract, needed to induce 50% of the maximum response, written as  $EC_{50}$ . After comparison with the standard curve, an estradiol equivalent (EEq) concentration was determined for each unknown sample.

A four-parameter logistic model was used to develop the standard and sample dose–response curves. This model allowed the analyst to define the lower limit, upper limit, slope, and  $EC_{50}$  values based on standard and experimental data. The four-parameter logistic model is described by the following:

$$f(x, (b, c, d, e)) = c + \frac{d - c}{1 + \exp\{b(\log(x) - \log(e))\}}$$

where  $b$ =slope,  $c$ =lower limit,  $d$ =upper limit, and  $e$ = $EC_{50}$ . The  $EC_{50}$  values were never forced upon a given model, but lower limit, upper limit, and slope were adjusted to achieve best fit and match the trends observed by the estradiol standards. Best fit was determined by iteratively adjusting model parameters to minimize standard error associated with deviation of data points from the model fit.

Model adjustments are particularly important for minimizing the errors associated with low dose–response, whereby the  $EC_{50}$  is underestimated because of failure of the sigmoidal dose–response curve to reach a maximum plateau. For example, Figure 2.8A illustrates an estradiol standard curve and a low-dose condition modeled with two different approaches: (1) using default settings and (2) using the maximum and minimum responses from the estradiol standards while manually shaping the curve to the low-dose sample data. The manual correction yields a more characteristic dose–response curve and ultimately a more accurate EEq concentration. The four-parameter logistic model is also able to account for early cell die-off, which is common in extracts that exert outright toxicity on the yeast or in aqueous samples with high biological activity. An example of an acute-toxicity condition is illustrated in Figure 2.8B. Again, manual adjustments to model parameters are necessary to eliminate the effects of toxicity and more accurately describe the dose–response curve.

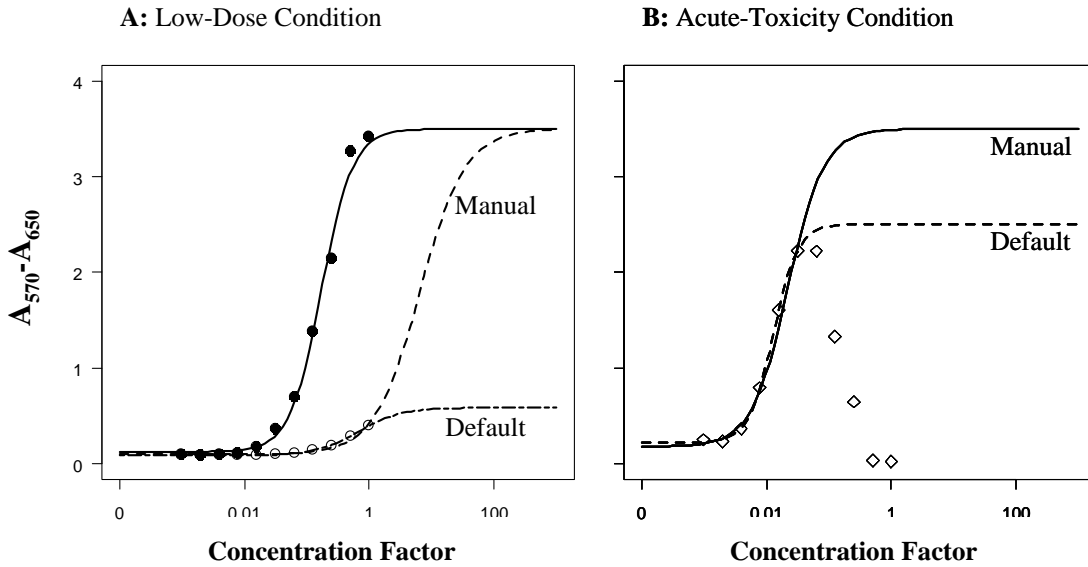


Figure 2.8. YES model corrections for low-dose and acute-toxicity conditions.

## 2.7 NDMA

NDMA was measured with a modification to EPA Method 521, which included SPE, analysis by gas chromatography tandem mass spectrometry, and corrections based on isotope dilution. The MRL for this method was 2.5 ng/L.

## 2.8 1,4-Dioxane

1,4-dioxane samples were shipped to Weck Laboratories, Inc. (Industry, CA) for analysis. Samples were prepared and analyzed using EPA Methods 3520C and 8270M.

## Chapter 3

# Bench-Scale Evaluation of Ozone for Water Reclamation

---

### 3.1 Clark County Water Reclamation District, Las Vegas, Nevada

CCWRD currently treats an average daily flow of approximately 100 MGD and discharges the tertiary-treated, UV-disinfected effluent into Lake Mead. Because Lake Mead is the immediate drinking water source for the Las Vegas metropolitan area and an additional 30 million people downstream, CCWRD is a significant contributor to water reuse. Past studies have observed increased feminization rates for fish populations in the effluent-dominated Las Vegas Bay, which is the discharge point into Lake Mead. In order to mitigate the potential environmental impacts of its discharged effluent, CCWRD is currently evaluating a number of treatment options to reduce the concentrations of TORCs. In addition to process optimization strategies (e.g., increasing SRTs in the activated sludge basins), CCWRD has also planned for a 30-MGD UF/ozone system, which is currently in the final phases of design. The UF system is intended as (1) a microbiological barrier, (2) a pretreatment system to reduce the TSS of the secondary effluent and increase ozone disinfection efficacy, and (3) an additional barrier for total phosphorus (TP) reductions. The ozone system targets reductions in estrogenicity in addition to disinfection for any microbes that pass through the membrane, particularly viruses.

The influent CCWRD wastewater is primarily municipal, but some industrial contributions are present. The CCWRD effluent is discharged into Lake Mead after treatment with bar screens; grit removal; primary clarification with ferric chloride addition; conventional activated sludge (SRT $\approx$ 7 days) with full nitrification ( $\text{NH}_{3,\text{eff}} < 0.1$  mg-N/L), partial denitrification, and biological phosphorus removal; secondary clarification; dual-media filtration with alum addition; and UV disinfection. A separate train treats a portion of the secondary effluent with flocculation, sedimentation, dual-media filtration with alum addition, and chlorine or UV disinfection. This UV-disinfected effluent is also discharged into Lake Mead, and the chlorine-disinfected effluent is pumped into the reclaimed water distribution system for irrigation and power plant cooling. With biological and chemical phosphorus removal, CCWRD is able to target TP levels of  $<100$   $\mu\text{g/L}$  in the finished effluent. A simplified treatment schematic for CCWRD is provided in Figure 3.1, and additional water quality data are provided herein.

Unfiltered secondary effluent from CCWRD was collected in April 2010, and the initial water quality data in Table 3.1 were obtained. Using the initial TOC and nitrite data, the ozone dosing conditions in Table 3.2 were calculated.

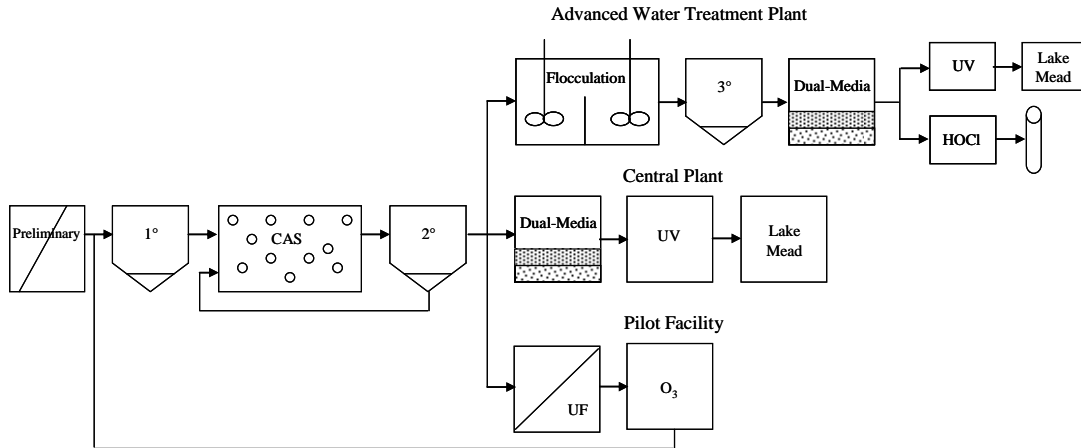


Figure 3.1. Simplified treatment schematic for CCWRD.

Table 3.1. Initial Water Quality Data for CCWRD

<b>Unfiltered Secondary Effluent</b>	alkalinity (mg/L CaCO <sub>3</sub> )	123
	bromide (µg/L)	174
	NDMA (ng/L)	<2.5
	NH <sub>3</sub> (mg-N/L)	0.09
	NO <sub>2</sub> (mg-N/L)	0.06
	NO <sub>3</sub> (mg-N/L)	14.0
	pH	6.9
	TKN (mg-N/L)	2.04
	TN (mg-N/L)	16.1
	TOC (mg/L)	7.1
	TON (mg-N/L)	1.95
	TSS (mg/L)	<5
	turbidity (NTU)	1.19
	UV <sub>254</sub> absorbance (cm <sup>-1</sup> )	0.132
<b>Filtered Secondary Effluent</b>	pH	6.9
	TOC (mg/L)	7.6
	TSS (mg/L)	<5
	turbidity (NTU)	0.55
	UV <sub>254</sub> absorbance (cm <sup>-1</sup> )	0.146
<b>Finished Effluent</b>	NDMA (ng/L)	<2.5
	TOC (mg/L)	5.8
	UV <sub>254</sub> absorbance (cm <sup>-1</sup> )	0.128

Notes: NDMA=N-nitrosodimethylamine; total Kjeldahl nitrogen (TKN)=sum of total organic nitrogen and ammonia; TN=total nitrogen; TOC=total organic carbon; total organic nitrogen (TON)=difference of total nitrogen and ammonia, nitrate, and nitrite; TSS=total suspended solids; UV=ultraviolet

**Table 3.2. Ozone Dosing Conditions for 1-L CCWRD Secondary Effluent Samples**

Concentration of O<sub>3</sub> stock solution=95 mg/L  
 Concentration of H<sub>2</sub>O<sub>2</sub> stock solution=10 g/L  
 Unfiltered dilution ratio=(899/1000)=0.899  
 Unfiltered TOC after dilution: 6.4 mg/L  
 Unfiltered NO<sub>2</sub> after dilution=0.051 mg/L as N=0.168 mg/L as NO<sub>2</sub>  
 Filtered dilution ratio=(892/1000)=0.892  
 Filtered TOC after dilution: 6.8 mg/L  
 Filtered NO<sub>2</sub> after dilution=0.051 mg/L as N=0.168 mg/L as NO<sub>2</sub>

Unfiltered						
O <sub>3</sub> :TOC/ H <sub>2</sub> O <sub>2</sub> :O <sub>3</sub>	Wastewater Volume (mL)	Nanopure Volume (mL)	O <sub>3</sub> Volume (mL)	O <sub>3</sub> Dose (mg/L)	H <sub>2</sub> O <sub>2</sub> Volume (μL)	H <sub>2</sub> O <sub>2</sub> Dose (mg/L)
Spike	899	101	0	0	0	0
0.25/0	899	82	19	1.8	0	0
0.25/0.5	899	82	19	1.8	57	0.6
0.25/1.0	899	82	19	1.8	115	1.2
0.5/0	899	65	36	3.4	0	0
0.5/0.5	899	65	36	3.4	115	1.2
0.5/1.0	899	65	36	3.4	230	2.3
1.0/0	899	32	69	6.6	0	0
1.0/0.5	899	32	69	6.6	226	2.3
1.0/1.0	899	32	69	6.6	452	4.5
1.5/0	899	0	101	9.6	0	0
1.5/0.5	899	0	101	9.6	339	3.4
1.5/1.0	899	0	101	9.6	678	6.8
Filtered						
O <sub>3</sub> :TOC/ H <sub>2</sub> O <sub>2</sub> :O <sub>3</sub>	Wastewater Volume (mL)	Nanopure Volume (mL)	O <sub>3</sub> Volume (mL)	O <sub>3</sub> Dose (mg/L)	H <sub>2</sub> O <sub>2</sub> Volume (μL)	H <sub>2</sub> O <sub>2</sub> Dose (mg/L)
Spike	892	108	0	0	0	0
0.25/0	892	88	20	1.9	0	0
0.25/0.5	892	88	20	1.9	61	0.6
0.25/1.0	892	88	20	1.9	122	1.2
0.5/0	892	70	38	3.6	0	0
0.5/0.5	892	70	38	3.6	123	1.2
0.5/1.0	892	70	38	3.6	246	2.5
1.0/0	892	35	73	7.0	0	0
1.0/0.5	892	35	73	7.0	242	2.4
1.0/1.0	892	35	73	7.0	483	4.8
1.5/0	892	0	108	10.3	0	0
1.5/0.5	892	0	108	10.3	363	3.6
1.5/1.0	892	0	108	10.3	725	7.3

Note: Some values are affected by rounding error and the precision of the ozone spike; TOC=total organic carbon

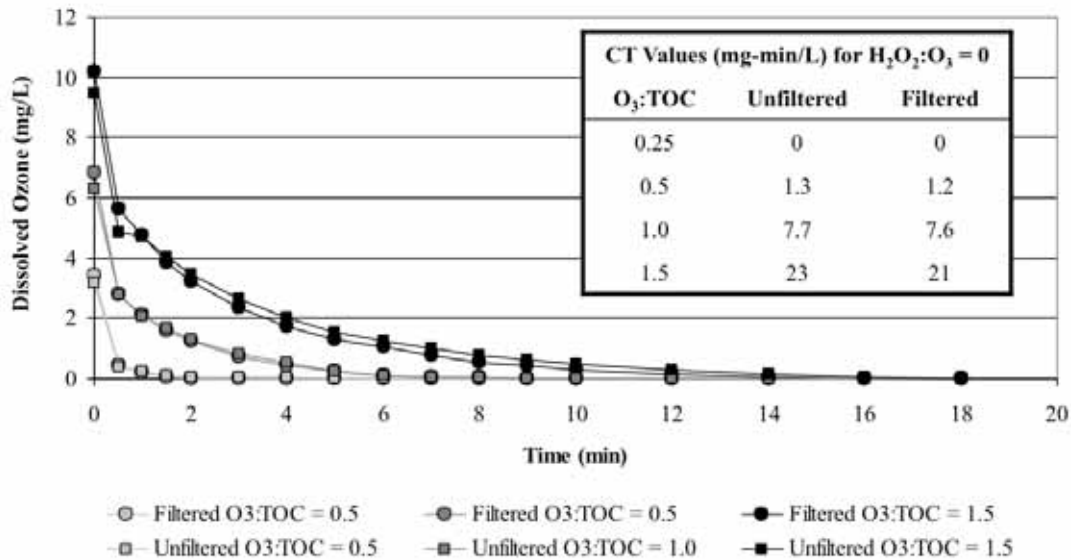


Figure 3.2. Ozone demand/decay curves for the CCWRD secondary effluent.

### 3.1.1 Ozone Demand/Decay

Figure 3.2 illustrates the ozone demand/decay curves for filtered and unfiltered CCWRD secondary effluent at the various dosing conditions in Table 3.2. The graph only includes dosing conditions with a measurable ozone residual after 30 seconds; corresponding CT values are also provided. For the  $O_3/H_2O_2$  samples, the addition of  $H_2O_2$  caused a nearly instantaneous reaction with the dissolved ozone, which led to the formation of  $\bullet OH$  but eliminated the dissolved ozone residual. Reactions with EfOM made the 0.25  $O_3:TOC$  ratio insufficient to establish a measurable ozone residual after 30 seconds. For the remaining dosing conditions, the graph illustrates the IOD (i.e., the precipitous drop between 0 and 30 seconds) and the decay over time. It also indicates that there was no significant difference between filtered and unfiltered secondary effluent as far as ozone demand and decay. This is consistent with the literature and indicates that the organic leaching from the cartridge filters did not impact the oxidation experiments for the CCWRD experiments.

### 3.1.2 Bromate Formation

One of the major factors limiting the widespread use of ozone in water and wastewater treatment is bromate formation. Although some studies indicate that more relaxed bromate guidelines should be applied to wastewater treatment, the EPA MCL of  $10 \mu g/L$  in drinking water is often used as a point of reference. As illustrated in Figure 3.3, significant bromate formation occurred during ozonation of CCWRD secondary effluent. The bromide values listed in each figure differ from the value in the previous table because of the dilution effect of the ozone stock. There was a noticeable difference in bromate formation for the unfiltered and filtered experiments, but it is unclear why cartridge filtration would affect bromate formation. The difference in the two data sets may be attributable to inherent variability during ozonation. Although the addition of  $H_2O_2$  provided some degree of bromate mitigation, the  $O_3:TOC$  ratios of 1.0 and 1.5 both exceeded  $10 \mu g/L$  in all samples, even exceeding  $90 \mu g/L$  in the absence of  $H_2O_2$ . In order to satisfy the  $10 \mu g/L$  benchmark,

O<sub>3</sub>:TOC ratios of 0.25 and 0.5 would be necessary unless further mitigation measures are implemented.

### 3.1.3 Hydroxyl Radical Exposure

Based on data from bench-scale experiments with pCBA spiked at 150 µg/L, Table 3.3 indicates the overall •OH exposure for each ozone and UV dosing condition. The •OH exposures for the UV/H<sub>2</sub>O<sub>2</sub> samples are corrected for the small level of pCBA degradation achieved by photolysis alone.

As mentioned earlier, ozone naturally decomposes into •OH, but the process can be expedited with the addition of H<sub>2</sub>O<sub>2</sub>. As indicated in Table 3.3, neither filtration nor the addition of H<sub>2</sub>O<sub>2</sub> has consistent impacts on •OH exposure. Therefore, assuming the dissolved ozone residual is allowed to react completely, the overall •OH exposure *in wastewater* is independent of H<sub>2</sub>O<sub>2</sub> dose. However, for the highest O<sub>3</sub>:TOC ratio, the overall reaction time can be reduced from nearly 16 minutes (see Figure 3.2) to several seconds with the addition of H<sub>2</sub>O<sub>2</sub>. Ozone-based oxidation also provided higher •OH exposures than the UV dosing conditions applied during these experiments. With 10 mg/L of H<sub>2</sub>O<sub>2</sub> for the UV AOP, UV doses of 225 mJ/cm<sup>2</sup> and 680 mJ/cm<sup>2</sup> were nearly equivalent to O<sub>3</sub>:TOC ratios of 0.25 and 0.5.

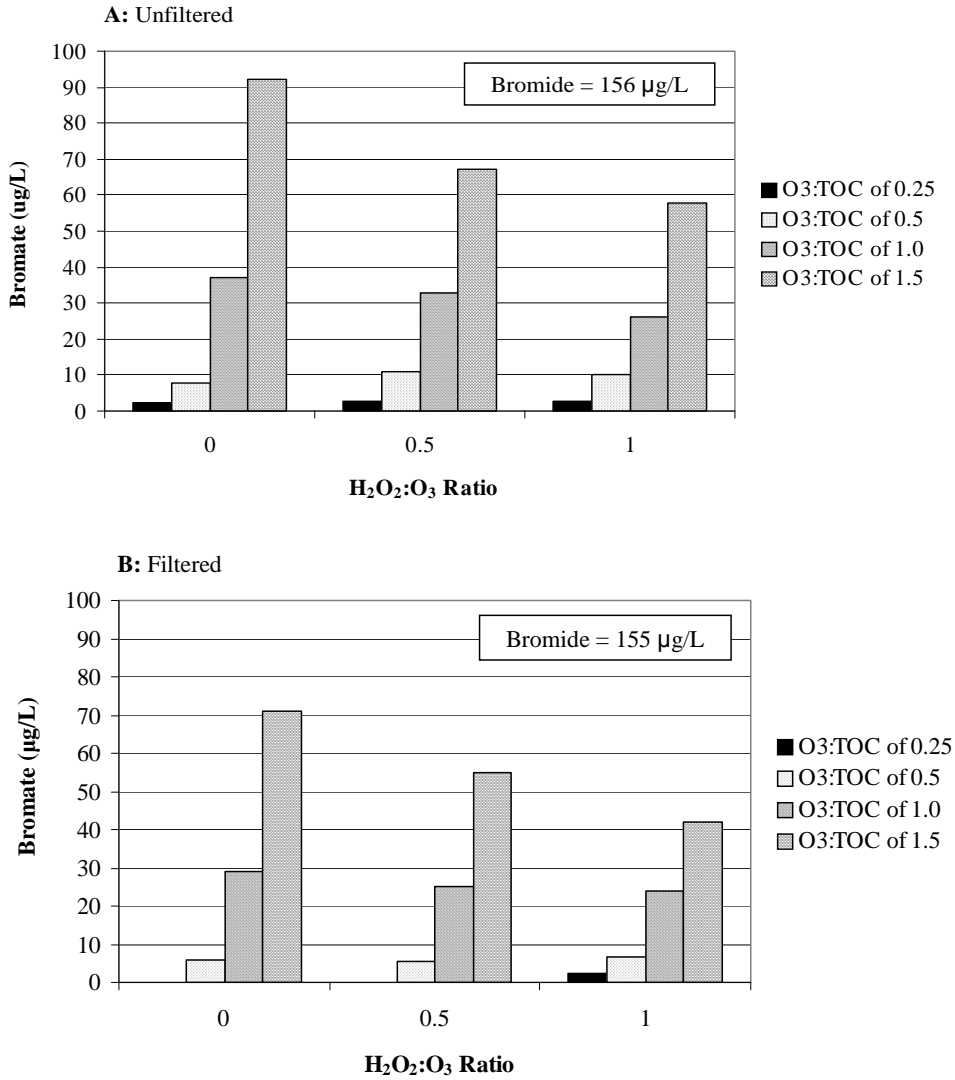


**Figure 3.3. Bromate formation during ozonation of CCWRD secondary effluent.**

**Table 3.3. •OH Exposure in the CCWRD Secondary Effluent**

Unfiltered Ozone ( $10^{-11}$ M-s)			
Ozone:TOC	H <sub>2</sub> O <sub>2</sub> :O <sub>3</sub> =0	H <sub>2</sub> O <sub>2</sub> :O <sub>3</sub> =0.5	H <sub>2</sub> O <sub>2</sub> :O <sub>3</sub> =1.0
0.25	6.7	6.7	7.9
0.5	20	23	25
1.0	39	35	35
1.5	[pCBA]<MRL	[pCBA]<MRL	49
Filtered Ozone ( $10^{-11}$ M-s)			
Ozone:TOC	H <sub>2</sub> O <sub>2</sub> :O <sub>3</sub> =0	H <sub>2</sub> O <sub>2</sub> :O <sub>3</sub> =0.5	H <sub>2</sub> O <sub>2</sub> :O <sub>3</sub> =1.0
0.25	8.1	8.1	9.2
0.5	19	22	24
1.0	39	37	37
1.5	[pCBA]<MRL	53	[pCBA]<MRL
Filtered UV ( $10^{-11}$ M-s)			
UV Dose (mJ/cm <sup>2</sup> )	H <sub>2</sub> O <sub>2</sub> = 0 mg/L	H <sub>2</sub> O <sub>2</sub> = 5 mg/L	H <sub>2</sub> O <sub>2</sub> = 10 mg/L
0	N/A	N/A	0.0*
23	N/A	N/A	0.41
45	N/A	N/A	2.0
225	N/A	N/A	4.4
680	N/A	N/A	14

Notes: \*=based on H<sub>2</sub>O<sub>2</sub> control; MRL=method reporting limit; pCBA=para-chlorobenzoic acid; TOC=total organic carbon; UV=ultraviolet

### 3.1.4 Title 22 Contaminants

In the past, CDPH Title 22 requirements for water recycling required reuse systems to demonstrate 1.2- and 0.5-log destruction or removal of NDMA and 1,4-dioxane. In order to satisfy these requirements, reuse systems often implemented the UV AOP (i.e., UV/H<sub>2</sub>O<sub>2</sub>) because NDMA is relatively susceptible to UV photolysis, and 1,4-dioxane can be eliminated with •OH oxidation.

Bench-scale experiments were performed with the filtered CCWRD wastewater to evaluate the use of ozone and UV for the destruction of spiked NDMA (200 ng/L) and 1,4-dioxane (700 µg/L). Figure 3.4 indicates that UV doses of approximately 500 and 625 mJ/cm<sup>2</sup> were required to satisfy the Title 22 requirement with UV and UV/H<sub>2</sub>O<sub>2</sub>. The additional energy required to reach the 1.2-log treatment goal with UV/H<sub>2</sub>O<sub>2</sub> is plausible because the H<sub>2</sub>O<sub>2</sub> will absorb a portion of the incident photons, and NDMA is highly resistant to •OH oxidation (Pisarenko et al., 2012). This was supported by a separate NDMA destruction experiment with ozone and ozone/H<sub>2</sub>O<sub>2</sub>. An O<sub>3</sub>:TOC ratio of 1.5 only achieved 0.05- to 0.14-log destruction of NDMA at H<sub>2</sub>O<sub>2</sub>:O<sub>3</sub> ratios of 0 and 0.5. Not only did ozone achieve limited levels of NDMA destruction, but it also led to a small level of NDMA *formation*. This should not be confused with NDMA *formation potential*, which incorporates chloramination to intentionally form NDMA. As indicated in Table 3.4, the ozone-induced NDMA formation remained relatively constant regardless of ozone or H<sub>2</sub>O<sub>2</sub> dose.

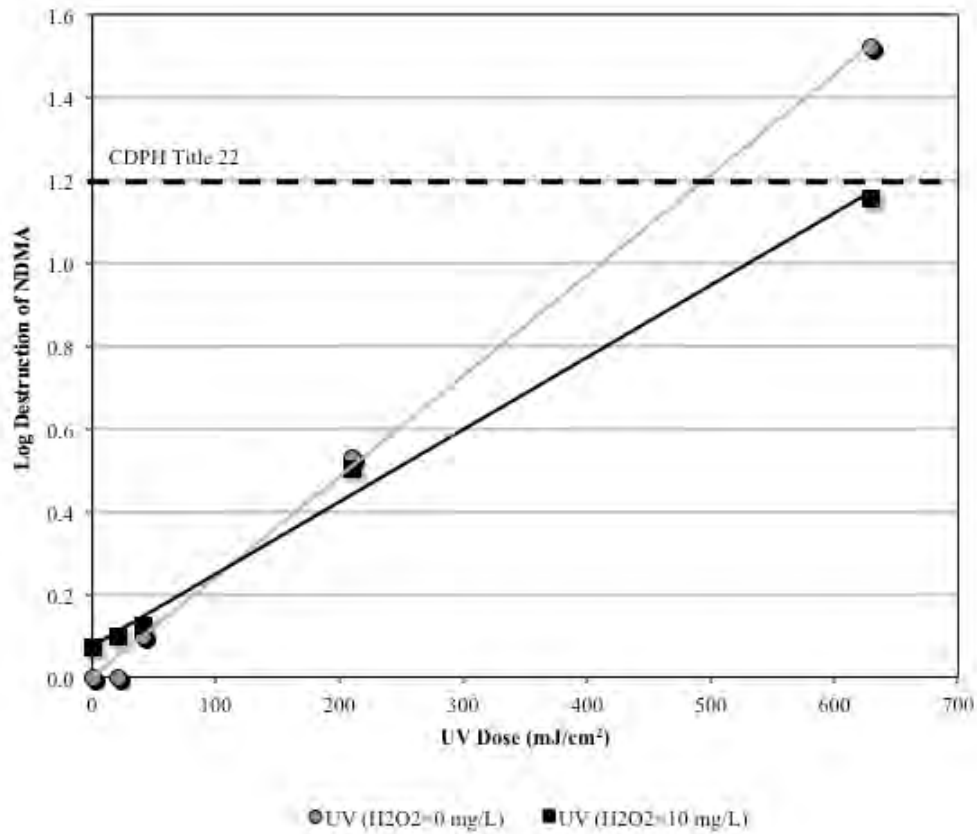
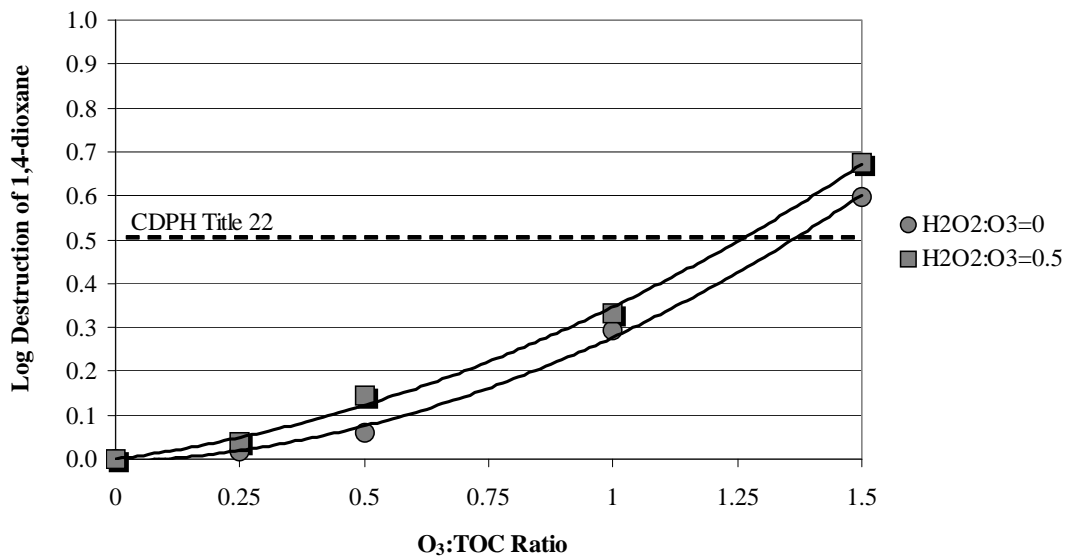


Figure 3.4. Destruction of NDMA in the filtered CCWRD secondary effluent.

Table 3.4. Direct NDMA Formation in the Filtered CCWRD Secondary Effluent

O <sub>3</sub> :TOC Ratio	H <sub>2</sub> O <sub>2</sub> :O <sub>3</sub> Ratio	NDMA (ng/L)
0	0	<2.5
0.5	0	48
0.5	0.5	45
1.0	0	42
1.0	0.5	36



**Figure 3.5. Destruction of 1,4-dioxane in the filtered CCWRD secondary effluent.**

Figure 3.5 illustrates the destruction of spiked 1,4-dioxane during the bench-scale ozone experiments. In general, O<sub>3</sub> and O<sub>3</sub>/H<sub>2</sub>O<sub>2</sub> achieved similar levels of treatment, although the trend lines suggest that O<sub>3</sub>/H<sub>2</sub>O<sub>2</sub> provided a slight advantage. On the basis of the CCWRD data, O<sub>3</sub>:TOC ratios of 1.25 to 1.35 are necessary to comply with the 0.5-log requirement.

### 3.1.5 Trace Organic Contaminants

Secondary and finished effluent samples from CCWRD were analyzed to determine the ambient concentrations of the target compounds, which are provided in Table 3.5. Only sulfamethoxazole was present at concentrations exceeding 1 µg/L, and a majority of the compounds were detected at concentrations less than 200 ng/L. The concentrations of some of the most bioamenable compounds, including naproxen and ibuprofen, were <MRL after biological treatment in the activated sludge process. Additional treatment with alum addition, sand filtration, and UV disinfection (40 mJ/cm<sup>2</sup>) reduced the concentrations of most of the target compounds even further. The compounds with higher concentrations in the finished effluent may have been influenced by temporal variability because the samples were not hydraulically linked. Notably, the total estrogenicity of the wastewater, which is measured in EEq, was reduced from 9.1 ng/L in the secondary effluent to <0.5 ng/L in the finished effluent.

**Table 3.5. Ambient TOrC Concentrations at CCWRD**

Parameter	Secondary Effluent (ng/L)	Finished Effluent (ng/L)
Atenolol	421	120
Atrazine	<10	<10
Bisphenol A	<50	<50
Carbamazepine	251	192
DEET	155	232
Diclofenac	131	57
Gemfibrozil	34	12
Ibuprofen	<25	<25
Meprobamate	629	362
Musk ketone	<100	<100
Naproxen	<25	<25
Phenytoin	216	113
Primidone	134	168
Sulfamethoxazole	1220	1150
TCEP	525	349
Total estrogenicity (EEq)	9.1	<0.074
Triclosan	29	38
Trimethoprim	256	43

Notes: DEET=*N,N*-diethyl-*meta*-toluamide; EEq=estradiol equivalents; TCEP tris-(2-chloroethyl)-phosphate

In order to evaluate each of the target compounds, a spiking stock was prepared prior to the bench-scale experiments. The spiking stock, which was prepared in deionized water, included approximately 2 mg/L of each target compound, and an aliquot was added to each sample bottle to target final concentrations of 1 µg/L. The target concentration did not account for the ambient concentrations in Table 3.5, so many of the target compounds were initially present at concentrations exceeding 1 µg/L. Excluding musk ketone, the concentrations of the spiking stock, and therefore the concentrations of the spiked controls, matched their expected concentrations. Musk ketone is an extremely volatile compound that experienced significant fluctuations between samples. Although this compound proved to be extremely resistant to oxidation, as expected, these data are less dependable because of their high variability. As a result, musk ketone is generally omitted from the data presentation. Finally, H<sub>2</sub>O<sub>2</sub> alone (i.e., 10 mg/L of H<sub>2</sub>O<sub>2</sub> with no ozone or UV exposure) had no noticeable effect on the concentrations of the target compounds.

Tables 3.6 and 3.7 show the relative oxidation levels of the 16 target compounds (musk ketone omitted) as a function of O<sub>3</sub>:TOC and H<sub>2</sub>O<sub>2</sub>:O<sub>3</sub> ratio in the unfiltered and filtered CCWRD secondary effluent. As described earlier, the target compounds were divided into five categories based on their second-order ozone and •OH rate constants, and “indicator” compounds were also defined as the average of the values within each group.

In general, there were no significant differences between the filtered versus unfiltered samples and the ozone versus ozone/H<sub>2</sub>O<sub>2</sub> samples. The compounds within each group experienced highly consistent levels of oxidation, thereby justifying the applicability of the indicator framework. The shading represents the dosing conditions required to achieve at least 80% oxidation of the target compounds, whereas the extreme resistance of TCEP limited its level of oxidation to <30%.

Table 3.8 shows the relative oxidation levels of the 16 target compounds as a function of UV and H<sub>2</sub>O<sub>2</sub> dose. The previously defined groups are not necessarily applicable to UV and UV/H<sub>2</sub>O<sub>2</sub> because of the compounds' variable susceptibility to UV photolysis. Two compounds (diclofenac and triclosan) experienced 90% removal with a UV dose of 225 mJ/cm<sup>2</sup>, three compounds (atrazine, phenytoin, and sulfamethoxazole) experienced greater than 50% removal with a UV dose of 680 mJ/cm<sup>2</sup>, and a majority of the target compounds experienced less than 20% removal at a UV dose of 680 mJ/cm<sup>2</sup>. As indicated by the light shading in Table 3.8, the high •OH rate constants for some of the compounds allowed for significant oxidation when UV doses were coupled with H<sub>2</sub>O<sub>2</sub> addition. Although UV/H<sub>2</sub>O<sub>2</sub> was more effective than UV photolysis, the UV AOP was still inferior to ozone and ozone/H<sub>2</sub>O<sub>2</sub> for a majority of the compounds. This is particularly evident for low UV doses (i.e., <50 mJ/cm<sup>2</sup>) where analytical variability, which is generally ±10%, was more significant than compound elimination.

Although it is important to understand the efficacy of various treatment processes in removing or oxidizing individual compounds, TOxCs are always present in complex mixtures for which aquatic impacts and health effects are unknown. Some assays are able to capture the aggregate effects of these mixtures based on a variety of endpoints. For example, the YES assay can be used to quantify the total estrogenicity of a sample. Figure 3.6 illustrates the change in total estrogenicity after (A) ozone- and (B) UV-based treatment processes. As indicated by the dashed lines, O<sub>3</sub>:TOC ratios of 0.5 and greater achieved the MRL (i.e., <0.074 ng/L) for all H<sub>2</sub>O<sub>2</sub> doses. UV photolysis demonstrated high variability and was unable to achieve the MRL for the UV doses in this experiment, whereas UV/H<sub>2</sub>O<sub>2</sub> was able to reach the MRL with 680 mJ/cm<sup>2</sup>. The addition of H<sub>2</sub>O<sub>2</sub> alone caused a small reduction in the initial EEq value, which is shown for the UV/H<sub>2</sub>O<sub>2</sub> data point at 0 mJ/cm<sup>2</sup>.

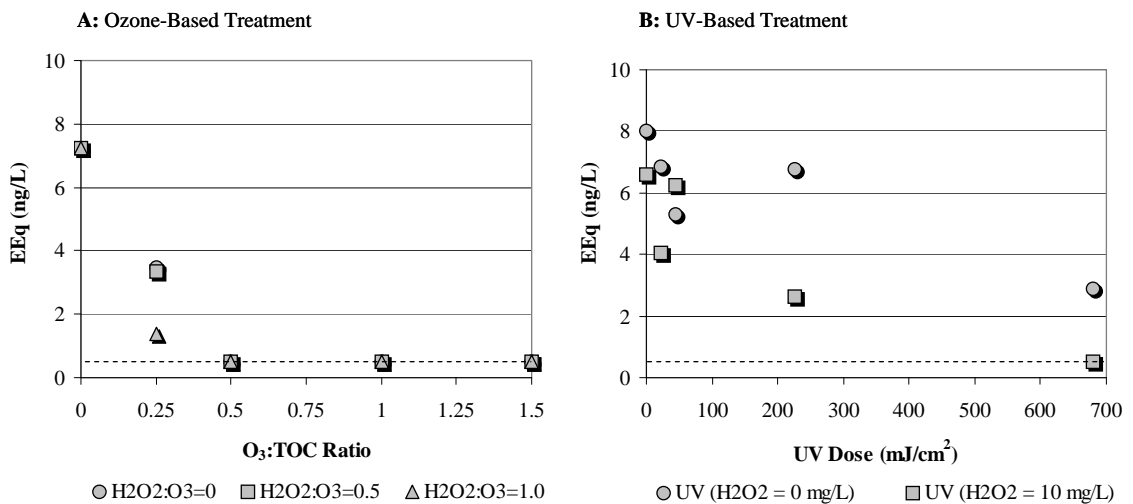


**Figure 3.6. Reduction in total estrogenicity in the filtered CCWRD secondary effluent.**

**Table 3.6. CCWRD TOrC Mitigation by Ozone (Unfiltered)**

Group	Contaminant	O <sub>3</sub> :TOC (mass) / H <sub>2</sub> O <sub>2</sub> :O <sub>3</sub> (molar)											
		0.25/0	0.25/0.5	0.25/1.0	0.5/0	0.5/0.5	0.5/1.0	1.0/0	1.0/0.5	1.0/1.0	1.5/0	1.5/0.5	1.5/1.0
1	Bisphenol A	75%	74%	72%	97%	91%	91%	97%	97%	97%	97%	97%	97%
	Carbamazepine	67%	66%	67%	99%	87%	87%	99%	99%	99%	99%	99%	99%
	Diclofenac	70%	69%	68%	97%	89%	89%	97%	97%	97%	97%	97%	97%
	Naproxen	65%	63%	65%	98%	88%	87%	98%	98%	98%	98%	98%	98%
	Sulfamethoxazole	64%	62%	62%	98%	85%	85%	99%	99%	99%	99%	99%	99%
	Triclosan	80%	76%	75%	97%	93%	93%	97%	97%	97%	97%	97%	97%
	Trimethoprim	67%	67%	67%	99%	88%	89%	99%	99%	99%	99%	99%	99%
	<b>Indicator</b>	<b>70%</b>	<b>68%</b>	<b>68%</b>	<b>98%</b>	<b>89%</b>	<b>89%</b>	<b>98%</b>	<b>98%</b>	<b>98%</b>	<b>98%</b>	<b>98%</b>	<b>98%</b>
2	Atenolol	36%	37%	37%	87%	69%	67%	98%	97%	89%	98%	98%	98%
	Gemfibrozil	55%	54%	54%	99%	79%	81%	99%	99%	99%	99%	99%	99%
	<b>Indicator</b>	<b>46%</b>	<b>46%</b>	<b>46%</b>	<b>93%</b>	<b>74%</b>	<b>74%</b>	<b>99%</b>	<b>98%</b>	<b>94%</b>	<b>99%</b>	<b>99%</b>	<b>99%</b>
3	DEET	24%	27%	27%	52%	54%	58%	87%	89%	82%	98%	98%	97%
	Ibuprofen	29%	35%	32%	62%	61%	65%	92%	92%	87%	97%	97%	97%
	Phenytoin	38%	31%	27%	67%	65%	65%	95%	96%	90%	99%	99%	99%
	Primidone	25%	25%	32%	54%	53%	59%	87%	88%	81%	99%	98%	97%
	<b>Indicator</b>	<b>29%</b>	<b>30%</b>	<b>30%</b>	<b>59%</b>	<b>58%</b>	<b>62%</b>	<b>90%</b>	<b>91%</b>	<b>85%</b>	<b>98%</b>	<b>98%</b>	<b>98%</b>
4	Atrazine	12%	15%	15%	25%	30%	34%	58%	64%	59%	85%	88%	86%
	Meprobamate	22%	24%	22%	37%	41%	46%	69%	76%	71%	91%	94%	92%
	<b>Indicator</b>	<b>17%</b>	<b>20%</b>	<b>19%</b>	<b>31%</b>	<b>36%</b>	<b>40%</b>	<b>64%</b>	<b>70%</b>	<b>65%</b>	<b>88%</b>	<b>91%</b>	<b>89%</b>
5	TCEP	0%	-2%	0%	4%	4%	6%	9%	13%	13%	22%	29%	27%

Notes: shading represents >80% oxidation; DEET=*N,N*-diethyl-*meta*-toluamide; TCEP=tris-(2-chloroethyl)-phosphate

**Table 3.7. CCWRD TOxC Mitigation by Ozone (Filtered)**

Group	Contaminant	O <sub>3</sub> :TOC (mass) / H <sub>2</sub> O <sub>2</sub> :O <sub>3</sub> (molar)											
		0.25/0	0.25/0.5	0.25/1.0	0.5/0	0.5/0.5	0.5/1.0	1.0/0	1.0/0.5	1.0/1.0	1.5/0	1.5/0.5	1.5/1.0
1	Bisphenol A	70%	73%	85%	98%	98%	98%	98%	98%	98%	98%	98%	98%
	Carbamazepine	69%	67%	71%	99%	99%	99%	99%	99%	99%	99%	99%	99%
	Diclofenac	72%	70%	80%	97%	97%	97%	97%	97%	97%	97%	97%	97%
	Naproxen	67%	67%	72%	98%	98%	97%	98%	98%	97%	98%	98%	97%
	Sulfamethoxazole	64%	63%	74%	98%	98%	97%	99%	99%	99%	99%	99%	99%
	Triclosan	79%	81%	95%	97%	97%	97%	97%	97%	97%	97%	77%	97%
	Trimethoprim	70%	69%	75%	99%	99%	99%	99%	99%	99%	99%	99%	99%
	<b>Indicator</b>	<b>70%</b>	<b>70%</b>	<b>79%</b>	<b>98%</b>	<b>95%</b>	<b>98%</b>						
2	Atenolol	37%	35%	41%	97%	82%	79%	98%	98%	97%	98%	98%	93%
	Gemfibrozil	55%	49%	53%	99%	99%	99%	99%	99%	99%	99%	99%	97%
	<b>Indicator</b>	<b>46%</b>	<b>42%</b>	<b>47%</b>	<b>98%</b>	<b>91%</b>	<b>89%</b>	<b>99%</b>	<b>99%</b>	<b>98%</b>	<b>99%</b>	<b>99%</b>	<b>95%</b>
3	DEET	27%	29%	32%	63%	66%	66%	94%	96%	94%	99%	99%	90%
	Ibuprofen	32%	33%	37%	70%	71%	72%	97%	97%	96%	97%	97%	92%
	Phenytoin	40%	38%	43%	78%	77%	76%	98%	99%	98%	99%	99%	95%
	Primidone	21%	22%	28%	64%	63%	63%	95%	96%	93%	99%	99%	90%
	<b>Indicator</b>	<b>30%</b>	<b>31%</b>	<b>35%</b>	<b>69%</b>	<b>69%</b>	<b>69%</b>	<b>96%</b>	<b>97%</b>	<b>95%</b>	<b>99%</b>	<b>99%</b>	<b>92%</b>
4	Atrazine	13%	15%	16%	32%	35%	35%	72%	76%	74%	89%	92%	77%
	Meprobamate	19%	24%	22%	46%	48%	48%	80%	85%	85%	94%	97%	84%
	<b>Indicator</b>	<b>16%</b>	<b>20%</b>	<b>19%</b>	<b>39%</b>	<b>42%</b>	<b>42%</b>	<b>76%</b>	<b>81%</b>	<b>80%</b>	<b>92%</b>	<b>95%</b>	<b>81%</b>
5	TCEP	2%	0%	2%	2%	5%	6%	14%	19%	21%	26%	30%	29%

Notes: shading represents >80% oxidation; DEET=*N,N*-diethyl-*meta*-toluamide; TCEP=tris-(2-chloroethyl)-phosphate

**Table 3.8. CCWRD TOrC Mitigation by UV (Filtered)**

Group	Contaminant	UV Dose (mJ/cm <sup>2</sup> ) / H <sub>2</sub> O <sub>2</sub> Dose (mg/L)							
		23/0	23/10	45/0	45/10	225/0	225/10	680/0	680/10
1	Bisphenol A	-5%	N/A	-3%	23%	13%	48%	4%	84%
	Carbamazepine	-3%	N/A	-5%	2%	7%	32%	12%	66%
	Diclofenac	21%	N/A	39%	47%	93%	95%	98%	98%
	Naproxen	-19%	N/A	-6%	-5%	10%	34%	18%	74%
	Sulfamethoxazole	9%	N/A	10%	22%	43%	51%	86%	93%
	Triclosan	22%	N/A	13%	38%	88%	89%	97%	97%
	Trimethoprim	-8%	N/A	-10%	5%	3%	24%	-1%	55%
2	Atenolol	6%	N/A	12%	11%	11%	32%	16%	58%
	Gemfibrozil	6%	N/A	-13%	17%	14%	37%	16%	65%
3	DEET	-6%	N/A	-1%	6%	8%	23%	4%	49%
	Ibuprofen	-11%	N/A	-6%	3%	9%	30%	8%	62%
	Phenytoin	24%	N/A	19%	47%	46%	66%	70%	90%
	Primidone	-8%	N/A	-12%	-2%	5%	14%	-5%	36%
4	Atrazine	-1%	N/A	3%	-3%	30%	24%	53%	59%
	Meprobamate	4%	N/A	-1%	5%	5%	14%	1%	30%
5	TCEP	-6%	N/A	-4%	24%	10%	26%	1%	25%

Notes: N/A=sample not analyzed; shading represents >80% photolysis or oxidation; groupings refer to ozone and OH rate constants;

DEET=*N,N*-diethyl-*meta*-toluamide; TCEP=tris-(2-chloroethyl)-phosphate

### 3.1.6 Disinfection

Ambient secondary (before and after laboratory filtration) and finished effluent samples from CCWRD were assayed for total and fecal coliforms, MS2, and *Bacillus* spores. The ambient microbial water quality data are provided in Table 3.9. On the basis of the microbial prevalence in the filtered secondary effluent, it is apparent that the laboratory filtration with a nominal pore size of 0.5 µm was highly ineffective.

**Table 3.9. Ambient Microbial Water Quality Data for CCWRD**

Microbial Surrogate	Unfiltered Secondary Effluent	Filtered Secondary Effluent	Finished Effluent
Bacillus spores (CFU/100 mL)	3.0x10 <sup>3</sup>	1.0x10 <sup>3</sup>	30
Coliforms, fecal (MPN/100 mL)	4.4x10 <sup>3</sup>	2.9x10 <sup>2</sup>	<1
Coliforms, total (MPN/100 mL)	7.3x10 <sup>4</sup>	3.3x10 <sup>3</sup>	8
MS2 (PFU/mL)	<1	<1	<1

In order to illustrate a wide range of inactivation, the ozone and UV disinfection samples were spiked with relatively high numbers of the surrogate microbes, as indicated in Table 3.10. The *E. coli* spiking stocks contained approximately 10<sup>9</sup> to 10<sup>10</sup> MPN/100 mL (after purification), the MS2 stocks contained approximately 10<sup>9</sup> to 10<sup>10</sup> PFU/mL (after

purification), and the *B. subtilis* spore stocks contained approximately  $10^8$  to  $10^9$  CFU/100 mL (after heat-shock and purification). Although the stocks were purified, only 250  $\mu$ L of the appropriate spiking stock was added to 250 mL of sample to target a sufficient microbial load while limiting the artificial organic loading associated with the culture media.

**Table 3.10. Microbial Spiking Levels for CCWRD Bench-Scale Experiments**

Microbial Surrogate	Unfiltered Ozone Disinfection	Filtered Ozone Disinfection	Filtered UV Disinfection
<i>B. subtilis</i> spores (CFU/100 mL)	$2.5 \times 10^5$	$2.6 \times 10^5$	$2.2 \times 10^5$
<i>E. coli</i> (MPN/100 mL)	$5.4 \times 10^7$	$5.4 \times 10^7$	$1.6 \times 10^7$
MS2 (PFU/mL)	$3.1 \times 10^7$	$2.0 \times 10^7$	$9.6 \times 10^7$

Note: UV-ultraviolet

Figure 3.7 illustrates the inactivation of spiked *E. coli* during the bench-scale ozone experiments. The disinfection results are reported based on log inactivation, which simplifies order-of-magnitude changes in microbial numbers. This nomenclature replaces percent inactivation (e.g., 90%, 99%, 99.9%) with its base-10 log equivalent (e.g., 1-log, 2-log, 3-log). The solid and dashed lines near the top of the figure represent the limits of inactivation based on the spiking levels in the filtered and unfiltered samples. In addition, there were four samples (Unfiltered 0.5/0.5, Unfiltered 0.5/1.0, Filtered 1.0/1.0, and Filtered 1.5/1.0) that could not be quantified because they were not sufficiently diluted during the assay period. The data points for these samples, which are indicated by arrows in the figure, represent the maximum level of inactivation based on the most diluted sample that was assayed. Therefore, the actual level of inactivation was less than that indicated by the data points.

In general, the filtered versus unfiltered comparison proved to be inconclusive because of the inherent variability in the data sets. On average, the addition of  $H_2O_2$  alone achieved less than 0.3-log inactivation, but when combined with ozonation, the addition of  $H_2O_2$  consistently hindered *E. coli* inactivation. This indicates that the increased reactivity of  $\bullet OH$  combined with the scavenging effects of EfOM were generally detrimental to the disinfection process. Although molecular ozone also decomposes into  $\bullet OH$  over time, the initial ozone exposure was critical for improving disinfection efficacy. The average log-inactivation values for each treatment condition after combining the unfiltered and filtered data sets are provided in Table 3.12.

Figure 3.8 illustrates the inactivation of spiked MS2 during the bench-scale ozone experiments. Similar to *E. coli*, there was no noticeable difference between the filtered and unfiltered samples, the addition of  $H_2O_2$  alone achieved less than 0.3-log inactivation, and when combined with ozonation, the addition of  $H_2O_2$  consistently hindered MS2 inactivation. To meet CDPH Title 22 requirements, an  $O_3$ :TOC ratio  $>1.0$  appears to be sufficient for 5-log MS2 inactivation, regardless of  $H_2O_2$  dose. With no  $H_2O_2$  addition, an  $O_3$ :TOC ratio greater than 1.0 is even sufficient for the 6.5-log alternative treatment goal. However, none of the  $H_2O_2$  treatment conditions satisfied the 6.5-log alternative for this particular set of samples. The average log-inactivation values for each treatment condition (combined unfiltered and filtered data) are provided in Table 3.13.

Figure 3.9 illustrates the inactivation of spiked *B. subtilis* spores during the bench-scale ozone experiments. *B. subtilis* proved to be an interesting test microbe because of its unique dose–response relationship for ozone and •OH. As expected, the spores proved to be extremely resistant to oxidation and only experienced significant inactivation for an O<sub>3</sub>:TOC ratio of 1.5 with no H<sub>2</sub>O<sub>2</sub> addition. In other words, a sufficient ozone CT had to be administered before ozone and •OH were able to penetrate the spore coat and inactivate the bacteria. This is consistent with the disinfection “lag phase” characteristic of many spore-forming microbes. Although there appears to be a significant difference between the unfiltered and filtered samples at an O<sub>3</sub>:TOC ratio of 1.5 (no H<sub>2</sub>O<sub>2</sub> addition), this is likely attributable to inherent variability rather than the effect of filtration. Furthermore, oxidation with •OH alone is extremely ineffective for spore inactivation, presumably because of the highly reactive nature of •OH and competition with EfOM. The average log-inactivation values for each treatment condition (combined unfiltered and filtered data) are provided in Table 3.14.

Finally, Figure 3.10 provides a summary of the ozone disinfection data for the three surrogate microbes as they pertain to the CT framework. Figure 3.10A illustrates the dose–response relationships for the filtered and unfiltered samples (combined) with no H<sub>2</sub>O<sub>2</sub> addition. Figure 3.10B illustrates the dose–response relationships for the filtered and unfiltered samples (combined) with H<sub>2</sub>O<sub>2</sub>:O<sub>3</sub> ratios of 0.5 and 1.0 (also combined). According to these data, the CT framework is not always appropriate because substantial levels of inactivation can be achieved when the apparent ozone CT is zero. However, the level of inactivation for vegetative bacteria and viruses is generally less than that observed when an ozone residual is present, and no inactivation of spore-forming bacteria can be achieved without a measurable CT.

Table 3.11 summarizes the efficacy of UV and UV/H<sub>2</sub>O<sub>2</sub> for the inactivation of the three surrogate microbes. The efficacy of UV-based disinfection differs dramatically from ozone-based disinfection because UV is highly effective against both vegetative and spore-forming bacteria, whereas some viruses demonstrate resistance. Even 45 mJ/cm<sup>2</sup> was sufficient to reach the limits of inactivation for *E. coli* and *Bacillus* spores, regardless of H<sub>2</sub>O<sub>2</sub> addition. On the other hand, MS2 inactivation occurred more slowly and only reached the limit of inactivation for UV doses of 225 and 680 mJ/cm<sup>2</sup> with 10 mg/L of H<sub>2</sub>O<sub>2</sub>. Under advanced oxidation dosing conditions (i.e., 225 or 680 mJ/cm<sup>2</sup> with 10 mg/L of H<sub>2</sub>O<sub>2</sub>), one can expect substantial inactivation of all microbes present in wastewater. This constitutes a significant advantage for UV-based treatment over the ozone-based alternatives.

Although the addition of H<sub>2</sub>O<sub>2</sub> appeared to be beneficial for the inactivation of the three microbes, the demonstrated resistance of *Bacillus* spores to oxidation indicates that the slightly higher level of inactivation with UV/H<sub>2</sub>O<sub>2</sub> was likely attributable to experimental variability. Because the incident germicidal light is only marginally impacted by the addition of H<sub>2</sub>O<sub>2</sub>, the higher inactivation levels for *E. coli* and MS2 with UV/H<sub>2</sub>O<sub>2</sub> are likely significant. In contrast to ozone/H<sub>2</sub>O<sub>2</sub>, where the H<sub>2</sub>O<sub>2</sub> immediately quenches the ozone residual, germicidal UV and photo-generated •OH are more synergistic in nature.

**Table 3.11. Summary of UV Inactivation in the CCWRD Secondary Effluent**

UV Dose (mJ/cm <sup>2</sup> )	<i>E. coli</i>		MS2		<i>Bacillus</i> spore	
	UV	UV/H <sub>2</sub> O <sub>2</sub> **	UV	UV/H <sub>2</sub> O <sub>2</sub> **	UV	UV/H <sub>2</sub> O <sub>2</sub> **
23	6.0	6.7	1.7	2.6	2.6	2.8
45	>7.2*	>7.2*	3.0	4.0	>3.3*	>3.3*
225	>7.2*	>7.2*	7.0	>8.0*	>3.3*	>3.3*
680	>7.2*	>7.2*	7.1	>8.0*	>3.3*	>3.3*

Notes: \*=limit of inactivation based on spiking level; \*\*=H<sub>2</sub>O<sub>2</sub>=10 mg/L; UV=ultraviolet

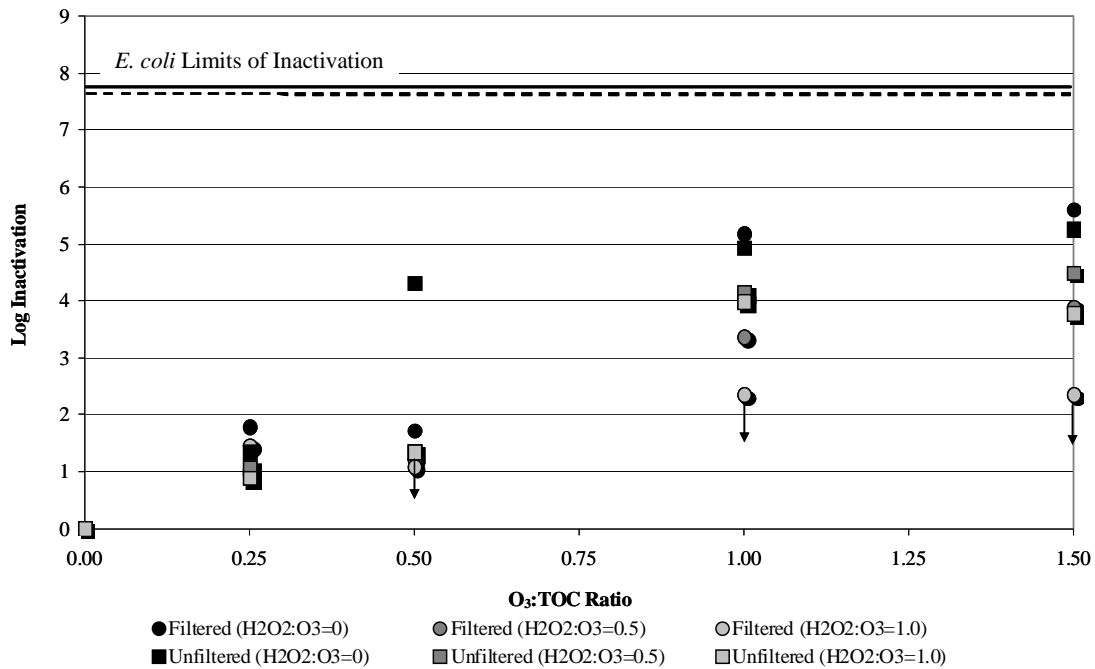


**Figure 3.7. Inactivation of spiked *E. coli* in the CCWRD secondary effluent.**

**Table 3.12. Summary of *E. coli* Inactivation in the CCWRD Secondary Effluent**

O <sub>3</sub> :TOC Ratio	H <sub>2</sub> O <sub>2</sub> :O <sub>3</sub> =0	H <sub>2</sub> O <sub>2</sub> :O <sub>3</sub> =0.5	H <sub>2</sub> O <sub>2</sub> :O <sub>3</sub> =1.0
0.25	1.6±0.3*	1.1±0.0	1.2±0.4
0.5	3.0±1.8	1.3±0.1**	1.2±0.2**
1.0	5.1±0.2	3.8±0.5	3.2±1.2**
1.5	5.4±0.2	4.2±0.4	3.1±1.0*

Notes: \*=average log inactivation ± span of filtered/unfiltered samples; \*\*=insufficient dilutions for one sample, so inactivation is slightly overestimated

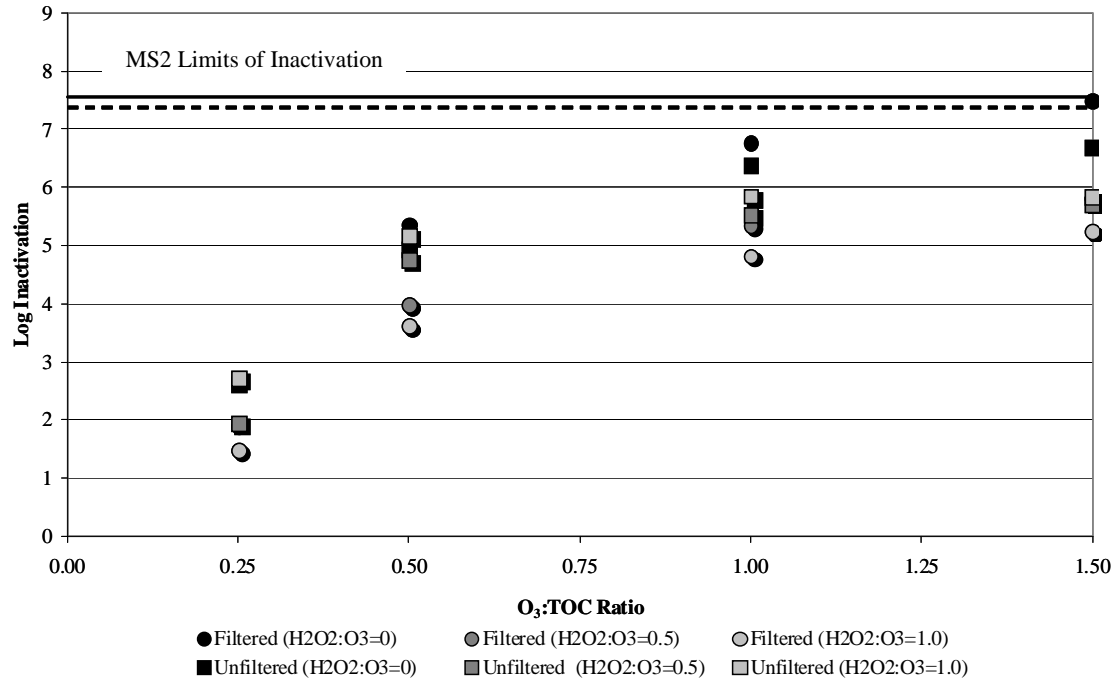
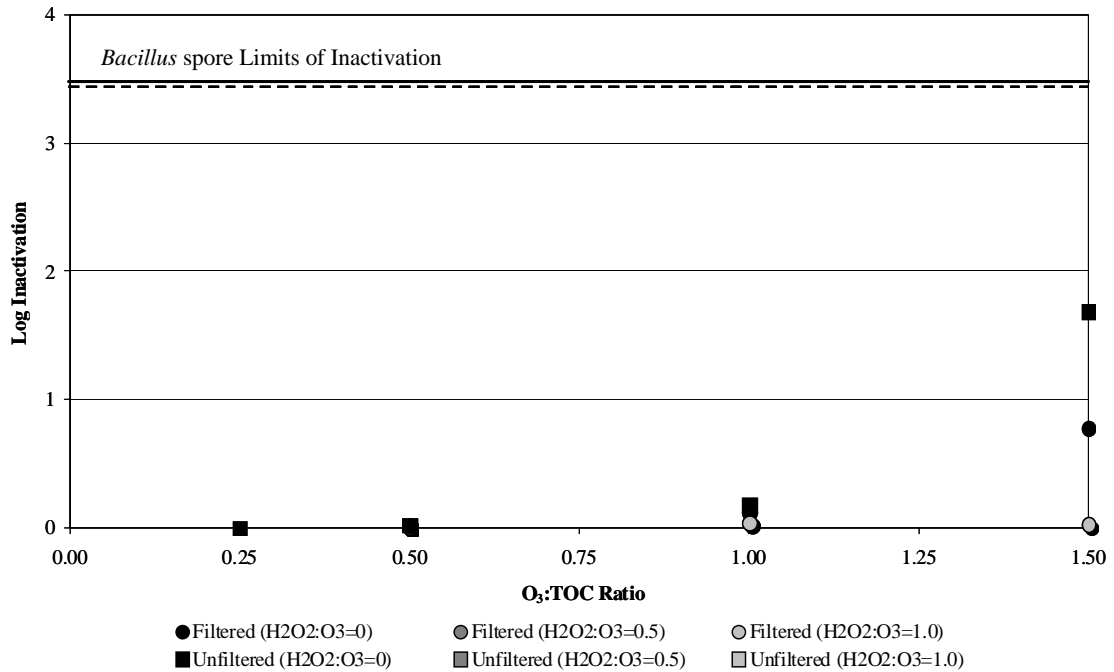


Figure 3.8. Inactivation of spiked MS2 in the CCWRD secondary effluent.

Table 3.13. Summary of MS2 Inactivation in the CCWRD Secondary Effluent

O <sub>3</sub> :TOC Ratio	H <sub>2</sub> O <sub>2</sub> :O <sub>3</sub> =0	H <sub>2</sub> O <sub>2</sub> :O <sub>3</sub> =0.5	H <sub>2</sub> O <sub>2</sub> :O <sub>3</sub> =1.0
0.25	2.2±0.5*	1.9±N/A**	2.1±0.9
0.5	5.1±0.3	4.4±0.5	4.4±1.1
1.0	6.6±0.3	5.4±0.1	5.3±0.7
1.5	7.1±0.6	5.8±0.1	5.5±0.4

Notes: \*=average log inactivation ± span of filtered/unfiltered samples; \*\*=N/A: filtered sample not collected, so value only represents unfiltered sample



**Figure 3.9. Inactivation of spiked *Bacillus* spores in the CCWRD secondary effluent.**

**Table 3.14. Summary of *Bacillus* Spore Inactivation in the CCWRD Secondary Effluent**

O <sub>3</sub> :TOC Ratio	H <sub>2</sub> O <sub>2</sub> :O <sub>3</sub> =0	H <sub>2</sub> O <sub>2</sub> :O <sub>3</sub> =0.5	H <sub>2</sub> O <sub>2</sub> :O <sub>3</sub> =1.0
0.25	0.0±0.0*	0.0±0.0	0.0±0.0
0.5	0.0±0.0	0.0±0.0	0.0±0.0
1.0	0.1±0.0	0.0±0.0	0.0±0.0
1.5	1.2±0.6	0.0±0.0	0.0±0.0

Note: \*=average log inactivation ± span of filtered/unfiltered samples

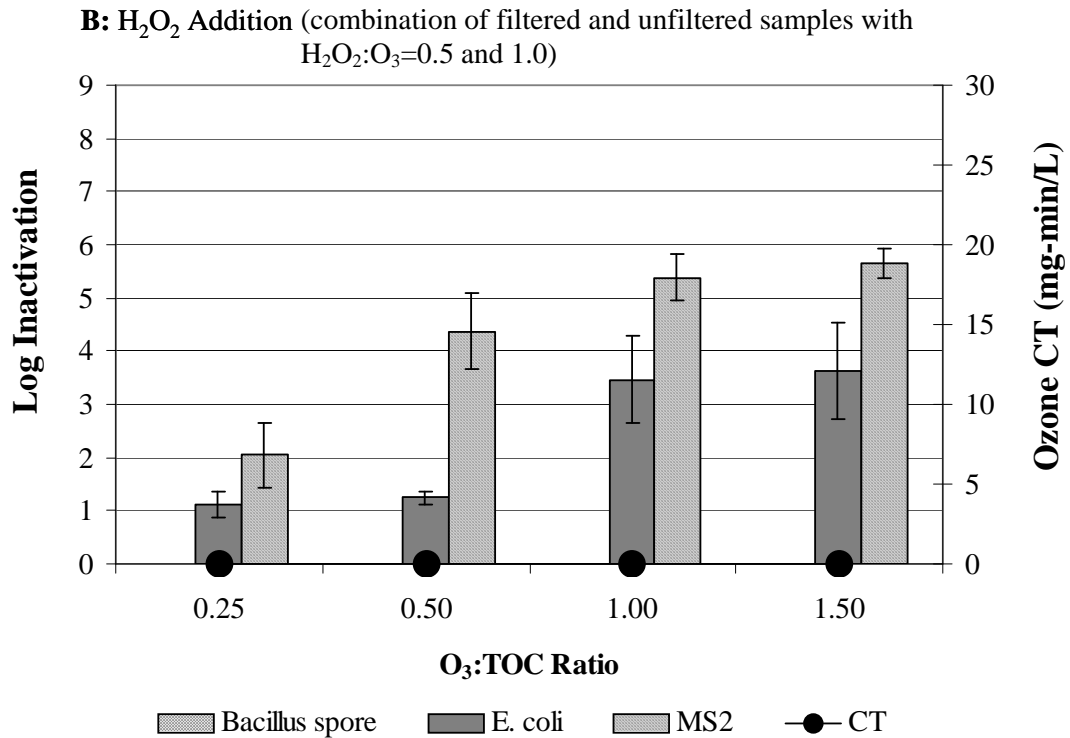
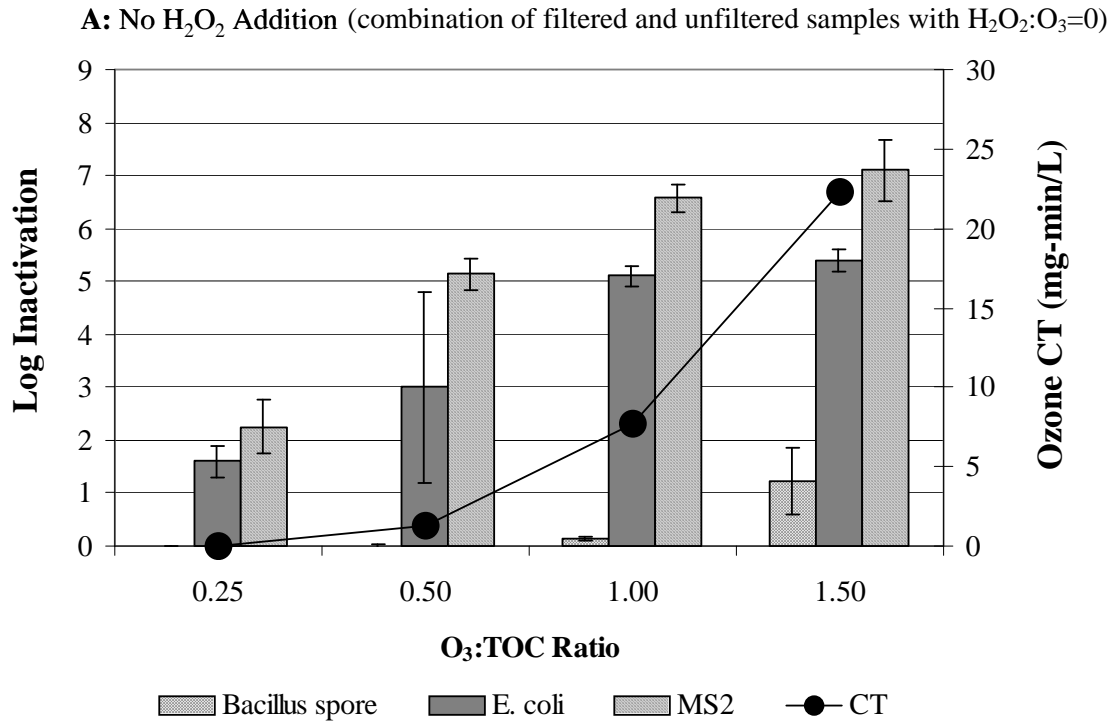


**Figure 3.10. Significance of CT for disinfection in the CCWRD secondary effluent.**

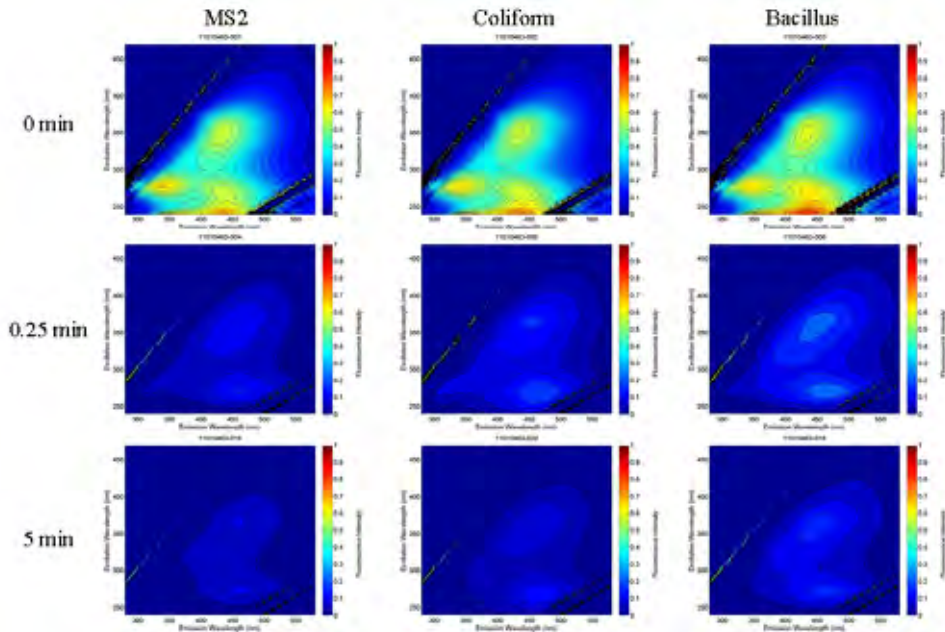


**Figure 3.11. Excitation emission matrices during the reaction time experiment.**

A separate set of experiments was performed to evaluate the significance of reaction time and TSS on disinfection efficacy. The literature suggests that the inactivation of vegetative bacteria and viruses occurs rapidly at low CT values; however, this is not reflected in the reported CT values in Figure 3.2 because they do not necessarily represent the actual ozone exposure required to achieve the reported levels of inactivation. Those CT values correspond to the actual ozone exposure achieved in each sample, whereas microbial inactivation may have occurred much faster. In the “reaction time” experiments, the same ozone doses were applied to the samples, but the samples were quenched after different exposure times. Particularly for the highest applied ozone dose ( $O_3:TOC=1.5$ ), a dissolved ozone residual would have been present for longer periods of time without the artificial quenching with sodium thiosulfate. Separate samples were spiked with MS2 and *Bacillus* spores, but the coliform experiments were based on indigenous microbes.

As demonstrated by the data in Table 3.15, the required CT values for coliform and MS2 inactivation are much lower than those actually achieved by an  $O_3:TOC$  value of 1.0 (~7.6 mg/min/L). Despite the fact that the dissolved ozone residual decays over 5 minutes, nearly all of the inactivation occurs in the first 15 seconds of the experiment. Changes in the bulk organic matter occur over a similar time frame, as indicated in Figure 3.11, which also indicates that the purification protocols for spiked MS2 and *Bacillus* spores are effective in reducing artificial impacts from the culture media.

For *Bacillus* spores, however, the entire decay period (CT of ~20 mg/min/L) is necessary to achieve the final level of inactivation for that particular dosing condition. Even an  $O_3:TOC$  ratio of 1.0 was insufficient to achieve a significant level of inactivation. Extended ozone exposure is necessary to allow time for the oxidant to diffuse across the spore coat and sufficiently damage the bacterium. Therefore, vegetative bacteria and viruses require minimal exposure times and CT values, but disinfectant-resistant microbes, including *Bacillus* spores, *Cryptosporidium* oocysts, and *Giardia* cysts, require much higher CT values for similar levels of inactivation.

**Table 3.15. Summary of Reaction Time Experiment**

Time (min)	Total Coliform <sup>a</sup>		Fecal Coliform <sup>a</sup>		MS2 <sup>a</sup>		<i>Bacillus</i> Spores <sup>b</sup>	
	MPN/100 mL	Log Inactivation	MPN/100 mL	Log Inactivation	PFU/mL	Log Inactivation	CFU/mL	Log Inactivation
0	26,130	0.0	5210	0	490,000	0	1940	0.0
0.25	2282	1.1	42	2.1	<1	>5.7	1257	0.2
0.5	1421	1.3	43	2.1	<1	>5.7	1030	0.3
1	696	1.6	120	1.6	<1	>5.7	510	0.6
2	943	1.4	77	1.8	<1	>5.7	143	1.1
5	596	1.6	163	1.5	<1	>5.7	38	1.7
20	908	1.5	35	2.2	<1	>5.7	32	1.8

Notes: <sup>a</sup>O<sub>3</sub>=5.1 mg/L → O<sub>3</sub>:TOC=1.0; <sup>b</sup>O<sub>3</sub>=6.7 mg/L → O<sub>3</sub>:TOC=1.5

**Table 3.16. Average Log Inactivation During TSS Experiment**

Microbe	Treatment	SRT=6 days	SRT=10 Days	SRT=40 Days
Coliform, fecal	O <sub>3</sub>	1.8±0.2	1.7±0.2	3.0±0.2
	O <sub>3</sub> /H <sub>2</sub> O <sub>2</sub>	1.4±0.1	1.3±0.8	3.1±0.2
Coliform, total	O <sub>3</sub>	1.9±0.2	1.4±0.1	2.9±0.5
	O <sub>3</sub> /H <sub>2</sub> O <sub>2</sub>	1.6±0.4	1.2±0.3	2.9±0.5
MS2	O <sub>3</sub>	5.9±0.1	5.0±0.1	5.0±0.1
	O <sub>3</sub> /H <sub>2</sub> O <sub>2</sub>	5.4±0.1	5.3±0.1	4.9±0.2

Note: ±1 standard deviation based on three replicate samples for each testing condition

Another experiment was performed to evaluate the impact of SRT on particle-associated microbes and ozone disinfection. At the time of the experiment, CCWRD was operating multiple SRTs in parallel activated sludge basins. Under normal conditions, CCWRD would operate each of the independent trains with a similar SRT optimized for biochemical oxygen demand (BOD) removal, nitrification, and biological phosphorus removal; however, it was operating with a wide range of SRTs to evaluate the effects of various operational parameters on TO<sub>r</sub>C mitigation during secondary treatment. For the “TSS” experiment, secondary effluent from the clarifiers associated with SRTs of 6, 10, and 40 days was collected and tested under various conditions. A summary of the data is provided in Table 3.16, and the complete data sets are provided in Table 3.17 and Table 3.18.

The TOC values of the three samples were initially assumed to be constant and similar to samples from past experiments. Therefore, a single ozone dose (3 mg/L) was applied to all of the samples; however, the subsequent TOC analysis indicated that the 40-day SRT was characterized by a lower TOC value (4.7 mg/L) than the 6- and 10-day SRTs (5.8 and 5.4 mg/L). After the dilution effect from the ozone, the O<sub>3</sub>:TOC ratios actually ranged from 0.6 to 0.8 for SRTs of 6 and 40 days, rather than the target value of 0.5. As expected, the TSS values for the three samples ranged from 9 to 40 mg/L for SRTs of 6 and 40 days.

The results of the TSS experiment appear to be inconclusive regarding the effects of SRT on particle-associated microbes and disinfection. For the indigenous total and fecal coliforms, the level of inactivation decreased as the SRT increased from 6 to 10 days, but the level of inactivation for the 40-day SRT was significantly higher. There are several possible explanations for this observation. Despite the higher TSS value for the 40-day SRT, this sample was actually a higher quality secondary effluent with regard to bulk organic matter. This is supported by the lower TOC value and the fact that the 40-day SRT had the least intense fluorescence fingerprint (Figure 3.12). Therefore, a constant ozone dose might be more effective than it would be for the lower quality 6-day SRT sample; however, this does not explain the reduction in performance for the 10-day SRT.

One other possibility is the higher total and fecal coliform counts in the ambient 40-day SRT sample, which were nearly an order of magnitude higher than both the 6- and 10-day SRTs. If a second-order reaction rate is assumed, this might lead to a greater level of inactivation for this sample. Again, this does not account for the difference in inactivation between the 6- and 10-day SRTs, although the difference in ambient coliform levels for these two samples was not as extreme. The independent samples for each SRT demonstrated similar levels of inactivation, as indicated by the relatively low standard deviations for most of the dosing conditions.

In contrast to the coliform data, the spiked MS2 samples demonstrated a lower level of inactivation for the 10- and 40-day SRTs. As with the coliform samples, this might partially be explained by the initial MS2 levels in each sample. The 6-day SRT also demonstrated the best performance despite its lower water quality and O<sub>3</sub>:TOC ratio. Although the MS2 data seem to indicate that suspended solids negatively impact disinfection, there were too many conflicting variables and results between the two experiments to draw any definitive conclusions. As a result, there is insufficient evidence to suggest that SRT has a consistent effect on disinfection efficacy, but there are certainly effects on a variety of water quality parameters.

**Table 3.17. TSS Experiment for Indigenous Total and Fecal Coliforms (MPN/100 mL)**

SRT (days)	TSS (mg/L)	TOC (mg/L)	Diluted TOC (mg/L)	O <sub>3</sub> (mg/L)	O <sub>3</sub> :TOC	H <sub>2</sub> O <sub>2</sub> :O <sub>3</sub>	Total Coliforms	Log Inactivation	Fecal Coliforms	Log Inactivation
6	9	5.8	4.9	Ambient			10,190	N/A	970	N/A
				3	0.6	0	86	2.1	<10	>2.0
							109	2.0	20	1.7
							249	1.6	20	1.7
				0.5	145	1.9	31	1.5		
					475	1.8	41	1.4		
					908	1.1	41	1.4		
10	10	5.4	4.5	Ambient			15,000	N/A	2620	N/A
				3	0.7	0	435	1.5	62	1.6
							697	1.3	75	1.5
							637	1.4	31	1.9
				0.5	1046	1.2	41	1.8		
					374	1.6	63	1.6		
					1725	0.9	1095	0.4		
40	40	4.7	3.9	Ambient			120,330	N/A	14,390	N/A
				3	0.8	0	203	2.8	20	2.9
							323	2.6	20	2.9
							41	3.5	<10	>3.2
				0.5	591	2.3	<10	>3.2		
					75	3.2	20	2.9		
					109	3.0	<10	>3.2		

Notes: MPN=most probable number; N/A=data not available; SRT=solids retention time; TOC=total organic carbon; TSS=total suspended solids

**Table 3.18. TSS Experiment for Spiked MS2 (PFU/mL)**

SRT (days)	TSS (mg/L)	TOC (mg/L)	Diluted TOC (mg/L)	O <sub>3</sub> (mg/L)	O <sub>3</sub> :TOC	H <sub>2</sub> O <sub>2</sub> :O <sub>3</sub>	MS2	Log Inactivation
6	9	5.8	4.9	Spike			9,500,000	N/A
				3	0.6	0	14	5.8
							10	6.0
							12	5.9
				0.5	39	5.4		
					36	5.4		
					31	5.5		
10	10	5.4	4.5	Spike			6,400,000	N/A
				3	0.7	0	55	5.1
							76	4.9
							72	5.0
				0.5	30	5.3		
					40	5.2		
					24	5.4		
40	40	4.7	3.9	Spike			5,866,667	N/A
				3	0.8	0	66	5.0
							61	5.0
							42	5.1
				0.5	95	4.8		
					83	4.9		
					42	5.2		

Notes: N/A=data not available; SRT=solids retention time; TOC=total organic carbon; TSS=total suspended solids

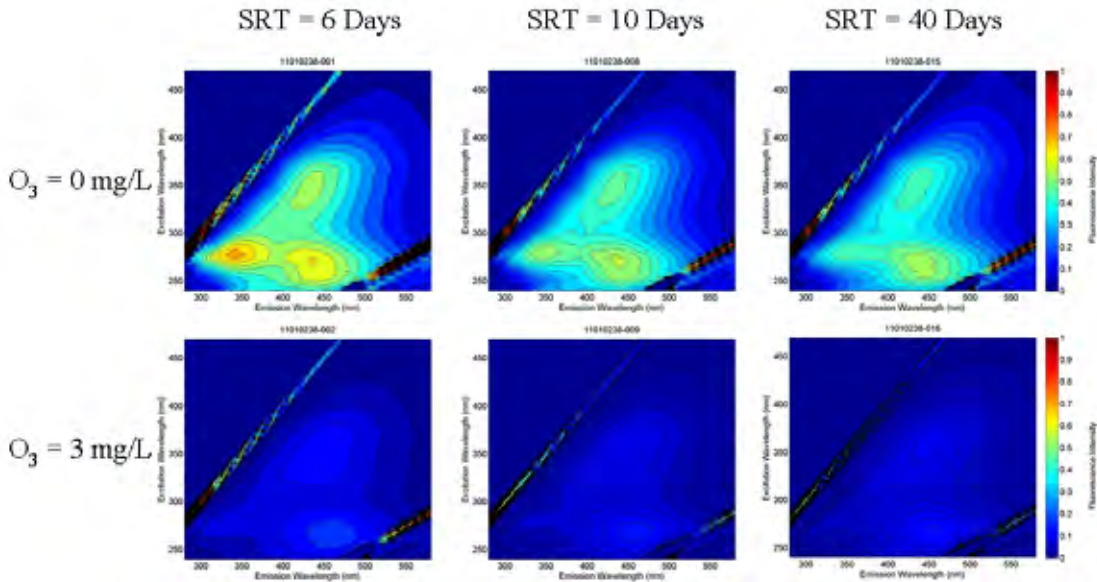


**Figure 3.12. Excitation emission matrices for the TSS coliform experiments.**

### 3.1.7 Organic Characterization

The full-spectrum scans in Figures 3.13 and 3.14, without (A) and with (B) H<sub>2</sub>O<sub>2</sub> addition, indicate that the absorbance profiles around 254 nm for the filtered CCWRD secondary effluent generally provide the greatest resolution between treatments. The unfiltered absorbance spectra demonstrated similar treatment profiles. Because of the limited efficacy of UV photolysis (Figure 3.14A), there is little resolution regardless of wavelength, although UV/H<sub>2</sub>O<sub>2</sub> achieved slight improvements over UV alone. Figure 3.15 focuses on the change in UV<sub>254</sub> absorbance with ozone, ozone/H<sub>2</sub>O<sub>2</sub>, UV, and UV/H<sub>2</sub>O<sub>2</sub> based on its suitability for future analyses and correlations. Regarding ozonation, reductions in UV<sub>254</sub> absorbance were hindered by cartridge filtration, which was likely attributable to the small amount of organic leaching, and the addition of H<sub>2</sub>O<sub>2</sub>. As would be expected with the synergistic aspect of the UV AOP, the addition of H<sub>2</sub>O<sub>2</sub> achieved a lower UV<sub>254</sub> absorbance.

As described earlier, 3D excitation emission matrices were developed for the unfiltered and filtered secondary effluent, the various treatment conditions, and the finished effluent from CCWRD. Figure 3.16 illustrates the ambient and finished effluent samples and also provides the total and regional fluorescence intensities based on arbitrary fluorescence units. The organic leaching from the cartridge filter is apparent from the higher fluorescence intensity in the filtered ambient sample. The reduced fluorescence in the finished effluent sample is due to the tertiary filtration with alum addition and UV disinfection applied at the full-scale wastewater treatment plant. Figure 3.17 provides a qualitative illustration of treatment efficacy after ozone- and UV-based oxidation. Similar to UV absorbance, UV photolysis and UV/H<sub>2</sub>O<sub>2</sub> are not nearly as effective in reducing fluorescence intensity as ozone-based oxidation.

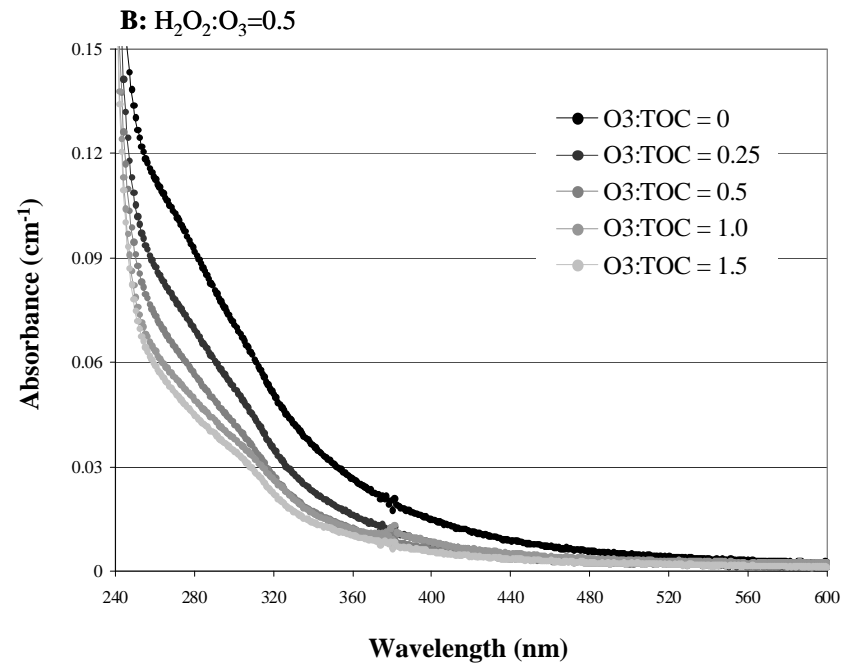
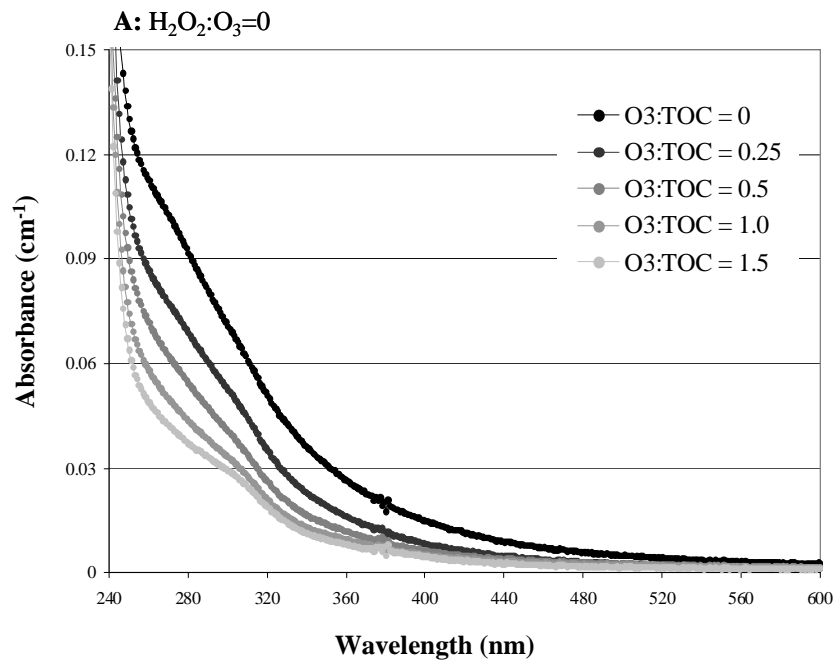


Figure 3.13. CCWRD absorbance spectra after ozonation.

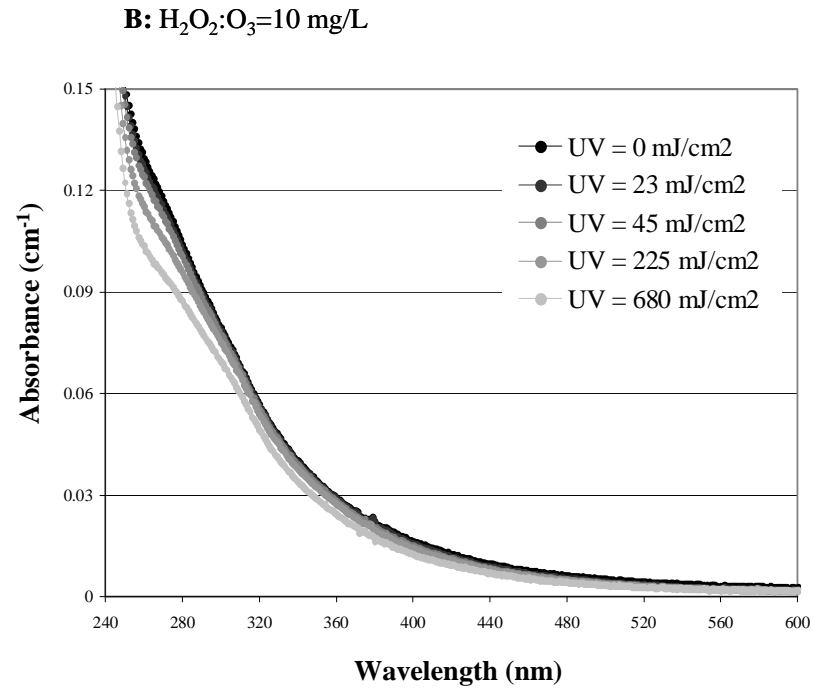
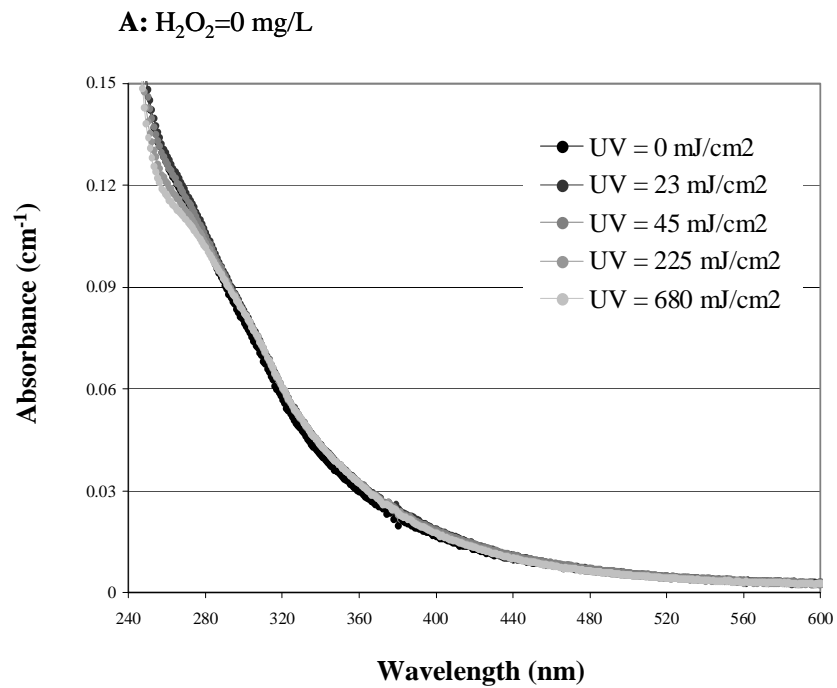


Figure 3.14. CCWRD absorbance spectra after UV and UV/H<sub>2</sub>O<sub>2</sub>.

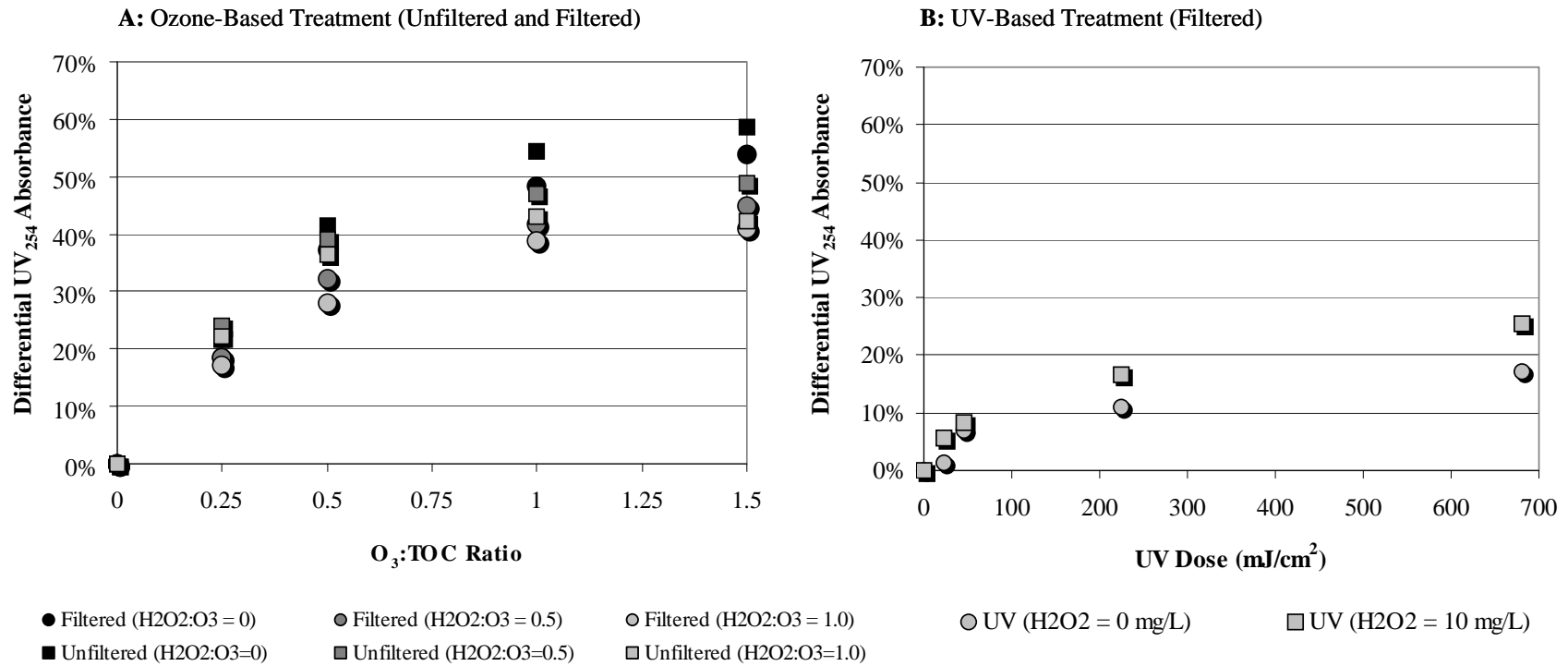


Figure 3.15. Differential UV<sub>254</sub> absorbance in the CCWRD secondary effluent.

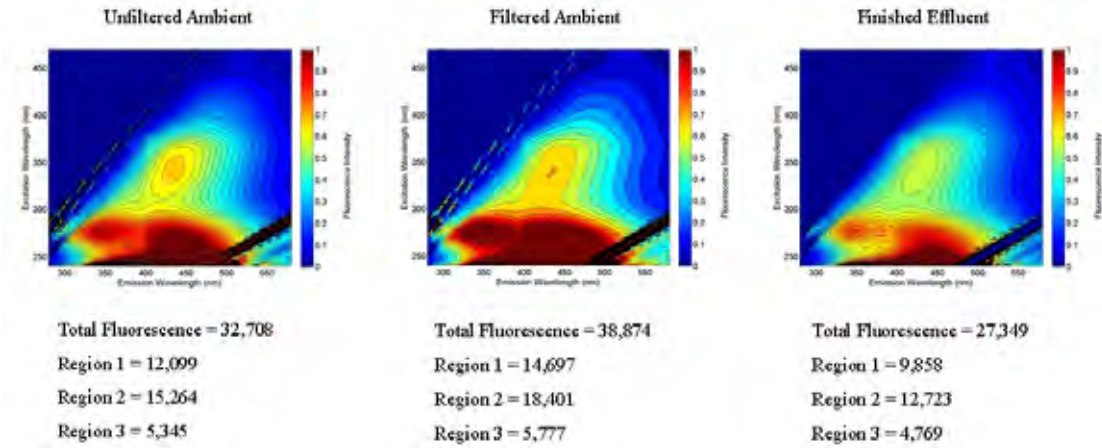


Figure 3.16. 3D EEMs for ambient samples from CCWRD.

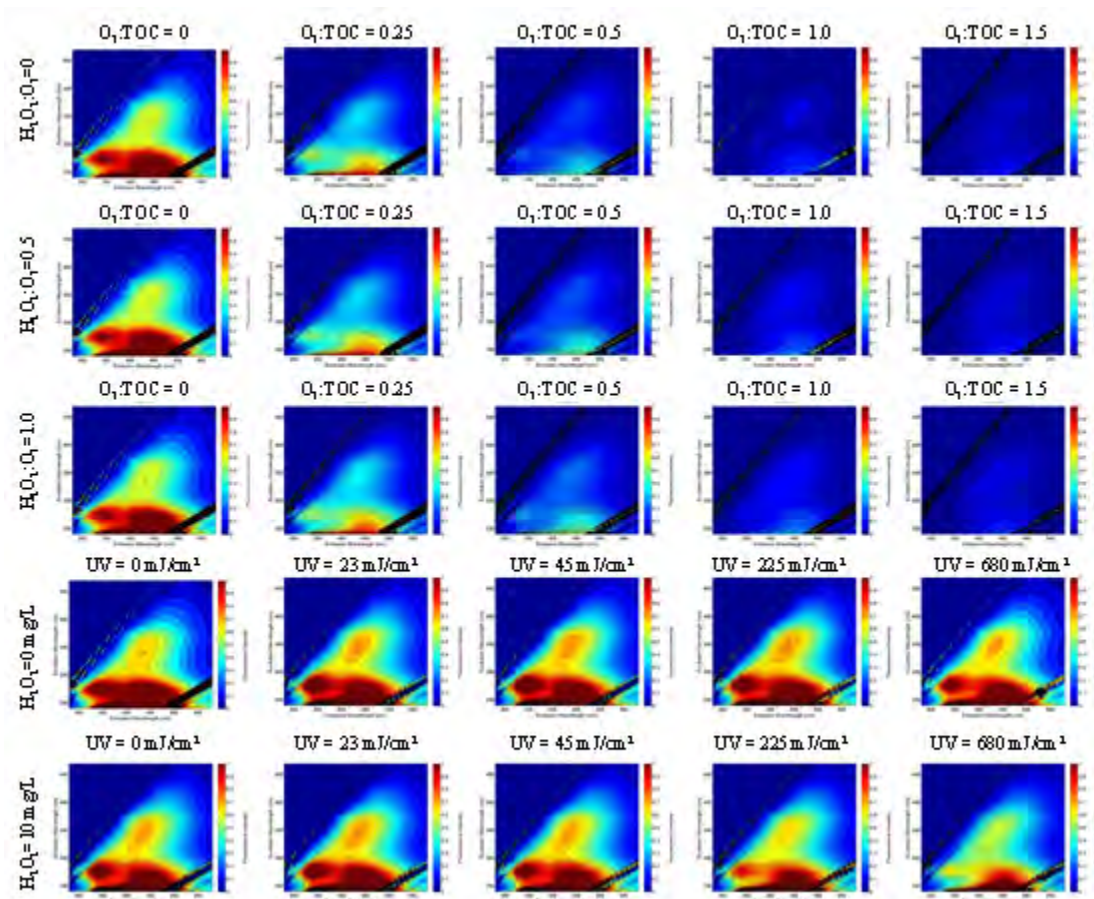


Figure 3.17. 3D EEMs after treatment for the filtered CCWRD secondary effluent.

In addition to the qualitative comparison between treatment conditions, 3D EEMs can be deconvoluted to identify quantitative changes in fluorescence intensity. These analyses include changes in fluorescence spectra, TF, FI, and TI. Figures 3.18 and 3.19 illustrate the fluorescence profiles at an excitation wavelength of 254 nm after ozonation and UV/H<sub>2</sub>O<sub>2</sub>. Because the addition of H<sub>2</sub>O<sub>2</sub> did not have a significant impact on ozone efficacy, and UV photolysis provided limited reductions in fluorescence intensity (see Figure 3.17), these fluorescence profiles are not shown. Fluorescence profiles are similar to absorbance spectra in that they demonstrate relatively consistent changes after oxidation, which is promising for their use as a surrogate for process efficacy. In order to develop process models, however, the optimal combination of excitation and emission wavelengths must be identified, which will be described later.

As shown in Figures 3.18 and 3.19, the maximum fluorescence intensity in secondary effluent EEMs often occurs near an excitation wavelength of 254 nm and an emission wavelength of 450 nm. Based on this observation, the TI was defined as the change in fluorescence intensity between ambient and treated samples at this particular point (i.e.,  $Ex_{254}Em_{450,T}/Ex_{254}Em_{450,A}$ ). The FI was defined earlier as the ratio of the emissions within a single EEM at 450 nm and 500 nm when excited by a wavelength of 370 nm (i.e.,  $Ex_{370}Em_{450}/Ex_{370}Em_{500}$ ). These indices are provided in Table 3.19.

Regarding ozonation, the FI values decreased consistently for O<sub>3</sub>:TOC ratios of 0.25 and 0.5 but started to stabilize with higher ozone doses. In other words, the organic matter associated with emissions at 450 nm experienced more rapid transformation with low ozone doses than the organic matter associated with emissions at 500 nm. Further transformation at higher ozone doses occurred at similar relative rates, thereby stabilizing the FI. These relative changes are illustrated in Figure 3.20, and similar trends are apparent in Figure 3.21, which illustrates the changes in total and regional fluorescence intensities (not to be confused with fluorescence *indices* [FI]) after ozonation. In Figure 3.21, the regional fluorescence intensities associated with soluble microbial products (Region I) and fulvic acids (Region II) decreased at a faster rate than those of the humic acids (Region III). The TI, which measures the extent of organic transformation, reached as low as 0.06 for the highest O<sub>3</sub>:TOC ratio, thereby indicating that 94% of the original fluorescence had been eliminated. In general, there was no consistent difference between the unfiltered and filtered wastewater, although the addition of H<sub>2</sub>O<sub>2</sub> hindered the ozone process slightly. Because of the limited reduction in fluorescence with UV and UV/H<sub>2</sub>O<sub>2</sub>, the corresponding FI and TI values did not change significantly. The corresponding changes in total and regional fluorescence intensities for UV and UV/H<sub>2</sub>O<sub>2</sub> are illustrated in Figure 3.22.

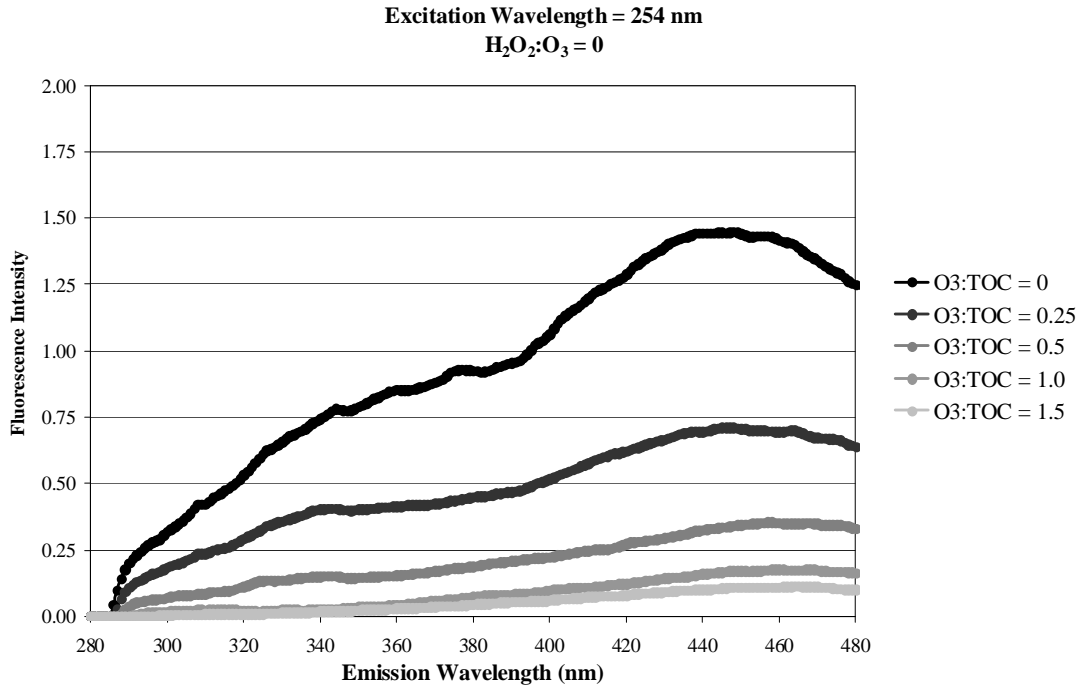


Figure 3.18. CCWRD fluorescence profiles (Ex<sub>254</sub>) after ozonation.

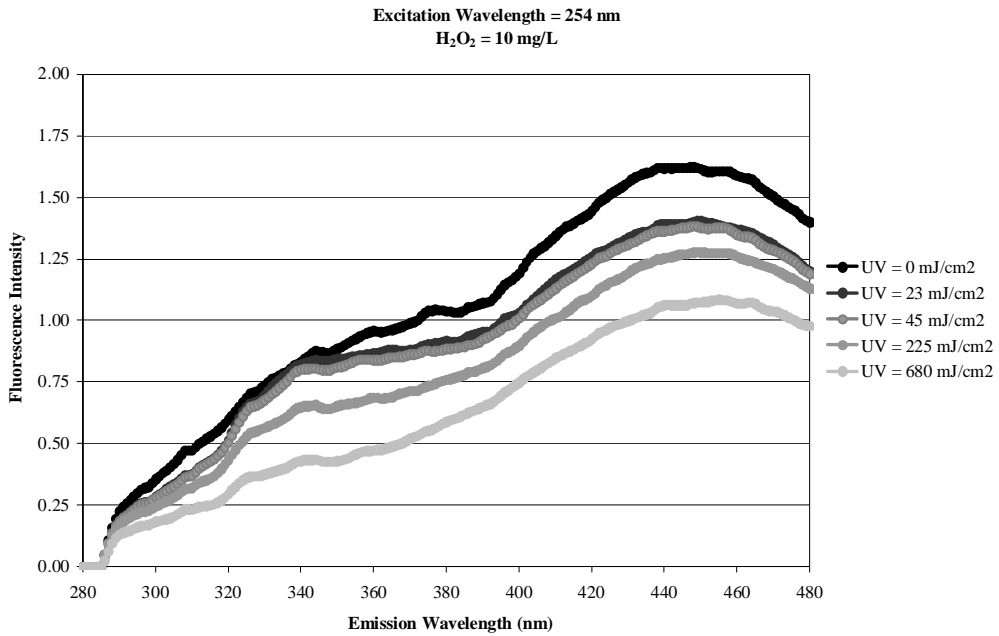


Figure 3.19. CCWRD fluorescence profiles (Ex<sub>254</sub>) after UV/H<sub>2</sub>O<sub>2</sub>.

**Table 3.19. FI and TI Values for the CCWRD Secondary Effluent**

<b>Unfiltered Ozone Exposure</b>						
<b>O<sub>3</sub>:TOC</b>	<b>H<sub>2</sub>O<sub>2</sub>:O<sub>3</sub>=0</b>		<b>H<sub>2</sub>O<sub>2</sub>:O<sub>3</sub>=0.5</b>		<b>H<sub>2</sub>O<sub>2</sub>:O<sub>3</sub>=1.0</b>	
	<b>FI</b>	<b>TI</b>	<b>FI</b>	<b>TI</b>	<b>FI</b>	<b>TI</b>
0	1.41	1.00	1.41	1.00	1.41	1.00
0.25	1.34	0.56	1.36	0.62	1.37	0.62
0.5	1.25	0.29	1.30	0.30	1.33	0.33
1.0	1.25	0.13	1.31	0.16	1.32	0.17
1.5	1.25	0.06	1.30	0.10	1.32	0.12

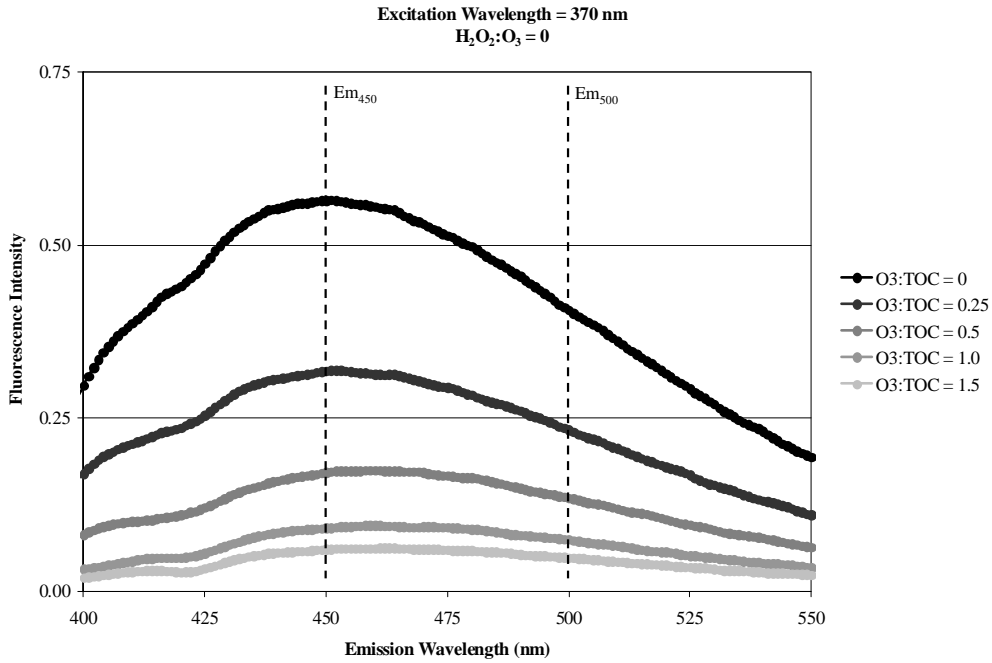
  

<b>Filtered Ozone Exposure</b>						
<b>O<sub>3</sub>:TOC</b>	<b>H<sub>2</sub>O<sub>2</sub>:O<sub>3</sub>=0</b>		<b>H<sub>2</sub>O<sub>2</sub>:O<sub>3</sub>=0.5</b>		<b>H<sub>2</sub>O<sub>2</sub>:O<sub>3</sub>=1.0</b>	
	<b>FI</b>	<b>TI</b>	<b>FI</b>	<b>TI</b>	<b>FI</b>	<b>TI</b>
0	1.39	1.00	1.39	1.00	1.39	1.00
0.25	1.37	0.49	1.39	0.51	1.39	0.53
0.5	1.27	0.24	1.30	0.28	1.34	0.29
1.0	1.22	0.12	1.31	0.14	1.33	0.16
1.5	1.24	0.08	1.33	0.09	1.35	0.10

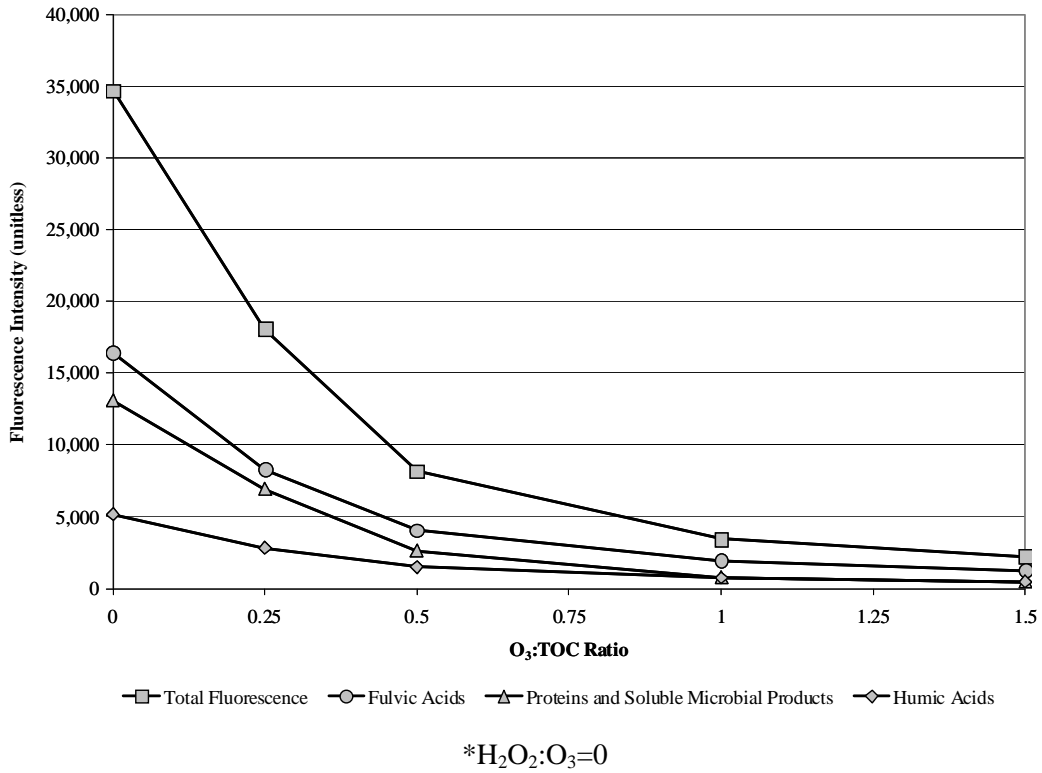
  

<b>Filtered UV Exposure</b>						
<b>UV Dose (mJ/cm<sup>2</sup>)</b>	<b>H<sub>2</sub>O<sub>2</sub>=0 mg/L</b>		<b>H<sub>2</sub>O<sub>2</sub>=5 mg/L</b>		<b>H<sub>2</sub>O<sub>2</sub>=10 mg/L</b>	
	<b>FI</b>	<b>TI</b>	<b>FI</b>	<b>TI</b>	<b>FI</b>	<b>TI</b>
0	1.39	1.00	N/A	N/A	1.39	1.00
23	1.42	0.86	N/A	N/A	1.42	0.87
45	1.40	0.87	N/A	N/A	1.42	0.85
225	1.40	0.88	N/A	N/A	1.40	0.79
680	1.40	0.84	N/A	N/A	1.37	0.66

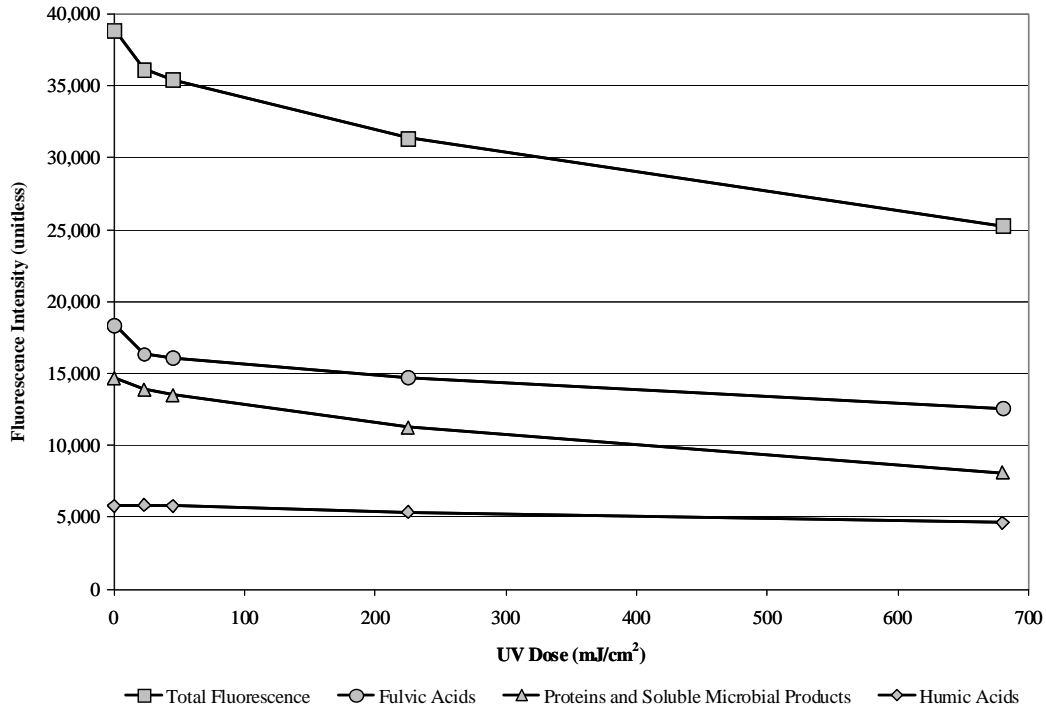
Notes: FI=fluorescence index; N/A=data not available; TI=treatment index; UV=ultraviolet



**Figure 3.20. CCWRD fluorescence profiles (Ex<sub>370</sub>) after ozonation.**



**Figure 3.21. Changes in fluorescence intensity after ozonation for CCWRD.**



\*H<sub>2</sub>O<sub>2</sub>=10 mg/L

Figure 3.22. Changes in fluorescence intensity after UV/H<sub>2</sub>O<sub>2</sub> for CCWRD.

### 3.2 Metropolitan Water Reclamation District of Greater Chicago, IL

The Metropolitan Water Reclamation District of Greater Chicago (MWRDGC) operates seven wastewater treatment facilities. The study site treats approximately 240 MGD of wastewater composed of primarily domestic flows with minor industrial contributions. The liquid treatment train consists of preliminary screening, grit removal, primary clarification, conventional activated sludge, and secondary clarification. The activated sludge process operates with an SRT ranging from 7 days in the summer to 14 days in the winter and achieves full nitrification and incidental partial denitrification. The secondary effluent is discharged to the North Shore Channel without filtration or disinfection; therefore, this data set does not include evaluations of finished effluent. A simplified treatment schematic of the facility is provided in Figure 3.23. Unfiltered secondary effluent from the MWRDGC facility was collected in August 2010, and the initial water quality data in Table 3.20 were obtained. Using the initial TOC and nitrite data, the ozone dosing conditions in Table 3.21 were calculated.

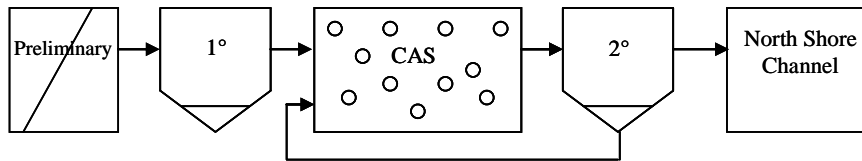


Figure 3.23. Simplified treatment schematic for MWRDGC facility.

Table 3.20. Initial Water Quality Data for MWRDGC

<b>Unfiltered Secondary Effluent</b>	Alkalinity (mg/L CaCO <sub>3</sub> )	134
	Bromide (µg/L)	93
	NDMA (ng/L)	<2.5
	NH <sub>3</sub> (mg/N/L)	0.07
	NO <sub>2</sub> (mg/N/L)	<0.05
	NO <sub>3</sub> (mg/N/L)	9.10
	pH	7.6
	TKN (mg/N/L)	0.70
	TN (mg/N/L)	9.80
	TOC (mg/L)	5.7
	TON (mg/N/L)	0.63
	TSS (mg/L)	<5
	Turbidity (NTU)	0.50
UV <sub>254</sub> absorbance (cm <sup>-1</sup> )	0.108	
<b>Filtered Secondary Effluent</b>	pH	7.6
	TOC (mg/L)	6.9
	TSS (mg/L)	<5
	Turbidity (NTU)	0.35
	UV <sub>254</sub> absorbance (cm <sup>-1</sup> )	0.131

Notes: NDMA=N-nitrosodimethylamine; TKN=total Kjeldahl nitrogen, the sum of TON and ammonia; TN=total nitrogen; TOC=total organic carbon; TON=total organic nitrogen, the difference of TN and ammonia, nitrate, and nitrite; TSS=total suspended solids; UV=ultraviolet

**Table 3.21. Ozone Dosing Conditions for 1-L MWRDGC Secondary Effluent Samples**Concentration of O<sub>3</sub> stock solution=80 mg/LConcentration of H<sub>2</sub>O<sub>2</sub> stock solution=10 g/L

Unfiltered dilution ratio=(903/1000)=0.903

Unfiltered TOC after dilution=5.1 mg/L

Unfiltered NO<sub>2</sub> after dilution< 0.05 mg/N/L (not considered in dosing calculations)

Unfiltered						
O <sub>3</sub> :TOC/ H <sub>2</sub> O <sub>2</sub> :O <sub>3</sub>	Wastewater Volume (mL)	Nanopure Volume (mL)	O <sub>3</sub> Volume (mL)	O <sub>3</sub> Dose (mg/L)	H <sub>2</sub> O <sub>2</sub> Volume (μL)	H <sub>2</sub> O <sub>2</sub> Dose (mg/L)
Spike	903	97	0	0	0	0
0.25/0	903	80	16	1.3	0	0
0.25/0.5	903	80	16	1.3	46	0.5
0.25/1.0	903	80	16	1.3	92	0.9
0.5/0	903	64	32	2.6	0	0
0.5/0.5	903	64	32	2.6	92	0.9
0.5/1.0	903	64	32	2.6	184	1.8
1.0/0	903	32	64	5.1	0	0
1.0/0.5	903	32	64	5.1	184	1.8
1.0/1.0	903	32	64	5.1	368	3.7
1.5/0	903	0	97	7.8	0	0
1.5/0.5	903	0	97	7.8	276	2.8
1.5/1.0	903	0	97	7.8	552	5.5

*Note:* Some values are affected by rounding error and the precision of the ozone spike.

Filtered dilution ratio=(885/1000)=0.885

Filtered TOC after dilution=6.1 mg/L

Filtered NO<sub>2</sub> after dilution<0.05 mg/N/L (not considered in dosing calculations)

Filtered						
O <sub>3</sub> :TOC/ H <sub>2</sub> O <sub>2</sub> :O <sub>3</sub>	Wastewater Volume (mL)	Nanopure Volume (mL)	O <sub>3</sub> Volume (mL)	O <sub>3</sub> Dose (mg/L)	H <sub>2</sub> O <sub>2</sub> Volume (μL)	H <sub>2</sub> O <sub>2</sub> Dose (mg/L)
Spike	885	115	0	0	0	0
0.25/0	885	96	19	1.5	0	0
0.25/0.5	885	96	19	1.5	54	0.5
0.25/1.0	885	96	19	1.5	108	1.1
0.5/0	885	77	38	3.0	0	0
0.5/0.5	885	77	38	3.0	108	1.1
0.5/1.0	885	77	38	3.0	216	2.2
1.0/0	885	38	76	6.1	0	0
1.0/0.5	885	38	76	6.1	216	2.2
1.0/1.0	885	38	76	6.1	432	4.3
1.5/0	885	0	115	9.2	0	0
1.5/0.5	885	0	115	9.2	324	3.2
1.5/1.0	885	0	115	9.2	648	6.5

*Note:* Some values are affected by rounding error and the precision of the ozone spike.

### 3.2.1 Ozone Demand/Decay

Figure 3.24 illustrates the ozone demand/decay curves for filtered and unfiltered MWRDGC secondary effluent at various dosing conditions. The graph only includes dosing conditions with a measurable ozone residual after 30 seconds; corresponding CT values are also provided. For the O<sub>3</sub>/H<sub>2</sub>O<sub>2</sub> samples, the addition of H<sub>2</sub>O<sub>2</sub> caused a nearly instantaneous reaction with the dissolved ozone, which led to the formation of •OH but eliminated the dissolved ozone residual. Because of reactions with EfOM, the 0.25 O<sub>3</sub>:TOC ratio was insufficient to establish a measurable ozone residual after 30 seconds. For the remaining dosing conditions, the graph illustrates the IOD (i.e., the precipitous drop between 0 and 30 seconds) and the decay over time.

As supported by the higher TOC value for the filtered secondary effluent, organic leaching may have impacted the ozone decay phase of the MWRDGC reactions, although the initial ozone demand was similar between the filtered and unfiltered samples. Although this affects the overall CT values for the higher applied ozone doses, the effect on oxidation efficacy may be insignificant; many of the reactions occur rapidly, as demonstrated by the reaction time experiments for the CCWRD secondary effluent.

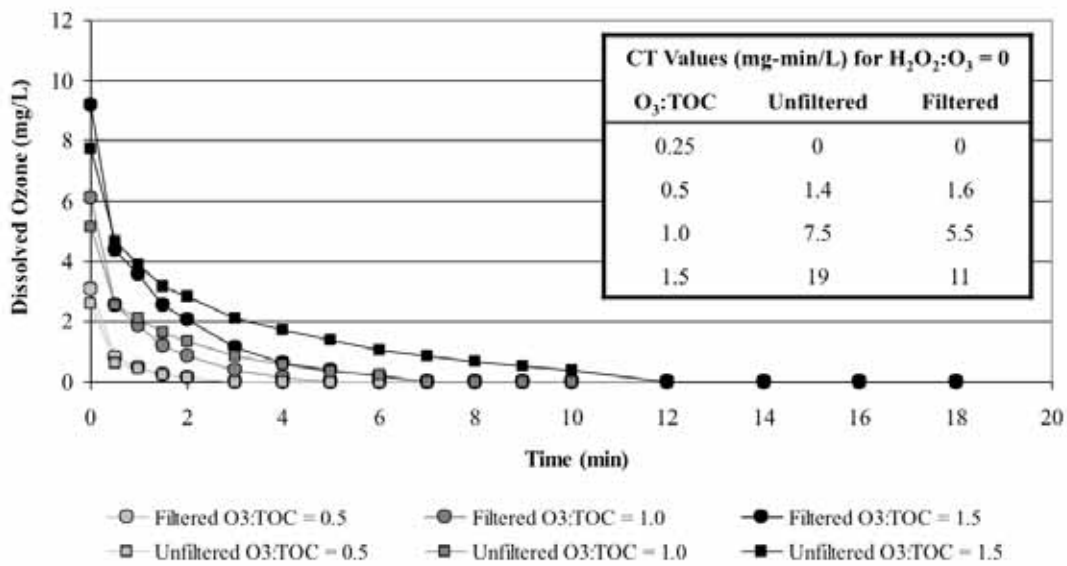


Figure 3.24. Ozone demand/decay curves for MWRDGC.

### 3.2.2 Bromate Formation

As illustrated in Figure 3.25, limited bromate formation occurred during ozonation of the MWRDGC secondary effluent. The bromate levels were lower than those observed during the CCWRD experiments, which is likely attributable to the lower bromide concentrations, and the filtered and unfiltered samples also yielded similar bromate formation. The O<sub>3</sub>:TOC ratio of 0.25 rarely produced bromate levels >MRL, and the O<sub>3</sub>:TOC ratio of 0.5 was also <MRL or <10 µg/L for all samples. The 1.0 and 1.5 O<sub>3</sub>:TOC ratios did not yield substantial bromate formation, but the samples did exceed the 10 µg/L benchmark in all samples. Similar to CCWRD, the addition of H<sub>2</sub>O<sub>2</sub> provided some degree of bromate mitigation. In order to

achieve the 10 µg/L treatment objective, the applied ozone dose would be limited to an O<sub>3</sub>:TOC ratio <1.0, or the process would have to be supplemented with substantial H<sub>2</sub>O<sub>2</sub> doses (assuming no other mitigation measures are implemented).

### 3.2.3 Hydroxyl Radical Exposure

Table 3.22 indicates the overall •OH exposure for each ozone and UV dosing condition based on data from bench-scale experiments with pCBA spiked at 500 µg/L. The •OH exposures for the UV/H<sub>2</sub>O<sub>2</sub> samples are corrected for the small level of pCBA degradation achieved by photolysis alone.

For MWRDGC, filtration had a slight negative impact on •OH exposure because of organic leaching from the cartridge filters, but, similar to CCWRD, H<sub>2</sub>O<sub>2</sub> addition had no significant impact on •OH exposure. Therefore, assuming the dissolved ozone residual is allowed to react completely, the overall •OH exposure *in wastewater* is independent of H<sub>2</sub>O<sub>2</sub> dose. However, for the highest O<sub>3</sub>:TOC ratio, the overall reaction time can be reduced from nearly 12 minutes (see Figure 3.24) to several seconds with the addition of H<sub>2</sub>O<sub>2</sub>. Ozone-based oxidation also provided higher •OH exposures than the UV dosing conditions applied during these experiments. With 10 mg/L of H<sub>2</sub>O<sub>2</sub> for the UV AOP, UV doses of 250 mJ/cm<sup>2</sup> and 500 mJ/cm<sup>2</sup> were nearly equivalent to O<sub>3</sub>:TOC ratios of 0.25 and 0.5.

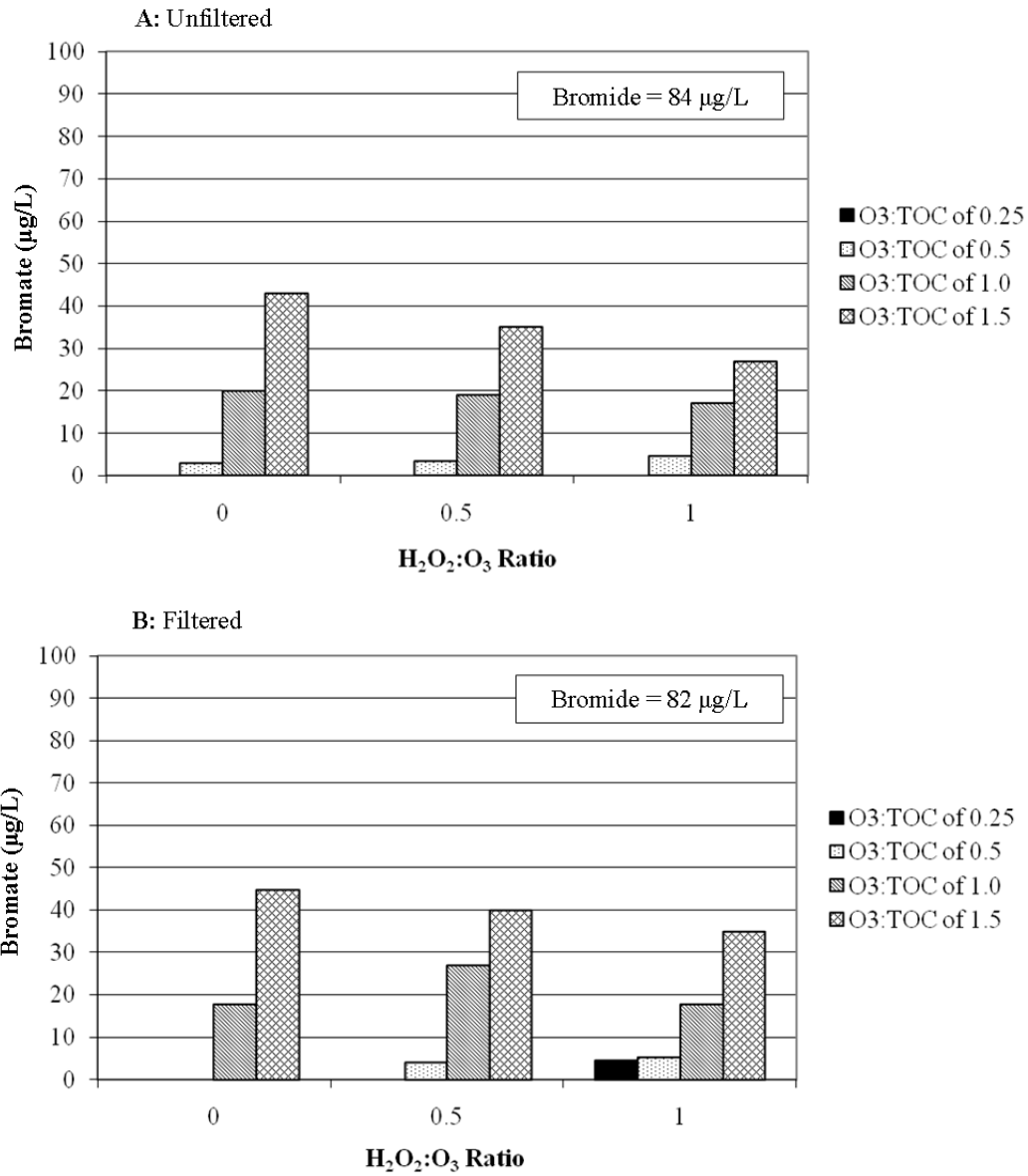


Figure 3.25. Bromate formation during ozonation of MWRDGC secondary effluent.

**Table 3.22. •OH Exposure in the MWRDGC Secondary Effluent**

<b>Unfiltered Ozone Exposure (<math>10^{-11}</math> M-s)</b>			
<b>Ozone:TOC</b>	<b>H<sub>2</sub>O<sub>2</sub>:O<sub>3</sub>=0</b>	<b>H<sub>2</sub>O<sub>2</sub>:O<sub>3</sub>=0.5</b>	<b>H<sub>2</sub>O<sub>2</sub>:O<sub>3</sub>=1.0</b>
0.25	5.6	5.9	6.1
0.5	14	11	16
1.0	39	41	33
1.5	71	79	61
<b>Filtered Ozone Exposure (<math>10^{-11}</math> M-s)</b>			
<b>Ozone:TOC</b>	<b>H<sub>2</sub>O<sub>2</sub>:O<sub>3</sub>=0</b>	<b>H<sub>2</sub>O<sub>2</sub>:O<sub>3</sub>=0.5</b>	<b>H<sub>2</sub>O<sub>2</sub>:O<sub>3</sub>=1.0</b>
0.25	3.8	4.4	5.0
0.5	10	12	11
1.0	26	28	26
1.5	47	52	48
<b>Filtered UV Exposure (<math>10^{-11}</math> M-s)</b>			
<b>UV Dose (mJ/cm<sup>2</sup>)</b>	<b>H<sub>2</sub>O<sub>2</sub>=0 mg/L</b>	<b>H<sub>2</sub>O<sub>2</sub>=5 mg/L</b>	<b>H<sub>2</sub>O<sub>2</sub>=10 mg/L</b>
0	N/A	N/A	0.61*
50	N/A	N/A	0.84
250	N/A	4.5	6.5
500	N/A	6.7	12

Note: \*=based on H<sub>2</sub>O<sub>2</sub> control; N/A=data not available

### 3.2.4 Title 22 Contaminants

Bench-scale experiments were performed with the filtered MWRDGC wastewater to evaluate the use of ozone and UV for the destruction of spiked NDMA (120 ng/L) and 1,4-dioxane (750 µg/L). Figure 3.26 indicates that UV doses ranging from 600 to 700 mJ/cm<sup>2</sup> were required to satisfy the Title 22 NDMA requirement. O<sub>3</sub>:TOC ratios >1.0 achieved net NDMA destruction (data not shown) by limited direct formation during ozonation (see Table 3.23); however, NDMA is highly resistant to •OH oxidation, so the extent of NDMA mitigation was insignificant (<0.1 log), particularly after considering the high ozone doses required.

Figure 3.27 illustrates the destruction of spiked 1,4-dioxane during the bench-scale ozone experiments. In general, O<sub>3</sub> and O<sub>3</sub>/H<sub>2</sub>O<sub>2</sub> achieved similar levels of treatment, although the trend lines suggest that O<sub>3</sub>/H<sub>2</sub>O<sub>2</sub> provided a slight advantage. For MWRDGC, O<sub>3</sub>:TOC ratios >1.5 are necessary to comply with the 0.5-log requirement.

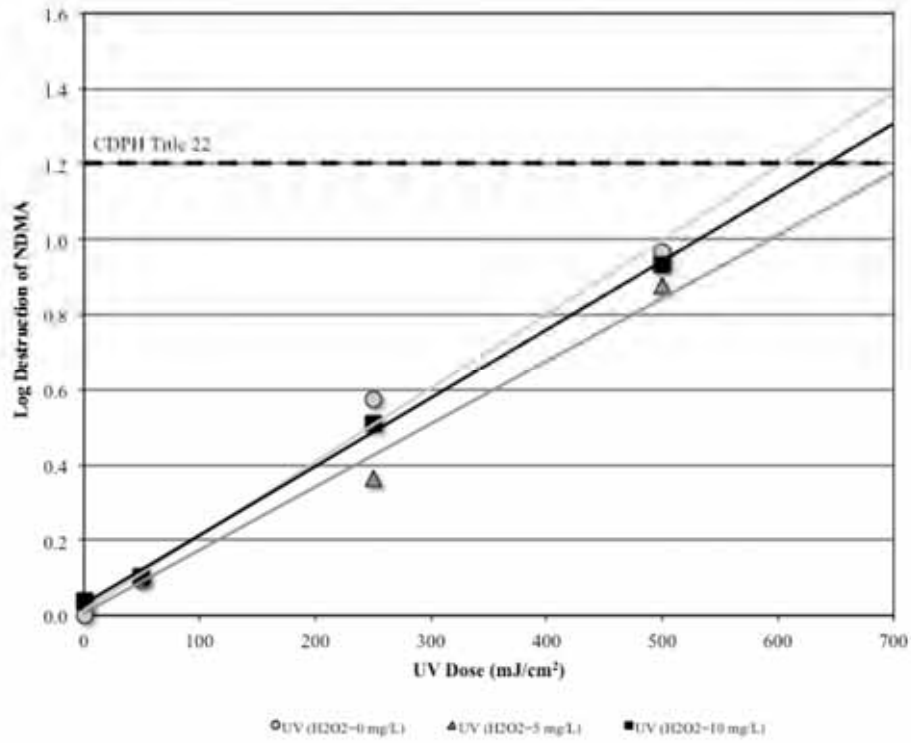


Figure 3.26. Destruction of NDMA in the filtered MWRDGC secondary effluent.

Table 3.23. Direct NDMA Formation in the Filtered MWRDGC Secondary Effluent

O <sub>3</sub> :TOC Ratio	H <sub>2</sub> O <sub>2</sub> :O <sub>3</sub> Ratio	NDMA (ng/L)
0	0	<2.5
0.5	0	9.8
0.5	0.5	11
1.0	0	9.2
1.0	0.5	10

Note: NDMA=N-nitrosodimethylamine

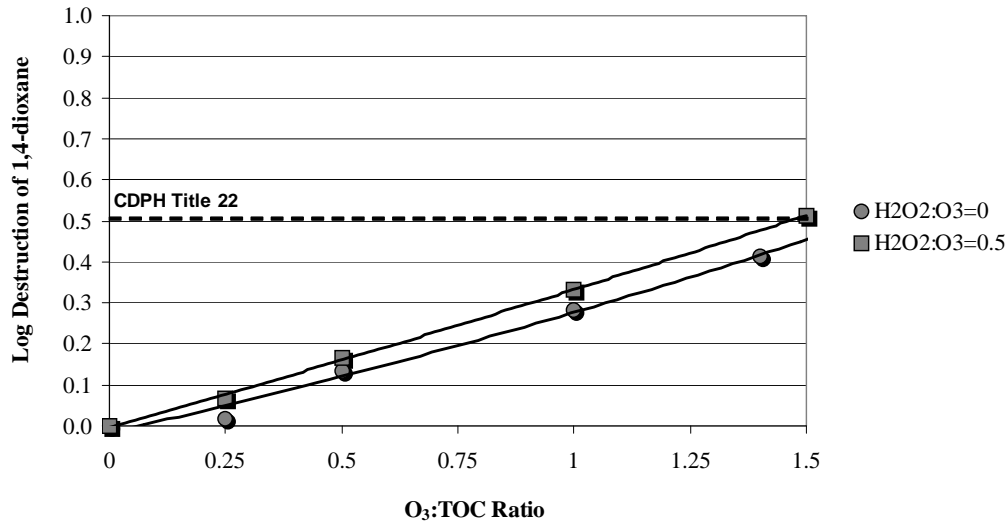


Figure 3.27. Destruction of 1,4-dioxane in the filtered MWRDGC secondary effluent.

### 3.2.5 Trace Organic Contaminants

Secondary effluent samples from MWRDGC were analyzed to determine the ambient concentrations of the target compounds, which are provided in Table 3.24. None of the compounds were present at concentrations exceeding 1 µg/L, and a majority of the compounds were detected at concentrations less than 100 ng/L. The concentrations of some of the most bioamenable compounds, including naproxen and ibuprofen, were <MRL after biological treatment in the activated sludge process. The total estrogenicity of the wastewater was determined to be 1.8 ng/L.

Table 3.24. Ambient TOrC Concentrations at MWRDGC

Parameter	Secondary Effluent (ng/L)
Atenolol	710
Atrazine	28
Bisphenol A	<50
Carbamazepine	140
DEET	54
Diclofenac	62
Gemfibrozil	31
Ibuprofen	<25
Meprobamate	41
Musk ketone	<100
Naproxen	<25
Phenytoin	110
Primidone	67
Sulfamethoxazole	570
TCEP	540
Total estrogenicity (EEq)	1.8
Triclosan	26
Trimethoprim	280

Notes: DEET=*N,N*-diethyl-*meta*-toluamide; EEq=estradiol equivalents; TCEP=tris-(2-chloroethyl)-phosphate

Bench-scale TOxC oxidation experiments were performed with spiking stocks similar to those described for CCWRD. Tables 3.25 and 3.26 show the relative oxidation levels of the 16 target compounds (musk ketone omitted) in the unfiltered and filtered MWRDGC secondary effluent. In general, there were no consistent differences between the ozone versus ozone/H<sub>2</sub>O<sub>2</sub> samples. There may have been slight improvements with H<sub>2</sub>O<sub>2</sub> addition for the ozone-resistant compounds (Groups 3, 4, and 5), but it would be difficult to justify H<sub>2</sub>O<sub>2</sub> addition for this reason alone. The slight differences in the filtered versus unfiltered samples for select compounds may have been attributable to the additional oxidant demand of the filtered secondary effluent (see Figure 3.24).

As described earlier, the target compounds were divided into five categories based on their second-order ozone and •OH rate constants. Despite the similar O<sub>3</sub>:TOC ratios, the level of oxidation experienced by the MWRDGC samples was slightly higher than that of CCWRD. In fact, nearly all of the Group 1 compounds were oxidized greater than 80% at an O<sub>3</sub>:TOC ratio of 0.25, and both of the Group 2 compounds were generally oxidized greater than 80% with an O<sub>3</sub>:TOC ratio of 0.5. The trends for MWRDGC and CCWRD were similar for the remaining compound groups.

Table 3.27 shows the relative photolysis and oxidation levels of the target compounds. Again, UV photolysis was quite ineffective in destroying the target compounds. Only two compounds (diclofenac and triclosan) experienced greater than 80% destruction with UV irradiation alone, whereas atrazine, phenytoin, and sulfamethoxazole experienced greater than 30% destruction with UV alone. Despite dramatic improvements in treatment efficacy, the addition of H<sub>2</sub>O<sub>2</sub> with a UV dose of 500 mJ/cm<sup>2</sup> was only able to achieve 80% destruction for one additional compound (sulfamethoxazole). A majority of the remaining compounds achieved destruction levels ranging from 50 to 75%.

Finally, the total estrogenicity of the secondary effluent was oxidized down to the MRL with every ozone and ozone/H<sub>2</sub>O<sub>2</sub> dosing condition. On the other hand, neither UV nor UV/H<sub>2</sub>O<sub>2</sub> was particularly effective for reducing total estrogenicity, but the MRL was eventually achieved with a UV dose of 500 mJ/cm<sup>2</sup> and an H<sub>2</sub>O<sub>2</sub> dose of 5 or 10 mg/L. These results are summarized in Figure 3.28.

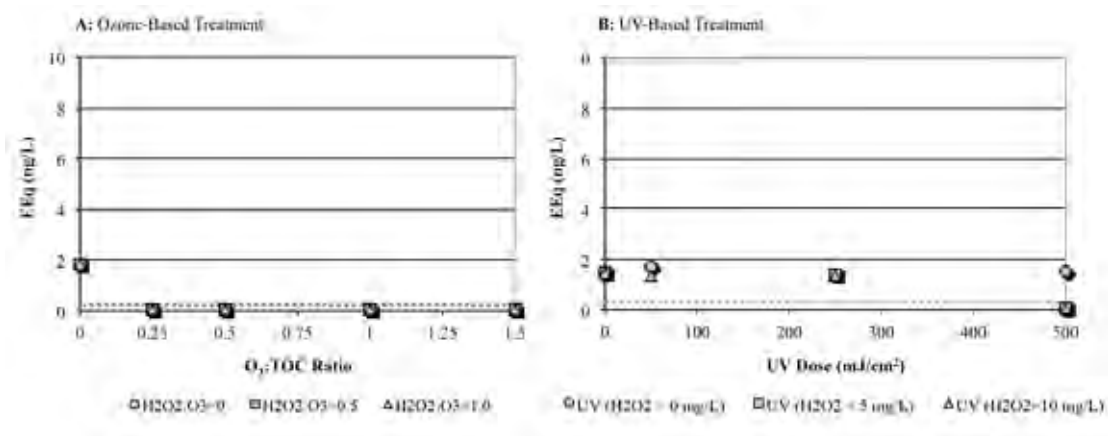


Figure 3.28. Reduction in total estrogenicity in the filtered MWRDGC secondary effluent.

**Table 3.25. MWRDGC TOrC Mitigation by Ozone (Unfiltered)**

Group	Contaminant	O <sub>3</sub> :TOC (mass) / H <sub>2</sub> O <sub>2</sub> :O <sub>3</sub> (molar)											
		0.25/0	0.25/0.5	0.25/1.0	0.5/0	0.5/0.5	0.5/1.0	1.0/0	1.0/0.5	1.0/1.0	1.5/0	1.5/0.5	1.5/1.0
1	Bisphenol A	97%	94%	85%	97%	97%	97%	97%	97%	97%	97%	97%	97%
	Diclofenac	93%	88%	81%	97%	97%	97%	97%	97%	97%	97%	97%	97%
	Carbamazepine	92%	88%	82%	99%	99%	99%	99%	99%	99%	99%	99%	99%
	Naproxen	91%	85%	79%	98%	98%	98%	98%	98%	98%	98%	98%	98%
	Sulfamethoxazole	90%	83%	76%	98%	98%	98%	98%	98%	98%	98%	98%	98%
	Triclosan	97%	97%	92%	97%	62%	97%	97%	97%	97%	97%	97%	97%
	Trimethoprim	91%	85%	77%	99%	99%	99%	99%	99%	99%	99%	99%	99%
	<b>Indicator</b>	<b>93%</b>	<b>89%</b>	<b>82%</b>	<b>98%</b>	<b>93%</b>	<b>98%</b>						
2	Atenolol	54%	51%	51%	84%	72%	94%	98%	98%	98%	98%	98%	98%
	Gemfibrozil	79%	77%	70%	99%	98%	99%	99%	99%	99%	99%	99%	99%
	<b>Indicator</b>	<b>67%</b>	<b>64%</b>	<b>61%</b>	<b>92%</b>	<b>85%</b>	<b>97%</b>	<b>99%</b>	<b>99%</b>	<b>99%</b>	<b>99%</b>	<b>99%</b>	<b>99%</b>
3	DEET	29%	35%	29%	46%	49%	74%	94%	95%	94%	99%	99%	99%
	Ibuprofen	34%	36%	34%	46%	55%	79%	97%	97%	96%	97%	97%	97%
	Phenytoin	31%	38%	28%	46%	51%	80%	97%	97%	96%	99%	99%	99%
	Primidone	22%	33%	28%	44%	39%	70%	94%	94%	92%	99%	99%	99%
	<b>Indicator</b>	<b>29%</b>	<b>36%</b>	<b>30%</b>	<b>46%</b>	<b>49%</b>	<b>76%</b>	<b>96%</b>	<b>96%</b>	<b>95%</b>	<b>99%</b>	<b>99%</b>	<b>99%</b>
4	Atrazine	11%	12%	9%	20%	20%	38%	69%	72%	71%	89%	91%	89%
	Meprobamate	19%	18%	15%	27%	25%	52%	78%	82%	81%	93%	96%	95%
	<b>Indicator</b>	<b>15%</b>	<b>15%</b>	<b>12%</b>	<b>24%</b>	<b>23%</b>	<b>45%</b>	<b>74%</b>	<b>77%</b>	<b>76%</b>	<b>91%</b>	<b>94%</b>	<b>92%</b>
5	TCEP	4%	5%	2%	2%	5%	7%	14%	19%	21%	23%	32%	30%

Notes: shading represents >80% oxidation; DEET=*N,N*-diethyl-*meta*-toluamide; TCEP=tris-(2-chloroethyl)-phosphate

**Table 3.26. MWRDGC TOrC Mitigation by Ozone (Filtered)**

Group	Contaminant	O <sub>3</sub> :TOC (mass) / H <sub>2</sub> O <sub>2</sub> :O <sub>3</sub> (molar)											
		0.25/0	0.25/0.5	0.25/1.0	0.5/0	0.5/0.5	0.5/1.0	1.0/0	1.0/0.5	1.0/1.0	1.5/0	1.5/0.5	1.5/1.0
1	Bisphenol A	97%	97%	97%	97%	97%	97%	97%	97%	97%	97%	97%	97%
	Carbamazepine	99%	99%	99%	99%	99%	99%	99%	99%	99%	99%	99%	99%
	Diclofenac	97%	97%	97%	97%	97%	97%	97%	97%	97%	97%	97%	97%
	Naproxen	98%	98%	94%	98%	98%	98%	98%	98%	98%	98%	98%	98%
	Sulfamethoxazole	95%	94%	91%	98%	98%	98%	98%	98%	98%	98%	98%	98%
	Triclosan	97%	97%	97%	97%	97%	97%	97%	97%	97%	97%	97%	97%
	Trimethoprim	99%	99%	98%	99%	99%	99%	99%	99%	99%	99%	99%	99%
	<b>Indicator</b>	<b>97%</b>	<b>97%</b>	<b>96%</b>	<b>98%</b>								
2	Atenolol	57%	53%	49%	98%	98%	94%	98%	98%	98%	98%	98%	98%
	Gemfibrozil	96%	90%	70%	99%	99%	99%	99%	99%	99%	99%	99%	99%
	<b>Indicator</b>	<b>77%</b>	<b>72%</b>	<b>60%</b>	<b>99%</b>	<b>99%</b>	<b>97%</b>	<b>99%</b>	<b>99%</b>	<b>99%</b>	<b>99%</b>	<b>99%</b>	<b>99%</b>
3	DEET	13%	19%	19%	43%	51%	52%	80%	85%	84%	95%	97%	93%
	Ibuprofen	27%	33%	33%	59%	65%	65%	89%	91%	90%	98%	98%	96%
	Phenytoin	12%	20%	24%	48%	61%	60%	89%	92%	89%	97%	99%	96%
	Primidone	24%	29%	33%	48%	58%	59%	84%	86%	86%	96%	96%	93%
	<b>Indicator</b>	<b>19%</b>	<b>25%</b>	<b>27%</b>	<b>50%</b>	<b>59%</b>	<b>59%</b>	<b>86%</b>	<b>89%</b>	<b>87%</b>	<b>97%</b>	<b>98%</b>	<b>95%</b>
4	Atrazine	9%	11%	11%	24%	29%	29%	53%	53%	56%	74%	76%	73%
	Meprobamate	10%	13%	15%	29%	36%	38%	62%	65%	67%	81%	86%	83%
	<b>Indicator</b>	<b>10%</b>	<b>12%</b>	<b>13%</b>	<b>27%</b>	<b>33%</b>	<b>34%</b>	<b>58%</b>	<b>59%</b>	<b>62%</b>	<b>78%</b>	<b>81%</b>	<b>78%</b>
5	TCEP	1%	10%	10%	13%	13%	13%	16%	11%	16%	20%	24%	26%

Notes: Shading represents >80% oxidation; DEET=*N,N*-diethyl-*meta*-toluamide; TCEP=tris-(2-chloroethyl)-phosphate

**Table 3.27. MWRDGC TOrC Mitigation by UV (Filtered)**

Group	Contaminant	UV Dose (mJ/cm <sup>2</sup> ) / H <sub>2</sub> O <sub>2</sub> Dose (mg/L)								
		50/0	50/10	250/0	250/5	250/10	500/0	500/5	500/10	
1	Bisphenol A	6%	-6%	6%	22%	46%	6%	28%	71%	
	Carbamazepine	9%	9%	0%	21%	43%	0%	22%	62%	
	Diclofenac	40%	41%	89%	94%	97%	97%	97%	97%	
	Naproxen	8%	17%	8%	31%	53%	18%	38%	73%	
	Sulfamethoxazole	-4%	-4%	37%	51%	58%	65%	71%	80%	
	Triclosan	10%	18%	70%	83%	89%	93%	95%	97%	
	Trimethoprim	3%	3%	3%	17%	34%	-3%	17%	54%	
2	Atenolol	10%	10%	-3%	16%	29%	3%	10%	55%	
	Gemfibrozil	8%	5%	3%	19%	40%	4%	5%	60%	
3	DEET	9%	9%	9%	21%	33%	9%	15%	52%	
	Ibuprofen	8%	8%	6%	25%	40%	7%	22%	62%	
	Phenytoin	6%	11%	32%	41%	56%	44%	55%	79%	
	Primidone	8%	8%	3%	18%	38%	8%	18%	52%	
4	Atrazine	7%	1%	17%	24%	35%	33%	27%	56%	
	Meprobamate	7%	3%	3%	10%	22%	2%	3%	36%	
5	TCEP	10%	17%	17%	18%	20%	13%	-4%	26%	

Notes: shading represents >80% photolysis or oxidation; groupings refer to ozone and OH rate constants; DEET=*N,N*-diethyl-*meta*-toluamide; TCEP=tris-(2-chloroethyl)-phosphate

**Table 3.28. Ambient Microbial Water Quality Data for MWRDGC**

Microbial Surrogate	Unfiltered Secondary Effluent	Filtered Secondary Effluent
<i>Bacillus</i> spores (CFU/100 mL)	2.5x10 <sup>3</sup>	2.1x10 <sup>3</sup>
Coliforms, fecal (MPN/100 mL)	1.6x10 <sup>2</sup>	1.1x10 <sup>2</sup>
Coliforms, total (MPN/100 mL)	1.9x10 <sup>3</sup>	6.3x10 <sup>2</sup>
MS2 (PFU/mL)	<1	<1

**Table 3.29. Microbial Spiking Levels for MWRDGC Bench-Scale Experiments**

Microbial Surrogate	Unfiltered Ozone Disinfection	Filtered Ozone Disinfection	Filtered UV Disinfection
<i>B. subtilis</i> spores (CFU/100 mL)	2.6x10 <sup>5</sup>	2.3x10 <sup>5</sup>	2.0x10 <sup>5</sup>
<i>E. coli</i> (MPN/100 mL)	1.3x10 <sup>8</sup>	1.1x10 <sup>8</sup>	2.1x10 <sup>7</sup>
MS2 (PFU/mL)	1.5x10 <sup>7</sup>	4.7x10 <sup>7</sup>	4.3x10 <sup>7</sup>

### 3.2.6 Disinfection

Ambient secondary effluent samples (before and after laboratory filtration) were assayed for total and fecal coliforms, MS2, and *Bacillus* spores. The ambient microbial water quality data are provided in Table 3.28. In order to illustrate a wide range of inactivation, the ozone and UV disinfection samples were spiked with relatively high numbers of the surrogate microbes, as indicated in Table 3.29.

Figure 3.29 illustrates the inactivation of spiked *E. coli* during the bench-scale ozone experiments. The solid and dashed lines near the top of the figure represent the limits of inactivation based on the spiking levels in the filtered and unfiltered samples.

Similar to CCWRD, the filtered versus unfiltered comparison proved to be inconclusive because of the inherent variability in the data sets. On average, the addition of H<sub>2</sub>O<sub>2</sub> alone achieved less than 0.3-log inactivation, but when combined with ozonation, the addition of H<sub>2</sub>O<sub>2</sub> generally hindered *E. coli* inactivation. This indicates that the increased reactivity of •OH combined with the scavenging effects of EfOM were generally detrimental to the disinfection process. Although molecular ozone also decomposes into •OH over time, the initial ozone exposure was critical for improving disinfection efficacy. For the ozone doses, inactivation for the O<sub>3</sub>:TOC ratio of 0.25 spanned nearly four orders of magnitude, whereas the remaining doses generally achieved >6-log inactivation. The average log-inactivation values for each treatment condition after combining the unfiltered and filtered data sets are provided in Table 3.30.

Figure 3.30 illustrates the inactivation of spiked MS2 during the bench-scale ozone experiments. As with *E. coli*, there was no noticeable difference between the filtered and unfiltered samples, and the addition of H<sub>2</sub>O<sub>2</sub> alone achieved less than 0.3-log inactivation; however, the negative impact of H<sub>2</sub>O<sub>2</sub> was not as consistent for MS2 inactivation. Pursuant to the CDPH Title 22 requirements, an O<sub>3</sub>:TOC ratio >0.5 was often sufficient for the 5- and 6.5-log inactivation requirements, but there were several samples within this dosing range that did not satisfy this treatment objective. The average log-inactivation values for each treatment condition (combined unfiltered and filtered data) are provided in Table 3.31.

Figure 3.31 illustrates the inactivation of spiked *B. subtilis* spores during the bench-scale ozone experiments. The spores proved to be extremely resistant to oxidation and only experienced significant inactivation for O<sub>3</sub>:TOC ratios >1.0 with no H<sub>2</sub>O<sub>2</sub> addition. In other words, a sufficient ozone CT had to be administered before ozone and •OH were able to penetrate the spore coat and inactivate the bacteria. Similar to CCWRD, there appears to be a significant difference between the unfiltered and filtered samples at an O<sub>3</sub>:TOC ratio of 1.0 (no H<sub>2</sub>O<sub>2</sub> addition), but this is likely attributable to inherent variability rather than the effect of filtration. It is important to reiterate that oxidation with •OH alone (i.e., with H<sub>2</sub>O<sub>2</sub> addition) is extremely ineffective for spore inactivation, presumably because of the highly reactive nature of •OH and competition with EfOM. The average log-inactivation values for each treatment condition (combined unfiltered and filtered data) are provided in Table 3.32.

Finally, Figure 3.32 provides a summary of the ozone disinfection data for the three surrogate microbes within the CT framework. Figure 3.32A illustrates the dose–response relationships for the filtered and unfiltered samples (combined) with no H<sub>2</sub>O<sub>2</sub> addition. Figure 3.32B illustrates the dose–response relationships for the filtered and unfiltered samples (combined) with H<sub>2</sub>O<sub>2</sub>:O<sub>3</sub> ratios of 0.5 and 1.0 (also combined). According to these data, the CT framework is not always appropriate because substantial levels of inactivation can be achieved when the apparent ozone CT is zero; however, the level of inactivation for vegetative bacteria and viruses is generally less than that observed when an ozone residual is present, and no inactivation of spore-forming bacteria can be achieved without a measurable CT.

Table 3.33 summarizes the efficacy of UV and UV/H<sub>2</sub>O<sub>2</sub> for the inactivation of the three surrogate microbes. The efficacy of UV-based disinfection differs dramatically from ozone-based disinfection because UV is highly effective against both vegetative and spore-forming bacteria, whereas some viruses demonstrate resistance. A dose of 50 mJ/cm<sup>2</sup> was sufficient to reach the limits of inactivation for *E. coli* and *Bacillus* spores, regardless of H<sub>2</sub>O<sub>2</sub> addition. On the other hand, MS2 inactivation occurred more slowly and only reached the limit of inactivation with a UV dose of 250 mJ/cm<sup>2</sup>. Although the 500 mJ/cm<sup>2</sup> sample did not technically reach the limit of inactivation, the MS2 levels in those samples were extremely low. Regarding advanced oxidation dosing conditions (i.e., >250 mJ/cm<sup>2</sup> with 10 mg/L of H<sub>2</sub>O<sub>2</sub>), one can expect substantial inactivation of all microbes present in wastewater. This constitutes a significant advantage for UV-based treatment over the ozone-based alternatives.

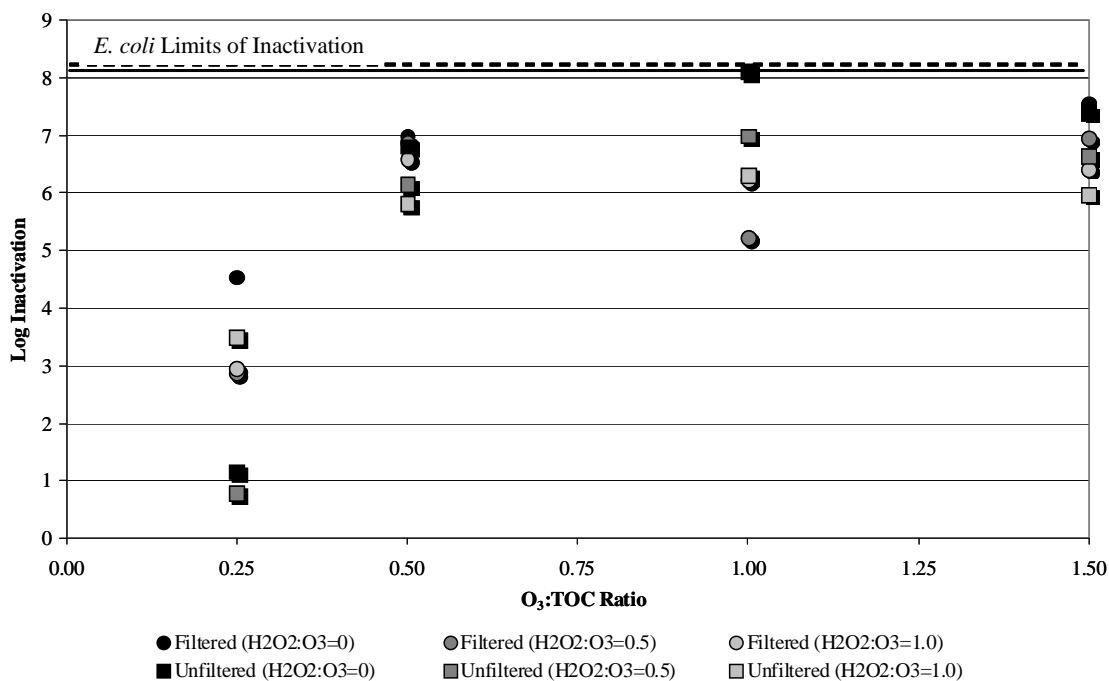


Figure 3.29. Inactivation of spiked *E. coli* in the MWRDGC secondary effluent.

Table 3.30. Summary of *E. coli* Inactivation in the MWRDGC Secondary Effluent

O <sub>3</sub> :TOC Ratio	H <sub>2</sub> O <sub>2</sub> :O <sub>3</sub> =0	H <sub>2</sub> O <sub>2</sub> :O <sub>3</sub> =0.5	H <sub>2</sub> O <sub>2</sub> :O <sub>3</sub> =1.0
0.25	2.9±2.4*	1.8±1.5	3.2±0.4
0.5	6.9±0.1	6.5±0.5	6.2±0.6
1.0	8.1±N/A**	6.1±1.3	6.3±0.1
1.5	7.5±0.1	6.8±0.2	6.2±0.3

Notes: \*=average log inactivation ± span of filtered/unfiltered samples; N/A=filtered sample not collected, so value only represents unfiltered sample

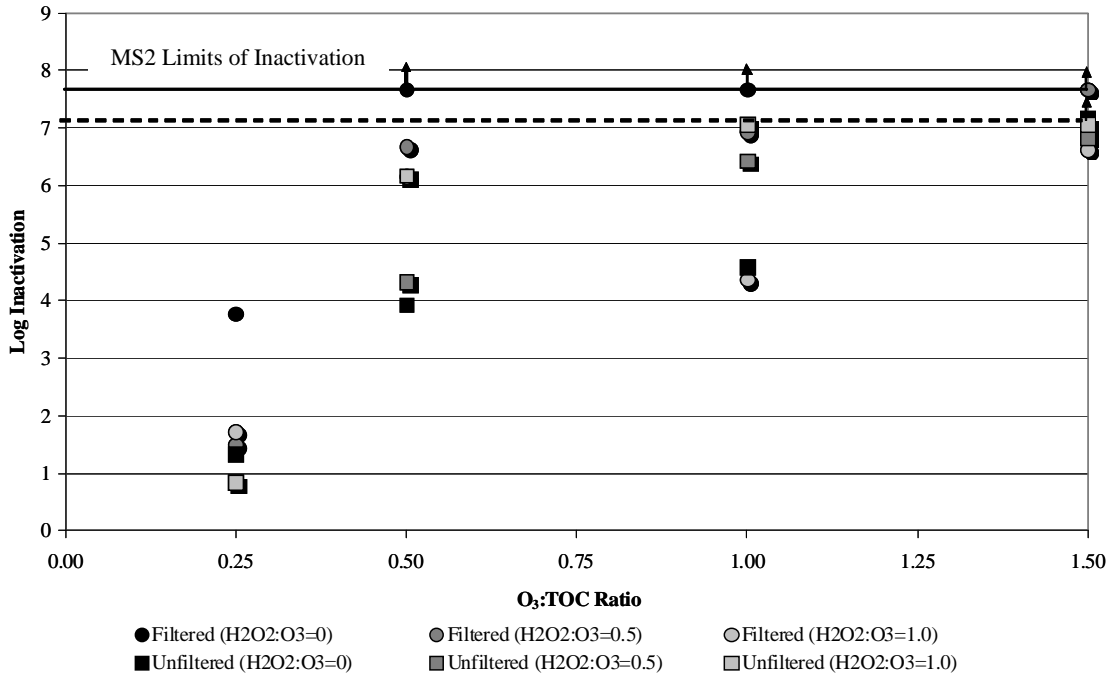


Figure 3.30. Inactivation of spiked MS2 in the MWRDGC secondary effluent.

Table 3.31. Summary of MS2 Inactivation in the MWRDGC Secondary Effluent

O <sub>3</sub> :TOC Ratio	H <sub>2</sub> O <sub>2</sub> :O <sub>3</sub> =0	H <sub>2</sub> O <sub>2</sub> :O <sub>3</sub> =0.5	H <sub>2</sub> O <sub>2</sub> :O <sub>3</sub> =1.0
0.25	2.6±1.7*	1.2±0.5	1.3±0.6
0.5	5.8±2.7	5.5±1.7	6.2±0.0
1.0	6.1±2.2	6.7±0.4	5.7±1.9
1.5	7.4±0.4	7.3±0.6	6.8±0.3

Note: \*=average log inactivation ± span of filtered/unfiltered samples

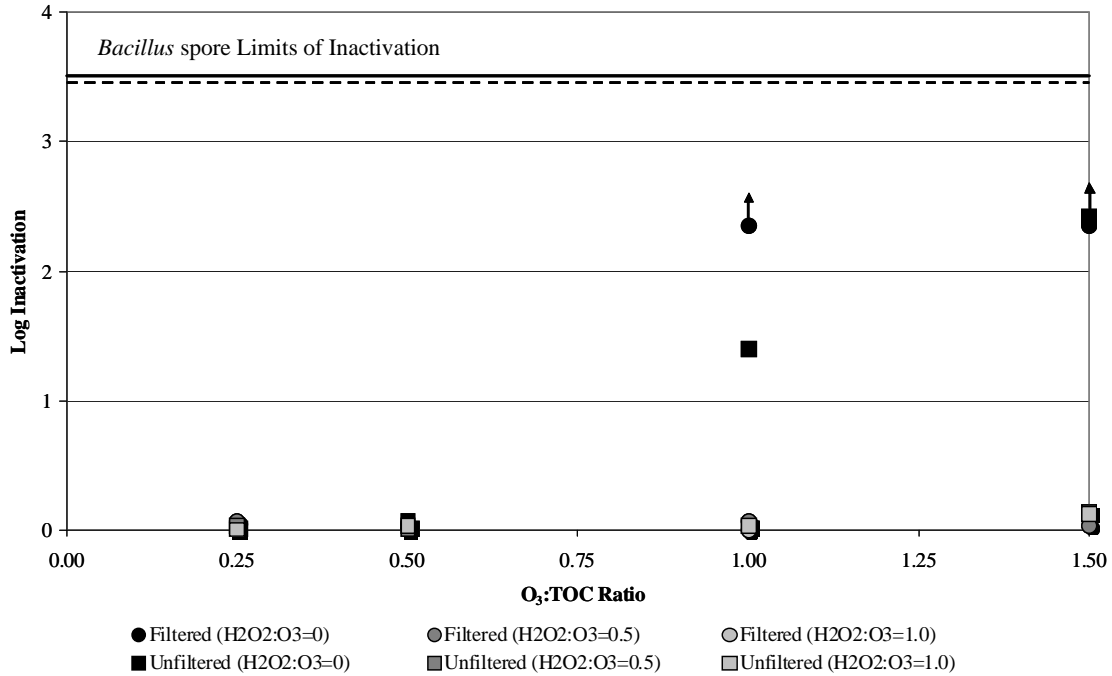
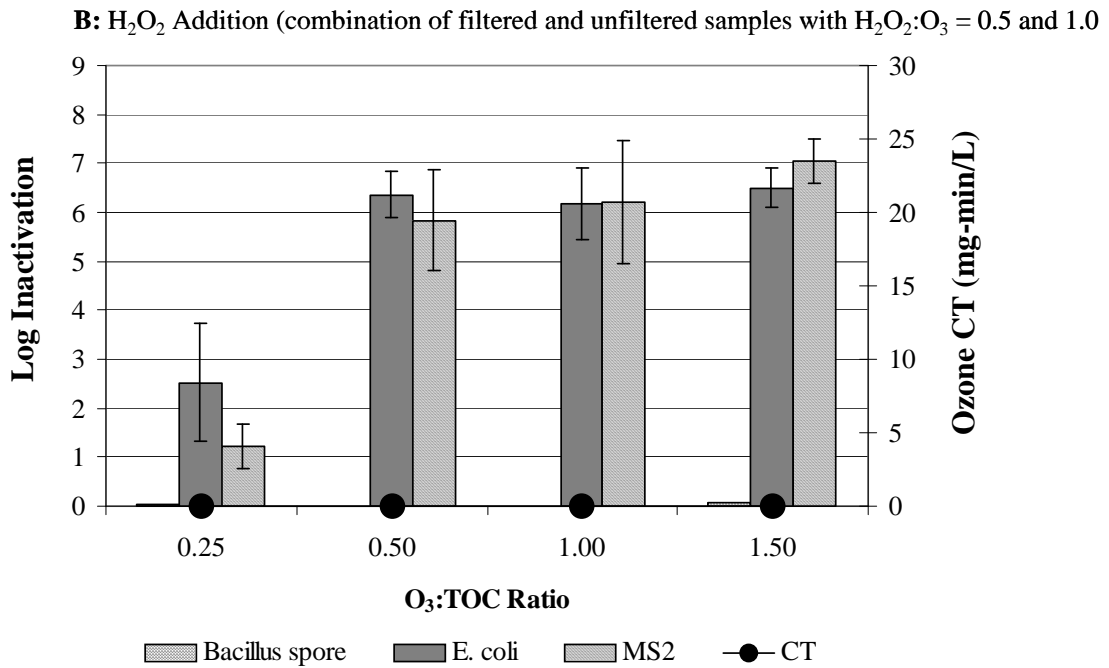
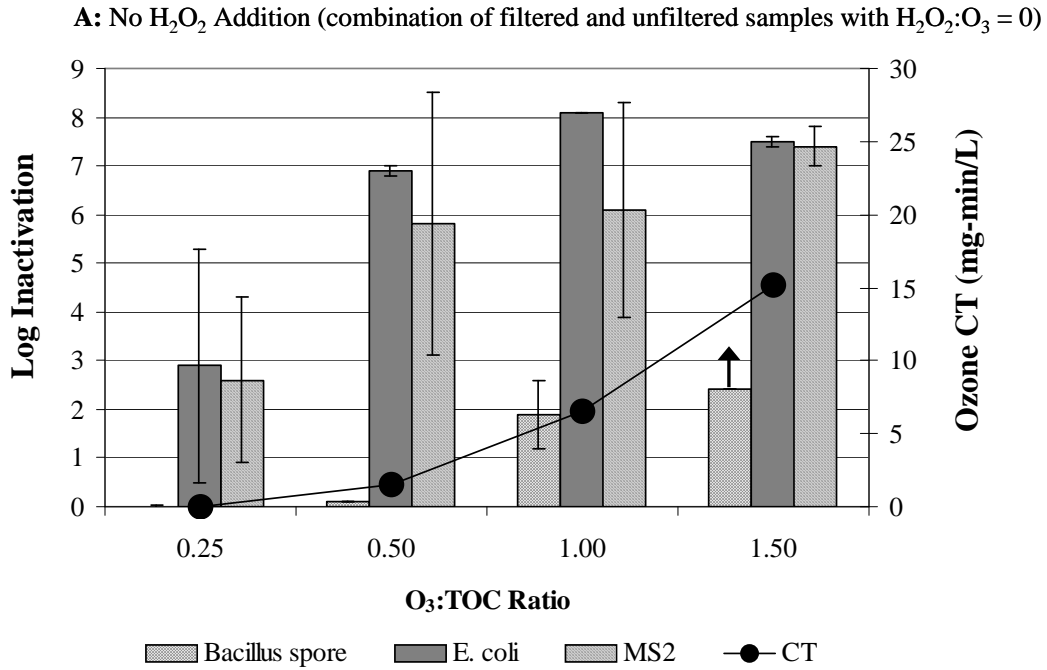


Figure 3.31. Inactivation of spiked *Bacillus* spores in the MWRDGC secondary effluent.

Table 3.32. Summary of *Bacillus* Spore Inactivation in the MWRDGC Secondary Effluent

O <sub>3</sub> :TOC Ratio	H <sub>2</sub> O <sub>2</sub> :O <sub>3</sub> =0	H <sub>2</sub> O <sub>2</sub> :O <sub>3</sub> =0.5	H <sub>2</sub> O <sub>2</sub> :O <sub>3</sub> =1.0
0.25	0.0±0.0*	0.1±0.0	0.0±0.0
0.5	0.1±0.0	0.0±0.0	0.0±0.1
1.0	1.9±0.7	0.0±0.1	0.0±0.0
1.5	>2.4** ±0.0	0.1±0.1	0.1±0.1

Notes: \*=average log inactivation ± span of filtered/unfiltered samples; \*\*=limit of inactivation based on sample dilutions



**Figure 3.32. Significance of CT for disinfection in the MWRDGC secondary effluent.**

**Table 3.33. Summary of UV Inactivation in the MWRDGC Secondary Effluent**

UV Dose (mJ/cm <sup>2</sup> )	<i>E. coli</i>		MS2		<i>Bacillus Spore</i>	
	UV	UV/H <sub>2</sub> O <sub>2</sub> <sup>*</sup>	UV	UV/H <sub>2</sub> O <sub>2</sub> <sup>*</sup>	UV	UV/H <sub>2</sub> O <sub>2</sub> <sup>*</sup>
25	5.3	N/A	N/A	N/A	2.9	3.2
50	>7.3 <sup>**</sup>	>7.3 <sup>**</sup>	2.9	3.8	>3.3 <sup>**</sup>	>3.3 <sup>**</sup>
250	>7.3 <sup>**</sup>	>7.3 <sup>**</sup>	>7.6 <sup>**</sup>	>7.6 <sup>**</sup>	>3.3 <sup>**</sup>	>3.3 <sup>**</sup>
500	>7.3 <sup>**</sup>	>7.3 <sup>**</sup>	7.5	7.2	>3.3 <sup>**</sup>	>3.3 <sup>**</sup>

Notes: <sup>\*</sup>=H<sub>2</sub>O<sub>2</sub> doses of 5 and 10 mg/L achieved similar levels of inactivation; <sup>\*\*</sup>=limit of inactivation based on spiking level

### 3.2.7 Organic Characterization

The full-spectrum scans in Figure 3.33 through Figure 3.35, without (A) and with (B) H<sub>2</sub>O<sub>2</sub> addition, indicate that the absorbance profiles around 254 nm generally provide the greatest resolution between treatments. The absorbance spectra for both sets of ozone experiments are shown because the filtered samples are characterized by discontinuity at 380 nm that may be attributable to organic leaching from the cartridge filters. Because of the limited efficacy of UV photolysis (Figure 3.35A), there is little resolution regardless of wavelength, although UV/H<sub>2</sub>O<sub>2</sub> achieved slight improvements over UV alone. Figure 3.36 focuses on the change in UV<sub>254</sub> absorbance with ozone, ozone/H<sub>2</sub>O<sub>2</sub>, UV, and UV/H<sub>2</sub>O<sub>2</sub>. As for ozonation, reductions in UV<sub>254</sub> absorbance were hindered by cartridge filtration, which was likely attributable to the small amount of organic leaching, and the addition of H<sub>2</sub>O<sub>2</sub>. As would be expected given the synergistic aspect of the UV AOP, the addition of H<sub>2</sub>O<sub>2</sub> during UV irradiation achieved a lower UV<sub>254</sub> absorbance.

As described earlier, 3D excitation emission matrices were developed for the unfiltered secondary effluent, the filtered secondary effluent, and the various treatment conditions. Figure 3.37 illustrates the fluorescence fingerprint of the secondary effluent samples and also provides the total and regional fluorescence intensities based on arbitrary fluorescence units. The organic leaching from the cartridge filter is apparent because of the higher fluorescence intensity in the filtered ambient sample. Figure 3.38 provides a qualitative illustration of treatment efficacy after ozone- and UV-based oxidation. Similar to UV absorbance, UV photolysis and UV/H<sub>2</sub>O<sub>2</sub> are not nearly as effective in reducing fluorescence intensity as ozone-based oxidation.

Figures 3.39 and 3.40 illustrate the fluorescence profiles at an excitation wavelength of 254 nm after ozonation and UV/H<sub>2</sub>O<sub>2</sub>. Because the addition of H<sub>2</sub>O<sub>2</sub> did not have a significant impact on ozone efficacy, and UV photolysis provided limited reductions in fluorescence intensity (see Figure 3.38), these fluorescence profiles are not shown.

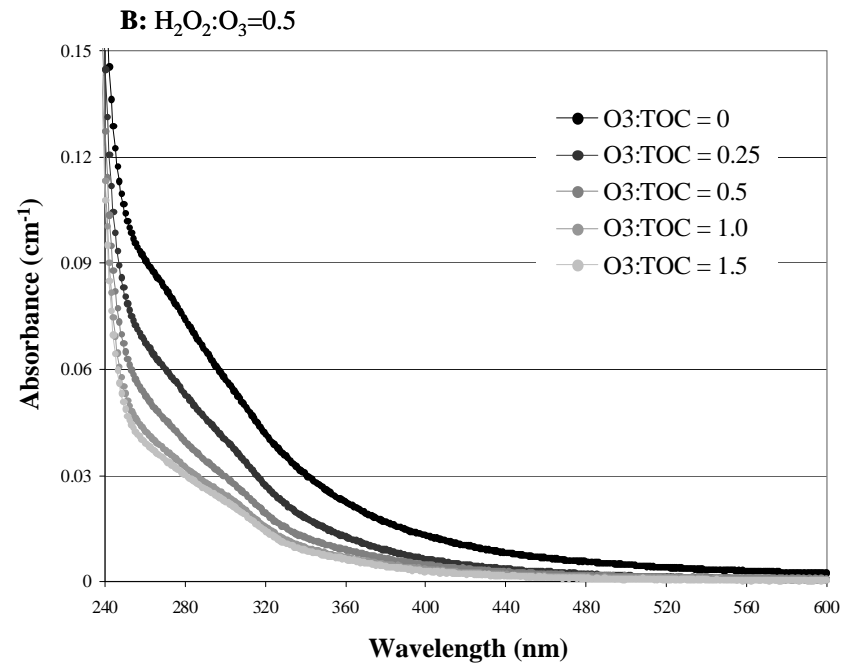
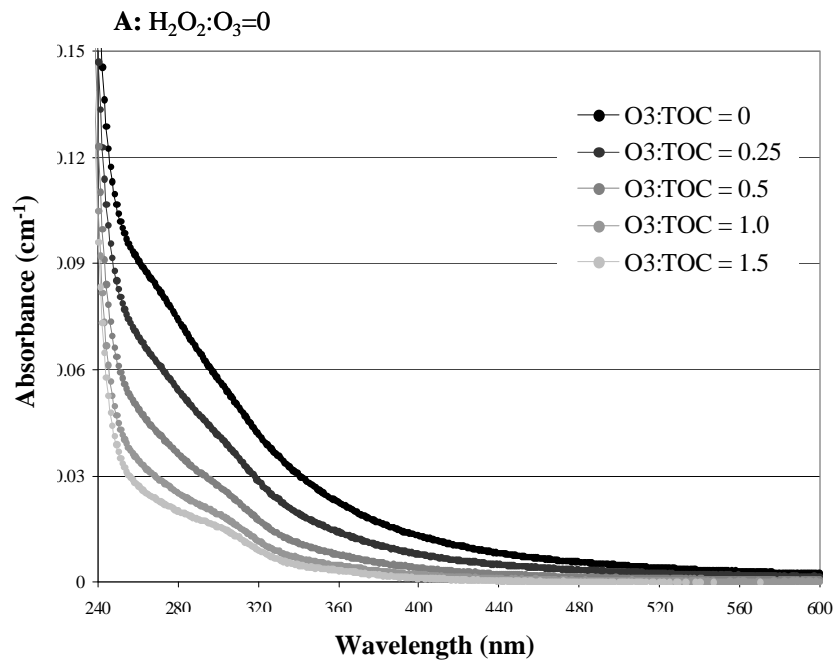


Figure 3.33. MWRDGC absorbance spectra after ozonation (unfiltered).

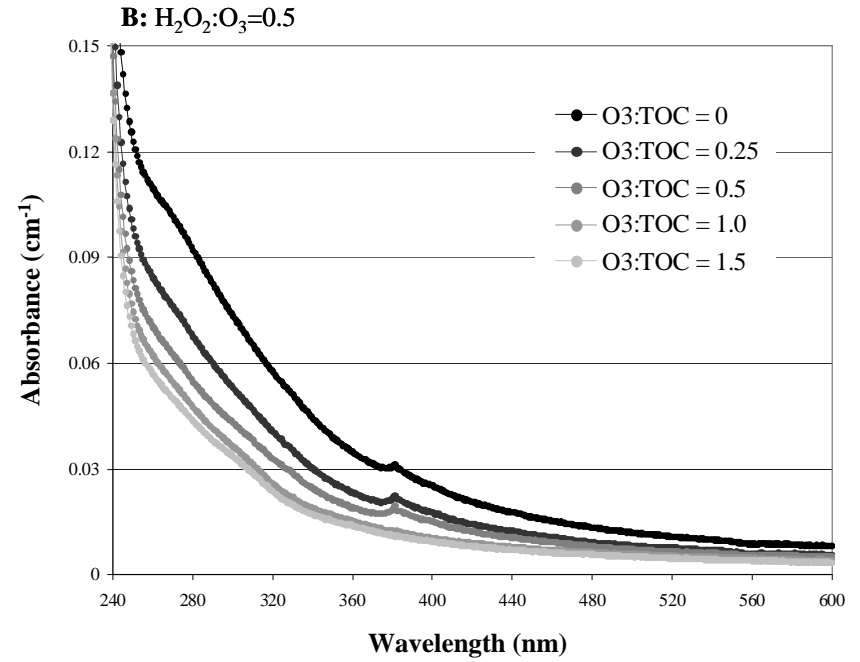
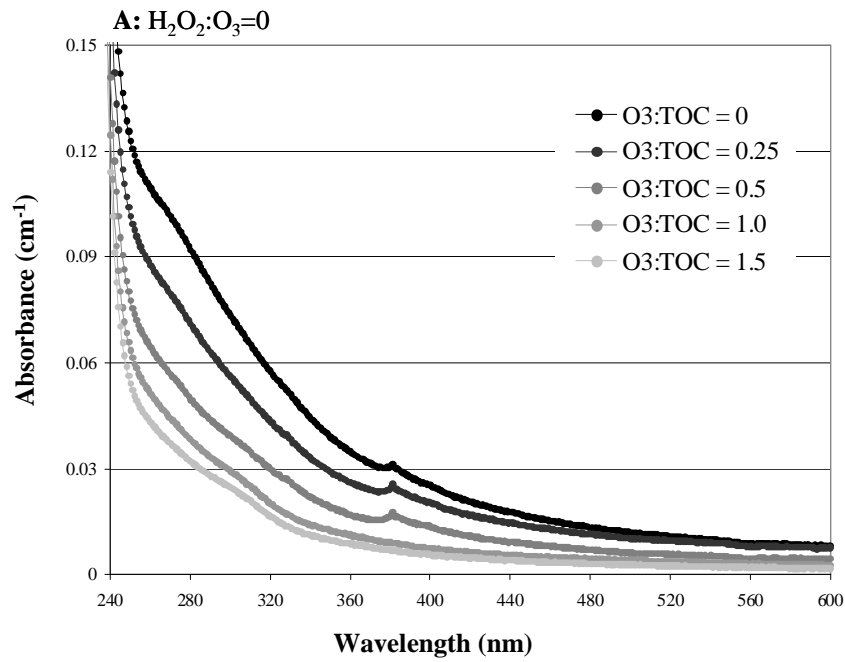


Figure 3.34. MWRDGC absorbance spectra after ozonation (filtered).

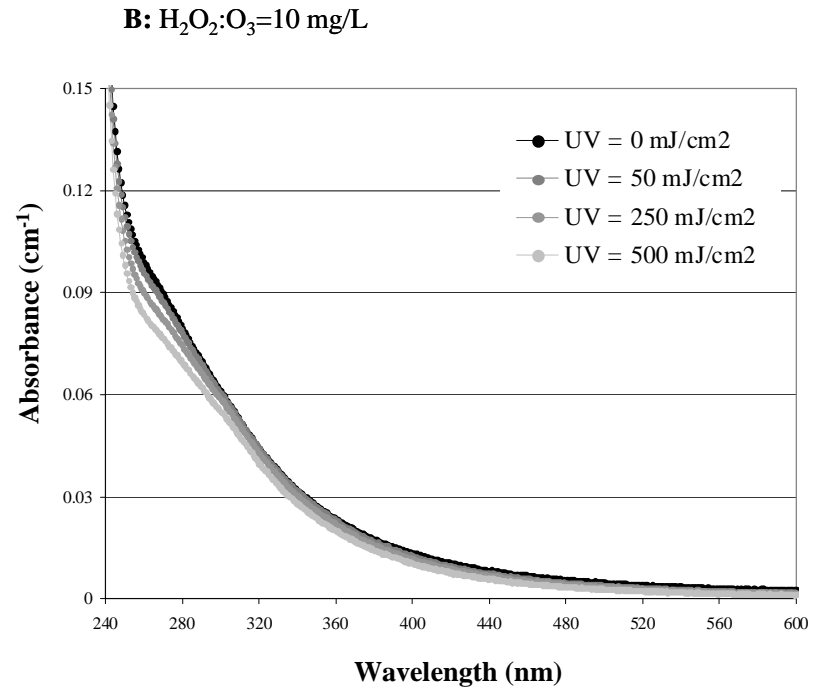
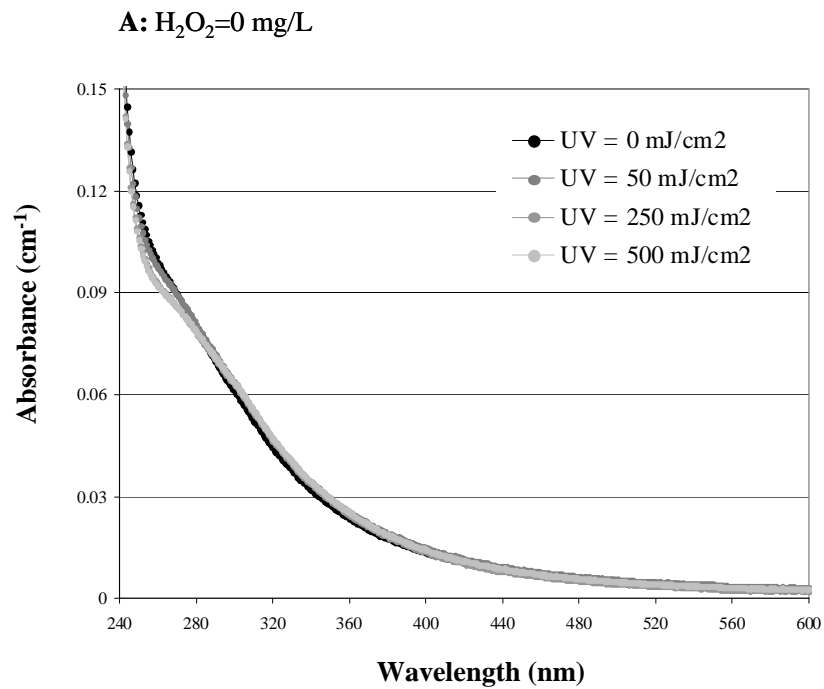


Figure 3.35. MWRDGC absorbance spectra after UV and UV/H<sub>2</sub>O<sub>2</sub>.

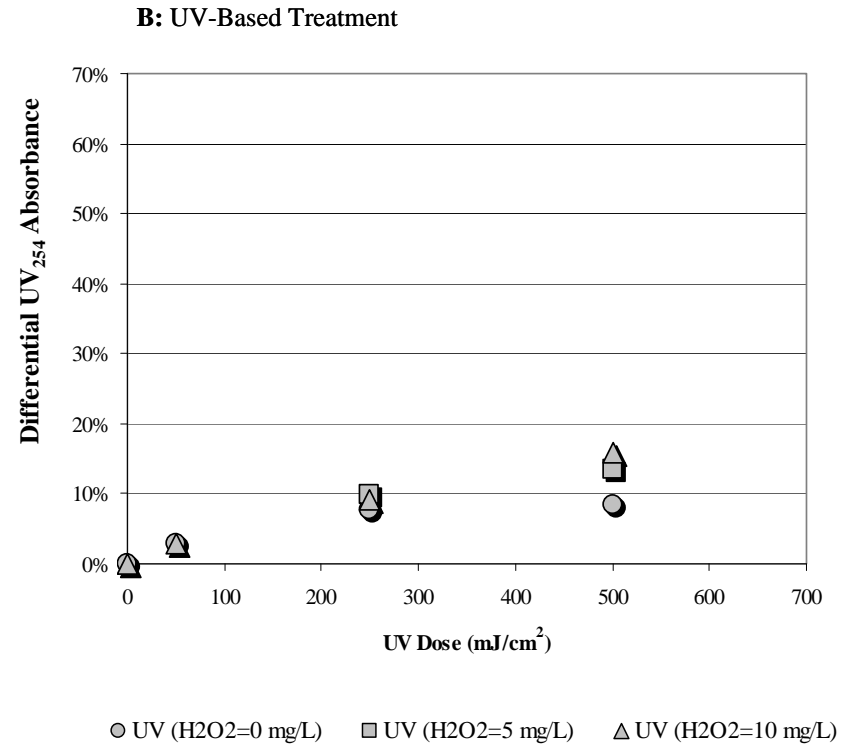
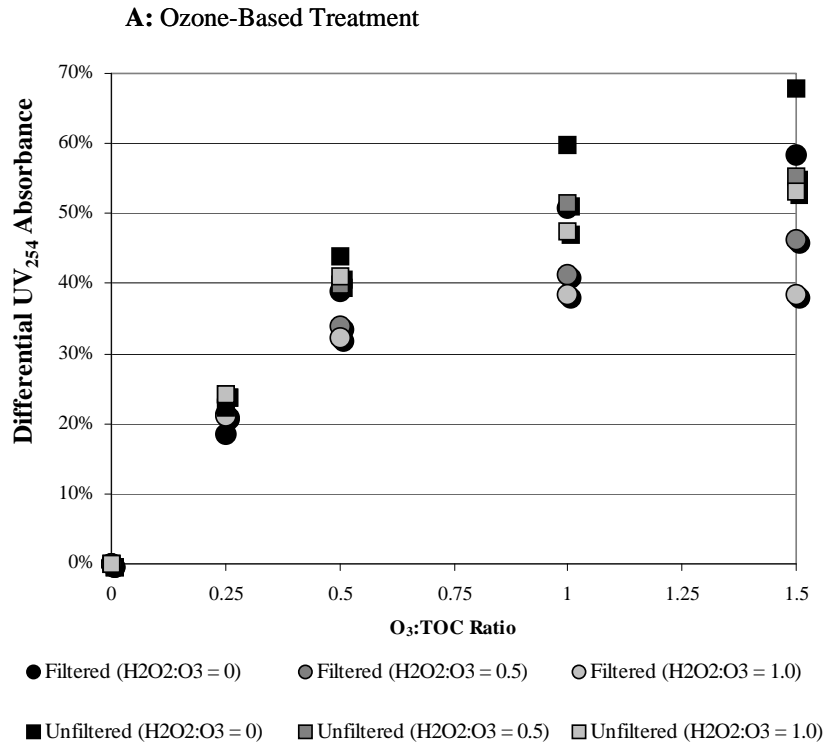


Figure 3.36. Differential UV<sub>254</sub> absorbance in the MWRDGC secondary effluent.

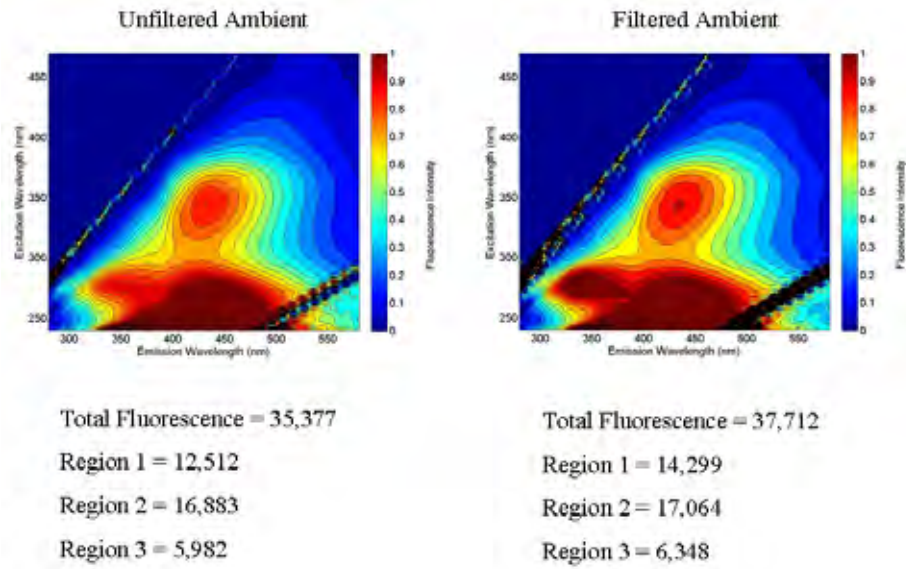


Figure 3.37. 3D EEMs for ambient samples from MWRDGC.

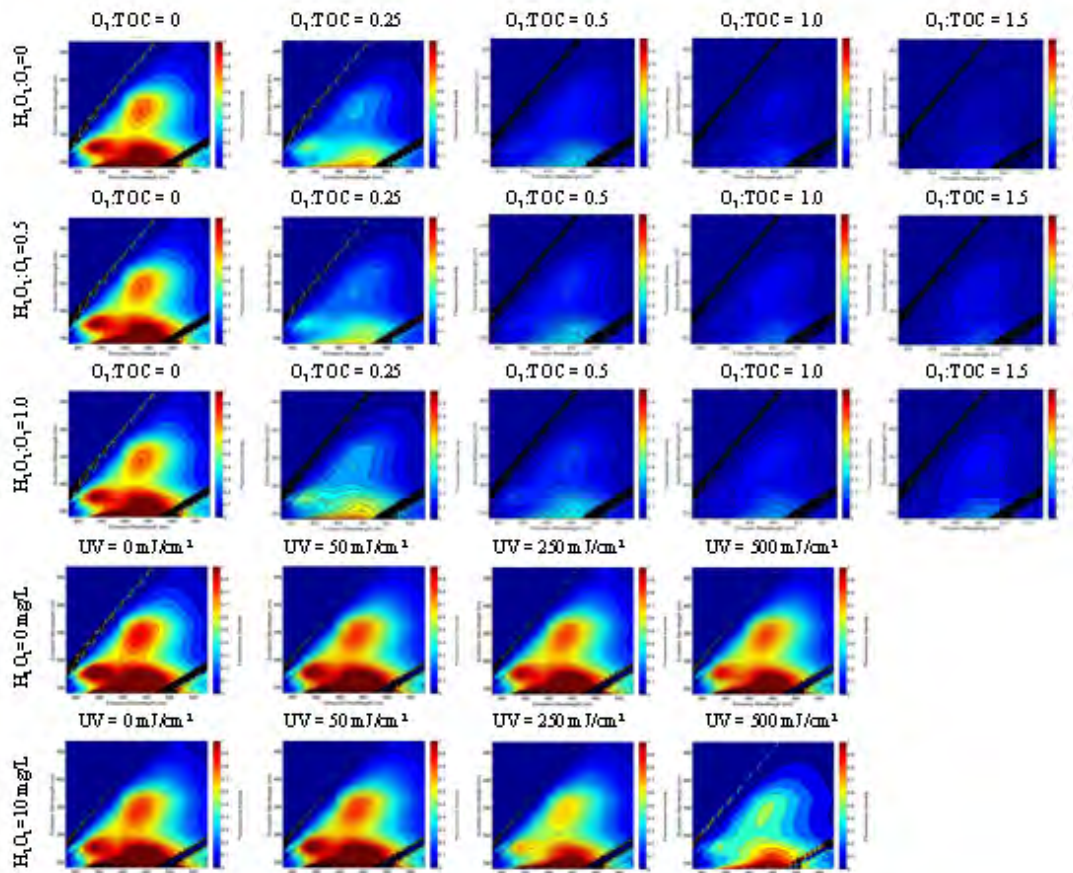


Figure 3.38. 3D EEMs after treatment for the filtered MWRDGC secondary effluent.

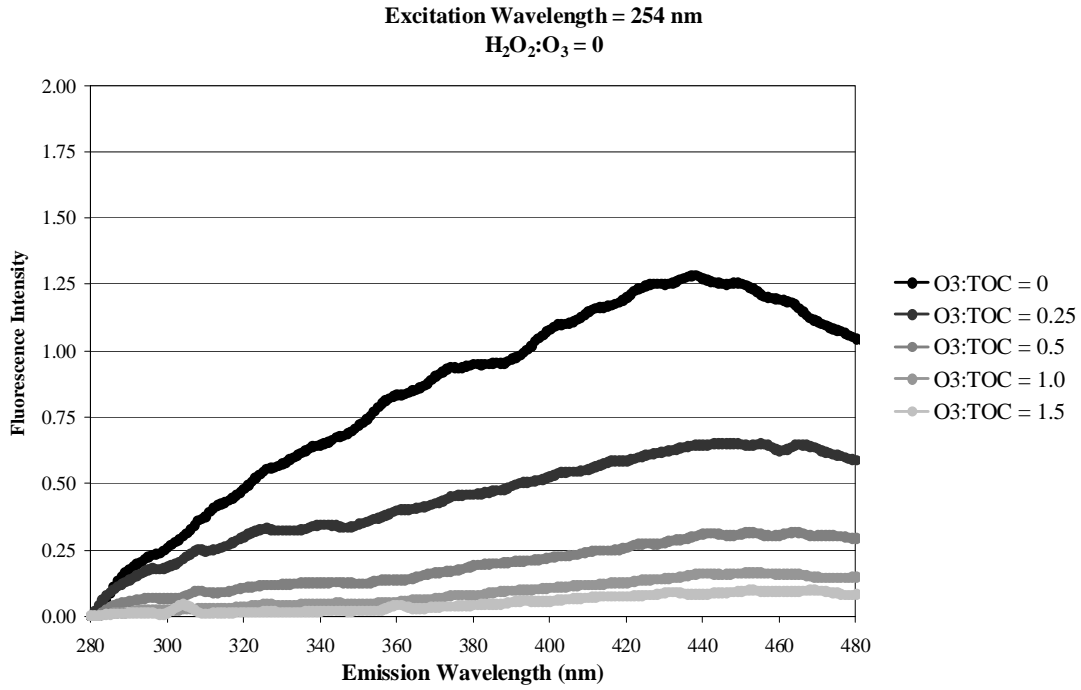


Figure 3.39. MWRDGC fluorescence profiles (Ex<sub>254</sub>) after ozonation.

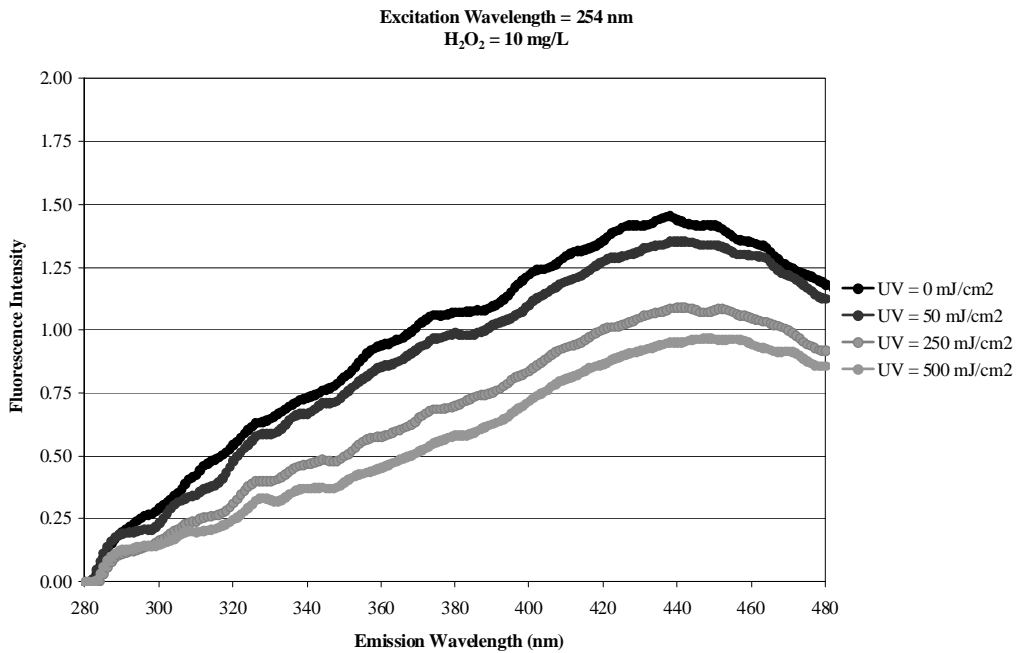


Figure 3.40. MWRDGC fluorescence profiles (Ex<sub>254</sub>) after UV/H<sub>2</sub>O<sub>2</sub>.

Table 3.34 provides the FI (i.e.,  $Ex_{370}Em_{450}/Ex_{370}Em_{500}$ ) and TI (i.e.,  $Ex_{254}Em_{450,T}/Ex_{254}Em_{450,A}$ ) for the MWRDGC experiments. Regarding ozonation, the FI values decreased consistently for  $O_3$ :TOC ratios of 0.25 and 0.5 but started to stabilize with higher ozone doses. In other words, the organic matter associated with emissions at 450 nm experienced more rapid transformation with low ozone doses than the organic matter associated with emissions at 500 nm. Further transformation at higher ozone doses occurred at similar relative rates, thereby stabilizing the FI. These relative changes are illustrated in Figure 3.41, and similar trends are apparent in Figure 3.42, which illustrates the changes in total and regional fluorescence intensities after ozonation. In Figure 3.42, the regional fluorescence intensities associated with soluble microbial products (Region I) and fulvic acids (Region II) decreased at a faster rate than those of the humic acids (Region III).

The TI, which measures the extent of organic transformation, reached as low as 0.04 for the highest  $O_3$ :TOC ratio, thereby indicating that 96% of the original fluorescence had been eliminated. In general, ozonation was slightly less effective in the filtered wastewater as a result of the organic leaching issue, and the addition of  $H_2O_2$  also hindered the ozone process slightly. Because of the limited reduction in fluorescence with UV and UV/ $H_2O_2$ , the corresponding FI and TI values did not change significantly. The corresponding changes in total and regional fluorescence intensities for UV and UV/ $H_2O_2$  are illustrated in Figure 3.43.

**Table 3.34. FI and TI Values for the MWRDGC Secondary Effluent**

Unfiltered Ozone Exposure						
$O_3$ :TOC	$H_2O_2$ : $O_3$ =0		$H_2O_2$ : $O_3$ =0.5		$H_2O_2$ : $O_3$ =1.0	
	FI	TI	FI	TI	FI	TI
0	1.55	1.00	1.55	1.00	1.55	1.00
0.25	1.32	0.45	1.33	0.47	1.40	0.50
0.5	1.26	0.20	1.24	0.22	1.28	0.22
1.0	1.22	0.09	1.26	0.13	1.31	0.14
1.5	1.21	0.04	1.32	0.07	1.32	0.10
Filtered Ozone Exposure						
$O_3$ :TOC	$H_2O_2$ : $O_3$ =0		$H_2O_2$ : $O_3$ =0.5		$H_2O_2$ : $O_3$ =1.0	
	FI	TI	FI	TI	FI	TI
0	1.53	1.00	1.53	1.00	1.53	1.00
0.25	1.33	0.52	1.24	0.44	1.35	0.52
0.5	1.23	0.25	1.26	0.26	1.27	0.29
1.0	1.24	0.13	1.24	0.17	1.27	0.22
1.5	1.29	0.08	1.25	0.15	1.23	0.19
Filtered UV Exposure						
UV Dose (mJ/cm <sup>2</sup> )	$H_2O_2$ =0 mg/L		$H_2O_2$ =5 mg/L		$H_2O_2$ =10 mg/L	
	FI	TI	FI	TI	FI	TI
0	1.53	1.00	1.53	1.00	1.53	1.00
50	1.47	0.97	N/A	N/A	1.48	0.94
250	1.49	0.95	1.47	0.85	1.45	0.76
500	1.45	0.86	1.42	0.81	1.41	0.68

Notes: FI=fluorescence index; N/A=not available; TI=treatment index; UV=ultraviolet

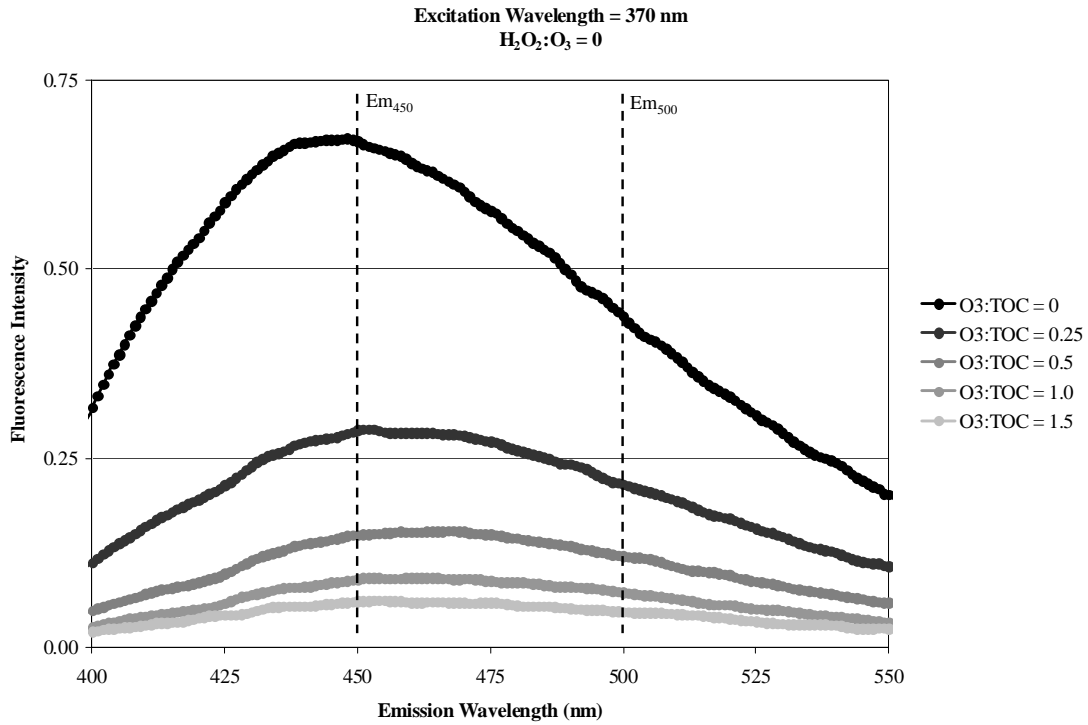


Figure 3.41. MWRDGC fluorescence profiles (Ex<sub>370</sub>) after ozonation.

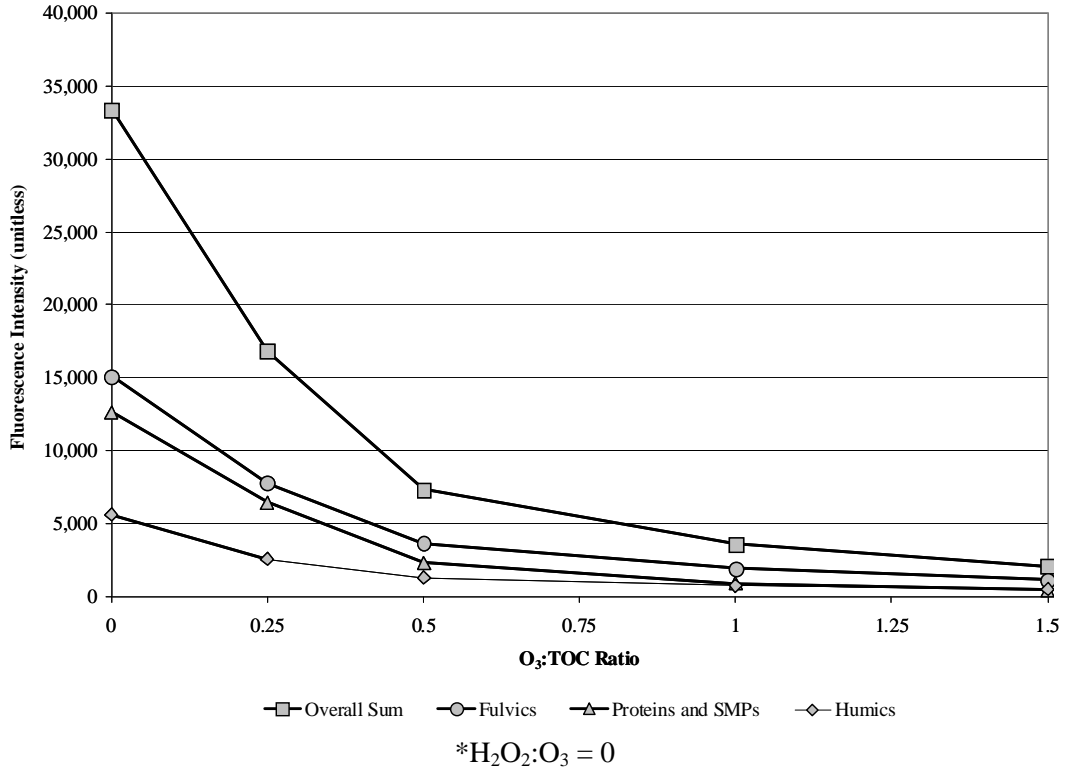


Figure 3.42. Changes in fluorescence intensity after ozonation for MWRDGC.

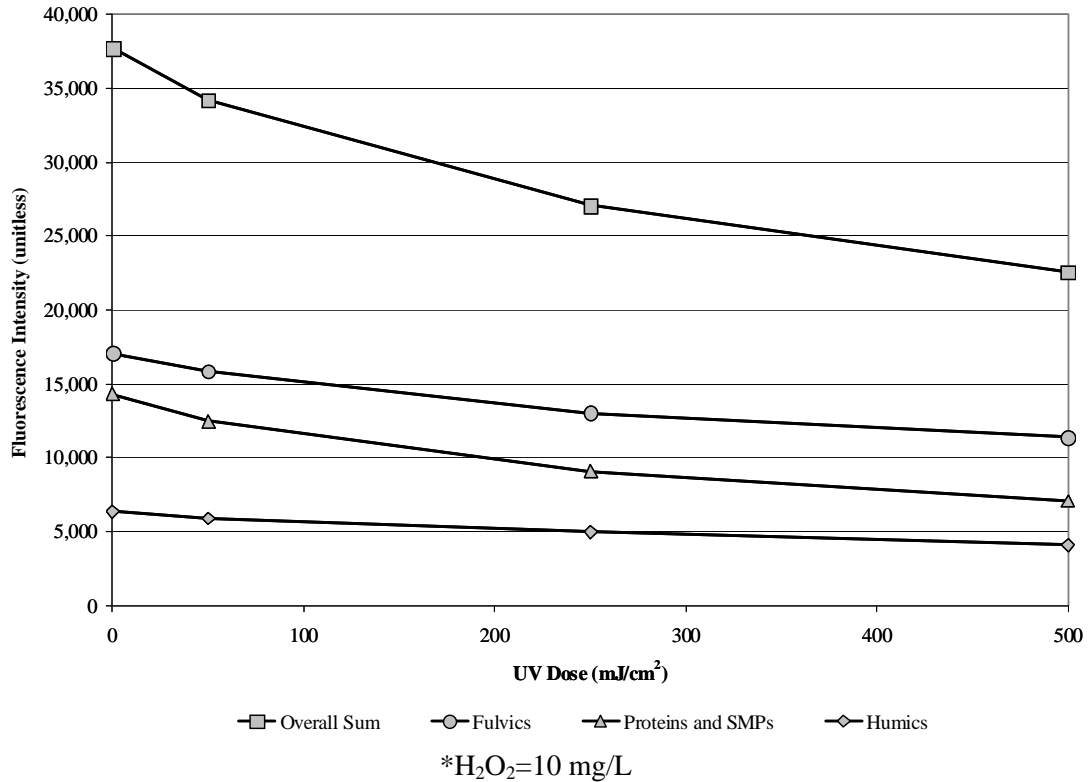


Figure 3.43. Changes in fluorescence intensity after UV/H<sub>2</sub>O<sub>2</sub> for MWRDGC.

### 3.3 West Basin Municipal Water District, Los Angeles, CA

The West Basin Municipal Water District (WBMWD) study site is a water recycling facility that receives secondary effluent from a nearby wastewater treatment plant. The wastewater treatment plant serves four million people and treats approximately 250 to 300 MGD of ~95% municipal wastewater. The liquid treatment train consists of primary clarification with coagulant addition, conventional activated sludge (SRT=1.5 days), and secondary clarification. Approximately 90% of the secondary effluent is discharged to Santa Monica Bay through a 5-mile outfall, and the remaining portion (~30 MGD) is pumped to the water recycling facility for advanced treatment. The advanced treatment can generally be described as two separate treatment trains serving a variety of final uses. One train consists of microfiltration (MF), RO, and UV/H<sub>2</sub>O<sub>2</sub> and is used as a saltwater intrusion barrier and for groundwater recharge.

As required by the CDPH Title 22 requirements, this advanced treatment train must achieve a total of 5-log removal/inactivation of poliovirus or MS2. MF provides 0.5-log removal, RO provides 2-log removal, and a target UV dose of 115 mJ/cm<sup>2</sup> is more than sufficient to achieve the remaining 2.5-log inactivation. The high UV dose is necessary to reach the NDMA NL of 10 ng/L, and the H<sub>2</sub>O<sub>2</sub> (3 mg/L) is required as an added barrier against unknown compounds that may be present in the RO permeate. Industrial customers receive water of a similar quality, but that stream is not treated with UV/H<sub>2</sub>O<sub>2</sub> (i.e., MF-RO or MF-RO-RO). The treatment train with conventional unit processes is described as a “Title 22” product and used for reclaimed water distribution systems. The sodium hypochlorite process

targets a residual of at least 4.1 mg/L to achieve a CT value of 450 mg/min/L, as required by Title 22. Simplified treatment schematics for the wastewater treatment plant and water recycling facility are provided in Figure 3.44.

The WBMWD facility is also piloting an ozone system as pretreatment for its MF process. The wastewater treatment plant sometimes experiences rapid irreversible fouling of its MF membranes, but the ozone pilot has demonstrated success in reducing transmembrane pressures by transforming the organic matter responsible for the fouling.

Influent from the WBMWD study site (i.e., secondary effluent from the associated wastewater treatment plant) was collected in September 2010, and the initial water quality data in Table 3.35 were obtained. Effluent samples from the MF-RO-UV/H<sub>2</sub>O<sub>2</sub> treatment train were also analyzed, and these data are reported as finished effluent. Using the initial TOC and nitrite data for the filtered secondary effluent, the ozone dosing conditions in Table 3.36 were calculated.

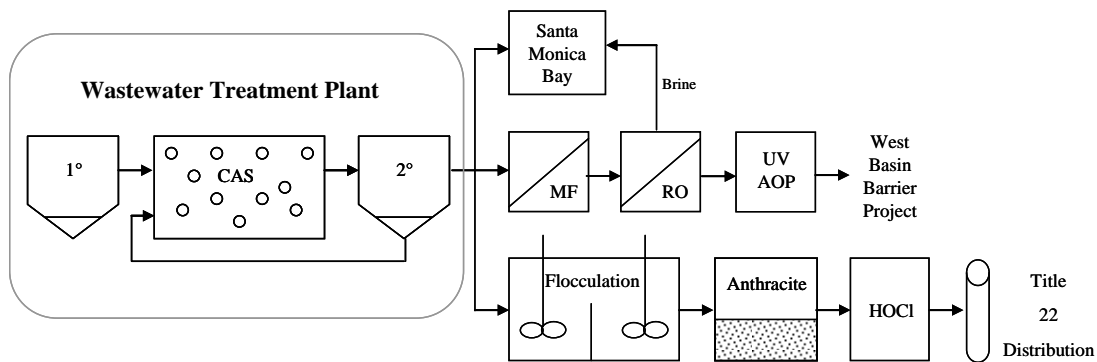


**Figure 3.44. Simplified treatment schematic for WBMWD.**

**Table 3.35. Initial Water Quality Data for WBMWD**

<b>Unfiltered Secondary Effluent</b>	alkalinity (mg/L CaCO <sub>3</sub> )	332
	bromide (µg/L)	409
	NDMA (ng/L)	20
	NH <sub>3</sub> (mg N/L)	46.9
	NO <sub>2</sub> (mg N/L)	0.17
	NO <sub>3</sub> (mg N/L)	0.11
	pH	7.3
	TKN (mg N/L)	46.9
	TN (mg N/L)	47.2
	TOC (mg/L)	15
	TON (mg N/L)	~0
	TSS (mg/L)	6.3
	turbidity (NTU)	3.38
<b>Filtered Secondary Effluent</b>	pH	7.3
	TOC (mg/L)	18
	TSS (mg/L)	<5
	turbidity (NTU)	2.65
	UV <sub>254</sub> absorbance (cm <sup>-1</sup> )	0.268
<b>Finished Effluent</b>	NDMA (ng/L)	6.5
	TOC (mg/L)	0.21
	UV <sub>254</sub> absorbance (cm <sup>-1</sup> )	0.018

*Notes:* NDMA=N-nitrosodimethylamine; TKN=total Kjeldahl nitrogen, sum of TON and ammonia; TN=total nitrogen; TOC=total organic carbon; TON=total organic nitrogen, difference of TN and ammonia, nitrate, and nitrite; TSS=total suspended solids

**Table 3.36. Ozone Dosing Conditions for 1-L Filtered WBMWD Samples**

Concentration of O<sub>3</sub> stock solution=86 mg/L  
 Concentration of H<sub>2</sub>O<sub>2</sub> stock solution=10 g/L  
 Filtered dilution ratio=(758/1000)=0.758  
 Filtered TOC after dilution=13.6 mg/L  
 Filtered NO<sub>2</sub> after dilution=0.13 mg/L as N=0.42 mg/L as NO<sub>2</sub>

O <sub>3</sub> :TOC/ H <sub>2</sub> O <sub>2</sub> :O <sub>3</sub>	Wastewater Volume (mL)	Nanopure Volume (mL)	O <sub>3</sub> Volume (mL)	O <sub>3</sub> Dose (mg/L)	H <sub>2</sub> O <sub>2</sub> Volume (μL)	H <sub>2</sub> O <sub>2</sub> Dose (mg/L)
Spike	758	242	0	0	0	0
0.25/0	758	198	44	3.8	0	0
0.25/0.5	758	198	44	3.8	124	1.2
0.25/1.0	758	198	44	3.8	248	2.5
0.5/0	758	159	83	7.2	0	0
0.5/0.5	758	159	83	7.2	245	2.5
0.5/1.0	758	159	83	7.2	490	4.9
1.0/0	758	79	163	14.0	0	0
1.0/0.5	758	79	163	14.0	487	4.9
1.0/1.0	758	79	163	14.0	975	9.8
1.5/0	758	0	242	20.8	0	0
1.5/0.5	758	0	242	20.8	730	7.3
1.5/1.0	758	0	242	20.8	1,459	14.6

Note: \*=Some values are affected by rounding error and the precision of the ozone spike.

### 3.3.1 Ozone Demand/Decay

Figure 3.45 illustrates the ozone demand/decay curves for the filtered WBMWD secondary effluent at various dosing conditions. The graph only includes dosing conditions with a measurable ozone residual after 30 seconds; corresponding CT values are also provided. As discussed earlier, the O<sub>3</sub>/H<sub>2</sub>O<sub>2</sub> samples are not included in the figure because the addition of H<sub>2</sub>O<sub>2</sub> led to the formation of •OH but eliminated the dissolved ozone residual. Because of reactions with EfOM, the 0.25 O<sub>3</sub>:TOC ratio was insufficient to establish a measurable ozone residual after 30 seconds. For the remaining dosing conditions, the graph illustrates the IOD (i.e., the precipitous drop between 0 and 30 seconds) and the decay over time. Although the applied ozone doses were significantly higher for WBMWD as compared to CCWRD and MWRDGC, the higher TOC concentration and ozone demand yielded CT values that were comparable to the other data sets.

### 3.3.2 Bromate Formation

As illustrated in Figure 3.46, bromate formation was considerably higher in the WBMWD secondary effluent as compared to CCWRD and MWRDGC because of the higher initial bromide concentration. The O<sub>3</sub>:TOC ratio of 0.25 was the only dosing condition that satisfied the 10 μg/L benchmark, whereas the highest dosing condition yielded a bromate concentration of 200 μg/L. The addition of H<sub>2</sub>O<sub>2</sub> provided some bromate mitigation for the lower applied ozone doses, but H<sub>2</sub>O<sub>2</sub> addition was associated with the highest level of bromate formation as well. In order to achieve the 10 μg/L treatment objective, the applied ozone dose would be limited to an O<sub>3</sub>:TOC ratio <0.25, or the process would have to be supplemented with substantial H<sub>2</sub>O<sub>2</sub> doses. The required H<sub>2</sub>O<sub>2</sub> dose for high O<sub>3</sub>:TOC ratios would likely be cost prohibitive unless other mitigation measures were employed.

### 3.3.3 Hydroxyl Radical Exposure

Based on data from bench-scale experiments with pCBA spiked at approximately 500 µg/L, Table 3.37 indicates the overall •OH exposure for each ozone and UV dosing condition. The •OH exposures for the UV/H<sub>2</sub>O<sub>2</sub> samples are corrected for the small level of pCBA degradation achieved by photolysis alone.

In contrast to CCWRD and MWRDGC, H<sub>2</sub>O<sub>2</sub> addition yielded higher overall •OH exposure at O<sub>3</sub>:TOC ratios of 1.0 and 1.5. Ozone-based oxidation also provided higher •OH exposures than the UV dosing conditions applied during these experiments. The poor water quality even necessitated UV doses greater than 500 mJ/cm<sup>2</sup> (with 10 mg/L H<sub>2</sub>O<sub>2</sub>) to achieve an •OH exposure similar to that of an O<sub>3</sub>:TOC ratio of 0.25.

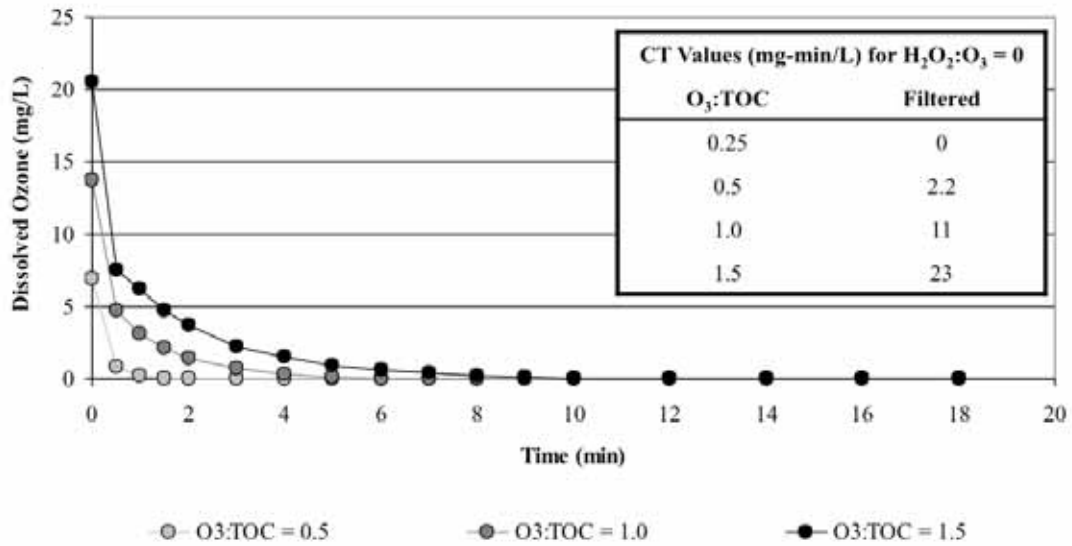


Figure 3.45. Ozone demand/decay curves for WBMWD (filtered).

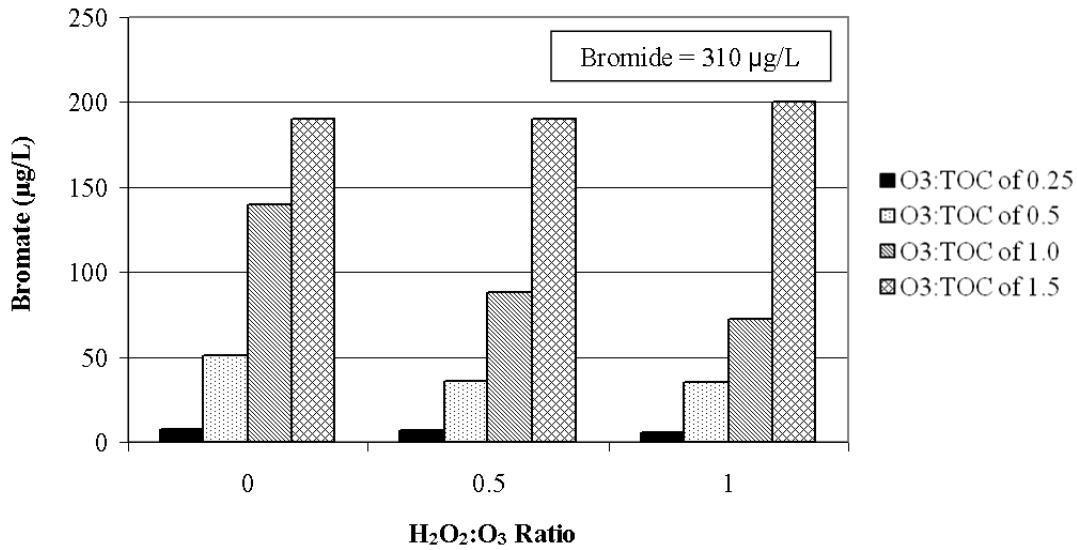


Figure 3.46. Bromate formation during ozonation of WBMWD secondary effluent.

Table 3.37. •OH Exposure in the WBMWD Secondary Effluent

Filtered Ozone Exposure ( $10^{-11}$ M-s)			
Ozone:TOC	H <sub>2</sub> O <sub>2</sub> :O <sub>3</sub> =0	H <sub>2</sub> O <sub>2</sub> :O <sub>3</sub> =0.5	H <sub>2</sub> O <sub>2</sub> :O <sub>3</sub> =1.0
0.25	7.8	7.9	8.4
0.5	20	21	23
1.0	49	63	60
1.5	73	96	94

Filtered UV Exposure ( $10^{-11}$ M-s)			
UV Dose (mJ/cm <sup>2</sup> )	H <sub>2</sub> O <sub>2</sub> =0 mg/L	H <sub>2</sub> O <sub>2</sub> =5 mg/L	H <sub>2</sub> O <sub>2</sub> =10 mg/L
0	N/A	N/A	0.0*
50	N/A	N/A	0.0
250	N/A	1.2	4.6
500	N/A	3.7	7.2

Notes: \*=based on H<sub>2</sub>O<sub>2</sub> control; UV=ultraviolet

### 3.3.4 Title 22 Contaminants

Bench-scale experiments were performed with the filtered WBMWD wastewater to evaluate the use of ozone and UV for the destruction of spiked NDMA (300 ng/L) and 1,4-dioxane (1 mg/L). In fact, the secondary effluent already contained 20 ng/L of NDMA prior to the spikes, whereas the MF-RO-UV/H<sub>2</sub>O<sub>2</sub> effluent contained 6.5 ng/L. Figure 3.47 indicates that UV doses ranging from 500 to 550 mJ/cm<sup>2</sup> were required to satisfy the Title 22 NDMA requirement. NDMA destruction with ozone proved to be completely impractical because of substantial direct NDMA formation (up to 150 ng/L), as indicated in Table 3.38. It is unclear what exactly contributed to this direct NDMA formation, but preliminary testing (data not shown) supported by the literature suggests that specific organic precursors are the most likely culprit. Because this wastewater was non-nitrified with minimal biotransformation and biodegradation of TOxCs, the tremendous NDMA yields are certainly plausible.

Figure 3.48 illustrates the destruction of spiked 1,4-dioxane during the bench-scale ozone experiments. The superior performance of the ozone/H<sub>2</sub>O<sub>2</sub> samples supports the previously reported pCBA data, which indicated that H<sub>2</sub>O<sub>2</sub> addition provided a slight benefit for overall •OH exposure. For WBMWD, O<sub>3</sub>:TOC ratios between 1.0 and 1.2 are necessary to comply with the 0.5-log requirement.

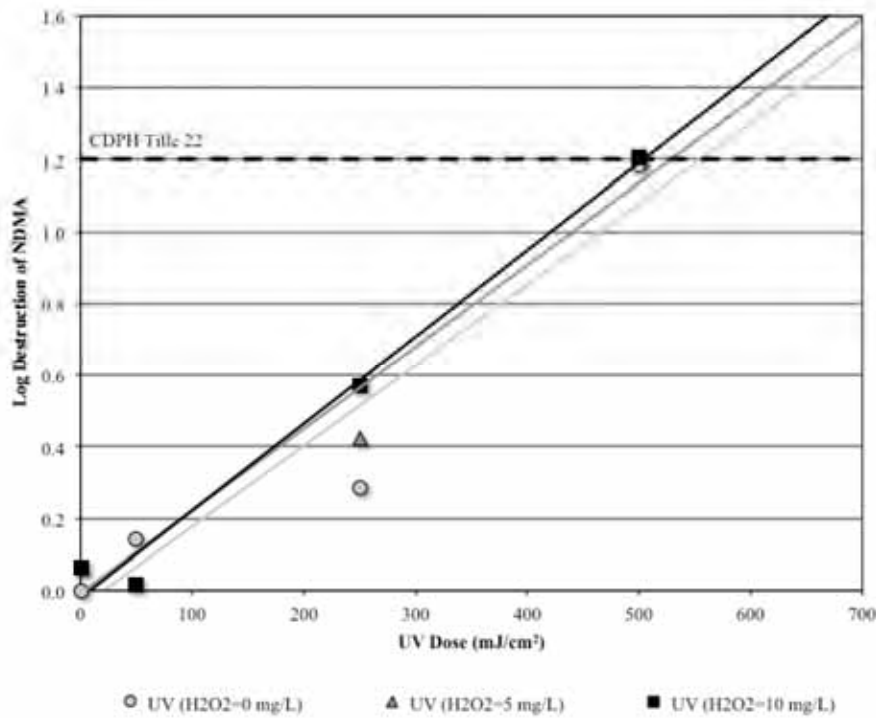
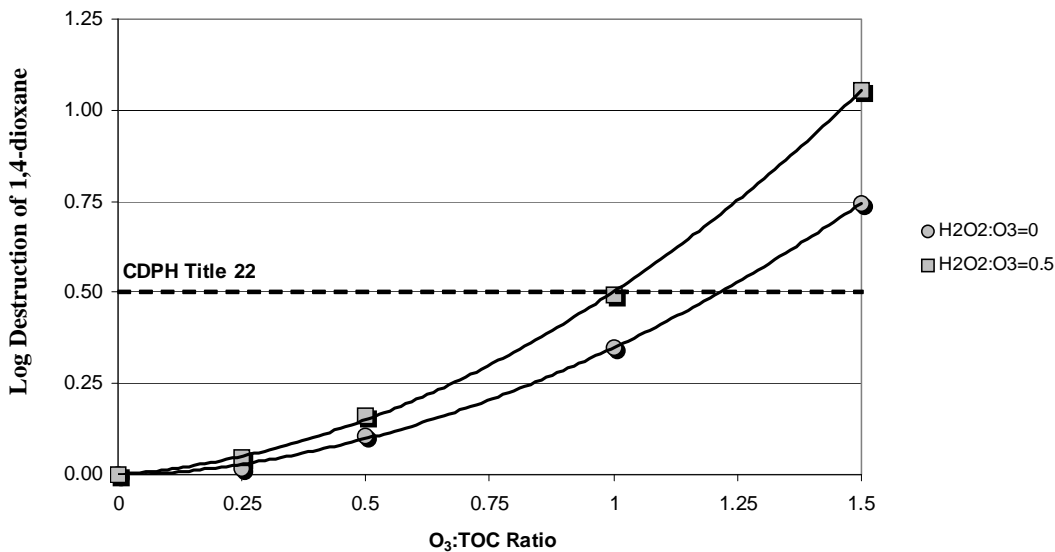


Figure 3.47. Destruction of NDMA in the filtered WBMWD secondary effluent.

**Table 3.38. Direct NDMA Formation in the Filtered WBMWD Secondary Effluent**

O <sub>3</sub> :TOC Ratio	H <sub>2</sub> O <sub>2</sub> :O <sub>3</sub> Ratio	NDMA (ng/L)
0	0	20
0.5	0	170
0.5	0.5	170
1.0	0	160
1.0	0.5	140



**Figure 3.48. Destruction of 1,4-dioxane in the filtered WBMWD secondary effluent.**

### 3.3.5 Trace Organic Contaminants

Secondary and finished (i.e., MF-RO-UV/H<sub>2</sub>O<sub>2</sub>) effluent samples from WBMWD were analyzed to determine the ambient concentrations of the target compounds, which are provided in Table 3.39. The effect of SRT during secondary treatment is quite apparent when comparing the secondary effluent concentrations of WBMWD with those of CCWRD and MWRDGC. The 1.5-day SRT provided minimal biological mitigation of TOrcs, which resulted in relatively high secondary effluent concentrations for all of the target compounds. In fact, even the highly bioamenable compounds (i.e., ibuprofen and naproxen) that were <MRL for CCWRD and MWRDGC were present at reportable concentrations in this water matrix. Furthermore, many of the target compounds were present at concentrations approaching 1 µg/L, and two of the compounds were present at concentrations exceeding 2 µg/L; however, it is important to note that despite the high concentrations relative to other secondary effluents, these concentrations likely pose little threat to public health. Atrazine, which is the only regulated contaminant on the target compound list, was even <MRL in the

secondary effluent. The total estrogenicity of the secondary effluent was determined to be 0.56 ng/L, but this number should be interpreted with caution because the highly concentrated secondary effluent may have had cytotoxic effects on the yeast cell line.

Finally, the multibarrier IPR treatment train achieved substantial removals for each of the target compounds, and all but one compound (bisphenol A) was <MRL after MF-RO-UV/H<sub>2</sub>O<sub>2</sub>. The exact reason for the breakthrough of bisphenol A is unclear, but it may have been an isolated occurrence captured by a single grab sample. Although bisphenol A is highly susceptible to biological treatment, little biotransformation was expected based on the low SRT. This compound is also relatively resistant to UV photolysis, but its •OH rate constant is relatively high, so there should have been significant destruction in the UV/H<sub>2</sub>O<sub>2</sub> process. It is important to note that there was no indication of sample contamination based on the experimental controls. More frequent sampling would be necessary to determine whether bisphenol A breakthrough is a significant problem in this system. Regardless, MF-RO-UV/H<sub>2</sub>O<sub>2</sub> is clearly an effective barrier against TOrC contamination in IPR applications.

**Table 3.39. Ambient TOrC Concentrations at WBMWD**

Parameter	Secondary Effluent (ng/L)	Finished Effluent (ng/L)
Atenolol	2100	<25
Atrazine	<10	<10
Bisphenol A	280	86
Carbamazepine	260	<10
Diclofenac	280	<25
DEET	640	<25
Gemfibrozil	2500	<10
Ibuprofen	47	<25
Meprobamate	290	<10
Musk ketone	<100	<100
Naproxen	320	<25
Phenytoin	160	<10
Primidone	96	<10
Sulfamethoxazole	700	<25
TCEP	630	<200
Total estrogenicity (EEq)	0.56	<0.074
Triclosan	150	<25
Trimethoprim	700	<10

Notes: DEET=*N,N*-diethyl-*meta*-toluamide; EEq=estradiol equivalents; TCEP=tris-(2-chloroethyl)-phosphate

Bench-scale TOxC oxidation experiments were performed with protocols and spiking stocks similar to those described for the previous wastewater matrices. A comparison of filtered versus unfiltered wastewater was not performed. Table 3.40 shows the relative oxidation levels of the 16 target compounds (musk ketone omitted) after ozonation. In contrast to the previous data sets, Table 3.40 supports the conclusion from the pCBA experiment (see Table 3.37) that H<sub>2</sub>O<sub>2</sub> addition increased •OH exposure at higher O<sub>3</sub>:TOC ratios. The impact of H<sub>2</sub>O<sub>2</sub> was most apparent for the ozone-resistant compounds (Groups 3, 4, and 5) and O<sub>3</sub>:TOC ratios of 1.0 and 1.5; however, the benefit was minimal and likely insufficient to warrant H<sub>2</sub>O<sub>2</sub> addition for this reason alone.

As described earlier, the target compounds were divided into five categories based on their second-order ozone and •OH rate constants. As highlighted by the shaded cells, in particular, the relative levels of oxidation were similar during the MWRDGC and WBMWD experiments. All of the Group 1 compounds were oxidized greater than 80% at an O<sub>3</sub>:TOC ratio of 0.25, and both of the Group 2 compounds were oxidized greater than 80% with an O<sub>3</sub>:TOC ratio of 0.5. Groups 3 and 4 required O<sub>3</sub>:TOC ratios of 1.0 and 1.5 to exceed 80% oxidation. Similar to the previous data sets, TCEP proved to be extremely resistant to ozonation, as the level of oxidation never exceeded 35%.

Table 3.41 shows the relative photolysis and UV/H<sub>2</sub>O<sub>2</sub> oxidation levels of the target compounds. Again, UV photolysis was quite ineffective in destroying the target compounds. Only two compounds (diclofenac and triclosan) experienced greater than 80% destruction with UV irradiation alone, whereas atrazine, phenytoin, and sulfamethoxazole experienced at least 25% destruction with UV alone. Photolysis appeared to be quite effective for DEET, meprobamate, and TCEP, but these numbers appear to be erroneous because they do not increase with increasing UV dose. The addition of H<sub>2</sub>O<sub>2</sub> with a UV dose of 500 mJ/cm<sup>2</sup> was also able to achieve 70% destruction of sulfamethoxazole, whereas a majority of the remaining compounds achieved destruction levels ranging from 20 to 50%.

Finally, the total estrogenicity of the secondary effluent was oxidized down to the MRL with every ozone and ozone/H<sub>2</sub>O<sub>2</sub> dosing condition. On the other hand, neither UV nor UV/H<sub>2</sub>O<sub>2</sub> was particularly effective for reducing total estrogenicity, as the highest dosing conditions were unable to achieve the MRL for the YES assay. These results are summarized in Figure 3.49.

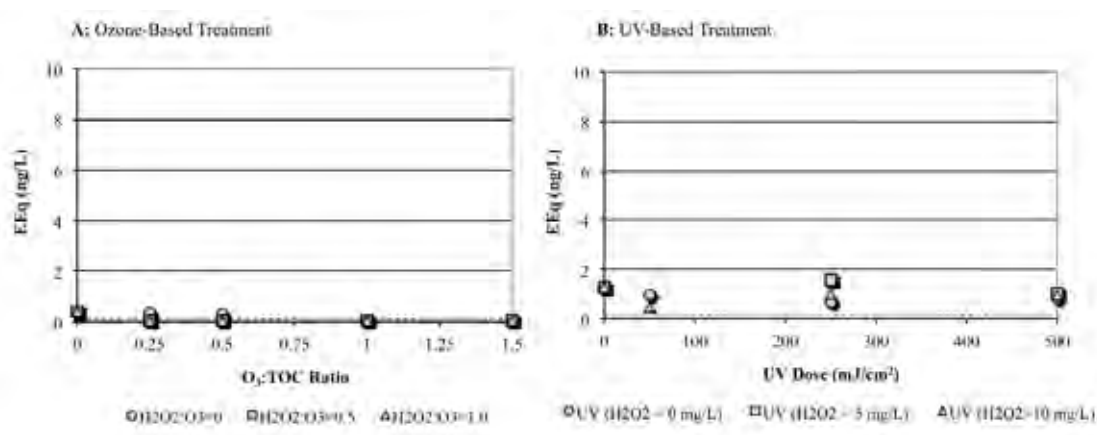


Figure 3.49. Reduction in total estrogenicity in the WBMWD secondary effluent.

**Table 3.40. WBMWD TOxC Mitigation by Ozone (Filtered)**

Group	Contaminant	O <sub>3</sub> :TOC (mass) / H <sub>2</sub> O <sub>2</sub> :O <sub>3</sub> (molar)											
		0.25/0	0.25/0.5	0.25/1.0	0.5/0	0.5/0.5	0.5/1.0	1.0/0	1.0/0.5	1.0/1.0	1.5/0	1.5/0.5	1.5/1.0
1	Bisphenol A	98%	98%	94%	98%	98%	98%	98%	98%	98%	98%	98%	98%
	Carbamazepine	99%	92%	85%	99%	99%	99%	99%	99%	99%	99%	99%	99%
	Diclofenac	98%	96%	91%	98%	98%	98%	98%	98%	98%	98%	98%	98%
	Naproxen	98%	93%	89%	98%	98%	98%	98%	98%	98%	98%	98%	98%
	Sulfamethoxazole	87%	83%	79%	98%	96%	95%	98%	98%	98%	98%	98%	98%
	Triclosan	97%	96%	94%	97%	97%	97%	97%	97%	97%	97%	97%	97%
	Trimethoprim	99%	93%	87%	99%	99%	99%	99%	99%	99%	99%	99%	99%
	<b>Indicator</b>	<b>97%</b>	<b>93%</b>	<b>88%</b>	<b>98%</b>								
2	Atenolol	44%	44%	44%	96%	86%	82%	99%	99%	99%	99%	99%	99%
	Gemfibrozil	89%	77%	73%	99%	99%	98%	99%	99%	99%	99%	99%	99%
	<b>Indicator</b>	<b>67%</b>	<b>61%</b>	<b>59%</b>	<b>98%</b>	<b>93%</b>	<b>90%</b>	<b>99%</b>	<b>99%</b>	<b>99%</b>	<b>99%</b>	<b>99%</b>	<b>99%</b>
3	DEET	35%	35%	35%	63%	68%	69%	92%	96%	96%	99%	99%	99%
	Ibuprofen	51%	44%	52%	75%	79%	80%	97%	98%	98%	98%	98%	98%
	Phenytoin	47%	44%	44%	72%	76%	77%	97%	99%	98%	99%	99%	99%
	Primidone	37%	32%	37%	65%	71%	68%	93%	97%	96%	99%	99%	99%
	<b>Indicator</b>	<b>43%</b>	<b>39%</b>	<b>42%</b>	<b>69%</b>	<b>74%</b>	<b>74%</b>	<b>95%</b>	<b>98%</b>	<b>97%</b>	<b>99%</b>	<b>99%</b>	<b>99%</b>
4	Atrazine	18%	12%	21%	36%	39%	40%	68%	77%	75%	87%	93%	93%
	Meprobamate	22%	22%	28%	43%	48%	49%	78%	86%	84%	92%	97%	97%
	<b>Indicator</b>	<b>20%</b>	<b>17%</b>	<b>25%</b>	<b>40%</b>	<b>44%</b>	<b>45%</b>	<b>73%</b>	<b>82%</b>	<b>80%</b>	<b>90%</b>	<b>95%</b>	<b>95%</b>
5	TCEP	-19%	2%	6%	10%	15%	5%	18%	24%	23%	24%	34%	35%

Notes: Shading represents >80% oxidation; DEET=*N,N*-diethyl-*meta*-toluamide; TCEP=tris-(2-chloroethyl)-phosphate

**Table 3.41. WBMWD TOrC Mitigation by UV (Filtered)**

Group	Contaminant	UV Dose (mJ/cm <sup>2</sup> ) / H <sub>2</sub> O <sub>2</sub> Dose (mg/L)								
		50/0	50/10	250/0	250/5	250/10	500/0	500/5	500/10	
1	Bisphenol A	5%	0%	0%	0%	0%	5%	10%	30%	
	Carbamazepine	-15%	0%	-23%	7%	7%	-15%	13%	27%	
	Diclofenac	39%	4%	92%	85%	89%	98%	97%	97%	
	Naproxen	7%	0%	7%	8%	15%	7%	23%	39%	
	Sulfamethoxazole	7%	-15%	49%	36%	42%	67%	68%	70%	
	Triclosan	17%	14%	78%	64%	76%	90%	90%	91%	
	Trimethoprim	5%	0%	0%	5%	5%	0%	5%	21%	
2	Atenolol	0%	0%	-3%	7%	17%	-7%	0%	23%	
	Gemfibrozil	3%	6%	0%	12%	15%	6%	18%	23%	
3	DEET	17%	0%	17%	5%	10%	4%	5%	20%	
	Ibuprofen	9%	0%	9%	7%	10%	9%	19%	29%	
	Phenytoin	16%	5%	35%	23%	30%	55%	48%	51%	
	Primidone	5%	-6%	0%	11%	6%	5%	-11%	0%	
4	Atrazine	-9%	0%	11%	17%	18%	27%	36%	39%	
	Meprobamate	29%	3%	31%	6%	6%	32%	3%	14%	
5	TCEP	14%	0%	13%	-4%	-4%	11%	7%	0%	

Notes: \*=groupings based on ozone and OH rate constants; shading represents >80% photolysis or oxidation; DEET=*N,N*-diethyl-*meta*-toluamide; TCEP=tris-(2-chloroethyl)-phosphate

### 3.3.6 Disinfection

Ambient secondary (before and after laboratory filtration) and finished effluent samples were assayed for total and fecal coliforms, MS2, and *Bacillus* spores. The ambient microbial water quality data are provided in Table 3.42. In comparison to the previous data sets, the number of indigenous microbes was slightly higher for WBMWD, and MS2 was even detected in the secondary effluent without filter concentration. In order to illustrate a wide range of inactivation, the ozone and UV disinfection samples were spiked with relatively high numbers of the surrogate microbes, as indicated in Table 3.43.

Figure 3.50 illustrates the inactivation of spiked *E. coli* during the bench-scale ozone experiments. The solid line near the top of the figure represents the limit of inactivation based on the spiking level in the filtered samples. Inactivation with H<sub>2</sub>O<sub>2</sub> alone was generally insignificant, and when combined with ozonation, the addition of H<sub>2</sub>O<sub>2</sub> generally hindered *E. coli* inactivation. The various dosing conditions were more consistent for WBMWD than for CCWRD and MWRDGC, with O<sub>3</sub>:TOC ratios >0.5 generally achieving >6-log inactivation of *E. coli*. The average log-inactivation values for each treatment condition are provided in Table 3.44.

**Table 3.42. Ambient Microbial Water Quality Data for WBMWD**

Microbial Surrogate	Unfiltered Secondary Effluent	Filtered Secondary Effluent	Finished Effluent
<i>Bacillus</i> spores (CFU/100 mL)	1.1x10 <sup>4</sup>	7.9x10 <sup>3</sup>	<1
Coliforms, fecal (MPN/100 mL)	9.4x10 <sup>3</sup>	7.7x10 <sup>3</sup>	<1
Coliforms, total (MPN/100 mL)	3.5x10 <sup>4</sup>	3.4x10 <sup>4</sup>	<1
MS2 (PFU/mL)	9	10	<1

**Table 3.43. Microbial Spiking Levels for WBMWD Bench-Scale Experiments**

Microbial Surrogate	Filtered Ozone Disinfection	Filtered UV Disinfection
<i>B. subtilis</i> spores (CFU/100 mL)	2.2x10 <sup>5</sup>	2.8x10 <sup>5</sup>
<i>E. coli</i> (MPN/100 mL)	2.4x10 <sup>7</sup>	9.3x10 <sup>6</sup>
MS2 (PFU/mL)	6.4x10 <sup>7</sup>	9.9x10 <sup>6</sup>

Figure 3.51 illustrates the inactivation of spiked MS2 during the bench-scale ozone experiments. Again, the inactivation achieved with the addition of H<sub>2</sub>O<sub>2</sub> alone was insignificant, and ozone/H<sub>2</sub>O<sub>2</sub> was slightly less effective than ozone alone. With respect to the CDPH Title 22 requirements, an O<sub>3</sub>:TOC ratio >0.5 was often sufficient for the 5-log inactivation requirement, and an O<sub>3</sub>:TOC ratio >1.0 was generally sufficient for the more stringent 6.5-log inactivation requirement. The average log-inactivation values for each treatment condition are provided in Table 3.45.

Figure 3.52 illustrates the inactivation of spiked *B. subtilis* spores during the bench-scale ozone experiments. As expected, the spores proved to be extremely resistant to oxidation and only experienced significant inactivation for O<sub>3</sub>:TOC ratios >1.0 with no H<sub>2</sub>O<sub>2</sub> addition. In other words, a sufficient ozone CT had to be administered before ozone and •OH were able to penetrate the spore coat and inactivate the bacteria. It is important to reiterate that oxidation with •OH alone (i.e., with H<sub>2</sub>O<sub>2</sub> addition) is extremely ineffective for spore inactivation, presumably because of the highly reactive nature of •OH and competition with EfOM. The average log-inactivation values for each treatment condition are provided in Table 3.46.

Finally, Figure 3.53 provides a summary of the ozone disinfection data for the three surrogate microbes as they pertain to the CT framework. Figure 3.53A illustrates the dose–response relationships for the samples with no H<sub>2</sub>O<sub>2</sub> addition, and Figure 3.53B illustrates the dose–response relationships for H<sub>2</sub>O<sub>2</sub>:O<sub>3</sub> ratios of 0.5 and 1.0 (combined). Similar to the previous data sets, the data indicate that the CT framework is not always appropriate because substantial levels of inactivation can be achieved when the apparent ozone CT is zero. Again, the level of inactivation for vegetative bacteria and viruses is generally less than that

observed when an ozone residual is present, and no inactivation of spore-forming bacteria can be achieved without a measurable CT.

Table 3.47 summarizes the efficacy of UV and UV/H<sub>2</sub>O<sub>2</sub> for the inactivation of the three surrogate microbes. The efficacy of UV-based disinfection differs dramatically from ozone-based disinfection because UV is highly effective against both vegetative and spore-forming bacteria, although some viruses demonstrate resistance. Regardless of H<sub>2</sub>O<sub>2</sub> addition, 50 mJ/cm<sup>2</sup> was sufficient to reach the limits of inactivation for *E. coli* and *Bacillus* spores. On the other hand, MS2 inactivation occurred more slowly and only reached the limit of inactivation with a UV dose of 250 mJ/cm<sup>2</sup>. There was no difference in UV/H<sub>2</sub>O<sub>2</sub> performance with H<sub>2</sub>O<sub>2</sub> doses of 5 and 10 mg/L. Particularly with advanced oxidation dosing conditions (i.e., >250 mJ/cm<sup>2</sup> with 10 mg/L of H<sub>2</sub>O<sub>2</sub>), one can expect substantial inactivation of all microbes present in wastewater. This constitutes a significant advantage for UV-based treatment over the ozone-based alternatives.

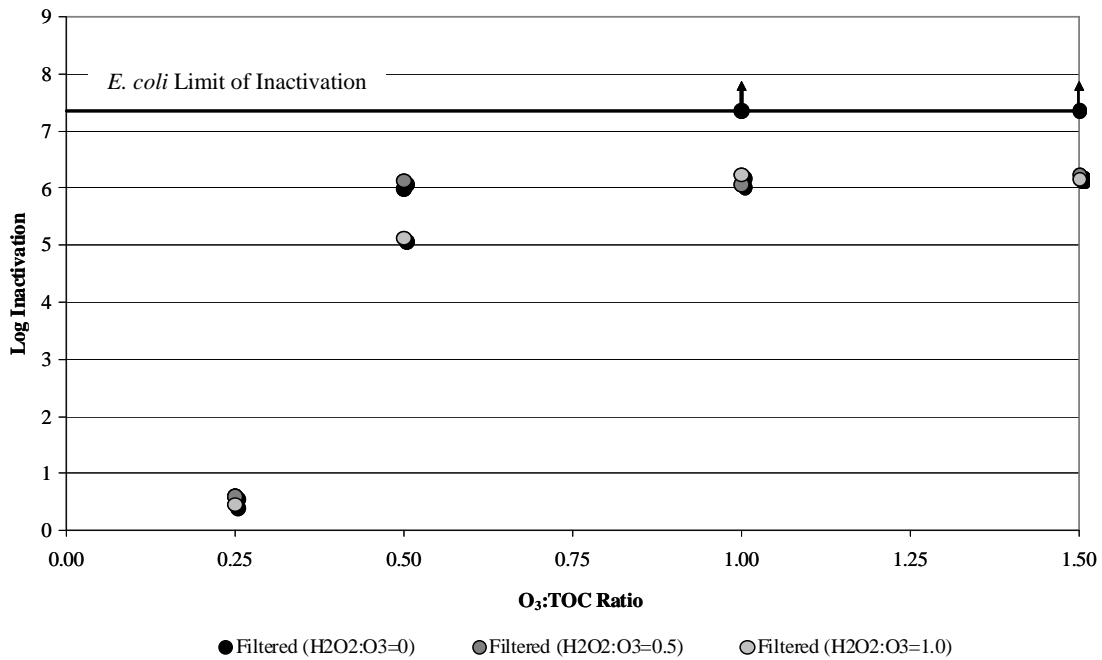
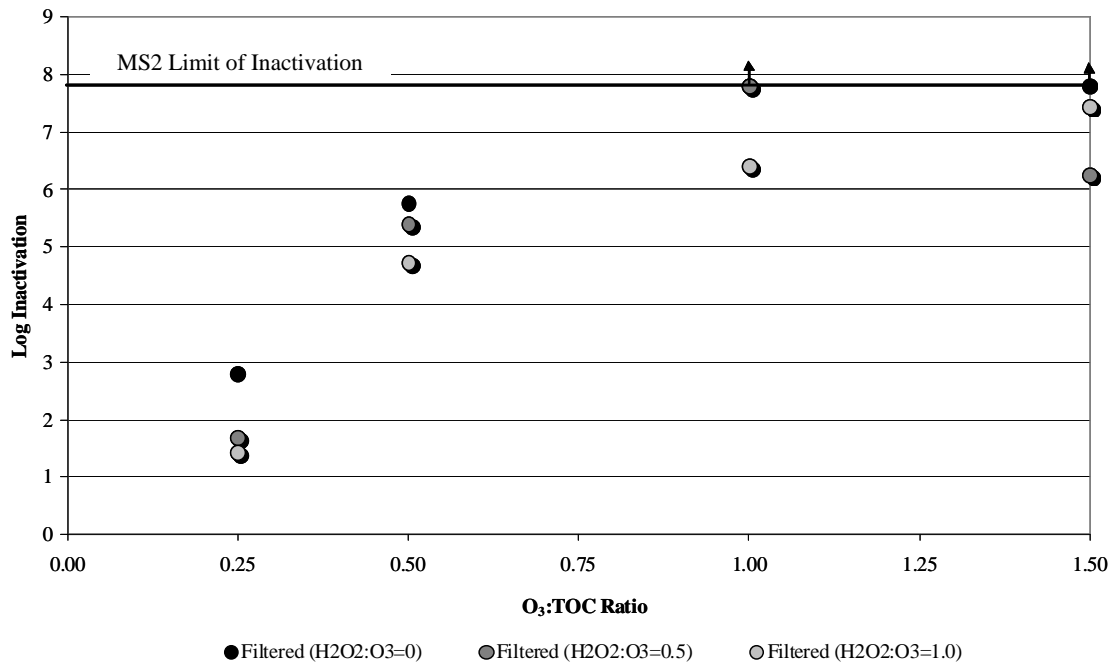


Figure 3.50. Inactivation of spiked *E. coli* in the WBMWD secondary effluent.

Table 3.44. Summary of *E. coli* Inactivation in the WBMWD Secondary Effluent

O <sub>3</sub> :TOC Ratio	H <sub>2</sub> O <sub>2</sub> :O <sub>3</sub> =0	H <sub>2</sub> O <sub>2</sub> :O <sub>3</sub> =0.5	H <sub>2</sub> O <sub>2</sub> :O <sub>3</sub> =1.0
0.25	0.6	0.6	0.5
0.5	6.0	6.1	5.1
1.0	>7.4*	6.1	6.2
1.5	>7.4*	6.2	6.2

Note: \*=limit of inactivation based on spiking level



**Figure 3.51. Inactivation of spiked MS2 in the WBMWD secondary effluent.**

**Table 3.45. Summary of MS2 Inactivation in the WBMWD Secondary Effluent**

O <sub>3</sub> :TOC Ratio	H <sub>2</sub> O <sub>2</sub> :O <sub>3</sub> =0	H <sub>2</sub> O <sub>2</sub> :O <sub>3</sub> =0.5	H <sub>2</sub> O <sub>2</sub> :O <sub>3</sub> =1.0
0.25	2.8	1.7	1.4
0.5	5.8	5.4	4.7
1.0	>7.8*	7.8	6.4
1.5	>7.8*	6.3	7.4

Note: \*=limit of inactivation based on spiking level

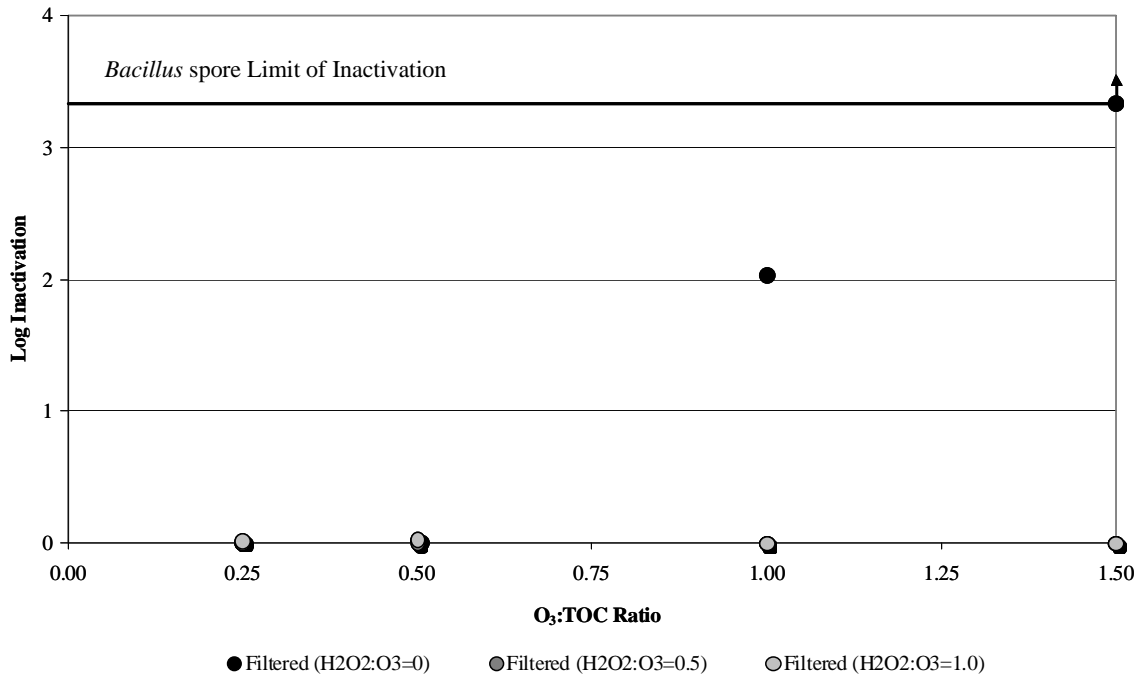


Figure 3.52. Inactivation of spiked *Bacillus* spores in the WBMWD secondary effluent.

Table 3.46. Summary of *Bacillus* Spore Inactivation in the WBMWD Secondary Effluent

O <sub>3</sub> :TOC Ratio	H <sub>2</sub> O <sub>2</sub> :O <sub>3</sub> =0	H <sub>2</sub> O <sub>2</sub> :O <sub>3</sub> =0.5	H <sub>2</sub> O <sub>2</sub> :O <sub>3</sub> =1.0
0.25	0.0	0.0	0.0
0.5	0.0	0.0	0.0
1.0	2.0	0.0	0.0
1.5	>3.3*	0.0	0.0

Note: \*=limit of inactivation based on spiking level

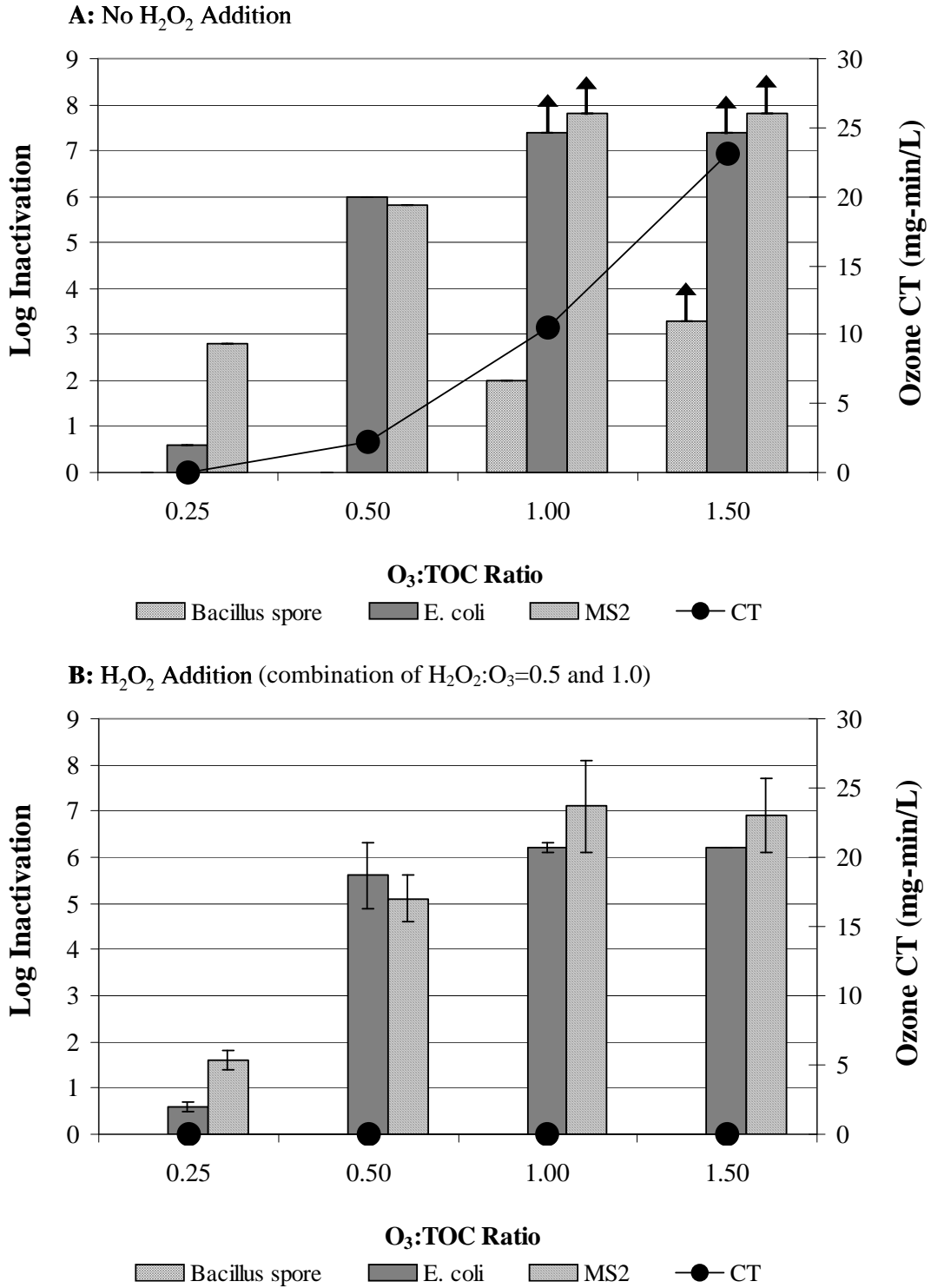


Figure 3.53. Significance of CT for disinfection in the WBMWD secondary effluent.

**Table 3.47. Summary of UV Inactivation in the WBMWD Secondary Effluent**

UV Dose (mJ/cm <sup>2</sup> )	<i>E. coli</i>		MS2		<i>Bacillus</i> Spores	
	UV	UV/H <sub>2</sub> O <sub>2</sub>	UV	UV/H <sub>2</sub> O <sub>2</sub> **	UV	UV/H <sub>2</sub> O <sub>2</sub>
25	>7.0*	5.9	N/A	N/A	1.9	1.7
50	7.0	>7.0*	3.1	3.4	>3.5*	>3.5*
250	>7.0*	>7.0*	>7.0*	>7.0*	>3.5*	>3.5*
500	>7.0*	>7.0*	>7.0*	>7.0*	>3.5*	>3.5*

Notes: \*=limit of inactivation based on spiking level; H<sub>2</sub>O<sub>2</sub> doses of 5 and 10 mg/L achieved similar levels of inactivation; UV=ultraviolet

### 3.3.7 Organic Characterization

Similar to the previous two data sets, the full-spectrum scans in Figures 3.54 and 3.55, without (A) and with (B) H<sub>2</sub>O<sub>2</sub> addition, indicate that the absorbance profiles around 254 nm generally provide the greatest resolution among treatments. Because of the limited efficacy of UV photolysis (Figure 3.55A), there is little resolution regardless of wavelength, and even UV/H<sub>2</sub>O<sub>2</sub> achieved minimal reductions in absorbance. Figure 3.56 focuses on the change in UV<sub>254</sub> absorbance with ozone, ozone/H<sub>2</sub>O<sub>2</sub>, UV, and UV/H<sub>2</sub>O<sub>2</sub>. As for ozonation, reductions in UV<sub>254</sub> absorbance were slightly hindered by the addition of H<sub>2</sub>O<sub>2</sub>. In contrast to CCWRD and MWRDGC, the synergistic aspect of the UV AOP provided minimal improvements over UV alone.

Three-dimensional excitation emission matrices were developed for the filtered secondary effluent, the MF-RO-UV/H<sub>2</sub>O<sub>2</sub> effluent, and the various treatment conditions. Figure 3.57 illustrates the fluorescence fingerprint of the secondary and finished effluent samples and also provides the total and regional fluorescence intensities based on arbitrary fluorescence units. The efficacy of the IPR treatment train is apparent based on the dramatic reduction in fluorescence intensity, from the most intense fingerprint of the various data sets to a fingerprint comparable to that of a blank sample. In fact, Regions I and II individually had higher TF intensities than Regions I, II, and III combined for CCWRD and MWRDGC. In contrast to CCWRD and MWRDGC, Region I (soluble microbial products and biopolymers) composed a larger portion of the TF than Region II (fulvic acids).

Figure 3.58 provides a qualitative illustration of treatment efficacy after ozone- and UV-based oxidation. It is interesting to note that an O<sub>3</sub>:TOC ratio of 0.25 yields a 3D EEM that is similar to the ambient secondary effluents of CCWRD and MWRDGC. Despite the poor water quality, ozone and ozone/H<sub>2</sub>O<sub>2</sub> are capable of achieving substantial reductions in regional and total fluorescence. Despite the corrections for UV absorbance in calculating UV doses, neither UV nor UV/H<sub>2</sub>O<sub>2</sub> are capable of significant reductions in fluorescence.

Figures 3.59 and 3.60 illustrate the fluorescence profiles at an excitation wavelength of 254 nm after ozonation and UV/H<sub>2</sub>O<sub>2</sub>. The addition of H<sub>2</sub>O<sub>2</sub> did not have a significant impact on ozone efficacy, and UV photolysis provided limited reductions in fluorescence intensity; therefore, these fluorescence profiles are not shown. They actually provide better resolution for the UV/H<sub>2</sub>O<sub>2</sub> samples in comparison to the full 3D EEMs. The fluorescence profiles also illustrate the prominence of Region I fluorescence because the WBMWD profiles are characterized by two distinct peaks, whereas CCWRD and MWRDGC are characterized by only a single peak associated with Region II.

Table 3.48 provides the FI (i.e.,  $E_{x_{370}}Em_{450}/E_{x_{370}}Em_{500}$ ) and TI (i.e.,  $E_{x_{254}}Em_{450,T}/E_{x_{254}}Em_{450,A}$ ) for the WBMWD experiments. In contrast to CCWRD and MWRDGC, the FI values remained relatively constant regardless of the treatment condition. In other words, the organic matter associated with emissions at 450 nm and 500 nm were oxidized at similar relative rates. These relative changes are illustrated in Figure 3.61, and Figure 3.62 illustrates the changes in total and regional fluorescence intensities. The fluorescence associated with soluble microbial products (Region I) and fulvic acids (Region II) decreased at a faster rate than that of the humic acids (Region III).

The TI, which measures the extent of organic transformation, reached as low as 0.06 for the highest  $O_3$ :TOC ratio, thereby indicating that 94% of the original fluorescence had been eliminated. This TI reduction is similar to those of CCWRD and MWRDGC, thereby highlighting the significance of relative changes in bulk organic matter for various water qualities. Also similar to CCWRD and MWRDGC, the addition of  $H_2O_2$  hindered the oxidation of the bulk organic matter. Because of the limited reduction in fluorescence with UV and UV/ $H_2O_2$ , the corresponding FI and TI values did not change significantly. The corresponding changes in total and regional fluorescence intensities for UV and UV/ $H_2O_2$  are illustrated in Figure 3.63.

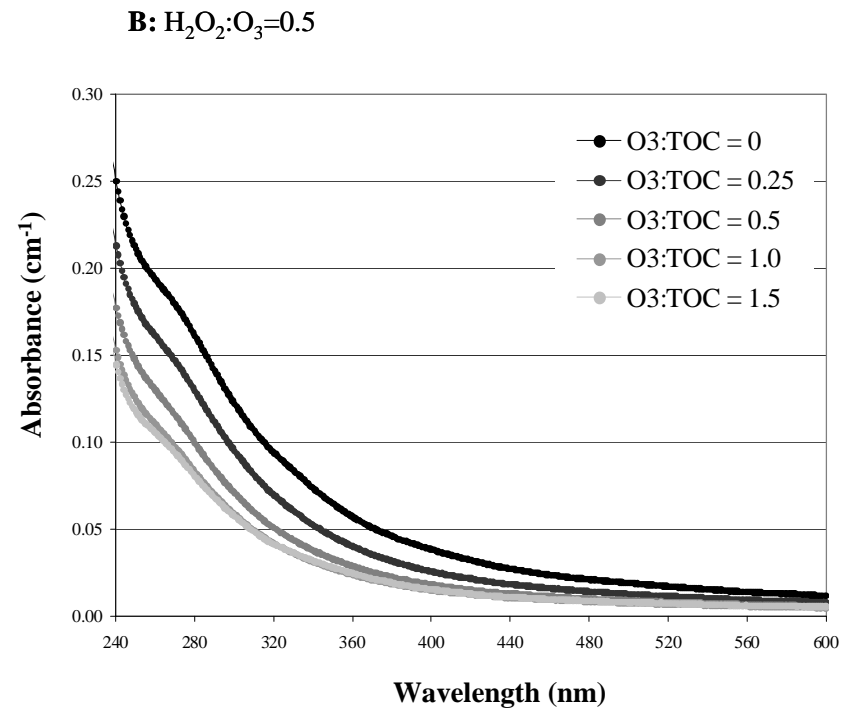
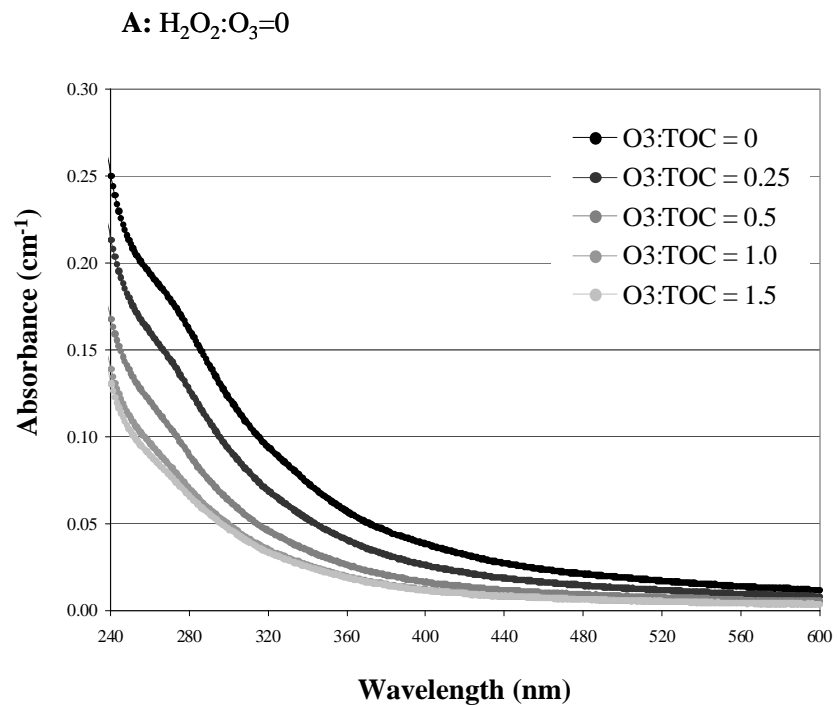


Figure 3.54. WBMWD absorbance spectra after ozonation.

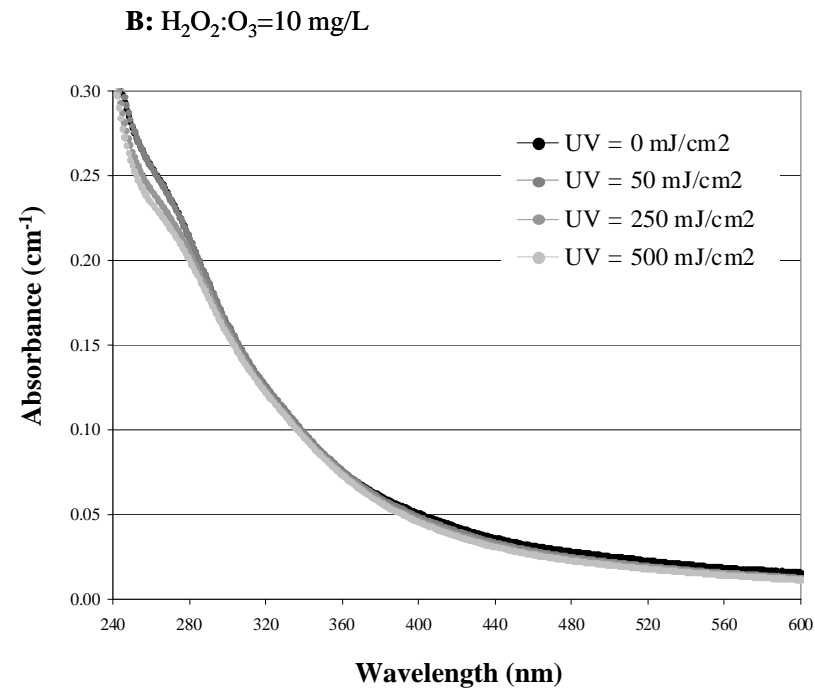
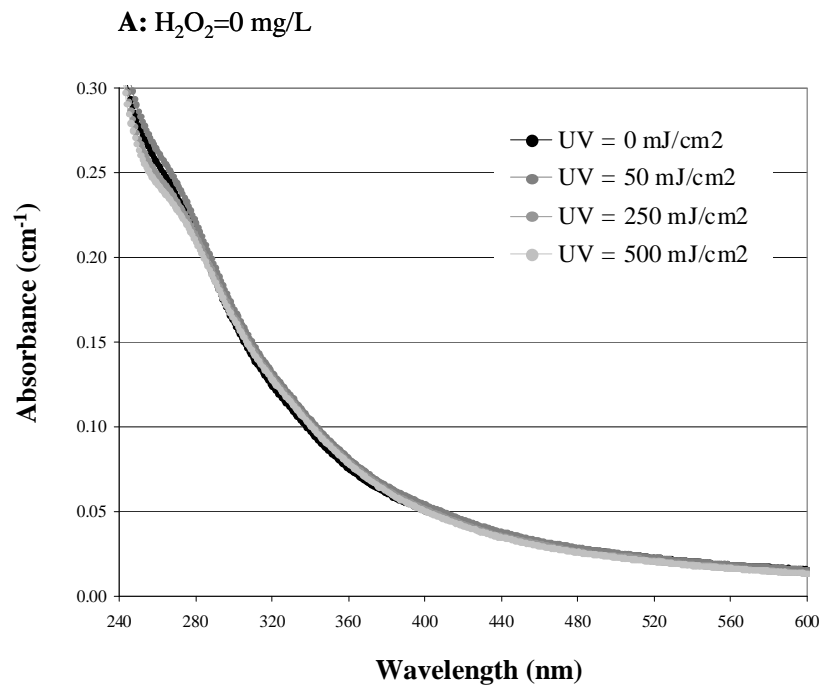


Figure 3.55. WBMWD absorbance spectra after UV and UV/H<sub>2</sub>O<sub>2</sub>.

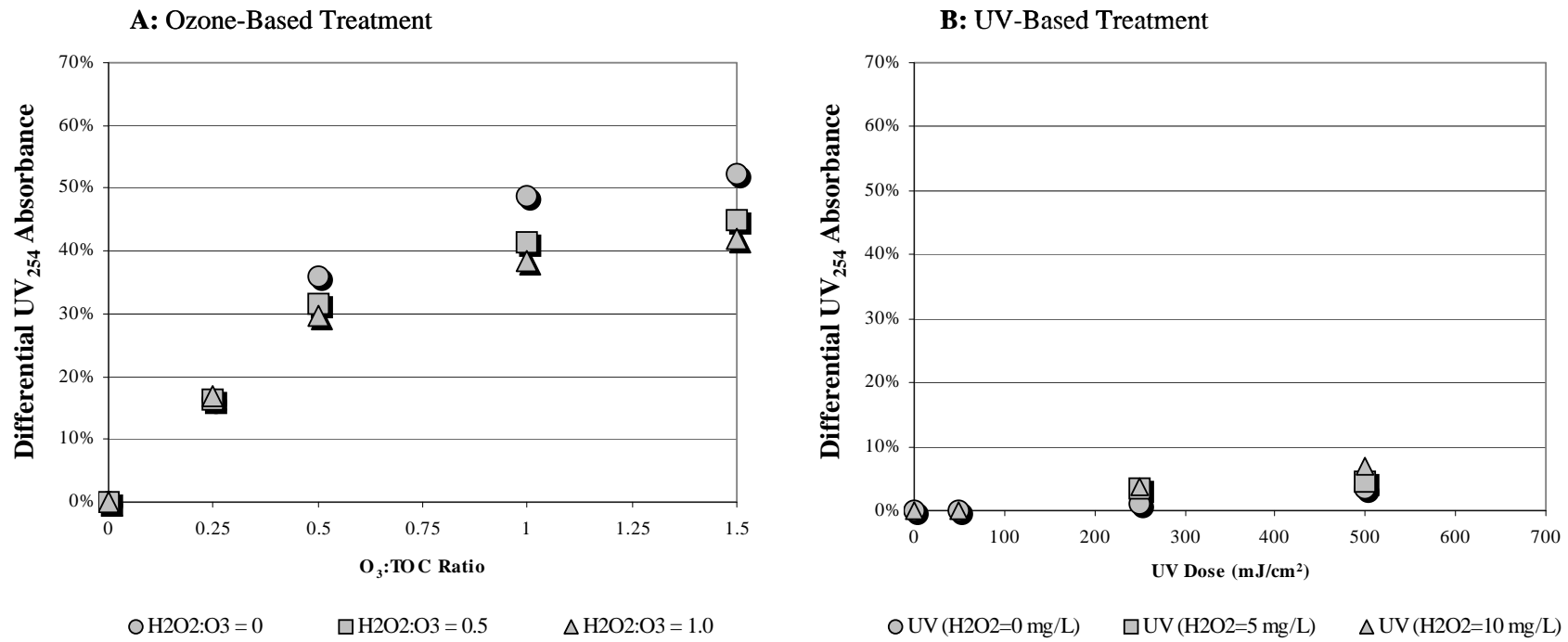


Figure 3.56. Differential UV<sub>254</sub> absorbance in the filtered WBMWD secondary effluent.

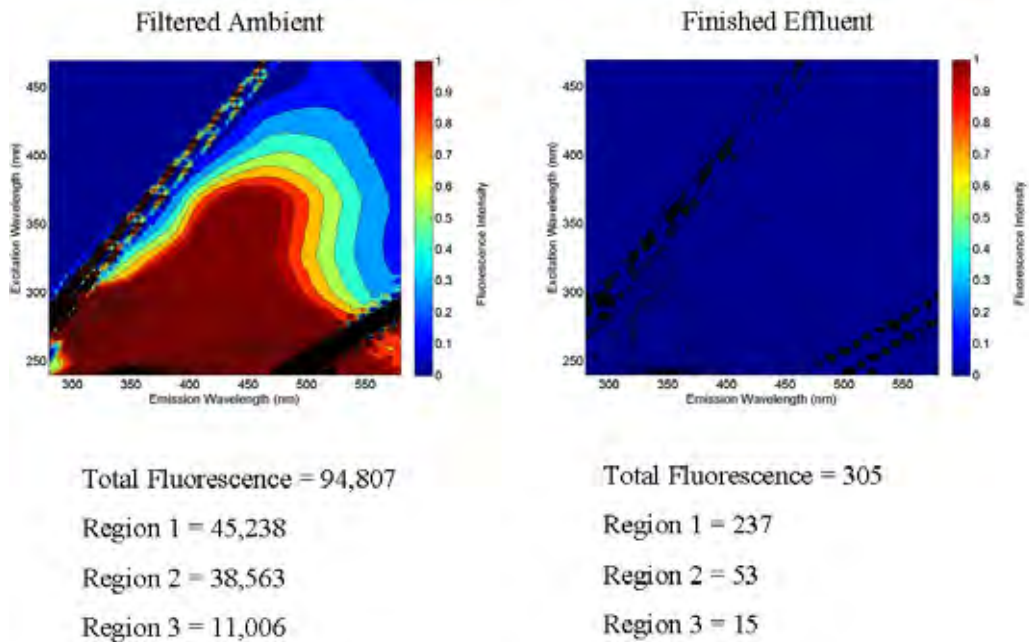


Figure 3.57. 3D EEMs for ambient samples from WBMWD.

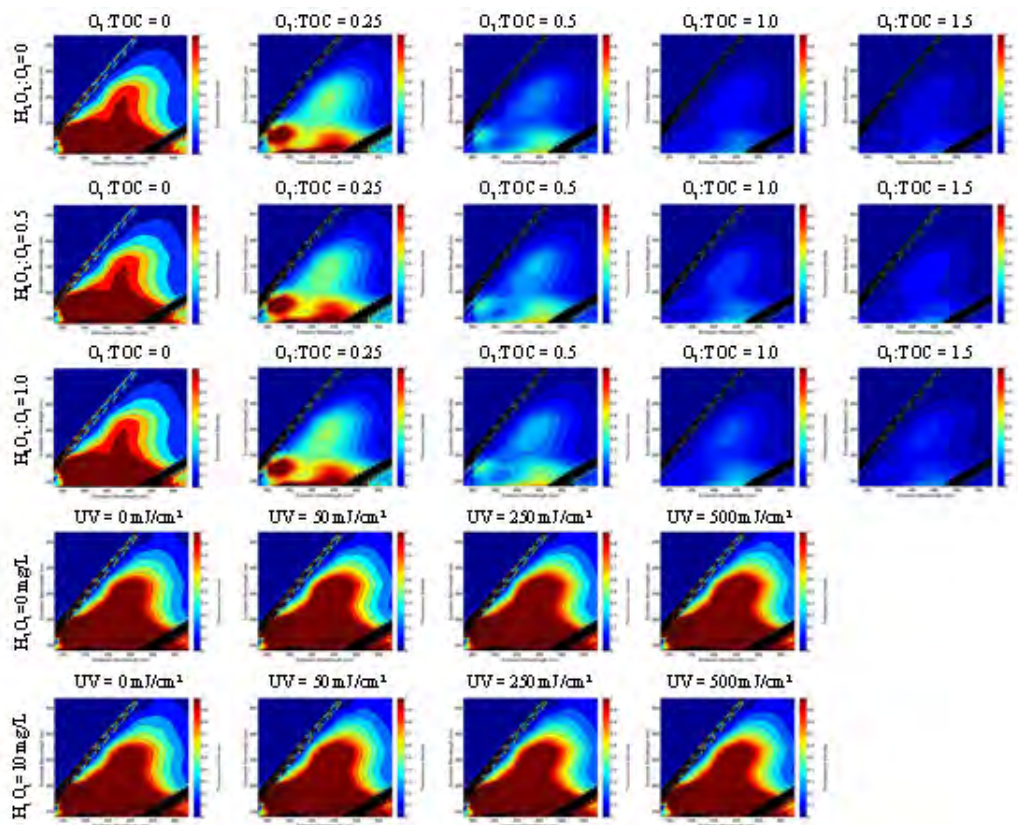
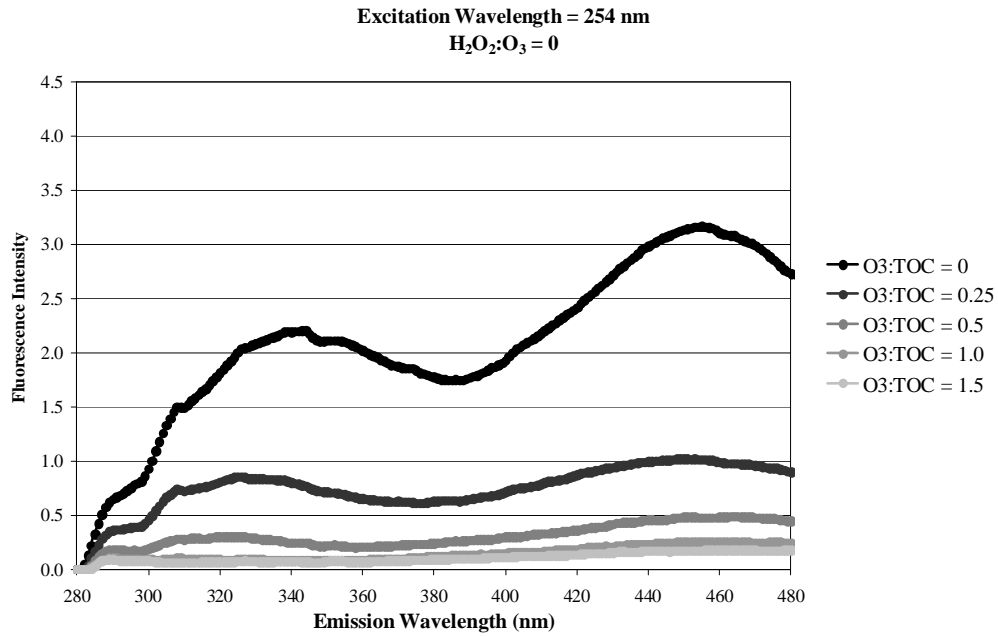
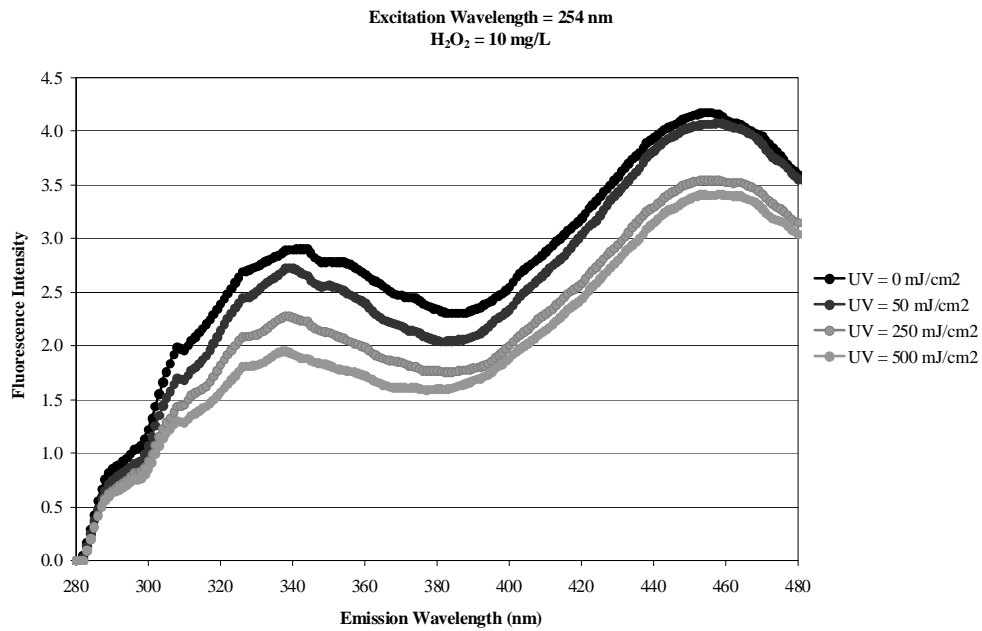


Figure 3.58. 3D EEMs after treatment for the filtered WBMWD secondary effluent.



**Figure 3.59. WBMWD fluorescence profiles (Ex<sub>254</sub>) after ozonation.**



**Figure 3.60. WBMWD fluorescence profiles (Ex<sub>254</sub>) after UV/H<sub>2</sub>O<sub>2</sub>.**

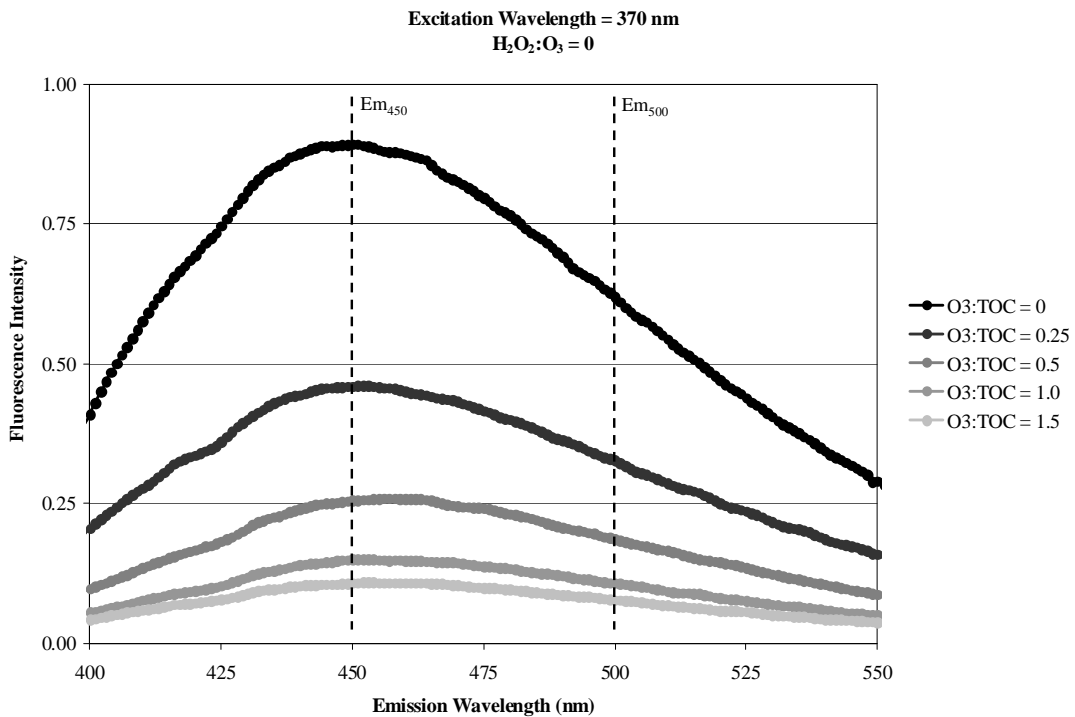
**Table 3.48. FI and TI Values for the WBMWD Secondary Effluent**

Filtered Ozone Exposure						
O <sub>3</sub> :TOC	H <sub>2</sub> O <sub>2</sub> :O <sub>3</sub> =0		H <sub>2</sub> O <sub>2</sub> :O <sub>3</sub> =0.5		H <sub>2</sub> O <sub>2</sub> :O <sub>3</sub> =1.0	
	FI	TI	FI	TI	FI	TI
0	1.44	1.00	1.44	1.00	1.44	1.00
0.25	1.40	0.33	1.42	0.32	1.46	0.32
0.5	1.37	0.15	1.40	0.17	1.41	0.18
1.0	1.39	0.08	1.50	0.09	1.45	0.10
1.5	1.38	0.06	1.43	0.07	1.47	0.07

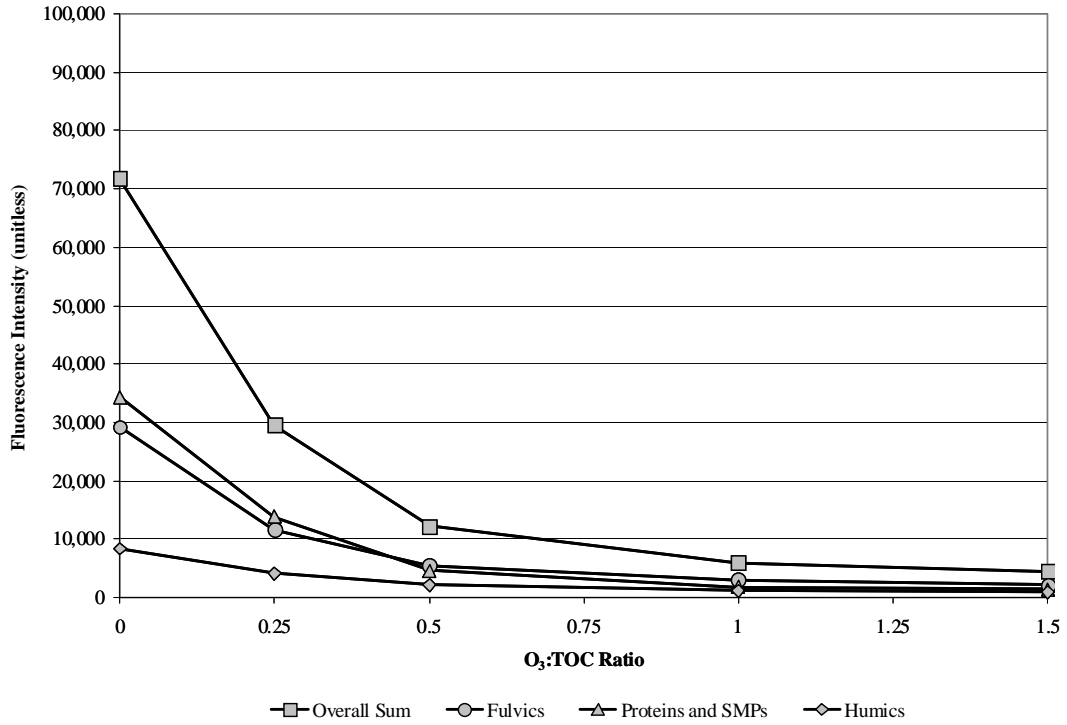
  

Filtered UV Exposure						
UV Dose (mJ/cm <sup>2</sup> )	H <sub>2</sub> O <sub>2</sub> =0 mg/L		H <sub>2</sub> O <sub>2</sub> =5 mg/L		H <sub>2</sub> O <sub>2</sub> =10 mg/L	
	FI	TI	FI	TI	FI	TI
0	1.44	1.00	1.44	1.00	1.44	1.00
50	1.40	1.03	N/A	N/A	1.40	0.98
250	1.39	0.95	1.39	0.91	1.40	0.85
500	1.38	0.91	1.38	0.89	1.39	0.82

Notes: FI=fluorescence index; TI=treatment index; UV=ultraviolet



**Figure 3.61. WBMWD fluorescence profiles (Ex<sub>370</sub>) after ozonation.**



\*H<sub>2</sub>O<sub>2</sub>:O<sub>3</sub>=0

Figure 3.62. Changes in fluorescence intensity after ozonation for WBMWD.

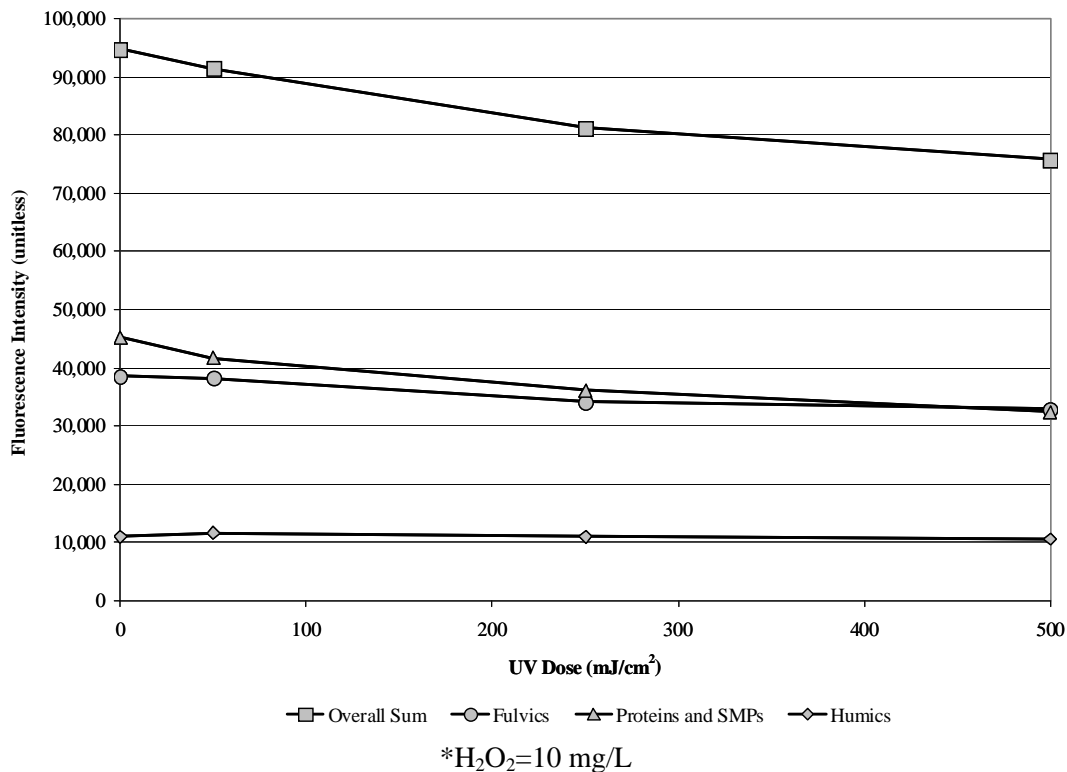


Figure 3.63. Changes in fluorescence intensity after UV/H<sub>2</sub>O<sub>2</sub> for WBMWD.

### 3.4 Pinellas County Utilities, St. Petersburg, FL

The secondary effluent provided by Pinellas County Utilities (PCU) is from a water reclamation facility in the Tampa Bay metropolitan area. PCU treats approximately 20 MGD of wastewater composed of >96% domestic and <4% industrial flows. The liquid treatment train consists of preliminary screening and grit removal; primary clarification; conventional activated sludge (SRT=11–13 days) with nitrification, denitrification (TN<sub>eff</sub>≈1.4 mg/L), and biological phosphorus removal (TP<sub>eff</sub>≈0.5 mg/L); secondary clarification; deep bed (sand) denitrification filters; and chlorination. The chlorine disinfection process targets a minimum residual of 1.0 mg/L at the end of the contact basin and a contact time of at least 15 minutes. The effluent is used in reclaimed water distribution systems for irrigation and as a Class 3 surface water discharge, which requires the effluent to comply with recreational water quality standards. The facility is currently being upgraded to include UV disinfection. A simplified treatment schematic of PCU is provided in Figure 3.64.

PCU is particularly interested in ozone technologies as a means to mitigate total trihalomethane concentrations in the finished effluent. The facility must specifically achieve annual averages of less than 22 µg/L and 34 µg/L for dichlorobromomethane and chlorodibromomethane. PCU has also tested for toxicological endpoints in the past but has not reached any definitive conclusions regarding the toxicity of its effluent.

Secondary effluent from PCU was collected in October 2010, and the initial water quality data in Table 3.49 were obtained. Post-chlorination finished effluent samples were also

analyzed. Using the initial TOC and nitrite data for the filtered secondary effluent, the ozone dosing conditions in Table 3.50 were calculated.

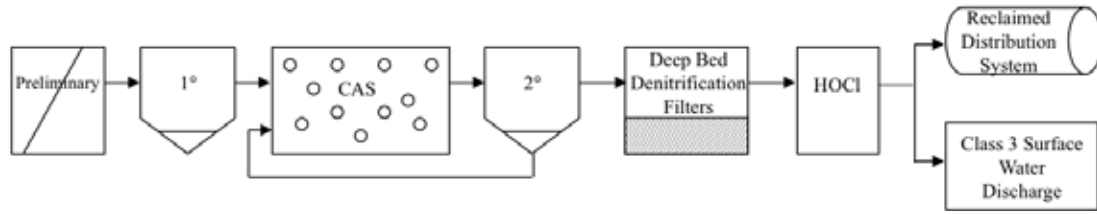


Figure 3.64. Simplified treatment schematic for PCU.

Table 3.49. Initial Water Quality Data for PCU

<b>Unfiltered Secondary Effluent</b>	Alkalinity (mg/L CaCO <sub>3</sub> )	205
	Bromide (µg/L)	730
	NDMA (ng/L)	7.1
	NH <sub>3</sub> (mg N/L)	0.02
	NO <sub>2</sub> (mg N/L)	<0.05
	NO <sub>3</sub> (mg N/L)	7.7
	pH	7.3
	TKN (mg N/L)	0.02
	TN (mg N/L)	7.9
	TOC (mg/L)	7.0
	TON (mg N/L)	~0
	TSS (mg/L)	<5
Turbidity (NTU)	0.51	
<b>Filtered Secondary Effluent</b>	pH	7.3
	TOC (mg/L)	7.2
	TSS (mg/L)	<5
	Turbidity (NTU)	0.33
<b>Finished Effluent</b>	UV <sub>254</sub> absorbance (cm <sup>-1</sup> )	0.187
	NDMA (ng/L)	3.9
	UV <sub>254</sub> absorbance (cm <sup>-1</sup> )	0.135

Notes: NDMA=N-nitrosodimethylamine; TKN=total Kjeldahl nitrogen, sum of TON and ammonia; TN=total nitrogen; TOC=total organic carbon; TON=total organic nitrogen, difference of TN and ammonia, nitrate, and nitrite; TSS=total suspended solids; UV=ultraviolet

**Table 3.50. Ozone Dosing Conditions for 1-L Filtered PCU Samples**Concentration of O<sub>3</sub> stock solution=85 mg/LConcentration of H<sub>2</sub>O<sub>2</sub> stock solution=10 g/L

Filtered dilution ratio=(887/1000)=0.887

Filtered TOC after dilution=6.4 mg/L

Filtered NO<sub>2</sub> after dilution< 0.05 mg-N/L (not considered in dosing calculations)

O <sub>3</sub> :TOC/ H <sub>2</sub> O <sub>2</sub> :O <sub>3</sub>	Wastewater Volume (mL)	Nanopure Volume (mL)	O <sub>3</sub> Volume (mL)	O <sub>3</sub> Dose (mg/L)	H <sub>2</sub> O <sub>2</sub> Volume (μL)	H <sub>2</sub> O <sub>2</sub> Dose (mg/L)
Spike	887	113	0	0	0	0
0.25/0	887	95	18	1.5	0	0
0.25/0.5	887	95	18	1.5	54	0.5
0.25/1.0	887	95	18	1.5	108	1.1
0.5/0	887	76	37	3.1	0	0
0.5/0.5	887	76	37	3.1	111	1.1
0.5/1.0	887	76	37	3.1	223	2.2
1.0/0	887	37	76	6.5	0	0
1.0/0.5	887	37	76	6.5	229	2.3
1.0/1.0	887	37	76	6.5	458	4.6
1.5/0	887	0	113	9.6	0	0
1.5/0.5	887	0	113	9.6	340	3.4
1.5/1.0	887	0	113	9.6	680	6.8

Note: \*=some values are affected by rounding error and the precision of the ozone spike

### 3.4.1 Ozone Demand/Decay

Figure 3.65 illustrates the ozone demand/decay curves for the filtered PCU secondary effluent at various dosing conditions. The graph only includes dosing conditions with a measurable ozone residual after 30 seconds; corresponding CT values are also provided. The O<sub>3</sub>/H<sub>2</sub>O<sub>2</sub> samples are not included in the figure because the addition of H<sub>2</sub>O<sub>2</sub> led to the formation of •OH but eliminated the dissolved ozone residual. Similar to the previous three data sets, the 0.25 O<sub>3</sub>:TOC ratio was insufficient to establish a measurable ozone residual after 30 seconds. For the remaining dosing conditions, the graph illustrates the IOD (i.e., the precipitous drop between 0 and 30 seconds) and the decay over time. In comparison to the previous data sets, the ozone residual in the PCU secondary effluent was more stable, which resulted in a significantly higher CT value for an O<sub>3</sub>:TOC ratio of 1.5. The O<sub>3</sub>:TOC ratios of 0.5 and 1.0 achieved similar CT values in comparison to the other wastewaters.

### 3.4.2 Bromate Formation

As illustrated in Figure 3.66, there was considerable bromate formation in the PCU secondary effluent because of the high initial bromide concentration of 648 μg/L (after dilution by the ozone stock). For an O<sub>3</sub>:TOC ratio of 1.5 with no peroxide addition, the bromate concentration approached 375 μg/L, but the addition of H<sub>2</sub>O<sub>2</sub> provided a tremendous reduction in bromate formation for this particular ozone dose. Bromate mitigation by peroxide was less apparent for the lower applied ozone doses. Similar to WBMWD, the applied ozone dose would be limited to an O<sub>3</sub>:TOC ratio <0.25, or the process would have to be supplemented with substantial H<sub>2</sub>O<sub>2</sub> doses to satisfy the 10 μg/L benchmark. Again, the required H<sub>2</sub>O<sub>2</sub> dose for high O<sub>3</sub>:TOC ratios would likely be cost prohibitive unless other mitigation measures were employed.

### 3.4.3 Hydroxyl Radical Exposure

Based on data from bench-scale experiments with pCBA spiked at approximately 2 mg/L for the ozone experiments and 500 µg/L for the UV experiments, Table 3.51 indicates the overall •OH exposure for each ozone and UV dosing condition. The •OH exposures for the UV/H<sub>2</sub>O<sub>2</sub> samples are corrected for the small level of pCBA degradation achieved by photolysis alone.

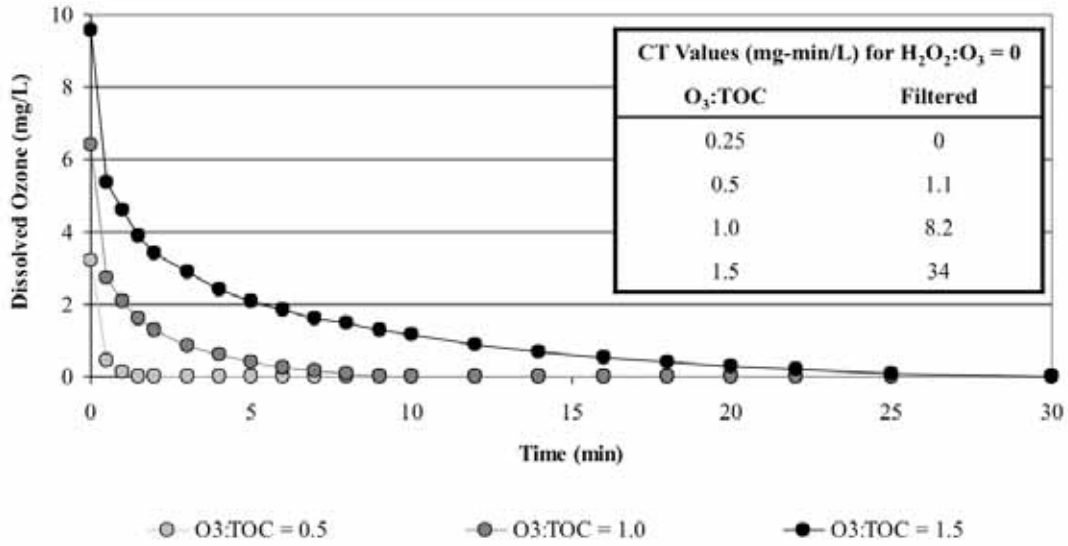


Figure 3.65. Ozone demand/decay curves for PCU (filtered).

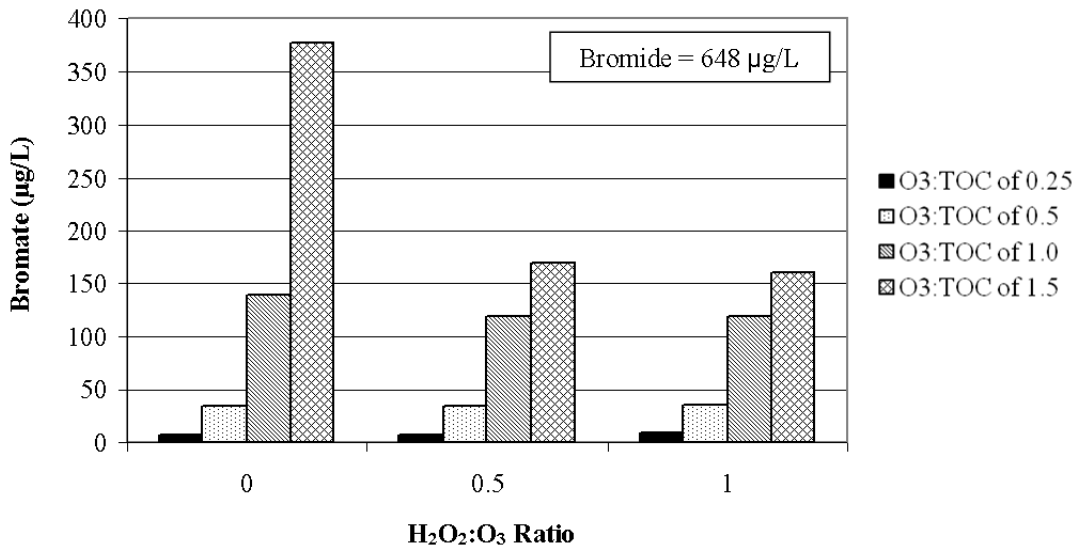


Figure 3.66. Bromate formation during ozonation of PCU secondary effluent.

**Table 3.51. •OH Exposure in the PCU Secondary Effluent**

Filtered Ozone Exposure ( $10^{-11}$ M/s)			
Ozone:TOC	H <sub>2</sub> O <sub>2</sub> :O <sub>3</sub> =0	H <sub>2</sub> O <sub>2</sub> :O <sub>3</sub> =0.5	H <sub>2</sub> O <sub>2</sub> :O <sub>3</sub> =1.0
0.25	3.8	3.8	3.9
0.5	6.8	8.4	7.8
1.0	27	25	22
1.5	41	42	32
Filtered UV Exposure ( $10^{-11}$ M/s)			
UV Dose (mJ/cm <sup>2</sup> )	H <sub>2</sub> O <sub>2</sub> =0 mg/L	H <sub>2</sub> O <sub>2</sub> =5 mg/L	H <sub>2</sub> O <sub>2</sub> =10 mg/L
0	N/A	N/A	0.0*
50	N/A	N/A	0.7
250	N/A	2.9	6.7
500	N/A	4.7	8.8

Notes: \*=based on H<sub>2</sub>O<sub>2</sub> control; N/A=not available; TOC=total organic carbon; UV=ultraviolet

Similar to CCWRD and MWRDGC but contrasting with WBMWD, H<sub>2</sub>O<sub>2</sub> addition did not have a consistent impact on overall •OH exposure. It is interesting to note that the longer ozone decay period also corresponded to lower overall •OH exposure in comparison to the previous data sets. This might indicate that the lower reactivity of the bulk organic matter affected the decomposition of ozone into •OH, but in this scenario, the addition of H<sub>2</sub>O<sub>2</sub> should have achieved higher overall •OH exposure, which was not observed. Therefore, it is unclear why the •OH exposure was lower for the various dosing conditions for the PCU secondary effluent. As with CCWRD and MWRDGC, UV doses between 250 and 500 mJ/cm<sup>2</sup> (with 10 mg/L H<sub>2</sub>O<sub>2</sub>) achieved •OH exposures similar to those of the lower O<sub>3</sub>:TOC ratios.

### 3.4.4 Title 22 Contaminants

Bench-scale experiments were performed with the filtered PCU wastewater to evaluate the use of ozone and UV for the destruction of spiked NDMA (100 ng/L) and 1,4-dioxane (1 mg/L). The secondary effluent already contained 7.1 ng/L of NDMA prior to the spikes, whereas the finished effluent contained 3.9 ng/L of NDMA. The reduction in ambient NDMA during full-scale treatment is likely attributable to the biological filtration employed at the PCU facility. Figure 3.67 indicates that UV doses >700 mJ/cm<sup>2</sup> are required to satisfy the Title 22 NDMA requirement. Because NDMA destruction with ozone proved to be impractical in the previous data sets, this experiment was eliminated for PCU, but additional experiments were included to evaluate the effect of laboratory filtration on direct NDMA formation during ozonation. Some polymers and other organics associated with full-scale membranes have been identified as NDMA precursors, so the intent of these additional samples was to eliminate this confounding factor. As indicated in Table 3.52, the potential organic leaching during laboratory filtration did not have any impact, and the direct NDMA formation was extremely consistent regardless of ozone or H<sub>2</sub>O<sub>2</sub> dose. Furthermore, the magnitude of direct NDMA formation (<6 ng/L above the ambient level) was considerably less than the previous data sets.

Figure 3.68 illustrates the destruction of spiked 1,4-dioxane during the bench-scale ozone experiments. Although each of the pCBA data sets indicates that H<sub>2</sub>O<sub>2</sub> addition had no impact

on overall  $\bullet\text{OH}$  exposure, ozone/ $\text{H}_2\text{O}_2$  consistently outperformed ozone alone during the 1,4-dioxane experiments. For PCU,  $\text{O}_3$ :TOC ratios between 1.2 and  $>1.5$  are necessary to comply with the 0.5-log requirement for ozone/ $\text{H}_2\text{O}_2$  and ozone.

### 3.4.5 Trace Organic Contaminants

Secondary and finished effluent samples from PCU were analyzed to determine the ambient concentrations of the target compounds, which are provided in Table 3.53. None of the target compounds were present at concentrations exceeding  $1\ \mu\text{g}/\text{L}$ , and a majority of the target compounds were present at  $<100\ \text{ng}/\text{L}$  in the secondary effluent. The efficacy of the secondary biological treatment process is evident in the absence of the bioamenable compounds (e.g., naproxen and ibuprofen), and the subsequent chlorination process was effective in oxidizing the more susceptible compounds (e.g., diclofenac and gemfibrozil). The total estrogenicity of the secondary and finished effluents was determined to be 0.66 and  $<0.074\ \text{ng}/\text{L}$ .

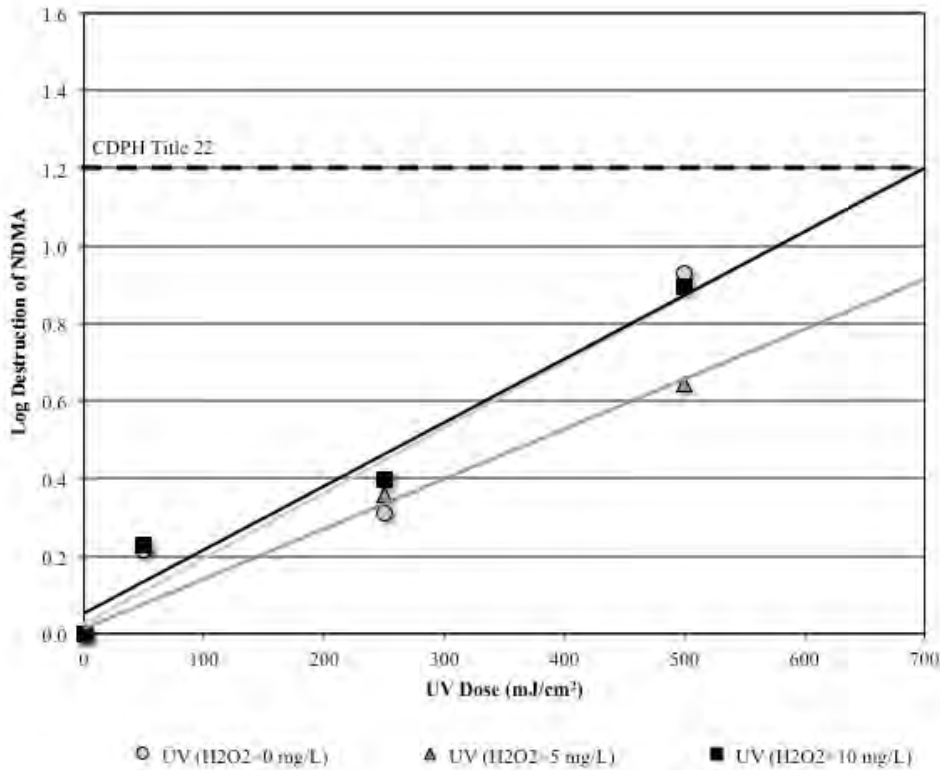
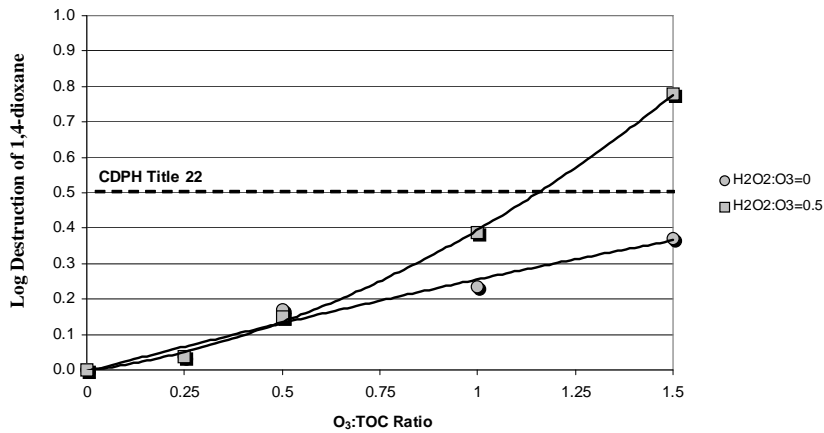


Figure 3.67. Destruction of NDMA in the filtered PCU secondary effluent.

**Table 3.52. Direct NDMA Formation in the PCU Secondary Effluent**

O <sub>3</sub> :TOC Ratio	H <sub>2</sub> O <sub>2</sub> :O <sub>3</sub> Ratio	Unfiltered NDMA (ng/L)	Filtered NDMA (ng/L)
0	0	N/A	7.1
0.25	0	11	10
0.25	0.5	9.6	9.9
0.5	0	13	11
0.5	0.5	11	11
1.0	0	12	11
1.0	0.5	11	11
1.5	0	12	13
1.5	0.5	12	10

Notes: N/A=not available; NDMA= N-nitrosodimethylamine; TOC=total organic carbon



**Figure 3.68. Destruction of 1,4-dioxane in the filtered PCU secondary effluent.**

**Table 3.53. Ambient TOrC Concentrations at PCU**

Parameter	Secondary Effluent (ng/L)	Finished Effluent (ng/L)
Atenolol	78	28
Atrazine	42	76
Bisphenol A	<50	<50
Carbamazepine	310	35
DEET	<25	30
Diclofenac	130	<25
Gemfibrozil	120	<10
Ibuprofen	<25	<25
Meprobamate	250	360
Musk ketone	<100	<100
Naproxen	<25	<25
Phenytoin	260	270
Primidone	240	270
Sulfamethoxazole	990	<25
TCEP	410	370
Total estrogenicity (EEq)	0.66	<0.074
Triclosan	<25	<25
Trimethoprim	16	<10

Notes: DEET=*N,N*-diethyl-*meta*-toluamide; EEq=estradiol equivalents; TCEP=tris-(2-chloroethyl)-phosphate

Bench-scale TOrC oxidation experiments were performed with spiking stocks and protocols similar to the previous bench-scale experiments. Again, the experiments focused on laboratory-filtered secondary effluent. Table 3.54 shows the relative oxidation levels of the 16 target compounds (musk ketone omitted) after ozonation. Although the pCBA data were inconsistent, the PCU data indicate that H<sub>2</sub>O<sub>2</sub> addition provided a slight benefit for some of the ozone-resistant compounds (Groups 3, 4, and 5) at higher O<sub>3</sub>:TOC ratios. As with WBMWD, the benefit may not be sufficient to warrant H<sub>2</sub>O<sub>2</sub> addition for this reason alone.

For the five rate constant categories, the trends were generally in agreement with the previous bench-scale experiments: an O<sub>3</sub>:TOC ratio of 0.25 was required to achieve greater than 80% oxidation of the Group 1 compounds, an O<sub>3</sub>:TOC ratio of 0.5 was required for the Group 2 compounds, an O<sub>3</sub>:TOC ratio of 1.0 was required for the Group 3 compounds, and an O<sub>3</sub>:TOC of 1.0 generally achieved 80 to 90% oxidation for the Group 4 compounds. TCEP proved to be highly resistant to both ozone and •OH; this compound barely exceeded 30% oxidation even for the highest dosing conditions.

Table 3.55 shows the relative photolysis and UV/H<sub>2</sub>O<sub>2</sub> oxidation levels of the target compounds. Similar to the previous data sets, only two compounds (diclofenac and triclosan) experienced greater than 80% destruction with UV irradiation alone, whereas atrazine, phenytoin, and sulfamethoxazole experienced greater than 30% destruction with UV alone. The addition of H<sub>2</sub>O<sub>2</sub> with a UV dose of 500 mJ/cm<sup>2</sup> was able to achieve approximately 70% destruction for sulfamethoxazole and phenytoin, whereas the remaining compounds (excluding TCEP) ranged from 20 to 65% destruction.

Finally, the total estrogenicity of the secondary effluent was oxidized down to the MRL with every ozone and H<sub>2</sub>O<sub>2</sub> dosing condition, whereas UV and UV/H<sub>2</sub>O<sub>2</sub> were unable to achieve the MRL with the dosing conditions used in this study. These data are summarized in

Figure 3.69. The total estrogenicity of the samples was quite low to start, so this might not be a significant concern.

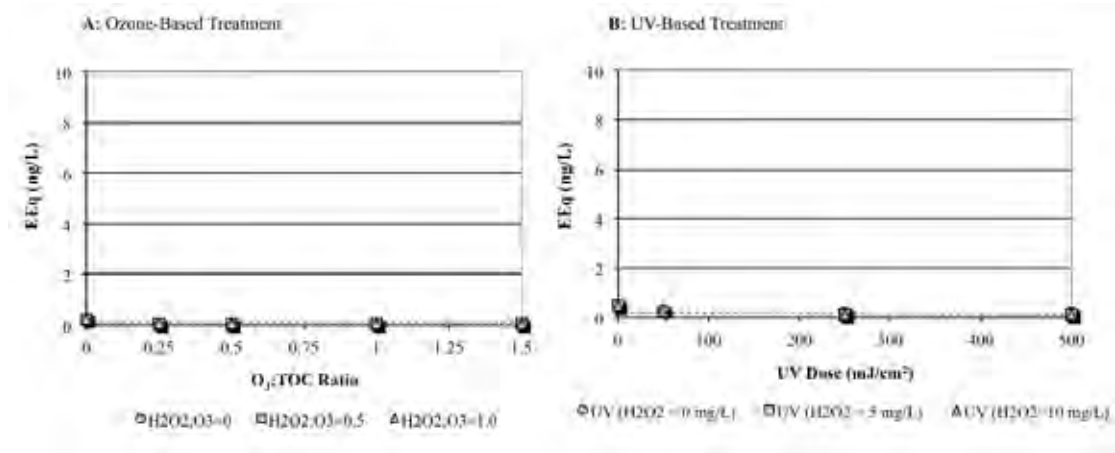


Figure 3.69. Reduction in total estrogenicity in the filtered PCU secondary effluent.

**Table 3.54. PCU TORc Mitigation by Ozone (Filtered)**

Group	Contaminant	O <sub>3</sub> :TOC (mass) / H <sub>2</sub> O <sub>2</sub> :O <sub>3</sub> (molar)											
		0.25/0	0.25/0.5	0.25/1.0	0.5/0	0.5/0.5	0.5/1.0	1.0/0	1.0/0.5	1.0/1.0	1.5/0	1.5/0.5	1.5/1.0
1	Bisphenol A	97%	97%	97%	97%	97%	97%	97%	97%	97%	97%	97%	97%
	Carbamazepine	99%	99%	93%	99%	99%	99%	99%	99%	99%	99%	99%	99%
	Diclofenac	98%	98%	98%	98%	98%	98%	98%	98%	98%	98%	98%	98%
	Naproxen	98%	98%	94%	98%	98%	98%	98%	98%	98%	98%	98%	98%
	Sulfamethoxazole	88%	88%	86%	98%	96%	95%	99%	99%	99%	99%	99%	99%
	Triclosan	98%	98%	98%	98%	98%	98%	98%	98%	98%	98%	98%	98%
	Trimethoprim	99%	99%	97%	99%	99%	99%	99%	99%	99%	99%	99%	99%
	<b>Indicator</b>	<b>97%</b>	<b>97%</b>	<b>95%</b>	<b>98%</b>								
2	Atenolol	49%	44%	52%	97%	92%	84%	97%	97%	97%	97%	97%	97%
	Gemfibrozil	84%	76%	73%	99%	99%	99%	99%	99%	99%	99%	99%	99%
	<b>Indicator</b>	<b>67%</b>	<b>60%</b>	<b>63%</b>	<b>98%</b>	<b>96%</b>	<b>92%</b>	<b>98%</b>	<b>98%</b>	<b>98%</b>	<b>98%</b>	<b>98%</b>	<b>98%</b>
3	DEET	29%	29%	35%	57%	62%	65%	85%	94%	92%	93%	99%	97%
	Ibuprofen	40%	42%	45%	70%	73%	75%	92%	97%	95%	98%	98%	98%
	Phenytoin	36%	42%	32%	70%	73%	77%	93%	97%	96%	97%	99%	99%
	Primidone	38%	33%	38%	62%	63%	66%	90%	95%	93%	95%	99%	97%
	<b>Indicator</b>	<b>36%</b>	<b>37%</b>	<b>38%</b>	<b>65%</b>	<b>68%</b>	<b>71%</b>	<b>90%</b>	<b>96%</b>	<b>94%</b>	<b>96%</b>	<b>99%</b>	<b>98%</b>
4	Atrazine	20%	18%	22%	38%	39%	42%	62%	74%	70%	75%	86%	84%
	Meprobamate	19%	21%	25%	42%	46%	43%	65%	82%	80%	77%	92%	89%
	<b>Indicator</b>	<b>20%</b>	<b>20%</b>	<b>24%</b>	<b>40%</b>	<b>43%</b>	<b>43%</b>	<b>64%</b>	<b>78%</b>	<b>75%</b>	<b>76%</b>	<b>89%</b>	<b>87%</b>
5	TCEP	11%	7%	14%	12%	14%	12%	12%	25%	21%	21%	32%	32%

Notes: DEET=*N,N*-diethyl-*meta*-toluamide; TCEP=tris-(2-chloroethyl)-phosphate

**Table 3.55. PCU TOrC Mitigation by UV (Filtered)**

Group	Contaminant	UV Dose (mJ/cm <sup>2</sup> ) / H <sub>2</sub> O <sub>2</sub> Dose (mg/L)								
		50/0	50/10	250/0	250/5	250/10	500/0	500/5	500/10	
1	Bisphenol A	20%	0%	20%	6%	13%	25%	31%	54%	
	Carbamazepine	0%	0%	0%	15%	15%	0%	50%	45%	
	Diclofenac	41%	3%	92%	83%	84%	98%	96%	96%	
	Naproxen	8%	0%	17%	25%	28%	22%	41%	60%	
	Sulfamethoxazole	6%	6%	44%	35%	24%	62%	65%	71%	
	Triclosan	37%	-9%	89%	76%	74%	97%	95%	95%	
	Trimethoprim	-8%	8%	-8%	15%	15%	0%	28%	45%	
2	Atenolol	3%	-2%	6%	20%	13%	0%	24%	34%	
	Gemfibrozil	7%	0%	5%	10%	12%	10%	23%	41%	
3	DEET	6%	0%	0%	7%	7%	6%	13%	27%	
	Ibuprofen	6%	-2%	5%	10%	12%	11%	30%	41%	
	Phenytoin	-11%	9%	16%	41%	36%	41%	57%	69%	
	Primidone	0%	9%	5%	18%	14%	9%	27%	36%	
4	Atrazine	9%	0%	25%	14%	12%	36%	34%	39%	
	Meprobamate	-2%	6%	4%	12%	7%	3%	16%	23%	
5	TCEP	3%	-4%	2%	4%	-2%	5%	2%	0%	

Notes: \*=groupings based on ozone and •OH rate constants; shading represents >80% photolysis or oxidation; DEET= *N,N*-diethyl-*meta*-toluamide; TCEP=tris-(2-chloroethyl)-phosphate

**Table 3.56. Ambient Microbial Water Quality Data for PCU**

Microbial Surrogate	Unfiltered Secondary Effluent	Filtered Secondary Effluent	Finished Effluent
<i>Bacillus</i> spores (CFU/100 mL)	5.2x10 <sup>3</sup>	4.0x10 <sup>3</sup>	73
Coliforms, fecal (MPN/100 mL)	2.7x10 <sup>2</sup>	1.5x10 <sup>2</sup>	<1
Coliforms, total (MPN/100 mL)	4.3x10 <sup>3</sup>	1.3x10 <sup>3</sup>	<1
MS2 (PFU/mL)	<1	<1	<1

**Table 3.57. Microbial Spiking Levels for PCU Bench-Scale Experiments**

Microbial Surrogate	Filtered Ozone Disinfection	Filtered UV Disinfection
<i>B. subtilis</i> spores (CFU/100 mL)	2.2x10 <sup>5</sup>	2.4x10 <sup>5</sup>
<i>E. coli</i> (MPN/100 mL)	1.1x10 <sup>8</sup>	6.9x10 <sup>6</sup>
MS2 (PFU/mL)	1.2x10 <sup>7</sup>	9.2x10 <sup>6</sup>

### 3.4.6 Disinfection

Ambient secondary (before and after laboratory filtration) and finished effluent samples were assayed for total and fecal coliforms, MS2, and *Bacillus* spores. The ambient microbial water quality data are provided in Table 3.56. Table 3.56 and appeared to be consistent with those of CCWRD and MWRDGC. In order to illustrate a wide range of inactivation, the ozone and UV disinfection samples were spiked with relatively high numbers of the surrogate microbes, as indicated in Table 3.57.

Figure 3.70 illustrates the inactivation of spiked *E. coli* during the bench-scale ozone experiments. The solid line near the top of the figure represents the limit of inactivation based on the spiking level in the filtered samples. Inactivation with H<sub>2</sub>O<sub>2</sub> alone was generally insignificant, and when combined with ozonation, the addition of H<sub>2</sub>O<sub>2</sub> significantly hindered *E. coli* inactivation. In fact, the addition of H<sub>2</sub>O<sub>2</sub> reduced the inactivation level by more than 5 logs for an O<sub>3</sub>:TOC ratio of 1.0. The average log-inactivation values for each treatment condition are provided in Table 3.58.

Figure 3.71 illustrates the inactivation of spiked MS2 during the bench-scale ozone experiments. Again, minimal inactivation was achieved with the addition of H<sub>2</sub>O<sub>2</sub> alone, and in contrast to the *E. coli* data, ozone and ozone/H<sub>2</sub>O<sub>2</sub> actually achieved similar levels of inactivation. Regarding the CDPH Title 22 requirements, an O<sub>3</sub>:TOC ratio >0.5 was often sufficient for the 5- and 6.5-log inactivation requirements, but compliance with this benchmark was not entirely consistent. The average log-inactivation values for each treatment condition are provided in Table 3.59.

Figure 3.72 illustrates the inactivation of spiked *B. subtilis* spores during the bench-scale ozone experiments. As expected, the spores proved to be extremely resistant to oxidation and only experienced significant inactivation for O<sub>3</sub>:TOC ratios >1.0 with no H<sub>2</sub>O<sub>2</sub> addition. In other words, a sufficient ozone CT had to be administered before ozone and •OH were able to penetrate the spore coat and inactivate the bacteria. The average log-inactivation values for each treatment condition are provided in Table 3.60.

Finally, Figure 3.73 provides a summary of the ozone disinfection data for the three surrogate microbes within the CT framework. Figure 3.73A illustrates the dose–response relationships for the samples with no H<sub>2</sub>O<sub>2</sub> addition, and Figure 3.73B illustrates the dose–response relationships for H<sub>2</sub>O<sub>2</sub>:O<sub>3</sub> ratios of 0.5 and 1.0 (combined). Similar to the previous data sets, the data indicate that the CT framework is not always appropriate because substantial levels of inactivation can be achieved when the apparent ozone CT is zero. Again, the level of inactivation for vegetative bacteria and viruses is sometimes less than that observed when an ozone residual is present, and no inactivation of spore-forming bacteria can be achieved without a measurable CT.

Table 3.61 summarizes the efficacy of UV and UV/H<sub>2</sub>O<sub>2</sub> for the inactivation of the three surrogate microbes. The efficacy of UV-based disinfection differs dramatically from ozone-based disinfection because UV is highly effective against both vegetative and spore-forming bacteria, whereas some viruses demonstrate resistance. Regardless of H<sub>2</sub>O<sub>2</sub> addition, 50 mJ/cm<sup>2</sup> was sufficient to reach the limits of inactivation for *E. coli* and *Bacillus* spores. On the other hand, MS2 inactivation occurred more slowly and only reached the limit of inactivation with a UV dose of 250 mJ/cm<sup>2</sup>. There was no difference in UV/H<sub>2</sub>O<sub>2</sub> performance with H<sub>2</sub>O<sub>2</sub> doses of 5 and 10 mg/L. Particularly with advanced oxidation dosing conditions (i.e., >250 mJ/cm<sup>2</sup> with 10 mg/L of H<sub>2</sub>O<sub>2</sub>), one can expect substantial inactivation

of all microbes present in wastewater. This constitutes a significant advantage for UV-based treatment over the ozone-based alternatives.

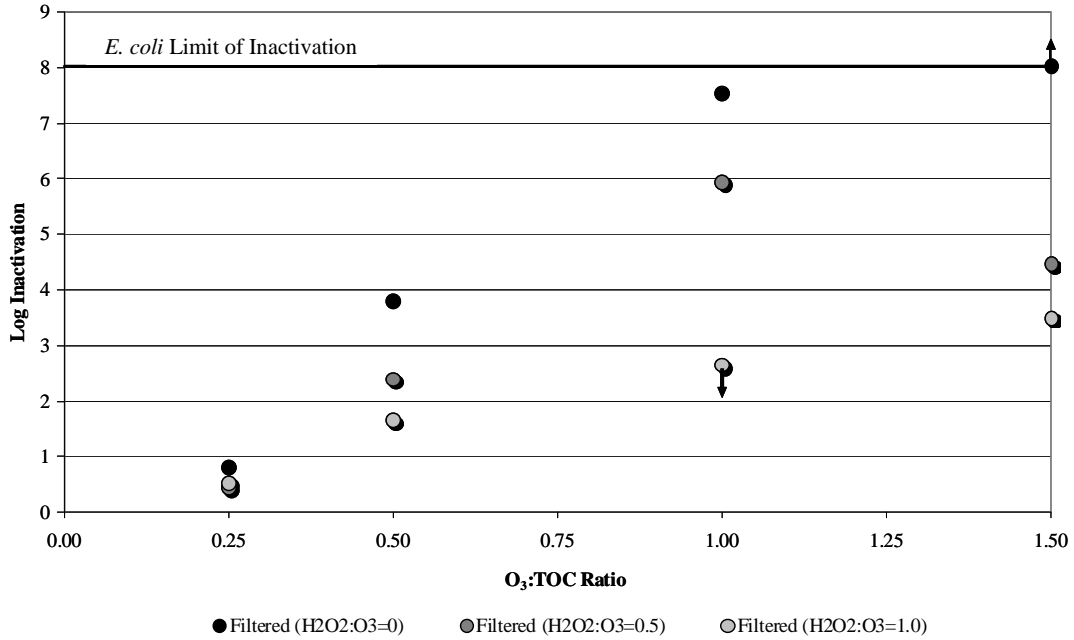


Figure 3.70. Inactivation of spiked *E. coli* in the PCU secondary effluent.

Table 3.58. Summary of *E. coli* Inactivation in the PCU Secondary Effluent

O <sub>3</sub> :TOC Ratio	H <sub>2</sub> O <sub>2</sub> :O <sub>3</sub> =0	H <sub>2</sub> O <sub>2</sub> :O <sub>3</sub> =0.5	H <sub>2</sub> O <sub>2</sub> :O <sub>3</sub> =1.0
0.25	0.8	0.5	0.5
0.5	3.8	2.4	1.7
1.0	7.6	6.0	<2.7**
1.5	>8.0*	4.5	3.5

Notes: \*=limit of inactivation based on spiking level; \*\*=insufficient dilutions to accurately quantify sample

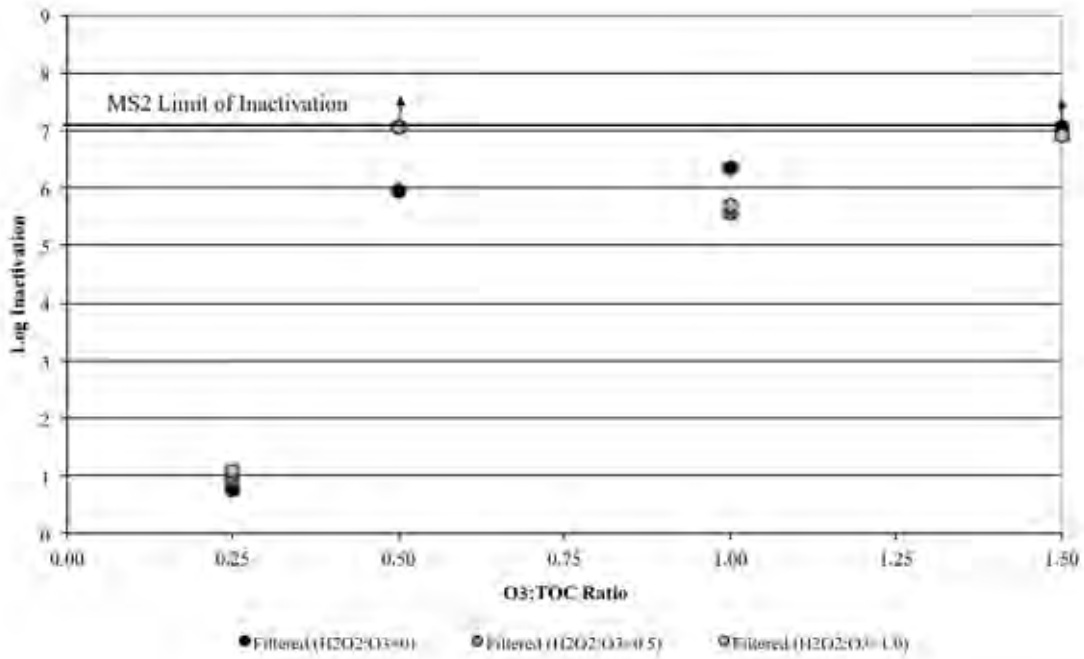


Figure 3.71. Inactivation of spiked MS2 in the PCU secondary effluent.

Table 3.59. Summary of MS2 Inactivation in the PCU Secondary Effluent

O <sub>3</sub> :TOC Ratio	H <sub>2</sub> O <sub>2</sub> :O <sub>3</sub> =0	H <sub>2</sub> O <sub>2</sub> :O <sub>3</sub> =0.5	H <sub>2</sub> O <sub>2</sub> :O <sub>3</sub> =1.0
0.25	0.8	0.9	1.1
0.5	6.0	>7.1*	>7.1*
1.0	6.4	5.6	5.7
1.5	>7.1*	6.9	6.9

Note: \*=limit of inactivation based on spiking level

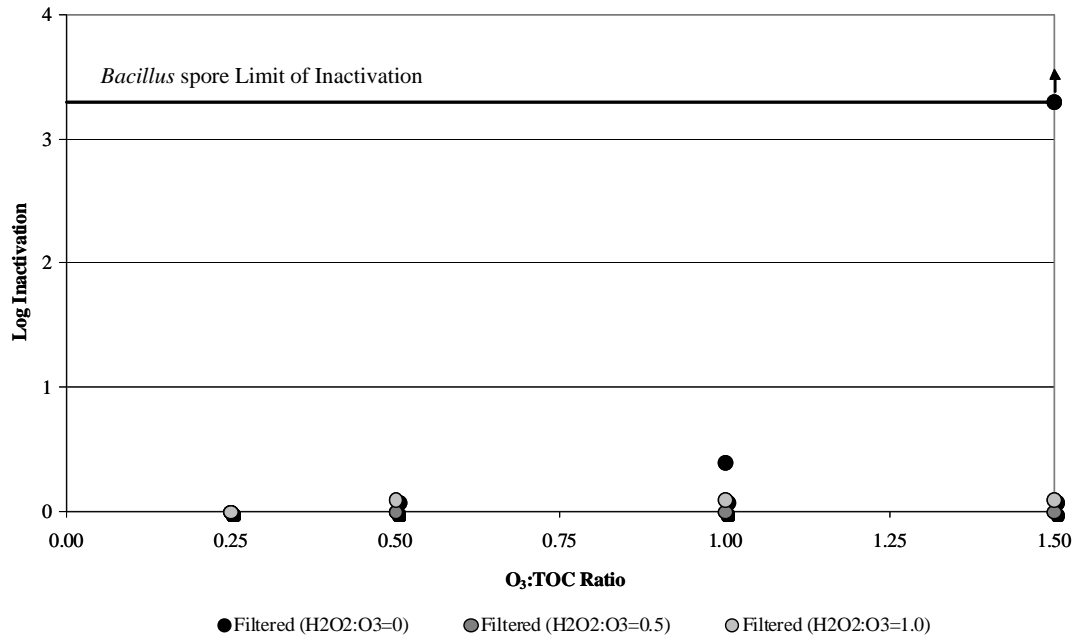


Figure 3.72. Inactivation of spiked *Bacillus* spores in the PCU secondary effluent.

Table 3.60. Summary of *Bacillus* Spore Inactivation in the PCU Secondary Effluent

O <sub>3</sub> :TOC Ratio	H <sub>2</sub> O <sub>2</sub> :O <sub>3</sub> =0	H <sub>2</sub> O <sub>2</sub> :O <sub>3</sub> =0.5	H <sub>2</sub> O <sub>2</sub> :O <sub>3</sub> =1.0
0.25	0.0	0.0	0.0
0.5	0.0	0.0	0.1
1.0	0.4	0.0	0.1
1.5	>3.3*	0.0	0.1

Note: \*=limit of inactivation based on spiking level

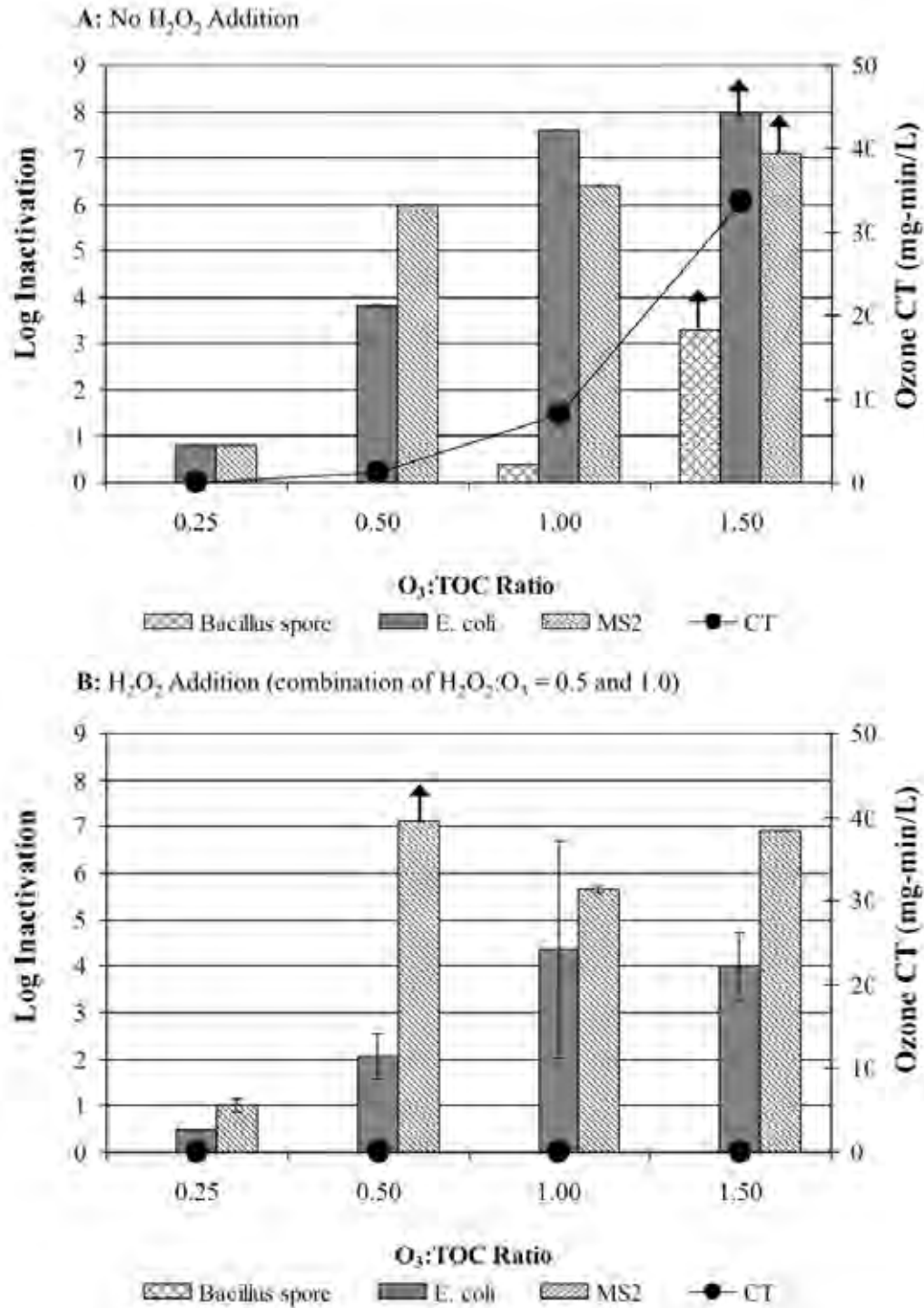


Figure 3.73. Significance of CT for disinfection in the PCU secondary effluent.

**Table 3.61. Summary of UV Inactivation in the PCU Secondary Effluent**

UV Dose (mJ/cm <sup>2</sup> )	<i>E. coli</i>		MS2		<i>Bacillus</i> Spores	
	UV	UV/H <sub>2</sub> O <sub>2</sub> <sup>*</sup>	UV	UV/H <sub>2</sub> O <sub>2</sub> <sup>*</sup>	UV	UV/H <sub>2</sub> O <sub>2</sub> <sup>*</sup>
25	2.5	>6.8 <sup>**</sup>	1.7	1.9	3.3	2.7
50	6.8	>6.8 <sup>**</sup>	2.8	3.1	>3.4 <sup>**</sup>	>3.4 <sup>**</sup>
250	>6.8 <sup>**</sup>	>6.8 <sup>**</sup>	>7.0 <sup>**</sup>	>7.0 <sup>**</sup>	>3.4 <sup>**</sup>	>3.4 <sup>**</sup>
500	>6.8 <sup>**</sup>	>6.8 <sup>**</sup>	>7.0 <sup>**</sup>	>7.0 <sup>**</sup>	>3.4 <sup>**</sup>	>3.4 <sup>**</sup>

Notes: <sup>\*</sup>=H<sub>2</sub>O<sub>2</sub> doses of 5 and 10 mg/L achieved similar levels of inactivation; <sup>\*\*</sup>=limit of inactivation based on spiking level; UV=ultraviolet

### 3.4.7 Organic Characterization

Similar to the previous three data sets, the full-spectrum scans in Figure 3.74 and Figure 3.75, without (A) and with (B) H<sub>2</sub>O<sub>2</sub> addition, indicate that the absorbance profiles around 254 nm generally provide the greatest resolution between treatments. Because of the limited efficacy of UV photolysis (Figure 3.75A), there is little resolution regardless of wavelength, whereas UV/H<sub>2</sub>O<sub>2</sub> (Figure 3.75B) provided slight improvements. Figure 3.76 focuses on the change in UV<sub>254</sub> absorbance with ozone, ozone/H<sub>2</sub>O<sub>2</sub>, UV, and UV/H<sub>2</sub>O<sub>2</sub>. Reductions in UV<sub>254</sub> absorbance were slightly hindered by the addition of H<sub>2</sub>O<sub>2</sub>, whereas the synergistic aspect of the UV AOP provided slight improvements over UV alone.

Three-dimensional excitation emission matrices were developed for the filtered secondary effluent, the finished effluent, and the various treatment conditions. Figure 3.77 illustrates the fluorescence fingerprint of the secondary and finished effluent samples and also provides the total and regional fluorescence intensities based on arbitrary fluorescence units. The fluorescence fingerprint pattern was similar to those of CCWRD and MWRDGC but at a higher intensity. The efficacy of the subsequent full-scale filtration and chlorination processes is apparent based on the reduction in fluorescence intensity from the secondary effluent to the finished effluent sample.

Figure 3.78 provides a qualitative illustration of treatment efficacy after ozone- and UV-based oxidation. Similar to the previous data sets, ozone and ozone/H<sub>2</sub>O<sub>2</sub> are capable of achieving substantial reductions in regional fluorescence and TF, whereas UV and UV/H<sub>2</sub>O<sub>2</sub> provide minimal reductions. It is interesting to note that the sample associated with an O<sub>3</sub>:TOC ratio of 1.5 and an H<sub>2</sub>O<sub>2</sub>:O<sub>3</sub> ratio of 0 was characterized by an unusual fluorescence peak in Region I. This peak is also evident in Figure 3.79.

Figure 3.79 and Figure 3.80 illustrate the fluorescence profiles at an excitation wavelength of 254 nm after ozonation and UV/H<sub>2</sub>O<sub>2</sub>. Because the addition of H<sub>2</sub>O<sub>2</sub> did not have a significant impact on ozone efficacy, and UV photolysis provided limited reductions in fluorescence intensity, these fluorescence profiles are not shown. In contrast to WBMWWD, which was characterized by two distinct peaks, PCU was similar to CCWRD and MWRDGC in that only one distinct peak was apparent.

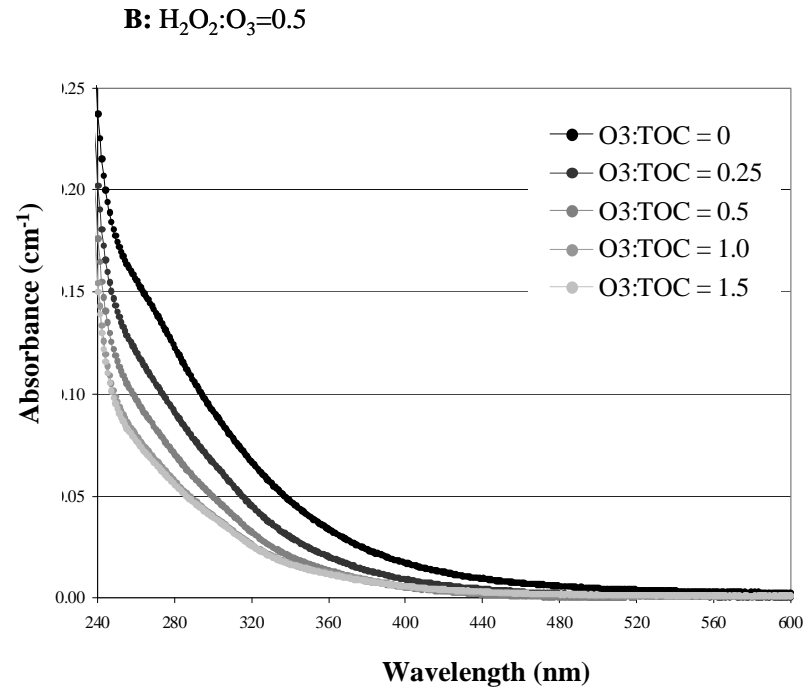
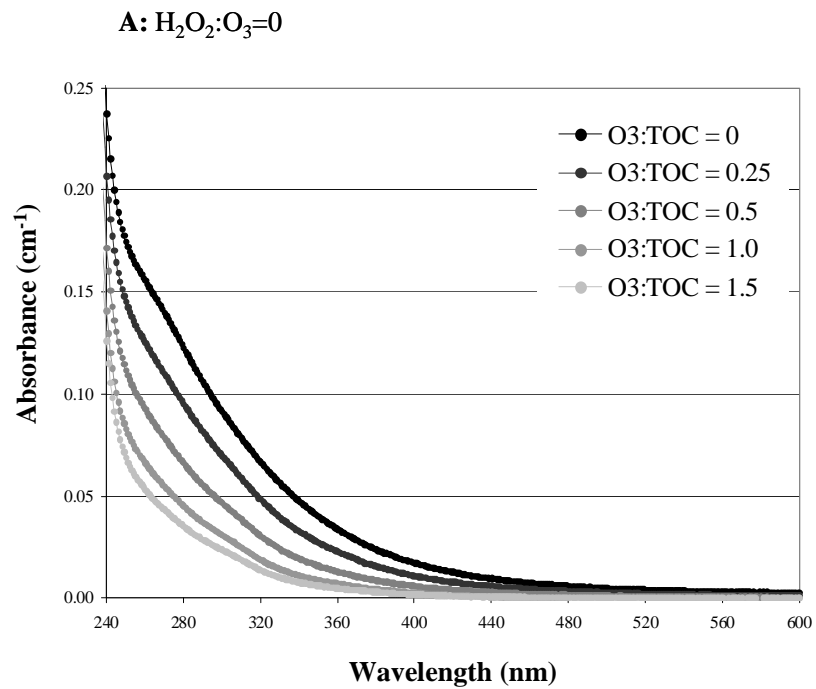


Figure 3.74. PCU absorbance spectra after ozonation.

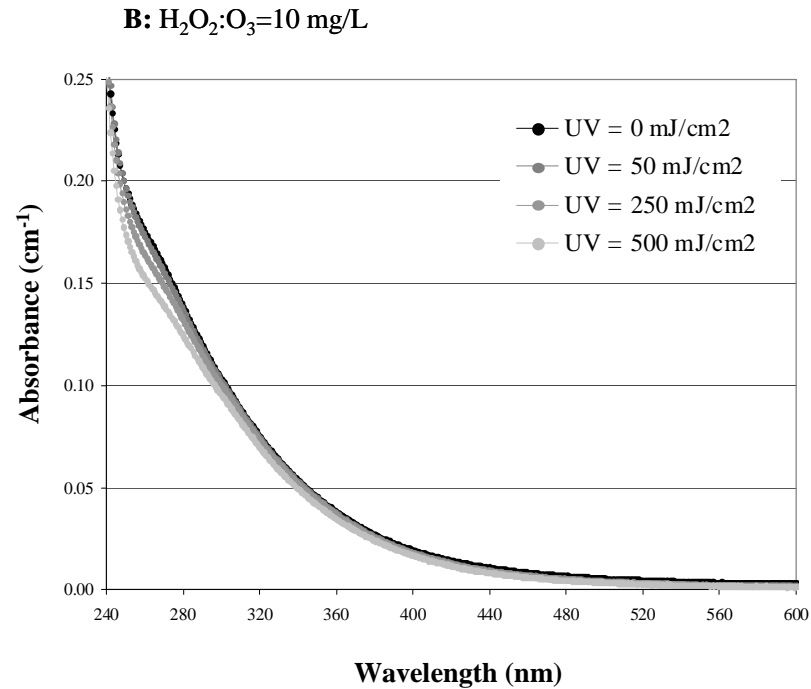
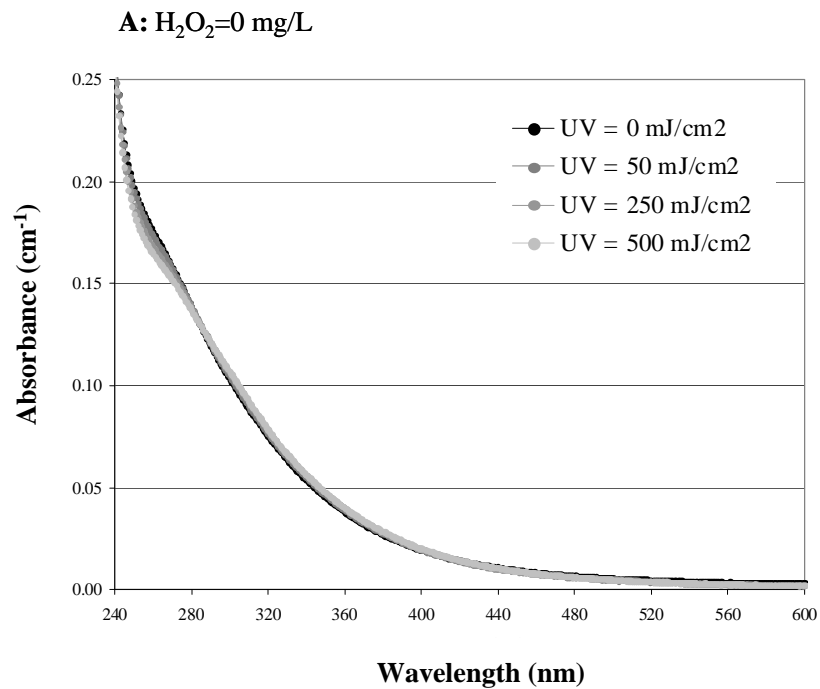
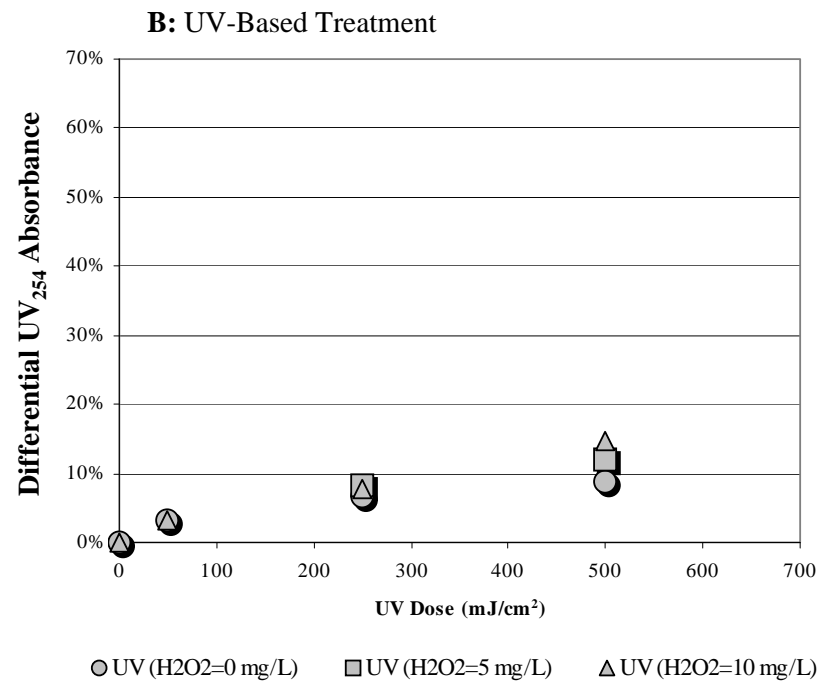
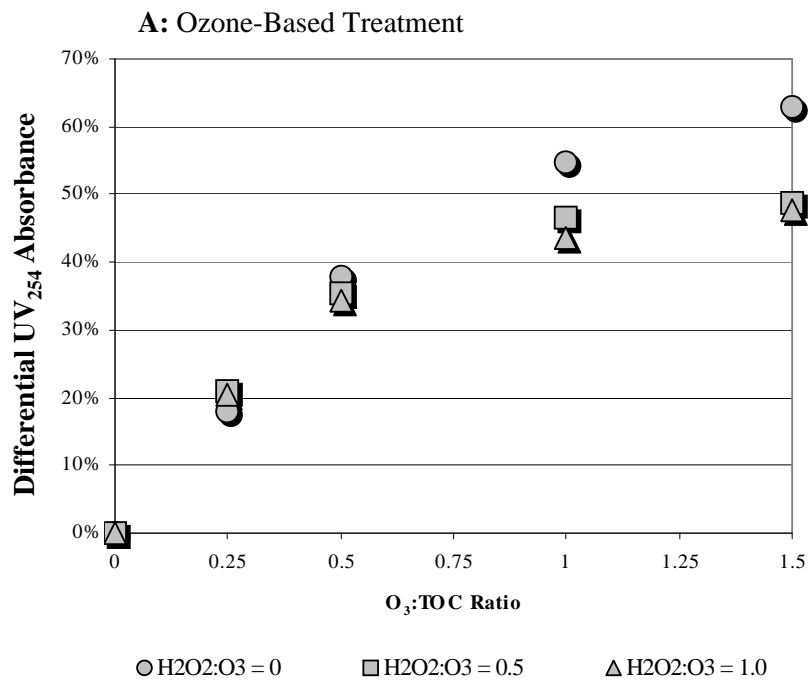


Figure 3.75. PCU absorbance spectra after UV and UV/H<sub>2</sub>O<sub>2</sub>.



**Figure 3.76. Differential UV<sub>254</sub> absorbance in the PCU secondary effluent.**

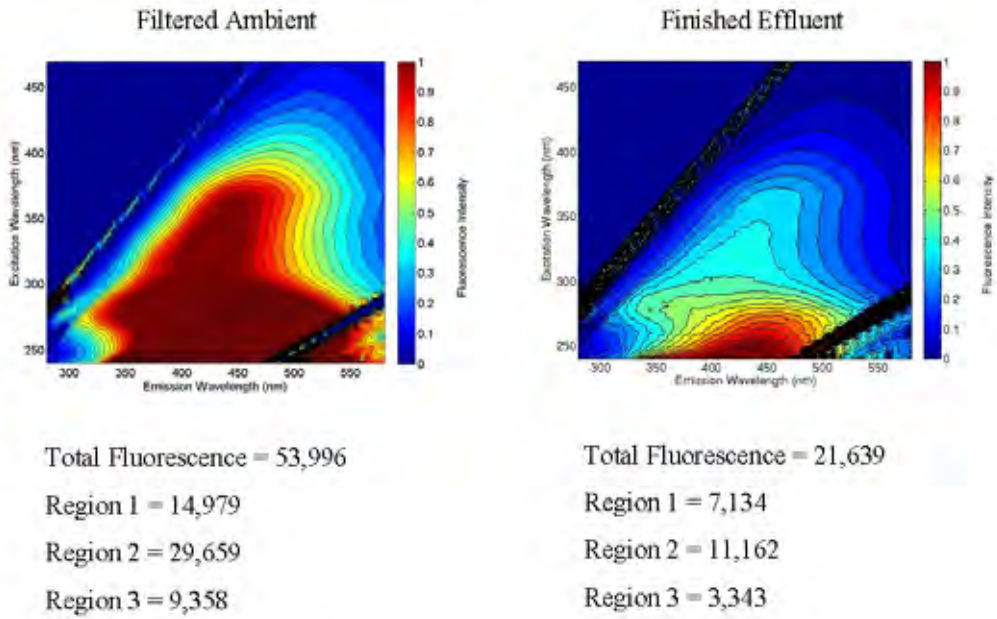


Figure 3.77. 3D EEMs for ambient samples from PCU.

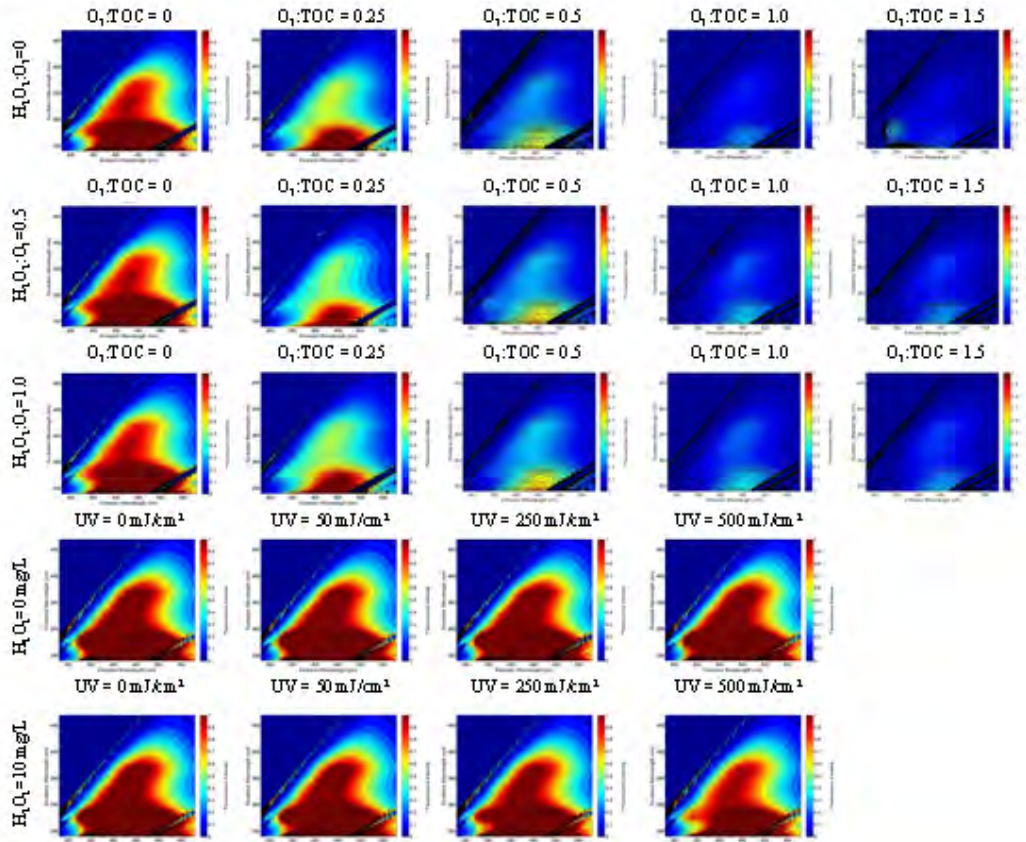


Figure 3.78. 3D EEMs after treatment for the filtered PCU secondary effluent.

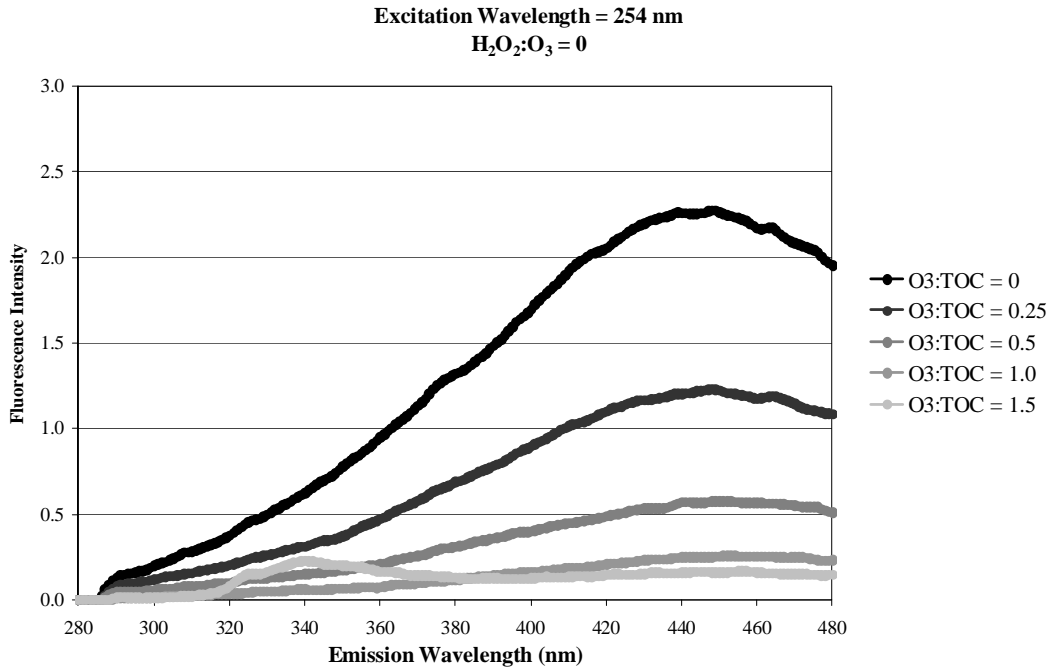


Figure 3.79. PCU fluorescence profiles (Ex<sub>254</sub>) after ozonation.

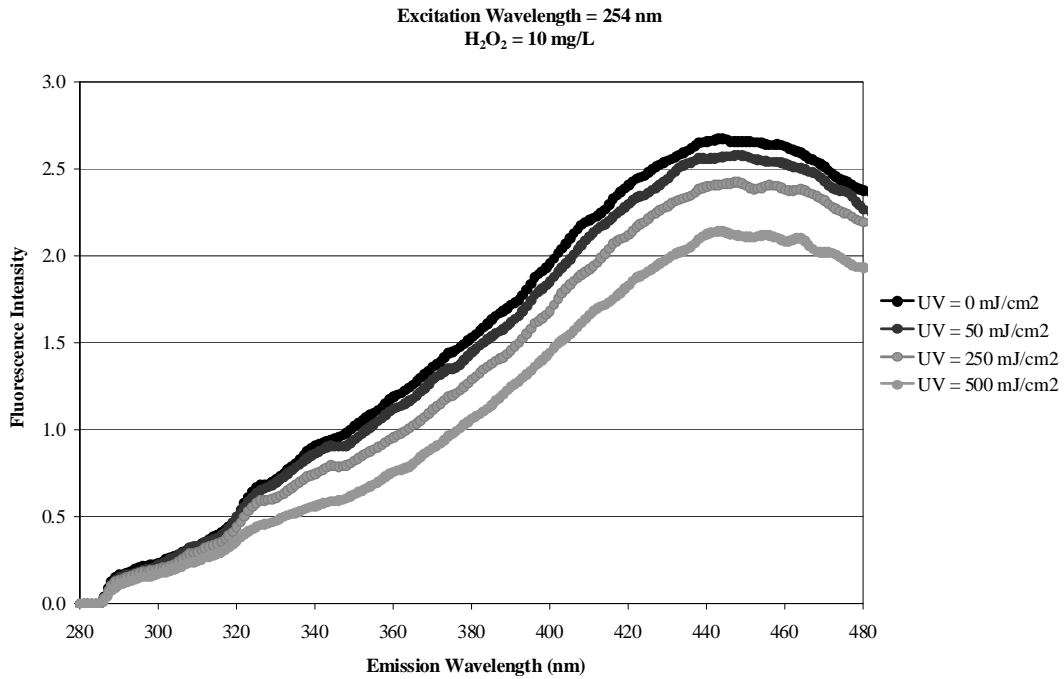


Figure 3.80. PCU fluorescence profiles (Ex<sub>254</sub>) after UV/H<sub>2</sub>O<sub>2</sub>.

Table 3.62 provides the FI (i.e.,  $Ex_{370}Em_{450}/Ex_{370}Em_{500}$ ) and TI (i.e.,  $Ex_{254}Em_{450,T}/Ex_{254}Em_{450,A}$ ) for the PCU experiments. Similar to WBMWD, the FI values remained relatively constant regardless of the treatment condition. In other words, the organic matter associated with emissions at 450 nm and 500 nm was oxidized at similar relative rates. These relative changes are illustrated in Figure 3.81, and Figure 3.82 and Figure 3.83 illustrate the changes in total and regional fluorescence intensities for ozone and UV/H<sub>2</sub>O<sub>2</sub>.

The TI, which measures the extent of organic transformation, reached as low as 0.07 for the highest O<sub>3</sub>:TOC ratio, thereby indicating that 93% of the original fluorescence had been eliminated. This TI reduction is similar to those of the previous three data sets, thereby highlighting the significance of relative changes in bulk organic matter for various water qualities. Also similar to the previous data sets, the addition of H<sub>2</sub>O<sub>2</sub> hindered the oxidation of the bulk organic matter. Because of the limited reduction in fluorescence with UV, the corresponding FI and TI values did not change significantly, although UV/H<sub>2</sub>O<sub>2</sub> provided slight improvements.

**Table 3.62. FI and TI Values for the PCU Secondary Effluent**

Filtered Ozone Exposure						
O <sub>3</sub> :TOC	H <sub>2</sub> O <sub>2</sub> :O <sub>3</sub> =0		H <sub>2</sub> O <sub>2</sub> :O <sub>3</sub> =0.5		H <sub>2</sub> O <sub>2</sub> :O <sub>3</sub> =1.0	
	FI	TI	FI	TI	FI	TI
0	1.30	1.00	1.30	1.00	1.30	1.00
0.25	1.28	0.54	1.26	0.48	1.28	0.50
0.5	1.25	0.26	1.25	0.28	1.27	0.29
1.0	1.24	0.11	1.25	0.14	1.28	0.16
1.5	1.27	0.07	1.28	0.12	1.27	0.12
Filtered UV Exposure						
UV Dose (mJ/cm <sup>2</sup> )	H <sub>2</sub> O <sub>2</sub> =0 mg/L		H <sub>2</sub> O <sub>2</sub> =5 mg/L		H <sub>2</sub> O <sub>2</sub> =10 mg/L	
	FI	TI	FI	TI	FI	TI
0	1.27	1.00	1.27	1.00	1.27	1.00
50	1.27	1.00	N/A	N/A	1.26	0.97
250	1.25	0.98	1.25	0.94	1.24	0.91
500	1.24	0.97	1.23	0.87	1.25	0.80

Notes: FI=fluorescence index; TI=treatment index; UV=ultraviolet

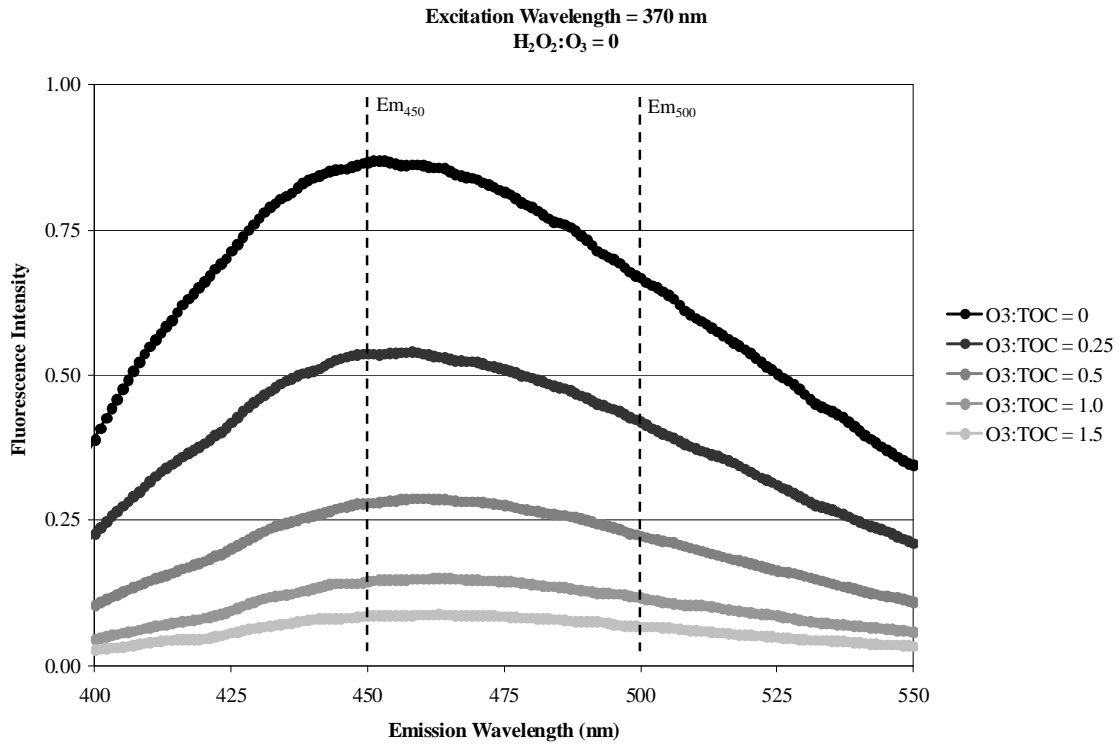


**Figure 3.81. PCU fluorescence profiles (Ex<sub>370</sub>) after ozonation.**

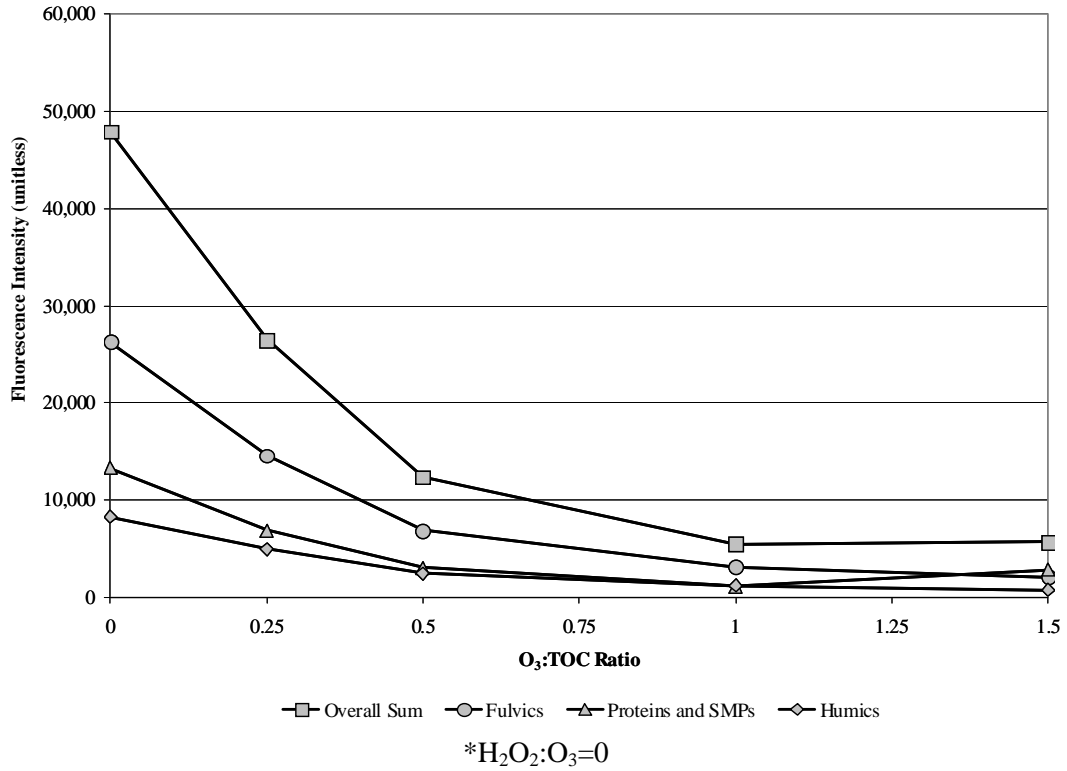


Figure 3.82. Changes in fluorescence intensity after ozonation for PCU.

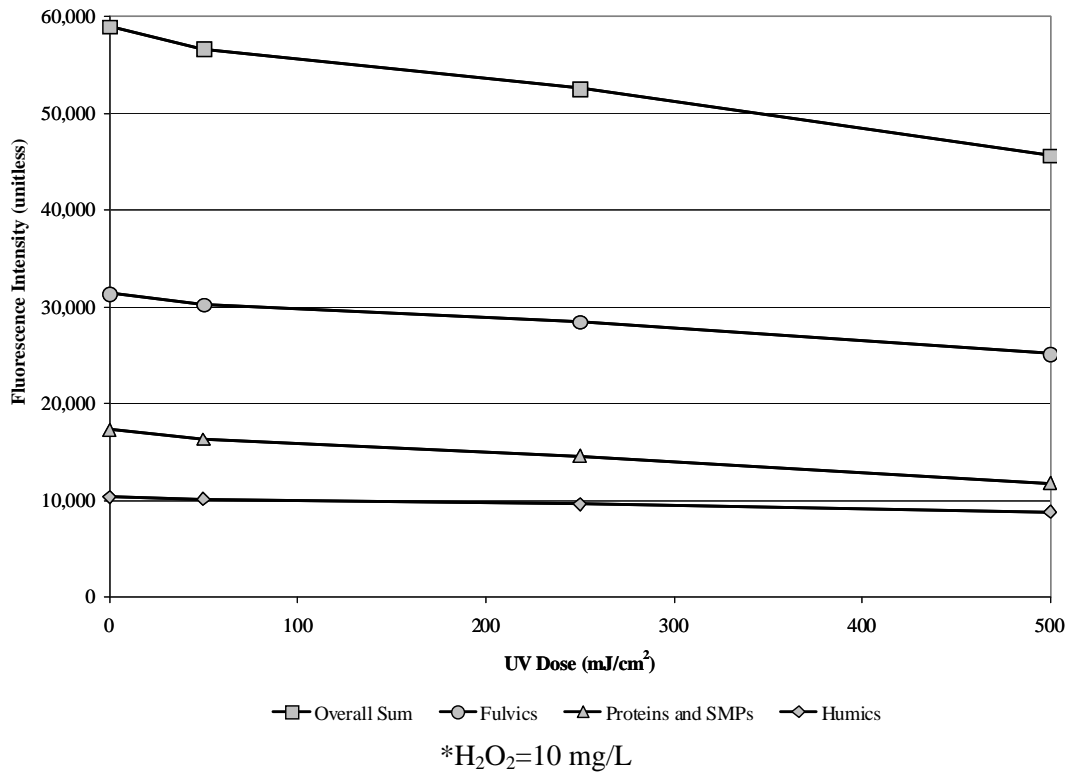


Figure 3.83. Changes in fluorescence intensity after UV/H<sub>2</sub>O<sub>2</sub> for PCU.

### 3.5 Gwinnett County, Atlanta, GA

The study site in Gwinnett County, Georgia, hereafter referred to as GCGA, is one of the largest UF wastewater treatment plants in the world. The GCGA treats approximately 60 MGD of wastewater composed of >98% domestic flows with minor industrial contributions. Multiple liquid treatment trains include the following processes: preliminary screening and grit removal; primary clarification; conventional activated sludge with full nitrification ( $\text{NH}_3 < 0.5 \text{ mg/L}$ ;  $\text{SRT}=11 \text{ days}$ ), denitrification, and biological phosphorus removal ( $\text{TP}_{\text{eff}} < 0.08 \text{ mg/L}$ ); secondary clarification; and high-pH lime clarification. One treatment train continues with recarbonation and trimedia filtration (sand, anthracite, and garnet), while another treatment train continues with strainers and UF. Both trains recombine for preozonation ( $\text{O}_3=1.0\text{--}1.5 \text{ mg/L}$ ), biologically active filtration (BAF;  $\text{EBCT}=15 \text{ minutes}$ ), and final ozone disinfection ( $\text{O}_3=1.0\text{--}1.5 \text{ mg/L}$ ). The BAF process actually contains BAC, but the media has not been replaced or regenerated, so its adsorption capacity is likely exhausted, thereby isolating the biological component. The effluent is discharged through a 20-mile pipeline to the Chattahoochee River. After years of litigation, Gwinnett County also has a permit to discharge the highly treated effluent directly into Lake Lanier, which is the Atlanta metropolitan area's primary drinking water source. A simplified treatment schematic of the GCGA facility is provided in Figure 3.84.

Secondary and finished effluent from GCGA were collected in January 2012, and the water quality data in Table 3.63 were obtained. Using the initial TOC and nitrite data for the filtered secondary effluent, the ozone dosing conditions in Table 3.64 were calculated.

Initially, nitrite was not factored into the dosing calculations because of its negligible effect in the previous bench-scale experiments. After analyzing the nitrite samples and evaluating the data from the other tests, it was apparent that the ambient nitrite concentrations ( $0.30 \text{ mg/L}$  as N or  $0.99 \text{ mg/L}$  as  $\text{NO}_2$ ) significantly impacted the efficacy of ozonation. Nitrite and ozone are known to react in a 1:1 ( $\text{NO}_2:\text{O}_3$ ) mass ratio, which can consume a significant fraction of the applied ozone for low dosing conditions. Because of the constant nature of this demand, the nitrite effect becomes less significant as the applied ozone dose increases. After recalculating the values on the basis of the applied ozone doses and initial nitrite concentration, the  $\text{O}_3:\text{TOC}$  ratios were actually 0.07, 0.32, 0.83, and 1.3. The  $\text{H}_2\text{O}_2:\text{O}_3$  ratios were also affected and are summarized in Table 3.64.

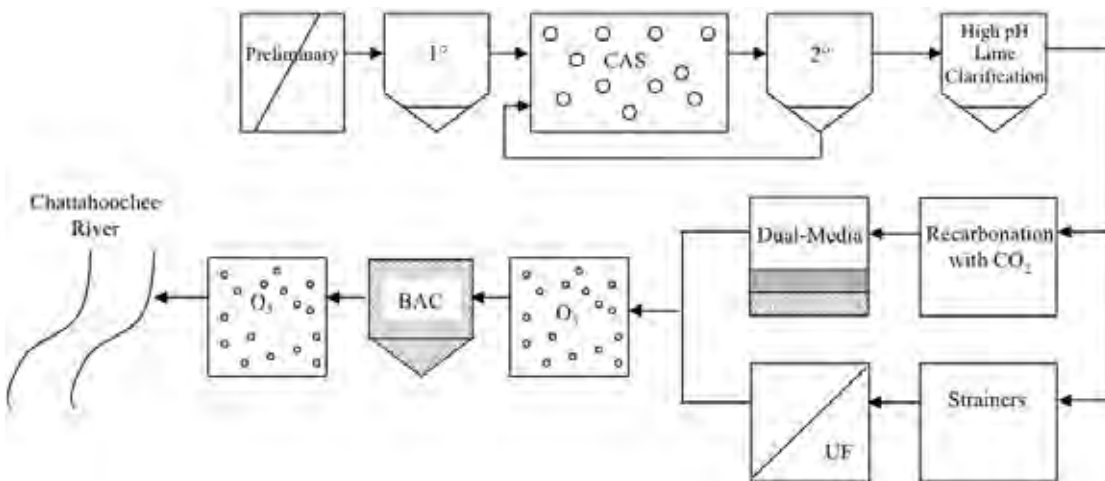


Figure 3.84. Simplified treatment schematic for the GCGA facility.

**Table 3.63. Initial Water Quality Data for GCGA**

<b>Unfiltered Secondary Effluent</b>	Alkalinity (mg/L CaCO <sub>3</sub> )	169
	Bromide (µg/L)	31
	NDMA (ng/L)	17
	NH <sub>3</sub> (mg-N/L)	5.8
	NO <sub>2</sub> (mg-N/L)	0.3
	NO <sub>3</sub> (mg-N/L)	8.6
	pH	7.3
	TKN* (mg-N/L)	5.8
	TN (mg-N/L)	14.7
	TOC (mg/L)	6.3
	TON** (mg-N/L)	~0
	TSS (mg/L)	6.4
	Turbidity (NTU)	3.22
<b>Filtered Secondary Effluent</b>	pH	7.3
	TOC (mg/L)	6.3
	TSS (mg/L)	<5
	Turbidity (NTU)	0.90
	UV <sub>254</sub> absorbance (cm <sup>-1</sup> )	0.130
<b>Finished Effluent</b>	NDMA (ng/L)	<2.5
	TOC (mg/L)	4.0
	UV <sub>254</sub> absorbance (cm <sup>-1</sup> )	0.053

Notes: NDMA=N-nitrosodimethylamine; TKN=total Kjeldahl nitrogen, sum of TON and ammonia; TN=total nitrogen; TOC=total organic carbon; TON=total organic nitrogen, difference of TN and ammonia, nitrate, and nitrite; TSS=total suspended solids

**Table 3.64. Ozone Dosing Conditions for 1-L Filtered GCGA Samples**

Concentration of O<sub>3</sub> stock solution=85 mg/L  
 Concentration of H<sub>2</sub>O<sub>2</sub> stock solution=10 g/L  
 Filtered dilution ratio=(900/1000)=0.900  
 Filtered TOC after dilution=5.7 mg/L  
 Filtered NO<sub>2</sub> after dilution=0.30 mg/L as N=0.99 mg/L as NO<sub>2</sub>

O <sub>3</sub> :TOC/ H <sub>2</sub> O <sub>2</sub> :O <sub>3</sub>	Wastewater Volume (mL)	Nanopure Volume (mL)	O <sub>3</sub> Volume (mL)	O <sub>3</sub> Dose (mg/L)	H <sub>2</sub> O <sub>2</sub> Volume (µL)	H <sub>2</sub> O <sub>2</sub> Dose (mg/L)
Spike	900	100	0	0	0	0
0.07/0	900	83	17	1.4	0	0
0.07/1.7	900	83	17	1.4	51	0.5
0.07/3.4	900	83	17	1.4	102	1.0
0.32/0	900	67	33	2.8	0	0
0.32/0.8	900	67	33	2.8	99	1.0
0.32/1.6	900	67	33	2.8	199	2.0
0.83/0	900	33	67	5.7	0	0
0.83/0.6	900	33	67	5.7	202	2.0
0.83/1.2	900	33	67	5.7	403	4.0
1.3/0	900	0	100	8.5	0	0
1.3/0.6	900	0	100	8.5	301	3.0
1.3/1.1	900	0	100	8.5	602	6.0

Notes: \*=O<sub>3</sub>:TOC ratios differ from previous data sets because NO<sub>2</sub> was not considered during dosing; \*\*=some values are affected by rounding error and the precision of the ozone spike

### 3.5.1 Ozone Demand/Decay

Figure 3.85 illustrates the ozone demand/decay curves for the filtered GCGA secondary effluent at various dosing conditions. The graph only includes dosing conditions with a measurable ozone residual after 30 seconds; corresponding CT values are also provided. The  $O_3/H_2O_2$  samples are not included in the figure because the addition of  $H_2O_2$  led to the formation of  $\bullet OH$  but eliminated the dissolved ozone residual. As expected, the 0.07  $O_3:TOC$  ratio was insufficient to establish a measurable ozone residual after 30 seconds. The low dissolved ozone exposure for the  $O_3:TOC$  ratio of 0.32 was also expected considering that an  $O_3:TOC$  ratio of 0.25 was insufficient to establish a residual for the other wastewaters. For the remaining dosing conditions, the graph illustrates the IOD (i.e., the precipitous drop between 0 and 30 seconds) and the decay over time. The additional demand exerted by ambient nitrite levels made the CT values significantly lower for GCGA in comparison to the other wastewaters.

### 3.5.2 Bromate Formation

As illustrated in Figure 3.86, there was minimal bromate formation for all of the ozone dosing conditions because of the low initial bromide concentration of  $55 \mu g/L$  (after dilution by the ozone stock). Even the highest applied ozone doses only formed 10 to  $15 \mu g/L$  of bromate, which indicates that this would not be a significant design concern for GCGA. The addition of  $H_2O_2$  did not have a consistent impact on bromate formation, but dilution after environmental discharge would be more than sufficient to reach the  $10 \mu g/L$  benchmark without any further mitigation measures.

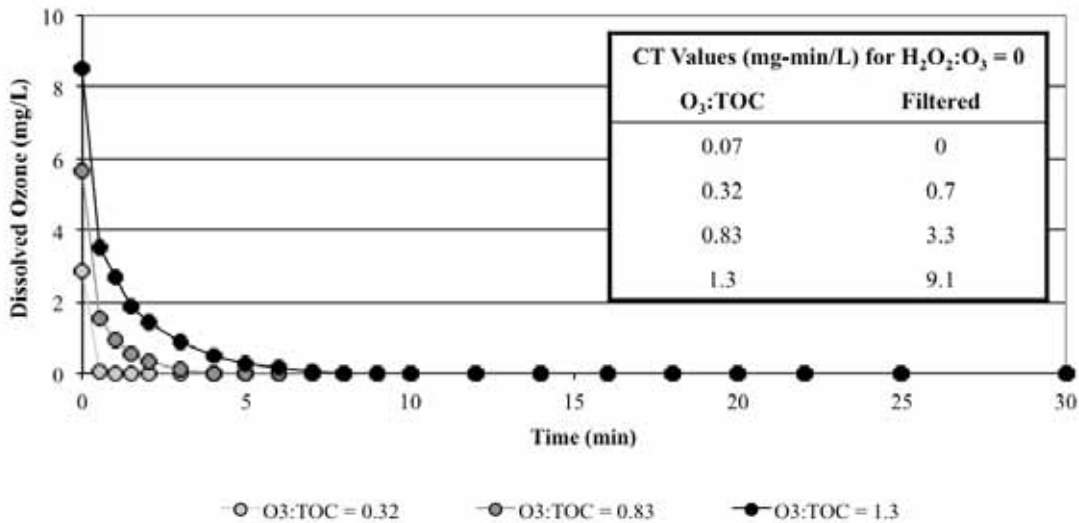
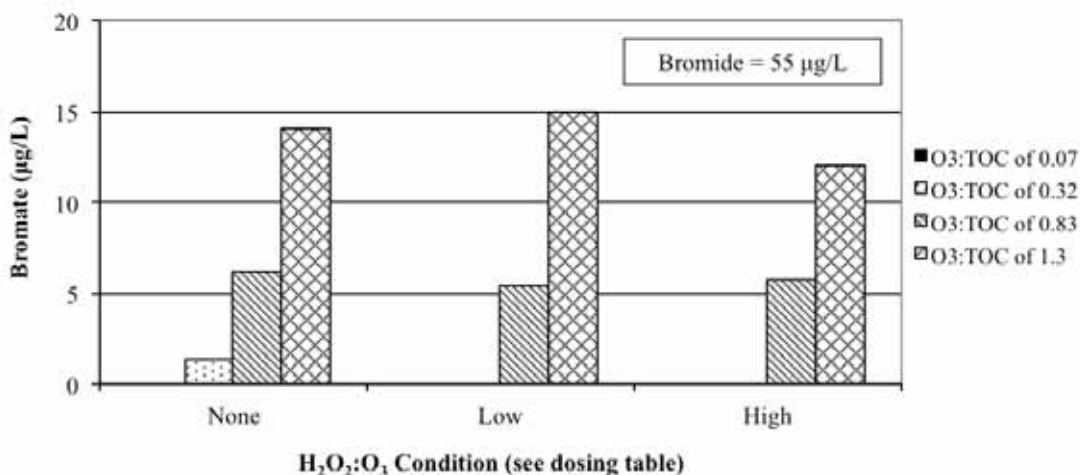


Figure 3.85. Ozone demand/decay curves for GCGA (filtered).



\*See Table 3.64 for H<sub>2</sub>O<sub>2</sub>:O<sub>3</sub> ratios

Figure 3.86. Bromate formation during ozonation of GCGA secondary effluent.

### 3.5.3 Hydroxyl Radical Exposure

On the basis of the data from bench-scale experiments with pCBA spiked at approximately 500 µg/L, Table 3.65 indicates the overall •OH exposure for each ozone and UV dosing condition. The •OH exposures for the UV/H<sub>2</sub>O<sub>2</sub> samples are corrected for the small level of pCBA degradation achieved by photolysis alone.

Similar to many of the previous experiments, the inconsistencies in the data made it difficult to determine whether H<sub>2</sub>O<sub>2</sub> addition impacted overall •OH exposures. The overall •OH exposures were also similar in magnitude to those of CCWRD, MWRDGC, and PCU, whereas WBMWD was characterized by higher •OH exposure because of its unique background organic matter. For GCGA, UV doses between 250 and 500 mJ/cm<sup>2</sup> (with 10 mg/L H<sub>2</sub>O<sub>2</sub>) achieved •OH exposures similar to those of the lower O<sub>3</sub>:TOC ratios.

### 3.5.4 Title 22 Contaminants

Bench-scale experiments were performed with the filtered GCGA wastewater to evaluate the use of ozone and UV for the destruction of spiked NDMA (170 ng/L) and 1,4-dioxane (2 mg/L). The secondary effluent contained 17 ng/L of NDMA prior to the spikes, but the full-scale treatment train was able to achieve the analytical MRL (<2.5 ng/L). The reduction in ambient NDMA during full-scale treatment may have been attributable to biodegradation during the BAC process, but the GCGA facility comprises a relatively complex treatment train. The initial ozonation step likely contributed a small amount of NDMA through a direct formation pathway, as indicated in Table 3.66. The initial ozonation step and the subsequent BAC process likely consumed, destroyed, or removed the remaining NDMA precursors. After biodegradation of the NDMA during the BAC process, the final ozonation step did not contribute any additional NDMA through direct formation, which resulted in the <2.5 ng/L value.

For the NDMA spiking experiment, Figure 3.87 indicates that UV doses of approximately 700 mJ/cm<sup>2</sup> are required to satisfy the Title 22 NDMA requirement. Regarding the direct

formation pathway, ozonation resulted in <10 ng/L of NDMA for all of the dosing conditions, which is comparable to of the results for PCU.

Figure 3.88 illustrates the destruction of spiked 1,4-dioxane during the bench-scale ozone experiments. Unlike any of the previous experiments, ozone was more effective than ozone/H<sub>2</sub>O<sub>2</sub> for the GCGA samples. In fact, ozone achieved the CDPH Title 22 requirement with an O<sub>3</sub>:TOC ratio of approximately 1.0, whereas ozone/H<sub>2</sub>O<sub>2</sub> only achieved 0.3-log destruction with an O<sub>3</sub>:TOC ratio of 1.3.

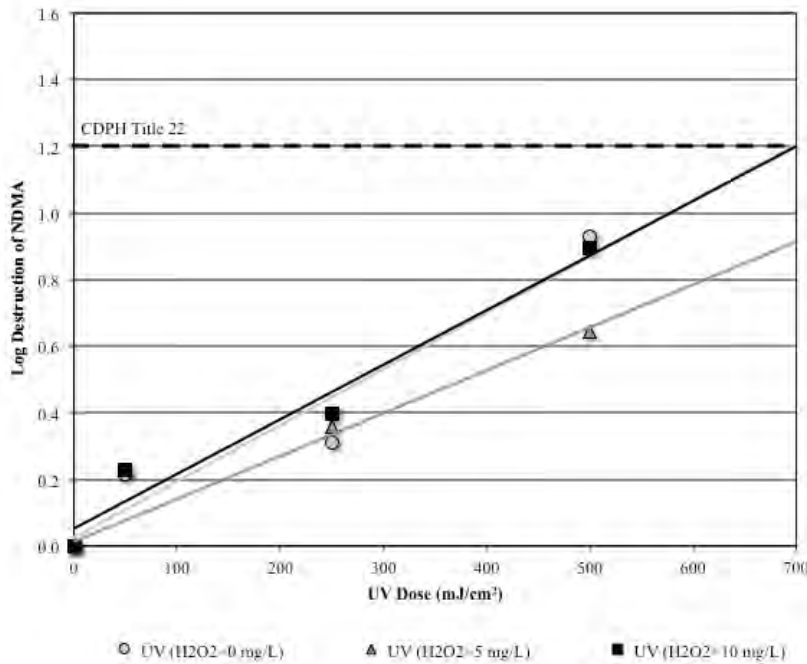
**Table 3.65. •OH Exposure in the GCGA Secondary Effluent**

Filtered Ozone Exposure (10 <sup>-11</sup> M/s)			
Ozone:TOC	H <sub>2</sub> O <sub>2</sub> :O <sub>3</sub> =None*	H <sub>2</sub> O <sub>2</sub> :O <sub>3</sub> =Low*	H <sub>2</sub> O <sub>2</sub> :O <sub>3</sub> =High*
0.07	3.6	4.0	4.4
0.32	9.2	8.9	8.5
0.83	26	32	31
1.3	54	65	53

Filtered UV Exposure (10 <sup>-11</sup> M/s)			
UV Dose (mJ/cm <sup>2</sup> )	H <sub>2</sub> O <sub>2</sub> =0 mg/L	H <sub>2</sub> O <sub>2</sub> =5 mg/L	H <sub>2</sub> O <sub>2</sub> =10 mg/L
0	N/A	N/A	0.0**
50	N/A	N/A	0.0
250	N/A	1.6	3.6
500	N/A	3.7	7.6

Notes: \*=see Table 3.64 for H<sub>2</sub>O<sub>2</sub>:O<sub>3</sub> ratios; \*\*=based on H<sub>2</sub>O<sub>2</sub> control



**Figure 3.87. Destruction of NDMA in the filtered GCGA secondary effluent.**

**Table 3.66. Direct NDMA Formation in the Filtered GCGA Secondary Effluent**

O <sub>3</sub> :TOC Ratio	H <sub>2</sub> O <sub>2</sub> :O <sub>3</sub> Condition*	NDMA (ng/L)
0	0	17
0.07	none	16
0.07	low	16
0.32	none	25
0.32	low	23
0.83	none	26
0.83	low	27
1.3	none	27
1.3	low	25

Note: \*=see Table 3.64 for H<sub>2</sub>O<sub>2</sub>:O<sub>3</sub> ratios

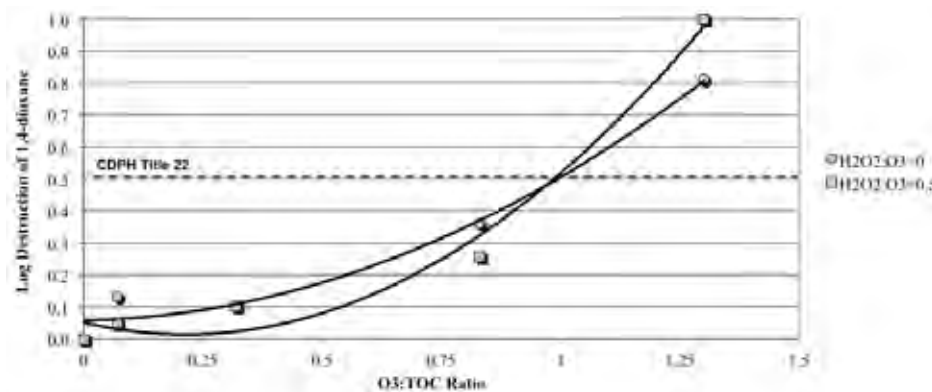


**Figure 3.88. Destruction of 1,4-dioxane in the filtered GCGA secondary effluent.**

### 3.5.5 Trace Organic Contaminants

Secondary and finished effluent samples from GCGA were analyzed to determine the ambient concentrations of the target compounds, which are provided in Table 3.67. The secondary effluent samples were generally consistent with other municipal wastewaters with effective activated sludge processes. For example, the most bioamenable compounds (e.g., naproxen and ibuprofen) were <MRL in the secondary effluent, and atenolol and sulfamethoxazole were present at the highest concentrations. It is interesting to note that TCEP, which is often present at relatively high concentrations in municipal wastewater, was <MRL. The finished effluent concentrations are also consistent with a treatment train composed of ozone and BAC, as will be discussed in Section 5.1. In other words, only the most biologically and ozone-resistant compounds were detected in the finished effluent. The total estrogenicity of the secondary and finished effluents was determined to be 0.66 and <0.074 ng/L.

**Table 3.67. Ambient TOxC Concentrations at GCGA**

Parameter	Secondary Effluent (ng/L)	Finished Effluent (ng/L)
Atenolol	800	<25
Atrazine	<10	<10
Bisphenol A	<50	<50
Carbamazepine	150	<10
DEET	32	<25
Diclofenac	250	<25
Gemfibrozil	150	<10
Ibuprofen	<25	<25
Meprobamate	300	190
Musk ketone	<100	<100
Naproxen	<25	<25
Phenytoin	110	33
Primidone	91	31
Sulfamethoxazole	1,000	<25
TCEP	<200	<200
Total estrogenicity (EEq)	3.2	<0.074
Triclosan	34	<25
Trimethoprim	400	<10

Notes: DEET=*N,N*-diethyl-*meta*-toluamide; EEq=estradiol equivalents; TCEP=tris-(2-chloroethyl)-phosphate

Table 3.68 shows the relative oxidation levels of the 16 target compounds (musk ketone omitted) in the filtered GCGA secondary effluent. As described earlier, the target compounds were divided into five categories based on their second-order ozone and •OH rate constants. Similar to some of the previous data sets, H<sub>2</sub>O<sub>2</sub> addition may have provided a slight advantage for the ozone-resistant compounds (Groups 3, 4, and 5). After accounting for the difference in O<sub>3</sub>:TOC ratios based on the nitrite demand, the GCGA oxidation levels were similar to those of previous data sets. Despite the low applied ozone dose, an O<sub>3</sub>:TOC ratio of 0.07 still achieved significant destruction of all of the target compounds, particularly those in Group 1. This dosing condition was unable to achieve 80% destruction of any compound, but an O<sub>3</sub>:TOC ratio of 0.32 was able to achieve 80% destruction of the Group 1 compounds and one of the Group 2 compounds. The remaining dosing conditions were similar to the previous data sets in that the third and fourth O<sub>3</sub>:TOC ratios achieved at least 80% destruction of the Groups 3 and 4 compounds. As expected, the maximum level of TCEP oxidation was 25%.

Table 3.69 shows the relative photolysis and UV/H<sub>2</sub>O<sub>2</sub> oxidation levels of the target compounds. UV photolysis only achieved 80% destruction of diclofenac and triclosan, whereas atrazine, phenytoin, and sulfamethoxazole experienced greater than 35% destruction with UV alone. The addition of H<sub>2</sub>O<sub>2</sub> with a UV dose of 500 mJ/cm<sup>2</sup> improved treatment efficacy, but a majority of the compounds only ranged from 20 to 40% oxidation. Neither UV nor UV/H<sub>2</sub>O<sub>2</sub> achieved significant destruction of TCEP.

During the ozone experiments, the total estrogenicity of the secondary effluent (3.2 ng/L) was oxidized down to the MRL with the higher ozone and H<sub>2</sub>O<sub>2</sub> dosing conditions (Figure 3.89). Although the reasons are unclear, the total estrogenicity of the secondary effluent during the UV and UV/H<sub>2</sub>O<sub>2</sub> experiments increased from 3.2 ng/L to approximately 8 ng/L. From a treatment perspective, UV and UV/H<sub>2</sub>O<sub>2</sub> achieved some reduction in total estrogenicity, although these treatment processes were unable to achieve the MRL of the YES assay.

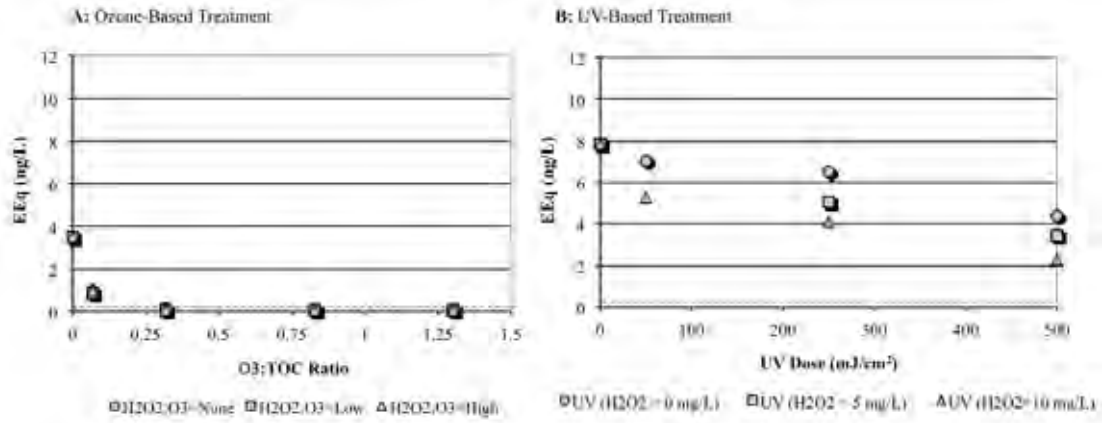


Figure 3.89. Reduction in total estrogenicity in the filtered GCGA secondary effluent.

**Table 3.68. GCGA TOxC Mitigation by Ozone (Filtered)**

Group	Contaminant	O <sub>3</sub> :TOC (mass) / H <sub>2</sub> O <sub>2</sub> :O <sub>3</sub> (molar)											
		0.07/0	0.07/1.7	0.07/3.4	0.32/0	0.32/0.8	0.32/1.6	0.83/0	0.83/0.6	0.83/1.2	1.3/0	1.3/0.6	1.3/1.1
1	Bisphenol A	66%	69%	67%	97%	97%	95%	97%	97%	97%	97%	97%	97%
	Carbamazepine	52%	53%	51%	99%	99%	91%	99%	99%	99%	99%	99%	99%
	Diclofenac	61%	62%	61%	98%	98%	94%	98%	98%	98%	98%	98%	98%
	Naproxen	55%	56%	49%	98%	98%	91%	98%	98%	98%	98%	98%	98%
	Sulfamethoxazole	45%	45%	43%	92%	91%	85%	98%	98%	98%	98%	98%	98%
	Triclosan	75%	79%	76%	97%	97%	97%	97%	97%	97%	97%	97%	97%
	Trimethoprim	56%	58%	56%	99%	99%	93%	99%	99%	99%	99%	99%	99%
	<b>Indicator</b>	<b>59%</b>	<b>60%</b>	<b>58%</b>	<b>97%</b>	<b>97%</b>	<b>92%</b>	<b>98%</b>	<b>98%</b>	<b>98%</b>	<b>98%</b>	<b>98%</b>	<b>98%</b>
2	Atenolol	25%	19%	13%	54%	51%	58%	98%	98%	97%	98%	98%	98%
	Gemfibrozil	30%	33%	30%	91%	85%	79%	99%	99%	99%	99%	99%	99%
	<b>Indicator</b>	<b>28%</b>	<b>26%</b>	<b>22%</b>	<b>73%</b>	<b>68%</b>	<b>69%</b>	<b>99%</b>	<b>99%</b>	<b>98%</b>	<b>99%</b>	<b>99%</b>	<b>99%</b>
3	DEET	13%	13%	19%	38%	38%	43%	84%	88%	89%	97%	98%	98%
	Ibuprofen	16%	18%	19%	43%	47%	49%	90%	92%	93%	97%	97%	97%
	Phenytoin	12%	15%	19%	44%	38%	51%	91%	94%	95%	99%	99%	99%
	Primidone	20%	20%	15%	40%	40%	45%	86%	88%	89%	98%	99%	98%
	<b>Indicator</b>	<b>15%</b>	<b>17%</b>	<b>18%</b>	<b>41%</b>	<b>41%</b>	<b>47%</b>	<b>88%</b>	<b>91%</b>	<b>92%</b>	<b>98%</b>	<b>98%</b>	<b>98%</b>
4	Atrazine	9%	8%	10%	23%	21%	25%	54%	59%	62%	80%	85%	84%
	Meprobamate	5%	8%	12%	22%	26%	31%	64%	71%	73%	87%	92%	92%
	<b>Indicator</b>	<b>7%</b>	<b>8%</b>	<b>11%</b>	<b>23%</b>	<b>24%</b>	<b>28%</b>	<b>59%</b>	<b>65%</b>	<b>68%</b>	<b>84%</b>	<b>89%</b>	<b>88%</b>
5	TCEP	4%	4%	2%	4%	4%	8%	8%	15%	13%	17%	25%	25%

Notes: Shading represents >80% oxidation; DEET=*N,N*-diethyl-*meta*-toluamide; TCEP=tris-(2-chloroethyl)-phosphate

**Table 3.69. GCGA TOxC Mitigation by UV (Filtered)**

Group	Contaminant	UV Dose (mJ/cm <sup>2</sup> ) / H <sub>2</sub> O <sub>2</sub> Dose (mg/L)								
		50/0	50/10	250/0	250/5	250/10	500/0	500/5	500/10	
1	Bisphenol A	-5%	0%	-5%	15%	20%	5%	20%	40%	
	Carbamazepine	1%	2%	0%	6%	14%	2%	12%	33%	
	Diclofenac	43%	0%	91%	83%	86%	98%	96%	96%	
	Naproxen	3%	1%	12%	13%	15%	25%	39%	41%	
	Sulfamethoxazole	12%	0%	47%	35%	34%	67%	64%	69%	
	Triclosan	30%	2%	82%	63%	69%	94%	92%	95%	
	Trimethoprim	6%	-7%	0%	7%	13%	6%	13%	27%	
2	Atenolol	0%	6%	-6%	18%	24%	12%	24%	29%	
	Gemfibrozil	12%	-2%	0%	4%	13%	9%	14%	30%	
3	DEET	11%	0%	6%	0%	13%	6%	13%	25%	
	Ibuprofen	5%	2%	1%	5%	11%	5%	23%	29%	
	Phenytoin	-1%	-5%	9%	17%	37%	35%	50%	58%	
	Primidone	5%	5%	0%	0%	5%	5%	5%	26%	
4	Atrazine	9%	-2%	21%	10%	16%	36%	32%	38%	
	Meprobamate	9%	1%	13%	0%	4%	11%	9%	18%	
5	TCEP	10%	-6%	3%	-6%	-2%	3%	-4%	-6%	

Notes: Groupings based on ozone and OH rate constants; shading represents >80% photolysis or oxidation; DEET=*N,N*-diethyl-*meta*-toluamide; TCEP=tris-(2-chloroethyl)-phosphate; UV=ultraviolet

### 3.5.6 Disinfection

Ambient secondary (before and after laboratory filtration) and finished effluent samples were assayed for total and fecal coliforms, MS2, and *Bacillus* spores. According to the ambient microbial water quality data provided in Figure 3.90 illustrates the inactivation of spiked *E. coli* during the bench-scale ozone experiments, and the average log-inactivation values for each treatment condition are provided in Table 3.72 The solid line near the top of the figure represents the limit of inactivation based on the spiking level in the filtered samples. Inactivation with H<sub>2</sub>O<sub>2</sub> alone was insignificant, and when combined with ozonation, the addition of H<sub>2</sub>O<sub>2</sub> significantly hindered *E. coli* inactivation. In fact, the addition of H<sub>2</sub>O<sub>2</sub> reduced the inactivation level by more than 5 logs for an O<sub>3</sub>:TOC ratio of 1.3. With the exception of one data point, the level of *E. coli* inactivation for GCGA was very low regardless of O<sub>3</sub>:TOC ratio, but it is unclear why the level of inactivation was consistently low in this particular wastewater. It is interesting to note that this facility uses ozone as a final disinfectant. Error! Not a valid bookmark self-reference. indicates that the finished effluent still contained 36.3 MPN/100 mL of total coliforms after two stages of ozonation.

Table 3.70, the total coliform, fecal coliform, and *Bacillus* spore values were an order of magnitude higher than those of the previous data sets, whereas MS2 was consistent with the previous wastewaters. In order to illustrate a wide range of inactivation, the ozone and UV disinfection samples were spiked with relatively high numbers of the surrogate microbes, as indicated in Table 3.71.

Figure 3.90 illustrates the inactivation of spiked *E. coli* during the bench-scale ozone experiments, and the average log-inactivation values for each treatment condition are provided in Table 3.72 The solid line near the top of the figure represents the limit of inactivation based on the spiking level in the filtered samples. Inactivation with H<sub>2</sub>O<sub>2</sub> alone

was insignificant, and when combined with ozonation, the addition of H<sub>2</sub>O<sub>2</sub> significantly hindered *E. coli* inactivation. In fact, the addition of H<sub>2</sub>O<sub>2</sub> reduced the inactivation level by more than 5 logs for an O<sub>3</sub>:TOC ratio of 1.3. With the exception of one data point, the level of *E. coli* inactivation for GCGA was very low regardless of O<sub>3</sub>:TOC ratio, but it is unclear why the level of inactivation was consistently low in this particular wastewater. It is interesting to note that this facility uses ozone as a final disinfectant, and Table 3.70 indicates that the finished effluent still contained 36.3 MPN/100 mL of total coliforms after two stages of ozonation.

**Table 3.70. Ambient Microbial Water Quality Data for GCGA**

Microbial Surrogate	Unfiltered Secondary Effluent	Filtered Secondary Effluent	Finished Effluent
<i>Bacillus</i> spores (CFU/100 mL)	2.3x10 <sup>4</sup>	1.3x10 <sup>4</sup>	9.3x10 <sup>3</sup>
Coliforms, fecal (MPN/100 mL)	1.1x10 <sup>3</sup>	1.0x10 <sup>3</sup>	<1
Coliforms, total (MPN/100 mL)	3.5x10 <sup>4</sup>	1.6x10 <sup>4</sup>	36.3
MS2 (PFU/mL)	<1	<1	<1

**Table 3.71. Microbial Spiking Levels for GCGA Bench-Scale Experiments**

Microbial Surrogate	Filtered Ozone Disinfection	Filtered UV Disinfection
<i>B. subtilis</i> spores (CFU/100 mL)	2.0x10 <sup>5</sup>	2.1x10 <sup>5</sup>
<i>E. coli</i> (MPN/100 mL)	1.2x10 <sup>8</sup>	1.4x10 <sup>7</sup>
MS2 (PFU/mL)	3.4x10 <sup>7</sup>	1.3x10 <sup>7</sup>

Note: UV=ultraviolet

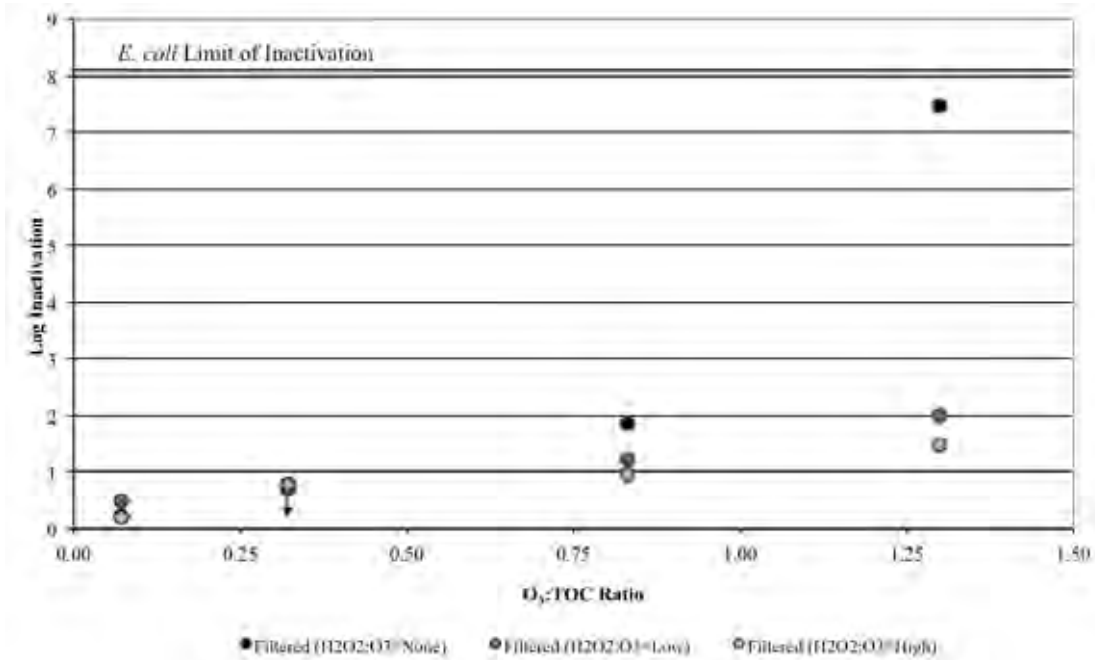
Figure 3.91 illustrates the inactivation of spiked MS2 during the bench-scale ozone experiments. Again, minimal inactivation was achieved with the addition of H<sub>2</sub>O<sub>2</sub> alone, and in contrast to the *E. coli* data, the addition of H<sub>2</sub>O<sub>2</sub> only had a slightly negative impact on MS2 inactivation during ozonation. To meet the CDPH Title 22 requirements, an O<sub>3</sub>:TOC ratio between 0.32 and 0.83 was often sufficient for the 5- and 6.5-log inactivation. An O<sub>3</sub>:TOC ratio of 1.3 achieved the Title 22 benchmarks for all H<sub>2</sub>O<sub>2</sub> conditions. The average log-inactivation values for each treatment condition are provided in Table 3.73.

Figure 3.92 illustrates the inactivation of spiked *Bacillus* spores during the bench-scale ozone experiments, and the average log-inactivation values for each treatment condition are provided in Table 3.74. As expected, the spores proved to be extremely resistant to oxidation and only experienced significant inactivation for an O<sub>3</sub>:TOC ratio of 1.3 with no H<sub>2</sub>O<sub>2</sub> addition. In other words, a sufficient ozone CT had to be administered before ozone and •OH were able to penetrate the spore coat and inactivate the bacteria. This is consistent with the

full-scale data in that limited spore inactivation was achieved despite two stages of ozonation (see Table 3.70).

Figure 3.93 provides a summary of the ozone disinfection data for the three surrogate microbes within the CT framework. Figure 3.93A illustrates the dose–response relationships for the samples with no H<sub>2</sub>O<sub>2</sub> addition, and Figure 3.93B illustrates the dose–response relationships for H<sub>2</sub>O<sub>2</sub>:O<sub>3</sub> ratios of 0.5 and 1.0 (combined). Similar to the previous data sets, the data indicate that the CT framework is not always appropriate because substantial levels of inactivation can be achieved when the apparent ozone CT is zero. Again, the level of inactivation for vegetative bacteria and viruses is sometimes less than that observed when an ozone residual is present, and no inactivation of spore-forming bacteria can be achieved without a measurable CT.

Table 3.75 summarizes the efficacy of UV and UV/H<sub>2</sub>O<sub>2</sub> for the inactivation of the three surrogate microbes. The efficacy of UV-based disinfection differs dramatically from ozone-based disinfection because UV is highly effective against both vegetative and spore-forming bacteria, whereas some viruses demonstrate resistance. Approximately 50 mJ/cm<sup>2</sup> was sufficient to reach the limits of inactivation for *E. coli* and *Bacillus* spores, regardless of H<sub>2</sub>O<sub>2</sub> addition. On the other hand, MS2 inactivation occurred more slowly and only reached the limit of inactivation with a UV dose of 250 mJ/cm<sup>2</sup>. There was no difference in UV/H<sub>2</sub>O<sub>2</sub> performance with H<sub>2</sub>O<sub>2</sub> doses of 5 and 10 mg/L. Particularly under advanced oxidation dosing conditions (i.e., >250 mJ/cm<sup>2</sup> with 10 mg/L of H<sub>2</sub>O<sub>2</sub>), one can expect substantial inactivation of all microbes present in wastewater. This constitutes a significant advantage for UV-based treatment over the ozone-based alternatives.



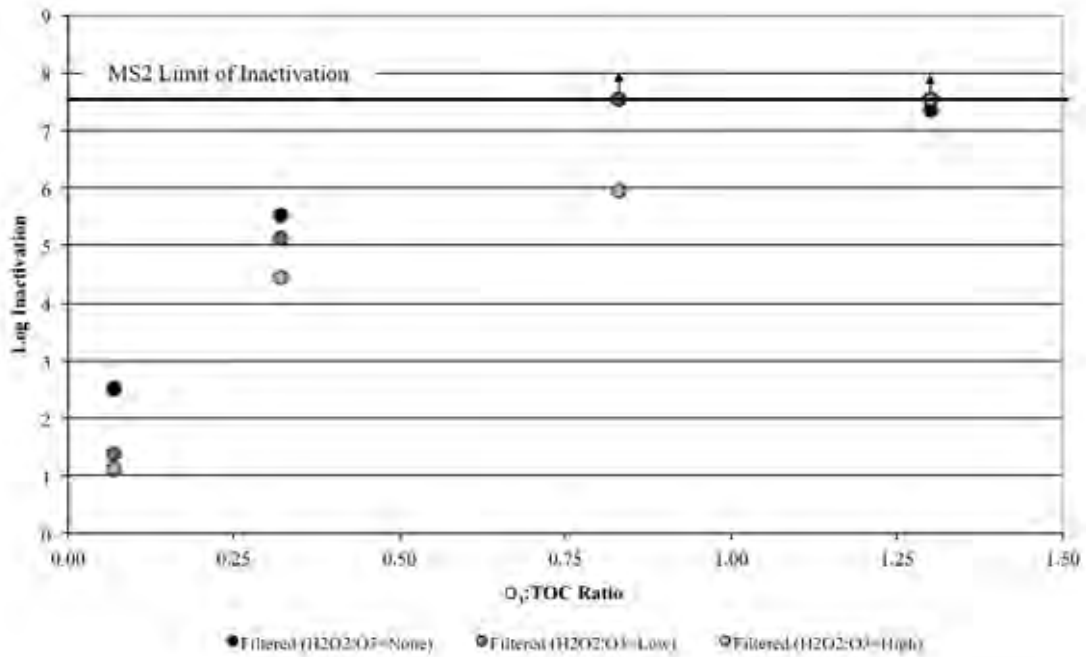
\*See Table 3.64 for H<sub>2</sub>O<sub>2</sub>:O<sub>3</sub> ratios

Figure 3.90. Inactivation of spiked *E. coli* in the GCGA secondary effluent.

Table 3.72. Summary of *E. coli* Inactivation in the GCGA Secondary Effluent

O <sub>3</sub> :TOC Ratio	H <sub>2</sub> O <sub>2</sub> :O <sub>3</sub> =None*	H <sub>2</sub> O <sub>2</sub> :O <sub>3</sub> =Low*	H <sub>2</sub> O <sub>2</sub> :O <sub>3</sub> =High*
0.07	0.2	0.5	0.2
0.32	0.8	0.7**	0.8
0.83	1.8	1.2	1.0
1.3	7.5	2.0	1.5

Notes: \*=see Table 3.64 for H<sub>2</sub>O<sub>2</sub>:O<sub>3</sub> ratios; \*\*=insufficient dilutions to accurately quantify sample



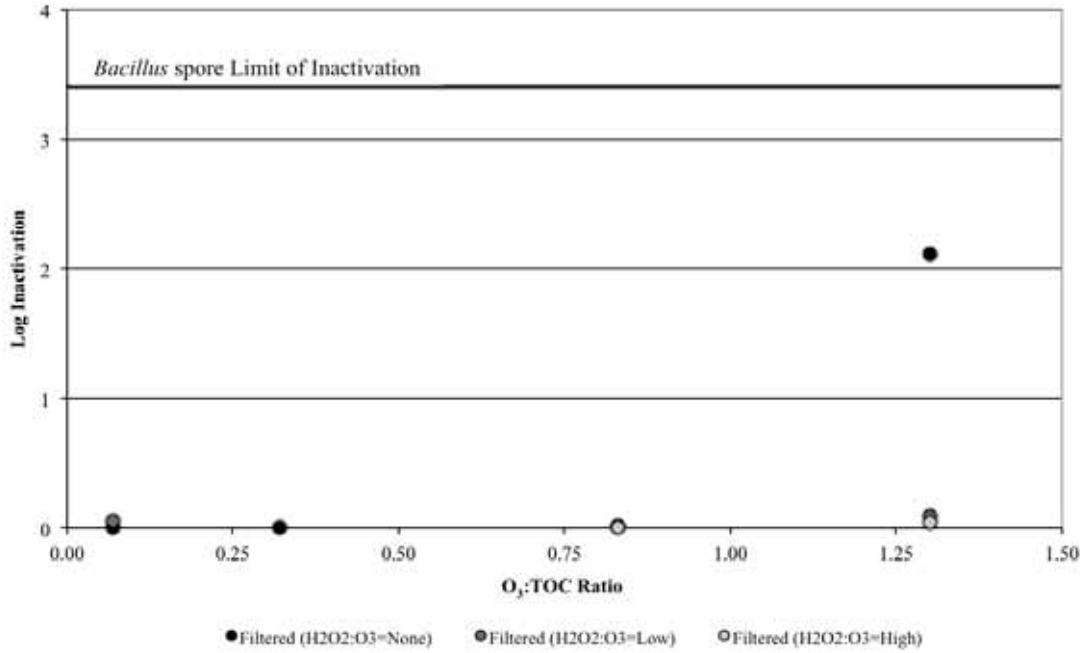
\*See Table 3.64 for H<sub>2</sub>O<sub>2</sub>:O<sub>3</sub> ratios

Figure 3.91. Inactivation of spiked MS2 in the GCGA secondary effluent.

Table 3.73. Summary of MS2 Inactivation in the GCGA Secondary Effluent

O <sub>3</sub> :TOC Ratio	H <sub>2</sub> O <sub>2</sub> :O <sub>3</sub> =None*	H <sub>2</sub> O <sub>2</sub> :O <sub>3</sub> =Low*	H <sub>2</sub> O <sub>2</sub> :O <sub>3</sub> =High*
0.07	2.5±0.0	1.4±0.0	1.1±0.0
0.32	5.5±0.0	5.1±0.0	4.5±0.0
0.83	>7.5±0.0**	>7.5±0.0**	6.0±0.0
1.3	7.3±0.4	>7.5±0.0**	>7.5±0.0**

Notes: \*=see Table 3.64 for H<sub>2</sub>O<sub>2</sub>:O<sub>3</sub> ratios; \*\*=limit of inactivation based on spiking level



\*See Table 3.64 for H<sub>2</sub>O<sub>2</sub>:O<sub>3</sub> ratios

Figure 3.92. Inactivation of spiked *Bacillus* spores in the GCGA secondary effluent.

Table 3.74. Summary of *Bacillus* Spore Inactivation in the GCGA Secondary Effluent

O <sub>3</sub> :TOC Ratio	H <sub>2</sub> O <sub>2</sub> :O <sub>3</sub> =None	H <sub>2</sub> O <sub>2</sub> :O <sub>3</sub> =Low	H <sub>2</sub> O <sub>2</sub> :O <sub>3</sub> =High
0.07	0.0±0.0	0.1±0.0	0.0±0.0
0.32	0.0±0.0	0.0±0.1	0.0±0.1
0.83	0.0±0.1	0.0±0.0	0.0±0.1
1.3	2.1±0.2	0.1±0.1	0.0±0.0

Note: See Table 3.64 for H<sub>2</sub>O<sub>2</sub>:O<sub>3</sub> ratios

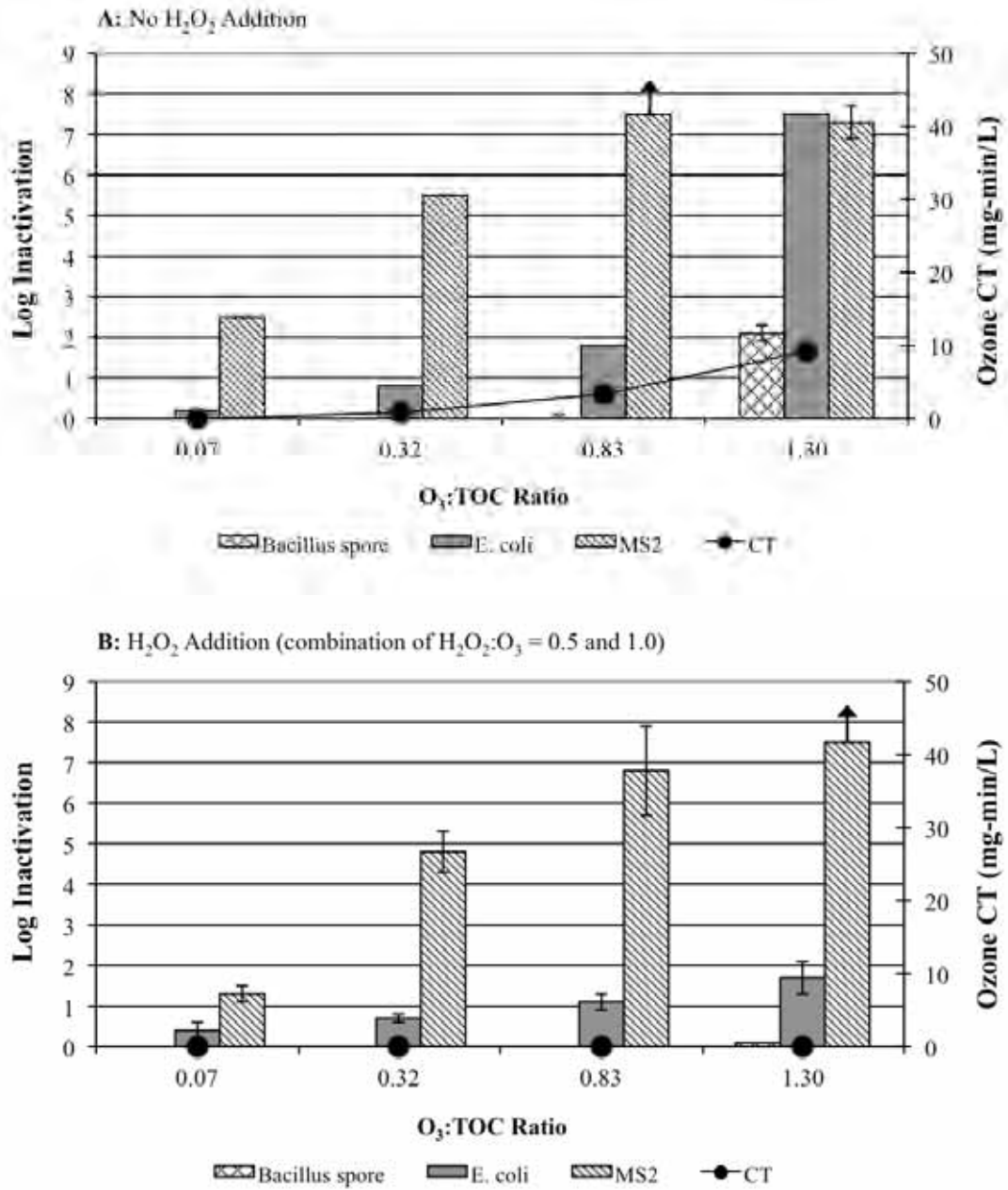


Figure 3.93. Significance of CT for disinfection in the GCGA secondary effluent.

**Table 3.75. Summary of UV Inactivation in the GCGA Secondary Effluent**

UV Dose (mJ/cm <sup>2</sup> )	<i>E. coli</i>		MS2		<i>Bacillus Spores</i>	
	UV	UV/H <sub>2</sub> O <sub>2</sub> *	UV	UV/H <sub>2</sub> O <sub>2</sub> *	UV	UV/H <sub>2</sub> O <sub>2</sub> *
25	6.5	6.3	1.8	2.1	2.2	2.6
50	7.1	7.1	3.0	3.2	>3.3**	>3.3**
250	>7.1**	>7.1**	>7.1**	>7.1**	>3.3**	>3.3**
500	>7.1**	>7.1**	>7.1**	>7.1**	>3.3**	>3.3**

Notes: \*=H<sub>2</sub>O<sub>2</sub> doses of 5 and 10 mg/L achieved similar levels of inactivation; \*\*=limit of inactivation based on spiking level

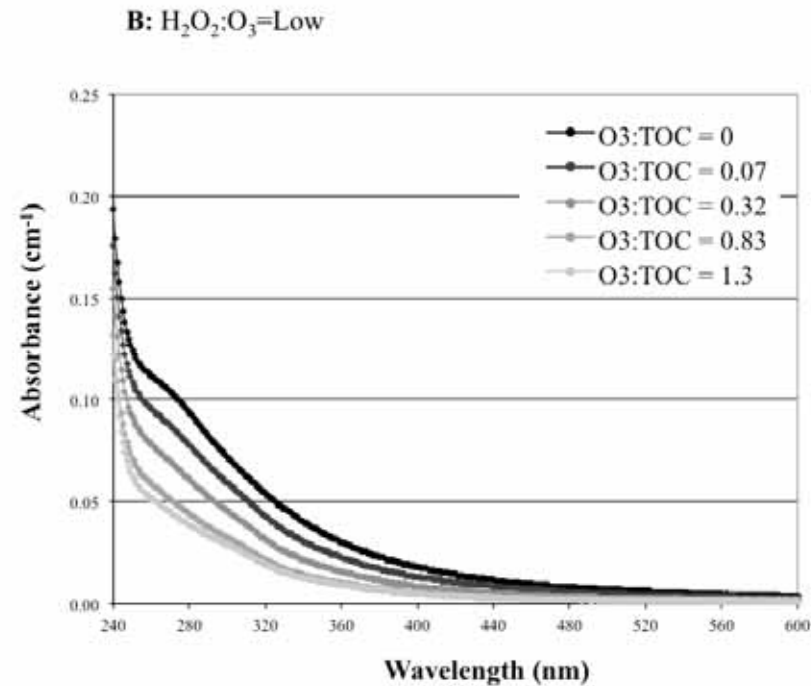
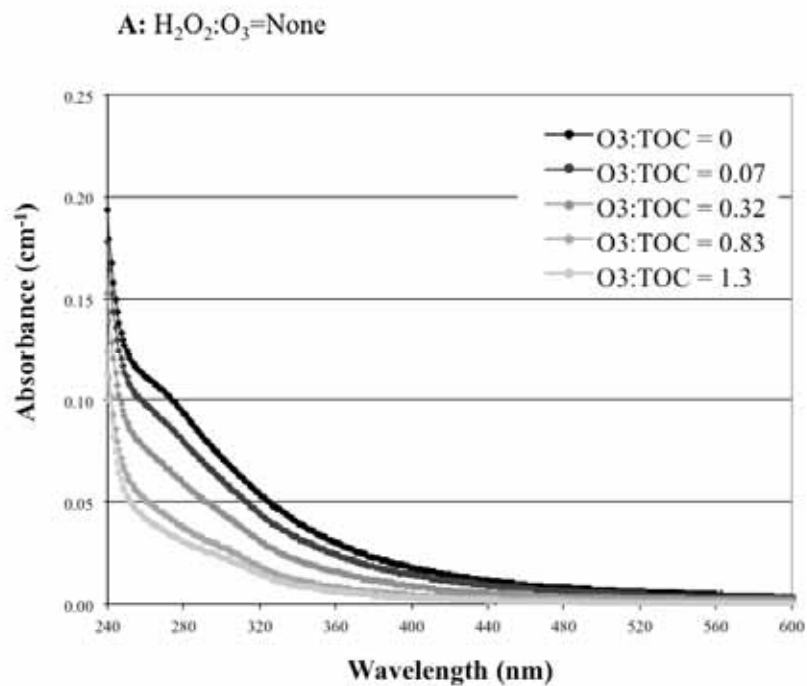
### 3.5.7 Organic Characterization

Similar to the previous data sets, the full-spectrum scans in Figure 3.94 and Figure 3.95, without (A) and with (B) H<sub>2</sub>O<sub>2</sub> addition, indicate that the absorbance profiles around 254 nm generally provide the greatest resolution between treatments. The addition of H<sub>2</sub>O<sub>2</sub> during ozonation decreased treatment efficacy for absorbance, whereas the addition of H<sub>2</sub>O<sub>2</sub> with UV irradiation provided a slight benefit, although the change in absorbance during both UV processes was much less significant than that of ozonation. Figure 3.96 focuses on the change in UV<sub>254</sub> absorbance with ozone, ozone/H<sub>2</sub>O<sub>2</sub>, UV, and UV/H<sub>2</sub>O<sub>2</sub>. Regarding ozonation, reductions in UV<sub>254</sub> absorbance were slightly hindered by the addition of H<sub>2</sub>O<sub>2</sub>. Similar to the absorbance profiles, there was limited reduction in UV<sub>254</sub> absorbance with UV or UV/H<sub>2</sub>O<sub>2</sub>.

Three-dimensional excitation emission matrices were developed for the filtered secondary effluent, the finished effluent, and the various treatment conditions. Figure 3.97 illustrates the fluorescence fingerprint of the secondary and finished effluent samples and also provides the total and regional fluorescence intensities based on arbitrary fluorescence units. The GCGA secondary effluent had a similar fluorescence fingerprint to those of CCWRD and MWRDGC, whereas the WBMWD and PCU secondary effluents had unique characteristics. It is interesting that the GCGA finished effluent is more comparable to WBMWD (MF-RO-UV/H<sub>2</sub>O<sub>2</sub>) than CCWRD (UV) or PCU (chlorine).

Figure 3.98 provides a qualitative illustration of treatment efficacy after ozone- and UV-based oxidation. Similar to the previous data sets, ozone and ozone/H<sub>2</sub>O<sub>2</sub> are capable of achieving substantial reductions in regional and total fluorescence, whereas UV and UV/H<sub>2</sub>O<sub>2</sub> provide minimal reductions. It is interesting to note that the samples associated with an O<sub>3</sub>:TOC ratio of 0.87 had similar fluorescence characteristics to the GCGA finished effluent.

Figure 3.99 and Figure 3.100 illustrate the fluorescence profiles at an excitation wavelength of 254 nm after ozonation and UV/H<sub>2</sub>O<sub>2</sub>. Because the addition of H<sub>2</sub>O<sub>2</sub> did not have a significant impact on ozone efficacy, and UV photolysis provided limited reductions in fluorescence intensity, these fluorescence profiles are not shown. In contrast to WBMWD, which was characterized by two distinct peaks, GCGA was similar to CCWRD, MWRDGC, and PCU in that only one distinct peak was apparent.



\*See Table 3.64 for H<sub>2</sub>O<sub>2</sub>:O<sub>3</sub> ratios

Figure 3.94. GCGA absorbance spectra after ozonation.

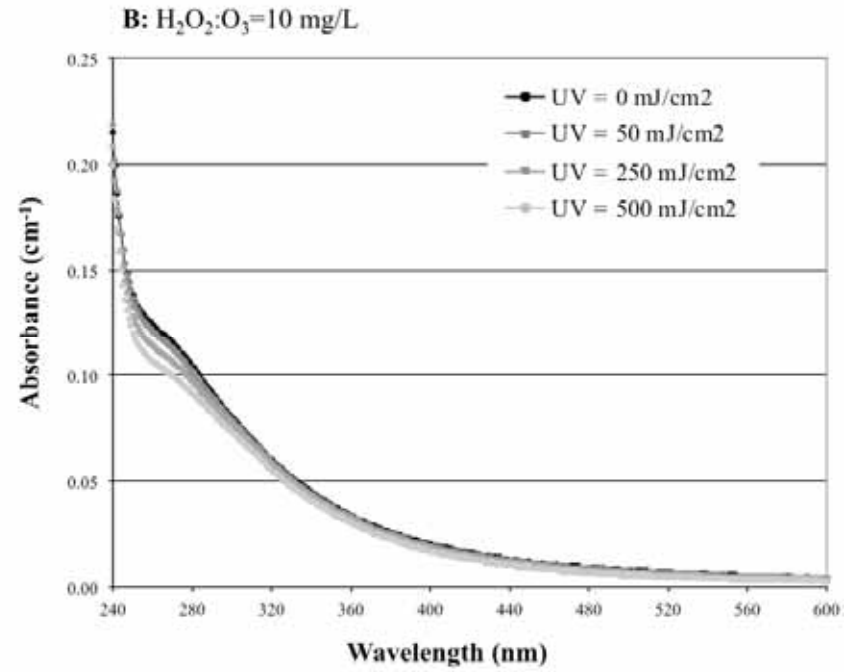
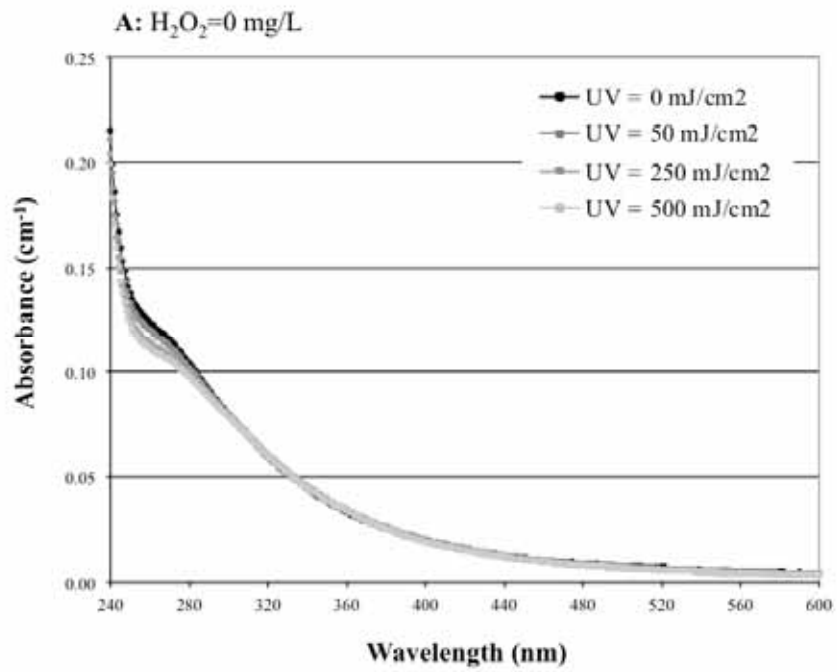
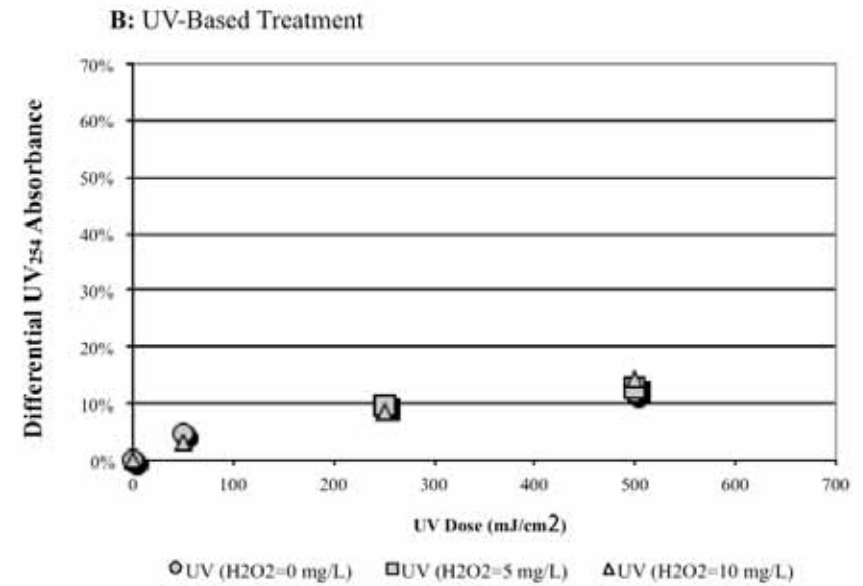
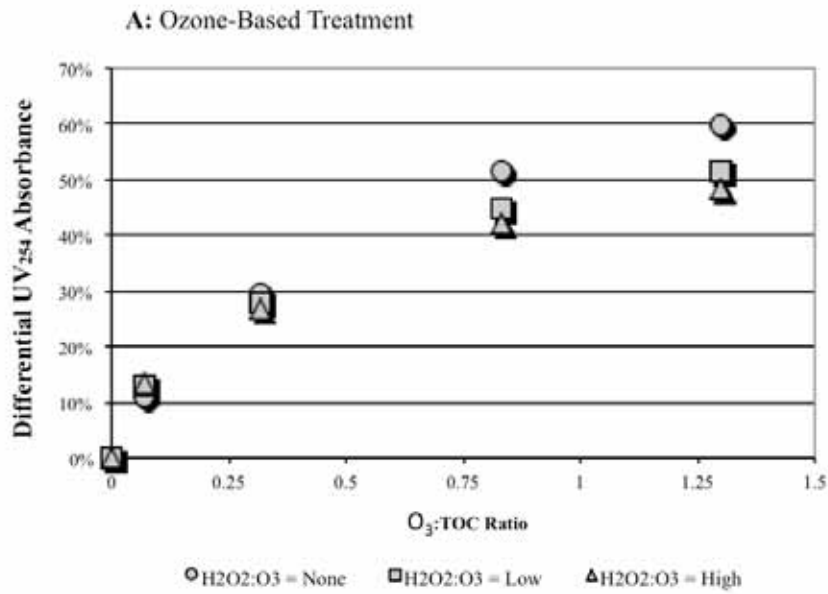


Figure 3.95. GCGA absorbance spectra after UV and UV/H<sub>2</sub>O<sub>2</sub>.



\*See Table 3.64 for H<sub>2</sub>O<sub>2</sub>:O<sub>3</sub> ratios

Figure 3.96. Differential UV<sub>254</sub> absorbance in the GCGA secondary effluent.

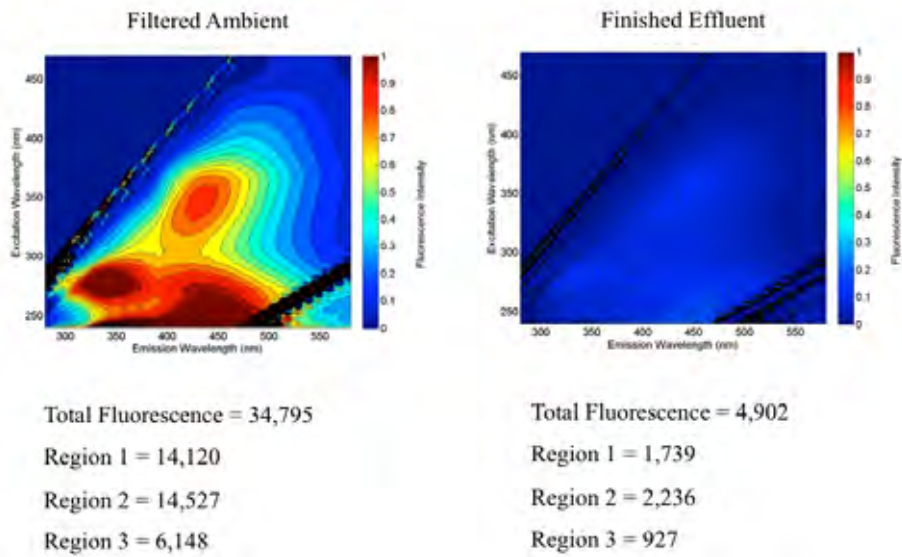
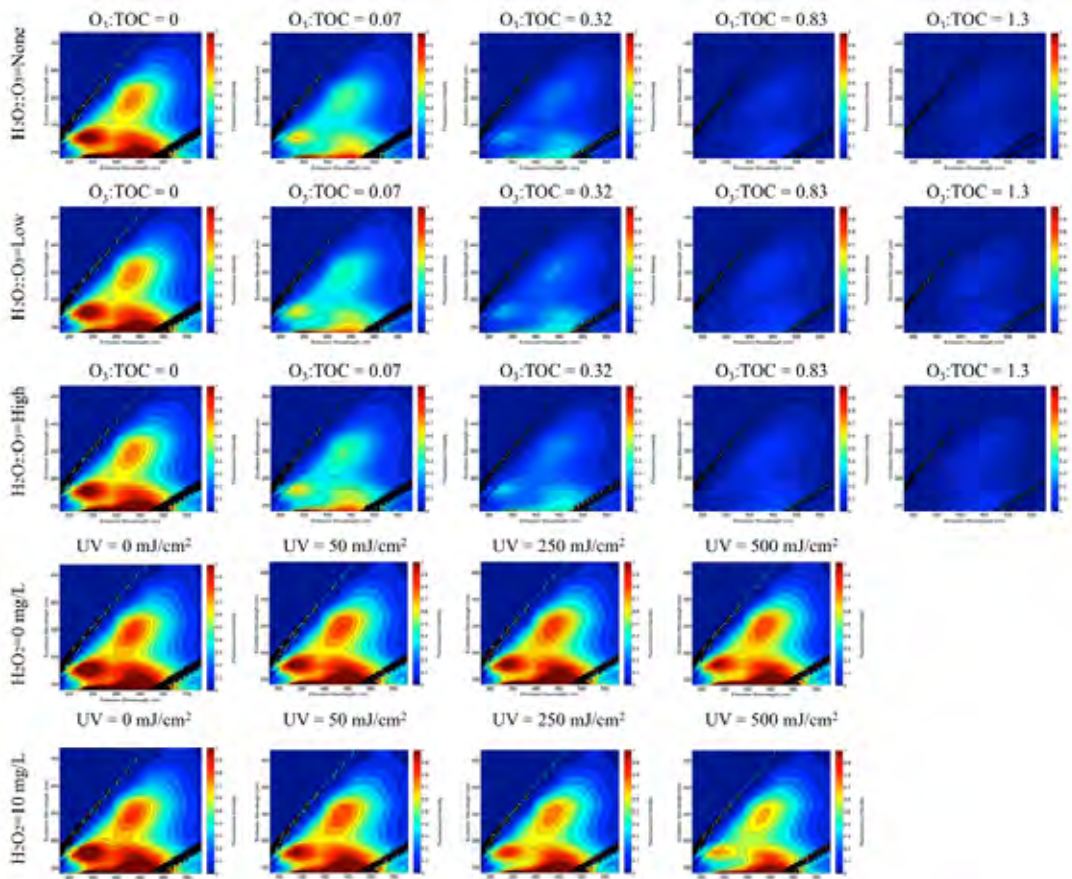


Figure 3.97. 3D EEMs for ambient samples from GCGA.



\*See Table 3.64 for H<sub>2</sub>O<sub>2</sub>:O<sub>3</sub> ratios

Figure 3.98. 3D EEMs after treatment for the filtered GCGA secondary effluent.

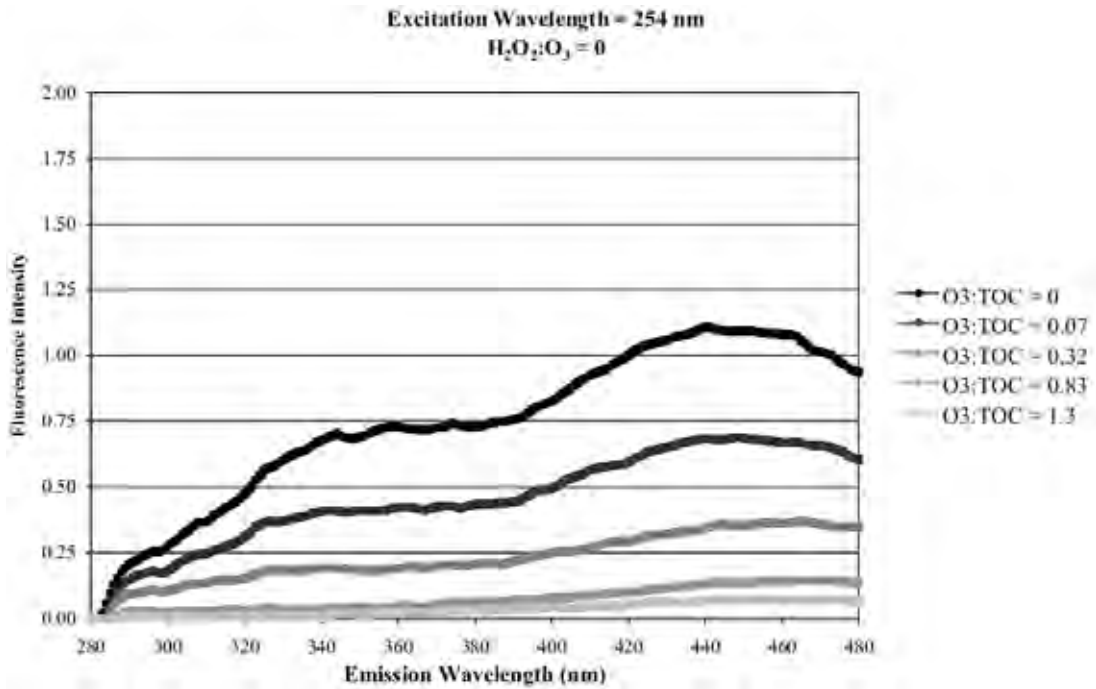


Figure 3.99. GCGA fluorescence profiles (Ex<sub>254</sub>) after ozonation.

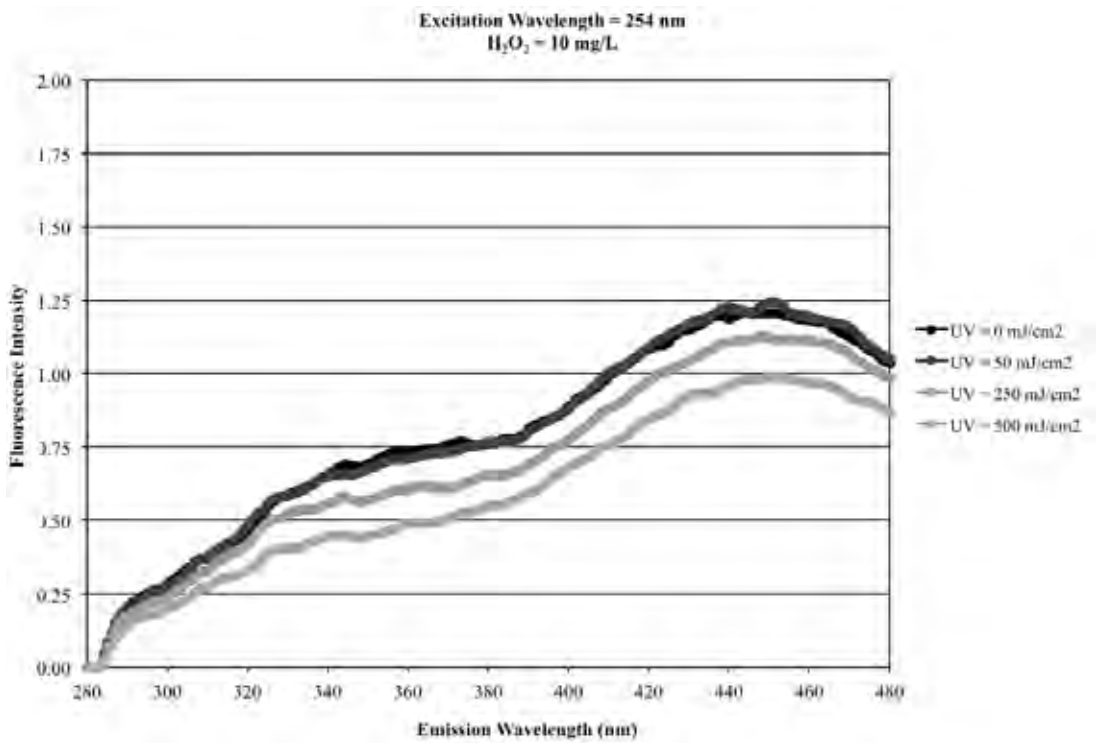


Figure 3.100. GCGA fluorescence profiles (Ex<sub>254</sub>) after UV/H<sub>2</sub>O<sub>2</sub>.

Table 3.62 Table 3.76 provides the FI (i.e.,  $E_{X_{370}}E_{M_{450}}/E_{X_{370}}E_{M_{500}}$ ) and TI (i.e.,  $E_{X_{254}}E_{M_{450,T}}/E_{X_{254}}E_{M_{450,A}}$ ) for the PCU experiments. The FI values dropped significantly for the ozonated samples but remained relatively constant during the UV and UV/H<sub>2</sub>O<sub>2</sub> processes. In other words, the organic matter associated with emissions at 450 nm was oxidized at a faster rate than that of 500 nm during ozonation. This causes a rapid flattening effect for the fluorescence profile associated with an excitation wavelength of 370 nm (Figure 3.101). The emissions at these particular points were photolyzed and oxidized at similar relative rates during UV and UV/H<sub>2</sub>O<sub>2</sub>. Figures 3.102 and 3.103 illustrate the changes in total and regional fluorescence intensities for ozone and UV/H<sub>2</sub>O<sub>2</sub>.

The TI, which measures the extent of organic transformation, reached as low as 0.06 for the highest O<sub>3</sub>:TOC ratio, thereby indicating that 94% of the original fluorescence had been eliminated. This TI reduction is similar to those of the previous data sets, thereby highlighting the significance of relative changes in bulk organic matter for various water qualities. Also similar to the previous data sets, the addition of H<sub>2</sub>O<sub>2</sub> hindered the oxidation of the bulk organic matter. Because of the limited reduction in fluorescence with UV, the corresponding FI and TI values did not change significantly, although UV/H<sub>2</sub>O<sub>2</sub> provided slight improvements.

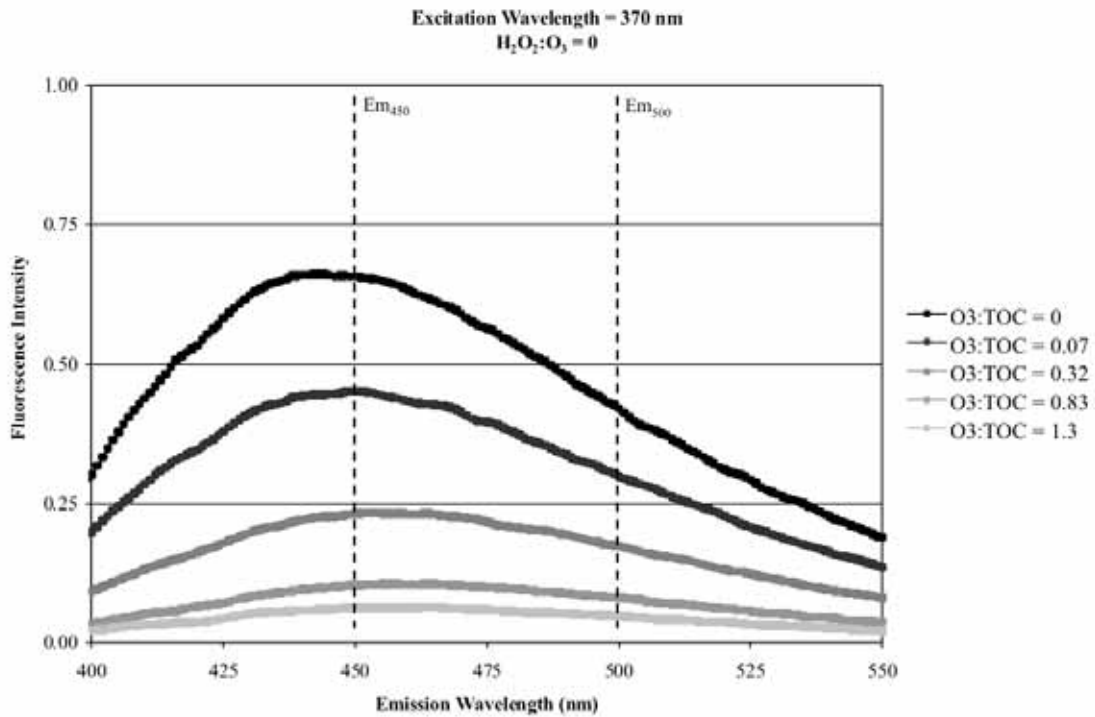
**Table 3.76. FI and TI Values for the GCGA Secondary Effluent**

Filtered Ozone Exposure						
O <sub>3</sub> :TOC	H <sub>2</sub> O <sub>2</sub> :O <sub>3</sub> =None*		H <sub>2</sub> O <sub>2</sub> :O <sub>3</sub> =Low*		H <sub>2</sub> O <sub>2</sub> :O <sub>3</sub> =High*	
	FI	TI	FI	TI	FI	TI
0	1.56	1.00	1.56	1.00	1.56	1.00
0.07	1.51	0.63	1.48	0.59	1.50	0.60
0.32	1.33	0.32	1.37	0.33	1.37	0.36
0.83	1.29	0.12	1.35	0.14	1.38	0.16
1.3	1.30	0.06	1.40	0.08	1.40	0.10

Filtered UV Exposure						
UV Dose (mJ/cm <sup>2</sup> )	H <sub>2</sub> O <sub>2</sub> =0 mg/L		H <sub>2</sub> O <sub>2</sub> =5 mg/L		H <sub>2</sub> O <sub>2</sub> =10 mg/L	
	FI	TI	FI	TI	FI	TI
0	1.57	1.00	1.57	1.00	1.57	1.00
50	1.53	1.01	N/A	N/A	1.53	1.03
250	1.50	1.03	1.51	0.97	1.53	0.94
500	1.53	0.96	1.51	0.92	1.53	0.82

Notes: See Table 3.64 for H<sub>2</sub>O<sub>2</sub>:O<sub>3</sub> dosing conditions; FI=fluorescence index; N/A=data not available; TI=treatment index; UV=ultraviolet



**Figure 3.101. GCGA fluorescence profiles (Ex<sub>370</sub>) after ozonation.**

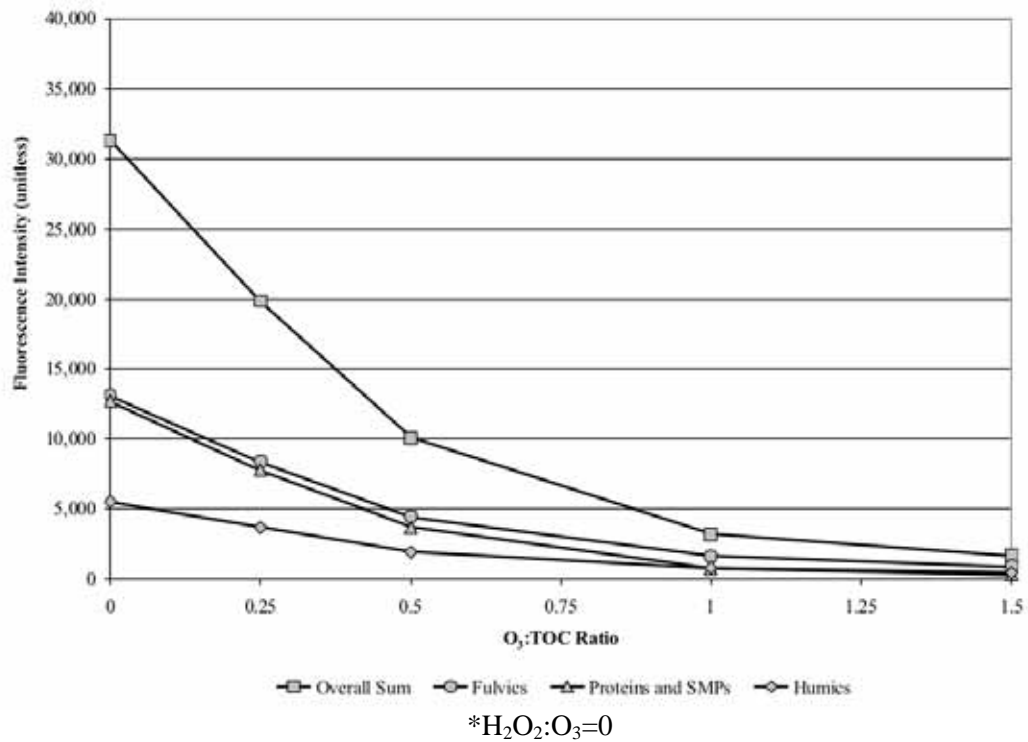


Figure 3.102. Changes in fluorescence intensity after ozonation for GCGA,

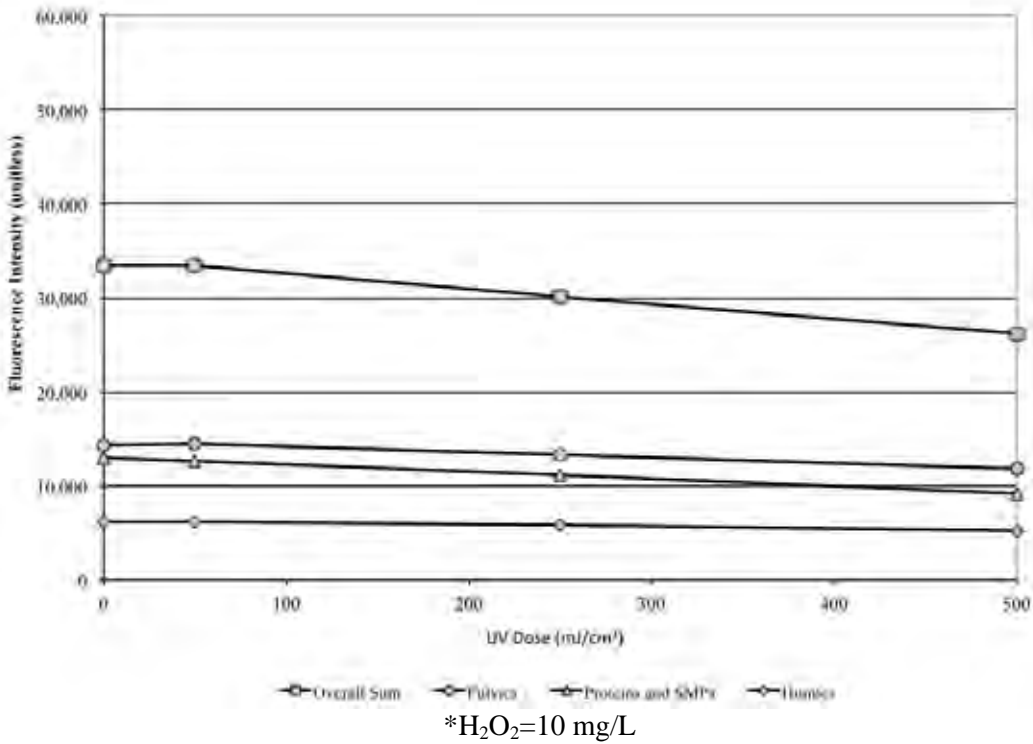


Figure 3.103. Changes in fluorescence intensity after UV/H<sub>2</sub>O<sub>2</sub> for GCGA.

## 3.6 Summary of Bench-Scale Experiments

The primary goal of this study was to provide the wastewater community with a simple, inexpensive tool to monitor the performance of AOPs, which generally rely on the formation of •OH for contaminant oxidation. Unlike free chlorine, chloramine, or even dissolved ozone in some instances, •OH reacts so rapidly that it is impractical to measure the oxidant residual. This becomes problematic for disinfection and the oxidation of some target compounds because the associated analyses may require days of processing before any performance metrics are available. Therefore, surrogate methods must be developed to aid in monitoring the performance of •OH-dominant processes, including UV/H<sub>2</sub>O<sub>2</sub>, ozone/H<sub>2</sub>O<sub>2</sub>, and even ozone. The bench-scale experiments presented earlier provide the data foundation necessary to develop such a surrogate framework. This section provides summaries of the various experiments performed for the five wastewaters. The intent is to (1) identify the rationale for the various analyses, (2) assimilate the data from the five sets of bench-scale experiments, and (3) identify the most significant conclusions.

### 3.6.1 Ozone Versus Ozone/H<sub>2</sub>O<sub>2</sub>

Regarding ozonation, the addition of H<sub>2</sub>O<sub>2</sub> is intended to drive the formation of •OH in order to target more recalcitrant compounds; however, ozonation alone is fully capable of generating •OH in wastewater applications because of side reactions with EfOM. Therefore, the following question can be posed: Why should H<sub>2</sub>O<sub>2</sub> be added to an ozone process? This question will be highlighted in the summaries of the various analyses, but the main points are summarized as follows.

- **Efficacy of ozone vs. •OH.** Second-order ozone and •OH rate constants vary significantly depending on the contaminant of interest. This is the basis for dividing the target compounds in this study into five different groups. Some compounds are susceptible to both ozone and •OH (e.g., Group 1: naproxen and carbamazepine; Group 2: gemfibrozil and atenolol), some are only susceptible to •OH (e.g., Group 3: ibuprofen and phenytoin; Group 4: atrazine and meprobamate), and some are resistant to both forms of oxidation (e.g., Group 5: TCEP). In order to oxidize the compounds in all five groups, the oxidation process must achieve excessively high ozone doses or provide moderate •OH exposure. In matrices with limited background organic matter, including surface water and groundwater, this may require the addition of H<sub>2</sub>O<sub>2</sub>.
- **Decomposition of ozone into •OH.** Although the combination of ozone and H<sub>2</sub>O<sub>2</sub> may be more appropriate in low TOC water matrices, ozone rapidly decomposes into •OH through reactions with EfOM in wastewater applications. In fact, ozone and ozone/H<sub>2</sub>O<sub>2</sub> generally provide similar overall •OH exposure in wastewater when sufficient reaction time is provided. Therefore, H<sub>2</sub>O<sub>2</sub> addition is often unnecessary for ozone to qualify as an AOP, but other issues may impact the design of the process and warrant H<sub>2</sub>O<sub>2</sub> addition.
- **Bromate control.** In previous studies, and to some extent in this study, H<sub>2</sub>O<sub>2</sub> addition has been shown to reduce bromate formation during ozonation. Some studies call for more relaxed bromate guidelines for environmental discharge (e.g., 3 mg/L), but the EPA MCL of 10 µg/L is often used as the benchmark for ozonation processes, particularly for IPR applications. Therefore, the combination of high applied ozone doses and high bromide levels may necessitate H<sub>2</sub>O<sub>2</sub> addition to meet the 10 µg/L

bromate benchmark. Other forms of bromate mitigation (e.g., the chlorine–ammonia process) are available as well.

- **Process footprint.** The addition of  $\text{H}_2\text{O}_2$  allows for rapid conversion of dissolved ozone to  $\bullet\text{OH}$ , which reduces the reaction time to a matter of seconds. High applied ozone doses without  $\text{H}_2\text{O}_2$  (e.g.,  $\text{O}_3$ :TOC ratios greater than 1.5) may require large contactors with more than 20 minutes of residence time. This translates into larger process footprints in full-scale applications. In order to achieve a combination of ozone residual and small process footprint,  $\text{H}_2\text{O}_2$  can be added after a target contact time has been reached to quench the remaining ozone residual while still capturing its oxidation benefits.
- **TOrCs.** As mentioned previously, some target compounds are highly resistant to ozone oxidation but are moderately susceptible to  $\bullet\text{OH}$  oxidation. Despite the fact that ozone naturally decomposes into  $\bullet\text{OH}$  in wastewater applications, the addition of  $\text{H}_2\text{O}_2$  may provide a slight benefit in the oxidation of ozone-resistant compounds (i.e., Groups 3, 4, and 5) when using higher applied ozone doses (i.e.,  $\text{O}_3$ :TOC > 0.5). The benefit generally amounts to less than a 10% increase in oxidation. In drinking water applications or groundwater remediation, the addition of  $\text{H}_2\text{O}_2$  will likely have a much more significant impact in comparison to ozone alone.
- **Microbes.** In the United States, oxidation-based disinfection is generally governed by the CT framework (i.e., disinfectant concentration x exposure time). This is a reasonable strategy for chlorine and chloramine because they can provide extended exposure times to relatively high oxidant concentrations. Although targeting a residual is possible with ozone, the residual is considerably less stable, so it is more difficult to follow the CT framework. Dissolved ozone is quite effective against nearly all microbes, including *Cryptosporidium* and *Giardia*, so it has become increasingly popular in disinfection applications. The natural decomposition of ozone into  $\bullet\text{OH}$  or the forced conversion with  $\text{H}_2\text{O}_2$  addition also achieves significant inactivation of certain microbes, including vegetative bacteria (e.g., *E. coli*) and viruses; however,  $\text{H}_2\text{O}_2$  addition generally reduces the level of inactivation achieved by ozone alone at the same  $\text{O}_3$ :TOC ratio, and the level of inactivation is less consistent. The reduced or absent CT also makes it nearly impossible to comply with current guidelines and regulations, which is the basis for this study. Furthermore, the inactivation of spore-forming microbes (e.g., *Bacillus* spores, *Cryptosporidium* oocysts, *Giardia* cysts) with  $\bullet\text{OH}$  is extremely inefficient, so  $\text{H}_2\text{O}_2$  addition is not recommended in applications targeting these microbes. In order to exploit the disinfection benefits of dissolved ozone and the smaller footprints associated with ozone/ $\text{H}_2\text{O}_2$ , it is possible to target a certain CT with dissolved ozone before adding  $\text{H}_2\text{O}_2$  to expedite the remaining reactions.
- **Organic matter.** Although there are few guidelines and regulations targeting bulk organic matter, aesthetic concerns sometimes necessitate reductions in UV absorbance or color, for example. Both dissolved ozone and ozone/ $\text{H}_2\text{O}_2$  are particularly effective in improving aesthetic parameters, but the addition of  $\text{H}_2\text{O}_2$  will slightly reduce treatment efficacy.
- **Cost.** The additional costs and complexities associated with chemical storage, handling, and injection may also limit the attractiveness of ozone/ $\text{H}_2\text{O}_2$ . On the basis of the following assumptions, which allow for simple process scaling, the  $\text{H}_2\text{O}_2$  chemical cost alone would amount to \$658 per year for each MGD of flow rate and mg/L of applied ozone. In comparison, the estimated cost for ozone generation

(energy only) would be \$1658 for each MGD of flow rate and mg/L of applied ozone. For a 100-MGD wastewater treatment plant targeting an applied ozone dose of 7 mg/L, the H<sub>2</sub>O<sub>2</sub> addition would cost approximately \$460,324 per year, whereas ozone generation would cost approximately \$1,160,481. Therefore, the costs associated with H<sub>2</sub>O<sub>2</sub> may be up to 40% of the overall operation and maintenance costs for ozone/H<sub>2</sub>O<sub>2</sub>.

- 50% H<sub>2</sub>O<sub>2</sub>=\$0.68/kg
  - Process flow rate=1 MGD
  - Ozone dose=1 mg/L
  - H<sub>2</sub>O<sub>2</sub>:O<sub>3</sub> ratio=0.5 → H<sub>2</sub>O<sub>2</sub>=0.35 mg/L
  - Ozone generation=0.012 kWh/g O<sub>3</sub>
  - Energy cost=\$0.10/kWh
- **UV vs. UV/H<sub>2</sub>O<sub>2</sub>.** In contrast to ozone-based treatment processes, the addition of H<sub>2</sub>O<sub>2</sub> is generally required for UV-based oxidation. Low- and medium-pressure UV irradiation are extremely effective for microbial inactivation and photolysis of NDMA, but UV light is generally insufficient to oxidize TOrCs. With the exception of certain compounds, including diclofenac and triclosan, significant oxidation often requires a combination of high UV doses (i.e., >250 mJ/cm<sup>2</sup>) and high concentrations of H<sub>2</sub>O<sub>2</sub> (i.e., >5 mg/L). This is the basis for the gold standard in IPR: UV photolysis for NDMA mitigation and H<sub>2</sub>O<sub>2</sub> addition for the oxidation of recalcitrant compounds such as 1,4-dioxane.
  - **H<sub>2</sub>O<sub>2</sub> quenching.** Residual H<sub>2</sub>O<sub>2</sub> is not a significant concern at this point, but there are benefits to optimizing the H<sub>2</sub>O<sub>2</sub> dose to prevent chemical waste and alleviate any concerns related to residual discharge. In ozone/H<sub>2</sub>O<sub>2</sub> applications, it may be possible to target appropriate H<sub>2</sub>O<sub>2</sub>:O<sub>3</sub> ratios to achieve complete consumption of H<sub>2</sub>O<sub>2</sub>. Based on stoichiometry, a molar H<sub>2</sub>O<sub>2</sub>:O<sub>3</sub> ratio of 0.5 would lead to complete consumption, but the complex interactions with other scavengers in the target water matrix often complicate the calculation. Therefore, a trial-and-error approach may be required in real-world applications. On the other hand, UV/H<sub>2</sub>O<sub>2</sub> processes will almost always have an H<sub>2</sub>O<sub>2</sub> residual because of the disconnect between the amount of chemical required to achieve a reasonable •OH exposure and the limited amount of chemical that is actually consumed in the process. If necessary, H<sub>2</sub>O<sub>2</sub> can be quenched with the addition of chemicals, such as calcium thiosulfate, or through catalytic decomposition in activated carbon beds, which are becoming popular in wastewater treatment trains with ozone-based oxidation.

### 3.6.2 Comparison of Filtered Secondary Effluents

**General water quality.** Secondary effluent samples were collected from five wastewater treatment plants with a range of operational conditions and water quality. The major water quality parameters affecting ozonation and the organic correlations developed later in the report are presented in Table 3.77. Four of the filtered secondary effluents fell within a TOC range of 6.3 to 7.6 mg/L, but WBMWD was clearly the outlier with a TOC of 18 mg/L. The low SRT of WBMWD also limited the biotransformation of bulk organic matter, as indicated by the extremely high UV<sub>254</sub> absorbance and TF values. The bulk organic matter in the PCU secondary effluent was unique in that its UV<sub>254</sub> and total fluorescence values were relatively high despite the high SRT at that facility. These observations were also evident in Figure 3.57 and Figure 3.77, which illustrated the unique fluorescence fingerprints of WBMWD and

PCU. As expected, the range of bromide values correlated to significant differences in bromate formation during ozonation. Finally, the nitrite values were relatively low and insignificant for three of the facilities. Although nitrite was higher at WBMWD, the 18 mg/L of TOC dominated the ozone demand, which rendered the nitrite demand negligible. On the other hand, GCGA had a relatively low TOC, so its high nitrite level had a significant impact on ozone demand and the final O<sub>3</sub>:TOC and H<sub>2</sub>O<sub>2</sub>:O<sub>3</sub> ratios, as described earlier.

**Ozone CT values.** The O<sub>3</sub>:TOC ratio is a convenient tool for determining the ozone dose for a particular application. As described in earlier sections, similar O<sub>3</sub>:TOC ratios achieve comparable levels of oxidation despite dramatic differences in water quality and dissolved ozone contact time (i.e., CT), which is summarized in Table 3.78. The filtered MWRDGC secondary effluent seemed to be most affected by the cartridge filter contamination reported earlier, which is likely the primary reason for its low CT relative to CCWRD and WBMWD. Again, PCU was a unique case in that its CT values were similar to CCWRD and WBMWD for O<sub>3</sub>:TOC ratios less than 1.5; however, the dissolved ozone residual at an O<sub>3</sub>:TOC ratio of 1.5 was more stable than that of the other wastewaters, which resulted in a much higher CT. The low CT values for GCGA were related to the incorrect applied ozone doses because of the unexpected nitrite demand.

**Table 3.77. Water Quality Summary for Filtered Secondary Effluent**

Parameter	CCWRD	MWRDGC	WBMWD	PCU	GCGA
Bromide (µg/L)	174	93	409	730	31
NO <sub>2</sub> (mg N/L)	0.06	<0.05	0.17	<0.05	0.30
pH	6.9	7.6	7.3	7.3	7.3
SRT (days)	7	7	1.5	12	11
TOC (mg/L)	7.6	6.9	18	7.2	6.3
Total fluorescence (unitless)	38,874	37,712	94,807	53,996	34,795
UV <sub>254</sub> (cm <sup>-1</sup> )	0.146	0.131	0.268	0.187	0.130

Notes: CCWRD=Clark County Water Reclamation District; GCGA=Gwinnett County, Georgia; MWRDGC=Metropolitan Water Reclamation District of Greater Chicago; PCU=Pinellas County Utilities; SRT=solids retention time; TOC=total organic carbon; UV=ultraviolet; WBMWD=West Basin Municipal Water District

**Table 3.78. Comparison of Ozone CT (mg/min/L) for Filtered Secondary Effluent**

O <sub>3</sub> :TOC	CCWRD	MWRDGC	WBMWD	PCU	GCGA*
0.00	0	0	0	0	0
0.25	0	0	0	0	0
0.50	1.2	1.6	2.2	1.1	0.7
1.00	7.6	5.5	11	8.2	3.3
1.50	21	11	23	34	9.1

Notes: \*=based on different O<sub>3</sub>:TOC ratios; CCWRD=Clark County Water Reclamation District; GCGA=Gwinnett County, Georgia; MWRDGC=Metropolitan Water Reclamation District of Greater Chicago; PCU=Pinellas County Utilities; SRT=solids retention time; TOC=total organic carbon; UV=ultraviolet; WBMWD=West Basin Municipal Water District

**Bromate formation.** The initial bromide concentrations for each secondary effluent were directly correlated to bromate formation, as summarized in Table 3.79. In other words, higher bromide concentrations lead to higher bromate formation unless some type of mitigation is employed. The bromide incorporation values provide a rough estimate, as indicated by the relatively high standard deviations, of expected bromate formation based on influent bromide concentrations. For an O<sub>3</sub>:TOC ratio of 1.5, approximately 31% of the initial bromide will be converted to bromate as bromide (Br=100 µg/L → BrO<sub>3</sub><sup>-</sup>=31 µg/L as Br → BrO<sub>3</sub><sup>-</sup>=50 µg/L). H<sub>2</sub>O<sub>2</sub> addition provided some degree of bromate mitigation during the bench-scale experiments, but the trends were not entirely consistent. Furthermore, the bromate concentrations were exceptionally high for some wastewaters, particularly WBMWD and PCU, so it would be difficult for these facilities to achieve the 10-µg/L benchmark without extensive optimization of mitigation strategies. Some researchers question the validity of using this benchmark in environmental discharge applications, but it may be relevant for IPR facilities.

**•OH exposure.** The goal of an AOP is to oxidize target contaminants with •OH. In wastewater applications, ozone, ozone/H<sub>2</sub>O<sub>2</sub>, and UV/H<sub>2</sub>O<sub>2</sub> all generate •OH, but ozone-based processes generally provide higher •OH exposures. Table 3.80 provides the average values from the five bench-scale experiments for O<sub>3</sub>:TOC and H<sub>2</sub>O<sub>2</sub>:O<sub>3</sub> ratios for the ozone-based processes and UV and H<sub>2</sub>O<sub>2</sub> doses for the UV-based processes. Although it was not entirely apparent in the individual bench-scale experiments, Table 3.80 indicates that H<sub>2</sub>O<sub>2</sub> addition yielded slightly higher •OH exposures during ozonation, but this relatively consistent trend in the averaged data may not be significant because of the high standard deviations.

**Table 3.79. Bromate Formation Summary for Filtered Secondary Effluent**

O <sub>3</sub> :TOC	CCWRD	MWRDGC	WBMWD	PCU	GCGA*	Bromide Incorporation (%)**
0.25	<1	<1	7.4	7.9	<1	1.2±0.5
0.50	5.7	<1	51	34	1.3	4.6±3.9
1.00	29	18	140	140	6.2	15±8
1.50	71	45	190	376	14	31±8

Notes: \*=based on different O<sub>3</sub>:TOC ratios; \*\*=includes GCGA data linearly adjusted based on O<sub>3</sub>:TOC ratio; CCWRD=Clark County Water Reclamation District; GCGA=Gwinnett County, Georgia; MWRDGC=Metropolitan Water Reclamation District of Greater Chicago; PCU=Pinellas County Utilities; WBMWD=West Basin Municipal Water District

**Table 3.80. Average •OH Exposures (10<sup>-11</sup> M-s) for Filtered Secondary Effluent**

O <sub>3</sub> :TOC*	H <sub>2</sub> O <sub>2</sub> :O <sub>3</sub> =0	H <sub>2</sub> O <sub>2</sub> :O <sub>3</sub> =0.5	H <sub>2</sub> O <sub>2</sub> :O <sub>3</sub> =1.0	UV Dose** (mJ/cm <sup>2</sup> )	H <sub>2</sub> O <sub>2</sub> =5 mg/L	H <sub>2</sub> O <sub>2</sub> =10 mg/L
0.25	7.3±3.8	7.7±4.2	8.4±4.6	0	N/A	0.1±0.3
0.50	14±5.7	16±5.9	16±7.3	50	N/A	0.7±0.8
1.00	35±9.6	38±15	37±15	250	2.6±1.5	5.2±1.4
1.50	56±15	64±22	59±26	500	4.7±1.4	8.9±2.2

Notes: \*=includes GCGA data linearly adjusted based on O<sub>3</sub>:TOC ratio; \*\*=includes CCWRD data for 45 (50) and 225 (250) mJ/cm<sup>2</sup>

**NDMA.** According to the previous draft of the CD PH Title 22 Requirements for Water Recycling, facilities were required to demonstrate 1.2-log (93.7%) destruction of NDMA prior to groundwater injection. Table 3.81 summarizes the UV doses required for 1.2-log destruction of NDMA during the UV and UV/H<sub>2</sub>O<sub>2</sub> experiments. Excluding WBMWD, H<sub>2</sub>O<sub>2</sub> addition negatively impacted NDMA destruction because of the relative efficacy of UV photolysis. Despite the lamp intensity corrections for UV<sub>254</sub> absorbance, the UV dose requirements varied significantly among the various matrices. On average, a UV dose of 600 to 700 mJ/cm<sup>2</sup> for the secondary effluents was required to achieve the CDPH Title 22 benchmark. Again, the UV exposures were corrected for UV absorbance, but it is unclear whether these doses would also apply for RO permeates, which is the common target matrix for UV photolysis of NDMA in IPR applications. According to the recent revisions to the draft CDPH regulations, facilities will no longer be required to achieve 1.2-log destruction of NDMA, but they will be required to comply with the 10 ng/L NL in IPR applications.

As described earlier, direct NDMA formation during ozonation was a relatively unexpected phenomenon, particularly at the magnitudes observed for CCWRD and WBMWD. Direct NDMA formation had previously been reported in the literature, but it was originally thought to be a more localized issue. The data in this study indicate that direct NDMA formation during ozonation in wastewater applications is a widespread issue, but the magnitudes can vary tremendously depending on the precursor loads. Unfortunately, the literature is currently insufficient to identify the most critical precursors or pretreatment strategies, but the potential concerns are sufficient to warrant future studies.

**Table 3.81. UV Dose (mJ/cm<sup>2</sup>) Required for 1.2-log NDMA Destruction**

H <sub>2</sub> O <sub>2</sub> Dose (mg/L)	CCWRD	MWRDGC	WBMWD	PCU	GCGA	Average
0	500	600	571	667	706	609±81
10	662	649	508	717	800	667±107

*Notes:* CCWRD=Clark County Water Reclamation District; GCGA=Gwinnett County, Georgia; MWRDGC=Metropolitan Water Reclamation District of Greater Chicago; PCU=Pinellas County Utilities; WBMWD=West Basin Municipal Water District

Table 3.82 summarizes the direct NDMA formation observed for several dosing conditions in the five secondary effluents. Direct NDMA formation appears to be independent of H<sub>2</sub>O<sub>2</sub>:O<sub>3</sub> and O<sub>3</sub>:TOC for ratios ranging from 0.5 to 1.0 and 0.25 to 1.50 (additional data shown previously). Depending on the organic precursor content, direct NDMA formation ranged from 4 to 150 ng/L during this study. Because of the direct formation issue and the relatively low rate constants, it would be difficult to employ ozone-based oxidation for NDMA destruction in most secondary effluents; however, additional studies are warranted to evaluate NDMA destruction in RO permeates, where the NDMA precursor load is expected to be much lower.

**Table 3.82. Summary of Direct NDMA Formation During Ozonation**

O <sub>3</sub> :TOC	H <sub>2</sub> O <sub>2</sub> :O <sub>3</sub>	CCWRD	MWRDGC	WBMWD	PCU	GCGA*
0.00	0	<2.5	<2.5	20	7.1	17
0.50	0	48	9.8	170	11	25
0.50	0.5	45	11	170	11	23
1.00	0	42	9.2	160	11	26
1.00	0.5	36	10	140	11	27

Notes: \*=based on O<sub>3</sub>:TOC ratios of 0.32 and 0.83; CCWRD=Clark County Water Reclamation District; GCGA=Gwinnett County, Georgia; MWRDGC=Metropolitan Water Reclamation District of Greater Chicago; PCU=Pinellas County Utilities; WBMWD=West Basin Municipal Water District

**Table 3.83. O<sub>3</sub>:TOC Ratio Required for 0.5-log Destruction of 1,4-dioxane**

H <sub>2</sub> O <sub>2</sub> :O <sub>3</sub>	CCWRD	MWRDGC	WBMWD	PCU	GCGA	Average
0	1.4	1.6	1.2	2.2	1.0	1.5±0.5
0.5	1.3	1.5	1.0	1.2	1.0	1.2±0.2

Notes: CCWRD=Clark County Water Reclamation District; GCGA=Gwinnett County, Georgia; MWRDGC=Metropolitan Water Reclamation District of Greater Chicago; PCU=Pinellas County Utilities; WBMWD=West Basin Municipal Water District

**1,4-dioxane.** In addition to the NDMA requirement, CDPH also requires 0.5-log (68.4%) destruction of 1,4-dioxane to satisfy Title 22. Typically, IPR facilities employ UV/H<sub>2</sub>O<sub>2</sub> for Title 22 compliance (i.e., UV for NDMA and H<sub>2</sub>O<sub>2</sub> addition to generate •OH for 1,4-dioxane destruction), but because of their efficacy in forming •OH, ozone and ozone/H<sub>2</sub>O<sub>2</sub> can also be employed for 1,4-dioxane destruction. Based on the data in Table 3.83, the average O<sub>3</sub>:TOC ratios required for 0.5-log destruction ranged from 1.3 to 1.5 for H<sub>2</sub>O<sub>2</sub>:O<sub>3</sub> ratios of 0.5 and 0. Similar to NDMA destruction, the O<sub>3</sub>:TOC ratios required for 0.5-log destruction of 1,4-dioxane in RO permeates would be significantly lower because of the reduction in oxidant scavengers.

**TOxCs.** Table 3.84 summarizes the ambient secondary effluent concentrations quantified during this study. Other than limited geographic variability (e.g., atrazine and meprobamate), the concentrations of the various target compounds were generally representative of most secondary effluents. The primary exception was WBMWD because of the low SRT associated with that matrix, which provided limited biotransformation and biodegradation of the target compounds. This was particularly apparent for the more bioamenable compounds, including atenolol, bisphenol A, gemfibrozil, ibuprofen, naproxen, triclosan, and trimethoprim. Despite the small magnitudes of the EEq values, the five wastewaters encompassed a wide range of total estrogenicity, and the values did not necessarily correlate to the other target compounds. Some of the wastewaters exhibited toxic effects on the assay cell line, however, so the final EEq values may have been impacted.

**Table 3.84. Summary of Secondary Effluent TOxC Concentrations (ng/L)**

Parameter	CCWRD	MWRDGC	WBMWD	PCU	GCGA
Atenolol	421	710	2100	78	800
Atrazine	<10	28	<10	42	<10
Bisphenol A	<50	<50	280	<50	<50
Carbamazepine	251	140	260	310	150
DEET	155	54	640	<25	32
Diclofenac	131	62	280	130	250
EEq	9.1	1.8	0.6	0.7	3.2
Gemfibrozil	34	31	2500	120	150
Ibuprofen	<25	<25	47	<25	<25
Meprobamate	629	41	290	250	300
Musk ketone	<100	<100	<100	<100	<100
Naproxen	<25	<25	320	<25	<25
Phenytoin	216	110	160	260	110
Primidone	134	67	96	240	91
Sulfamethoxazole	1220	570	700	990	1000
TCEP	525	540	630	410	<200
Triclosan	29	26	150	<25	34
Trimethoprim	256	280	700	16	400

Notes: CCWRD=Clark County Water Reclamation District; DEET=*N,N*-diethyl-*meta*-toluamide; EEq=estradiol equivalents; GCGA=Gwinnett County, Georgia; MWRDGC=Metropolitan Water Reclamation District of Greater Chicago; PCU=Pinellas County Utilities; TCEP=tris-(2-chloroethyl)-phosphate; WBMWD=West Basin Municipal Water District

Table 3.85 summarizes the concentrations of the target compounds in the finished effluents. In conjunction with the secondary effluent concentrations, these values basically illustrate the impact of the disinfection processes. UV irradiation at typical disinfection doses (i.e., <100 mJ/cm<sup>2</sup>) is relatively ineffective for most TOxCs, whereas chlorine disinfection achieves additional destruction of some compounds. It is interesting that the efficacy of BAC and ozonation is quite similar to that of RO-UV/H<sub>2</sub>O<sub>2</sub>, with the exception of the most oxidant-resistant compounds (e.g., meprobamate, phenytoin, and primidone). TCEP would likely be included in this oxidant-resistant list as well, but it was already <MRL in the GCGA secondary effluent. The total estrogenicity of the wastewaters was <MRL for every site with post-secondary treatment.

**Table 3.85. Summary of Finished Effluent TOxC Concentrations**

Parameter	CCWRD (UV)	MWRDGC (None)	WBMWD (RO-UV/H <sub>2</sub> O <sub>2</sub> )	PCU (Cl <sub>2</sub> )	GCGA (BAC-O <sub>3</sub> )
Atenolol	120	710	<25	28	<25
Atrazine	<10	28	<10	76	<10
Bisphenol A	<50	<50	86	<50	<50
Carbamazepine	192	140	<10	35	<10
DEET	232	54	<25	30	<25
Diclofenac	57	62	<25	<25	<25
EEq	<0.074	1.8	<0.074	<0.074	<0.074
Gemfibrozil	12	31	<10	<10	<10
Ibuprofen	<25	<25	<25	<25	<25
Meprobamate	362	41	<10	360	190
Musk ketone	<100	<100	<100	<100	<100
Naproxen	<25	<25	<25	<25	<25
Phenytoin	113	110	<10	270	33
Primidone	168	67	<10	270	31
Sulfamethoxazole	1,150	570	<25	<25	<25
TCEP	349	540	<200	370	<200
Triclosan	38	26	<25	<25	<25
Trimethoprim	43	280	<10	<10	<10

Notes: BAC=biological activated carbon; CCWRD=Clark County Water Reclamation District; DEET=*N,N*-diethyl-*meta*-toluamide; EEq=estradiol equivalents; GCGA=Gwinnett County, Georgia; MWRDGC=Metropolitan Water Reclamation District of Greater Chicago; PCU=Pinellas County Utilities; RO=reverse osmosis; TCEP=tris-(2-chloroethyl)-phosphate; UV=ultraviolet; WBMWD=West Basin Municipal Water District

Tables 3.86 and 3.87 provide summaries of ozone- and UV-based destruction of the target compounds. The countless number of TOxCs in the environment make it impractical to develop oxidation profiles for every known chemical and dosing condition. Grouping contaminants based on their relative resistance/susceptibility to oxidation is a much more reasonable strategy. This strategy is also robust in that compounds with unknown oxidation profiles can often be modeled based on their structural properties, a concept known as QSAR. The groupings used in Table 3.86 indicate the following, with the corresponding rate constant ranges presented earlier:

- Group 1: Very susceptible to both ozone and •OH
- Group 2: Moderately susceptible to ozone/highly susceptible to •OH
- Group 3: Very resistant to ozone/highly susceptible to •OH
- Group 4: Very resistant to ozone/moderately susceptible to •OH
- Group 5: Very resistant to both ozone and •OH

A generic indicator also provides an estimate of the expected level of oxidation for an unknown compound with similar structural characteristics and rate constants. The indicator was calculated as the average of the target compounds in each group. The grouping and indicator framework proved to be quite useful in that each stepwise increase in O<sub>3</sub>:TOC ratio led to an additional group of contaminants experiencing greater than 80% oxidation. As described in the literature review, there are few existing guidelines for TOxC destruction, so relative oxidation (i.e., % destruction) is the most useful descriptor of process performance. Similar to the pCBA/•OH exposure experiments, H<sub>2</sub>O<sub>2</sub> addition yielded slightly higher destruction of the ozone-resistant compounds (Groups 3, 4, and 5), whereas H<sub>2</sub>O<sub>2</sub> addition was slightly detrimental to the ozone-susceptible compounds. Again, the differences were

minimal and insignificant because of the high standard deviations across the bench-scale experiments. Finally, given the rapid destruction of many of the target compounds, it is likely that the compounds in Groups 4 and 5 will control the design of ozone systems for TOC mitigation.

The groupings are also presented in Table 3.87 to describe the resistance of the compounds to  $\bullet\text{OH}$ , but the utility of the grouping framework is compromised because of the impact of UV photolysis. Although most compounds are highly resistant to UV photolysis alone, some compounds, particularly diclofenac and triclosan, are photolyzed rapidly by UV light. Other compounds that are highly resistant to oxidation, particularly phenytoin and atrazine, also experience moderate levels of photolysis. These UV-susceptible compounds are typically characterized by aromatic ring structures that more effectively absorb UV light. Regardless, ozone oxidation typically achieves higher levels of contaminant mitigation at relevant dosing levels.

Table 3.86. Average TOxC Mitigation (%) During Ozonation

Group	Contaminant	O <sub>3</sub> :TOC (mass) / H <sub>2</sub> O <sub>2</sub> :O <sub>3</sub> (molar)											
		0.25/0	0.25/0.5	0.25/1.0	0.50/0	0.50/0.5	0.50/1.0	1.0/0	1.0/0.5	1.0/1.0	1.5/0	1.5/0.5	1.5/1.0
1	Bisphenol A	91±14	91±12	93±6	98±1	98±1	98±1	98±1	98±1	98±1	98±1	98±1	98±1
	Carbamazepine	92±15	89±15	87±12	99±0	99±0	99±0	99±0	99±0	99±0	99±0	99±0	99±0
	Diclofenac	91±13	90±14	92±8	98±1	98±1	98±1	98±1	98±1	98±1	98±1	98±1	98±1
	Naproxen	90±16	89±15	87±10	98±0	98±0	98±1	98±0	98±0	98±1	98±0	98±0	98±1
	Sulfamethoxazole	84±13	82±13	83±8	98±0	97±1	96±2	99±1	99±1	99±1	99±1	99±1	99±1
	Triclosan	93±9	93±8	96±2	97±1	97±1	97±1	97±1	97±1	97±1	97±1	92±10	97±1
	Trimethoprim	92±15	90±14	89±11	99±0	99±0	99±0	99±0	99±0	99±0	99±0	99±0	99±0
	<b>Indicator</b>	90±14	89±13	90±8	98±0	98±0	98±0	98±0	98±0	98±0	98±0	97±2	98±0
2	Atenolol	47±8	44±7	47±5	97±1	90±7	85±7	98±1	98±1	98±1	98±1	98±1	97±3
	Gemfibrozil	81±18	73±17	67±10	99±0	99±0	99±1	99±0	99±0	99±0	99±0	99±0	99±1
	<b>Indicator</b>	64±13	59±12	57±7	98±1	95±4	92±4	99±1	99±1	99±1	99±1	99±1	98±2
	DEET	26±9	28±7	30±8	57±9	62±8	63±8	88±6	93±5	92±5	97±3	99±1	95±4
3	Ibuprofen	38±10	38±6	42±8	69±7	72±6	73±6	94±4	96±3	95±3	98±1	98±1	96±3
	Phenytoin	34±15	36±11	36±10	67±13	72±7	73±8	94±4	97±3	95±4	98±1	99±0	97±2
	Primidone	30±9	29±5	34±5	60±8	64±5	64±4	91±5	94±5	92±4	97±2	98±2	95±4
	<b>Indicator</b>	32±10	33±6	36±6	63±9	68±6	68±7	92±5	95±4	93±4	98±2	99±1	96±3
4	Atrazine	15±5	14±3	18±5	33±6	36±5	37±6	64±8	70±11	69±9	81±8	87±8	82±9
	Meprobamate	18±5	20±5	23±6	40±8	45±6	45±5	71±9	80±10	79±8	86±8	93±5	88±6
	<b>Indicator</b>	17±5	17±4	20±5	37±6	41±5	41±5	68±8	75±11	74±9	84±8	90±7	85±8
5	TCEP	-1±13	5±5	8±5	9±5	12±5	9±4	15±3	20±6	20±3	23±3	30±4	31±4

Notes: Shading represents >80% oxidation; \*=GCGA omitted because of differences in O<sub>3</sub>:TOC ratios and the nonlinearity of contaminant oxidation; DEET=*N,N*-diethyl-*meta*-toluamide; TCEP=tris-(2-chloroethyl)-phosphate

**Table 3.87. Average TOxC Mitigation (%) for UV and UV/H<sub>2</sub>O<sub>2</sub>**

Group	Contaminant	UV Dose (mJ/cm <sup>2</sup> ) / H <sub>2</sub> O <sub>2</sub> Dose (mg/L)							
		50/0	50/10	250/0	250/5	250/10	500/0	500/5	500/10
1	Bisphenol A	5±10	3±11	7±10	11±10	25±21	10±10	22±9	49±18
	Carbamazepine	-2±9	3±4	-3±11	12±7	22±15	-3±8	24±18	42±15
	Diclofenac	40±2	19±23	91±2	86±5	90±6	98±1	97±1	97±1
	Naproxen	4±6	3±8	11±4	19±11	29±16	18±8	35±8	53±16
	Sulfamethoxazole	6±6	2±14	44±5	39±8	42±13	65±2	67±3	73±5
	Triclosan	21±12	13±18	81±8	72±10	79±9	94±3	93±2	95±3
	Trimethoprim	-1±8	2±6	0±5	11±6	18±11	1±4	16±10	37±15
2	Atenolol	5±6	5±6	1±7	15±6	23±8	2±8	15±12	35±14
	Gemfibrozil	3±10	5±7	4±6	11±6	23±14	7±3	15±8	39±16
3	DEET	8±7	3±4	8±6	8±9	17±11	6±2	12±4	31±14
	Ibuprofen	4±6	2±4	6±3	12±9	21±14	8±3	24±5	40±16
	Phenytoin	6±12	13±20	28±15	31±12	45±15	44±8	53±4	64±12
	Primidone	1±8	3±7	3±3	12±9	15±13	7±2	10±17	29±22
4	Atrazine	4±8	-1±2	21±7	16±6	21±9	33±4	32±4	43±9
	Meprobamate	8±12	4±2	11±12	7±5	11±7	12±14	8±6	23±10
5	TCEP	7±7	6±13	9±6	3±11	8±14	8±5	0±5	5±14

Notes: Groupings based on ozone and •OH rate constants; shading represents >80% oxidation; includes CCWRD data for 45 (50) and 225 (250) mJ/cm<sup>2</sup>; DEET=*N,N*-diethyl-*meta*-toluamide; TCEP=tris-(2-chloroethyl)-phosphate

**Disinfection.** Wastewater contains a countless number of bacteria, viruses, and parasites, but only a small fraction of these microbes are actually pathogenic. Pathogenicity even varies between strains of the same species. Ideally, evaluations of disinfection efficacy would focus only on the pathogenic microbes, but the related assays are sometimes impractical because of limited ambient prevalence, complex infectivity assays (e.g., *Cryptosporidium* oocysts), or the complete lack of established infectivity assays (e.g., noroviruses). In order to compile useful databases of disinfection efficacy, researchers often use surrogate microbes that are assumed to have similar disinfection profiles as the target pathogens.

Table 3.88 and Table 3.89 provide the average levels of inactivation for *E. coli* and the bacteriophage MS2 with ozone and ozone/H<sub>2</sub>O<sub>2</sub>. *E. coli* was more resistant than MS2 to ozone-based oxidation, and *E. coli* inactivation was also more variable among the wastewater matrices. Although dissolved ozone residuals and CTs are often required to demonstrate regulatory compliance, the addition of H<sub>2</sub>O<sub>2</sub>, which rapidly quenches any ozone residual, still achieved significant levels of inactivation for *E. coli* and MS2. However, ozone/H<sub>2</sub>O<sub>2</sub> was generally less effective and slightly more variable than ozone alone for *E. coli* and MS2 inactivation. In order to achieve the modified CDPH Title 22 benchmark of 6.5-log viral inactivation, O<sub>3</sub>:TOC ratios of 1.0 to 1.5 were required for ozone and ozone/H<sub>2</sub>O<sub>2</sub>. Based on the reaction time experiment (see Table 3.15), achieving a dissolved ozone residual provided greater inactivation, but a majority of the microbial inactivation was complete within 15 seconds regardless of H<sub>2</sub>O<sub>2</sub> dose.

**Table 3.88. Average Log Inactivation for *E. coli* During Ozonation**

O <sub>3</sub> :TOC	H <sub>2</sub> O <sub>2</sub> :O <sub>3</sub> =0	H <sub>2</sub> O <sub>2</sub> :O <sub>3</sub> =0.5	H <sub>2</sub> O <sub>2</sub> :O <sub>3</sub> =1.0
0.25	1.5±1.0	1.0±0.6	1.4±1.3
0.50	4.9±1.8	4.1±2.6	3.6±2.5
1.00	7.1±1.3*	5.5±1.1	5.2±1.8
1.50	7.1±1.1*	5.4±1.3	4.8±1.7

Notes: \*=limited by spiking level in some samples; GCGA omitted because of differences in O<sub>3</sub>:TOC ratios

**Table 3.89. Average Log Inactivation for MS2 During Ozonation**

O <sub>3</sub> :TOC	H <sub>2</sub> O <sub>2</sub> :O <sub>3</sub> =0	H <sub>2</sub> O <sub>2</sub> :O <sub>3</sub> =0.5	H <sub>2</sub> O <sub>2</sub> :O <sub>3</sub> =1.0
0.25	2.1±0.9	1.4±0.5	1.5±0.4
0.50	5.7±0.4	5.6±1.1*	5.6±1.3*
1.00	6.7±0.7*	6.4±1.1	5.8±0.5
1.50	7.4±0.3*	6.6±0.7	6.7±0.8

Notes: \*=limited by spiking level in some samples; GCGA omitted because of differences in O<sub>3</sub>:TOC ratios

**Table 3.90. Average Log Inactivation for *B. subtilis* Spores During Ozonation**

O <sub>3</sub> :TOC	H <sub>2</sub> O <sub>2</sub> :O <sub>3</sub> =0	H <sub>2</sub> O <sub>2</sub> :O <sub>3</sub> =0.5	H <sub>2</sub> O <sub>2</sub> :O <sub>3</sub> =1.0
0.25	0.0±0.0	0.0±0.1	0.0±0.0
0.50	0.0±0.1	0.0±0.0	0.0±0.1
1.00	1.1±1.0	0.0±0.0	0.0±0.1
1.50	2.6±1.0*	0.0±0.1	0.1±0.1

Notes: \*=limited by spiking level in some samples; GCGA omitted because of differences in O<sub>3</sub>:TOC ratios

**Table 3.91. Average Inactivation During UV and UV/H<sub>2</sub>O<sub>2</sub>**

UV Dose (mJ/cm <sup>2</sup> )	<i>E. coli</i>		MS2		<i>Bacillus</i> Spores	
	UV	UV/H <sub>2</sub> O <sub>2</sub>	UV	UV/H <sub>2</sub> O <sub>2</sub>	UV	UV/H <sub>2</sub> O <sub>2</sub>
25	5.5±1.8*	6.4±0.4*	1.7±0.1	2.2±0.4	2.5±0.6	2.5±0.5
50	7.1±0.2*	7.1±0.2*	3.0±0.1	3.5±0.4	3.3±0.2*	3.3±0.1*
250	7.1±0.2*	7.1±0.2*	7.1±0.3*	7.3±0.4*	3.4±0.1*	3.4±0.1*
500	7.1±0.2*	7.1±0.2*	7.2±0.2*	7.1±0.1*	3.4±0.1*	3.4±0.1*

Notes: \*Limited by spiking level in some samples; includes CCWRD data for 23 (25), 45 (50), and 225 (250) mJ/cm<sup>2</sup>; UV=ultraviolet

Table 3.90 provides the average levels of inactivation for *B. subtilis* spores, which are generally used as surrogates for pathogenic *Cryptosporidium* oocysts and *Giardia* cysts. In comparison to chlorine, ozone achieves greater levels of inactivation of spore-forming microbes, but the spores still provide significant protection against ozone and •OH. In fact, extended contact with dissolved ozone is required before the oxidant is able to diffuse across the spore coat and inactivate the microbe (see Table 3.15). Therefore, applications targeting spore/oocyst/cyst inactivation should only use O<sub>3</sub>:TOC ratios >1.0 with no H<sub>2</sub>O<sub>2</sub> addition. The level of inactivation will still be lower than that of vegetative bacteria and viruses.

Table 3.91 provides the average levels of inactivation of all three surrogate microbes with UV and UV/H<sub>2</sub>O<sub>2</sub>. UV and UV/H<sub>2</sub>O<sub>2</sub> are extremely effective for the inactivation of both vegetative (e.g., *E. coli*) and spore-forming microbes (e.g., *B. subtilis* spores, *Cryptosporidium* oocysts, and *Giardia* cysts), which clearly provides an advantage over ozone-based oxidation. In fact, a common disinfection dose of 50 mJ/cm<sup>2</sup> achieved the limit of inactivation for *E. coli* and *B. subtilis* spores. MS2 was more resistant to UV than the bacterial surrogates, but the modified CDPH Title 22 benchmark of 6.5-log viral inactivation was easily achieved with moderate advanced oxidation dosing conditions (i.e., UV dose >250 mJ/cm<sup>2</sup>). Viral resistance to germicidal UV light (λ=254 nm) is also reported in the literature and is the basis for the high dose requirements established by the LT2ESWTR for drinking water applications.

**Organic characterization.** Many of the analyses described previously are time-consuming, costly, and require tremendous analytical expertise to ensure high-quality results. In contrast, organic characterization methods such as simple measurements of UV absorbance are quite simple and easy to interpret, which highlights their utility as surrogate measures of oxidation efficacy for contaminant destruction and microbial inactivation. Furthermore, relative changes in bulk organic matter are often quite similar among wastewater matrices despite significant differences in water quality. For example, the UV absorbance profiles for the different wastewater matrices exhibited very similar trends, although the magnitudes varied significantly. The relative changes in UV<sub>254</sub> absorbance for the ozone- and UV-based treatment processes are illustrated in Figure 3.104. The relative changes during the ozone-based treatment processes can also be described by the following models. On the other hand, relative changes in UV<sub>254</sub> absorbance during the UV/H<sub>2</sub>O<sub>2</sub> process varied significantly between wastewater matrices, which prevented the development of useful models.

- H<sub>2</sub>O<sub>2</sub>:O<sub>3</sub>=0:             $\Delta UV_{254} (\%) = 100 * 0.5077(O_3:TOC)^{0.5968} \quad R^2=0.92$
- H<sub>2</sub>O<sub>2</sub>:O<sub>3</sub>=0.5:            $\Delta UV_{254} (\%) = 100 * 0.4343(O_3:TOC)^{0.4608} \quad R^2=0.89$
- H<sub>2</sub>O<sub>2</sub>:O<sub>3</sub>=1.0:            $\Delta UV_{254} (\%) = 100 * 0.4023(O_3:TOC)^{0.4252} \quad R^2=0.86$
- Combined:                 $\Delta UV_{254} (\%) = 100 * 0.4460(O_3:TOC)^{0.4943} \quad R^2=0.86$

Because measurements of TF require more complex equipment, this analysis is less common in wastewater treatment operations, but TF provides a more sensitive alternative to UV<sub>254</sub> absorbance and is capable of differentiating high-quality matrices. This makes it a relatively straightforward concept with the potential to act as a surrogate measure of treatment efficacy for contaminant oxidation and microbial inactivation. Similar to absorbance, the magnitude of TF may vary considerably among different wastewater matrices, but the relative changes are quite consistent. The relative changes in TF for the ozone- and UV-based treatment processes are illustrated in Figure 3.105. The relative changes during ozone-based oxidation can also be described by the following models.

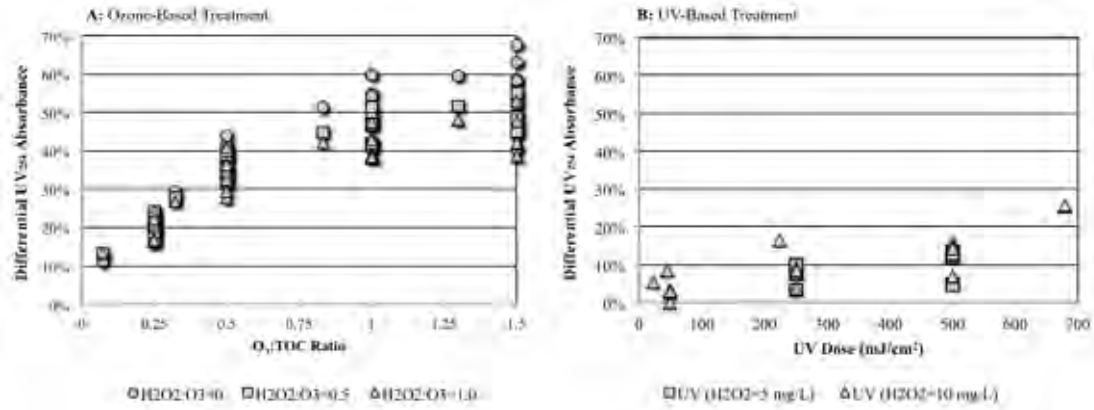


Figure 3.104. Summary of differential UV<sub>254</sub> absorbance.

- H<sub>2</sub>O<sub>2</sub>:O<sub>3</sub>=0:  $\Delta TF (\%) = 100 * 0.8758(O_3:TOC)^{0.3376}$   $R^2=0.86$
- H<sub>2</sub>O<sub>2</sub>:O<sub>3</sub>=0.5:  $\Delta TF (\%) = 100 * 0.8525(O_3:TOC)^{0.3041}$   $R^2=0.84$
- H<sub>2</sub>O<sub>2</sub>:O<sub>3</sub>=1.0:  $\Delta TF (\%) = 100 * 0.8345(O_3:TOC)^{0.3193}$   $R^2=0.83$
- Combined:  $\Delta TF (\%) = 100 * 0.8541(O_3:TOC)^{0.3204}$   $R^2=0.84$

The data presented throughout this chapter provide the foundation for the organic correlations developed in the next section. The intent of the organic correlations is to simplify process performance monitoring by substituting all of the complex analyses with measurements of absorbance or fluorescence.

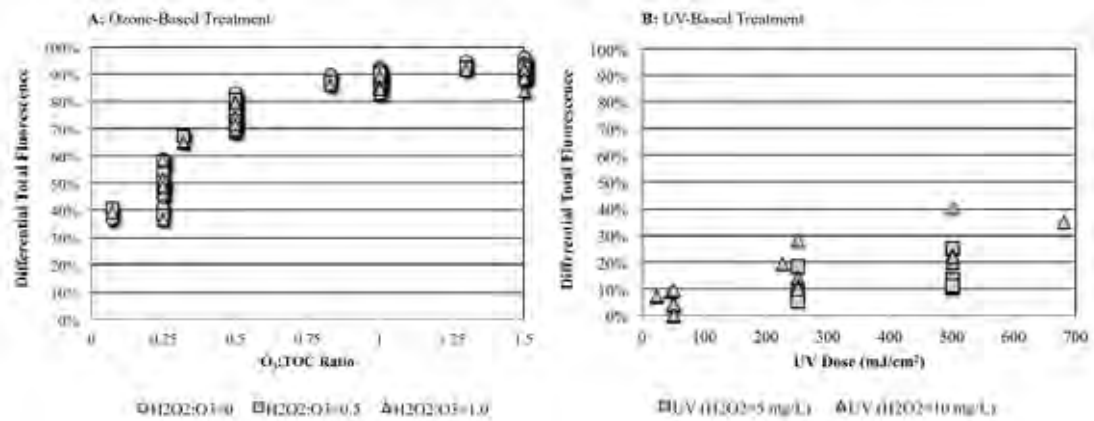


Figure 3.105. Summary of total fluorescence.



## Chapter 4

# Development of Organic Correlations

---

### 4.1 Characterization of Surrogate Parameters

The effects of advanced oxidation on EfOM were quantified with several different approaches, including differential absorbance spectroscopy, numerically processed fluorescence data, and high-performance size exclusion chromatography (HPSEC). In all cases, vast data sets were generated for each examined wastewater and each set of treatment conditions. Despite the wide variety of experimental conditions, the AOP-induced transformation of EfOM proved to be relatively consistent among the various secondary effluents. Because the AOP-induced changes were more prominent in the ozone and ozone/H<sub>2</sub>O<sub>2</sub> samples, the ensuing discussion is primarily focused on data obtained for ozone-based oxidation. Similar correlations were developed for UV-based oxidation, but the extent of transformation was generally less conspicuous.

Absorbance and fluorescence spectroscopy and size exclusion chromatography (SEC) provide a seemingly endless spectrum of data (e.g., different excitation emission wavelengths, different molecular weights) from which correlations can be developed. Therefore, it is important to optimize these elements of organic characterization so they can be used as surrogate parameters. The following sections characterize the use of EfOM as a potential surrogate framework and highlight the most appropriate conditions for evaluating treatment process efficacy. For results that were similar among the various secondary effluents, the report focuses on CCWRD, but the discussion is supported and enhanced, when necessary, with data from the other sites.

#### 4.1.1 Absorbance Spectroscopy

For a specific wavelength ( $\lambda$ ), the absorbance of any treated sample was subtracted from the absorbance of the untreated sample (i.e., secondary effluent) to obtain differential absorbance values:

$$\Delta A_{\lambda, \text{treated}} = A_{\lambda, \text{untreated}} - A_{\lambda, \text{treated}}$$

The differential absorbance spectra in Figures 4.1 and 4.2 illustrate the existence of common and highly reproducible transformations of EfOM. The increase in differential absorbance illustrates the degradation of a wide range of EfOM chromophores. In previous sections, the discussion focused on the *actual* absorbance spectra, which decrease with treatment, as opposed to these *differential* absorbance spectra, which increase with treatment, thereby illustrating organic transformation. The increase is particularly evident for wavelengths <240 nm, which is similar to observations reported in the literature (Nanaboina and Korshin, 2010). However, changes in absorbance at wavelengths below 240 nm are more difficult to interpret because of potential interference from other species (e.g., nitrate) and more extensive particulate-induced light scattering. For these reasons, analyses of EfOM transformation were limited to wavelengths >240 nm. After limiting the data accordingly, the differential absorbance spectra for CCWRD exhibited a maximum, or a fairly pronounced plateau, in the range of wavelengths from 250 to 280 nm. At higher O<sub>3</sub>:TOC ratios, the maximum/plateau

was replaced by a less pronounced “shoulder.” As described earlier and illustrated again in Figure 4.2, the addition of H<sub>2</sub>O<sub>2</sub> did not have a significant effect on the trends in EfOM transformation, but H<sub>2</sub>O<sub>2</sub> addition did reduce the extent of transformation slightly.

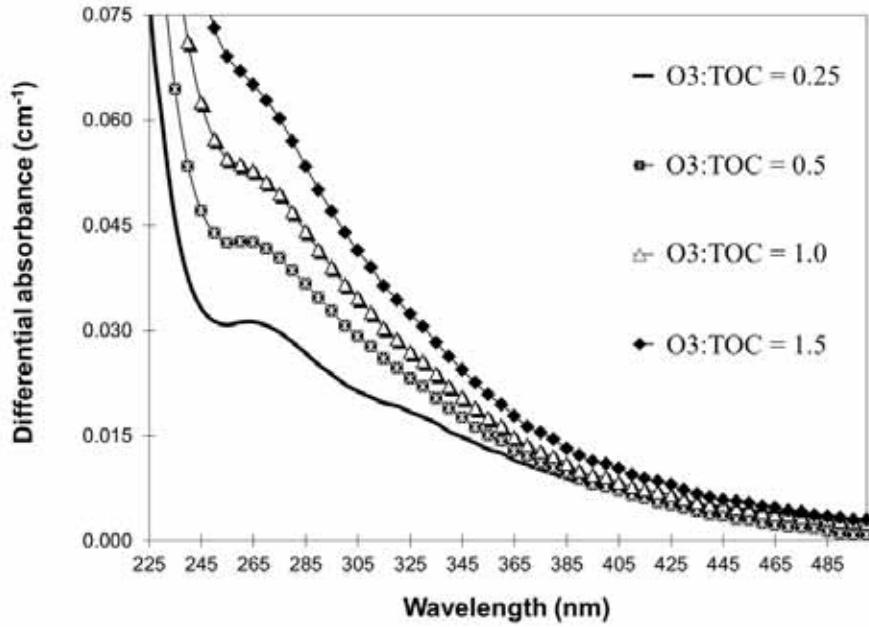


Figure 4.1. Differential absorbance spectra for CCWRD (H<sub>2</sub>O<sub>2</sub>:O<sub>3</sub>=0).

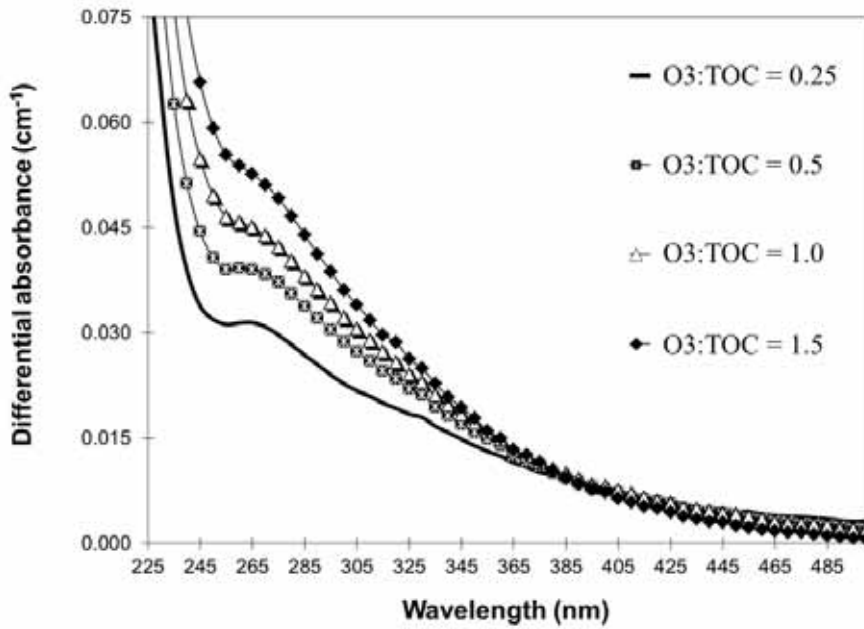


Figure 4.2. Differential absorbance spectra for CCWRD (H<sub>2</sub>O<sub>2</sub>:O<sub>3</sub>=1.0).

EfOM transformation was also evaluated with *normalized* differential spectra, as illustrated in Figure 3.3 and Figure 3.4. The spectra were normalized against the differential absorbance at 270 nm, which was the approximate location of the maximum/plateau for each sample, according to the following equation:

$$\Delta A_{\lambda,treated}^{normalized} = \frac{\Delta A_{\lambda,treated}}{\Delta A_{270nm,treated}}$$

As shown in these figures, the shape of the normalized differential spectra remains largely the same irrespective of ozone dose or H<sub>2</sub>O<sub>2</sub> addition. The only notable difference in the spectra is the presence of a relatively small bump for lower ozone doses in the wavelength range from 320 to 330 nm. The spike is fairly distinct in some samples and more shoulderlike in other samples. The reason for this feature has not been determined, but results of prior research (Nanaboina and Korshin, 2010) indicate that this shoulder may correspond to changes in the most rapidly reacting group of EfOM, which some consider to be biopolymers.

Although the differential spectra reach their maxima near a wavelength of 270 nm, the relative changes in absorbance spectra (i.e., percent reduction in absorbance) exhibit a different pattern. Relative changes in absorbance were calculated according to the following equation, and the examples for CCWRD are shown in Figure 3.5 and Figure 3.6:

$$\frac{\Delta A_{\lambda}}{A_{0,\lambda}} = \frac{A_{\lambda,untreated} - A_{\lambda,treated}}{A_{\lambda,untreated}}$$

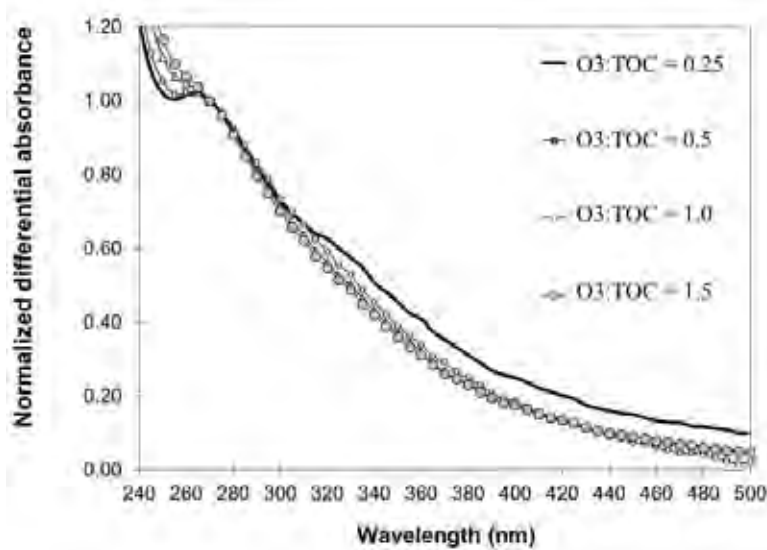
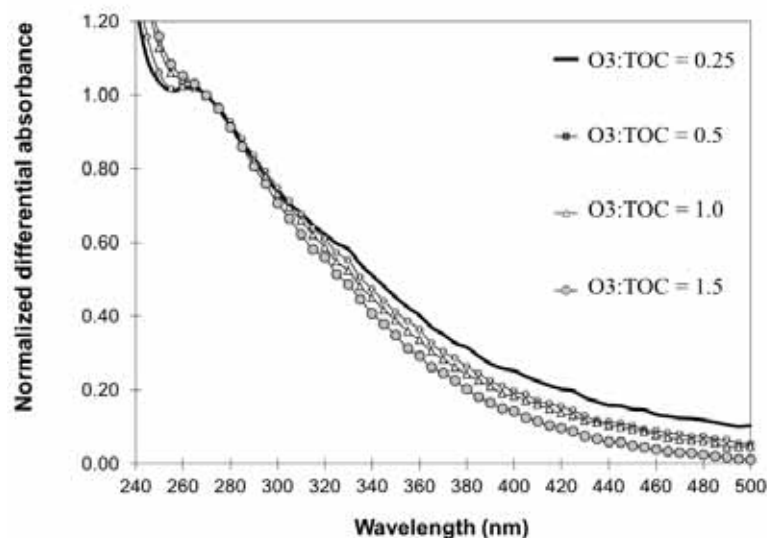


Figure 4.3. Normalized differential absorbance spectra for CCWRD (H<sub>2</sub>O<sub>2</sub>:O<sub>3</sub>=0).



**Figure 4.4. Normalized differential absorbance spectra for CCWRD ( $\text{H}_2\text{O}_2:\text{O}_3=1.0$ ).**

The figures demonstrate the existence of four wavelength ranges with characteristic  $\Delta A/A_0$  behavior. In the range of wavelengths from 225 to 245 nm, the  $\Delta A/A_0$  values increase rapidly with wavelength. The magnitude of  $\Delta A/A_0$  is initially low in this range, which reflects the presence of species unaffected by AOP treatment. As the wavelength increases, the representative species experience significant transformation, which is reflected in the rapid increase in  $\Delta A/A_0$ . In the range of wavelengths from 250 to 300 nm,  $\Delta A/A_0$  values exhibit a plateau and remain relatively consistent regardless of wavelength. Furthermore, this range often exhibits the largest differential across AOP conditions, which highlights its usefulness in evaluating treatment process efficacy.

In the range of wavelengths from 300 to 330 nm,  $\Delta A/A_0$  values increase once again before plateauing at wavelengths  $>330$  nm. The latter two wavelength ranges also show potential for quantifying treatment efficacy, but the differences between the treatment conditions are not entirely consistent (e.g.,  $\lambda=400$  nm in Figure 3.6), and the absolute absorbance values are generally lower at higher wavelengths, thereby limiting sensitivity. For surrogate frameworks, the selection of wavelengths  $>330$  nm may have distinct benefits, such as reduced spectral interference by competing species, reduced particulate-induced light scattering, and the use of inexpensive absorbance spectrometers operating in the visible light range. The limitations described previously indicate that shorter wavelengths, particularly 254 nm, may provide a more robust surrogate parameter.

Changes in absorbance were more subtle and complex for the UV/ $\text{H}_2\text{O}_2$  process. In contrast to the data for ozone-based oxidation, UV/ $\text{H}_2\text{O}_2$  resulted in differential absorbance spectra with a maximum close to 250 nm, but the shape of the differential absorbance spectra remained the same regardless of the matrix or  $\text{H}_2\text{O}_2$  concentration (Figure 3.7). Because of the shift toward 250 nm, the equation for the normalized differential absorbance spectra was modified accordingly, and an example is provided in Figure 3.8.

Despite the differences in the absolute and differential absorbance spectra for ozone- and UV-based oxidation, the relative changes in the absorbance spectra displayed similar features for

both treatment processes (Figure 3.9). The relative absorbance increased rapidly for wavelengths <240 nm and remained fairly constant between 250 and 300 nm. These features, combined with the maximum differential near 250 nm, further justify the selection of 254 nm for the surrogate framework. Fortunately, this is also one of the most common parameters for water quality monitoring.

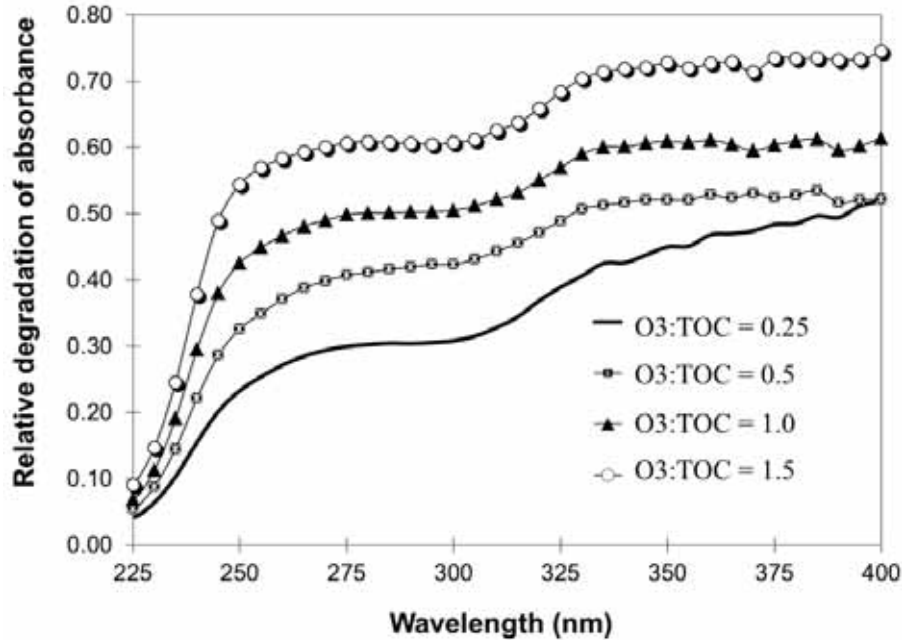


Figure 4.5. Relative changes in absorbance spectra for CCWRD ( $H_2O_2:O_3=0$ ).

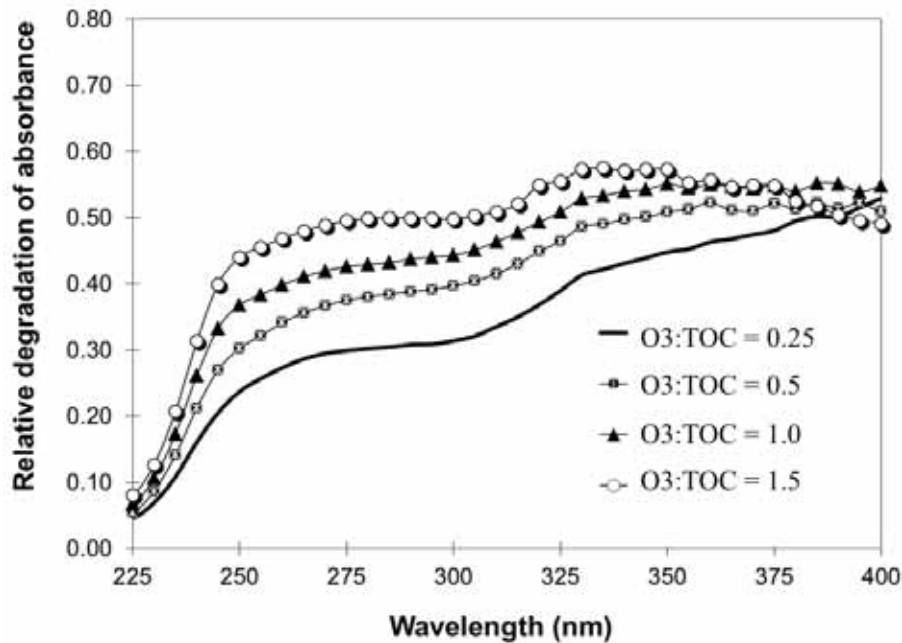


Figure 4.6. Relative changes in absorbance spectra for CCWRD ( $H_2O_2:O_3=1.0$ ).

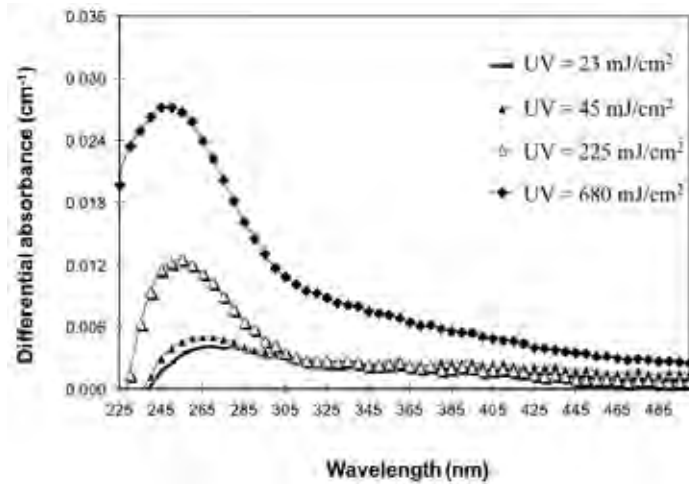


Figure 4.7. Differential absorbance spectra for CCWRD ( $H_2O_2=10$  mg/L).

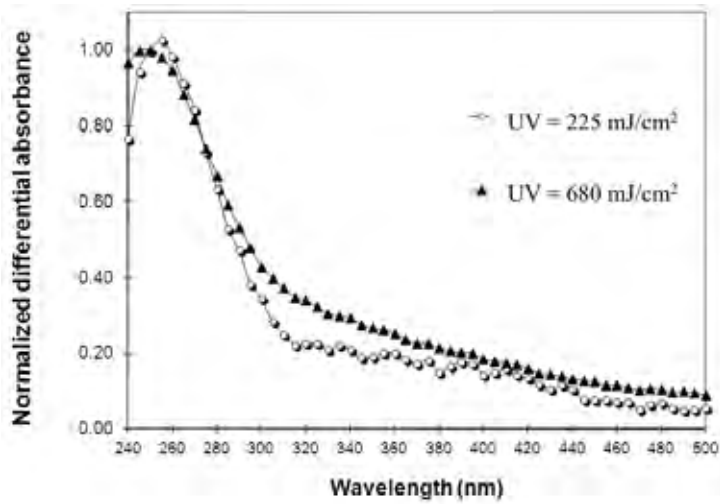


Figure 4.8. Normalized differential absorbance spectra for CCWRD ( $H_2O_2=10$  mg/L).

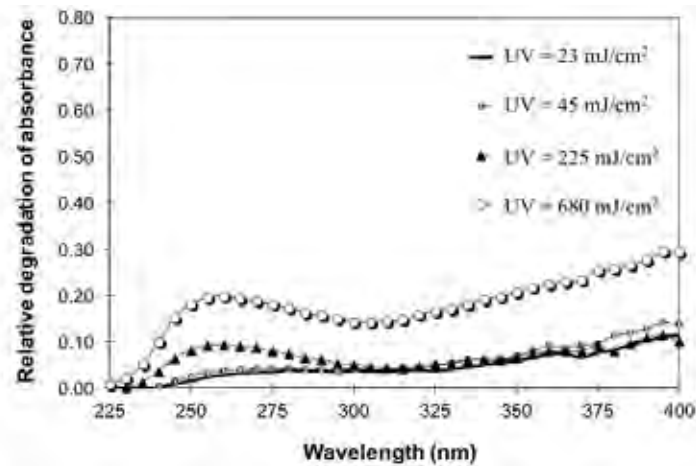


Figure 4.9. Relative changes in absorbance spectra for CCWRD ( $H_2O_2=10$  mg/L).

### 4.1.2 Fluorescence Spectra

Table 4.1 summarizes the excitation and emission wavelengths and the corresponding intensities of the most prominent fluorescence maxima for the five secondary effluents. These data indicate that the positions of Regions I, II, and III were relatively consistent between the five secondary effluents, although the intensities of these regions exhibited considerable variability. This indicates that the relative composition of the EfOM was similar among the matrices, but they contained different concentrations of the various EfOM constituents, including fluorophores associated with microbial biopolymers, fulvic-, and humic-like species. Because the regions sometimes contained multiple peaks, the original boundaries for Regions I and II (Figure 4.3) were also divided into subregions (I, IA, II, and IIA) for this analysis.

As shown in earlier sections of this report, fluorescence intensity exhibited a monotonic decrease with increasing oxidation and transformation. In fact, decreases in EEM intensity were more dramatic than those of absorbance, particularly for high ozone doses that resulted in nearly 100% reductions in TF. Similar to the absorbance spectra, the effects of H<sub>2</sub>O<sub>2</sub> addition were generally insignificant in comparison to ozone alone.

To characterize the effects of advanced oxidation on fluorescence, differential fluorescence spectra were developed for the various matrices. The calculations were performed in a similar manner to those of the differential absorbance spectra:

$$\Delta F_{\lambda_{ex}, \lambda_{em}, treated} = F_{\lambda_{ex}, \lambda_{em}, untreated} - F_{\lambda_{ex}, \lambda_{em}, treated}$$

Examples of the differential 3D EEMs are shown in Figure 3.10 and Figure 3.11 for CCWRD. As the applied ozone dose increased, the intensities of the differential spectra increased as well, thereby indicating an increase in organic transformation. In each matrix, the features associated with Groups I, II, and III as well as IA and IIA were clearly visible, and their relative intensities were largely similar to those in the initial 3D EEMs.

Careful observation of the normalized differential 3D EEMs, which were created as follows and are exemplified in Figure 3.12 and Figure 3.13, indicate that changes in fluorescence were consistent (relative to the maximum differential) regardless of the applied ozone dose:

$$\Delta F_{\lambda_{ex}, \lambda_{em}, treated}^{normalized} = \frac{\Delta F_{\lambda_{ex}, \lambda_{em}, treated}}{\Delta F_{GroupIII\_max, treated}}$$

In other words, the fluorescence within each region decreased at a relatively constant rate regardless of applied ozone dose (i.e., consistency between EEMs representing different ozone doses). However, the variability in intensity within a single EEM indicates that some regions were transformed at a slightly faster rate. This was also illustrated in previous sections.

The relative changes in the 3D EEMs (denoted as  $\Delta F_{ij}/F_{ij}^0$ , where I and j correspond to the excitation and emission wavelengths) can be defined as follows:

$$\frac{\Delta F_{\lambda_{ex}, \lambda_{em}}}{F_{\lambda_{ex}, \lambda_{em}}^0} = \frac{F_{\lambda_{ex}, \lambda_{em}, untreated} - F_{\lambda_{ex}, \lambda_{em}, treated}}{F_{\lambda_{ex}, \lambda_{em}, untreated}}$$

Three-dimensional  $\Delta F_{ij}/F_{ij}^0$  matrices illustrate the removal of both major and minor components of EfOM regarding their original contribution to 3D fluorescence. Examples of 3D  $\Delta F_{ij}/F_{ij}^0$  matrices are presented in Figure 3.14 and Figure 3.15. Although significant transformation occurred in all regions, the organic matter associated with Region I was transformed extensively and at a particularly rapid rate. This observation indicates that EfOM biopolymers are particularly reactive compounds during advanced oxidation.

**Table 4.1. Notable Features of the 3D EEMs for the Five Secondary Effluents**

Matrix/Region	Max. Excitation Wavelength (nm)	Max. Emission Wavelength (nm)	Max. Intensity (arbitrary fluorescence units)
<b>CCWRD</b>			
I	285	355	317
IA	240	350	550
II	285	420	287
IIA	245	425	491
III	340	425	383
<b>MWRDGC</b>			
I	285	375	259
IA	240	365	517
II	285	425	285
IIA	245	425	541
III	340	425	392
<b>WBMWD</b>			
I	285	350	467
IA	245	355	516
II	285	420	397
IIA	250	450	775
III	340	425	506
<b>PCU</b>			
I	285	375	458
IA	240	395	680
II	285	445	432
IIA	240	430	819
III	335	390	995
<b>GCGA</b>			
I	285	370	358
IA	240	360	570
II	285	420	325
IIA	245	425	558
III	340	415	543

Notes: CCWRD=Clark County Water Reclamation District; GCGA=Gwinnett County, Georgia; MWRDGC=Metropolitan Water Reclamation District of Greater Chicago; PCU=Pinellas County Utilities; WBMWD=West Basin Municipal Water District

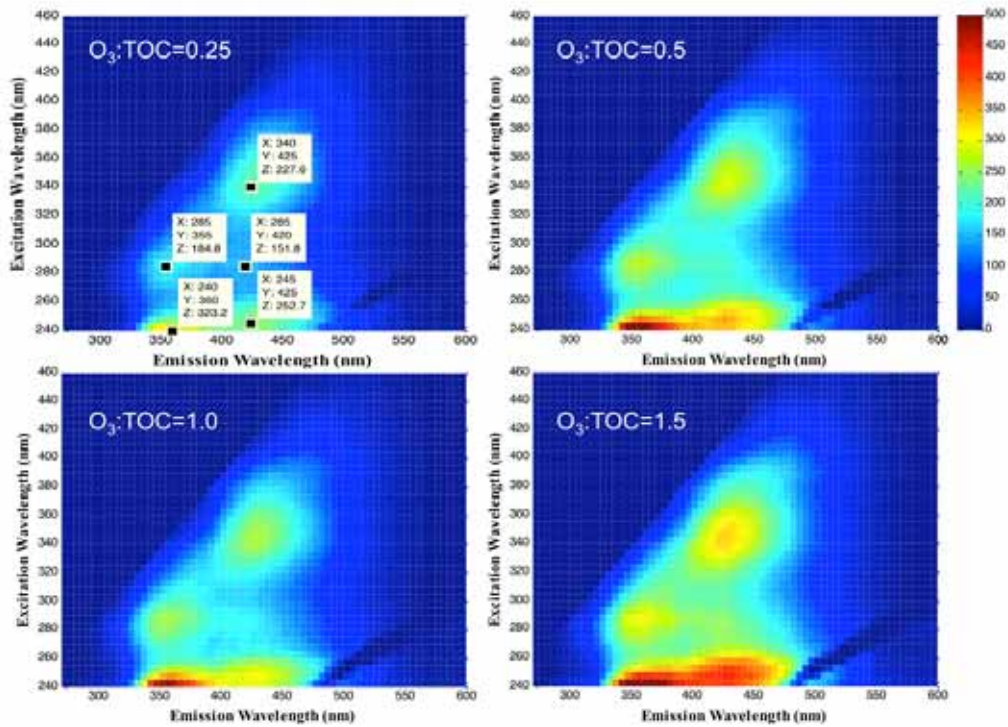


Figure 4.10. Differential 3D EEMs for CCWRD ( $H_2O_2:O_3=0$ ).

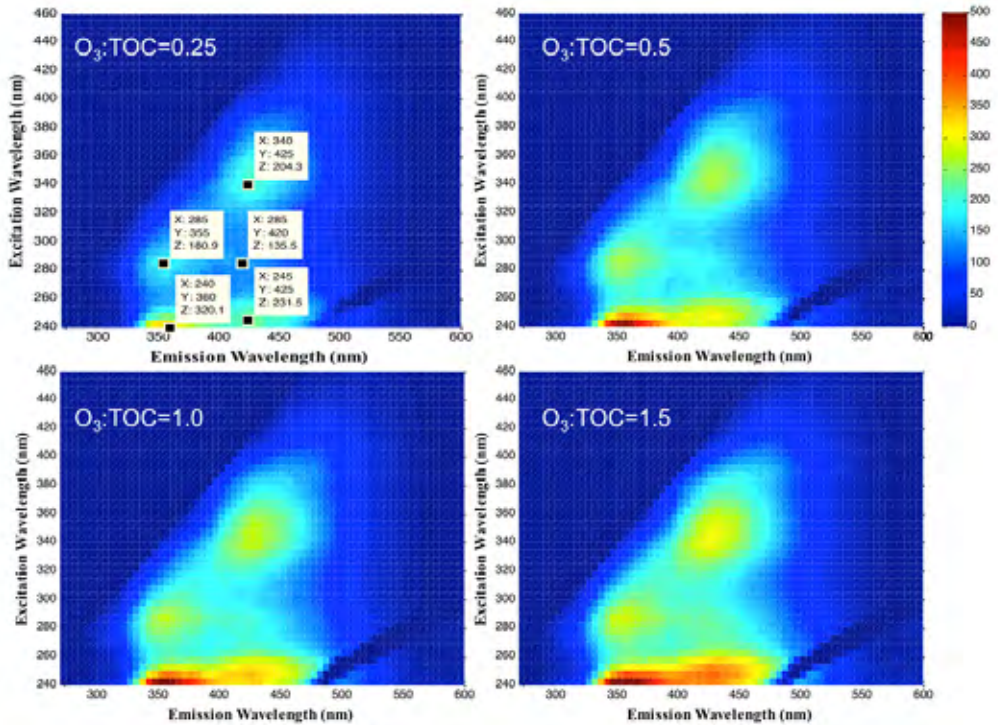


Figure 4.11. Differential 3D EEMs for CCWRD ( $H_2O_2:O_3=1.0$ ).

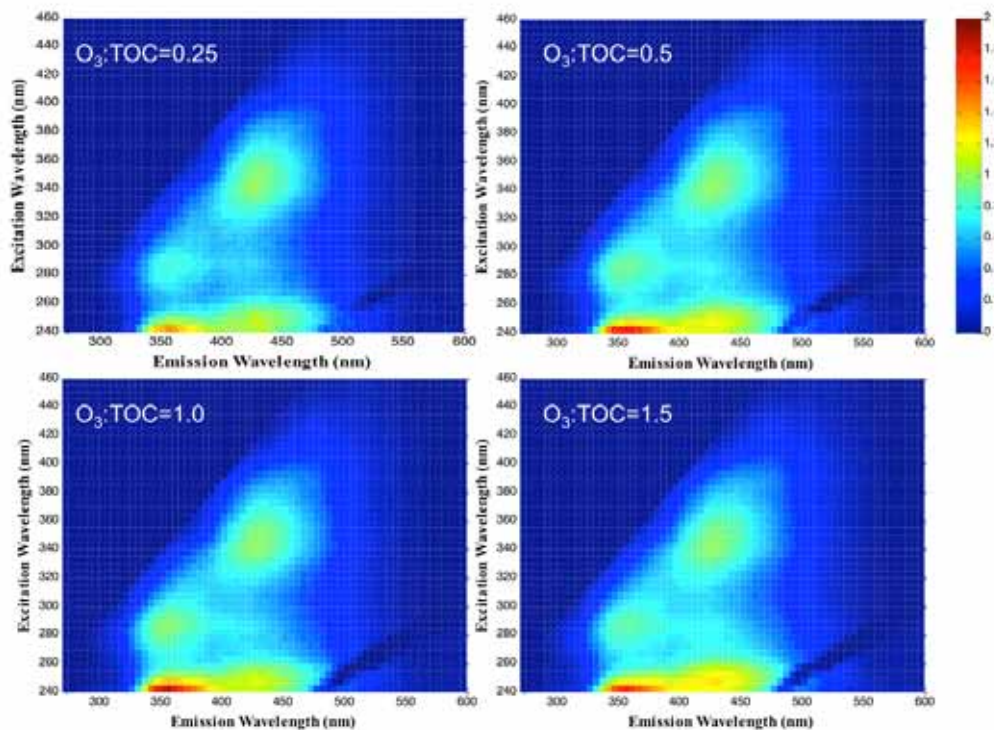


Figure 4.12. Normalized differential 3D EEM for CCWRD ( $H_2O_2:O_3=0$ ).

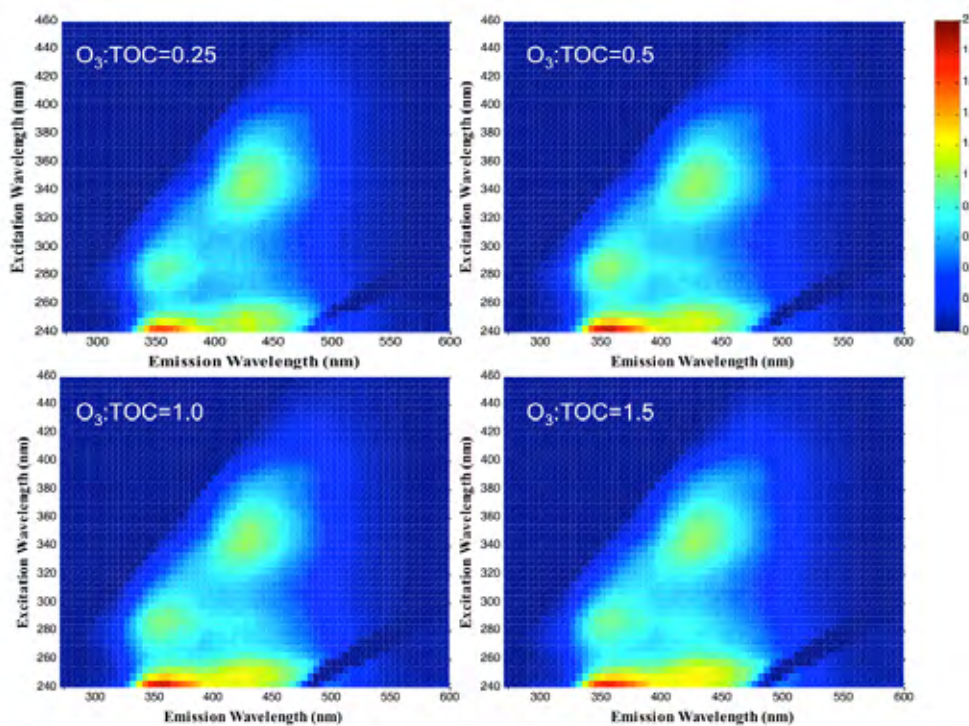


Figure 4.13. Normalized differential 3D EEM for CCWRD ( $H_2O_2:O_3=1.0$ ).

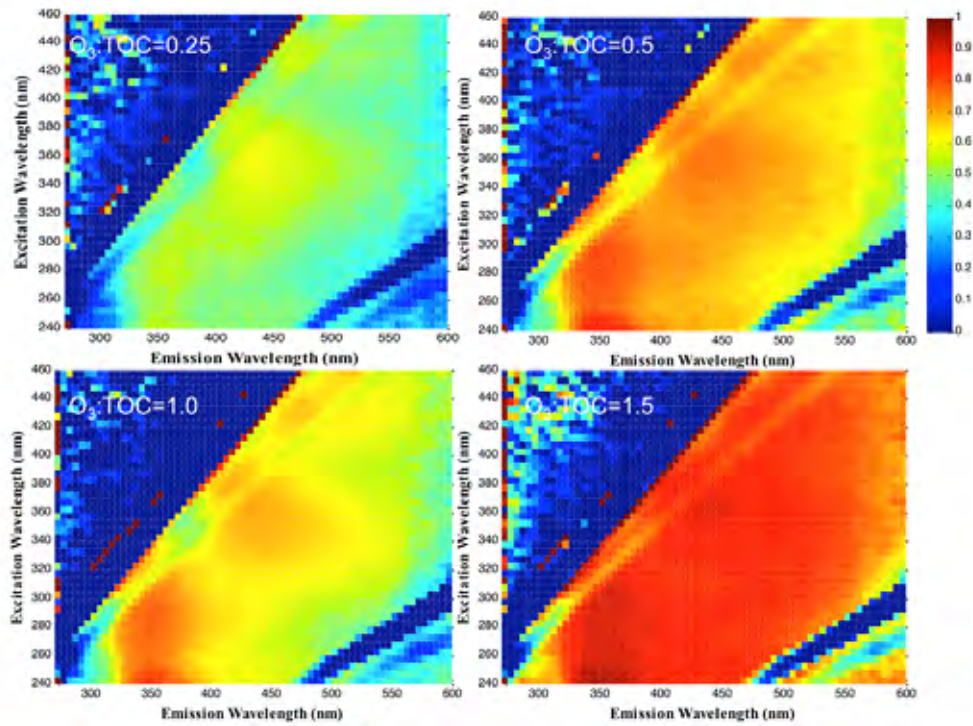


Figure 4.14. Relative changes in fluorescence intensity for CCWRD ( $H_2O_2:O_3=0$ ).

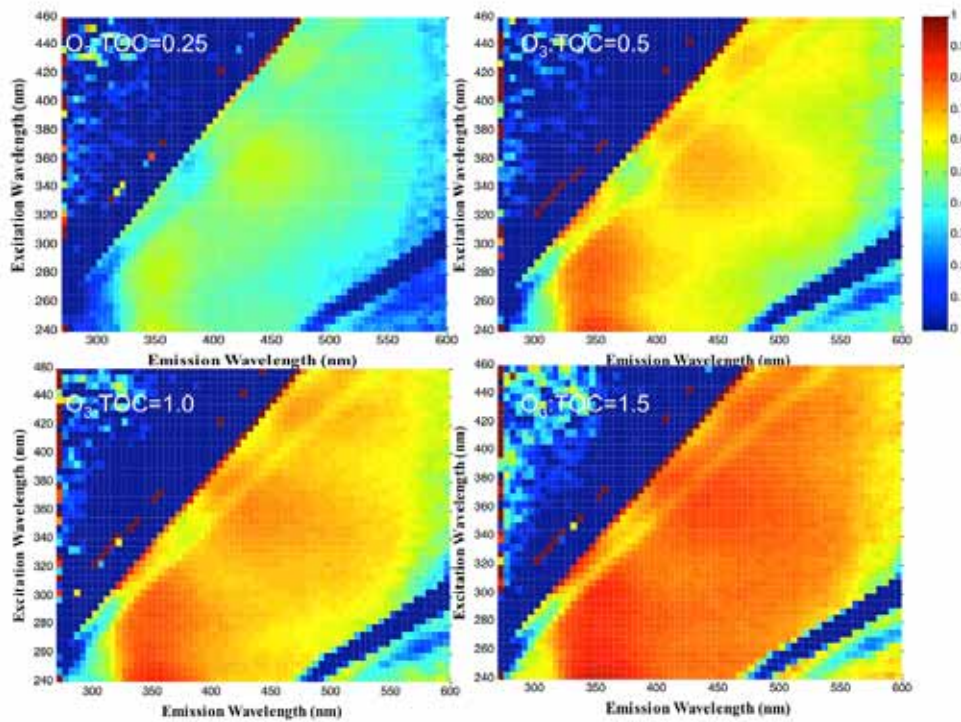


Figure 4.15. Relative changes in fluorescence intensity for CCWRD ( $H_2O_2:O_3=1.0$ ).

The fact that some types of organic matter are preferentially transformed during ozone- and UV-based oxidation highlights the possibility of correlating contaminant oxidation to changes in regional, rather than overall, fluorescence. The 3D EEMs presented earlier illustrate the fluorescence of a broad mixture of organic compounds. It is also possible to characterize the fluorescence of a single compound, which can be described as that compound's fluorescence fingerprint. If the fluorophores of a particular contaminant are predominantly associated with Region I, for example, the oxidation of that contaminant might show the strongest correlation with changes in the bulk organic matter associated with that same region. This concept will be evaluated in greater detail following the discussion of HPSEC.

### 4.1.3 High Performance Size Exclusion Chromatography

Organic characterization by HPSEC was achieved through molecular weight separation and downstream analysis by UV<sub>254</sub> absorbance. In other words, the untreated and treated samples were passed through an SEC column, which separated the organic compounds according to their molecular weights, and the eluent was analyzed over time with a UV detector. HPSEC is able to characterize the organic matter in a sample because the compounds with higher molecular weights elute off of the column faster than the compounds with lower molecular weights (i.e., inverse relationship between molecular weight and elution time). Several distinct features of the SEC chromatograms from this study are summarized in Table 4.2, and example chromatograms are provided in Figures 4.16 and 4.17.

**Table 4.2. Locations and Magnitudes of SEC Peaks**

<b>Matrix/Retention Time (min)</b>	<b>Intensity (mAU)</b>
<b>CCWRD</b>	
14.33	8.78
15.30	9.69
16.08	3.75
16.70	5.62
<b>MWRDGC</b>	
14.18	8.73
14.77	6.36
15.82	2.39
16.28	4.67
<b>WBMWD</b>	
14.35	10.08
15.08	13.82
16.08	6.21
<b>PCU</b>	
14.23	18.66
15.05	11.38
16.10	3.66
16.75	3.76
<b>GCGA</b>	
14.20	18.06
14.80	18.90
15.93	4.73
16.30	5.40

*Notes:* CCWRD=Clark County Water Reclamation District; GCGA=Gwinnett County, Georgia; MWRDGC=Metropolitan Water Reclamation District of Greater Chicago; PCU=Pinellas County Utilities; WBMWD=West Basin Municipal Water District

For both the filtered and unfiltered CCWRD samples (unfiltered data not shown), the SEC chromatograms contained four peaks at elution times of 14.33, 15.30, 16.08, and 16.70 min. For the purposes of this analysis, the elution times were correlated to broad molecular weight classes, specifically high molecular weight (HMW), intermediate molecular weight (IMW), and low molecular weight (LMW). Based on a general standard curve, the molecular weight classes can be grouped as follows: HMW > 1300 Da, IMW=1300 to 300 Da, and LMW < 300 Da. It is important to note that these HMW, IMW, and LMW ranges are defined operationally, so the thresholds are only estimated. Therefore, the following discussion will focus on changes in bulk organic matter as it pertains to the larger groupings rather than apparent molecular weights. With this classification scheme, the 14.33-min peak corresponded to a HMW fraction, the 15.30-min peak corresponded to an IMW fraction, and the 16.08- and 16.70-min peaks corresponded to a LMW fraction.

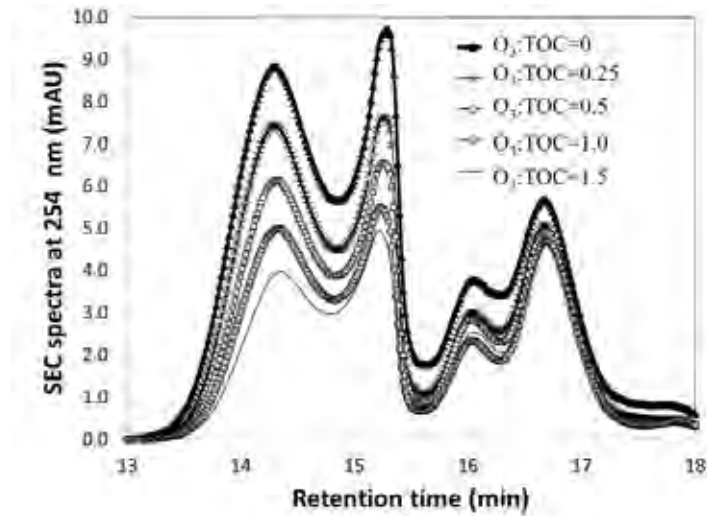


Figure 4.16. SEC chromatograms for CCWRD ( $H_2O_2:O_3=0$ ).

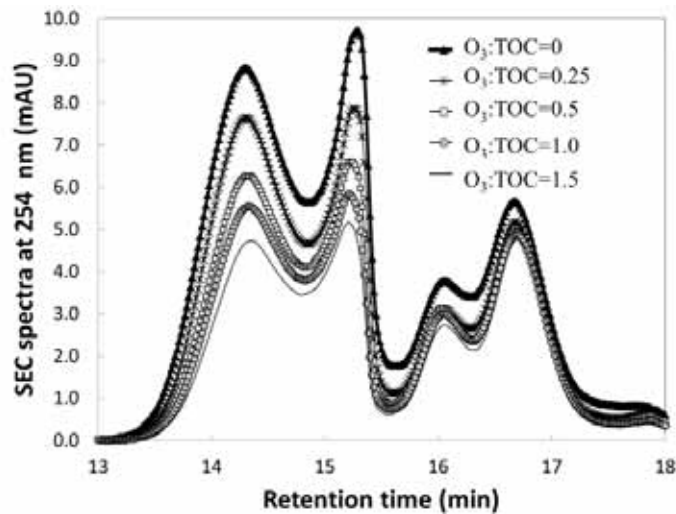


Figure 4.17. SEC chromatograms for CCWRD ( $H_2O_2:O_3=1.0$ ).

The preceding figures indicate that all molecular weights were transformed during oxidation. This observation is also evident in the differential and normalized HPSEC profiles, which were developed in a similar manner to those of absorbance and fluorescence:

$$\Delta A_{elution\_time,treated}^{HPSEC,254nm} = A_{elution\_time,untreated}^{HPSEC,254nm} - A_{elution\_time,treated}^{HPSEC,254nm}$$

Differential HPSEC profiles for CCWRD are shown in Figure 3.18 and Figure 3.19. These profiles generally have the same features as those of the initial (nondifferential) HPSEC data, thereby indicating that nearly all molecular weights undergo degradation by oxidation. In general, a seemingly monotonic increase in the intensity of differential HPSEC was observed for HMW and IMW ranges; however, this trend was less consistent and less prominent in the case of LMW organic matter. For the ozone-only condition, a portion of the LMW fraction in Figure 3.18 was higher, with an O<sub>3</sub>:TOC ratio of 1.0 as compared to 1.5. At both H<sub>2</sub>O<sub>2</sub> doses (H<sub>2</sub>O<sub>2</sub>:O<sub>3</sub> of 0.5 not shown), no significant intensity change was observed for the LMW fraction as the O<sub>3</sub>:TOC ratio increased from 0.5 to 1.0. This highlights a potential issue with using SEC data to develop correlations for treatment efficacy. Oxidation provides a monotonic reduction in UV absorbance, which is the basis for quantification during SEC. Therefore, UV absorbance may not always provide an accurate representation of the molecular weight distribution. Furthermore, certain molecular weight fractions are simultaneously experiencing increases due to decomposition of higher molecular weight compounds and decreases due to decomposition of the fraction in question. These issues may have contributed to the inconsistencies.

The unique properties of the LMW fraction were also evaluated based on normalized SEC profiles (Figures 4.20 and 4.21), which were developed in relation to the IMW peak according to the following equation:

$$A_{elution\_time,treated}^{normalized\_HPSEC,254nm} = \frac{A_{elution\_time,treated}^{HPSEC,254nm}}{A_{IMW\_max,treated}^{HPSEC,254nm}}$$

In contrast to the previous absorbance and fluorescence data, these normalized chromatograms were not based on differential data. The normalized chromatograms effectively illustrate the transformation of higher molecular weight compounds into lower molecular weights during oxidation. In other words, as the ozone dose increased, the LMW compounds accounted for an increasingly higher level of absorbance relative to the other fractions.

Changes in apparent molecular weight were also characterized by integrating the absorbance within each molecular weight class and calculating the relative contribution of each class. Similar to the normalized HPSEC data, these integrations clearly highlight the conversion of HMW to LMW compounds. The increase in the LMW fraction appeared to be related to the transformation of HMW rather than IMW EfOM. The extent of these changes was largely similar in the presence and absence of H<sub>2</sub>O<sub>2</sub>, although the molecular weight shift was less apparent in the ozone/H<sub>2</sub>O<sub>2</sub> samples.

Although this analysis focused on HPSEC with UV detection at 254 nm, higher wavelengths might also provide useful data because of potential reductions in spectroscopic interferences, which are more prominent at lower wavelengths. Again, detection at 254 nm is the most common analytical method, so it offers the most promise for the surrogate framework.

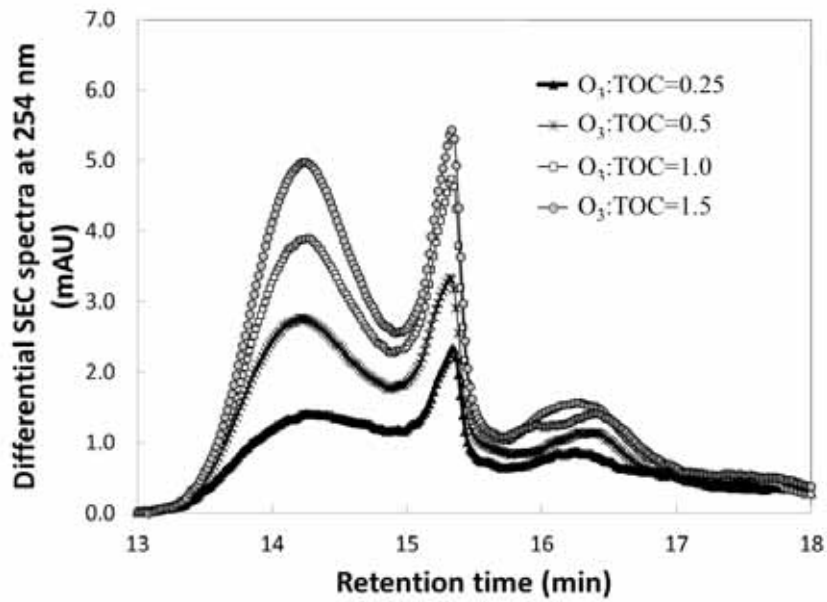


Figure 4.18. Differential SEC chromatograms for CCWRD ( $H_2O_2:O_3=0$ ).

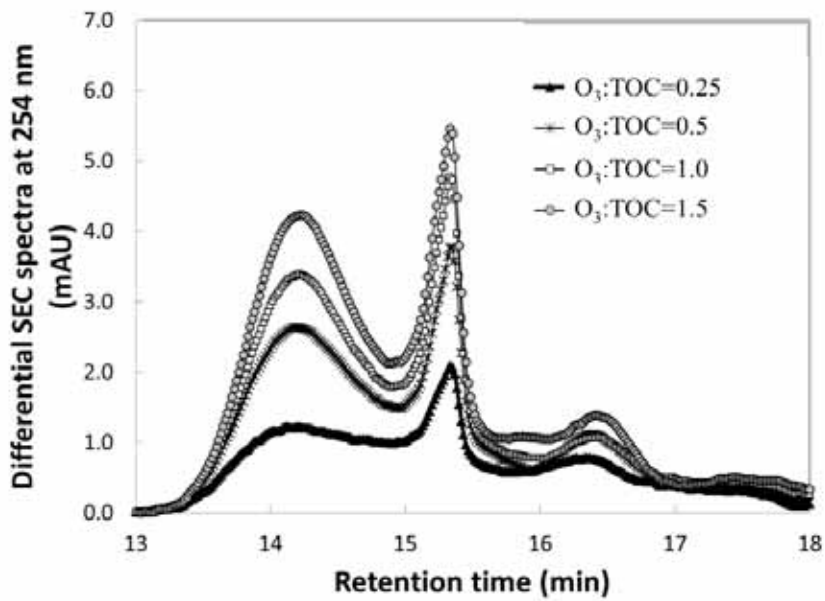


Figure 4.19. Differential SEC chromatograms for CCWRD ( $H_2O_2:O_3=1.0$ ).

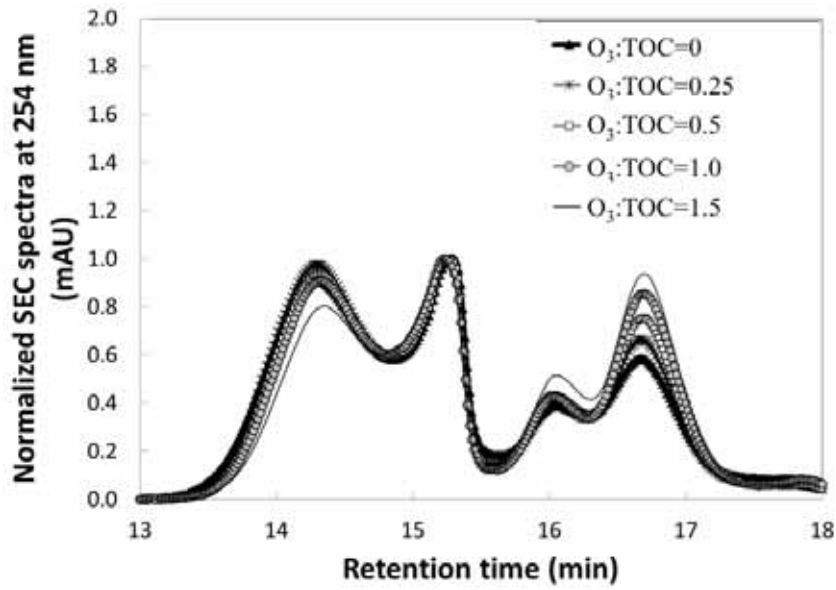


Figure 4.20. Normalized SEC chromatograms for CCWRD ( $H_2O_2:O_3=0$ ).

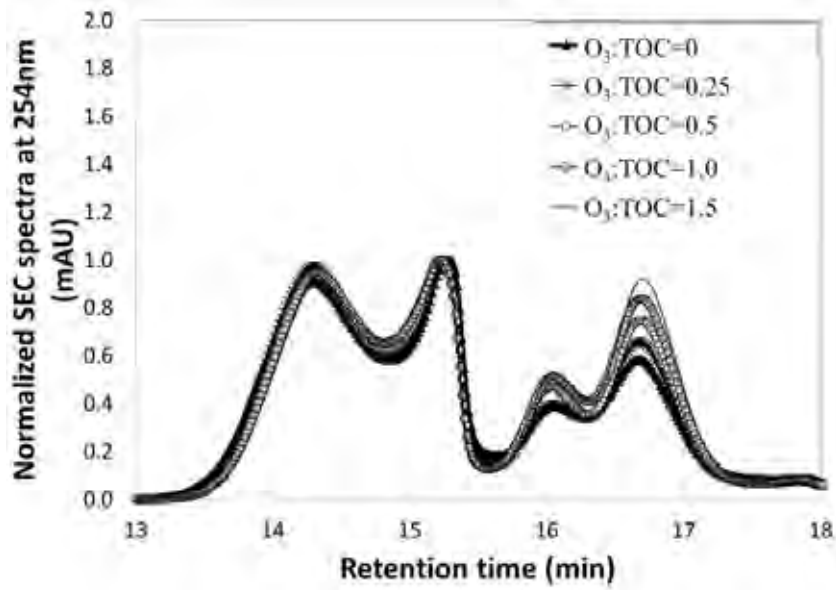


Figure 4.21. Normalized SEC chromatograms for CCWRD ( $H_2O_2:O_3=1.0$ ).

**Table 4.3. Molecular Weight Distributions by Group**

<b>Molecular Weight Class</b>	<b>O<sub>3</sub>:TOC=0</b>	<b>O<sub>3</sub>:TOC=0.25</b>	<b>O<sub>3</sub>:TOC=0.5</b>	<b>O<sub>3</sub>:TOC=1.0</b>	<b>O<sub>3</sub>:TOC=1.5</b>
<b>CCWRD: H<sub>2</sub>O<sub>2</sub>:O<sub>3</sub>=0</b>					
HMW	24.7%	24.6%	21.9%	20.6%	16.9%
IMW	44.4%	44.0%	43.6%	42.9%	41.7%
LMW	30.9%	31.4%	34.5%	36.5%	41.3%
<b>CCWRD: H<sub>2</sub>O<sub>2</sub>:O<sub>3</sub>=1.0</b>					
HMW	24.7%	24.3%	22.0%	20.6%	18.8%
IMW	44.4%	44.2%	43.3%	42.2%	41.9%
LMW	30.9%	31.5%	34.7%	37.1%	39.2%
<b>MWRDGC: H<sub>2</sub>O<sub>2</sub>:O<sub>3</sub>=0</b>					
HMW	43.1%	32.4%	44.3%	41.3%	36.6%
IMW	31.1%	30.1%	28.8%	29.0%	30.6%
LMW	25.8%	37.5%	26.9%	29.7%	32.8%
<b>MWRDGC: H<sub>2</sub>O<sub>2</sub>:O<sub>3</sub>=1.0</b>					
HMW	43.1%	35.0%	44.7%	42.2%	29.7%
IMW	31.1%	30.4%	29.0%	29.3%	33.8%
LMW	25.8%	34.5%	26.3%	28.6%	36.5%
<b>WBMWD: H<sub>2</sub>O<sub>2</sub>:O<sub>3</sub>=0</b>					
HMW	24.6%	27.3%	25.3%	23.0%	22.6%
IMW	47.6%	46.6%	49.2%	48.1%	47.1%
LMW	27.8%	26.1%	25.5%	28.9%	30.4%
<b>WBMWD: H<sub>2</sub>O<sub>2</sub>:O<sub>3</sub>=1.0</b>					
HMW	24.6%	27.6%	26.7%	26.7%	25.7%
IMW	47.6%	46.3%	46.8%	45.0%	44.0%
LMW	27.8%	26.0%	26.6%	28.3%	30.4%
<b>PCU: H<sub>2</sub>O<sub>2</sub>:O<sub>3</sub>=0</b>					
HMW	32.8%	33.7%	33.0%	29.8%	26.3%
IMW	36.7%	36.1%	36.2%	35.9%	35.6%
LMW	30.5%	30.2%	30.8%	34.3%	38.1%
<b>PCU: H<sub>2</sub>O<sub>2</sub>:O<sub>3</sub>=1.0</b>					
HMW	32.8%	33.5%	32.7%	31.4%	29.7%
IMW	36.7%	35.9%	35.8%	34.3%	33.8%
LMW	30.5%	30.6%	31.5%	34.2%	36.5%
<b>GCGA: H<sub>2</sub>O<sub>2</sub>:O<sub>3</sub>=1.0</b>					
HMW	32.8%	33.7%	33.0%	29.8%	26.3%
IMW	36.7%	36.1%	36.2%	35.9%	35.6%
LMW	30.5%	30.2%	30.8%	34.3%	38.1%
<b>GCGA: H<sub>2</sub>O<sub>2</sub>:O<sub>3</sub>=0</b>					
HMW	32.8%	33.5%	32.7%	31.4%	29.7%
IMW	36.7%	35.9%	35.8%	34.3%	33.8%
LMW	30.5%	30.6%	31.5%	34.2%	36.5%

*Notes:* CCWRD=Clark County Water Reclamation District; GCGA=Gwinnett County, Georgia; HMW=high molecular weight; IMW=intermediate molecular weight; LMW=low molecular weight; MWRDGC=Metropolitan Water Reclamation District of Greater Chicago; PCU=Pinellas County Utilities; WBMWD=West Basin Municipal Water District

#### 4.1.4 Optimization of Surrogate Parameters

Organic characterization based on absorbance, fluorescence, and SEC generally relies on specific analytical parameters (e.g., wavelengths) that have been linked to unique properties of organic matter, such as the relationship between  $UV_{254}$  absorbance and aromaticity. The heterogeneous nature of TOrCs and microbes can create a variety of wavelengths that yield strong correlations between transformation of bulk organic matter, contaminant destruction, and microbial inactivation. Proposing an infinite number of correlations does not benefit the water reuse community, so it is critical to identify the most appropriate parameters to serve as the foundation of the surrogate framework. The following observations facilitate this goal:

- Ozone, ozone/ $H_2O_2$ , and UV/ $H_2O_2$  caused prominent and monotonic decreases in absorbance at all wavelengths.
- The shapes of the differential absorbance spectra were highly reproducible from one site to another.
- The maximum differentials occurred at wavelengths of 250 and 270 nm for UV- and ozone-based oxidation.
- Relative changes in absorbance spectra were most prominent for wavelengths  $>325$  nm, but there was also a comparable plateau between 250 nm and 300 nm.
- All major constituents of EfOM (i.e., microbial biopolymers, fulvic- and humic-like species) experienced significant reductions in fluorescence, although the rates of transformation differed among the major groups.
- Nearly all molecular weights experienced significant transformation during oxidation.

These observations confirm the point that changes in absorbance and fluorescence reflect the behavior of the entire ensemble of compounds composing EfOM. Furthermore, these observations support the conclusion that treatment efficacy can theoretically be evaluated based on measurements at practically any wavelength or, in the case of fluorescence, using any reasonable combination of excitation and emission wavelengths.

One issue that has not been sufficiently addressed in the literature is the effect of contaminant properties on correlation models. In order to explore this concept in greater detail, the absorbance and fluorescence fingerprints of the target compounds were evaluated individually (Appendix 1). Of the compounds that demonstrated significant absorbance, the maximum values generally occurred near lower wavelengths. Specific wavelengths of note include 254 nm, which is often associated with aromaticity, and 280 nm, which is often associated with proteinaceous organic matter. Wavelengths lower than 240 nm are often unreliable because of absorbance by the water itself, and wavelengths higher than 280 nm rarely demonstrate any response regarding individual target compounds. Because of the practical nature of measuring  $UV_{254}$  absorbance and its efficacy in relation to the various target compounds, this particular wavelength appears to be the most appropriate parameter for the correlation models. Measuring  $UV_{254}$  absorbance is also simple, inexpensive, and common in water and wastewater operations, and  $UV_{254}$  absorbance also coincides with the observations listed previously. In fact, the existing correlation models in the literature also focus on 254 nm for these reasons.

Appendix 1 also provides the fluorescence fingerprints (i.e., 3D EEMs) for the various target compounds. Although some of the target compounds exhibited a limited response or none at all, many of the compounds exhibited strong responses that were generally associated with

Region I, which is associated with proteinaceous organic matter or soluble microbial products. In addition, some of the target compounds were characterized by distinctive fingerprints that stretched across multiple regions. These unique fingerprints initially offered promise for developing compound-specific correlation models. This is supported by the preferential transformation of EfOM associated with specific regions, as described earlier; however, models correlating contaminant oxidation and regional fluorescence intensity provided no significant benefit over the models based on TF intensity. For example, DEET exhibited an intense fluorescence signal in Region I, but, as indicated in Figure 3.22, this compound's TF correlation for the CCWRD experiments was actually stronger than the Region I correlation, albeit by an extremely small margin. Therefore, the fluorescence correlation models presented in this report are based on TF intensity rather than regional fluorescence intensity.

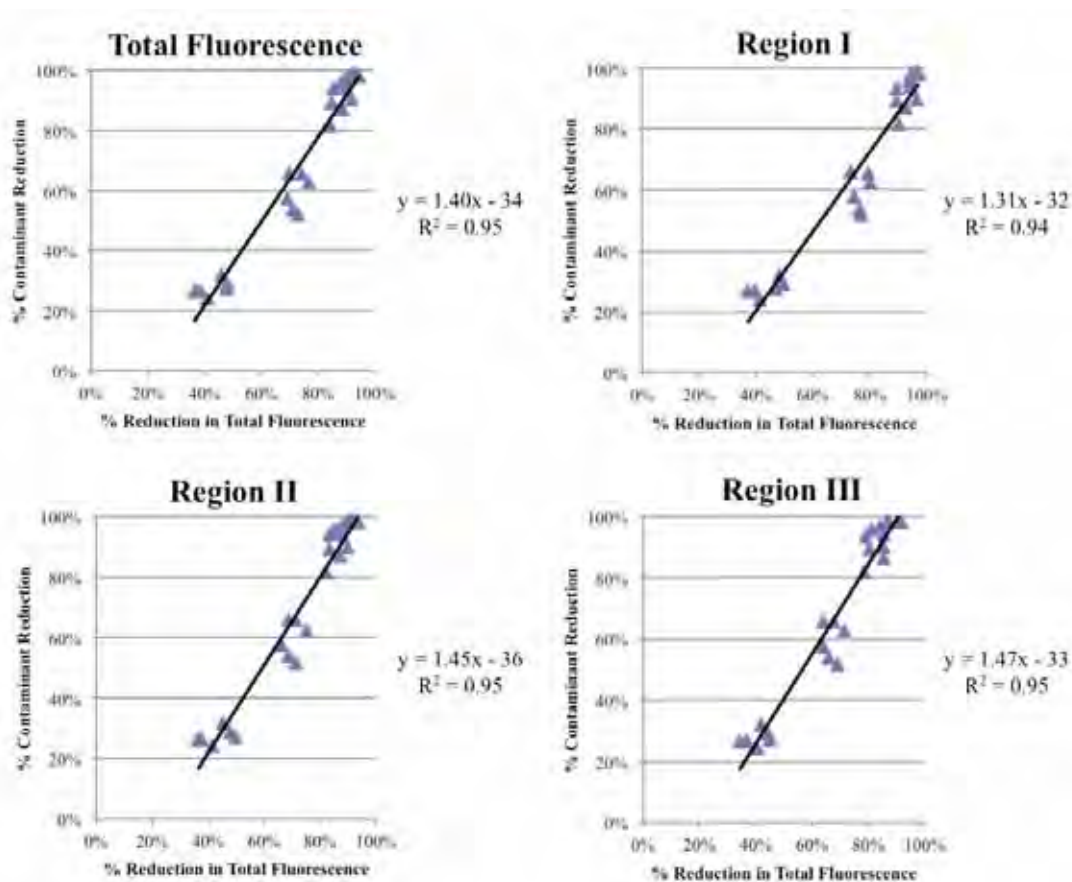


**Figure 4.22. Comparison of total and regional fluorescence correlation models for DEET.**

difficult to differentiate simultaneous increases (i.e., decomposition of higher molecular weight compounds) and decreases (i.e., decomposition of the fraction in question) in the signal. Finally, SEC is the most complex of the three potential surrogate methods, and it also has limited applicability in online field applications. As a result of these limitations, SEC is excluded from further consideration.

The following sections describe two different methods for developing correlations using the organic characterization data listed earlier. The first section describes a set of simple, empirical correlations that relate organic transformation, contaminant destruction, and

microbial inactivation using linear regression. The second section uses a more mechanistic approach based on differential equations to model changes in chromophore and fluorophore concentrations over time. Both approaches use  $UV_{254}$  absorbance and TF as the foundation of the models, and both approaches can provide utilities with a surrogate framework that can be used to monitor the performance of full-scale AOPs. As an example, Figure 3.23 illustrates how this framework could be applied in a full-scale application using secondary effluent data from WBMWD and the empirical model developed during the study.

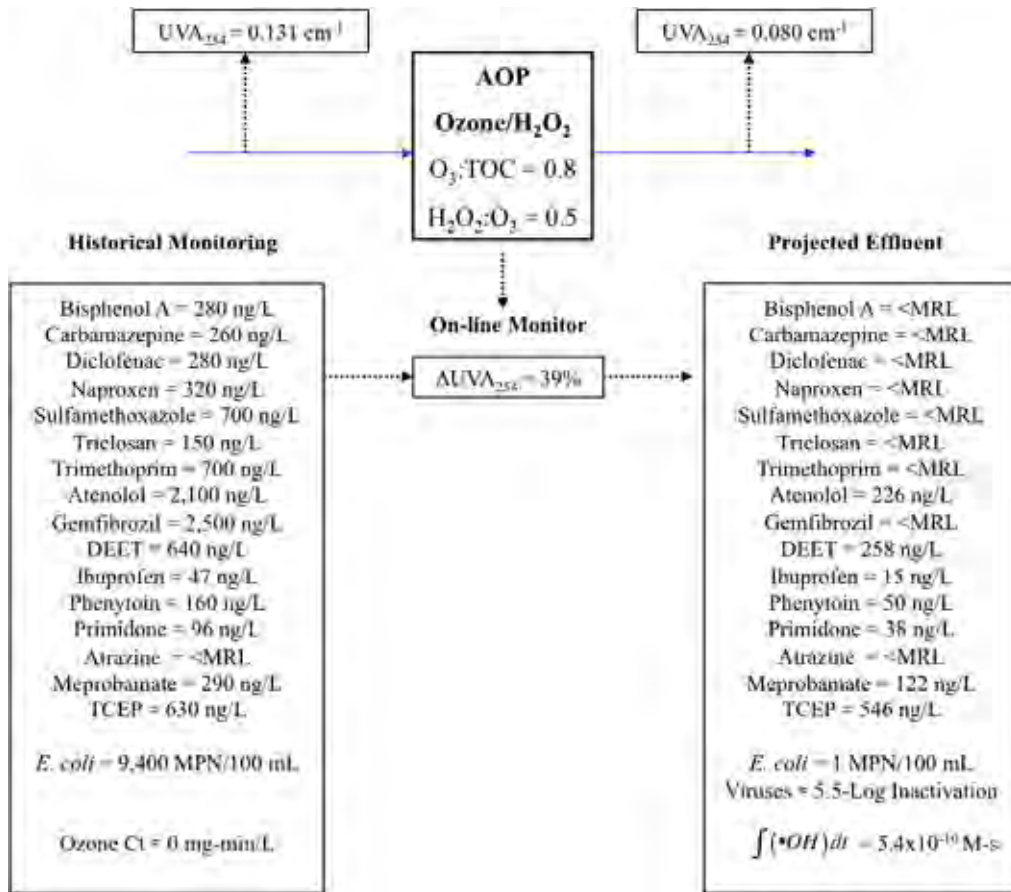


Figure 4.23 Application of surrogate framework.

## 4.2 Empirical Organic Correlations

The first step in developing the empirical correlation models was to plot the relative reductions in target compound concentrations against the relative changes in both  $UV_{254}$  absorbance and TF. The general equation for the empirical correlation models is as follows:

$$\left(1 - \frac{[C]}{[C]_0}\right) * 100(\%) = Slope * \left[\left(1 - \frac{UV \text{ or } TF}{UV_0 \text{ or } TF_0}\right) * 100(\%)\right] + Intercept$$

Appendix 2 provides individual scatter plots for each target compound that differentiate the various water matrices. Each marker represents a single ozone and H<sub>2</sub>O<sub>2</sub> dosing condition.

Filtered versus unfiltered (as shown in Appendix 3) and ozone versus ozone/H<sub>2</sub>O<sub>2</sub> samples (as shown in Appendix 4) were not differentiated because they did not yield noticeably different results. As for peroxide addition (Appendix 4), several of the plots indicate that H<sub>2</sub>O<sub>2</sub>:O<sub>3</sub> ratios have a very slight impact on the correlation models. As discussed previously, the addition of H<sub>2</sub>O<sub>2</sub> caused slight decreases in process efficacy for reducing UV<sub>254</sub> absorbance and fluorescence, but the corresponding changes in contaminant concentrations were generally insignificant. This causes a horizontal translation (to the left) in the correlation data, as the higher peroxide concentrations result in lower reductions in absorbance and fluorescence but similar reductions in contaminant concentrations. Because the impact is minimal, however, grouping all of the data for each compound into a single data set prior to developing the correlations was assumed to be reasonable.

Some degree of scatter in the plots is reasonable because they illustrate empirical correlations, but, based on the overlapping data points, there was no apparent difference among the various water matrices on a compound-specific basis. On the other hand, there were dramatic differences among contaminants, which can be explained by their relative resistance or susceptibility to oxidation. ; DEET=N,N-diethyl-meta-toluamide; pCBA=para-chlorobenzoic acid; TCEP=tris-(2-chloroethyl)-phosphate

Table 4.5 provides a summary of the linear regression parameters for the ozone correlation models. The target compounds were separated into five groups based on their relative susceptibility to ozone and •OH, which also affected the magnitudes of their correlation parameters (i.e., slopes and vertical intercepts). The table also provides regression parameters for a representative “Indicator” in each group based on all of the constituent compounds combined.

Gemfibrozil and atenolol proved to be slightly problematic because they are both moderately resistant to ozone and highly susceptible to •OH, but their respective rate constants still differ by an order of magnitude. This translated into noticeable differences in their regression models, but they were still sufficiently different from the other groups to warrant a separate classification. For the compounds with high ozone and •OH rate constants, particularly for Group 1, the contaminant concentrations rapidly approached their respective MRLs. Because the inclusion of these data points would distort the linear regression analyses, some of them were excluded, as indicated by the “n” parameter for each compound. The compounds in each group were treated similarly in order to reduce any artificial biases.

For Group 1, which includes the compounds that are most susceptible to oxidation, the contaminant concentrations rapidly approached their respective MRLs even with the lowest O<sub>3</sub>:TOC ratio (i.e., nearly vertical lines). Therefore, it was not possible to accurately describe the removal rate based on changes in UV<sub>254</sub> absorbance. Although it was possible to develop correlation models with TF, the correlations were relatively weak (i.e., R<sup>2</sup><0.63). With respect to the TF models, the Group 1 compounds were generally characterized by high slopes (>1.6) with low vertical intercepts (<10) or low slopes (<1.6) with high vertical intercepts (>10). The high slopes indicate rapid reaction rates, as would be expected for these compounds, and the low vertical intercepts indicate that reductions in these particular compounds initiated at the same time as reductions in the bulk organic parameters. On the other hand, the fastest reacting compounds, including triclosan, bisphenol A, and diclofenac, had lower slopes because their oxidation initiated quicker than that of the bulk organic matter, which translated into vertical shifts in the regressions. Finally, for nearly complete oxidation

of the Group 1 compounds, utilities should target >30% and >70% reductions in UV<sub>254</sub> absorbance and TF.

As mentioned previously, the Group 2 compounds were quite different from the other compounds, thereby warranting their own group, but the reaction rates for the constituent compounds (gemfibrozil and atenolol) also differed by an order of magnitude. This was apparent in the different regression properties, but the models still indicated fast reaction rates by either a high slope or vertical intercept. Furthermore, fewer data points were excluded from the Group 2 analysis because of the greater resistance of these compounds to oxidation. Reduced reactivity made regression analyses for both UV<sub>254</sub> absorbance and TF possible.

For the Group 3 compounds, the UV<sub>254</sub> absorbance models consistently had slopes <1.7 and vertical intercepts <10. This indicates that contaminant oxidation initiated at the same time as the changes in UV<sub>254</sub> absorbance but at a much faster rate. For the TF models, the slopes were generally <1.1, whereas the vertical intercepts were consistently negative. Therefore, the Group 3 compounds experience a lag in oxidation in comparison to reductions in TF, but the changes then occur at approximately the same rate. For nearly complete removal of the Group 3 compounds, utilities would have to target >70% and >90% reductions in UV<sub>254</sub> absorbance and TF.

The Group 4 compounds demonstrated significant lags in oxidation compared to the bulk organic matter, as indicated by the negative vertical intercepts, and the fluorescence models were also characterized by slightly exponential trends. This is consistent with the group's high to moderate resistance to both ozone and •OH oxidation. For complete removal of the Group 4 compounds, utilities would have to target >70 to 90% and >90% reductions in UV<sub>254</sub> absorbance and TF.

As would be expected, TCEP was characterized by extremely small slopes and negative intercepts, which indicate that TCEP oxidation initiates much later and at a much slower rate than changes in the bulk organic matter. It is important to note that musk ketone would also be included in Group 5, but its volatility made it extremely unstable during the bench-scale experiments. Therefore, it was not possible to generate valid data and correlations for musk ketone, so it was omitted from the study. It was not possible to achieve 100% removal of the Group 5 compounds with practical dosing conditions.

In contrast to the target compounds, the microbial correlations are based on log inactivation rather than percent reductions in concentrations:

$$-Log\left(\frac{N}{N_0}\right) = Slope * \left[\left(1 - \frac{UV \text{ or } TF}{UV_0 \text{ or } TF_0}\right) * 100(\%)\right] + Intercept$$

Therefore, the slopes and intercepts cannot be compared directly to those of the target compounds. It is interesting to note that the inactivation of both *E. coli* and MS2 was quite comparable, but MS2 demonstrated stronger correlations than *E. coli*. For CDPH Title 22 compliance, 6.5-log inactivation of MS2 corresponds to 46% and 59% reductions in UV<sub>254</sub> absorbance and TF. As shown in the reaction time CCWRD data (see Table 3.15), the *Bacillus* spores required extended exposure to dissolved ozone before any inactivation was observed. Therefore, it was not possible to accurately correlate *Bacillus* inactivation with changes in the bulk organic matter. In fact, nearly 50% and 90% reductions in UV<sub>254</sub> absorbance and TF were required before any inactivation was observed. Inactivation was very rapid after that threshold was achieved.

Appendices 5 and 6 illustrate the correlation models for the bench-scale UV/H<sub>2</sub>O<sub>2</sub> experiments. In order to identify any differences in the data sets, Appendix 5 differentiates the various wastewater matrices, whereas Appendix 6 differentiates the two H<sub>2</sub>O<sub>2</sub> doses. Similar to the ozone correlation models, the different experimental conditions had little effect on the relationship between contaminant oxidation and changes in the bulk organic matter. Therefore, all of the data for each compound was combined into a single data set prior to developing the UV/H<sub>2</sub>O<sub>2</sub> regression equations. The resulting models are summarized in

Table 4.4. The UV<sub>254</sub> and fluorescence intercepts were generally insignificant, so the relative oxidation rates for the target compounds can be described almost entirely by their respective slopes. Exceptions to this observation include the compounds that were susceptible to photolysis alone, including triclosan, diclofenac, sulfamethoxazole, and phenytoin. Inactivation of MS2, *E. coli*, and *Bacillus* spores was extremely rapid during the UV/H<sub>2</sub>O<sub>2</sub> experiments. Because nearly complete inactivation was achieved with low UV doses, it was not possible to develop correlations with the bulk organic parameters. In other words, the three microbes reached their limits of inactivation prior to any significant change in UV<sub>254</sub> absorbance or TF.

**Table 4.4. Summary of Regression Parameters for UV/H<sub>2</sub>O<sub>2</sub> Correlations**

Contaminant	N	UV <sub>254</sub> Absorbance			Total Fluorescence		
		Slope	Intercept	R <sup>2</sup>	Slope	Intercept	R <sup>2</sup>
Atenolol	23	2.19	0	0.76	1.25	1	0.68
Atrazine	23	2.26	2	0.61	1.50	0	0.74
Bisphenol A	23	3.35	-6	0.80	2.07	-7	0.81
Carbamazepine	23	2.59	-2	0.68	1.68	-3	0.77
DEET	23	1.84	-2	0.64	1.35	-5	0.92
Diclofenac	13	6.70	16	0.62	4.98	18	0.51
Gemfibrozil	23	2.26	0	0.62	1.54	-3	0.77
Ibuprofen	23	2.41	-1	0.70	1.64	-4	0.88
Meprobamate	23	1.15	0	0.56	0.81	-1	0.73
Naproxen	23	3.02	1	0.70	1.96	-1	0.81
pCBA	23	2.23	0	0.73	1.42	-1	0.83
Phenytoin	23	3.68	8	0.80	2.03	12	0.74
Primidone	23	1.70	-1	0.48	1.21	-4	0.62
Sulfamethoxazole	23	3.97	7	0.68	2.25	11	0.63
TCEP	23	0.85	-3	0.21	0.65	-5	0.31
Triclosan	13	6.21	10	0.65	4.74	10	0.53
Trimethoprim	23	2.22	-2	0.71	1.45	-4	0.81

*Notes:* Contaminant reduction and organic surrogate reduction reported as percent instead of decimal; DEET=*N,N*-diethyl-*meta*-toluamide; pCBA=*para*-chlorobenzoic acid; TCEP=*tris*-(2-chloroethyl)-phosphate

**Table 4.5. Summary of Regression Parameters for Ozone Correlations**

Contaminant	N	UV <sub>254</sub> Absorbance			Total Fluorescence		
		Slope	Intercept	R <sup>2</sup>	Slope	Intercept	R <sup>2</sup>
<b>Group 1 (% Contaminant Reduction vs. % Organic Surrogate Reduction)</b>							
Bisphenol A	21		N/A		1.36	20	0.63
Carbamazepine	21		N/A		1.75	-4	0.58
Diclofenac	21		N/A		1.51	10	0.60
Naproxen	21		N/A		1.77	-5	0.60
Sulfamethoxazole	21		N/A		1.69	-7	0.57
Triclosan	21		N/A		1.02	40	0.63
Trimethoprim	21		N/A		1.63	3	0.55
<b>Indicator</b>	<b>147</b>		<b>N/A</b>		<b>1.53</b>	<b>8</b>	<b>0.53</b>
<i>~100% Removal</i>			<i>&gt;30%</i>			<i>&gt;70%</i>	
<b>Group 2 (% Contaminant Reduction vs. % Organic Surrogate Reduction)</b>							
Atenolol	42	2.34	-2	0.77	1.49	-30	0.82
Gemfibrozil	42	1.72	34	0.56	1.23	5	0.75
<b>Indicator</b>	<b>84</b>	<b>2.03</b>	<b>16</b>	<b>0.57</b>	<b>1.36</b>	<b>-13</b>	<b>0.67</b>
<i>~100% Removal</i>			<i>&gt;50%</i>			<i>&gt;90%</i>	
<b>Group 3 (% Contaminant Reduction vs. % Organic Surrogate Reduction)</b>							
DEET	42	1.53	0	0.63	1.02	-22	0.75
Ibuprofen	42	1.56	7	0.59	1.10	-18	0.76
pCBA	42	1.31	3	0.48	0.86	-15	0.54
Phenytoin	42	1.68	3	0.56	1.13	-22	0.67
Primidone	42	1.44	4	0.61	0.98	-17	0.73
<b>Indicator</b>	<b>210</b>	<b>1.50</b>	<b>3</b>	<b>0.54</b>	<b>1.02</b>	<b>-19</b>	<b>0.65</b>
<i>~100% Removal</i>			<i>&gt;70%</i>			<i>&gt;90%</i>	
<b>Group 4 (% Contaminant Reduction vs. % Organic Surrogate Reduction)</b>							
1,4-dioxane	39	1.57	-18	0.69	1.29	-57	0.70
Atrazine	84	1.79	-19	0.72	1.42	-59	0.77
Meprobamate	84	1.87	-15	0.73	1.50	-57	0.80
<b>Indicator</b>	<b>207</b>	<b>1.78</b>	<b>-17</b>	<b>0.69</b>	<b>1.42</b>	<b>-57</b>	<b>0.74</b>
<i>~100% Removal</i>			<i>&gt;70-90%</i>			<i>&gt;90%</i>	
<b>Group 5 (% Contaminant Reduction vs. % Organic Surrogate Reduction)</b>							
TCEP	84	0.52	-7	0.45	0.43	-19	0.53
<i>~100% Removal</i>			<i>N/A</i>			<i>N/A</i>	
<b>Microbial Inactivation (Log Inactivation vs. % Organic Surrogate Reduction)</b>							
<i>Bacillus</i> spores	14	N/A	N/A				
<i>E. coli</i>	83	0.13	-1.1	0.50	0.10	-3.5	0.47
MS2	83	0.14	0.0	0.69	0.11	-3.1	0.76

Notes: Contaminant reduction and organic surrogate reduction reported as percent instead of decimal; DEET=*N,N*-diethyl-*meta*-toluamide; pCBA=*para*-chlorobenzoic acid; TCEP=tris-(2-chloroethyl)-phosphate

In addition to estimating reductions in target compounds, the aforementioned correlations can also be used to estimate overall •OH exposure during ozonation or UV/H<sub>2</sub>O<sub>2</sub> processes. The first equation represents the linear correlation model developed during this study for differential UV<sub>254</sub> absorbance or TF, and the second equation illustrates the process for calculating overall •OH exposure based on changes in pCBA concentration. By combining these equations and the pCBA correlation models described previously, the various •OH exposure models in Table 4.6 can be derived. Therefore, instead of spiking and analyzing for changes in pCBA concentration, which requires access to expensive instrumentation and analytical expertise, one can rely on changes in UV<sub>254</sub> absorbance or TF to estimate overall •OH exposure.

$$\left(1 - \frac{[pCBA]}{[pCBA]_0}\right) * 100(\%) = Slope * \left(1 - \frac{UV \text{ or } TF}{UV_0 \text{ or } TF_0}\right) * 100(\%) + Intercept$$

$$\int (\bullet OH) dt = \frac{\ln\left(\frac{[pCBA]}{[pCBA]_0}\right)}{-5 \times 10^9 \text{ M}^{-1} \text{ s}^{-1}}$$

(•OH exposure is reported as M-s)

**Table 4.6. Summary of pCBA Surrogate Model**

Process	UV <sub>254</sub> Absorbance	Total Fluorescence
Ozone or Ozone/H <sub>2</sub> O <sub>2</sub>	$\int (\bullet OH) dt = \frac{\ln\left(-0.0131 * \left[1 - \frac{UV}{UV_0}\right] * 100(\%) + 0.97\right)}{-5 \times 10^9}$	$\int (\bullet OH) dt = \frac{\ln\left(-0.0086 * \left[1 - \frac{TF}{TF_0}\right] * 100(\%) + 1.15\right)}{-5 \times 10^9}$
UV/H <sub>2</sub> O <sub>2</sub>	$\int (\bullet OH) dt = \frac{\ln\left(-0.0223 * \left[1 - \frac{UV}{UV_0}\right] * 100(\%) + 1.00\right)}{-5 \times 10^9}$	$\int (\bullet OH) dt = \frac{\ln\left(-0.0142 * \left[1 - \frac{TF}{TF_0}\right] * 100(\%) + 1.01\right)}{-5 \times 10^9}$

Note: •OH exposure is calculated with units of M-s.

DEET=*N,N*-diethyl-*meta*-toluamide; pCBA=*para*-chlorobenzoic acid; TCEP=tris-(2-chloroethyl)-phosphate

This method for calculating •OH exposures can then be used to estimate the elimination of recalcitrant TOrCs (i.e., contribution from ozone assumed to be negligible) based on kinetics, particularly for compounds that do not have established correlation models. For example, a 35% reduction in UV<sub>254</sub> absorbance during ozonation of secondary effluent corresponds to an •OH exposure of 1.34x10<sup>-10</sup> M-s based on the aforementioned pCBA model.

$$\Delta UV_{254}=35\%: \int [\bullet OH] dt \text{ (M-s)} = \frac{\ln(-0.0131 * 35 + 0.97)}{-5 \times 10^9} = 1.34 \times 10^{-10} \text{ M-s}$$

The corresponding elimination of meprobamate can be estimated directly from its  $UV_{254}$  absorbance correlation (50%; see Table 3.5 for regression parameters):

$$\Delta UV_{254}=35\%: \left(1 - \frac{[C]}{[C]_0}\right) * 100(\%) = 1.87 * 35 - 15 = 50\%$$

The elimination of meprobamate can also be estimated from kinetics (42%) using a combination of the estimated  $\bullet OH$  exposure listed herein ( $1.34 \times 10^{-10}$  M-s) and its rate constant with  $\bullet OH$  ( $4.0 \times 10^9$   $M^{-1}s^{-1}$ ; see Table 3.4):

$$\ln(C/C_0) = -(k_{OH})(\int \bullet OH dt),$$

where the contribution from ozone is assumed to be negligible.

$$\ln(C/C_0) = -(4.0 \times 10^9 \text{ M}^{-1}\text{s}^{-1})(1.34 \times 10^{-10} \text{ M-s}) = -0.54$$

$$C/C_0 = \exp(-0.54)$$

$$1 - C/C_0 = 1 - \exp(-0.54) = 1 - 0.58 = 0.42 \rightarrow 42\%$$

#### 4.2.1 Relevance to November 2011 CDPH Regulations

CDPH published a revised set of draft regulations for direct injection after FAT (i.e., MF-RO-AOP) that outlines required removals for indicator compounds based on their chemical structures and functional groups (CDPH, 2011). For context, the RO process in every FAT facility in California must achieve specified TOC and sodium chloride rejection criteria, and the downstream AOP must demonstrate 0.5-log (Groups A-G) and 0.3-log (Groups H-I) removal of at least one indicator compound in each group. The groups are described as follows:

- (A) Hydroxy aromatic
- (B) Amino/acylamino aromatic
- (C) Nonaromatic with carbon double bonds
- (D) Deprotonated amine
- (E) Alkoxy polyaromatic
- (F) Alkoxy aromatic
- (G) Alkyl aromatic
- (H) Saturated aliphatic
- (I) Nitro aromatic

This classification system is shown in Table 4.7 in relation to the target compounds from this study. Musk ketone is the only nitro aromatic in the target compound list, but this compound was omitted from the study because of its high volatility and difficulty in achieving consistent spiking levels. However, musk ketone (Group I) and TCEP (Group H) are characterized by similar resistance to oxidation, so the regression parameters for these compounds would likely be similar. Therefore, TCEP was used as a surrogate for Group I compounds. As an alternative to this new framework, FAT facilities may demonstrate 0.5-log removal of 1,4-dioxane in accordance with the previous draft regulations.

In addition to the specified removals, CDPH also requires FAT facilities to identify at least one surrogate parameter that can be monitored continuously, predict the level of oxidation for the indicator compounds, and alert operators to process inefficiencies and failures. The proposed correlation framework and the results from this study would appear to be directly applicable to these new regulations; however, the CDPH requirements apply only to advanced oxidation in FAT applications (i.e., RO permeate), whereas this study is based on secondary and tertiary wastewater effluents.

Because the UV<sub>254</sub> absorbance and TF of RO permeates are low (see Table 3.35 and Figure 3.57), the correlations from WRF-09-10 are likely inapplicable to FAT applications. It may be possible to demonstrate the specified TO<sub>r</sub>C removals upstream of RO, in which case the WRF-09-10 correlations would apply, but this alternative would have to be approved by CDPH. For example, WBMWD is planning to incorporate ozone upstream of MF to reduce organic fouling on its membranes. Although the primary objective of this upgrade is improved energy efficiency and increased capacity, the ozonation process will also achieve significant TO<sub>r</sub>C reductions and microbial inactivation, thereby providing an opportunity to demonstrate the specified removals and integrate the WRF-09-10 correlations. Regardless of whether the CDPH requirements actually apply, the framework can still be applied more broadly as a TO<sub>r</sub>C mitigation baseline because treatment criteria are limited or nonexistent in many regions.

**Table 4.7. Classification of Target Compounds in Relation to CDPH Requirements**

Compound	WRF-09-10 Group	CDPH <sup>1</sup> G rroup	Required Removal	UV <sub>254</sub> Reduction	TF Reduction
Bisphenol A	1	A	0.5 log (69%)	N/A <sup>3</sup>	>36%
Carbamazepine	1	C	0.5 log (69%)	N/A <sup>3</sup>	>42%
Diclofenac	1	D	0.5 log (69%)	N/A <sup>3</sup>	>39%
Naproxen	1	E	0.5 log (69%)	N/A <sup>3</sup>	>42%
Sulfamethoxazole	1	B	0.5 log (69%)	N/A <sup>3</sup>	>45%
Triclosan	1	A	0.5 log (69%)	N/A <sup>3</sup>	>28%
Trimethoprim	1	D	0.5 log (69%)	N/A <sup>3</sup>	>40%
Atenolol	2	D	0.5 log (69%)	>30%	>66%
Gemfibrozil	2	F	0.5 log (69%)	>20%	>52%
DEET	3	G	0.5 log (69%)	>45%	>89%
Ibuprofen	3	G	0.5 log (69%)	>40%	>79%
pCBA	3	G	0.5 log (69%)	>50%	>98%
Phenytoin	3	G	0.5 log (69%)	>39%	>81%
Primidone	3	G	0.5 log (69%)	>45%	>88%
1,4-dioxane	4	Alt <sup>2</sup>	0.5 log (69%)	>55%	>98%
Atrazine	4	D	0.5 log (69%)	>49%	>90%
Meprobamate	4	H	0.3 log (50%)	>35%	>71%
Musk ketone	5	I	0.3 log (50%)	--	--
TCEP	5	H	0.3 log (50%)	N/A <sup>4</sup>	N/A <sup>4</sup>

Notes: 1=CDPH, 2011: Groups A–G require 0.5-log removal, and Groups H–I require 0.3-log removal; 2=alternative to revised framework; 3=slope was too steep to develop and accurate correlation (conservative estimate: >30%); 4=required percent reduction could not be determined (exceeds 100%); DEET=*N,N*-diethyl-*meta*-toluamide; pCBA=*para*-chlorobenzoic acid; TCEP=*tris*-(2-chloroethyl)-phosphate

Table 3.7 also specifies the percent reductions in UV<sub>254</sub> absorbance and TF that would need to be demonstrated to satisfy the CDPH treatment objectives. The surrogate models from WRF-09-10 proved to be useful for a majority of the contaminants, although TCEP (and

presumably musk ketone) required reductions greater than 100% to achieve the 0.3-log benchmark. The 0.3-log requirement for TCEP and musk ketone could be achieved with high ozone doses, but this dosing condition would exceed the capabilities of the UV<sub>254</sub> absorbance and TF surrogates. As an alternative, indicator compounds from Groups H and I with higher reactivity with ozone and •OH could be selected to satisfy the CDPH requirements. The 6.5-log inactivation requirement for disinfection for MS2 would require 46% and 91% reductions in UV<sub>254</sub> absorbance and TFTF.

### 4.3 Mechanistic Organic Correlations

Similar to the empirical correlations, the mechanistic correlations were developed by treating all data from the study sites as a single data set. In other words, the various ozone dosing conditions, the H<sub>2</sub>O<sub>2</sub> dosing conditions, and the filtered versus unfiltered samples for the five secondary effluents were all grouped into a single data set when developing the regression models. In order to validate this assumption, the various experimental conditions are still differentiated by symbol in the figures.

For the following discussion, relative changes in TOxC concentrations, UV<sub>254</sub> absorbance, and TF are denoted as  $\Delta C/C_0$ ,  $\Delta A/A_0$  and  $\Delta F/F_0$ , respectively. To explore the nature of the observed  $\Delta C/C_0$  vs.  $\Delta A/A_0$  and  $\Delta C/C_0$  vs.  $\Delta F/F_0$  relationships, models were developed based on kinetic laws, as described in the literature (Nanaboina and Korshin, 2010; Liu et al., 2012). The approach utilized in this study assumes that EfOM is composed of at least two kinetically and spectroscopically distinct functionalities (denoted S<sub>1</sub> and S<sub>2</sub>). These moieties undergo degradation by both •OH and ozone. In terms of formal kinetics, the removal of these moieties can be described by the following equations:

$$\frac{d[S_1]}{dt} = -(k_{S_1}^{OH} [OH\cdot] + k_{S_1}^{O_3} [O_3])[S_1]$$

$$\frac{d[S_2]}{dt} = -(k_{S_2}^{OH} [OH\cdot] + k_{S_2}^{O_3} [O_3])[S_2]$$

The oxidation of a target TOxC (denoted as C) takes place simultaneously with the oxidation of EfOM substrates S<sub>1</sub> and S<sub>2</sub>, and the process can likewise be described as follows:

$$\frac{d[C]}{dt} = -(k_C^{OH} [OH\cdot] + k_C^{O_3} [O_3])[C]$$

The major goal of the approach is to relate AOP-induced changes in the concentration of C with those of S<sub>1</sub> and S<sub>2</sub>, which approximate the behavior of EfOM chromophores and fluorophores. Detailed mathematics associated with the derivation of pertinent mathematical expressions have been presented elsewhere (Nanaboina and Korshin, 2010; Liu et al., 2012). Briefly, the modeling of  $\Delta C/C_0$  vs.  $\Delta A/A_0$  and  $\Delta C/C_0$  vs.  $\Delta F/F_0$  requires simultaneous numerical integration of the following expressions, which are derived from the previous equations:

$$\varepsilon_1 [S_1^0] \left( \frac{[S_2]}{[S_2^0]} \right)^{r_{S_1/S_2}} + \varepsilon_2 [S_2] = A - A_F$$

$$\int_{C_0}^C d[\ln C] = \int_{A_0}^A \frac{r_{C/S_2} dA}{\left( \varepsilon_1 r_{S_1/S_2} [S_1^0] \left( \frac{[S_2]}{[S_2^0]} \right)^{r_{S_1/S_2}} + \varepsilon_2 [S_2] \right)}$$

$$\phi_1 [S_1^0] \left( \frac{[S_2]}{[S_2^0]} \right)^{r_{S_1/S_2}} + \phi_2 [S_2] = F - F_F$$

$$\int_{C_0}^C d[\ln C] = \int_{A_0}^A \frac{r_{C/S_2} dF}{\left( \phi_1 r_{S_1/S_2} [S_1^0] \left( \frac{[S_2]}{[S_2^0]} \right)^{r_{S_1/S_2}} + \phi_2 [S_2] \right)}$$

In these expressions, A and F correspond to the absorbance (e.g., at 254 nm) and TF of the treated secondary effluent,  $\varepsilon_1$  and  $\varepsilon_2$  are molar extinction coefficients of chromophores  $S_1$  and  $S_2$ , and  $\phi_1$  and  $\phi_2$  correspond to the emissivity of EfOM fluorophores associated with substrates  $S_1$  and  $S_2$ .  $A_F$  and  $F_F$  correspond to the absorbance of chromophores and emission of fluorophores that are not degraded by the oxidation processes. The notation  $r_{C/S_2}$  corresponds to the dimensionless ratio of the apparent rates of oxidation of compound C divided by that of the less reactive EfOM substrate  $S_2$ . The notation  $r_{S_1/S_2}$  is the dimensionless ratio of the apparent oxidation rates of the rapidly reacting substrate  $S_1$  divided by that of substrate  $S_2$ .

This derivation implies that the functional shape of any correlation between the degradation of target trace-level contaminants and changes in absorbance or fluorescence are defined by factors intrinsic to that contaminant and its matrix. These factors include the molar absorptivities and concentrations of substrates  $S_1$  and  $S_2$ , the fraction of absorbance and fluorescence of unreactive EfOM chromophores and fluorophores ( $A_F$  and  $F_F$ ), and ratios of reaction rates between  $\bullet\text{OH}$  and the substrates  $S_1$ ,  $S_2$ , and C. The values of  $A_F$  and  $F_F$  can be established experimentally, and other system parameters (e.g.,  $\varepsilon_1 [S_1]_0$ ,  $\varepsilon_2 [S_2]_0$ ,  $r_{S_1/S_2}$ , and  $r_{C/S_2}$ ) can be determined based on fitting of experimentally generated  $\Delta C/C_0$  vs.  $\Delta A/A_0$  relationships.

The same  $r_{S_1/S_2}$  ratio was used to fit the  $C/C_0$  vs.  $\Delta A/A_0$  and  $\Delta C/C_0$  vs.  $\Delta F/F_0$  relationships for all observed species and wastewaters. Because there were differences in the EfOM properties of the five secondary effluents, this can be considered an oversimplification, but this assumption allows for the development of a general model that is applicable to practically any AOP-treated wastewater. Likewise, the values of  $\varepsilon_1 [S_1]_0$ ,  $\varepsilon_2 [S_2]_0$  and  $A_F$ , which were used in the modeling of  $\Delta C/C_0$  vs.  $\Delta A/A_0$ , and those of  $\phi_1$ ,  $\phi_2$  and  $F_F$ , which were used in the modeling of  $\Delta C/C_0$  vs.  $\Delta F/F_0$ , were assumed to be the same for the entire data set. The ratio  $r_{C/S_2}$ , which characterized the relative reactivity of any TOxC compared to that of

the slowly reacting EfOM moiety  $S_2$ , was the same in the modeling of  $\Delta C/C_0$  vs.  $\Delta A/A_0$  and  $\Delta C/C_0$  vs.  $\Delta F/F_0$ .

The previous assumptions yield a series of global fits for the entire data set irrespective of the site specificity of the matrices; however, this approach does not negate the effects of site-specific EfOM composition but rather allows for examination of the data set in its entirety. These assumptions were employed in the previous numerical integrations and subsequently used to develop correlation models for the target compounds with widely different chemical structures and reactivities. The following parameters were used in these global fits:

- $r_{S_1/S_2} = 15$
- $\varepsilon_1[S_1]_0 = 0.010$
- $\varepsilon_2[S_2]_0 = 0.015$
- $A_F = 0.01$
- $\phi_1 = 1.0$
- $\phi_2 = 9.0$
- $F_F = 0.08$

The value of  $r_{S_1/S_2}$  utilized for the global fit in this study is lower than the value previously published in the literature, which only included data for a single wastewater (Nanaboina and Korshin, 2010). This is expected, however, because the current study included matrices with kinetically different EfOM compositions. Despite the anticipated diversity of these substrates, the resulting models demonstrate that the concept of monitoring changes in bulk organic parameters as a surrogate for process efficacy is robust and applicable to diverse matrices and contaminants.

The mechanistic models developed for the target contaminants are provided in Appendix 9. The modeling approach yielded reasonably precise  $r_{C/S_2}$  values for nearly all of the target contaminants, excluding musk ketone (omitted from the study). The lowest  $r_{C/S_2}$  value was associated with TCEP ( $r_{C/S_2} = 0.4$ ), which indicates that the apparent degradation rate for TCEP was approximately 2.5 times slower than that of the average EfOM substrate  $S_2$ . On the other hand, the degradation of more reactive TOrCs, such as bisphenol A, carbamazepine, diclofenac, naproxen, sulfamethoxazole, triclosan, and trimethoprim, occurred at very low ozone doses, which were associated with low  $\Delta A/A_0$  and  $\Delta F/F_0$  values. Accordingly, the  $r_{C/S_2}$  values for these contaminants ranged from 24 to 42. Given that the  $r_{S_1/S_2}$  ratio was 15 in all cases, this demonstrates that these compounds were degraded faster than the most reactive moiety of EfOM. By comparing the  $\Delta C/C_0$  vs.  $\Delta A/A_0$  and  $\Delta C/C_0$  vs.  $\Delta F/F_0$  relationships for the various TOrCs, it is apparent that the effect of  $H_2O_2$  addition was minimal in nearly all cases. As mentioned earlier,  $H_2O_2$  addition provided a slightly higher level of oxidation for the more recalcitrant compounds, including TCEP, atrazine, meprobamate, and 1,4-dioxane. All of these species have low  $r_{C/S_2}$  values ranging from 0.4 for TCEP to 2.5 for meprobamate. The  $r_{C/S_2}$  values are summarized in Table 4.8, and their correlations with the corresponding TOrC's ozone and  $\bullet OH$  rate constants are illustrated in Figure 4.24.

Finally, the quality of the model fit was generally similar for the  $\Delta C/C_0$  vs.  $\Delta A/A_0$  and  $\Delta C/C_0$  versus  $\Delta F/F_0$  relationships, but the fluorescence data yielded a slightly stronger correlation for certain TOxCs, including atrazine, DEET, 1,4-dioxane, and meprobamate.

On the basis of the empirical and mechanistic correlations in this study, it is clear that changes in bulk organic parameters, specifically  $UV_{254}$  absorbance and TF, can be used as a surrogate measure of treatment efficacy during advanced oxidation. Using either approach, one can develop relatively accurate predictors of TOxC oxidation with simple laboratory measurements or even online instruments. This concept is further validated in the following sections based on independent data from the literature and online  $UV_{254}$  measurements in a pilot-scale treatment train. Because the linear (empirical) regression models are easier to implement in a full-scale application, the final sections focus on these correlations.

**Table 4.8. Dimensionless  $r_{C/S_2}$  Ratios for the Mechanistic Modeling Approach**

Contaminant	$r_{C/S_2}$	$k_{O_3}$ ( $M^{-1}s^{-1}$ )	$k_{OH}$ ( $M^{-1}s^{-1}$ )
<b>Group 1</b>			
Bisphenol A	38	$7 \times 10^5$	$1 \times 10^{10}$
Carbamazepine	29	$3 \times 10^5$	$9 \times 10^9$
Diclofenac	33	$1 \times 10^6$	$8 \times 10^9$
Naproxen	23	$2 \times 10^5$	$1 \times 10^{10}$
Sulfamethoxazole	24	$3 \times 10^6$	$6 \times 10^9$
Triclosan	42	$4 \times 10^7$	$1 \times 10^{10}$
Trimethoprim	28	$3 \times 10^5$	$7 \times 10^9$
<b>Indicator</b>	<b>31</b>	<b><math>6.5 \times 10^6</math></b>	<b><math>9 \times 10^9</math></b>
<b>Group 2</b>			
Atenolol	9.5	$2 \times 10^3$	$8 \times 10^9$
Gemfibrozil	18	$2 \times 10^4$	$1 \times 10^{10}$
<b>Indicator</b>	<b>13.8</b>	<b><math>1.1 \times 10^4</math></b>	<b><math>9 \times 10^9</math></b>
<b>Group 3</b>			
DEET	4.5	<10	$5 \times 10^9$
Ibuprofen	6.5	10	$7 \times 10^9$
pCBA	3.5	<0.15	$5 \times 10^9$
Phenytoin	5.0	<10	$6 \times 10^9$
Primidone	5.0	<10	$7 \times 10^9$
<b>Indicator</b>	<b>4.9</b>	<b>&lt;10</b>	<b><math>6 \times 10^9</math></b>
<b>Group 4</b>			
1,4-dioxane	1.4	0.32	$2 \times 10^9$
Atrazine	2.2	6	$3 \times 10^9$
Meprobamate	2.5	<1	$4 \times 10^9$
<b>Indicator</b>	<b>2.0</b>	<b>&lt;10</b>	<b><math>3 \times 10^9</math></b>
<b>Group 5</b>			
TCEP	0.4	<1	$7 \times 10^8$
<b>Surrogate Microbes</b>			
<i>Bacillus</i> spores	0.2	N/A	N/A
<i>E. coli</i>	2	N/A	N/A
MS2	4	N/A	N/A

Notes: DEET=*N,N*-diethyl-*meta*-toluamide; pCBA=*para*-chlorobenzoic acid; TCEP=*tris*-(2-chloroethyl)-phosphate

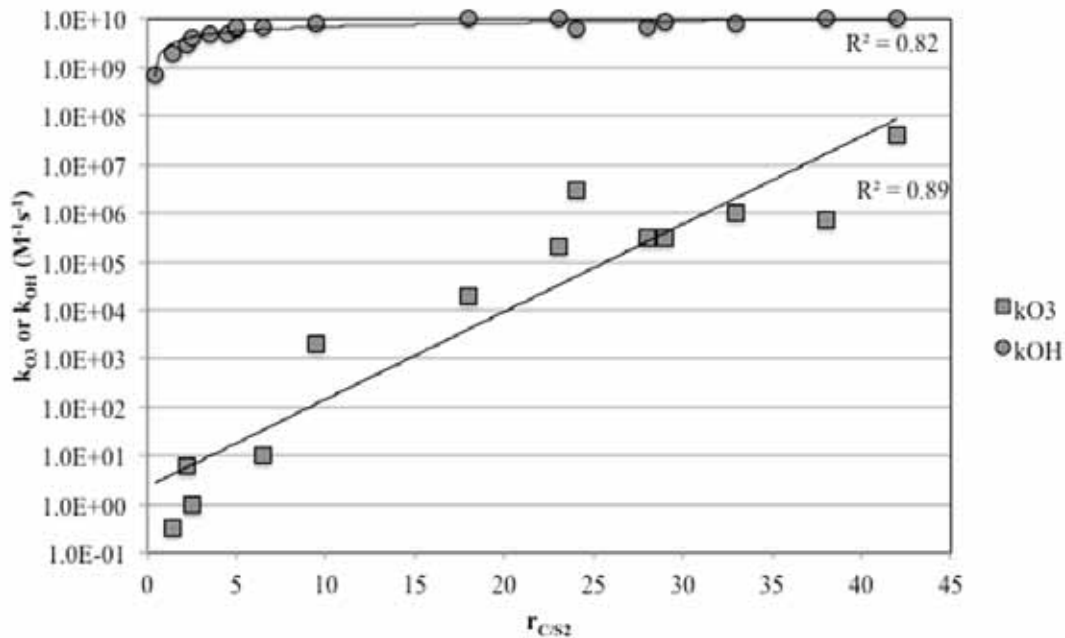


Figure 4.24. Correlation between experimental  $r_{C/S2}$  values and ozone rate constants.

#### 4.4 Future Research

Our experimental data show that the introduction of  $H_2O_2$  in the system did not result in major effects but it did cause a slight decrease in the removal of absorbance and fluorescence of EfOM. This appears to indicate that degradation of EfOM in  $O_3/H_2O_2$  system could primarily be due to ozone. Though the changes induced by the presence of  $H_2O_2$  are relatively minor, we speculate that the decrease of the effective ozone concentrations caused by  $H_2O_2$  could be of major importance. This shows that the oxidation of EfOM chromophores is caused by both  $O_3$  and OH radicals, with possibly higher relative contribution from  $O_3$ . However, the separation of the contributions of these oxidants was not possible using solely the absorbance and fluorescence data reported in this report, and this needs to be done in independent experiments with varying level of well-characterized OH radical probes and scavengers (e.g., pCBA, tert-butanol).

3D EEM data also show Group I and Group III fluorophores to be more sensitive to treatment. As pointed out in the results and discussion section, Group III can further be divided into two categories in terms of the sensitivity of its subfractions to AOP oxidation. This is a somewhat unexpected result, and the chemical identity of these subregions and their practical significance needs to be ascertained through more research.

Our HPSEC data discussed in the context of this report only for the observation wavelength of 254 nm show that AOP effects of EfOM fractions with varying molecular weights are largely nonspecific. This point needs to be explored in more detail using HPSEC data for varying wavelengths as well as HPSEC detectors other than absorbance (e.g., online DOC and fluorescence). By using a HPSEC fluorescence detector, we are likely to be more capable of understanding the apparent molecular weight distribution for the various groups observed in the fluorescence spectra.

Although the data of this study demonstrate the similarity of AOP effects on the absorbance and fluorescence of all studied wastewaters, more research is needed to ascertain effects of their site-specificity in more detail. This may be important for practical applications of the online monitoring options examined in this study. It is also necessary to examine in detail changes of EfOM absorbance and/or fluorescence, as well as the degradation of EDC/PPCPs and pathogenic microorganisms. This issue goes beyond the scope of this report, but it is vitally important for practical implementation of the online monitoring of AOP of wastewater based on changes of its spectroscopic properties.



## Chapter 5

# Pilot-Scale Evaluation of Oxidation Technologies for Water Reclamation

---

The pilot-scale portion of the report is divided into three main sections: (1) a detailed summary of the City of Reno pilot, which was composed of ozone and BAC; (2) validation of the bench-scale correlation models with independent pilot-scale data from this study and the literature; and (3) online monitoring of UV absorbance to demonstrate the applicability of this concept in an actual water reuse application. The Reno pilot provides a general overview of an alternative advanced water treatment train for IPR, but some of the data from the pilot were also used to validate the models.

### 5.1 Reno-Stead Water Reclamation Facility Pilot System

In an effort to establish water quality criteria for aquifer injection of reclaimed water, Reno and the Nevada Department of Environmental Protection conducted extensive pilot testing of UF, ozone/H<sub>2</sub>O<sub>2</sub> (HiPOx), and BAC at the RSWRF. The gold standard treatment train for IPR is generally considered to be membrane filtration (MF or UF), RO, UV/H<sub>2</sub>O<sub>2</sub>, and aquifer injection. The goal of the RSWRF pilot system was to generate a data set to validate membrane filtration, ozone-based oxidation, BAC, and aquifer injection as a viable alternative to the gold standard, particularly for inland applications where brine disposal is an issue. This type of treatment train has already demonstrated promise in pilot- and full-scale installations in Europe and Australia, as discussed previously.

The evaluation of the IPR treatment train included extensive monitoring of TOxCs, DBPs, transformation products, microbial indicators, and microbial characterization in the BAC column. The pilot study, which was performed by Reno, ECO:LOGIC Engineering (now Stantec; Rocklin, CA), and the Southern Nevada Water Authority, included approximately 20 months of continuous operation and was separated into two phases. The first phase (September 2008 to December 2009) evaluated full-scale secondary treatment, pilot-scale UF (WesTech Engineering, Salt Lake City, UT), pilot-scale ozone/H<sub>2</sub>O<sub>2</sub> (HiPOx, APTwater, Pleasant Hill, CA), and pilot-scale BAC (WesTech Engineering). The second phase (January to May 2010) evaluated full-scale secondary treatment, full-scale sand filtration, pilot-scale ozone/H<sub>2</sub>O<sub>2</sub>, and pilot-scale BAC. One of the objectives of the different phases was to determine whether UF provided significant improvements to the downstream ozone (i.e., increased contaminant destruction and disinfection) and BAC (i.e., reductions in backwash frequency) processes.

Secondary effluent (SRT of 25 days) from the RSWRF was fed into the 40 L/min (10.7 gpm) pilot-scale treatment train (Figure 5.1). During both phases, ozone was dosed at an O<sub>3</sub>:TOC ratio of approximately 0.8 to 1.0 (5 mg/L), and H<sub>2</sub>O<sub>2</sub> was added at a molar ratio of 1.0 (3.5 mg/L). The H<sub>2</sub>O<sub>2</sub> was added immediately prior to the ozone, and both were added via direct injection through single injection ports. The dosing conditions were selected based on preliminary testing of TOxC oxidation and bromate mitigation (<5 µg/L) during Phase 1. The BAC column was 1 m in diameter and contained approximately 570 kg of Filtrasorb F-400 carbon (Calgon Carbon, Pittsburgh, PA) at a bed depth of 1.4 m. The BAC was operated with an EBCT of 30 minutes. During the UF phase (Phase 1), BAC backwashing was performed

once every 14 days, but because of the higher solids loading during the sand filtration phase (Phase 2), backwashing frequency was increased to once every 7 days. The full-scale DynaSand (Parkson Corporation, Fort Lauderdale, FL) media filters were operated in an upflow configuration with continuous backwash and air scour. The conical cells are approximately 2 m in diameter, with an average bed depth of 3 m. The filters are operated with an average daily loading rate of 1.6 gpm/ft<sup>2</sup> and a peak loading rate of 2.5 gpm/ft<sup>2</sup>.

Each phase of the project consisted of three separate sampling events to evaluate the consistency in operational performance. For Phase 1, samples were collected in August, November, and December of 2009, and for Phase 2, samples were collected in February, April, and May of 2010. The operational period from September 2008 to August 2009 was used to identify the optimal ozone and H<sub>2</sub>O<sub>2</sub> doses and establish a stable microbial community in the BAC column.

In contrast to the previous bench-scale experiments, this part of the project targeted a slightly different set of TOxCs. The more sensitive analytical methods allowed for lower MRLs and quantification of additional compounds, including steroid hormones. The samples were processed with SPE and analyzed with LC-MS/MS with isotope dilution according to previously published methods (Vanderford et al., 2003; Trenholm et al., 2006; Vanderford and Snyder, 2006). Reporting limits for the target compounds ranged from 0.25 to 2000 ng/L. The TOxC analyses were supplemented with organic characterization, quantification of total estrogenicity, and the inactivation and removal of surrogate microbes.

In addition to the samples described earlier, UF (TOC=4.9 mg/L) and sand effluent (TOC=5.6 mg/L) were also evaluated at bench-scale to develop ozone demand/decay curves and assess changes in UV<sub>254</sub> absorbance. It is important to note that H<sub>2</sub>O<sub>2</sub> was not applied because the primary objective of the bench-scale experiments was to characterize the demand of the wastewater, which would not have been possible after quenching the ozone residual with H<sub>2</sub>O<sub>2</sub>. Figure 5.2 illustrates the demand/decay curves for the two wastewater qualities at three O<sub>3</sub>:TOC ratios. As for decay rates, neither form of pretreatment had a significant effect on ozonation, which is supported by similar studies in the literature. Figure 5.3 illustrates the reduction in UV<sub>254</sub> absorbance during bench-scale ozonation. As shown earlier with the previous bench-scale experiments, reductions in UV<sub>254</sub> absorbance are relatively consistent after ozonation despite differences in wastewater quality and pretreatment.

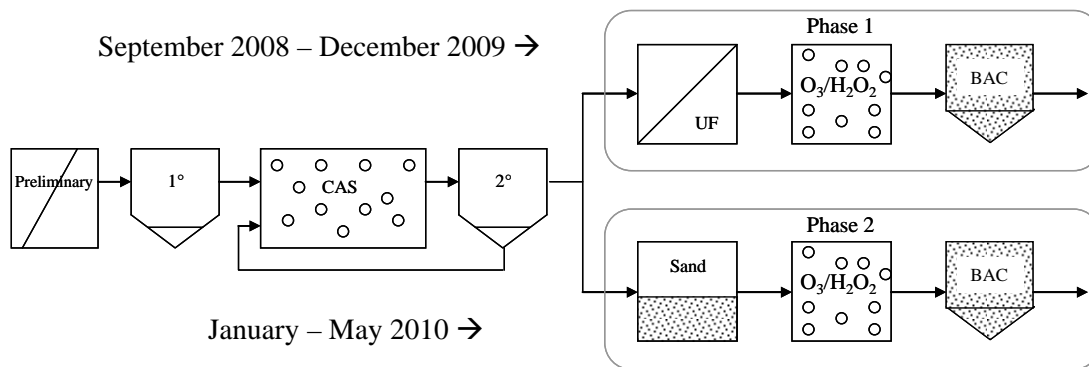


**Figure 5.1. Pilot-scale treatment trains at RSWRF.**

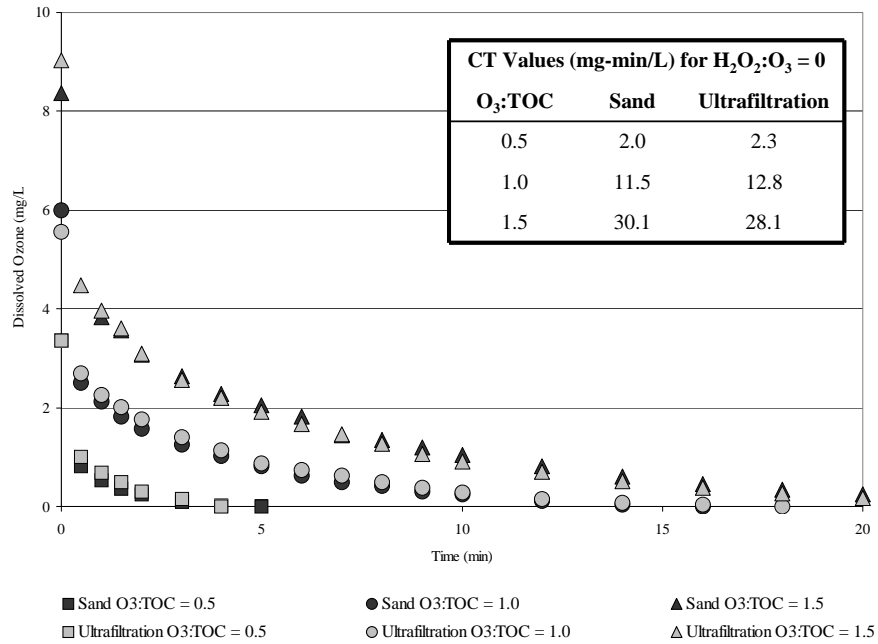


Figure 5.2. Ozone demand/decay comparison for RSWRF.

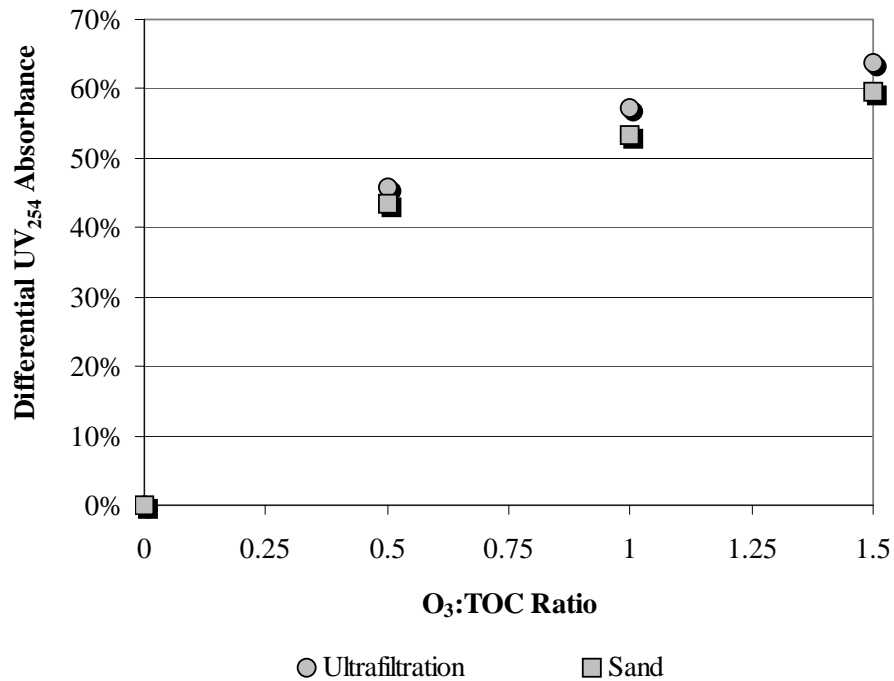


Figure 5.3. Differential  $UV_{254}$  absorbance for RSWRF after ozonation.

### 5.1.1 TOxC Mitigation in the RSWRF Pilot Treatment Train

Table 5.1 describes the effects of the various pilot- and full-scale treatment processes on TOxC concentrations. Regarding the secondary effluent, 27 of the 31 target compounds were detected in at least one sample event, but only the compounds listed in Table 5.1 were detected in all six sample events. Iopromide, ethynylestradiol, testosterone, and progesterone were not detected in any of the sample events. The bold values represent compounds with considerable variability throughout the six sample events. For example, the anticonvulsant phenytoin ranged from 1300 ng/L in February to less than 300 ng/L in April and May. Because phenytoin is dosed throughout the day in most patients, the concentrations should have been relatively stable in each sample event. However, phenytoin is not readily biodegraded in secondary treatment, so its effluent concentration is more susceptible to temporal fluctuations, which are exacerbated by grab sampling as opposed to composite sampling. Despite the variability of some compounds, the concentrations in the secondary effluent were generally similar across the six sample events and ranged from <MRL for iopromide, testosterone, progesterone, and ethynylestradiol to more than 1 µg/L for atenolol and TCPP. A majority of the target compounds were present at concentrations <100 ng/L in the secondary effluent. In Table 5.1, the percent removals were calculated based on the respective secondary effluent concentrations in each sample event, and then the averages over the sample events were calculated and presented in the table.

In general, UF and sand filtration provided limited and sporadic reductions in the concentrations of most TOxCs. Some of the highest removals were experienced by compounds with log  $K_{OW}$  values >3 (e.g., gemfibrozil, bisphenol A, and estrone), which would indicate particle-assisted removal by the filtration process; however, several compounds with high log  $K_{OW}$  values also experienced low removals during the filtration process (e.g., diclofenac and naproxen). Some of the observed filter removals for the TOxCs were consistent with the literature (e.g., bisphenol A, carbamazepine, DEET, naproxen, TCEP, and trimethoprim), whereas others demonstrated opposite trends (e.g., atenolol, gemfibrozil, ibuprofen, musk ketone, triclosan, and TCPP; Stevens-Garmon et al., 2011). Furthermore, a small number of compounds experienced different removal profiles after UF versus sand filtration. Some of the more bioamenable compounds (e.g., atenolol and gemfibrozil) experienced greater removals during sand filtration because of the likelihood of biofilm formation on the media, whereas the compounds with greater sorption potential (e.g., fluoxetine and triclosan) experienced greater removal during UF because of solids rejection. In general, it appears that biophysicochemical properties are not always a reliable indicator of treatment efficacy during filtration.

**Table 5.1. TOxC Summary Data for the Six Sample Events at RSWRF**

Compound	Concentration	Average % Removal		Average % Removal	
	Secondary Effluent (ng/L)	Ultrafiltration Effluent	Sand Effluent	Ozone/H <sub>2</sub> O <sub>2</sub> Effluent	BAC Effluent
Atenolol	1110	6	46	99	>99
Atorvastatin	39	44	6	>98	>98
Atrazine	2.2	-18	5	66	>85
Benzophenone	218	11	16	>64	>64
BHA	69	45	4	>98	>98
Carbamazepine	218	4	-4	>99	>99
DEET	224	-3	-5	94	>99
Diazepam	2.7	-8	-9	>90	>90
Estrone	68	82	66	>99	>99
Fluoxetine	51	36	-5	>99	>99
Gemfibrozil	484	20	55	>99	>99
Meprobamate	648	-3	-4	83	98
Naproxen	50	7	-10	>98	>98
Phenytoin	427	35	33	98	>99
Primidone	198	-11	0	94	99
Sulfamethoxazole	688	6	-3	99	>99
TCEP	520	1	2	16	96
Triclosan	135	98	3	>99	>99
Trimethoprim	525	30	30	>99	>99

Notes: BAC=biological activated carbon; BHA=butylated hydroxyanisole; DEET=*N,N*-diethyl-*meta*-toluamide; TCEP=tris-(2-chloroethyl)-phosphate

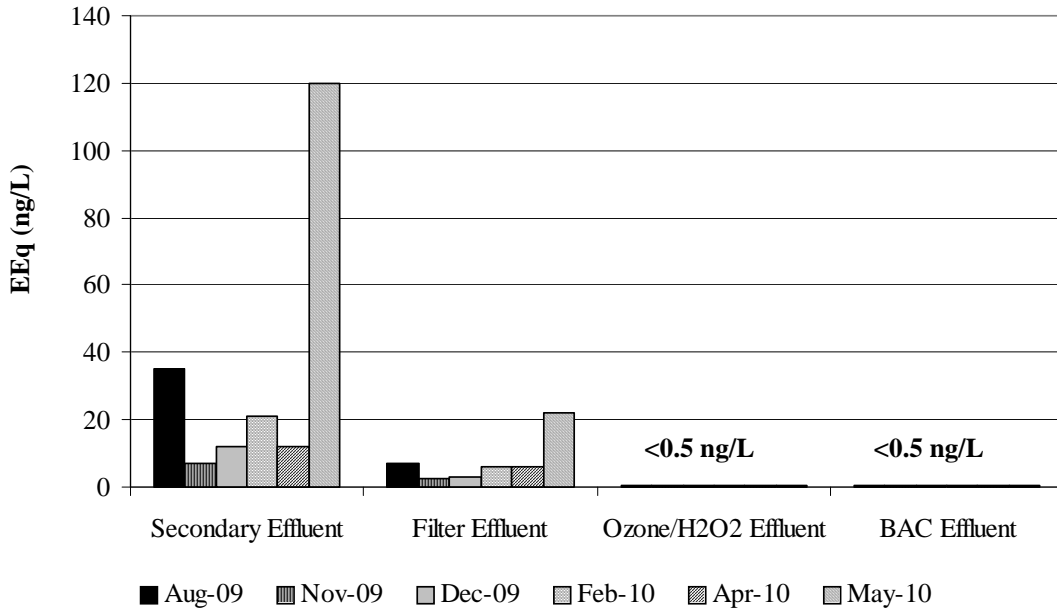


**Figure 5.4. Summary of YES data for RSWRF.**

The subsequent ozone/H<sub>2</sub>O<sub>2</sub> process demonstrated significant reductions in nearly all of the target contaminants. Only a small number of compounds (e.g., meprobamate, atrazine, and TCEP) failed to achieve their respective MRLs in at least one sample event. Meprobamate and atrazine still experienced removals of 60 to 90%, and only TCEP, which is specifically designed to resist oxidation, experienced less than 30% removal. The remaining target contaminants were removed by more than 90% or to the extent of quantification. Although temporal variability may have affected the secondary effluent and filter effluent concentrations, the ozone/H<sub>2</sub>O<sub>2</sub> process overcame the effects of sampling error with extensive oxidation. In other words, the consistency and effectiveness of the ozone process correlates to a high degree of confidence in the effluent concentrations and calculated removal percentages.

Finally, the BAC process achieved the limit of quantification or at least 95% removal for every target contaminant. Benzophenone (130 and 130 ng/L), meprobamate (11, 17, and 29 ng/L), TCEP (21, 34, and 35 ng/L), and TCPP (100 and 250 ng/L) were the only target contaminants with effluent concentrations exceeding 10 ng/L in some sample events. DEET, ibuprofen, primidone, and sulfamethoxazole were detected at less than 2 ng/L in the BAC effluent.

In addition to concentrations of individual contaminants, the YES assay was used to quantify the total estrogenicity of each sample (Figure 5.4). Similar to some of the estrogenic target compounds, the secondary effluent EEq values experienced significant variability (i.e., 7 to 120 ng/L) because of relatively low values in Sample Events 2–5 and spikes in Sample Events 1 and 6. The analytical methods used in this study do not identify all of the individual compounds contributing to estrogenicity; however, the target compound list does include several estrogenic compounds, and these compounds demonstrated trends consistent with the YES assay, as shown in Table 5.2.

**Table 5.2. Estrogenicity of RSWRF Secondary Effluent**

<b>Estrogenic Compound</b>	<b>Sample Event 1 (ng/L)</b>	<b>Sample Events 2–5 (ng/L)</b>	<b>Sample Event 6 (ng/L)</b>
Bisphenol A	<5	<5	72
EEq (YES assay)	35	13±6	120
Estradiol	6	<0.5	3
Estrone	113	38±17	140
Octylphenol	31	<25	31

*Notes:* EEq=estradiol equivalents; YES=yeast estrogen screen

Although filtration was not particularly effective for most TOxCs, both UF and sand filtration were effective in removing estrogenic compounds and total estrogenicity. The subsequent ozone/H<sub>2</sub>O<sub>2</sub> process was then capable of oxidizing any residual estrogenic activity, as demonstrated by EEq values <MRL (i.e., 0.5 ng/L) in all sample events. Except for the apparent contamination in Sample Events 1 and 6, in which estrone was detected at 7.6 ng/L, the individual steroid hormones were also <MRL after secondary clarification or ozone.

### 5.1.2 Microbial Inactivation and Removal at RSWRF

Figure 5.5 illustrates the prevalence of indicator and surrogate bacteria (i.e., total coliforms, fecal coliforms, and *Bacillus* spores) in the effluent from the various treatment processes. In contrast to UF (data not shown), sand filtration provided limited physical removal of bacteria. The subsequent ozone process achieved approximately 2- to 3-log inactivation of total coliforms and 3- to 4-log inactivation of fecal coliforms, but the dosing conditions were insufficient to comply with the most stringent reuse criteria given the concentration of total ( $761 \pm 419$  MPN/100 mL) and fecal coliforms ( $16 \pm 18$  MPN/100 mL) in the ozone/H<sub>2</sub>O<sub>2</sub> effluent. Moreover, the number of total ( $1819 \pm 254$  MPN/100 mL) and fecal ( $25 \pm 16$  MPN/100 mL) coliforms increased slightly in the BAC effluent, presumably because of regrowth on the BAC media. Advanced oxidation has the potential to convert recalcitrant organic matter to more bioavailable forms (e.g., carboxylic acids). This is important for BAC considering that the carbon provides a substrate for vegetative bacteria to attach and develop biofilm communities. Coupled with the continuous supply of biodegradable organic carbon, the contactor provides an ideal environment for bacteria to thrive. This is beneficial for reductions in residual TOxCs and oxidation byproducts, but it provides a regrowth opportunity for indicator bacteria, such as total and fecal coliforms and even pathogenic bacteria. Despite consistent decreases in each treatment process, the overall treatment train achieved less than 0.7-log reduction in viable *Bacillus* spores. This is reasonable given the resistance of *Bacillus* to ozonation, particularly with H<sub>2</sub>O<sub>2</sub> addition.

On the basis of these bacterial data, a downstream disinfection process (e.g., low-pressure UV irradiation) would certainly be necessary unless membrane filtration or modified dosing conditions were implemented. Even with more stringent pretreatment, it would still be possible for the subsequent BAC process to trigger coliform violations due to regrowth. Therefore, a final disinfection process may be warranted regardless of whether membrane filtration is implemented.

Because of the limited number of indigenous MS2 (<1 PFU/mL), concentrated MS2 was spiked into the ozone/H<sub>2</sub>O<sub>2</sub> influent in order to evaluate the process based on the Title 22 viral inactivation criteria. Five replicate samples were analyzed from two different sample ports on the HiPOx reactor. Sample Port 4 corresponds to approximately 3 seconds of reaction time, and Sample Port 6 corresponds to approximately 5 seconds of reaction time. H<sub>2</sub>O<sub>2</sub> was added into the HiPOx reactor, so these reaction times are sufficient for the oxidation process to reach completion. The MS2 inactivation data, including the simultaneous inactivation of indigenous total and fecal coliforms, are summarized in Figure 5.6. With 5 mg/L of applied ozone and 3.5 mg/L of H<sub>2</sub>O<sub>2</sub>, the HiPOx reactor consistently satisfied the 5- and 6.5-log inactivation criteria established by CDPH and Ishida et al. (2008). The simultaneous inactivation of total and fecal coliforms was consistent with the values determined during the full sample events.

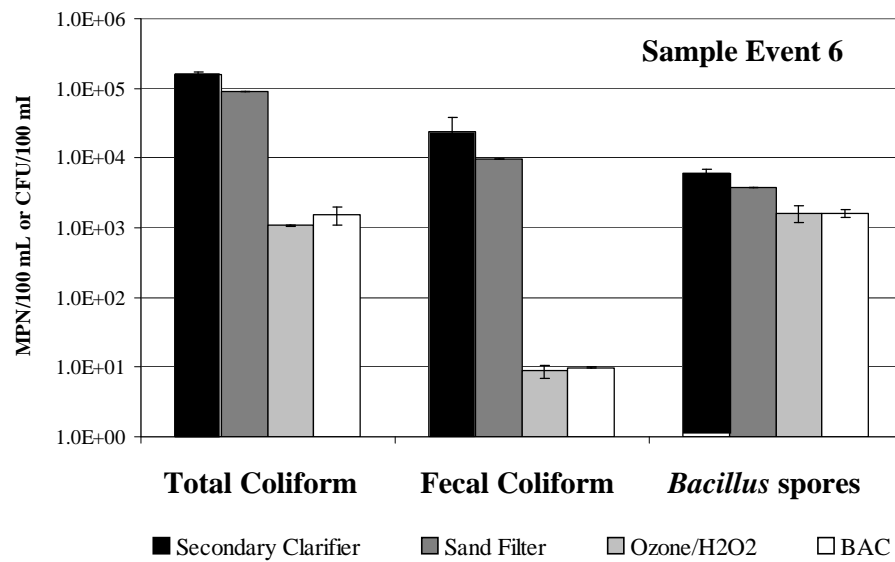
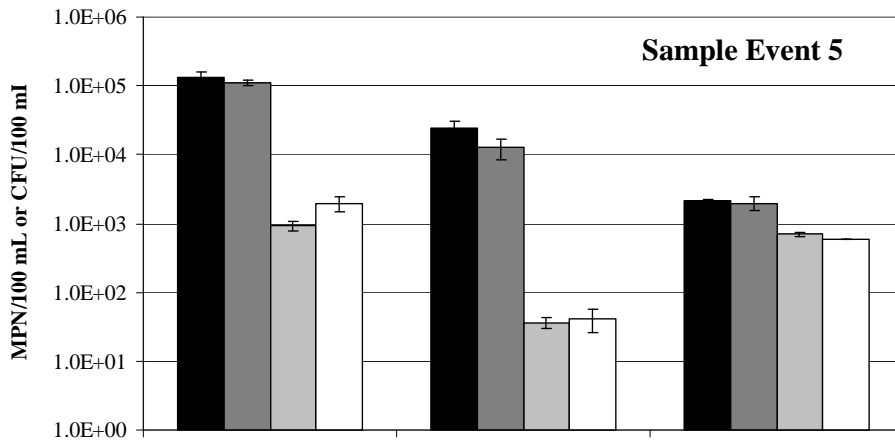
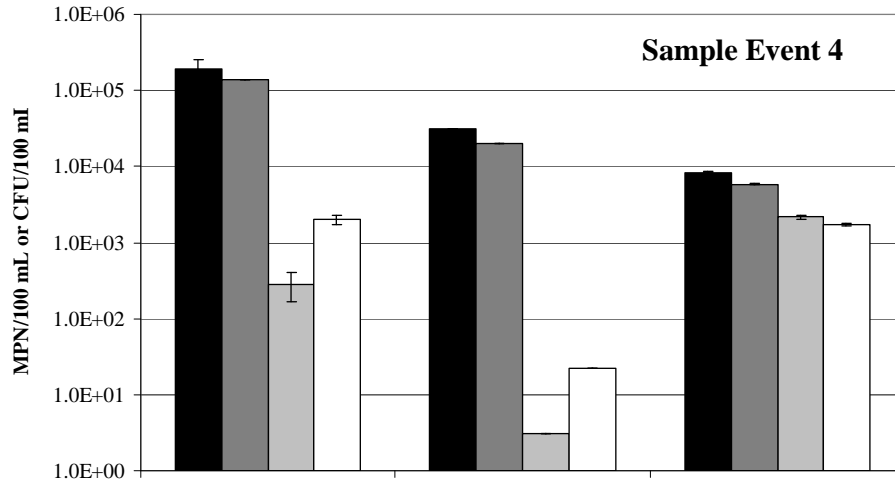


**Figure 5.5. Coliform and spore removal/inactivation at RSWRF.**

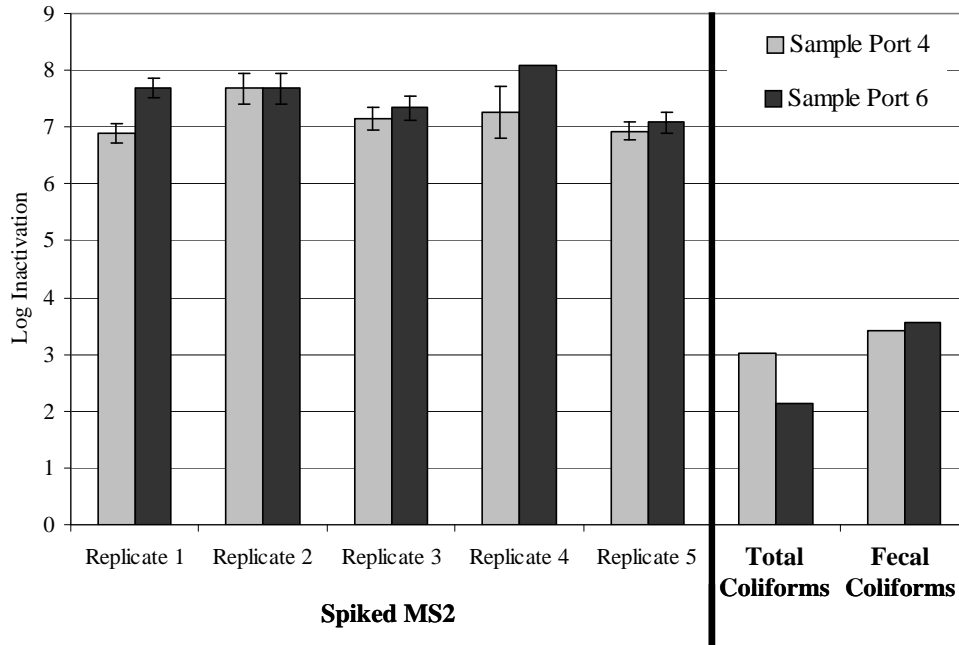


Figure 5.6. MS2 and coliform inactivation during spiking study.

### 5.1.3 Organic Characterization

During the first phase of the project, the average TOC of the secondary effluent was approximately 6.0 mg/L, but the average TOC increased slightly to approximately 6.8 mg/L during Phase 2. Neither UF nor sand filtration had a significant impact on TOC based on effluent values of 5.9 and 6.6 mg/L. Because moderate ozone/H<sub>2</sub>O<sub>2</sub> doses are incapable of achieving significant mineralization, the slight decrease in TOC during Phase 1 was reasonable; however, there was a noticeable increase in TOC after ozone/H<sub>2</sub>O<sub>2</sub> during Phase 2. This is likely attributable to biological growth on the walls of the HiPOx reactor. The lack of a dissolved ozone residual, high bacterial counts in the HiPOx, and conversion of complex organic matter to AOC created a suitable environment for biofilm growth, which was visually apparent along the walls of the reactor. This biofilm may have been sloughing off periodically, which would explain the increase in TOC.

Finally, the BAC process achieved considerable TOC reductions during Phase 1 (51%) because the column still maintained a relatively high adsorption capacity, but Phase 2 only achieved an average TOC reduction of 33%, which could be attributed to the higher TOC loading from the ozone/H<sub>2</sub>O<sub>2</sub> effluent, a reduction in adsorption capacity over time, or a combination of both. This theory was supported by a multidepth analysis of the BAC contactor during Phase 2. This analysis indicated that the first half of the contactor had reached exhaustion (i.e., no reduction in TOC), and the lower depths were approaching exhaustion with each sample event; however, even after 20 months of continuous operation, the BAC contactor still retained some adsorption capacity. The TOC data are summarized in Table 5.3.

As shown in Table 5.4, the UV<sub>254</sub> values for the RSWRF were very consistent across the six sample events. Neither UF nor sand filtration provided a significant reduction in UV<sub>254</sub>.

absorbance, but ozone/H<sub>2</sub>O<sub>2</sub> achieved consistent 50% reductions in UV<sub>254</sub> absorbance, and the final BAC process provided additional 50% and 29% reductions in Phases 1 and 2. Figure 5.9 provides an example (Sample Event 1) of the absorbance spectra for the various unit processes. The secondary effluent and UF spectra are nearly identical, so it is difficult to distinguish them in the graph.

Figure 5.7 illustrates the transformation of organic matter during the various full- and pilot-scale treatment processes. The secondary effluent images indicate that there was some variability in the EfOM over the duration of the project, but the major organic fractions (i.e., fluorescence peaks) are still apparent in each sample event. As expected, there is little change in the organic matter after UF or sand filtration, but the ozone/H<sub>2</sub>O<sub>2</sub> process dramatically reduced the fluorescence of the wastewater matrix.

In general, the subsequent BAC process was able to reduce the fluorescence even further. Similar to the bench-scale experiments, Figure 3.8 illustrates the changes in TF and the different organic fractions (i.e., region) during treatment. In addition, Table 5.5 summarizes FI and TI across the various treatment processes and sample events. On average, each step of the treatment train results in a small decrease in fluorescence intensity, and the TI indicate that the various unit processes are quite consistent in their ability to reduce the fluorescence of the EfOM. This indicates that the treatment train was very stable throughout the entire duration of the project, which is particularly important for the applicability of the correlation models. As demonstrated in each of these figures and tables, the RSWRF pilot-scale treatment train achieves significant transformation of the EfOM, which causes the matrix to lose its wastewater identity and approach that of a more pristine source water.

**Table 5.3. TOC Values (mg/L) for RSWRF**

Sample Location	Phase 1 – Ultrafiltration				Phase 2 – Sand Filtration			
	Aug. 2009	Nov. 2009	Dec. 2009	Average	Feb. 2010	Apr. 2010	May 2010	Average
Secondary	6.2	6.2	5.6	6.0	6.8	6.9	6.8	6.8
Filter	6.8	5.9	5.1	5.9	6.5	6.2	7.2	6.6
Ozone/H <sub>2</sub> O <sub>2</sub>	6.2	6.0	5.0	5.7	7.6	7.1	7.3	7.3
BAC	2.5	3.1	2.7	2.8	4.8	5.0	4.8	4.9

Note: BAC=biological activated carbon

**Table 5.4. UV<sub>254</sub> Values (cm<sup>-1</sup>) for RSWRF**

Sample Location	Phase 1 – Ultrafiltration				Phase 2 – Sand Filtration			
	Aug. 2009	Nov. 2009	Dec. 2009	Average	Feb. 2010	Apr. 2010	May 2010	Average
Secondary	0.13	0.13	0.13	0.13	0.15	0.13	0.15	0.14
Filter	0.13	0.13	0.11	0.12	0.14	0.13	0.14	0.14
Ozone/H <sub>2</sub> O <sub>2</sub>	0.06	0.06	0.05	0.06	0.08	0.07	0.07	0.07
BAC	0.02	0.03	0.03	0.03	0.05	0.05	0.05	0.05

Note: BAC=biological activated carbon

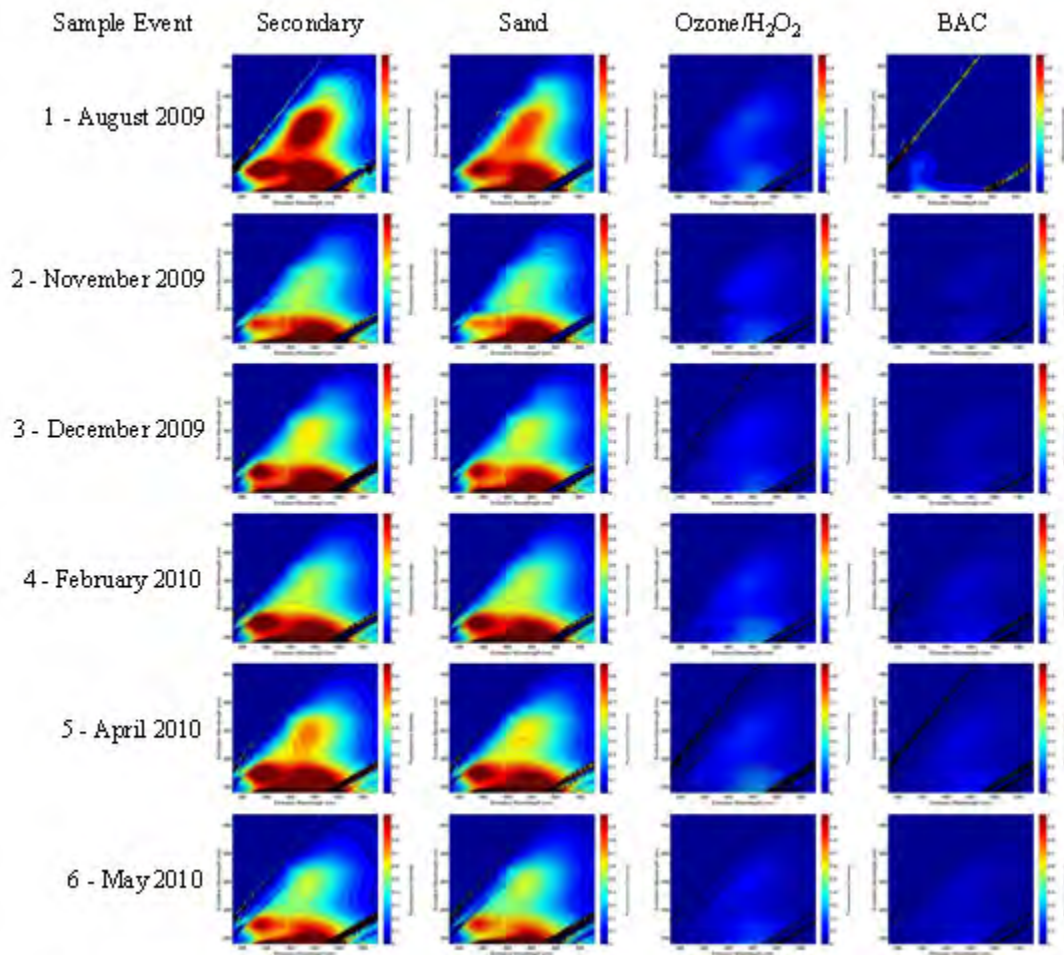


Figure 5.7. EEMs after treatment for RSWRF.

Table 5.5. Summary of Treatment and Fluorescence Indices for RSWRF

Sample Event	Fluorescence Indices				Treatment Indices			
	Sec.	Filter	Ozone	BAC	Sec.	Filter	Ozone	BAC
1	1.55	1.49	1.36	1.30	1.00	0.89	0.17	0.05
2	1.31	1.30	1.31	1.27	1.00	1.02	0.15	0.05
3	1.37	1.36	1.34	1.27	1.00	0.91	0.13	0.05
4	1.34	1.33	1.37	1.31	1.00	0.97	0.19	0.08
5	1.42	1.37	1.35	1.30	1.00	0.93	0.17	0.08
6	1.45	1.49	1.39	1.31	1.00	0.90	0.15	0.08
<b>Average</b>	<b>1.41</b>	<b>1.39</b>	<b>1.35</b>	<b>1.29</b>	<b>1.00</b>	<b>0.94</b>	<b>0.16</b>	<b>0.07</b>

Note: BAC=biological activated carbon

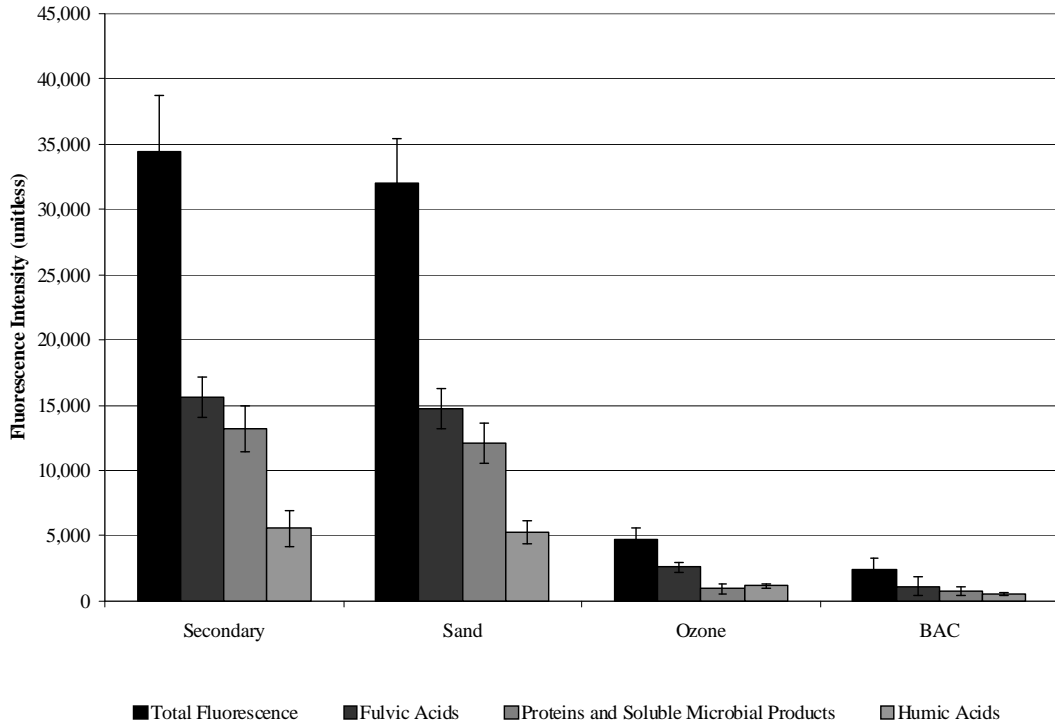


Figure 5.8. Regional fluorescence intensities for RSWRF.

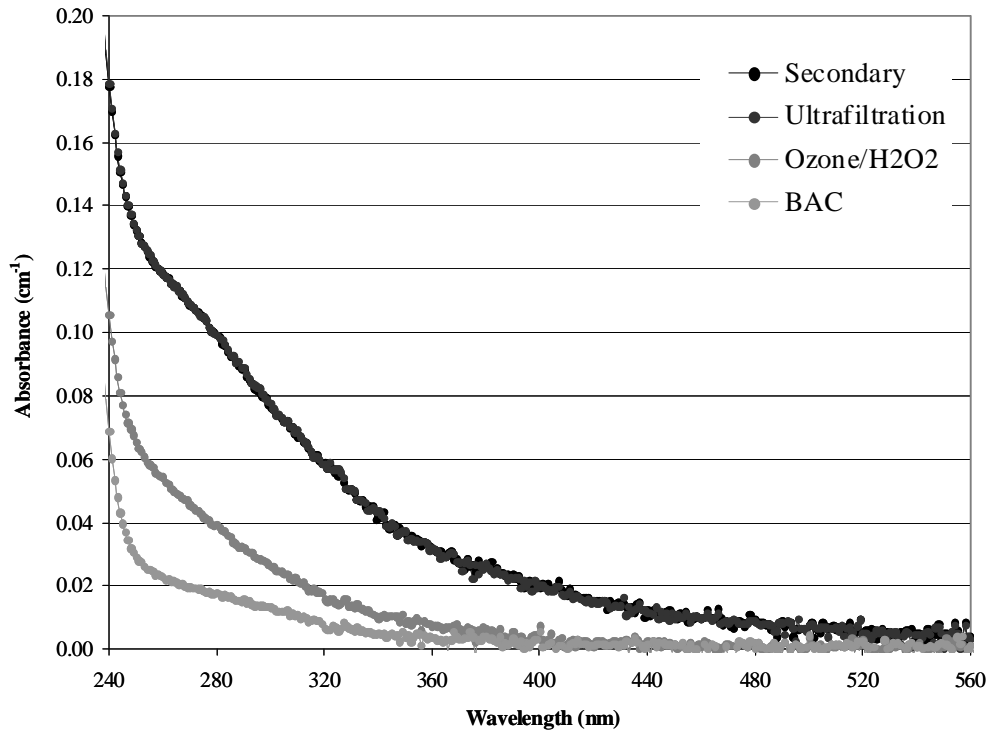


Figure 5.9. Absorbance spectra for Sample Event 1 at RSWRF.

## 5.2 Validation of Correlation Models

The bench-scale correlations developed in Section 0 proved to be highly consistent across wastewater matrices, but a more critical issue is whether these correlations can be applied to other reactors, particularly large-scale oxidation systems. Independent data from the literature and several pilot-scale reactors were compiled and overlaid with the correlation plots in the appendices. These validation plots are provided in Appendices 7 and 8 for ozone- and UV-based oxidation, respectively. Because the target compound list varied by study, some compounds only include data points from the WRF-09-10 data set. On the other hand, some compounds include data points from up to five independent sets of experiments incorporating 11 different wastewater matrices. The data sets also include varying levels of pretreatment, including secondary effluent, secondary effluent with sand filtration, secondary effluent with UF, and an MBR filtrate. The data sets include the following, which are described in greater detail:

1. Wert et al. (2009b)
2. Rosario-Ortiz et al. (2010)
3. City of Las Vegas Water Pollution Control Facility (CLV) Pilot ( $O_3$ )
4. RSWRF Pilot ( $O_3/H_2O_2$ )
5. Green Valley Water Reclamation Facility Pilot ( $O_3$ ,  $O_3/H_2O_2$ ,  $UV/H_2O_2$ )

### 5.2.1 Wert et al. (2009b)

Wert et al. (2009b), which is referred to as “Wert” in Appendix 7, was the first peer-reviewed publication demonstrating the strong correlation between changes in  $UV_{254}$  absorbance and contaminant oxidation during ozone-based oxidation processes. The authors developed the correlations with a combination of bench- and pilot-scale ozone and ozone/ $H_2O_2$  in three different wastewater matrices. Two of their wastewaters were also tested in the current study, but the water qualities and sampling locations (tertiary instead of secondary effluent) were slightly different. Applied ozone doses ranged from 0 to 12 mg/L ( $O_3:TOC=0-1.2$ ), and some samples were supplemented with an  $H_2O_2:O_3$  ratio of 0.5. The study targeted atenolol, carbamazepine, phenytoin, iopromide, meprobamate, and primidone.

### 5.2.2 Rosario-Ortiz et al. (2010)

Rosario-Ortiz et al. (2010), which is referred to as “Rosario” in Appendix 8, was the first peer-reviewed publication demonstrating correlations between changes in  $UV_{254}$  absorbance and contaminant oxidation during UV-based oxidation processes. The study evaluated bench-scale  $UV/H_2O_2$  with low-pressure UV light (i.e., 254 nm); UV doses of 300, 500, and 700  $mJ/cm^2$ ; and  $H_2O_2$  doses of 2, 5, 10, 15, and 20 mg/L. The same wastewater matrices were used in this study and Wert et al. (2009b), and correlations were developed for atenolol, carbamazepine, phenytoin, meprobamate, primidone, trimethoprim, and pCBA.

### 5.2.3 City of Las Vegas Water Pollution Control Facility

In conjunction with another WateReuse Research Foundation project evaluating the effect of preoxidation on RO fouling (WRF-08-08), pilot-scale experiments were performed at the CLV in Las Vegas, NV. The filtrate from a 20 gpm, pilot-scale MBR (Hydranautics, Nitto Denko, Oceanside, CA) was divided into two separate trains: one train fed a 10 gpm, pilot-scale, RO membrane (Hydranautics), and the other train fed a 10 gpm, pilot-scale, HiPOx<sup>®</sup>

reactor (APTwater, Pleasant Hill, CA) as pretreatment for a separate pilot-scale RO membrane. A picture of the pilot-scale treatment train is provided in Figure 5.10.

The goal of WRF-08-08 was to validate bench-scale studies demonstrating reductions in RO fouling after preoxidation with ozone and ozone/H<sub>2</sub>O<sub>2</sub>. Even at extremely low ozone doses (e.g., 1.5 mg/L or a O<sub>3</sub>:TOC ratio of approximately 0.25), preoxidation makes EfOM more hydrophilic and less likely to accumulate on membrane surfaces. Ultimately, this leads to improved performance, stable transmembrane pressures, reduced maintenance, and possibly lowered costs. Another goal of WRF-08-08 was to determine whether the reductions in organic fouling offset the additional capital and operation and maintenance costs associated with preoxidation.

For WRF-09-10, the HiPOx ozone system was evaluated as a stand-alone process for contaminant oxidation. MBR filtrate was exposed to applied ozone doses ranging from 0 to 10 mg/L (O<sub>3</sub>:TOC=0–2.0) and H<sub>2</sub>O<sub>2</sub>:O<sub>3</sub> ratios of 0 and 0.5. Samples were analyzed for all of the target compounds in the current study, but some compounds were not present in the MBR filtrate because of the efficacy of the preceding biological treatment or their absence in the influent wastewater. This pilot was also operated with an online UV absorbance monitor to measure real-time changes in UV<sub>254</sub> absorbance, which is discussed in Section 5.3.

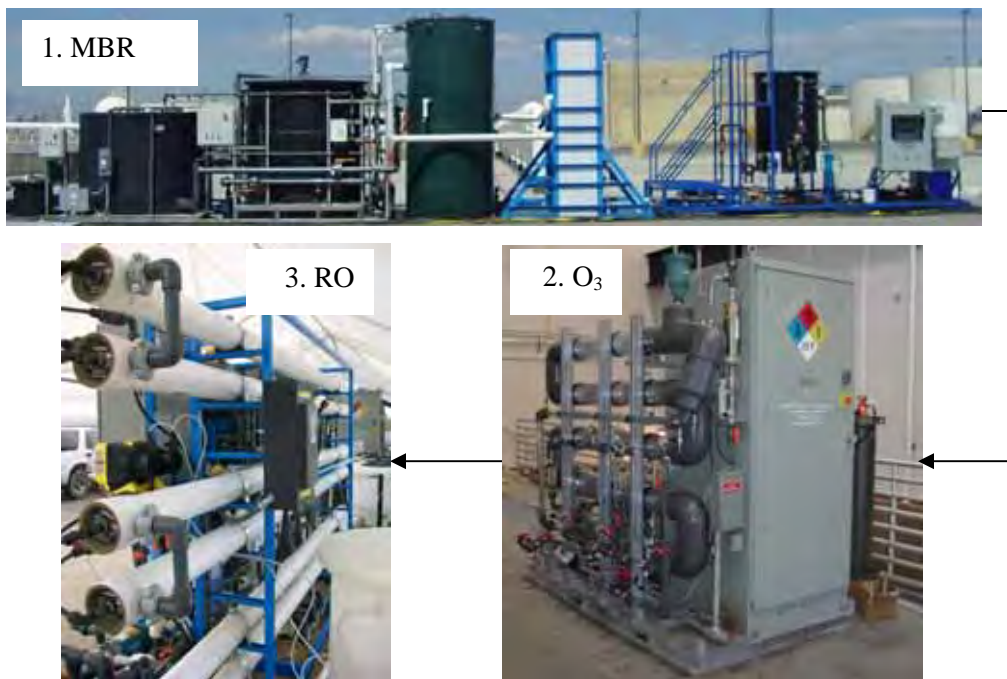


**Figure 5.10.** CLV pilot-scale MBR-O<sub>3</sub>-RO treatment train.



**Figure 5.11. Green Valley Water Reclamation Facility pilot.**

### **5.2.4 Reno-Stead Water Reclamation Facility**

The six sample events described in Section 5.1 are included in the correlation comparison in Appendix 7.

### **5.2.5 Green Valley Water Reclamation Facility**

In conjunction with WRF-08-05 (Use of Ozone in Water Reclamation for Contaminant Oxidation), pilot-scale experiments were performed at the Green Valley Water Reclamation Facility in Tucson, AZ. Sand filtered effluent from a conventional wastewater treatment train was fed to a 10-gpm, Wedeco/ITT pilot reactor (Herford, Germany). The versatility of the pilot system allowed for a variety of treatment configurations, including ozone, ozone/H<sub>2</sub>O<sub>2</sub>, UV, UV/H<sub>2</sub>O<sub>2</sub>, ozone/UV, and ozone/UV/H<sub>2</sub>O<sub>2</sub>. In order to simplify the presentation of data, only the ozone, ozone/H<sub>2</sub>O<sub>2</sub>, and UV/H<sub>2</sub>O<sub>2</sub> samples are included in Appendices 7 and 8. Based on a TOC of approximately 6 mg/L, ozone doses of 1.5, 3.0, 6.0, and 9.0 mg/L, which corresponded to O<sub>3</sub>:TOC ratios of 0.25, 0.50, 1.0, and 1.5, respectively, were applied to the tertiary effluent. For the ozone/H<sub>2</sub>O<sub>2</sub> experiments, peroxide was applied at molar H<sub>2</sub>O<sub>2</sub>:O<sub>3</sub> ratios of 0 and 1.0. For the UV/H<sub>2</sub>O<sub>2</sub> experiments, UV doses ranged from 250 to 1000 mJ/cm<sup>2</sup>, and H<sub>2</sub>O<sub>2</sub> was dosed at 10 mg/L. Samples from three separate sample events were analyzed for TOCs and bulk organic matter. Photos of the pilot skid and reactor are provided in Figure 5.11.

### **5.2.6 Comparison of Studies**

For ozone and ozone/H<sub>2</sub>O<sub>2</sub> (Appendix 7) and UV/H<sub>2</sub>O<sub>2</sub> (Appendix 8), there was relatively strong agreement between the bench-scale correlations and the independent correlations from previous studies. This highlights the widespread applicability of this concept to diverse water qualities and treatment technologies; however, the contaminant correlations proved to be much stronger than the microbial correlations, particularly in the case of *E. coli*. Therefore, the use of differential organic parameters may be limited to general process performance and contaminant oxidation, whereas disinfection may still require more traditional measures of performance to increase confidence in advanced treatment trains.

### 5.3 Online Absorbance Analyzer

In addition to the grab samples during the initial ozone dosing experiment (Section 5.2.3), the HiPOx unit at CLV was evaluated with an online absorbance analyzer from s::can Messtechnik (Vienna, Austria). The s::can spectro::lyser™ (Figure 3.12) was used to store the entire absorption spectrum of the target water matrix at 5-minute time intervals. In addition to automatic absorbance logging for a range of wavelengths (220–720 nm), the analyzer is also capable of using built-in algorithms to convert absorption spectra into numerous water quality parameters, including COD, BOD, TOC, DOC, nitrate, nitrite, ammonia, and AOC. For the purposes of this project, the following discussion will focus on the use of real-time, online UV<sub>254</sub> absorbance readings for continuous monitoring of process performance.

The analyzer can either be submerged in the target water matrix during operation or mounted for a more permanent and stable installation. For this project, the analyzer was externally mounted on the HiPOx unit, and a sidestream of ozonated effluent was continuously fed through the flow cell. Although it is not shown in Figure 5.12, the flow cell was encapsulated in a plastic housing with inlet and outlet ports during operation. The housing was removed periodically, and the internal surfaces were cleaned with dilute hydrochloric acid and Kimwipes to reduce interference by biofilms, attached solids, and scaling. The s::can spectro::lyser can also be equipped with an automatic cleaning system with a brush and compressed air, but the unit provided for this study required manual cleaning.

For a period of approximately 10 weeks, the performance of the HiPOx unit was continuously evaluated based on differential UV<sub>254</sub> absorbance. The goal of this phase was to further validate the bench-scale correlations while monitoring the stability of the water quality and ozone oxidation at the pilot. The project team was only able to acquire one s::can spectro::lyser. Therefore, the instrument received MBR filtrate (i.e., ozone influent) and ozonated MBR filtrate (i.e., ozone effluent) at different times during the monitoring period. Figure 5.13 illustrates the fluctuation in UV<sub>254</sub> absorbance for the ozone influent, which was monitored from May 21 through May 31. Figure 5.13 also indicates the UV<sub>254</sub> absorbance of a grab sample that was analyzed in the laboratory to validate the online reading from the s::can spectro::lyser. More frequent grab samples were performed during the ozone effluent monitoring period. During the initial ozone influent monitoring period, the instrument was quite stable and able to detect fluctuations in influent water quality due to typical diurnal variability. The data collected during this time indicated that the UV<sub>254</sub> absorbance of the ozone influent ranged from 0.095 to 0.155 cm<sup>-1</sup> and had an average value of 0.111 cm<sup>-1</sup>. After May 31, the ozone influent was assumed to follow a similar trend, which allowed the project team to focus on the water quality of the ozone effluent.

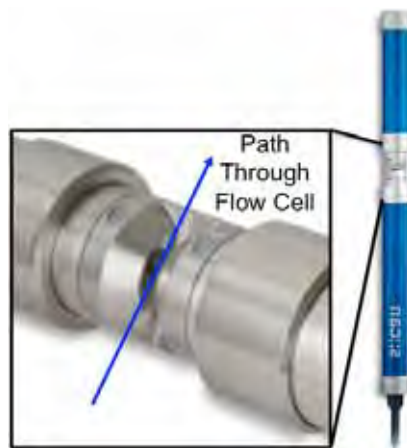


**Figure 5.12. Online absorbance analyzer (spectrolyser).**

Figure 5.14 illustrates the  $UV_{254}$  absorbance of the ozone effluent from May 31 to July 4. In contrast to the relatively stable ozone influent, the ozone effluent experienced dramatic fluctuations in water quality that resulted in numerous  $UV_{254}$  absorbance spikes in the raw data. In order to improve the clarity of the data, any values  $>0.100\text{ cm}^{-1}$  were removed from the data set. These points were assumed to be invalid for the purposes of this project for a variety of possible reasons:

- unexpected or planned shutdowns of the pilot systems
- scaling or biological fouling of the spectrolyser
- spikes in turbidity or air bubbles that interrupted the light path in the flow cell

The gaps in the ozone effluent values indicate data that were removed. During the effluent monitoring period, there were numerous operational problems with the MBR and ozone pilots. For example, the cooling system of the HiPOx unit malfunctioned, which caused periodic overheating and shutdowns of the ozone generator. The spectrolyser continued to collect absorbance data despite the shutdown and lack of flow through the unit. Although this did not benefit the model validation, it indicated that this type of online monitoring system would provide redundancy in alerting plant personnel of operational problems.

As mentioned previously, scaling, biological fouling, and periodic spikes in turbidity also impacted the data provided by the spectrolyser. Therefore, several modifications related to these issues are recommended for future online monitoring efforts. First, a more consistent and frequent cleaning schedule—perhaps daily—would improve the quality of the data generated by the unit. If available, the automatic cleaning system could be programmed to initiate an hourly cleaning cycle to minimize the formation and impacts of the various types of fouling. Manual cleaning with dilute acid may still be warranted to address potential scaling impacts. Finally, incorporating a filter into the spectrolyser housing may prevent artificial spikes in UV absorbance related to turbidity, although, a separate online turbidimeter may be warranted to identify spikes in turbidity that may impact microbial inactivation during ozonation.

In addition to the  $UV_{254}$  absorbance spikes (or data gaps), several low points are also evident in Figure 5.14. The cyclical low points are indicative of diurnal variability in the influent water quality. Because differential absorbance (i.e., percent reduction) during ozonation is

relatively consistent, the effluent data will generally track the trends in influent water quality, as indicated by Figure 3.15. The dramatic dips in the effluent  $UV_{254}$  absorbance—June 14 as an example—are indicative of variable dosing experiments that were used to assess TO<sub>RC</sub> oxidation or other experimental objectives. During these experiments, the applied ozone doses ranged from 0.6 to 9.0 mg/L, which corresponded to  $O_3$ :TOC ratios ranging from 0.1 to 1.5. At all other times, a single ozone dose of 1.5 mg/L ( $O_3$ :TOC of 0.25) was maintained to evaluate the impacts of preoxidation on RO membrane fouling (WRF-08-08).

Most of the operational and data quality issues evident in the data gaps in Figure 3.14 can be mitigated in future applications. After addressing the issues and implementing the previous recommendations, the s::can spectro::lyser would certainly provide useful data for operators of water reuse facilities. This is demonstrated by the consistency in the absorbance values detected by the s::can instrument versus the corresponding grab samples. During continuous operation, there are some fluctuations in water quality that would not be captured by periodic grab samples. The s::can spectro::lyser is capable of capturing this temporal variability and ultimately incorporating the online data into a model—whether the TO<sub>RC</sub> oxidation model developed during this study or the proprietary s::can algorithms—to evaluate a range of water quality parameters.

In order to evaluate the TO<sub>RC</sub> correlation models developed during the bench-scale phase, a variable ozone dosing experiment was performed on June 14. The  $UV_{254}$  absorbance data from this experiment, including data for influent grab samples, effluent grab samples, and online monitoring of the ozone effluent, are illustrated in Figure 3.16. During the short timeframe of the dosing experiment, the influent water quality (shaded circles) was relatively stable considering that the  $UV_{254}$  absorbance only ranged from 0.102 to 0.113  $cm^3$ . The numbered boxes indicate different ozone dosing conditions for effluent, as described in Table 5.6. The data demonstrate tremendous consistency between online (empty triangles) and grab sample (black squares) throughout the testing period.

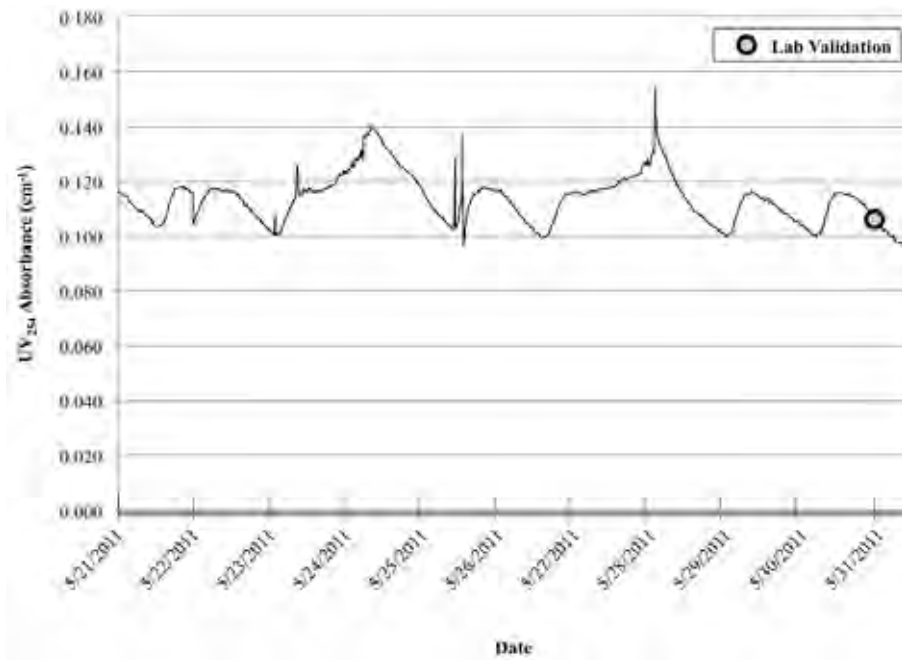


Figure 5.13. Influent UV<sub>254</sub> absorbance monitoring with s::can spectro::lyser.

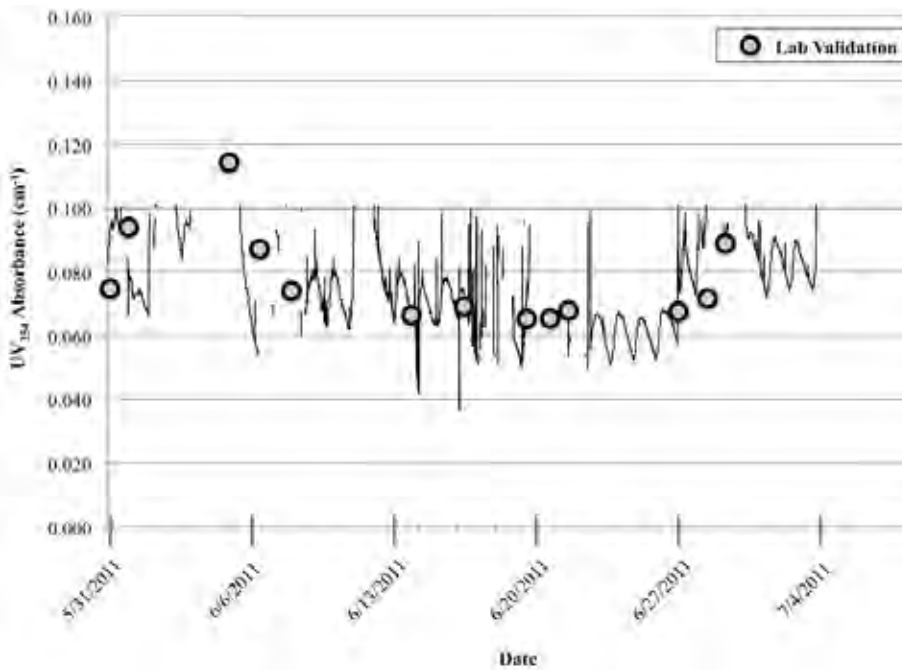


Figure 5.14. Effluent UV<sub>254</sub> absorbance monitoring with s::can spectro::lyser.

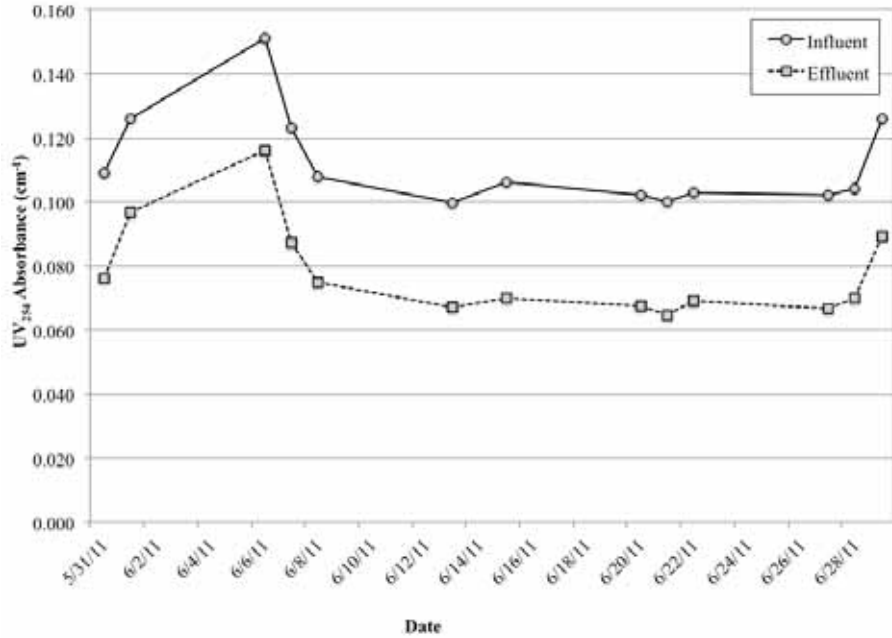


Figure 5.15. UV<sub>254</sub> absorbance monitoring with routine grab samples.

Table 5.6. Ozone Dosing Conditions During Variable Dosing Experiment

Ozone Dosing Condition	O <sub>3</sub> :TOC Ratio	Applied Ozone Dose (mg/L)
1	0.1	0.6
2	0.2	1.2
3	0.3	1.8
4	0.4	2.4
5	0.5	3.0
6	0.6	3.6
7	0.7	4.2
8	0.8	4.8
9	0.9	5.4
10	1.0	6.0
11 (Duplicate)	1.0	6.0
12	1.2	7.2
13	1.3	7.8
14	1.4	8.4
15	1.5	9.0

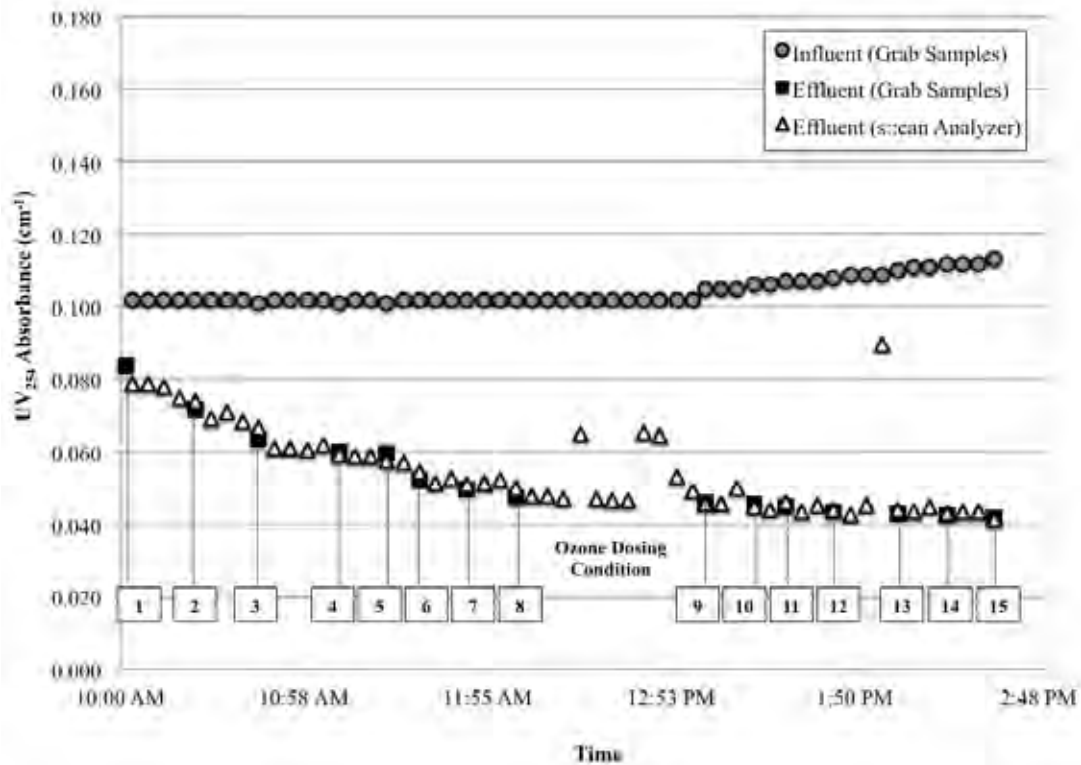


Figure 5.16. UV<sub>254</sub> absorbance monitoring during variable dosing experiment.

Regarding WRF-09-10, the most significant question was whether the online absorbance data could be used to predict the extent of oxidation for the target compound list. Appendix 10 illustrates the scan validation data for changes in UV<sub>254</sub> absorbance (grab and online samples) and corresponding changes in TF (only grab samples). Correlations for some compounds are not available because they were <MRL in the MBR filtrate.

With the exception of ibuprofen and TCEP, the predictive model based on the online absorbance readings and the actual levels of destruction based on the grab samples were quite consistent. This was particularly true for the highly susceptible Group 1 compounds, which were almost always <MRL, but the data were also relatively consistent for the Groups 2, 3, and 4 compounds. It is unclear exactly why the actual data and the predictive model for ibuprofen and TCEP were dissimilar, but the bench-scale TCEP data that were used to develop the correlation also showed more variability than the other compounds. Finally, the predictive model tended to overestimate the level of oxidation for some compounds, so a conservative correction factor may be warranted in critical applications.



## Chapter 6

# Conclusions

---

Depending on upstream treatment processes, secondary effluent can vary considerably among treatment plants. This was evident in the secondary effluent water quality for the five study sites, considering that some facilities employed extensive biological secondary treatment targeting nutrient removal and others employed low SRTs targeting BOD removal alone. This could seemingly make it difficult to optimize downstream oxidation processes targeting disinfection or contaminant oxidation; however, the results of this study indicate that there are certain parameters that can be monitored (e.g., differential UV<sub>254</sub> absorbance or TF) or targeted (e.g., O<sub>3</sub>:TOC ratio) to achieve similar water quality objectives regardless of the wastewater matrix. Other parameters, such as bromate formation, also demonstrated some consistency among matrices, but the trends exhibited greater variability.

In general, both ozone- and UV-based oxidation proved to be effective alternatives for contaminant oxidation and microbial inactivation, but the inherent limitations of each treatment process must be considered when tailoring a treatment train to a particular system. For example, ozone-based oxidation achieved significantly higher levels of contaminant oxidation as compared to UV-based oxidation, but the process was hindered by relatively high direct NDMA formation in some matrices and limited inactivation of spore-forming microbes. On the other hand, UV-based oxidation was extremely effective for disinfection because of high UV doses and synergistic •OH oxidation, but the required energy consumption and H<sub>2</sub>O<sub>2</sub> addition for contaminant oxidation may be prohibitive in some applications, particularly when the matrix has limited UV transmittance. Therefore, ozone- and UV-based treatment processes both have potential applications in advanced treatment trains, but the site's regulatory requirements and treatment objectives will determine the appropriate alternative.

After the treatment train is designed and constructed, the major limitation of advanced oxidation is real-time monitoring of process performance. As such, the motivation for this project was the industry's current inability to identify breakdowns and inefficiencies in AOP performance because of the reliance on •OH chemistry. Because •OH are highly reactive and short-lived, it is impractical, if not impossible, to measure an •OH residual. Disinfectant residuals are critical components of the existing CT framework, and they are a common surrogate for oxidation process performance. Current strategies rely on spiking and monitoring of probe compounds, such as pCBA, to estimate •OH exposure in AOPs, but this may not be possible for many agencies.

This project demonstrated that transformation of bulk organic matter—on relative terms (e.g., percent reduction in TF)—is a highly reproducible and consistent outcome of any AOP. In fact, the correlations between EfOM transformation, contaminant oxidation, and microbial inactivation were consistent regardless of the study site, upstream filtration, or H<sub>2</sub>O<sub>2</sub> dose. Furthermore, quantifying these EfOM transformations requires minimal equipment, expertise, time, and money compared to full-scale monitoring of target contaminants and pathogens. Automated online analyzers, such as the spectro::lyser manufactured by s::can Messtechnik, are also available for UV absorbance and fluorescence, so full-scale implementation of the empirical or mechanistic models developed in this project is entirely feasible. Although there is a certain amount of variability inherent in the models, the pilot-scale validation efforts and

comparisons with previous studies in the literature indicate that the models are valuable, accurate, and robust. The correlations may not yet be strong enough to warrant disinfection credits for microbial inactivation, but the models still provide a useful estimate of expected log inactivation. Additional studies would be necessary to further refine the microbial inactivation models and integrate them into a regulatory framework.

The results of this study are particularly relevant considering the revisions to the Draft Groundwater Replenishment Reuse regulations recently published by CDPH. The regulations stipulate that IPR agencies must identify an acceptable surrogate parameter that can be monitored continuously to ensure process integrity. The regulations further stipulate that agencies must identify target compounds encompassing a range of structural properties and susceptibilities, similar to the indicator framework proposed in this study, and the agencies must demonstrate that their AOPs achieve a specific removal objective for each group. In this context, WRF-09-10 provides a wealth of information that can be used to tailor the surrogate framework to an individual system. If the target compound removals and surrogate validation required by CDPH can be applied to a secondary or tertiary effluent, the results of this study are directly applicable. If the treatment objectives must be demonstrated following RO, the correlations may need to be modified to account for this significant change in matrix quality. In other words, the ambient  $UV_{254}$  absorbance and TF of a typical RO permeate may not be sufficient to achieve relevant differentials given the sensitivity of the analyses. Therefore, it may be necessary to identify a new surrogate parameter, such as chloramine residual, but the approach for model development will be identical to the one described in this report.

## References

---

- Adams, M. *Bacteriophages*; Interscience Publishers: New York, 1959.
- Australia. Guidelines for Water Recycling: Augmentation of Drinking Water Supplies. Canberra, Australia. Environment Protection Heritage Council, National Health and Medical Research Council, National Resource Management Ministerial Council, 2008.
- Benner, J.; Salhi, E.; Ternes, T.; von Gunten, U. Ozonation of reverse osmosis concentrate: Kinetics and efficiency of beta blocker oxidation. *Water Res.* **2008**, *42*, 3003–3012.
- Benotti, M. J.; Trenholm, R. A.; Vanderford, B. J.; Holady, J. C.; Stanford, B. D.; Snyder, S. A. Pharmaceuticals and endocrine disrupting compounds in U.S. drinking water. *Environ. Sci. Technol.* **2009**, *43*, 597–603.
- Bolton, J.; Linden, K. Standardization of methods for fluence (UV dose) determination in bench-scale UV experiments. *J. Environ. Eng.* **2003**, *129*, 209–215.
- Boxall, A. B. A.; Johnson, P.; Smith, E. J.; Sinclair, C. J.; Stutt, E.; Levy, L. S. Uptake of veterinary medicines from soils into plants. *J. Agric. Food Chem.* **2006**, *54*, 2288–2297.
- Buffle, M. O.; Schumacher, J.; Meylan, S.; Jekel, M.; von Gunten, U. Ozonation and advanced oxidation of wastewater: Effect of O<sub>3</sub> dose, pH, DOM and HO• scavengers on ozone decomposition and HO• generation. *Ozone: Science & Engineering* **2006a**, *28*, 247–259.
- Buffle, M. O.; Schumacher, J.; Salhi, E.; Jekel, M.; von Gunten, U. Measurement of the initial phase of ozone decomposition in water and wastewater by means of a continuous quench-flow system: Application to disinfection and pharmaceutical oxidation. *Water Res.* **2006b**, *40*, 1884–1894.
- Burns, N.; Hunter, G.; Jackman, A.; Hulsey, B.; Coughenour, J.; Walz, T. The return of ozone and the hydroxyl radical to wastewater disinfection. *Ozone: Science & Engineering* **2007**, *29*, 303–306.
- California Department of Public Health (CDPH). NDMA and other nitrosamines - Drinking water issues. <http://www.cdph.ca.gov/certlic/drinkingwater/Pages/NDMA.aspx>. 2009a (accessed: Feb. 22, 2013).
- CDPH. Regulations related to recycled water. California Code of Regulations. Titles 22 and 17; 2009b.
- CDPH. Groundwater replenishment reuse draft regulations. <http://www.cdph.ca.gov/certlic/drinkingwater/Documents/Recharge/DraftRechargeReg-2011-11-21.pdf>. 2011 (accessed: Feb. 22, 2013).
- Camacho-Munoz, D.; Martin, J.; Santos, J. L.; Aparicio, I.; Alonso, E. An affordable method for the simultaneous determination of the most studied pharmaceutical compounds as wastewater and surface water pollutants. *J. Sep. Sci.* **2009**, *32*, 3064–3073.
- Chen, W.; Westerhoff, P.; Leenheer, J. A.; Booksh, K. Fluorescence excitation-emission matrix regional integration to quantify spectra for dissolved organic matter. *Environ. Sci. Technol.* **2003**, *37*, 5701–5710.

- Daughton, C. G.; Ternes, T. A. Pharmaceuticals and personal care products in the environment: Agents of subtle change? *Environ. Health Perspect.* **1999**, *107*, 907–938.
- de Velasquez, T. O.; Rojas-Valencia, N.; Ayala, A. Wastewater disinfection using ozone to remove free-living, highly pathogenic bacteria and amoebae. *Ozone: Science & Engineering* **2008**, *30*, 367–375.
- Deborde, M.; Rabouan, S.; Duguet, J. P.; Legube, B. Kinetics of aqueous ozone-induced oxidation of some endocrine disrupters. *Environ. Sci. Technol.* **2005**, *39*, 6086–6092.
- Dietrich, J. P.; Loge, F. J.; Ginn, T. R.; Basagaoglu, H. Inactivation of particle-associated microorganisms in wastewater disinfection: Modeling of ozone and chlorine reactive diffusive transport in polydispersed suspensions. *Water Res.* **2007**, *41*, 2189–2201.
- Dodd, M. C.; Buffle, M. O.; von Gunten, U. Oxidation of antibacterial molecules by aqueous ozone: Moiety-specific reaction kinetics and application to ozone-based wastewater treatment. *Environ. Sci. Technol.* **2006**, *40*, 1969–1977.
- Environmental Protection Agency (EPA). Design Manual: Municipal Wastewater Disinfection. Office of Research and Development. Cincinnati. EPA/625/1-86/021; 1986.
- EPA. Guidelines for Water Reuse. EPA/600/R-12/618. Washington, DC: EPA, Office of Water. <http://nepis.epa.gov/Adobe/PDF/P100FS7K.pdf>. 2012 (accessed: Feb. 22, 2013).
- Escher, B. I.; Bramaz, N.; Ort, C. JEM Spotlight: Monitoring the treatment efficiency of a full scale ozonation on a sewage treatment plant with a mode-of-action based test battery. *J. Environ. Monit.* **2009**, *11*, 1836–1846.
- Escher, B. I.; Bramaz, N.; Quayle, P.; Rutishauser, S.; Vermeirssen, E. L. M. Monitoring of the ecotoxicological hazard potential by polar organic micropollutants in sewage treatment plants and surface waters using a mode-of-action based test battery. *J. Environ. Monit.* **2008**, *10*, 622–631.
- European Union (EU). Directive 2000/60/EC of the European Parliament and of the Council; 2000.
- Fent, K.; Weston, A. A.; Caminada, D. Ecotoxicology of human pharmaceuticals. *Aquat. Toxicol.* **2006**, *76*, 122–159.
- Gagnon, C.; Lajeunesse, A.; Cejka, P.; Gagnon, F.; Hausler, R. Degradation of selected acidic and neutral pharmaceutical products in a primary-treated wastewater by disinfection processes. *Ozone: Science & Engineering* **2008**, *30*, 387–392.
- Gehr, R.; Wagner, M.; Veerasubramanian, P.; Payment, P. Disinfection efficiency of peracetic acid, UV and ozone after enhanced primary treatment of municipal wastewater. *Water Res.* **2003**, *37*, 4573–4586.
- Gerrity, D.; Ryu, H.; Crittenden, J.; Abbaszadegan, M. UV inactivation of adenovirus type 4 measured by integrated cell culture qPCR. *J. Environ. Sci. Health, Part A* **2008**, *43*, 1628–1638.
- Gerrity, D.; Stanford, B. D.; Trenholm, R. A.; Snyder, S. A. An evaluation of a pilot-scale nonthermal plasma advanced oxidation process for trace organic compound degradation. *Water Res.* **2010**, *44*, 493–504.

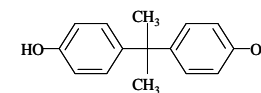
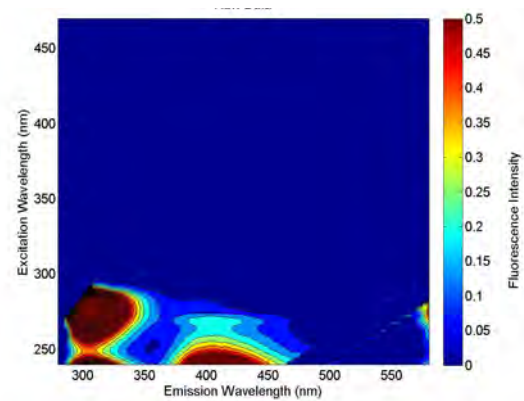
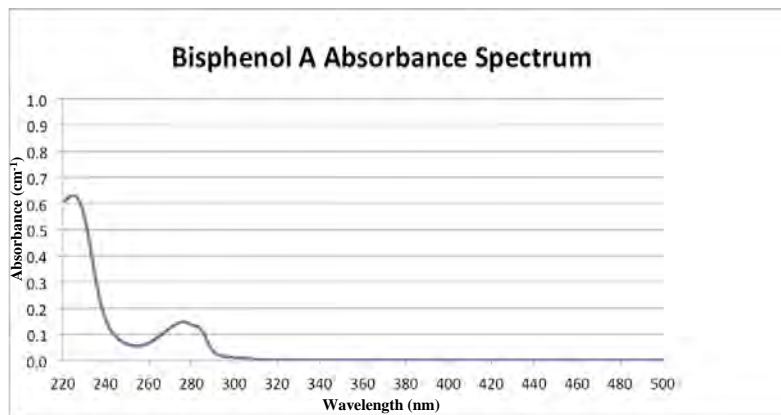
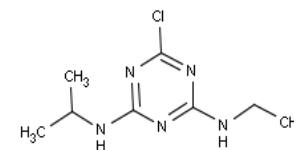
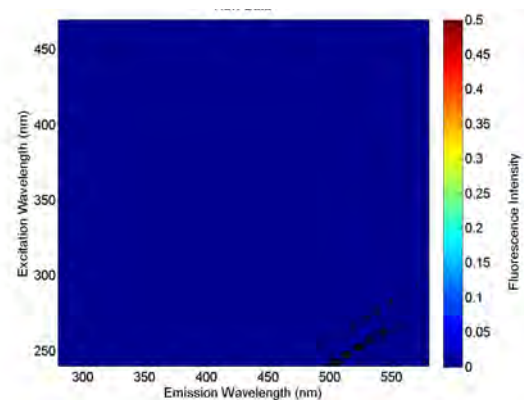
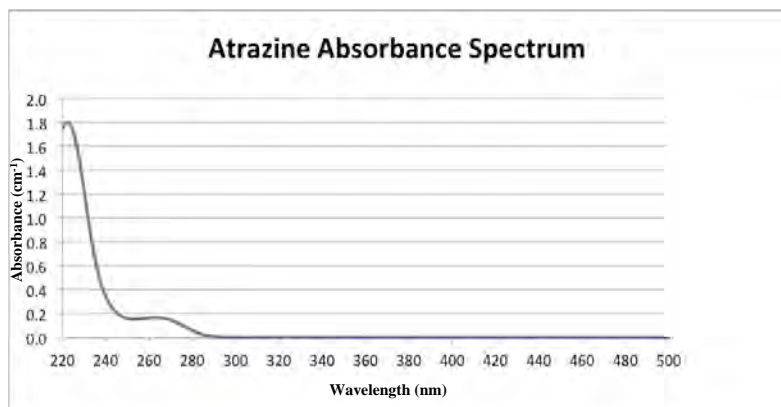
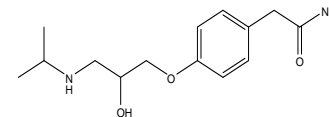
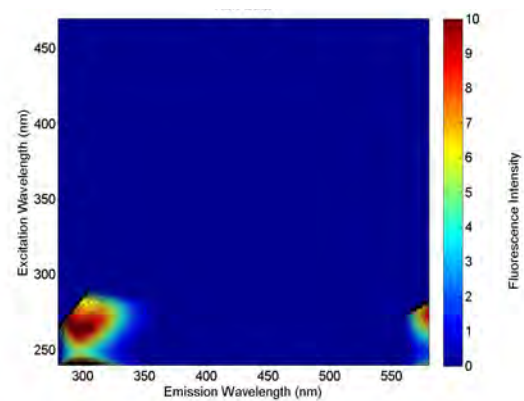
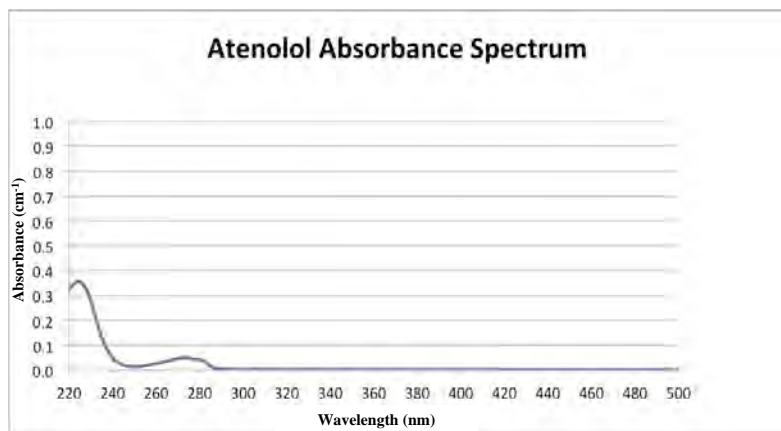
- Hollender, J.; Zimmermann, S. G.; Koepke, S.; Krauss, M.; McArdell, C. S.; Ort, C.; Singer, H.; von Gunten, U.; Siegrist, H. Elimination of organic micropollutants in a municipal wastewater treatment plant upgraded with a full-scale post-ozonation followed by sand filtration. *Environ. Sci. Technol.* **2009**, *43*, 7862–7869.
- Huber, M. M.; Canonica, S.; Park, G. Y.; von Gunten, U. Oxidation of pharmaceuticals during ozonation and advanced oxidation processes. *Environ. Sci. Technol.* **2003**, *37*, 1016–1024.
- Huber, M. M.; Goebel, A.; Joss, A.; Hermann, N.; Loeffler, D.; McArdell, C. S.; Ried, A.; Siegrist, H.; Ternes, T. A.; von Gunten, U. Oxidation of pharmaceuticals during ozonation of municipal wastewater effluents: A pilot study. *Environ. Sci. Technol.* **2005**, *39*, 4290–4299.
- Ishida, C.; Salvesson, A.; Robinson, K.; Bowman, R.; Snyder, S. Ozone disinfection with the HiPOx reactor: Streamlining an "old technology" for wastewater reuse. *Water Sci. Technol.* **2008**, *58*, 1765–1773.
- Kim, S. D.; Cho, J.; Kim, I. S.; Vanderford, B. J.; Snyder, S. A. Occurrence and removal of pharmaceuticals and endocrine disruptors in South Korean surface, drinking, and waste waters. *Water Res.* **2007**, *41*, 1013–1021.
- Kolpin, D. W.; Furlong, E. T.; Meyer, M. T.; Thurman, E. M.; Zaugg, S. D.; Barber, L. B.; Buxton, H. T. Pharmaceuticals, hormones, and other organic wastewater contaminants in U.S. streams, 1999–2000: A national reconnaissance. *Environ. Sci. Technol.* **2002**, *36*, 1202–1211.
- Kuo, J.; Chen, C.; Nellor, M. Standardized collimated beam testing protocol for water/wastewater ultraviolet disinfection. *J. Environ. Eng.* **2003**, *129*, 774–779.
- Lange, A.; Paull, G. C.; Coe, T. S.; Katsu, Y.; Urushitani, H.; Iguchi, T.; Tyler, C. R. Sexual reprogramming and estrogenic sensitization in wild fish exposed to ethinylestradiol. *Environ. Sci. Technol.* **2009**, *43*, 1219–1225.
- Langlais, R. T.; Reckhow, D. A.; Brink, D. R. *Ozone in Water Treatment: Application and Engineering*; Lewis Publishers: Boca Raton, FL, 1991.
- Latch, D. E.; Packer, J. L.; Stender, B. L.; VanOverbeke, J.; Arnold, W. A.; McNeill, K. Aqueous photochemistry of triclosan: Formation of 2,4-dichlorophenol, 2,8-dichlorodibenzo-p-dioxin, and oligomerization products. *Environ. Toxicol. Chem.* **2005**, *24*, 517–525.
- Lienert, J.; Gudel, K.; Escher, B. I. Screening method for ecotoxicological hazard assessment of 42 pharmaceuticals considering human metabolism and excretory routes. *Environ. Sci. Technol.* **2007**, *41*, 4471–4478.
- Liu, C.; Nanaboina, V.; Korshin, G. Spectroscopic study of the degradation of antibiotics and the generation of representative EfOM oxidation products in ozonated wastewater. *Chemosphere* **2012**, *86*, 774–782.
- MacDonald, B. C.; Lvin, S. J.; Patterson, H. Correction of fluorescence inner filter effects and the partitioning of pyrene to dissolved organic carbon. *Anal. Chim. Acta* **1997**, *338*, 155–162.
- Macova, M.; Escher, B. I.; Reungoat, J.; Carswell, S.; Chue, K. L.; Keller, J.; Mueller, J. F. Monitoring the biological activity of micropollutants during advanced wastewater treatment with ozonation and activated carbon filtration. *Water Res.* **2010**, *44*, 477–492.

- Maier, R. M.; Pepper, I. L.; Gerba, C. P. *Environmental Microbiology*; Academic Press: San Diego, CA, 2000.
- McKnight, D. M.; Boyer, E. W.; Westerhoff, P. K.; Doran, P. T.; Kulbe, D. T.; Andersen, D. T. Spectrofluorometric characterization of dissolved organic matter for indication of precursor organic material and aromaticity. *Limnol. Oceanogr.* **2001**, *46*, 38–48.
- Mesquita, M. M. F.; Stimson, J.; Chae, G.-T.; Tufenkji, N.; Ptzcek, C. J.; Blowes, D. W.; Emelko, M. B. Optimal preparation and purification of PRD1-like bacteriophages for use in environmental fate and transport studies. *Water Res.* **2010**, *44*, 1114–1125.
- Mezzanotte, V.; Antonelli, M.; Citterio, S.; Nurizzo, C. Wastewater disinfection alternatives: Chlorine, ozone, peracetic acid, and UV light. *Water Environ. Res.* **2007**, *79*, 2373–2379.
- Nakada, N.; Shinohara, H.; Murata, A.; Kiri, K.; Managaki, S.; Sato, N.; Takada, H. Removal of selected pharmaceuticals and personal care products (PPCPs) and endocrine-disrupting chemicals (EDCs) during sand filtration and ozonation at a municipal sewage treatment plant. *Water Res.* **2007**, *41*, 4373–4382.
- Nanaboina, V.; Korshin, G. V. Evolution of absorbance spectra of ozonated wastewater and its relationship with the degradation of trace-level organic species. *Environ. Sci. Technol.* **2010**, *44*, 6130–6137.
- Packer, J. L.; Werner, J. J.; Latch, D. E.; McNeill, K.; Arnold, W. A. Photochemical fate of pharmaceuticals in the environment. *Aquat. Sci.* **2003**, *65*, 342–351.
- Pisarenko, A. N.; Stanford, B. D.; Yan, D.; Gerrity, D.; Snyder, S. A. Effects of ozone and ozone/peroxide on trace organic contaminants and NDMA in drinking water and water reuse applications. *Water Res.* **2012**, *46*, 316–326.
- R\_Development\_Core\_Team. R: A language and environment for statistical computing, v. 2.4.0; The R Foundation for Statistical Computing: Vienna, Austria, 2006.
- Razavi, B.; Song, W.; Cooper, W. J.; Greaves, J.; Jeong, J. Free-radical-induced oxidative and reductive degradation of fibrate pharmaceuticals: Kinetic studies and degradation mechanisms. *J. Phys. Chem. A* **2009**, *113*, 1287–1294.
- Reungoat, J.; Macova, M.; Escher, B. I.; Carswell, S.; Mueller, J. F.; Keller, J. Removal of micropollutants and reduction of biological activity in a full scale reclamation plant using ozonation and activated carbon filtration. *Water Res.* **2010**, *44*, 625–637.
- Ritz, C.; Streibig, J. C. Bioassay analysis using R. *Journal of Statistical Software* **2005**, *12*.
- Rosario-Ortiz, F. L.; Wert, E. C.; Snyder, S. A. Evaluation of UV/H<sub>2</sub>O<sub>2</sub> treatment for the oxidation of pharmaceuticals in wastewater. *Water Res.* **2010**, *44*, 1440–1448.
- Rosenfeldt, E. J.; Linden, K. G.; Canonica, S.; von Gunten, U. Comparison of the efficiency of •OH radical formation during ozonation and the advanced oxidation processes O<sub>3</sub>/H<sub>2</sub>O<sub>2</sub> and UV/H<sub>2</sub>O<sub>2</sub>. *Water Res.* **2006**, *40*, 3695–3704.
- Routledge, E. J.; Sumpter, J. P. Estrogenic activity of surfactants and some of their degradation products assessed using a recombinant yeast screen. *Environ. Toxicol. Chem.* **1996**, *15*, 241–248.
- Schriks, M.; Heringa, M. B.; van der Kooi, M. M. E.; de Voogt, P.; van Wezel, A. P. Toxicological relevance of emerging contaminants for drinking water quality. *Water Res.* **2010**, *44*, 461–476.

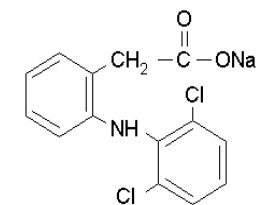
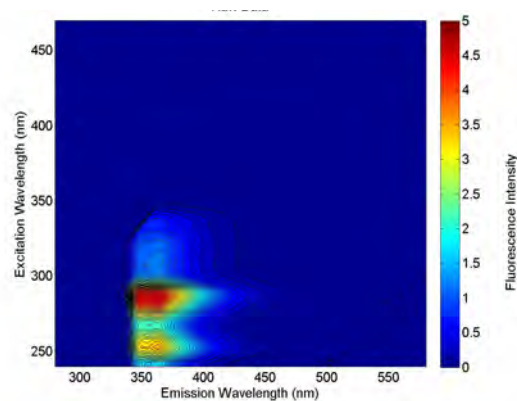
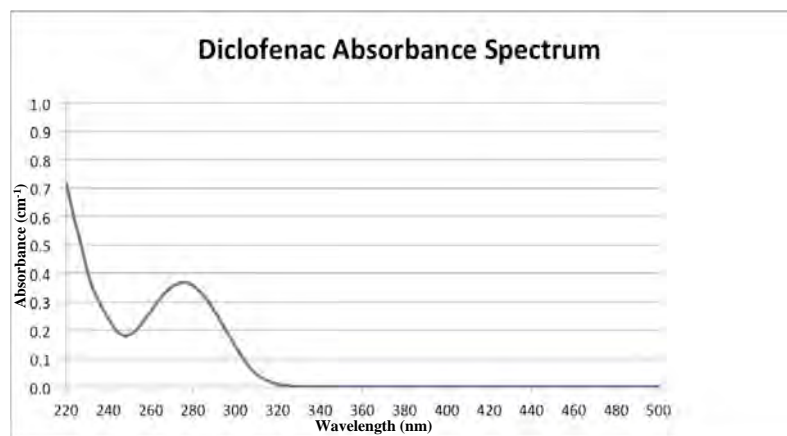
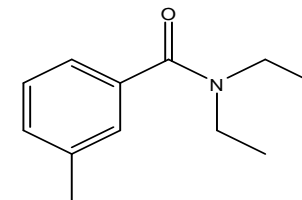
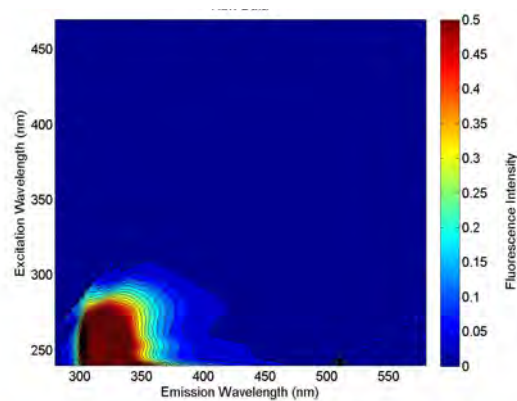
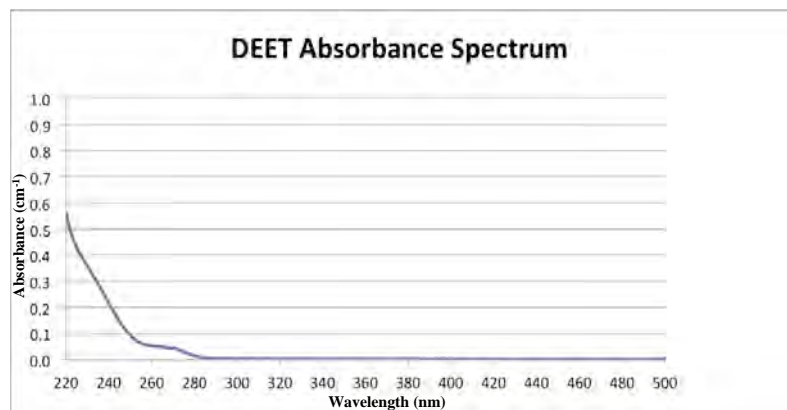
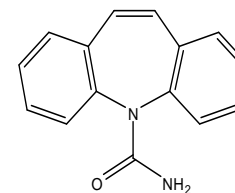
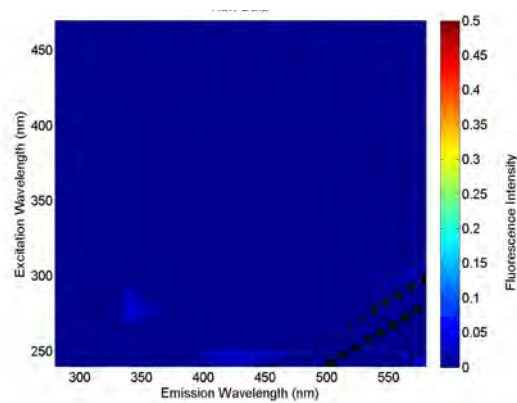
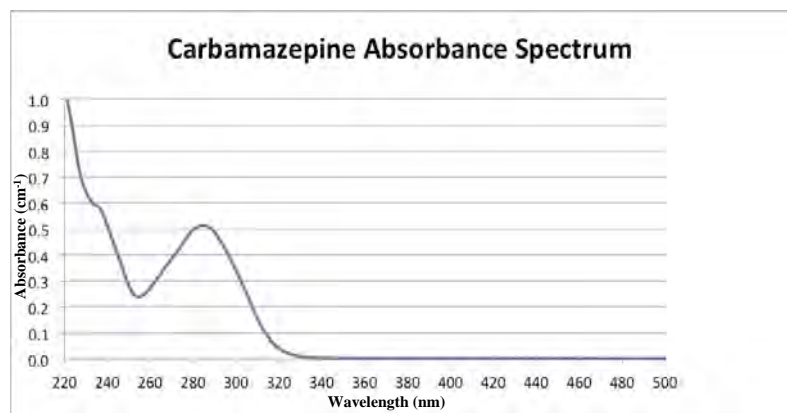
- Snyder, S.; Vanderford, B.; Pearson, R.; Quinones, O.; Yoon, Y. Analytical methods used to measure endocrine disrupting compounds in water. *Pract. Periodical Hazard., Toxic, Radioact. Waste Manage.* **2003a**, *7*, 224–234.
- Snyder, S. A.; Westerhoff, P.; Yoon, Y.; Sedlak, D. L. Pharmaceuticals, personal care products, and endocrine disruptors in water: Implications for the water industry. *Environ. Engin. Sci.* **2003b**, *20*, 449–469.
- Snyder, S. A.; Wert, E. C.; Rexing, D. J.; Zegers, R. E.; Drury, D. D. Ozone oxidation of endocrine disruptors and pharmaceuticals in surface water and wastewater. *Ozone: Science & Engineering* **2006**, *28*, 445–460.
- Snyder, S. A.; Wert, E. C.; Lei, H.; Westerhoff, P.; Yoon, Y. *Removal of EDCs and Pharmaceuticals in Drinking and Reuse Treatment Processes*; American Water Works Association Research Foundation. IWA Publishing: London, UK, 2007.
- Snyder, S. A.; Trenholm, R. A.; Snyder, E. M.; Bruce, G. M.; Pleus, R. C.; Hemming, J. D. C. *Toxicological Relevance of EDCs and Pharmaceuticals in Drinking Water*; American Water Works Association Research Foundation. IWA Publishing: London, UK, 2008a.
- Snyder, S. A.; Vanderford, B. J.; Drewes, J.; Dickenson, E.; Snyder, E. M.; Bruce, G. M.; Pleus, R. C. *State of Knowledge of Endocrine Disruptors and Pharmaceuticals in Drinking Water*; American Water Works Association Research Foundation. IWA Publishing: London, UK, 2008b.
- Song, W.; Cooper, W. J.; Peake, B. M.; Mezyk, S. P.; Nickelsen, M. G.; O'Shea, K. E. Free-radical induced oxidative and reductive degradation of N,N-diethyl-meta-toluamide (DEET): Kinetic studies and degradation pathways. *Water Res.* **2009**, *43*, 635–642.
- Stalter, D.; Magdeburg, A.; Oehlmann, J. Comparative toxicity assessment of ozone and activated carbon treated sewage effluents using an in vivo test battery. *Water Res.* **2010a**, *44*, 2610–2620.
- Stalter, D.; Magdeburg, A.; Weil, M.; Knacker, T.; Oehlmann, J. Toxication or detoxication? In vivo toxicity assessment of ozonation as advanced wastewater treatment with the rainbow trout. *Water Res.* **2010b**, *44*, 439–448.
- Stevens-Garmon, J.; Drewes, J. E.; Khan, S. J.; McDonald, J. A.; Dickenson, E. R. Sorption of emerging trace organic compounds onto wastewater sludge solids. *Water Res.* **2011**, *45*, 3417–3426.
- Suarez, S.; Dodd, M. C.; Omil, F.; von Gunten, U. Kinetics of triclosan oxidation by aqueous ozone and consequent loss of antibacterial activity: Relevance to municipal wastewater ozonation. *Water Res.* **2007**, *41*, 2481–2490.
- Sundaram, V.; Emerick, R. W.; Shumaker, S. E. Field evaluation of MF-Ozone-BAC process train for the removal of microconstituents from wastewater effluent. 24th Annual WateReuse Symposium, Seattle, WA, September 13–16, 2009.
- Ternes, T. A. Occurrence of drugs in German sewage treatment plants and rivers. *Water Res.* **1998**, *32*, 3245–3260.
- Ternes, T. A.; Meisenheimer, M.; McDowell, D.; Sacher, F.; Brauch, H. J.; Haist-Gulde, B.; Preuss, G.; Wilme, U.; Zulei-Seibert, N. Removal of pharmaceuticals during drinking water treatment. *Environ. Sci. Technol.* **2002**, *36*, 3855–3863.

- Thurston-Enriquez, J. A.; Haas, C. N.; Jacangelo, J.; Riley, K.; Gerba, C. P. Inactivation of feline calicivirus and adenovirus type-40 by UV radiation. *Appl. Environ. Microbiol.* **2003**, *69*, 577–582.
- Trenholm, R. A.; Vanderford, B. J.; Holady, J. C.; Rexing, D. J.; Snyder, S. A. Broad range analysis of endocrine disruptors and pharmaceuticals using gas chromatography and liquid chromatography tandem mass spectrometry. *Chemosphere* **2006**, *65*, 1990–1998.
- Trenholm, R. A.; Vanderford, B. J.; Snyder, S. A. On-line solids phase extraction LC-MS/MS analysis of pharmaceutical indicators in water: A green alternative to conventional methods. *Talanta* **2009**, *79*, 1425–1432.
- Tyler, C. R.; Jobling, S. Roach, sex, and gender-bending chemicals: The feminization of wild fish in English rivers. *Bioscience* **2008**, *58*, 1051–1059.
- Vanderford, B. J.; Pearson, R. A.; Rexing, D. J.; Snyder, S. A. Analysis of endocrine disruptors, pharmaceuticals, and personal care products in water using liquid chromatography/tandem mass spectrometry. *Anal. Chem.* **2003**, *75*, 6265–6274.
- Vanderford, B. J.; Snyder, S. A. Analysis of pharmaceuticals in water by isotope dilution liquid chromatography/tandem mass spectrometry. *Environ. Sci. Technol.* **2006**, *40*, 7312–7320.
- Vanderford, B. J.; Rosario-Ortiz, F. L.; Snyder, S. A. Analysis of p-chlorobenzoic acid in water by liquid chromatography-tandem mass spectrometry. *J. Chromatogr.* **2007**, *1164*, 219–223.
- Vanderford, B. J.; Mawhinney, D. B.; Rosario-Ortiz, F. L.; Snyder, S. A. Real-time detection and identification of aqueous chlorine transformation products using QTOF MS. *Anal. Chem.* **2008**, *80*, 4193–4199.
- Watts, M. J.; Linden, K. G. Advanced oxidation kinetics of aqueous trialkyl phosphate flame retardants and plasticizers. *Environ. Sci. Technol.* **2009**, *43*, 2937–2942.
- Wert, E. C.; Rosario-Ortiz, F. L.; Snyder, S. A. Effect of ozone exposure on the oxidation of trace organic contaminants in wastewater. *Water Res.* **2009a**, *43*, 1005–1014.
- Wert, E. C.; Rosario-Ortiz, F. L.; Snyder, S. A. Using ultraviolet absorbance and color to assess pharmaceutical oxidation during ozonation of wastewater. *Environ. Sci. Technol.* **2009b**, *43*, 4858–4863.
- Westerhoff, P.; Chen, W.; Esparza, M. Fluorescence analysis of a standard fulvic acid and tertiary treated wastewater. *J. Environ. Qual.* **2001**, *30*, 2037–2046.
- Westerhoff, P.; Yoon, Y.; Snyder, S.; Wert, E. Fate of endocrine-disruptor, pharmaceutical, and personal care product chemicals during simulated drinking water treatment processes. *Environ. Sci. Technol.* **2005**, *39*, 6649–6663.
- Xu, P.; Janex, M.; Savoye, P.; Cockx, A.; Lazarova, V. Wastewater disinfection by ozone: Main parameters for process design. *Water Res.* **2002**, *36*, 1043–1055.
- Yates, M. V.; Malley, J.; Rochelle, P.; Hoffman, R. Effect of adenovirus resistance on UV disinfection requirements: A report on the state of adenovirus science. *JAWWA* **2006**, *98*, 93–106.

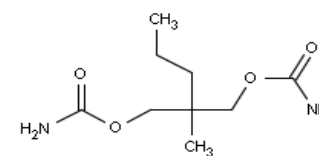
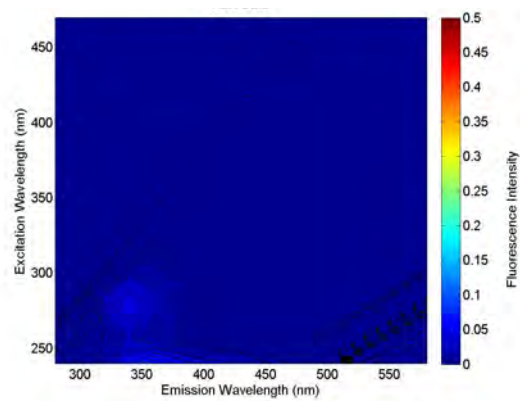
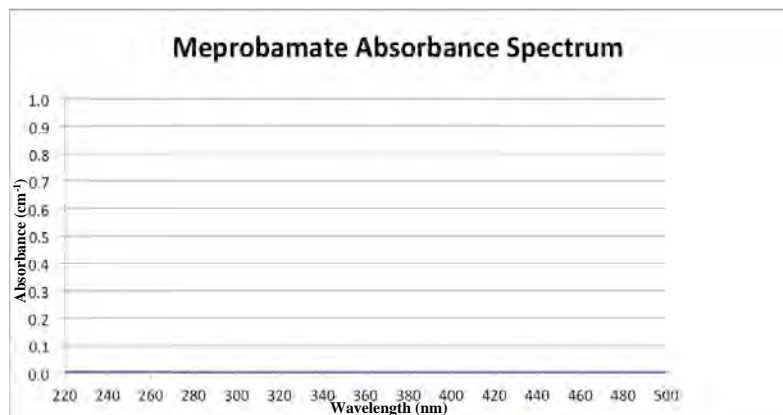
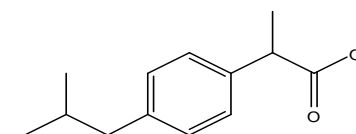
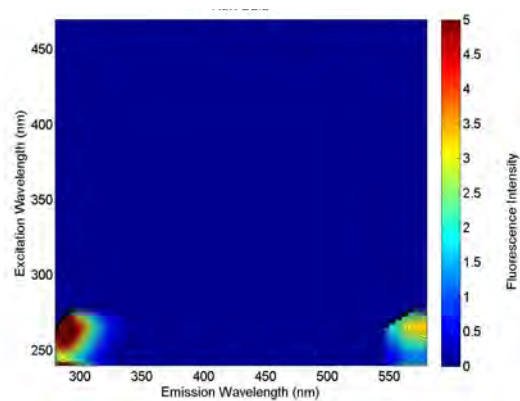
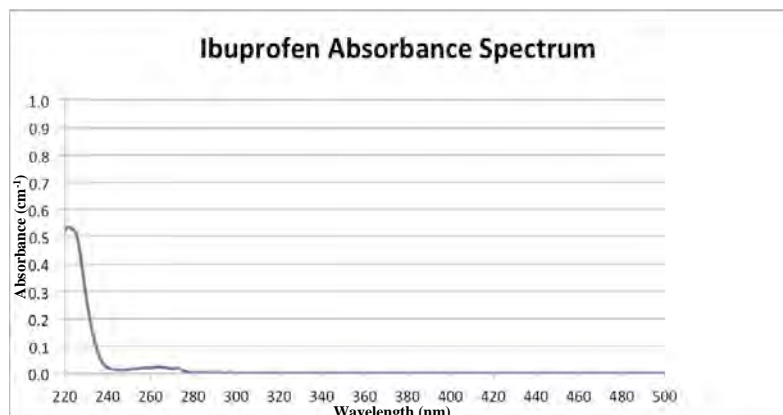
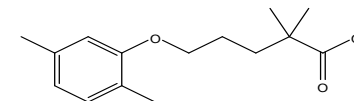
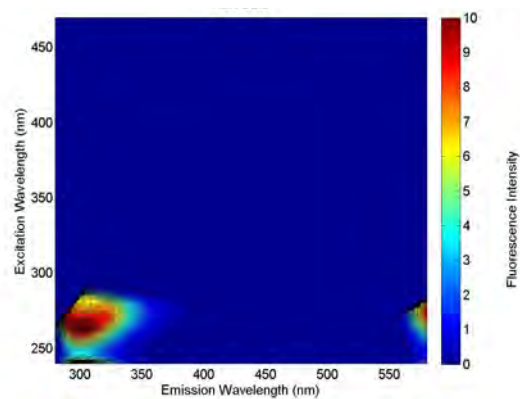
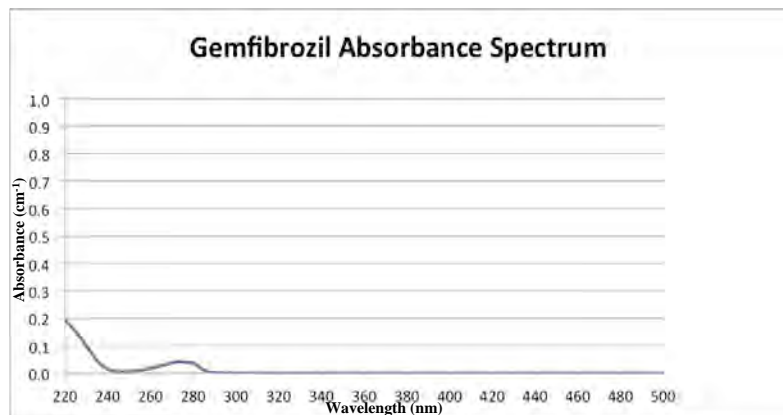
Appendix 1  
Organic Characterization of Target Compounds



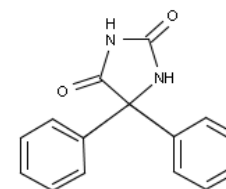
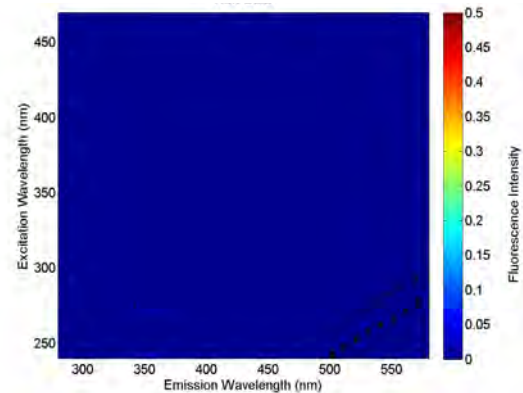
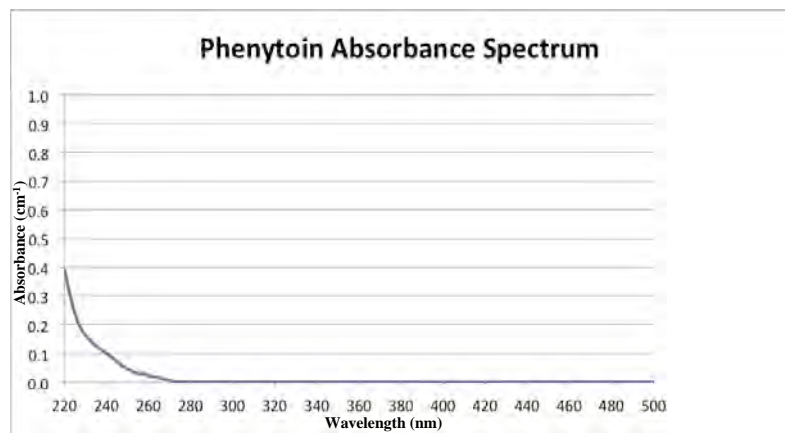
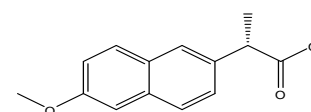
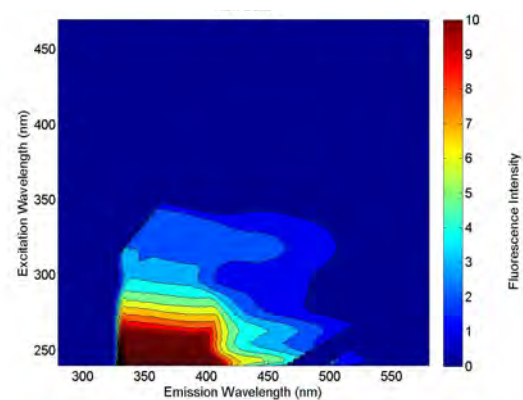
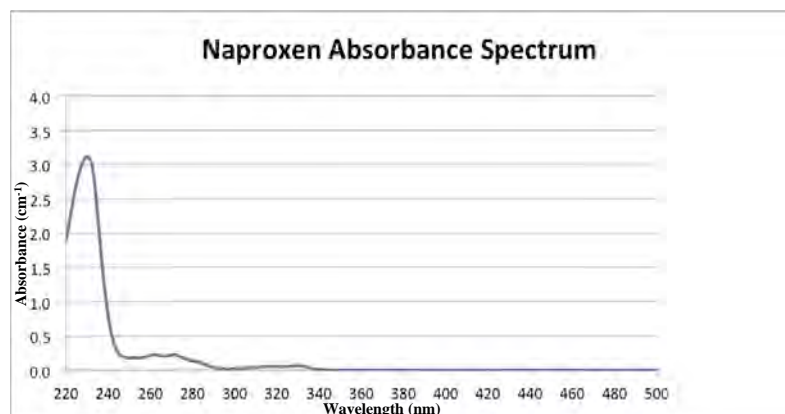
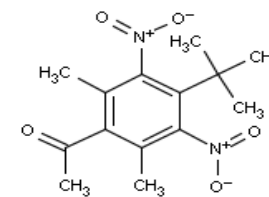
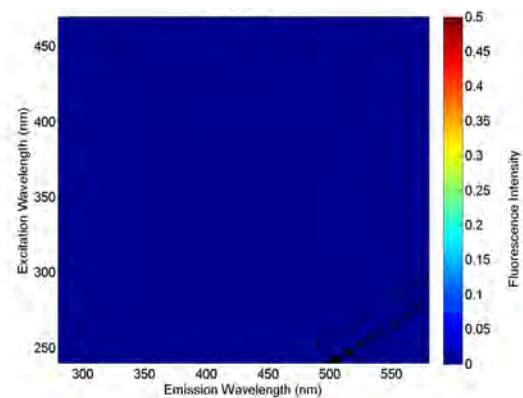
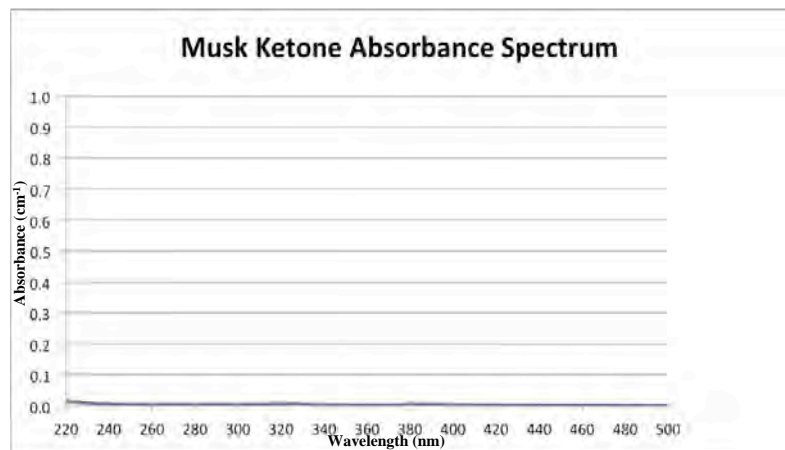
Appendix 1  
Organic Characterization of Target Compounds



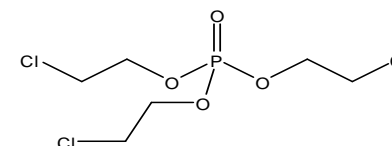
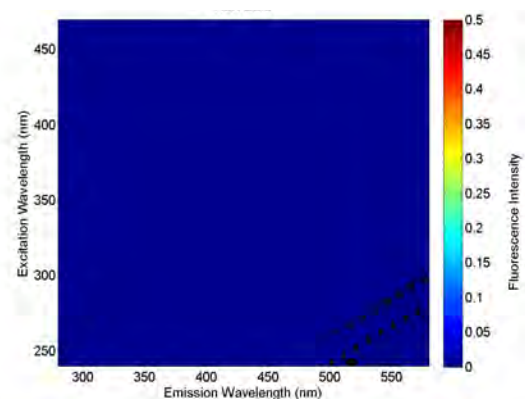
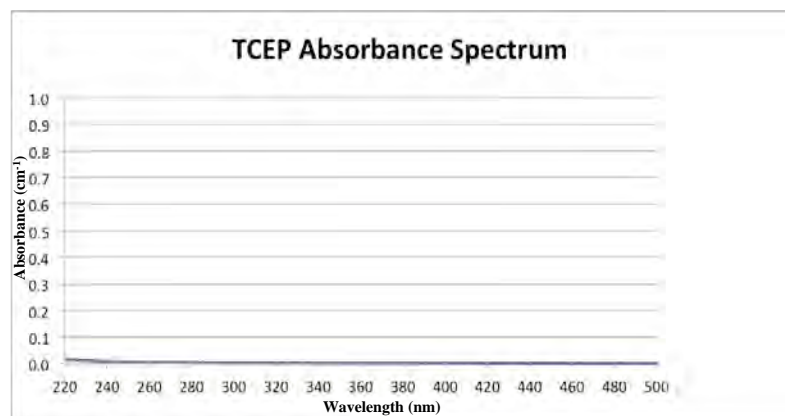
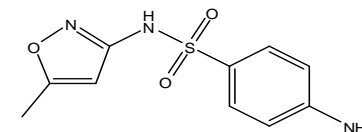
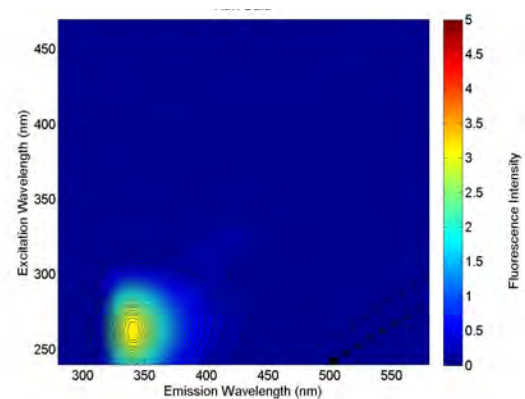
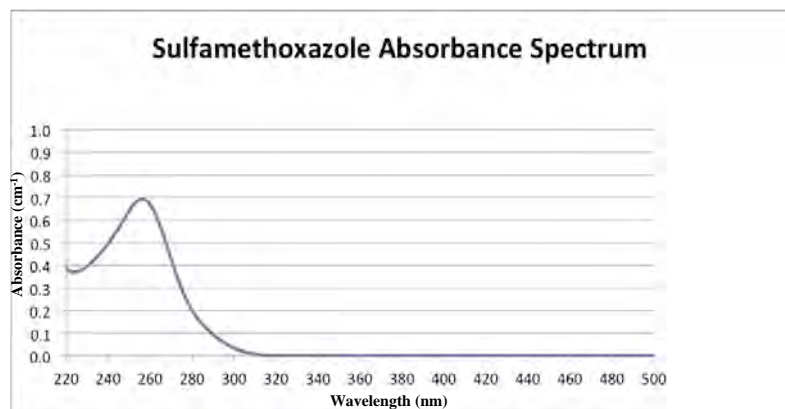
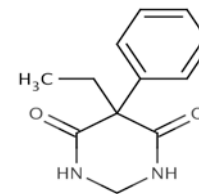
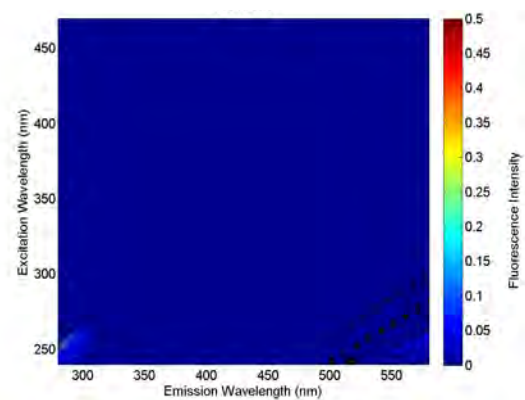
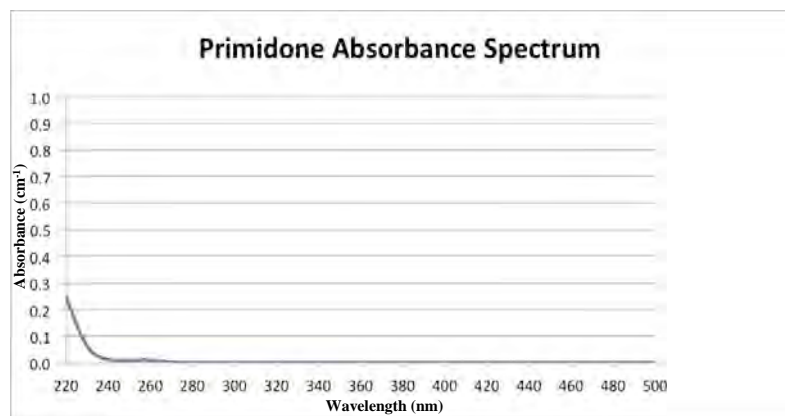
Appendix 1  
Organic Characterization of Target Compounds



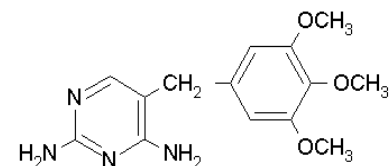
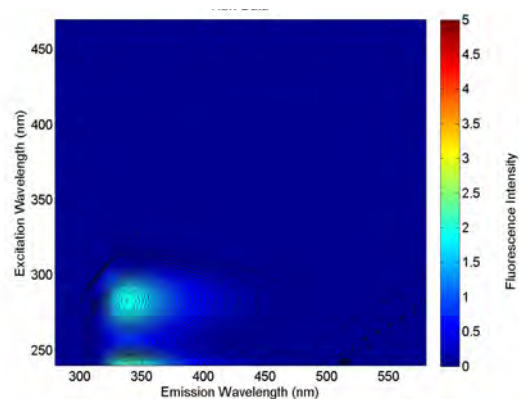
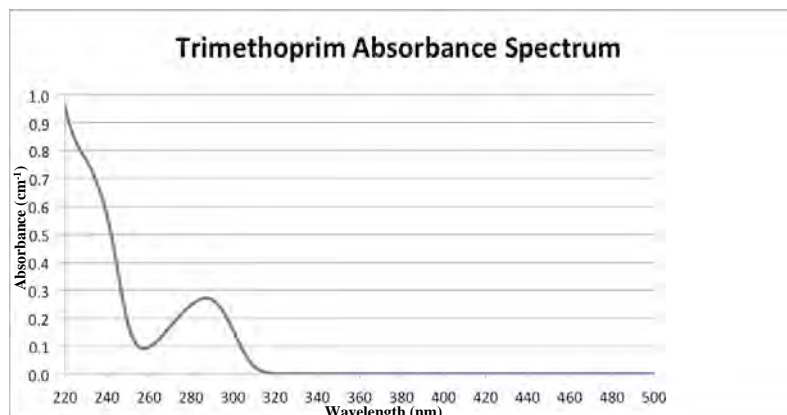
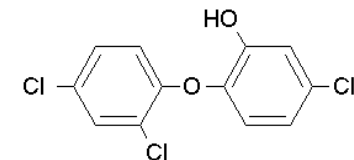
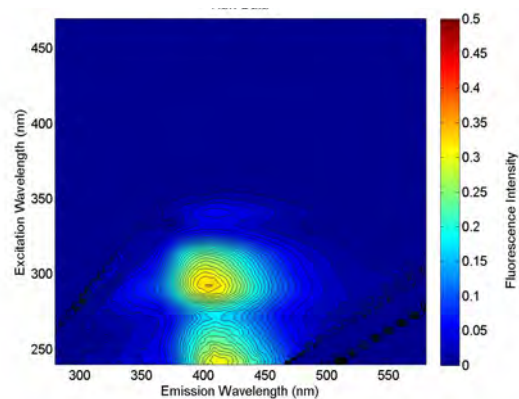
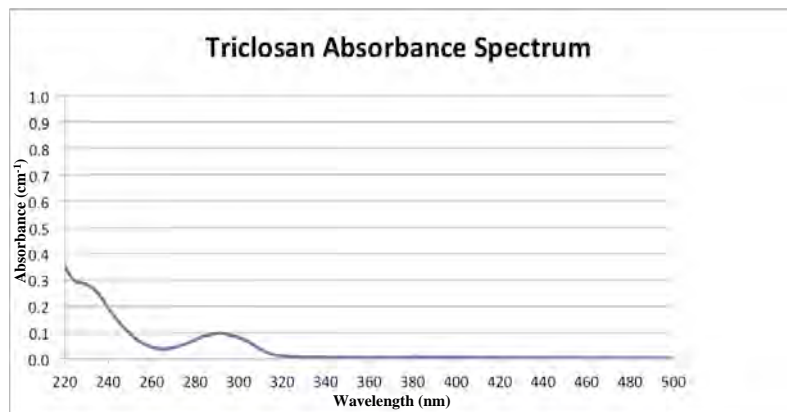
Appendix 1  
Organic Characterization of Target Compounds



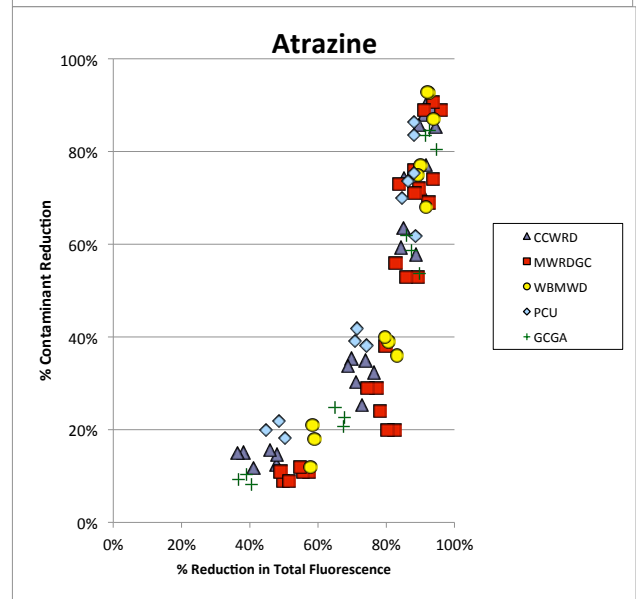
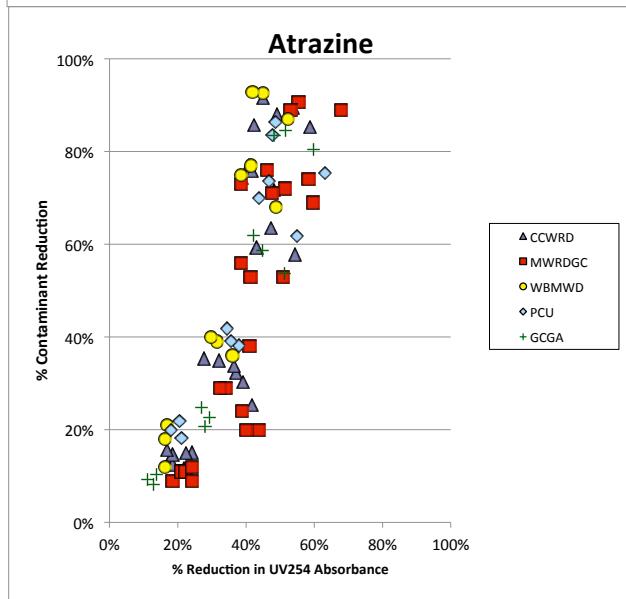
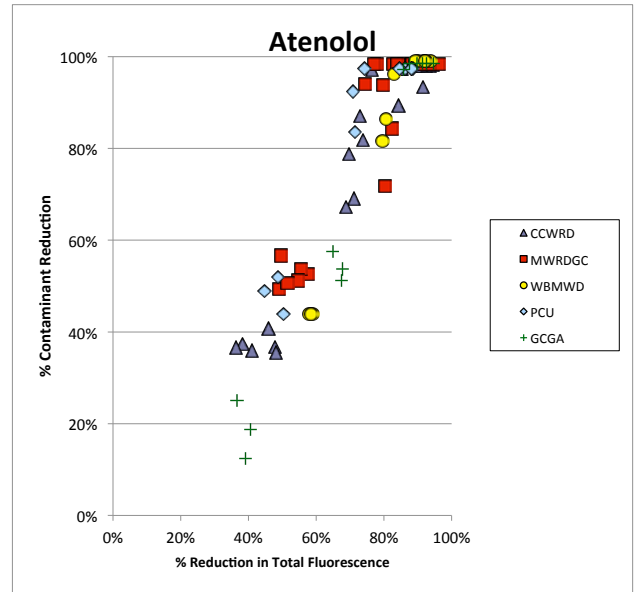
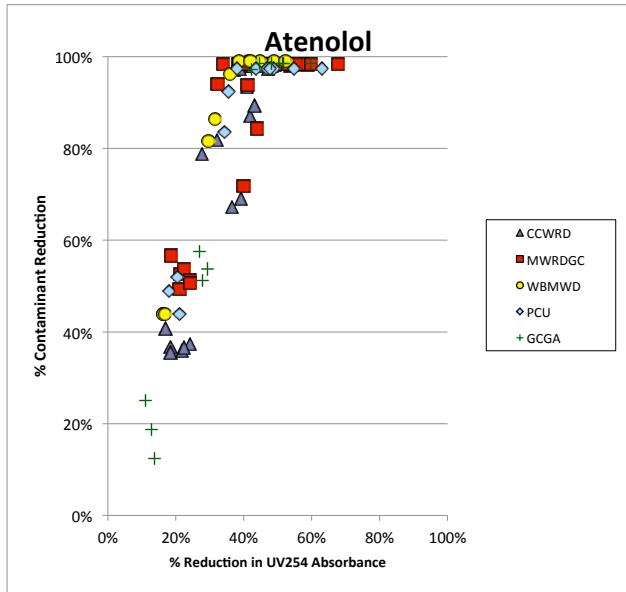
Appendix 1  
Organic Characterization of Target Compounds



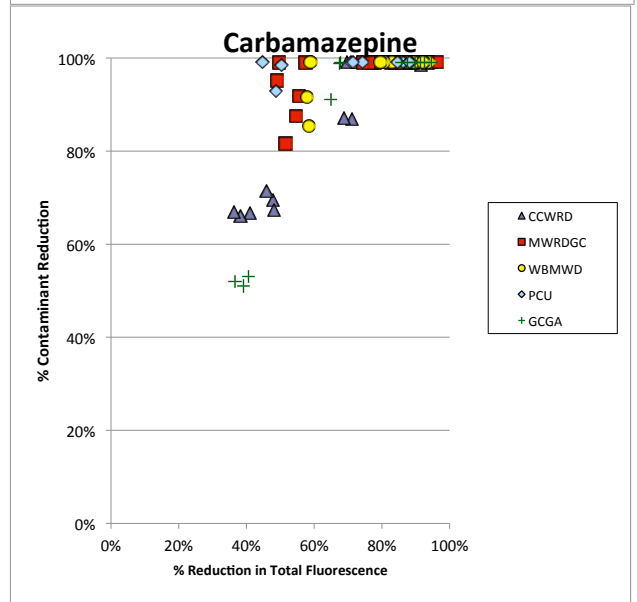
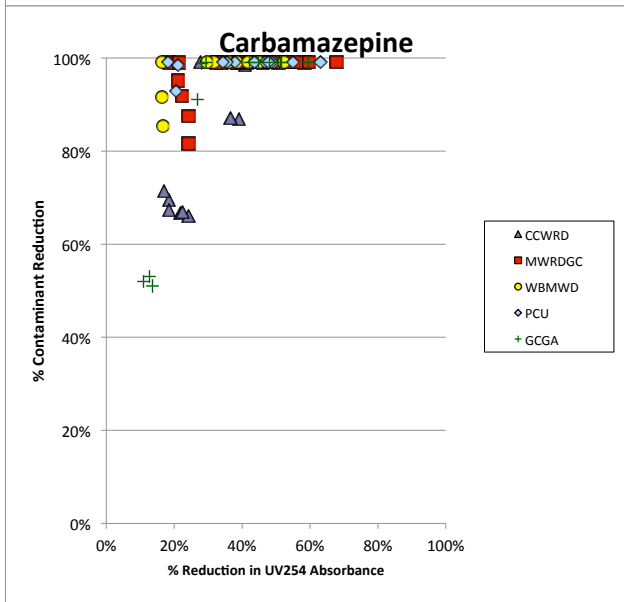
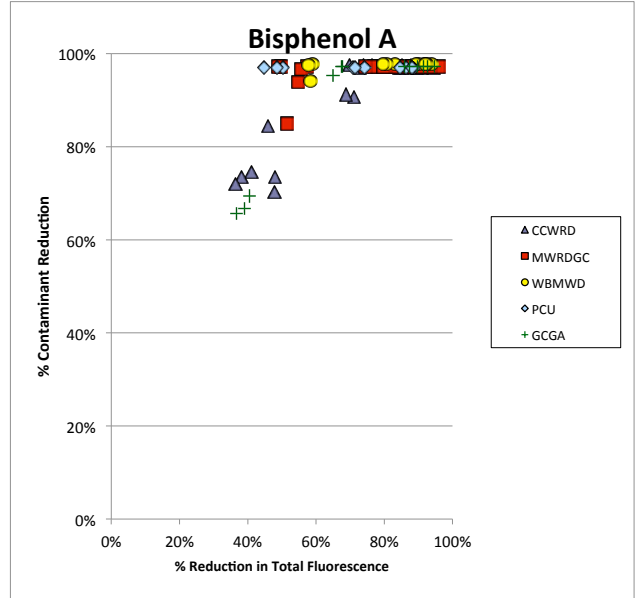
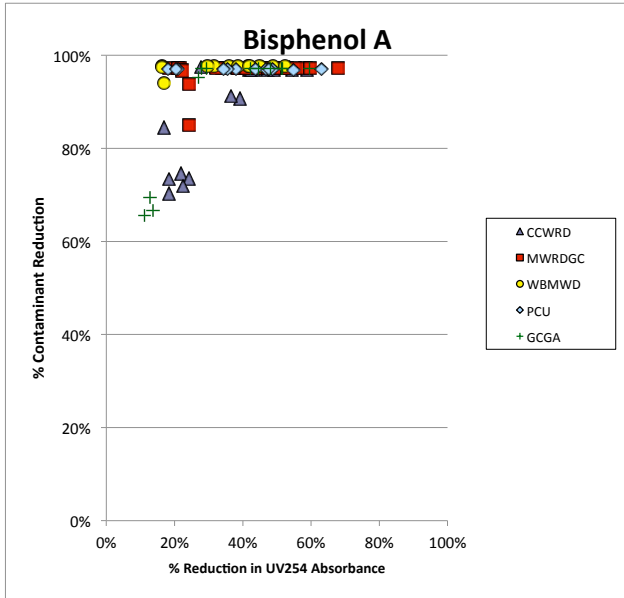
Appendix 1  
Organic Characterization of Target Compounds



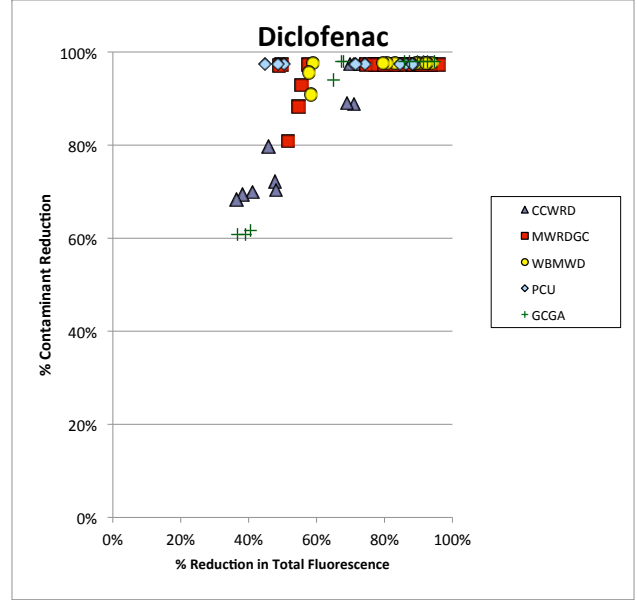
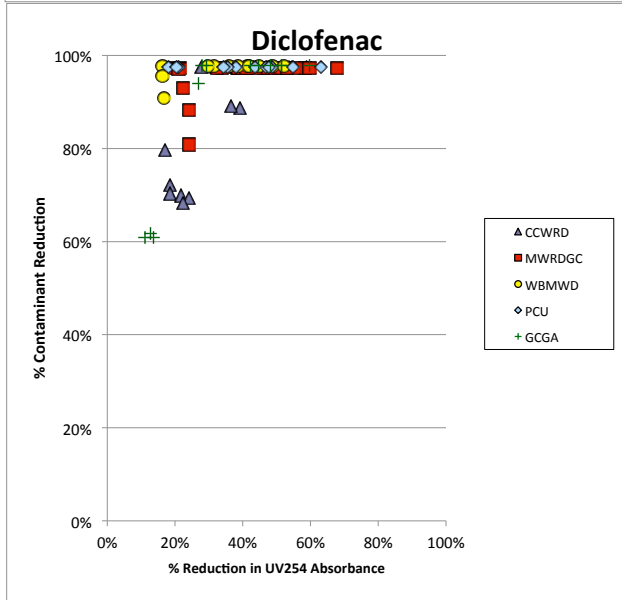
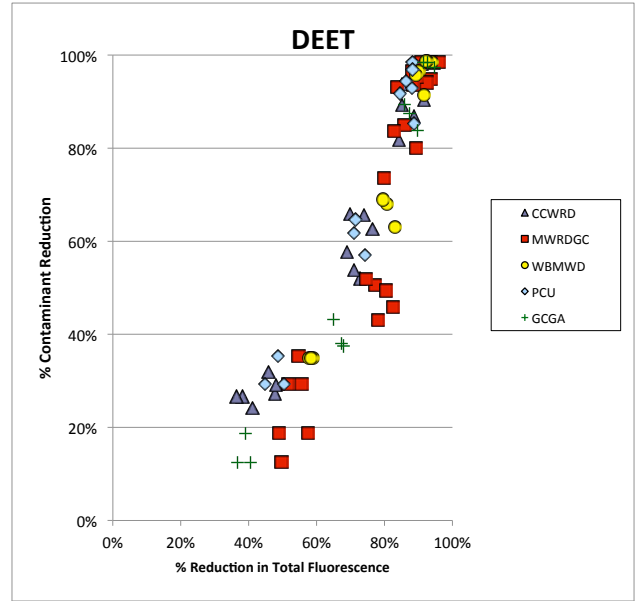
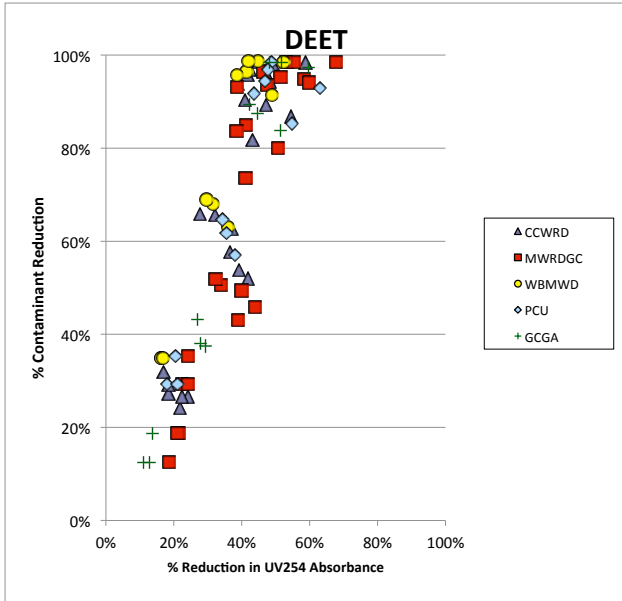
## Appendix 2 Comparison of Secondary Effluents Ozone and Ozone/H2O2 Correlations



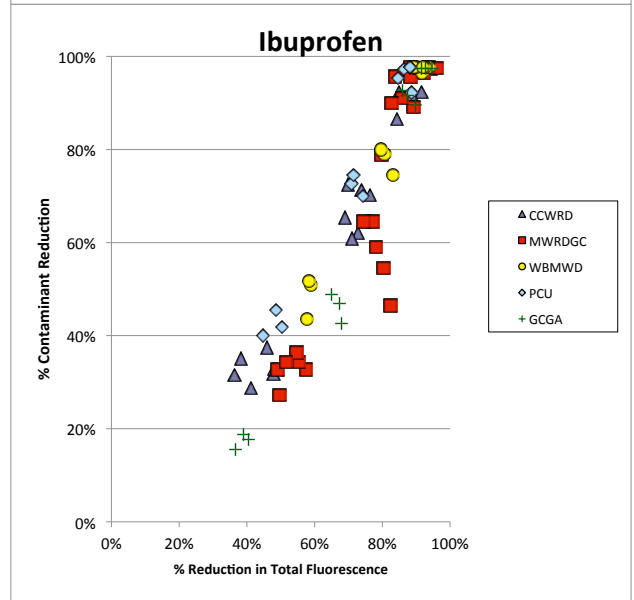
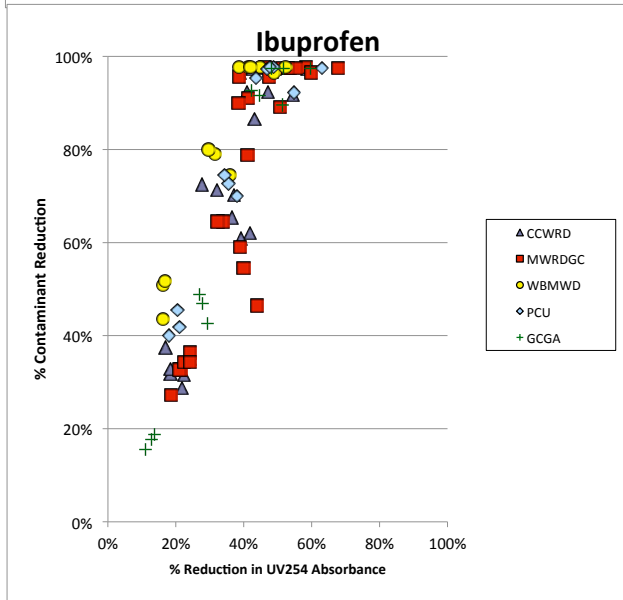
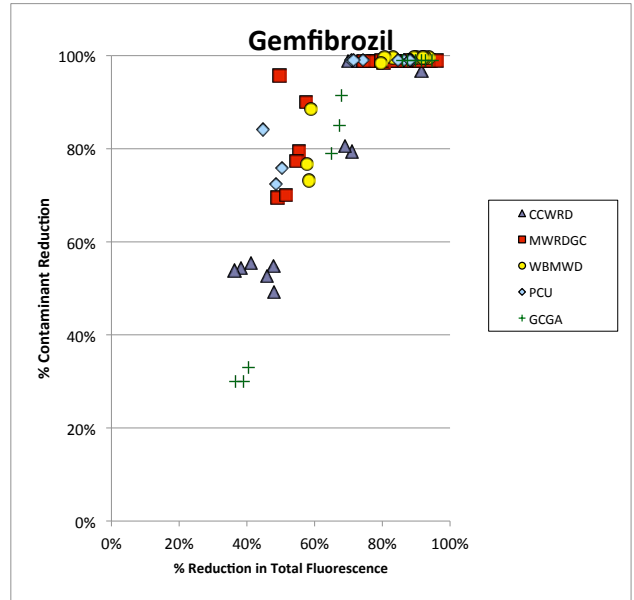
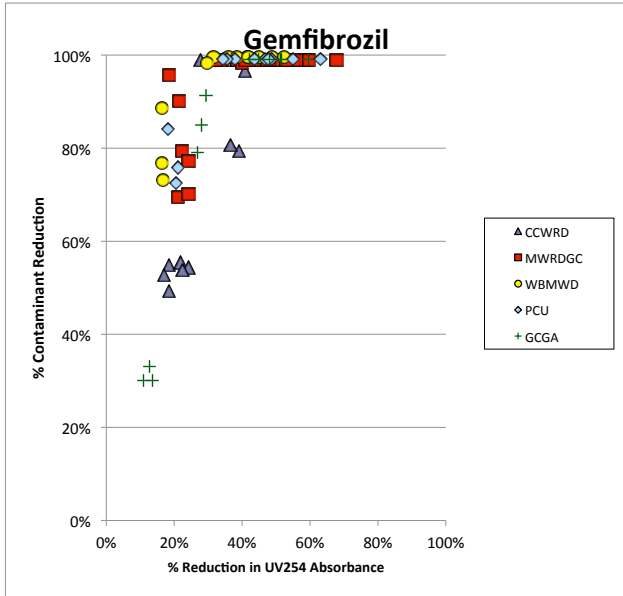
## Appendix 2 Comparison of Secondary Effluents Ozone and Ozone/H2O2 Correlations



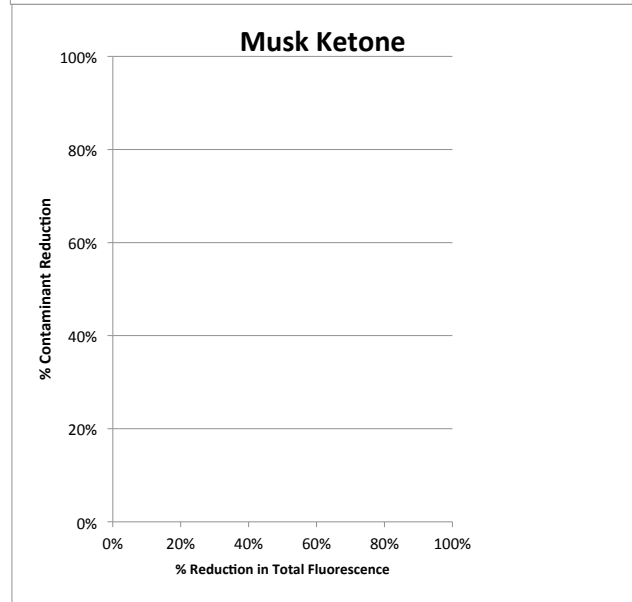
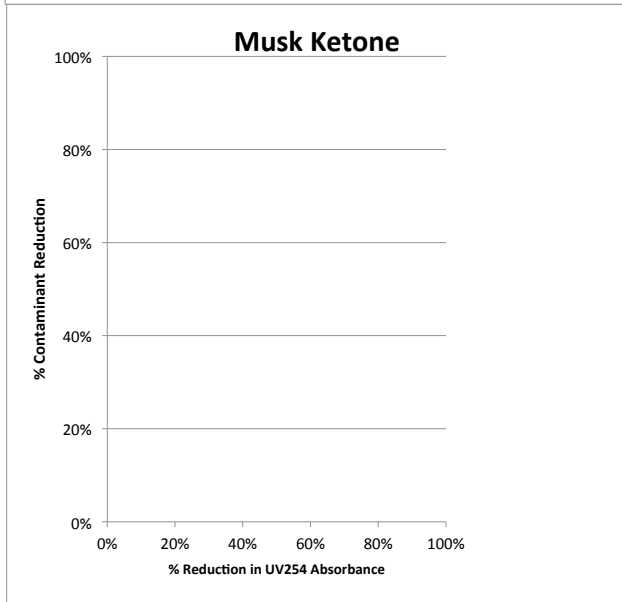
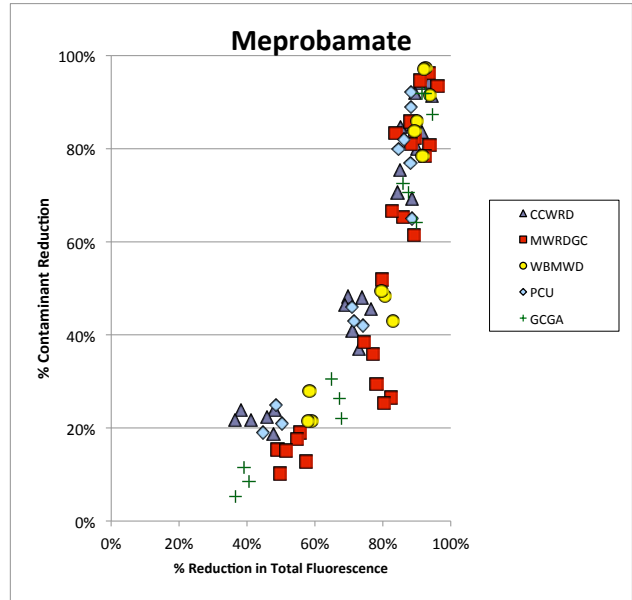
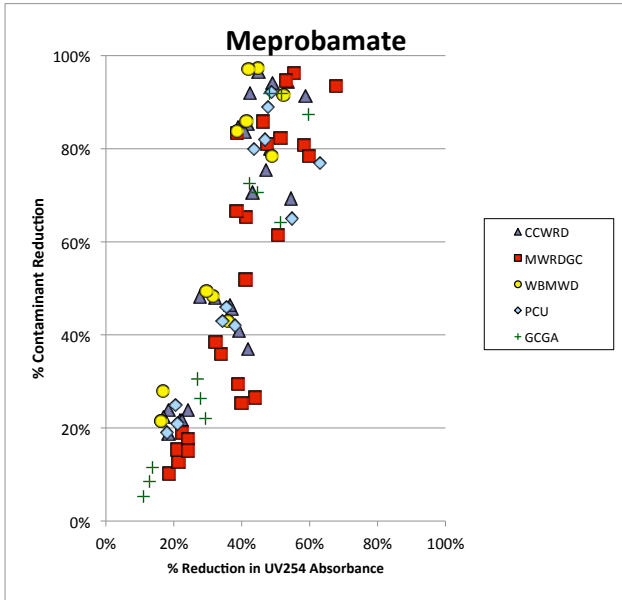
## Appendix 2 Comparison of Secondary Effluents Ozone and Ozone/H2O2 Correlations



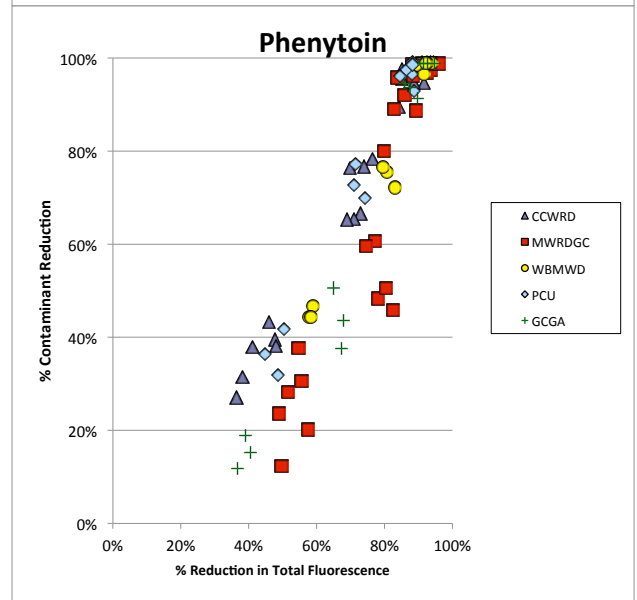
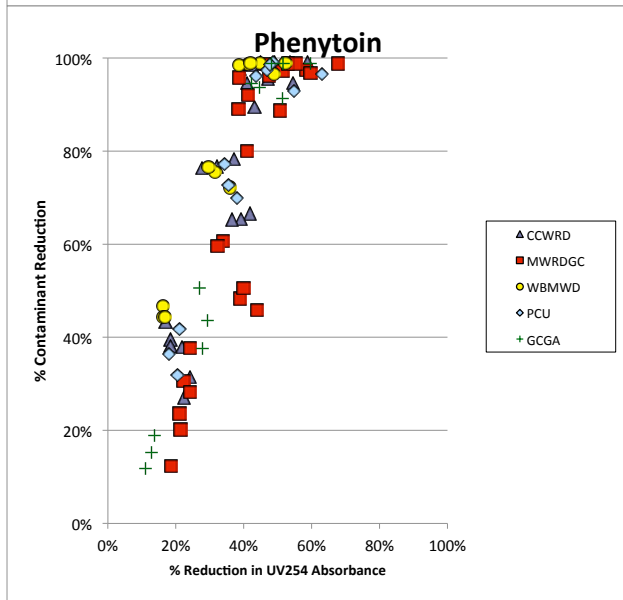
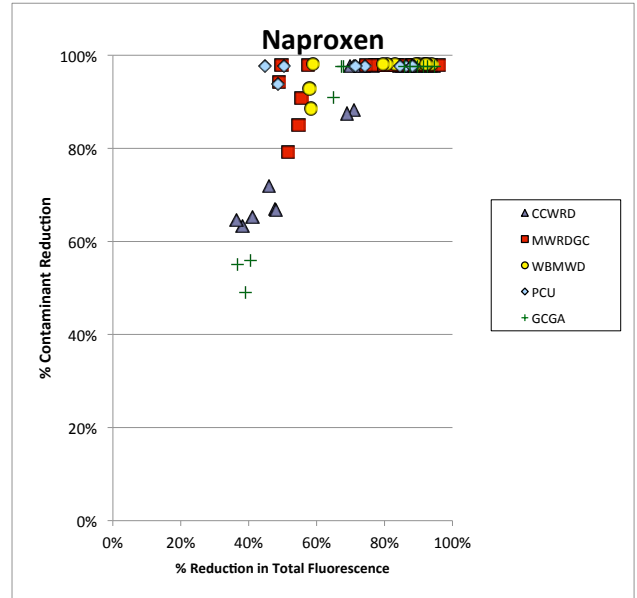
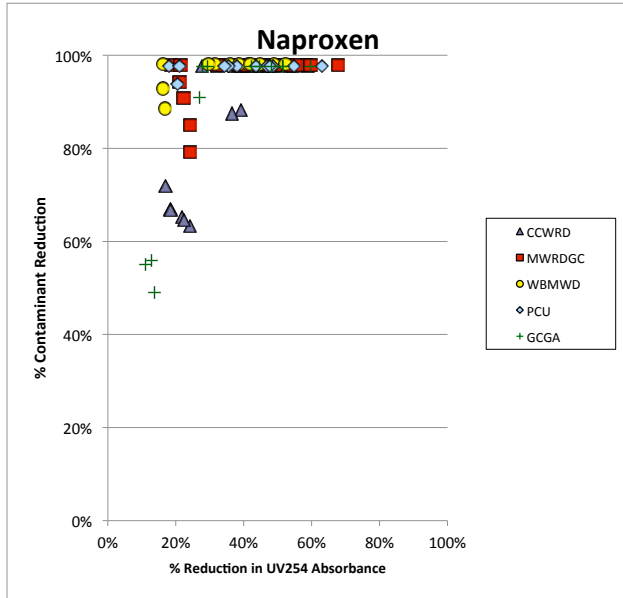
## Appendix 2 Comparison of Secondary Effluents Ozone and Ozone/H2O2 Correlations



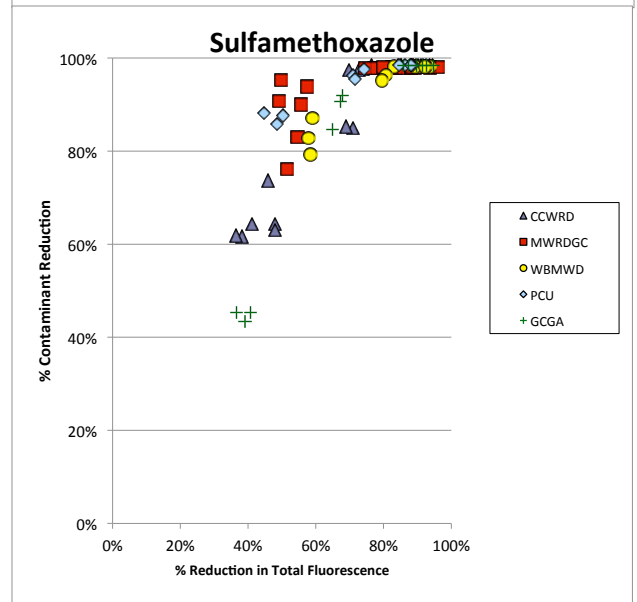
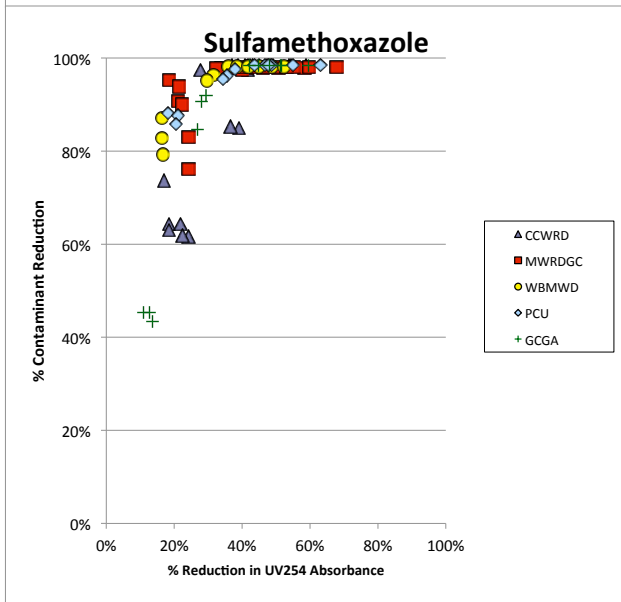
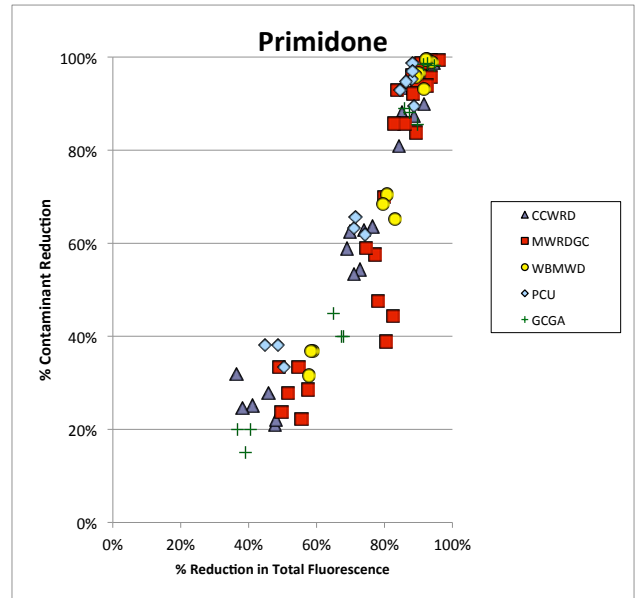
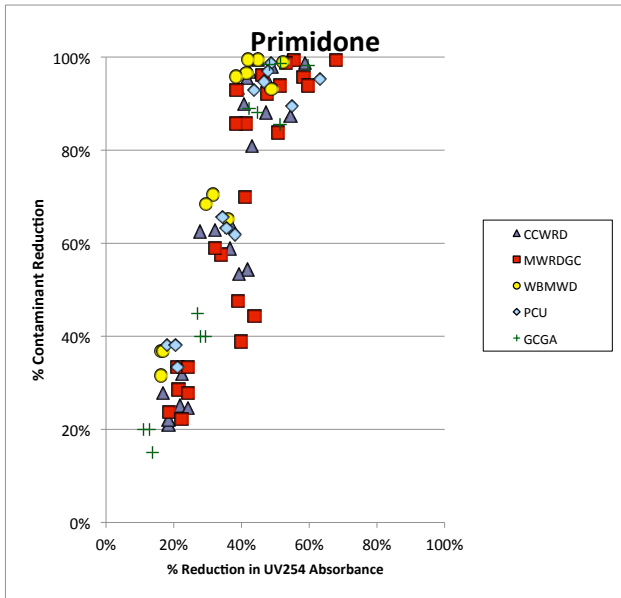
## Appendix 2 Comparison of Secondary Effluents Ozone and Ozone/H2O2 Correlations



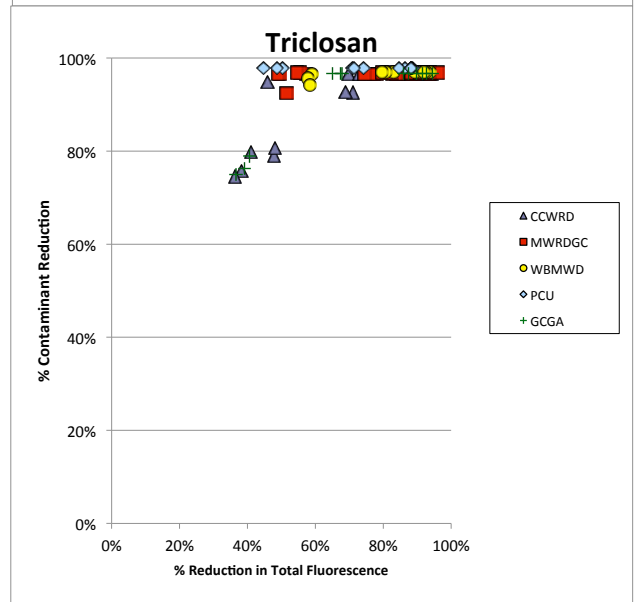
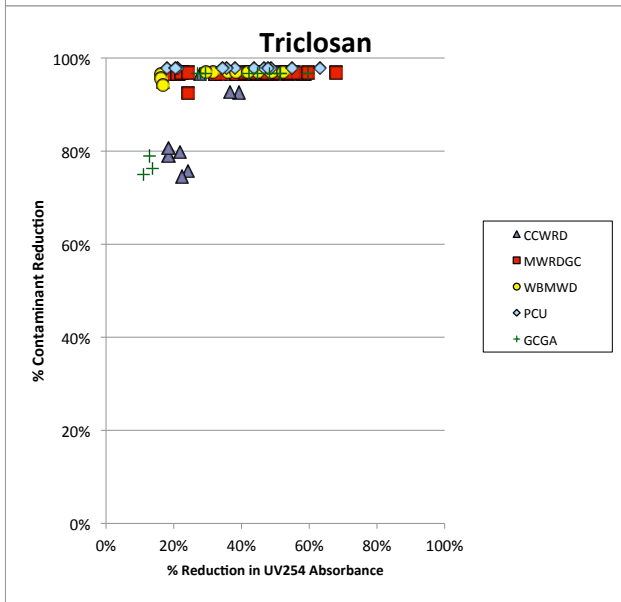
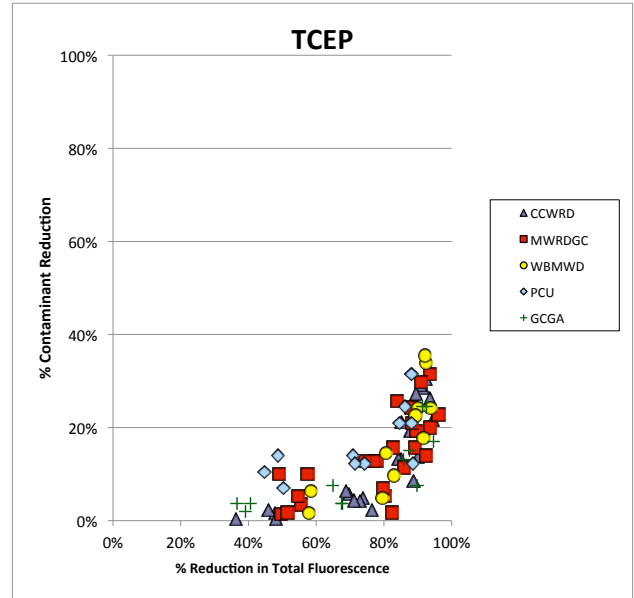
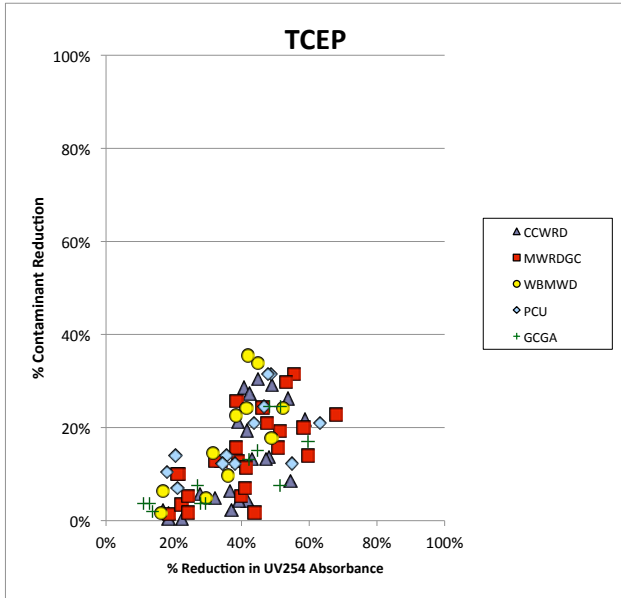
## Appendix 2 Comparison of Secondary Effluents Ozone and Ozone/H2O2 Correlations



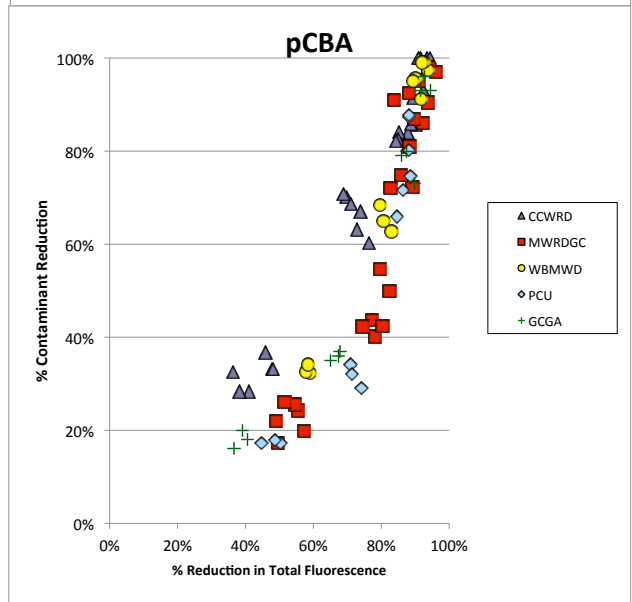
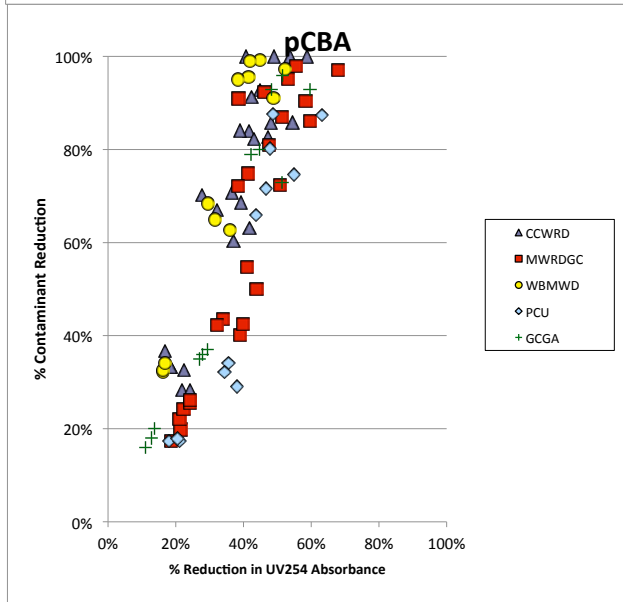
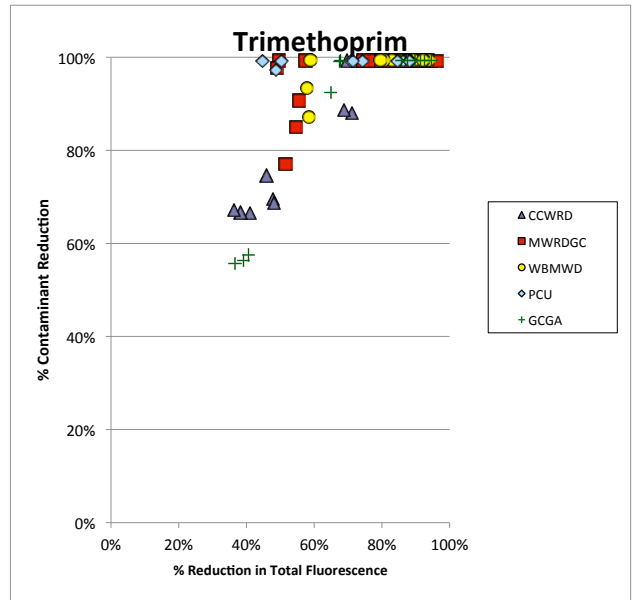
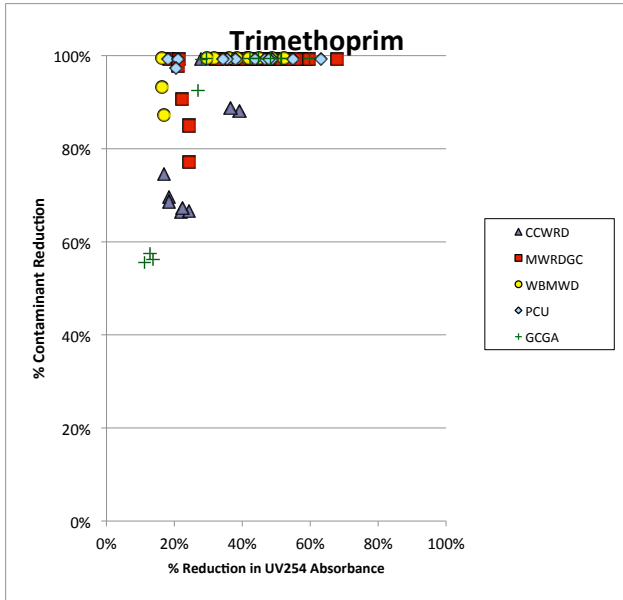
## Appendix 2 Comparison of Secondary Effluents Ozone and Ozone/H2O2 Correlations



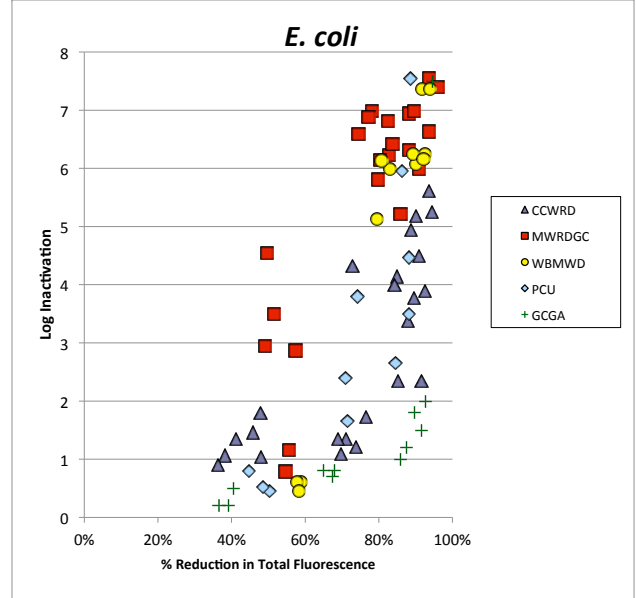
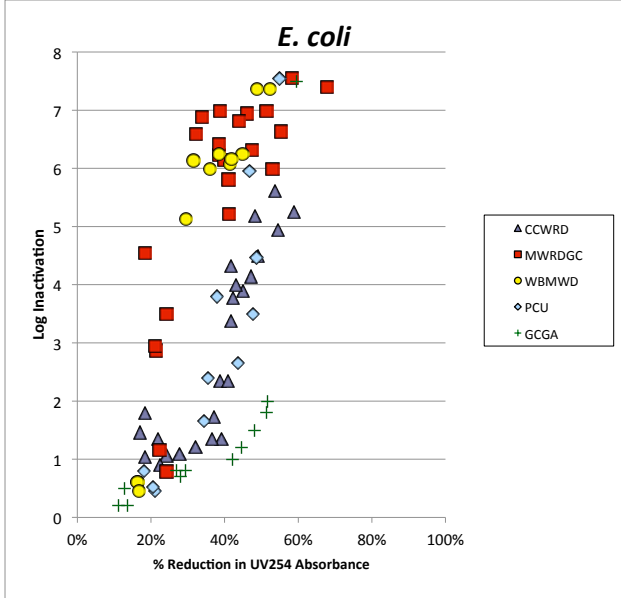
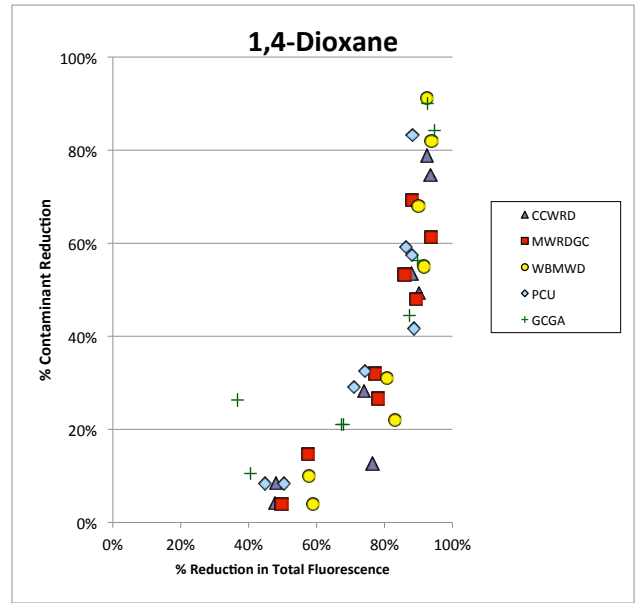
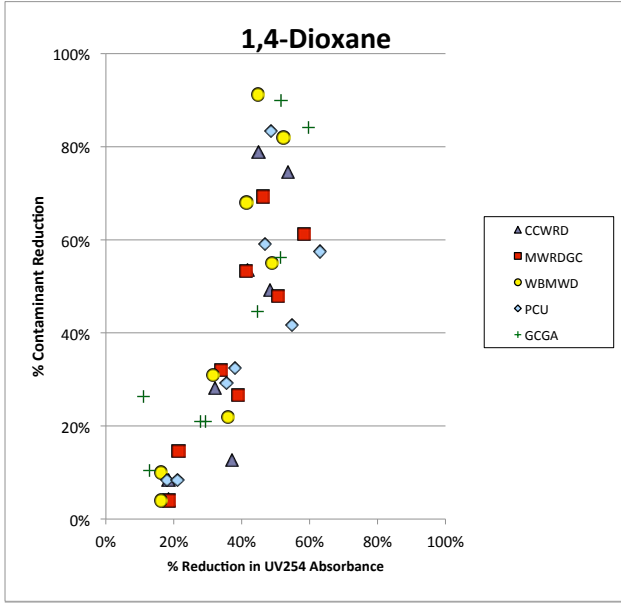
## Appendix 2 Comparison of Secondary Effluents Ozone and Ozone/H2O2 Correlations



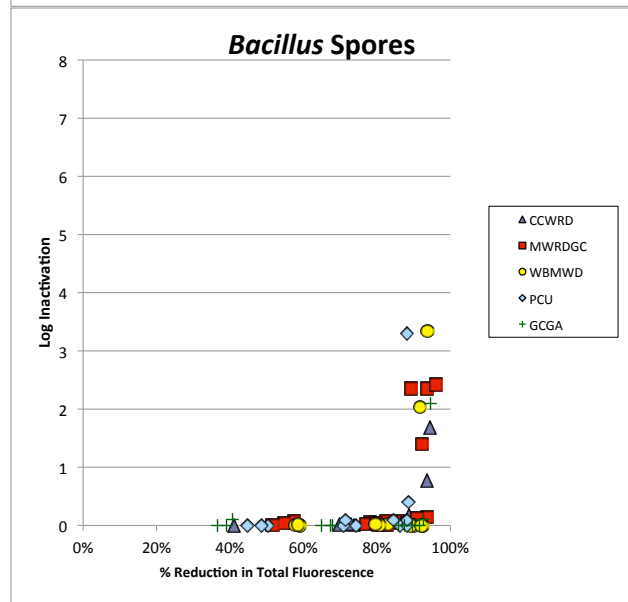
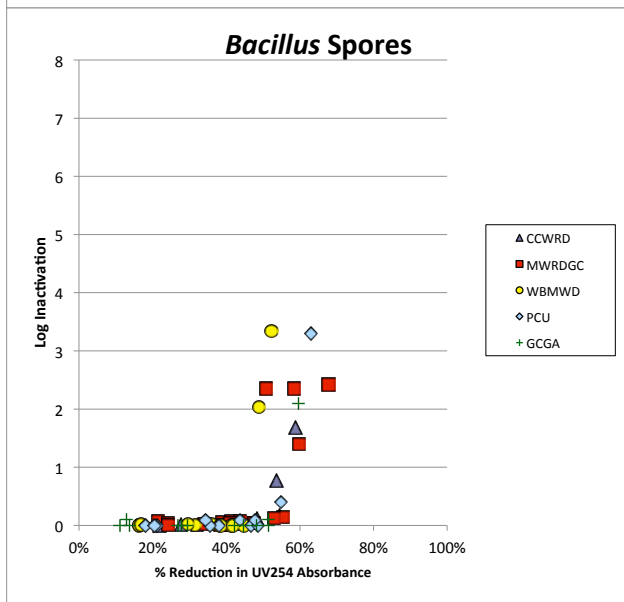
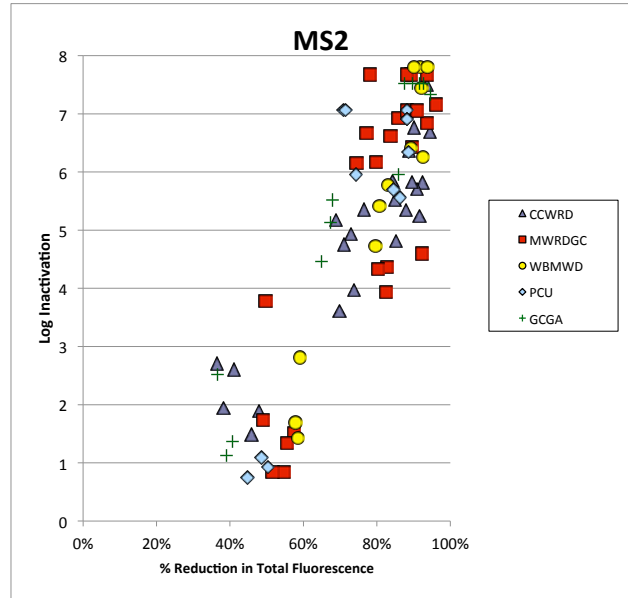
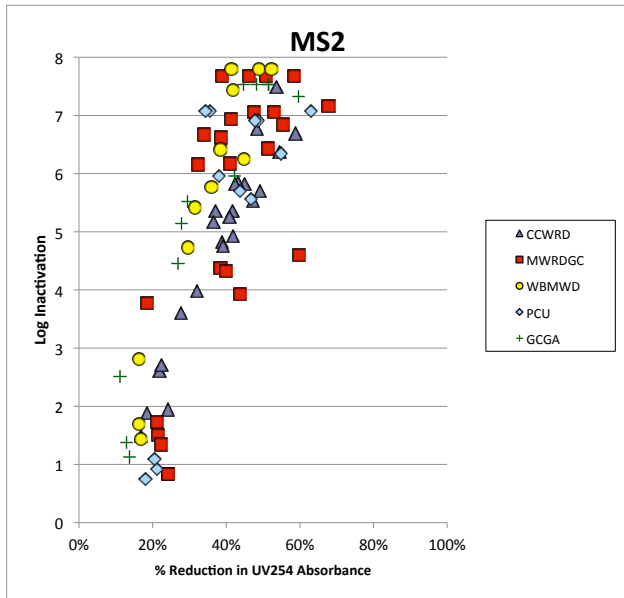
## Appendix 2 Comparison of Secondary Effluents Ozone and Ozone/H2O2 Correlations



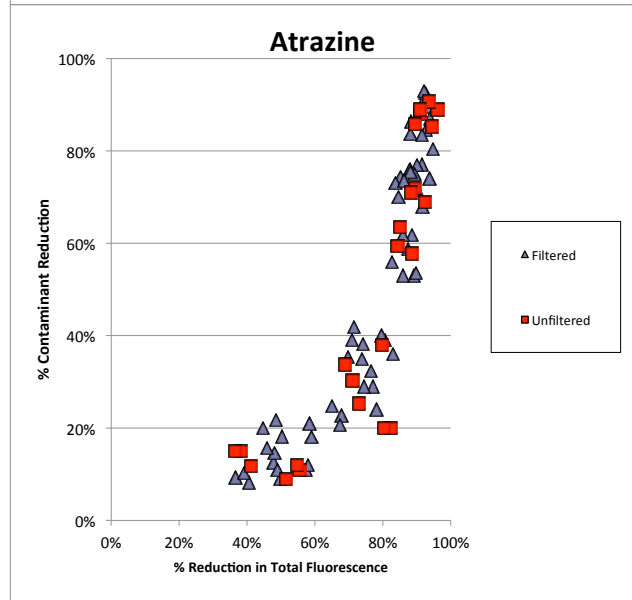
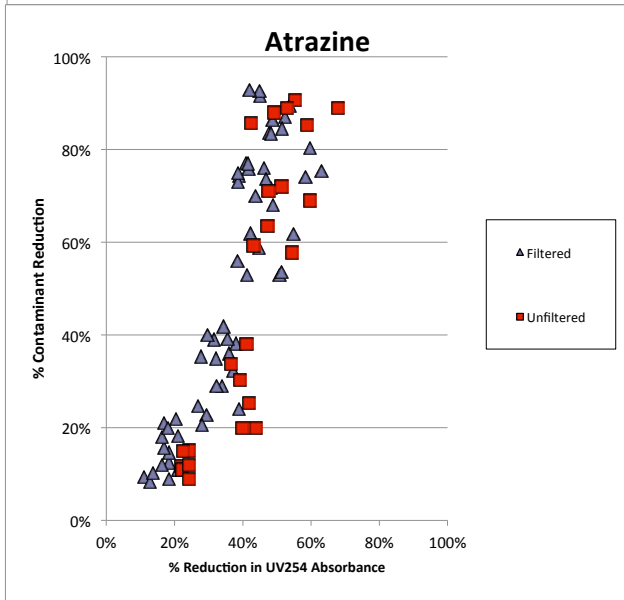
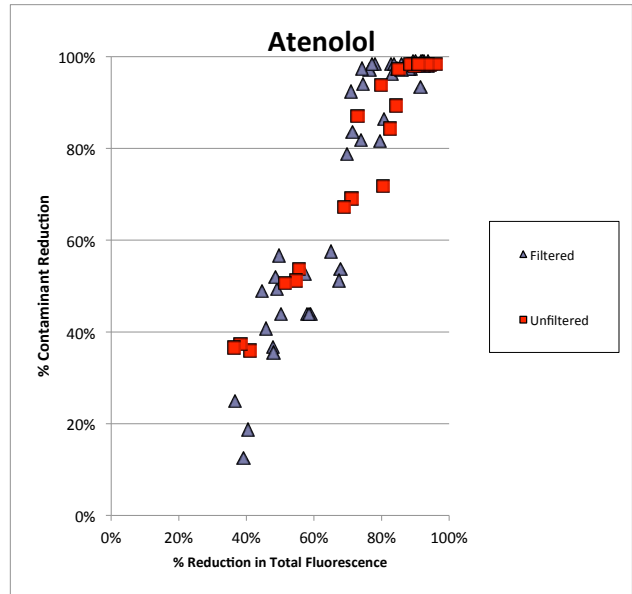
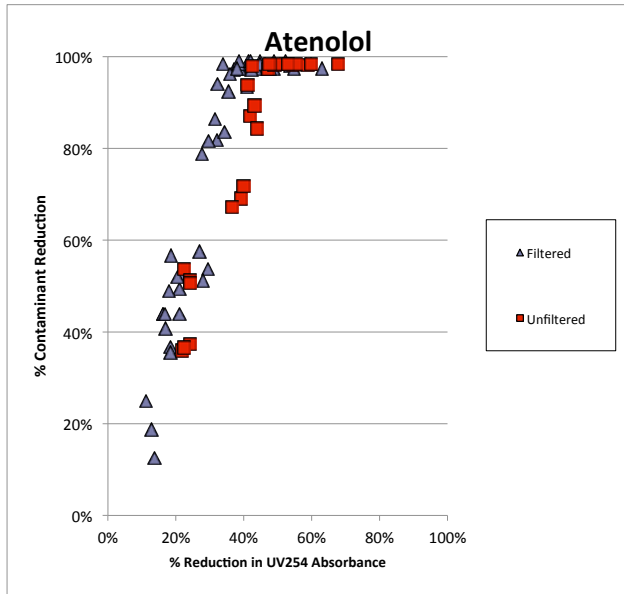
## Appendix 2 Comparison of Secondary Effluents Ozone and Ozone/H2O2 Correlations



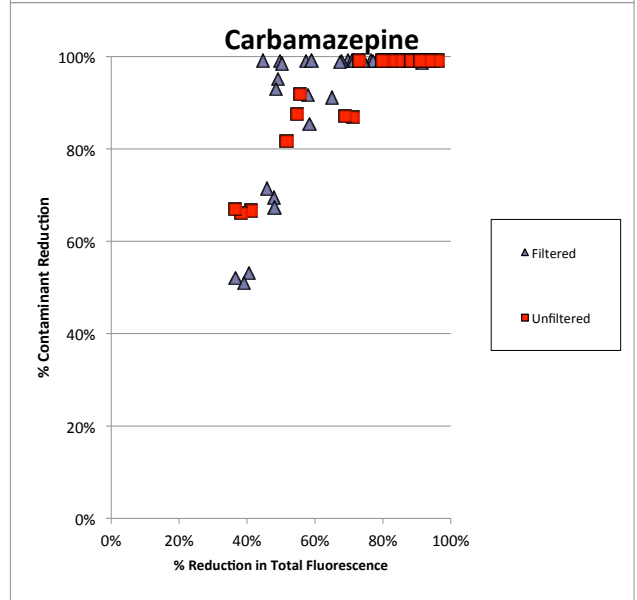
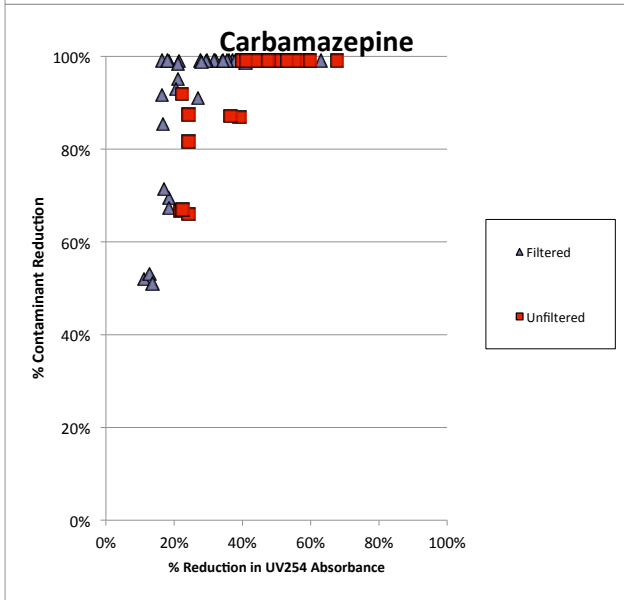
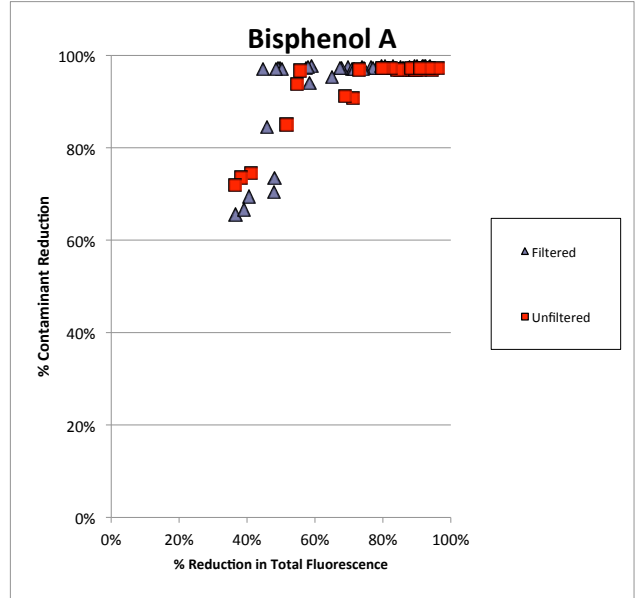
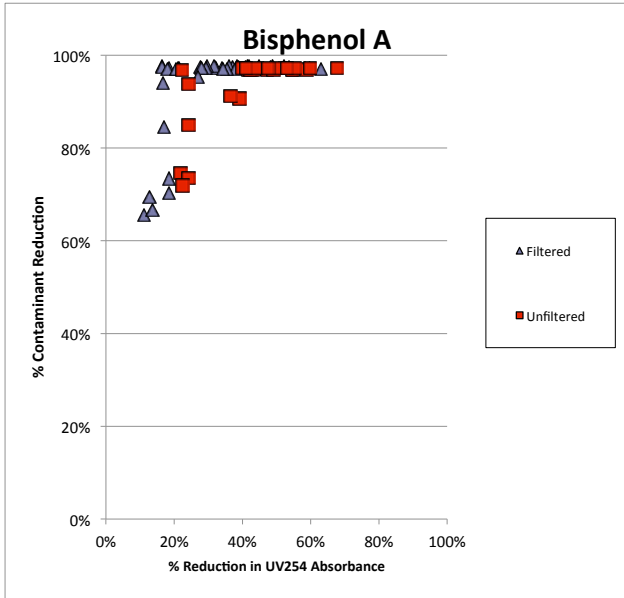
## Appendix 2 Comparison of Secondary Effluents Ozone and Ozone/H2O2 Correlations



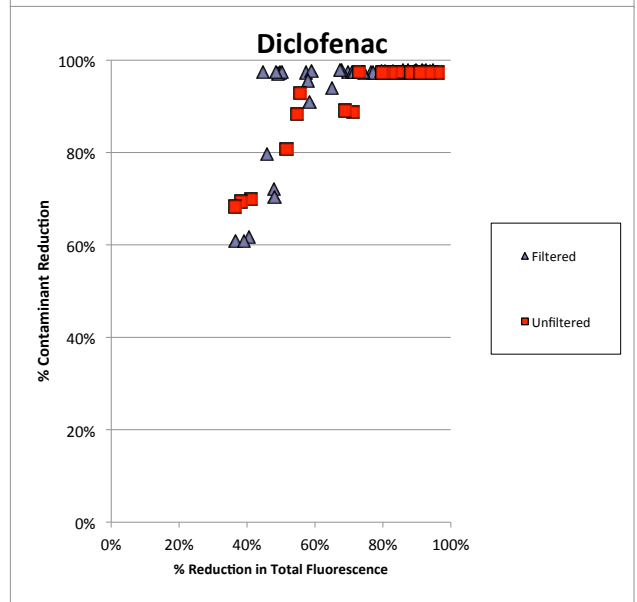
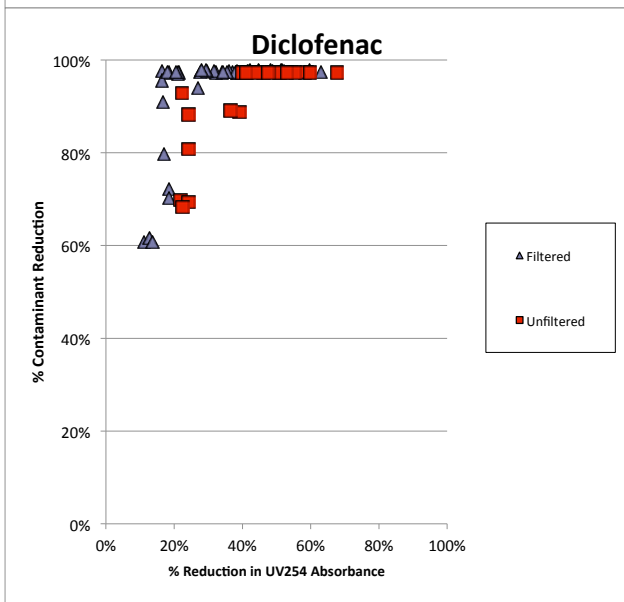
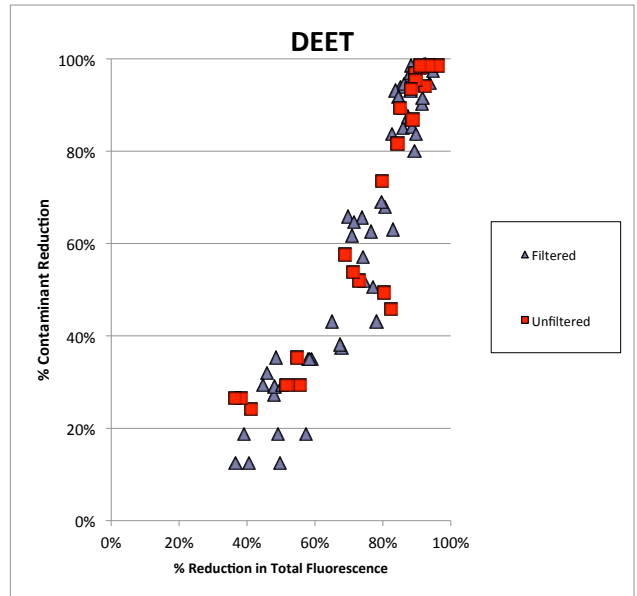
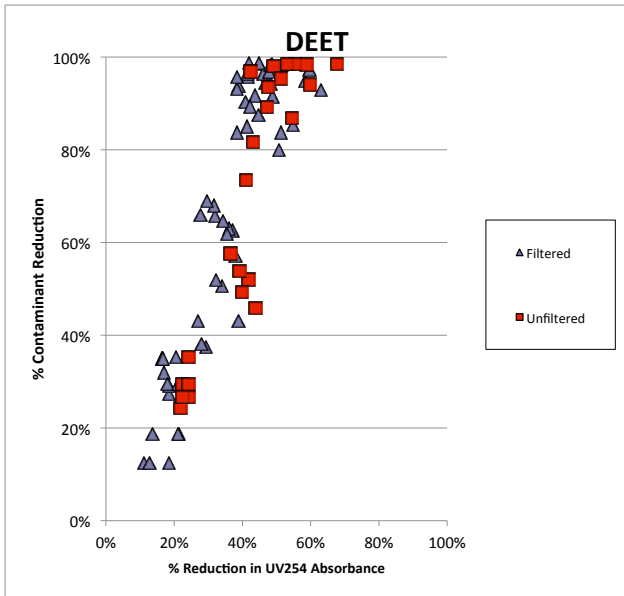
**Appendix 3**  
**Comparison of Filtered and Unfiltered Secondary Effluents**  
**Ozone and Ozone/H2O2**



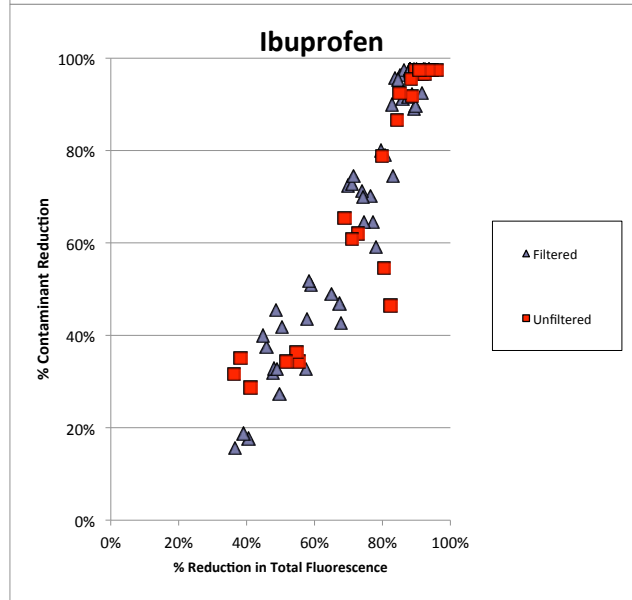
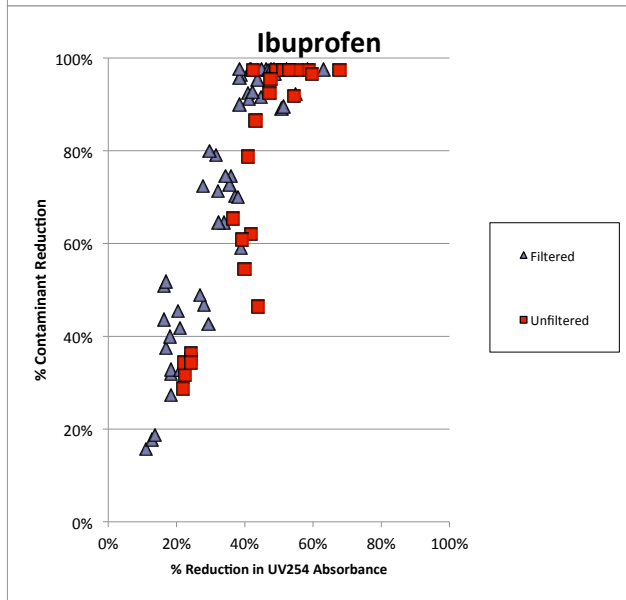
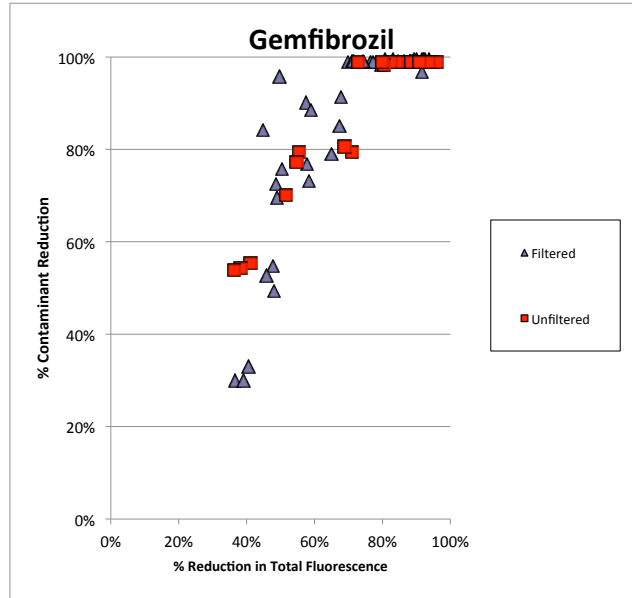
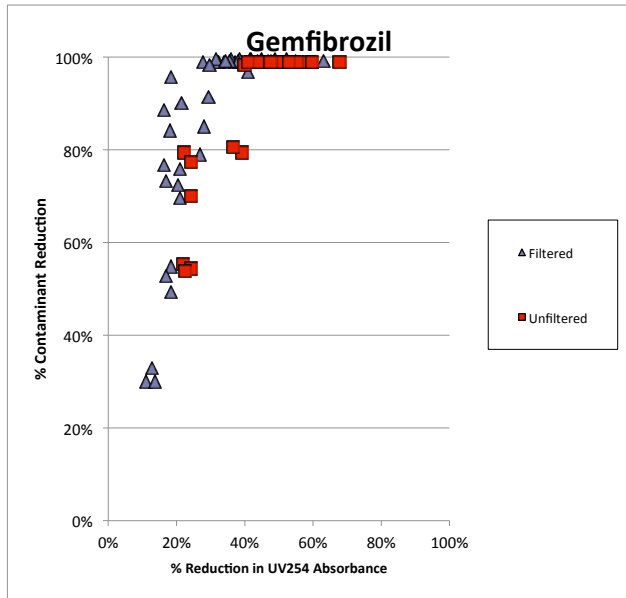
### Appendix 3 Comparison of Filtered and Unfiltered Secondary Effluents Ozone and Ozone/H2O2



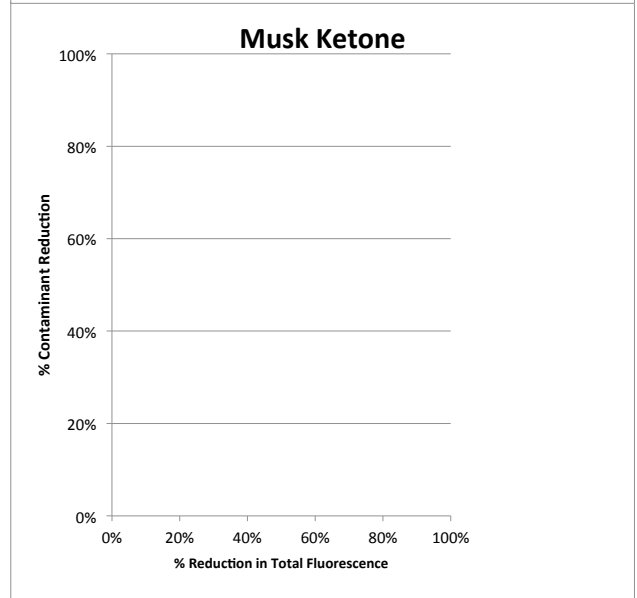
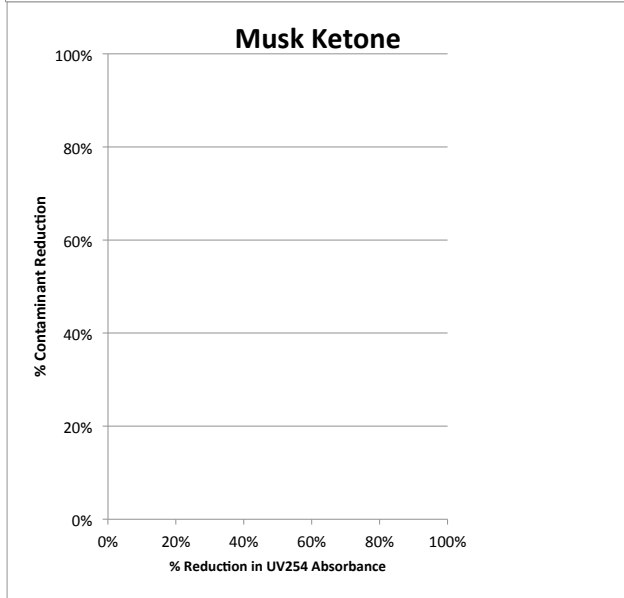
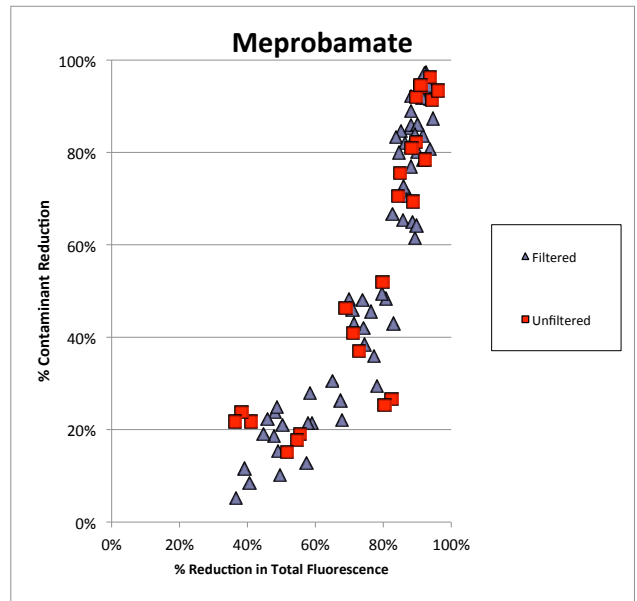
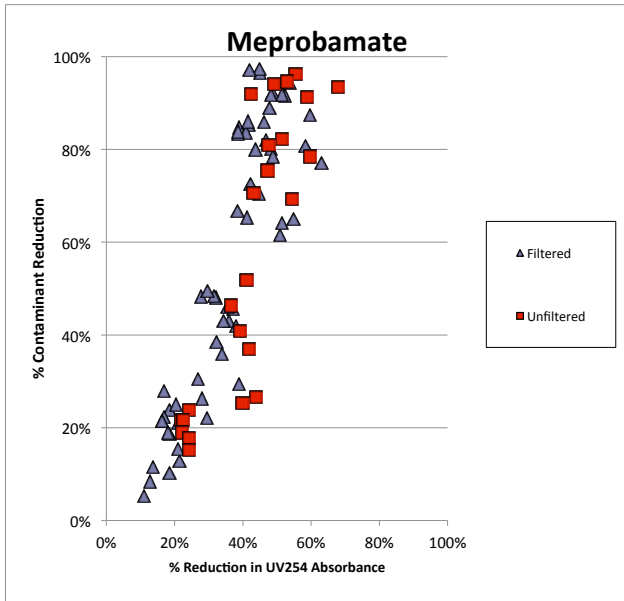
**Appendix 3**  
**Comparison of Filtered and Unfiltered Secondary Effluents**  
**Ozone and Ozone/H2O2**



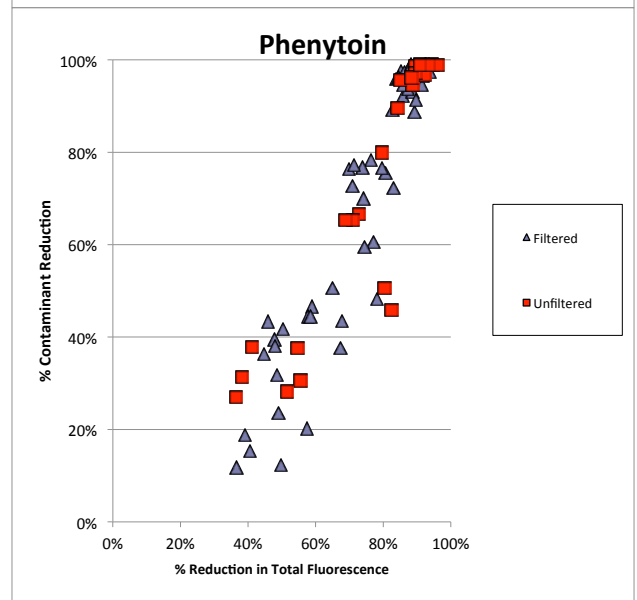
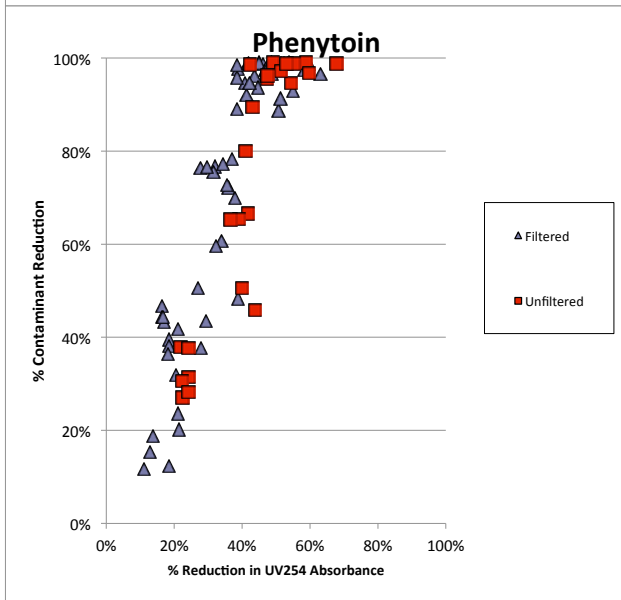
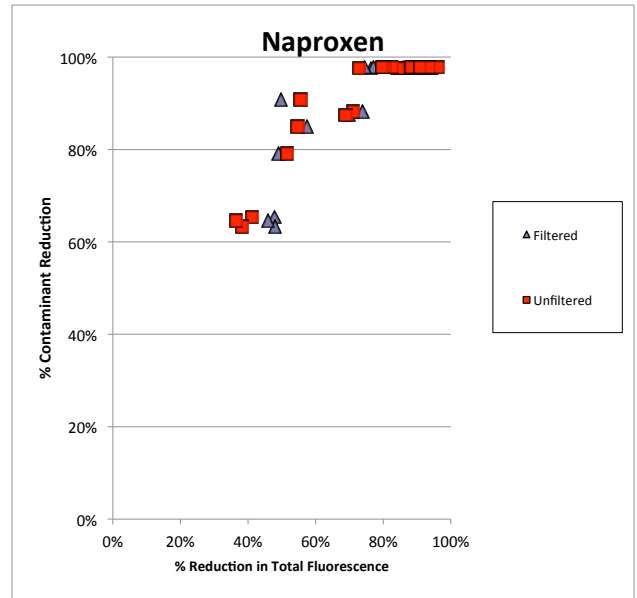
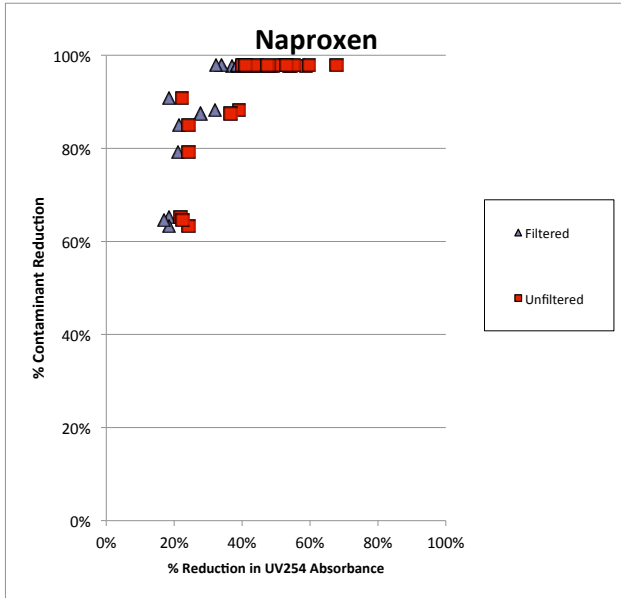
**Appendix 3**  
**Comparison of Filtered and Unfiltered Secondary Effluents**  
**Ozone and Ozone/H2O2**



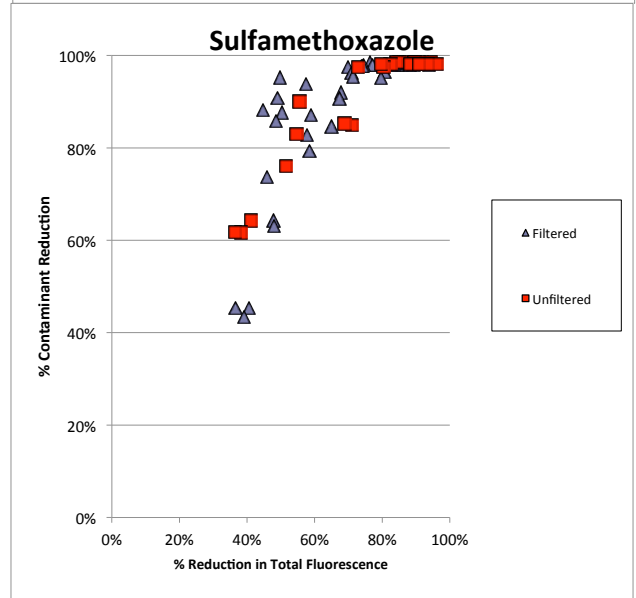
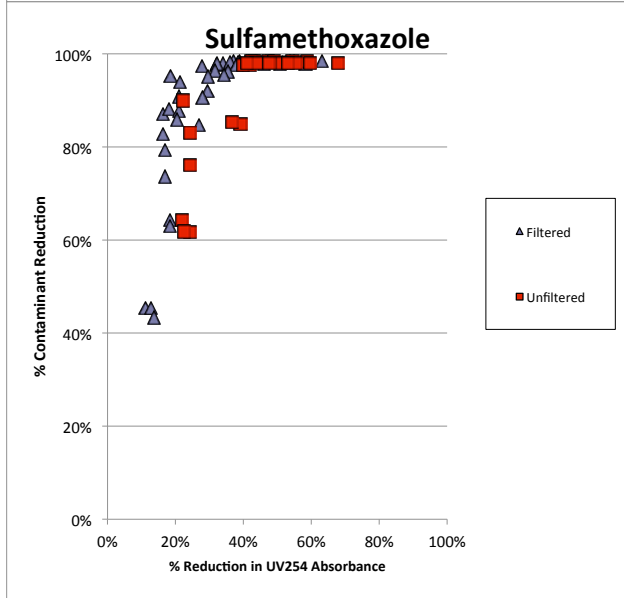
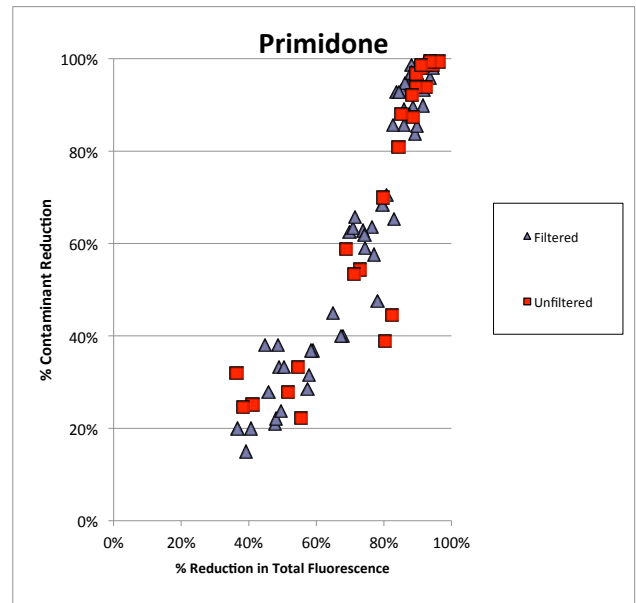
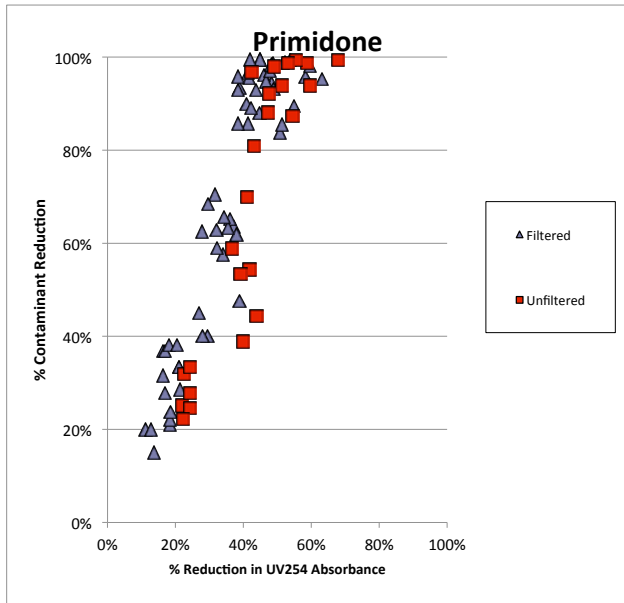
**Appendix 3**  
**Comparison of Filtered and Unfiltered Secondary Effluents**  
**Ozone and Ozone/H2O2**



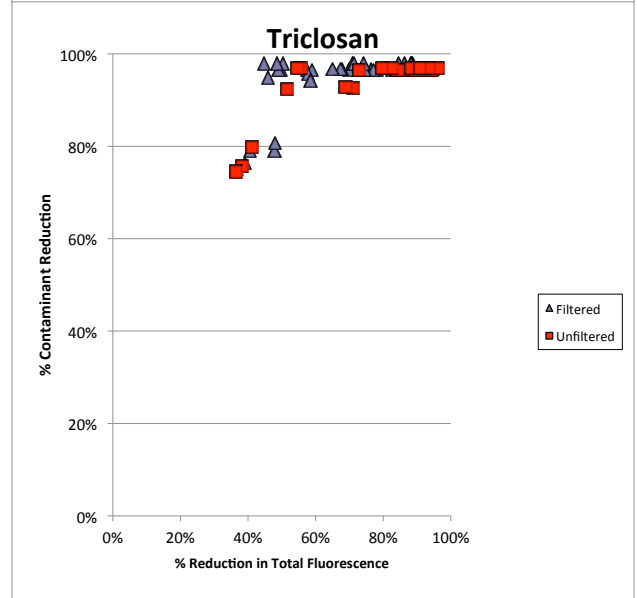
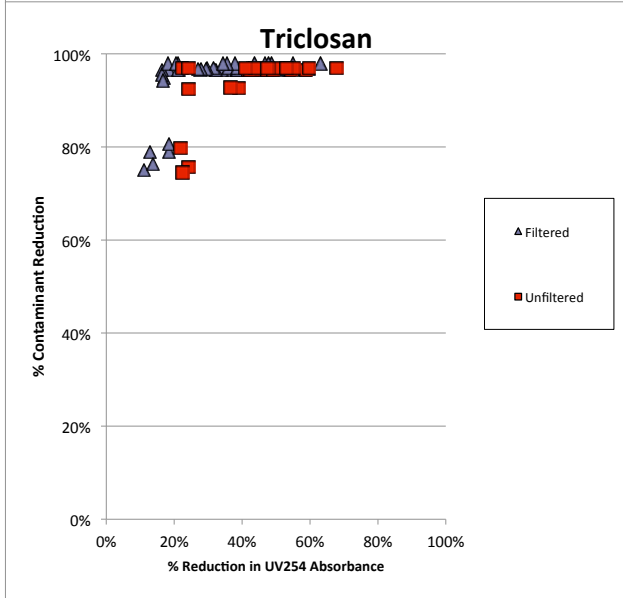
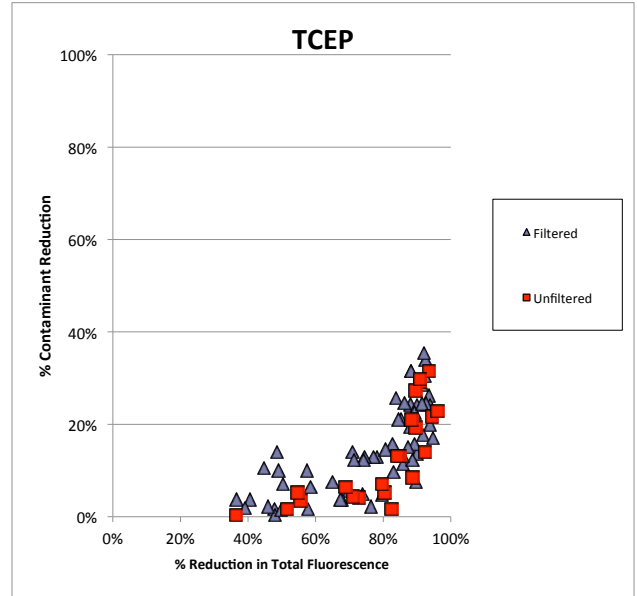
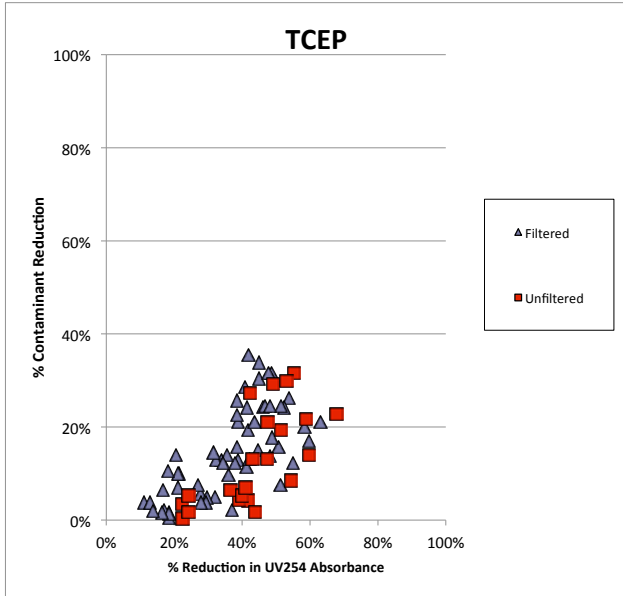
### Appendix 3 Comparison of Filtered and Unfiltered Secondary Effluents Ozone and Ozone/H2O2



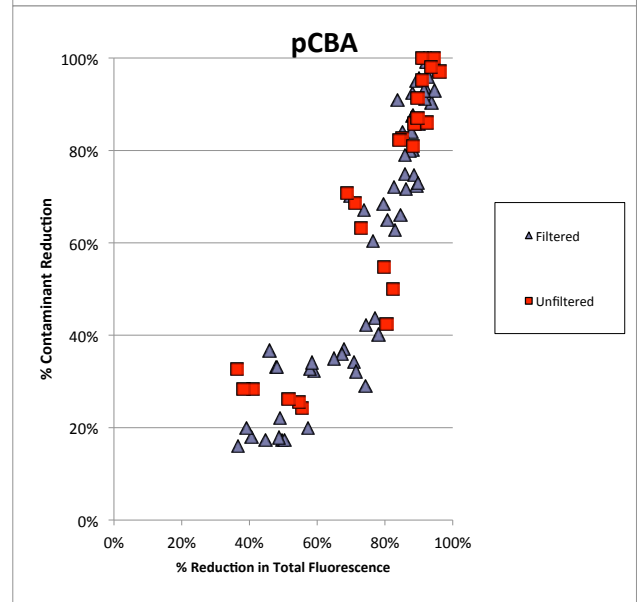
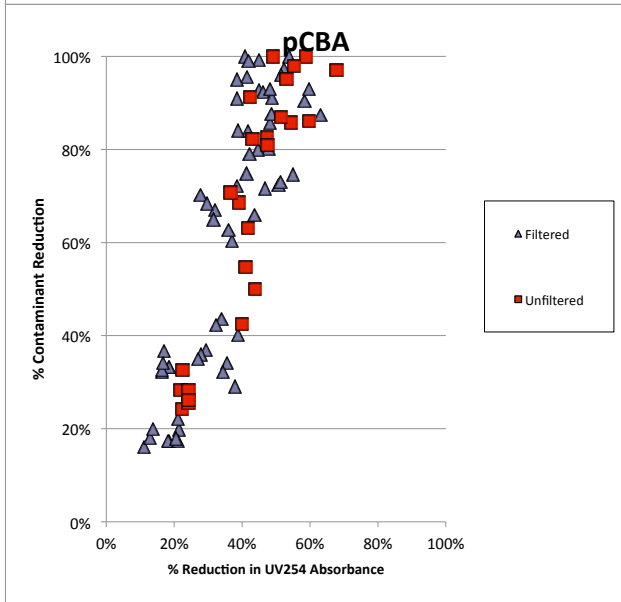
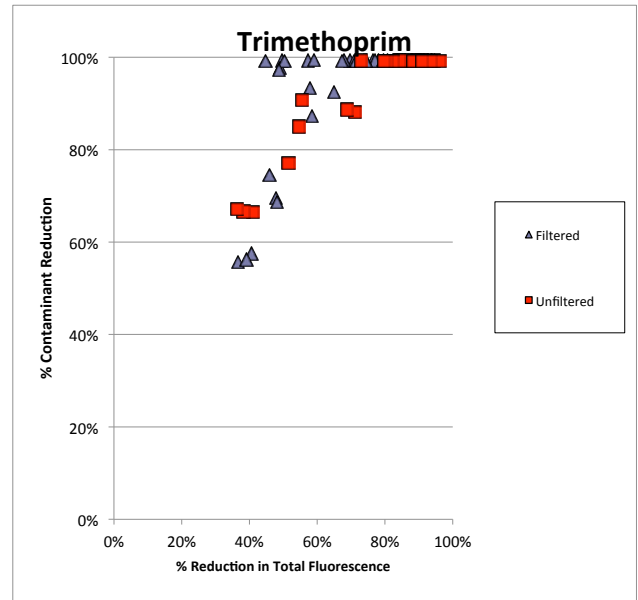
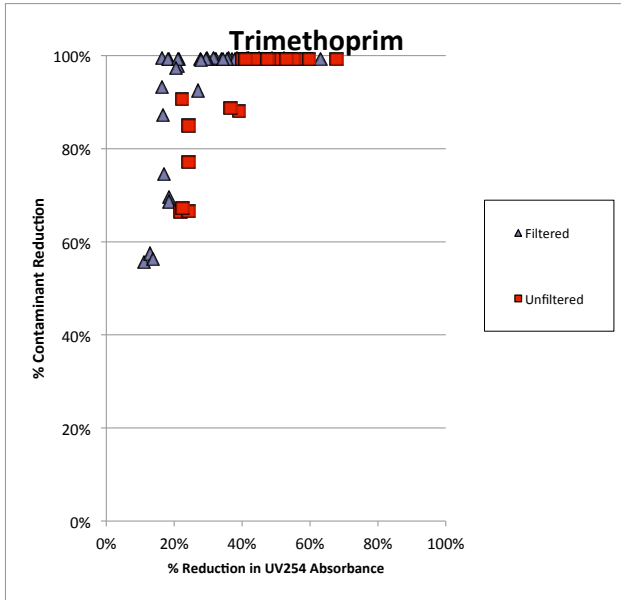
### Appendix 3 Comparison of Filtered and Unfiltered Secondary Effluents Ozone and Ozone/H2O2



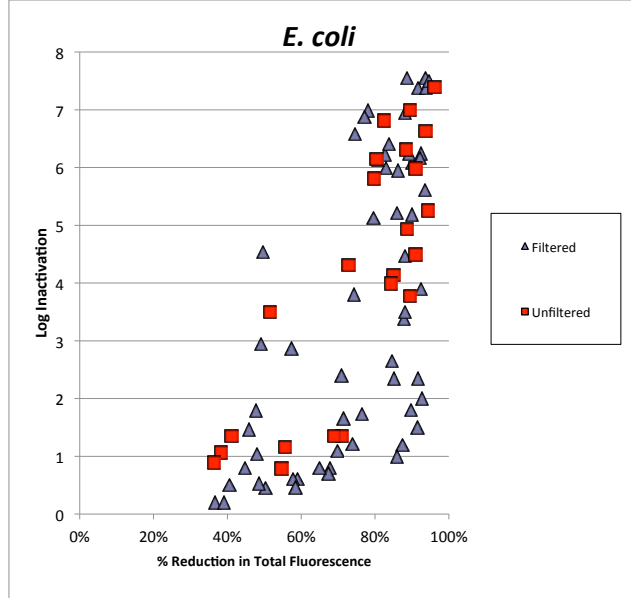
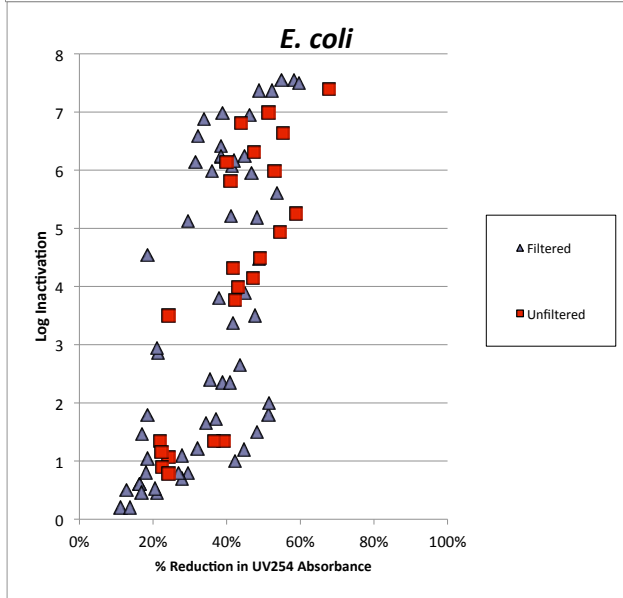
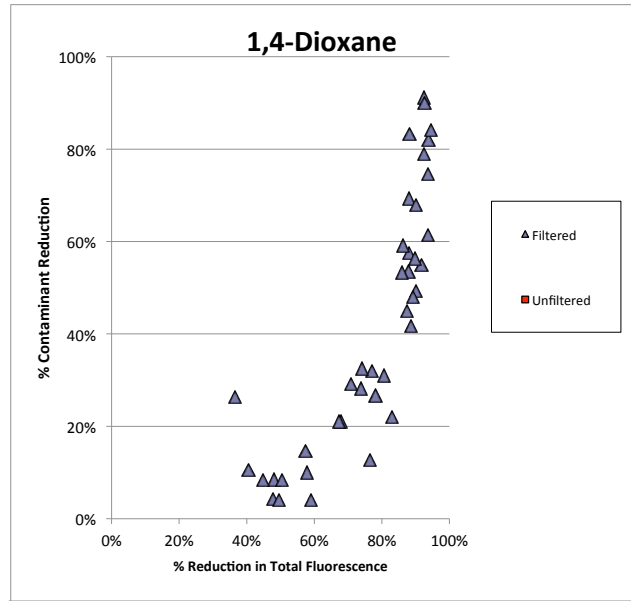
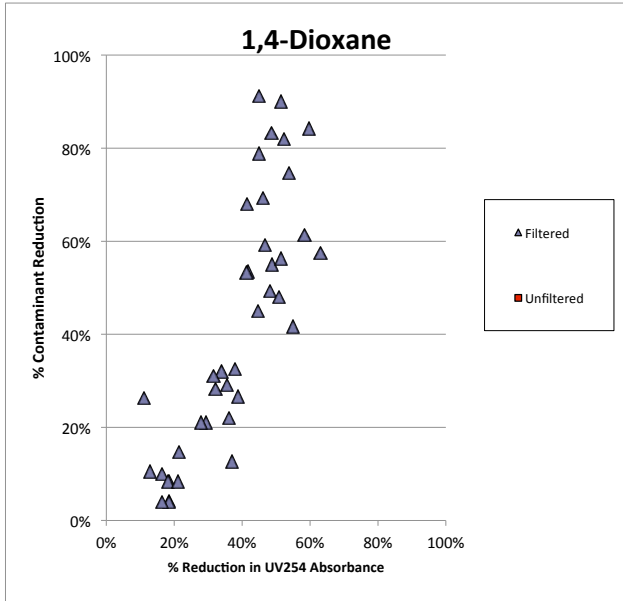
### Appendix 3 Comparison of Filtered and Unfiltered Secondary Effluents Ozone and Ozone/H2O2



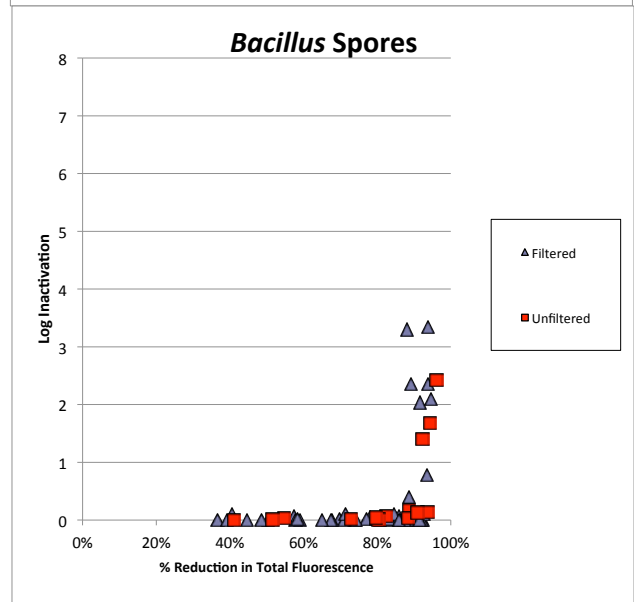
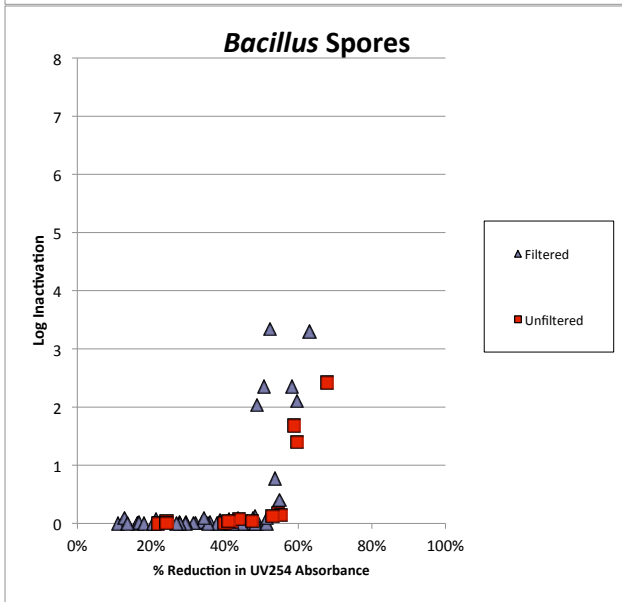
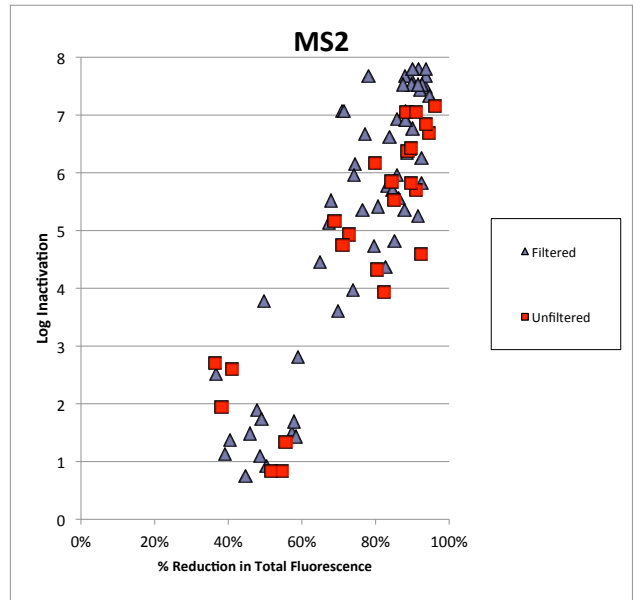
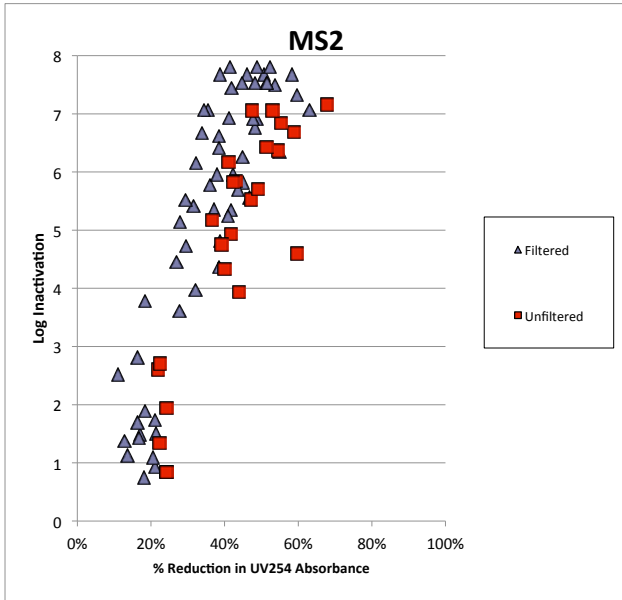
### Appendix 3 Comparison of Filtered and Unfiltered Secondary Effluents Ozone and Ozone/H2O2



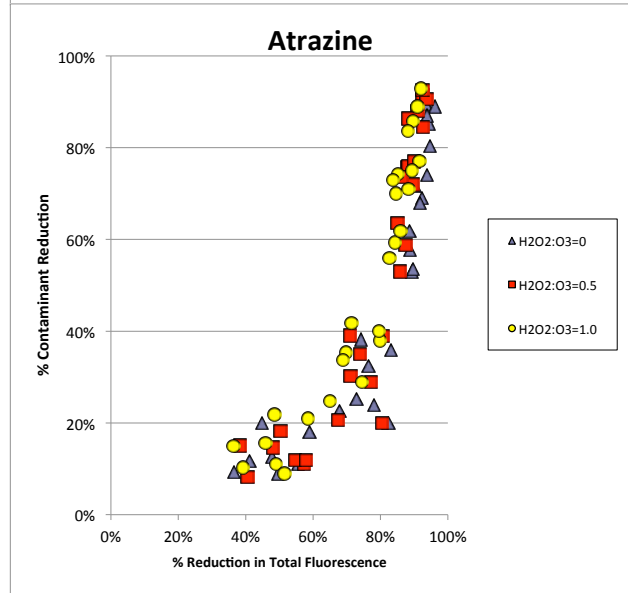
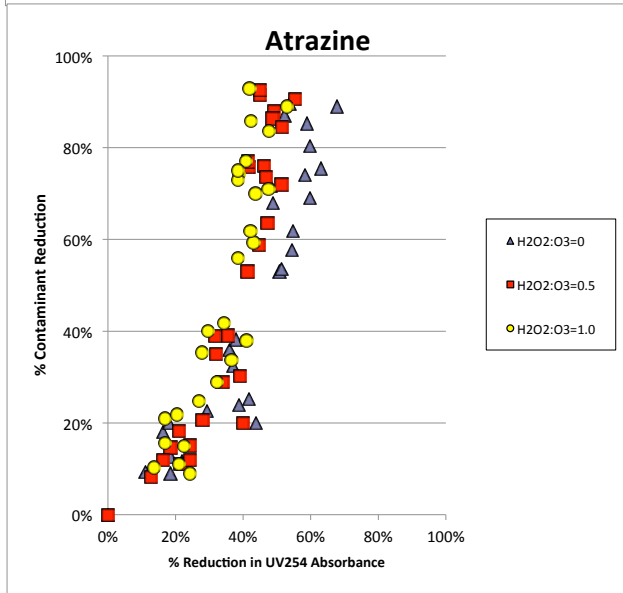
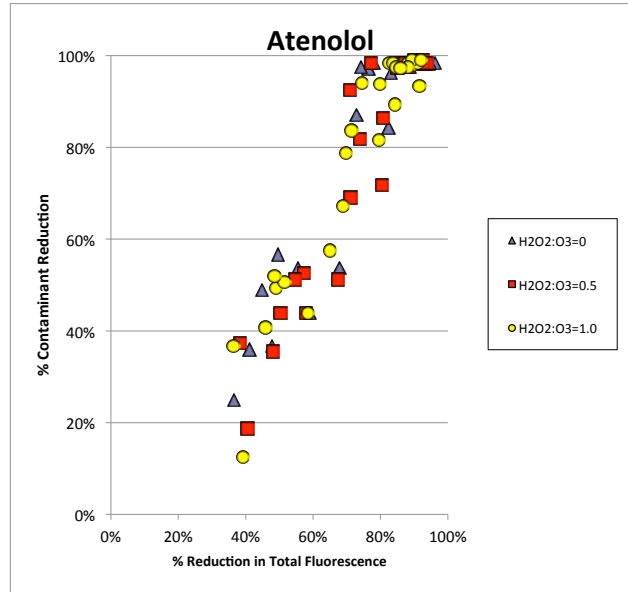
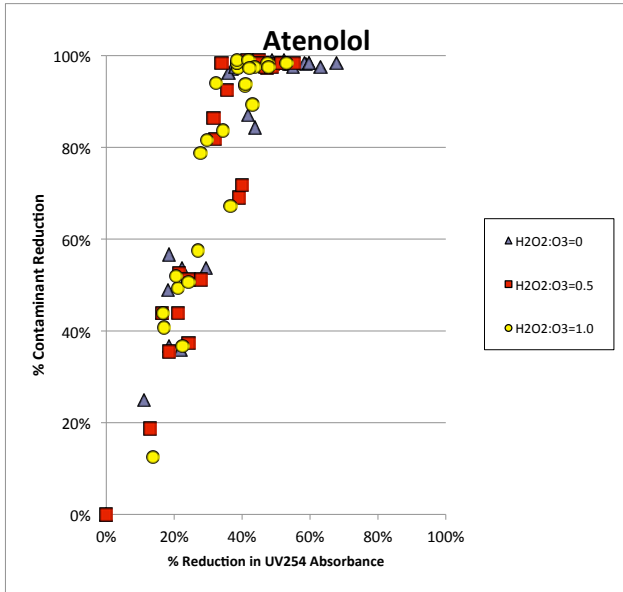
**Appendix 3**  
**Comparison of Filtered and Unfiltered Secondary Effluents**  
**Ozone and Ozone/H2O2**



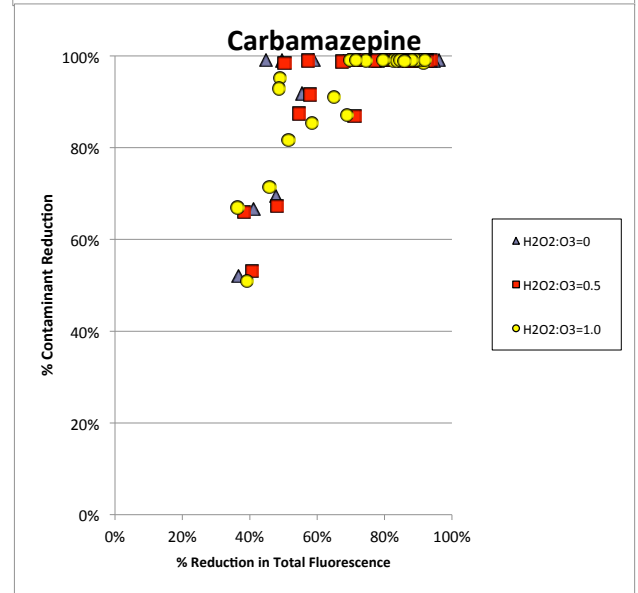
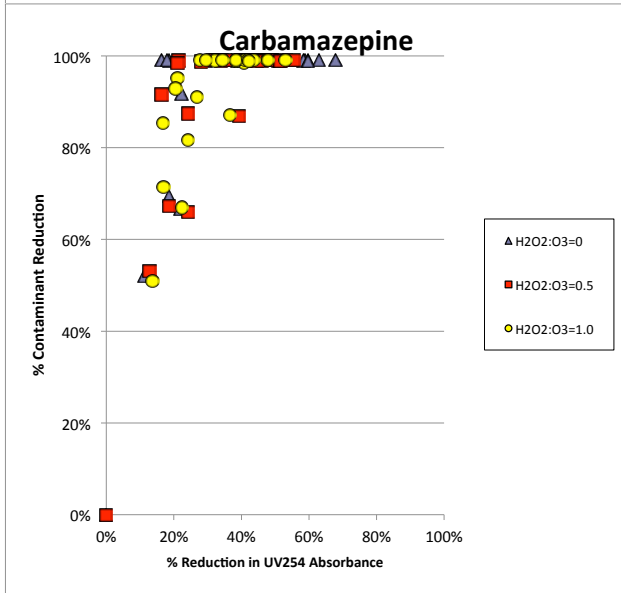
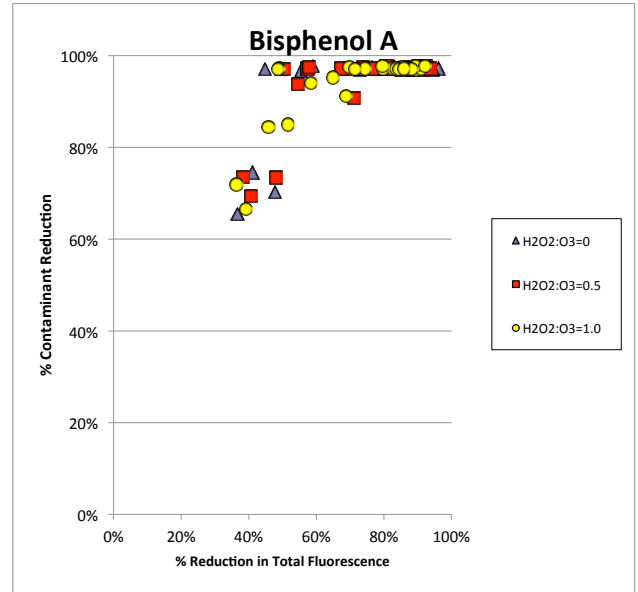
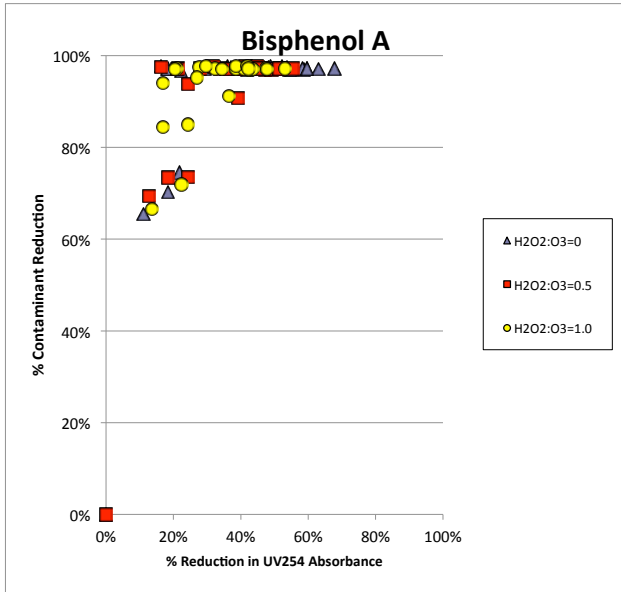
**Appendix 3**  
**Comparison of Filtered and Unfiltered Secondary Effluents**  
**Ozone and Ozone/H2O2**



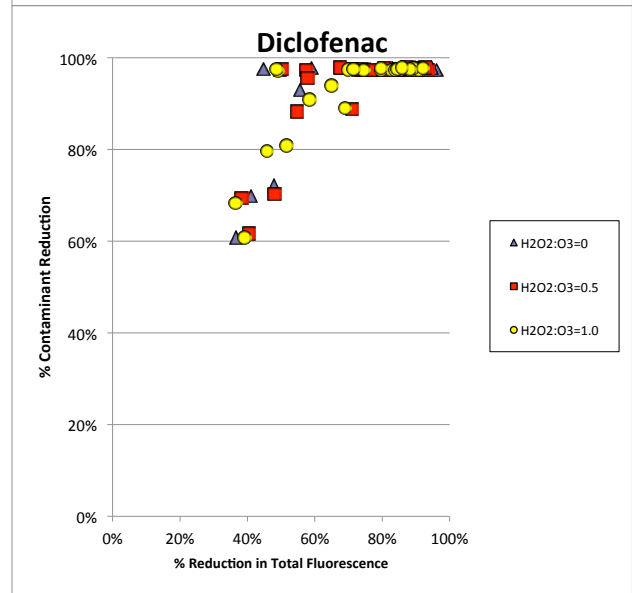
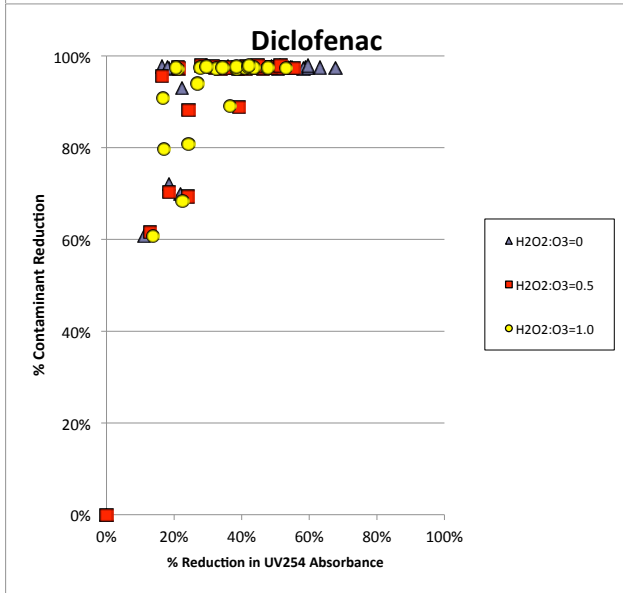
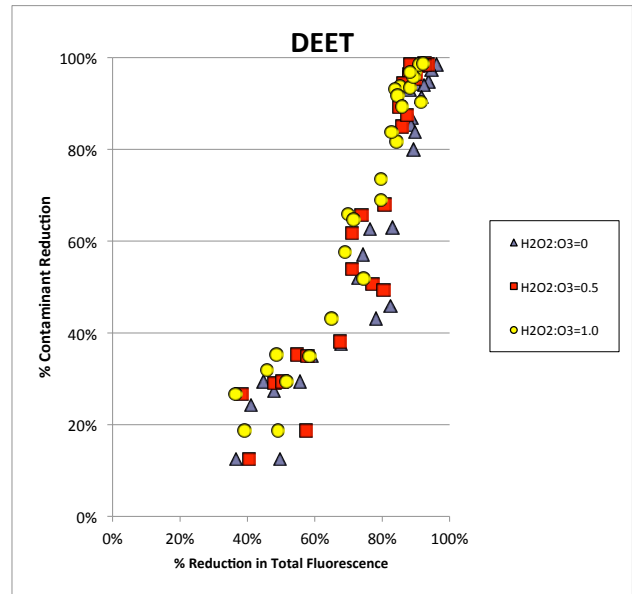
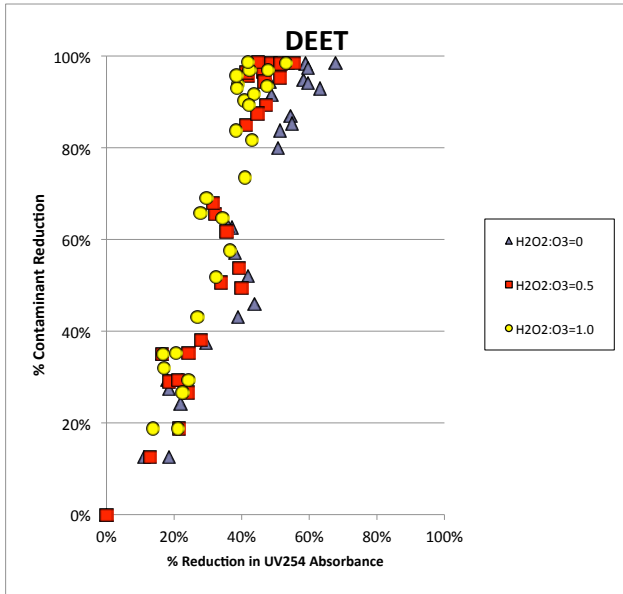
## Appendix 4 Comparison of H2O2 Doses Ozone and Ozone/H2O2



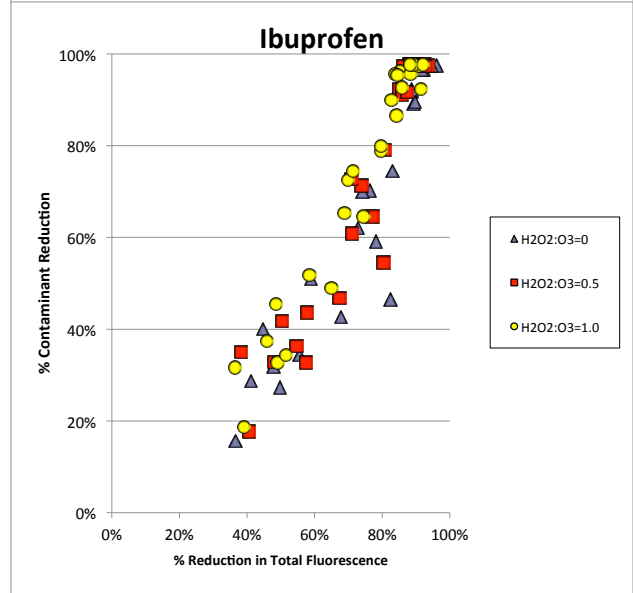
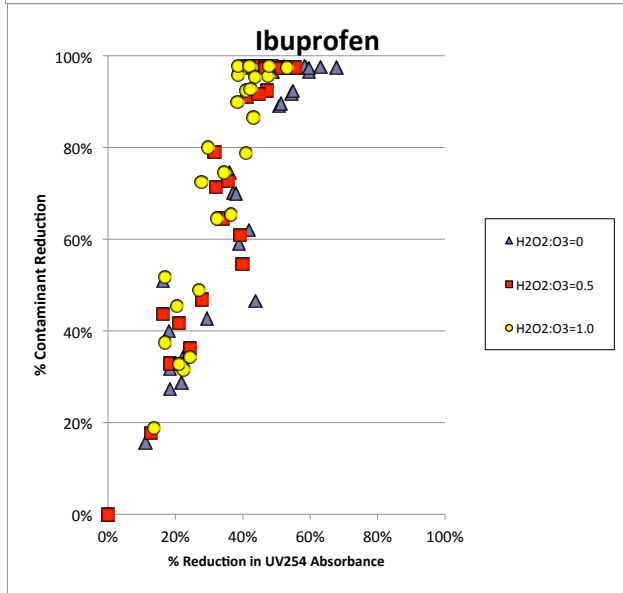
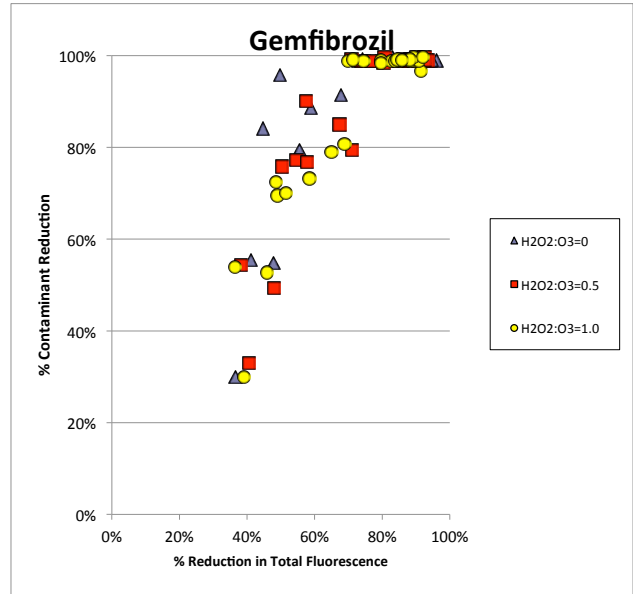
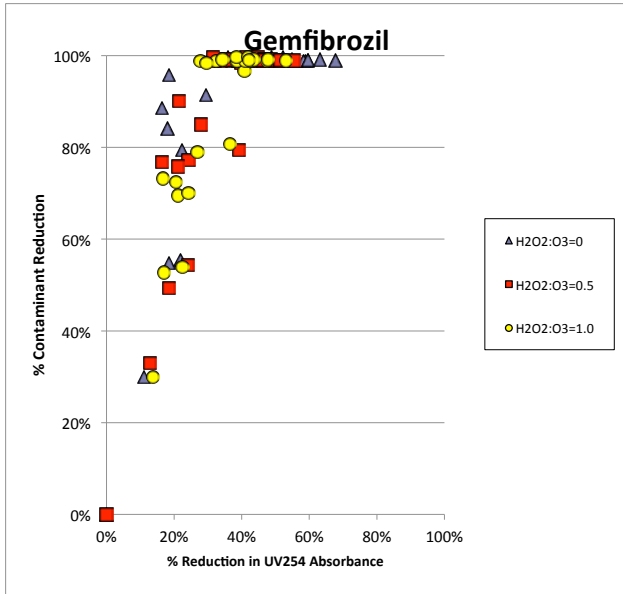
## Appendix 4 Comparison of H2O2 Doses Ozone and Ozone/H2O2



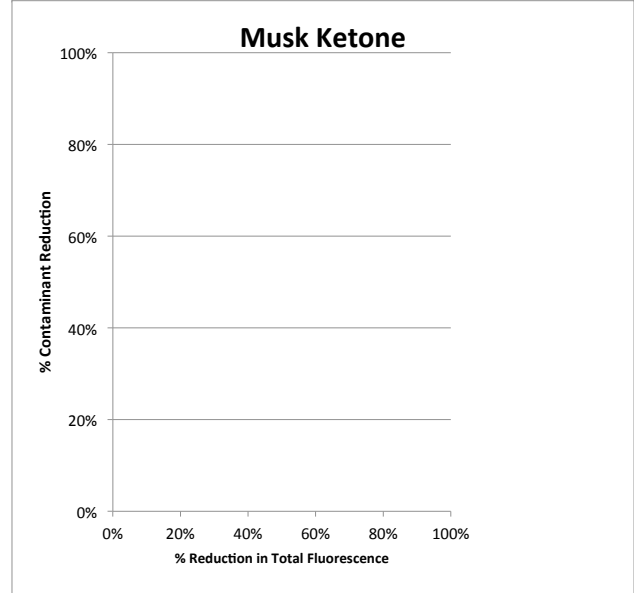
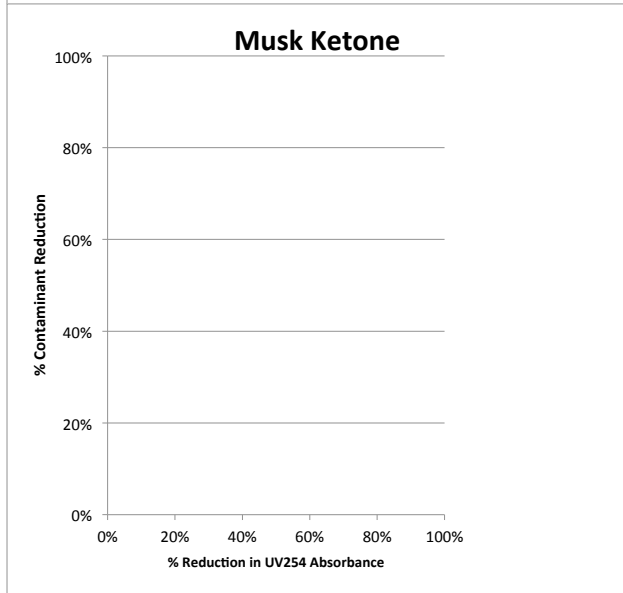
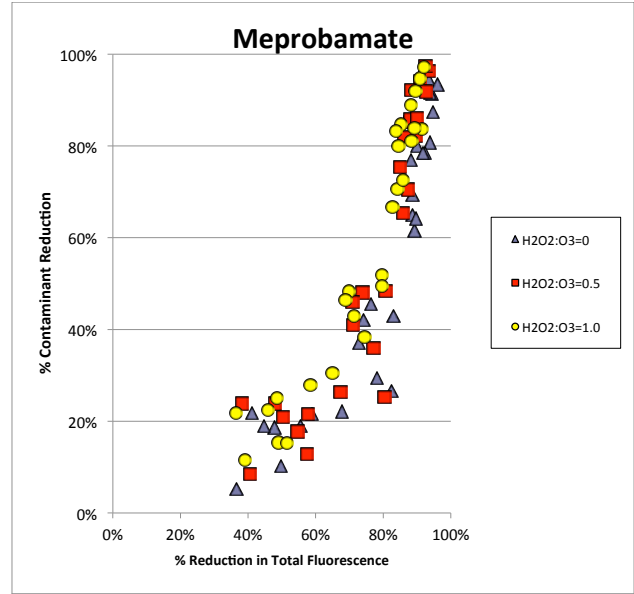
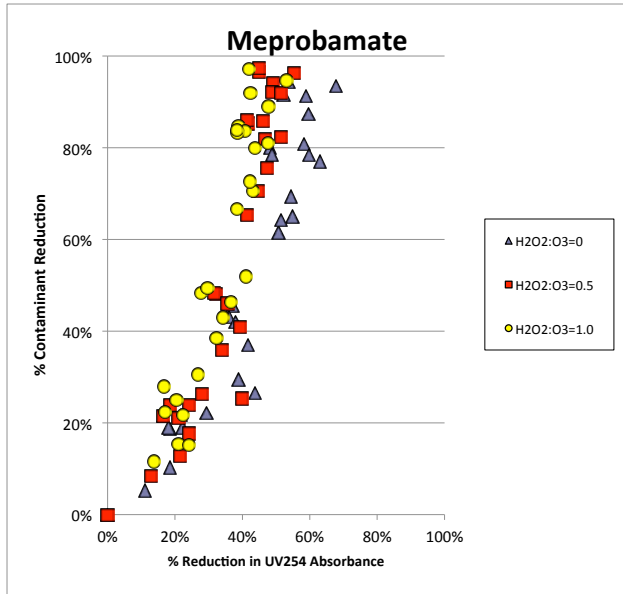
## Appendix 4 Comparison of H2O2 Doses Ozone and Ozone/H2O2



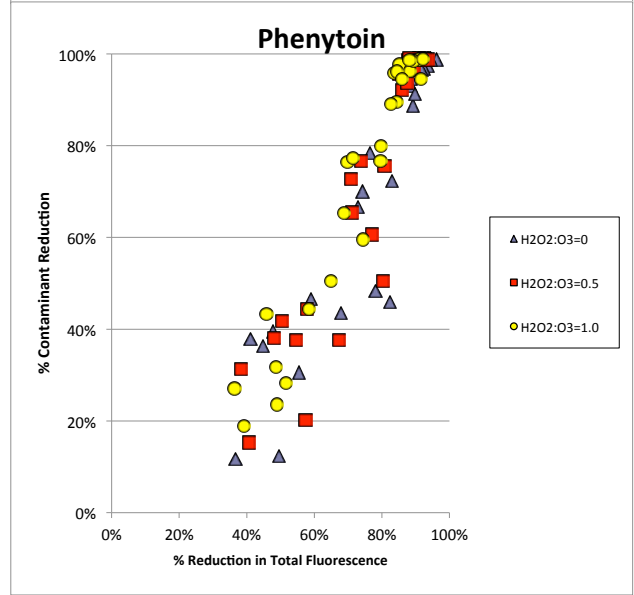
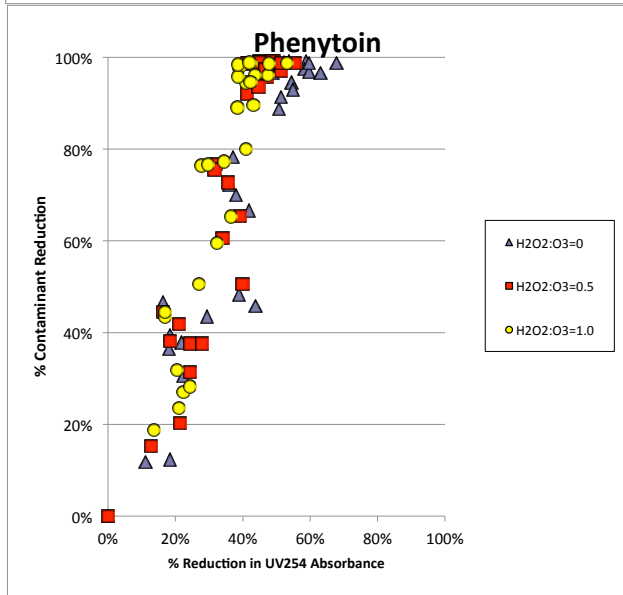
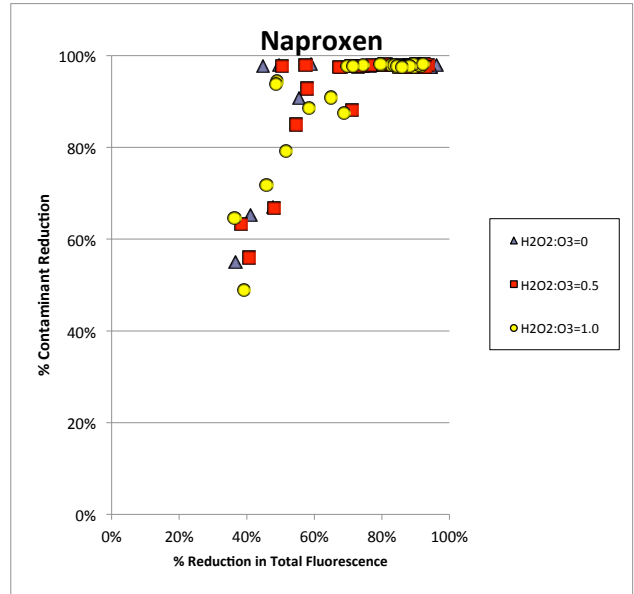
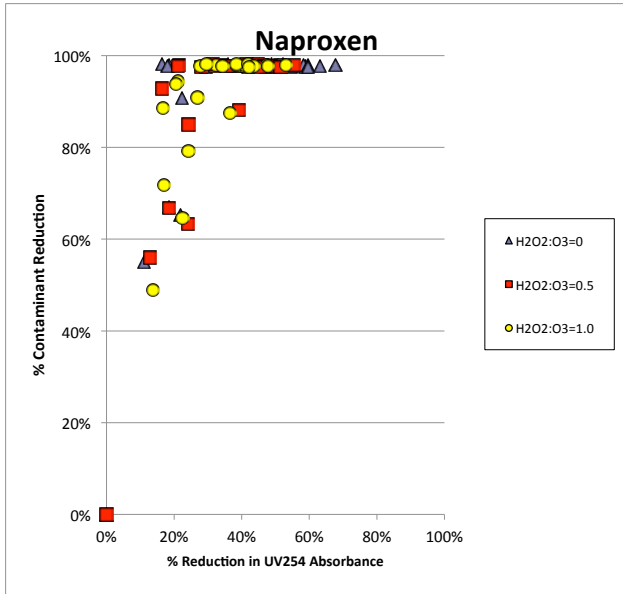
## Appendix 4 Comparison of H2O2 Doses Ozone and Ozone/H2O2



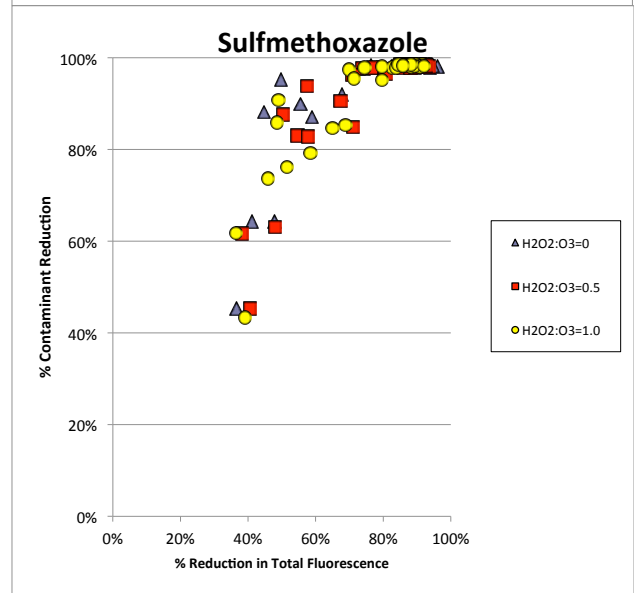
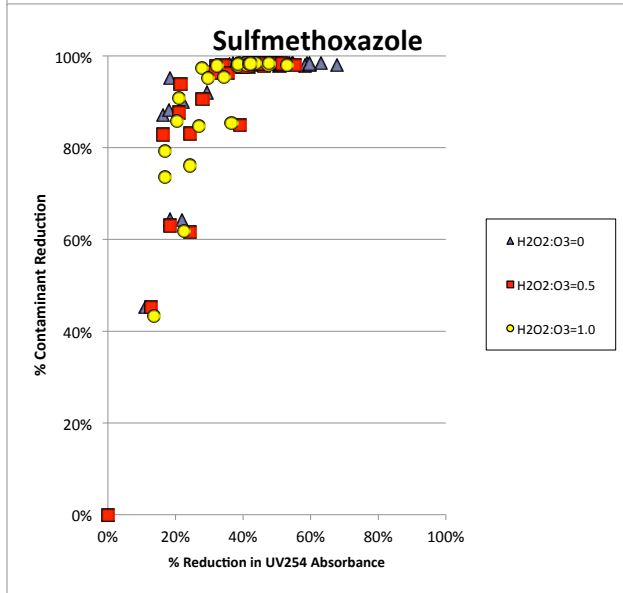
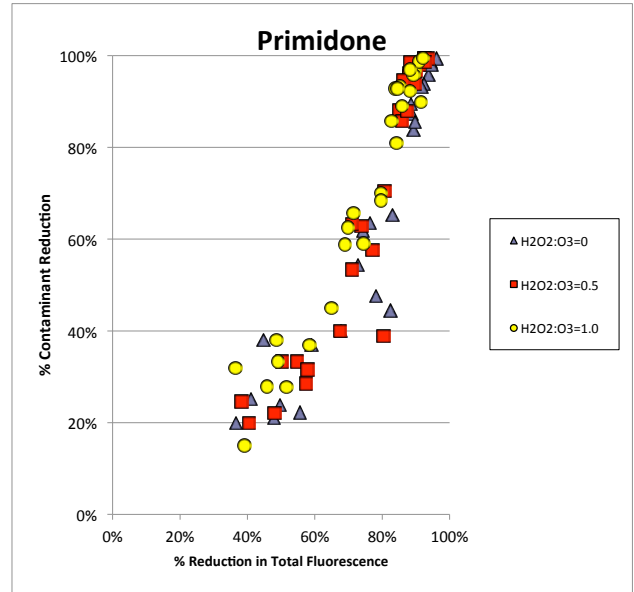
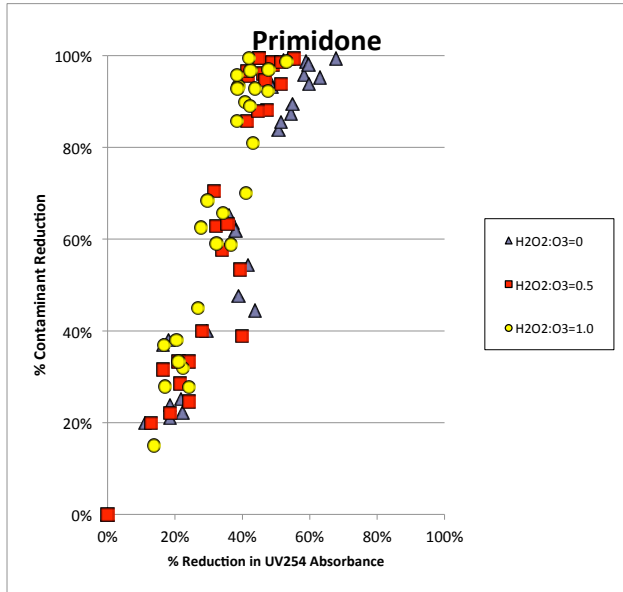
## Appendix 4 Comparison of H2O2 Doses Ozone and Ozone/H2O2



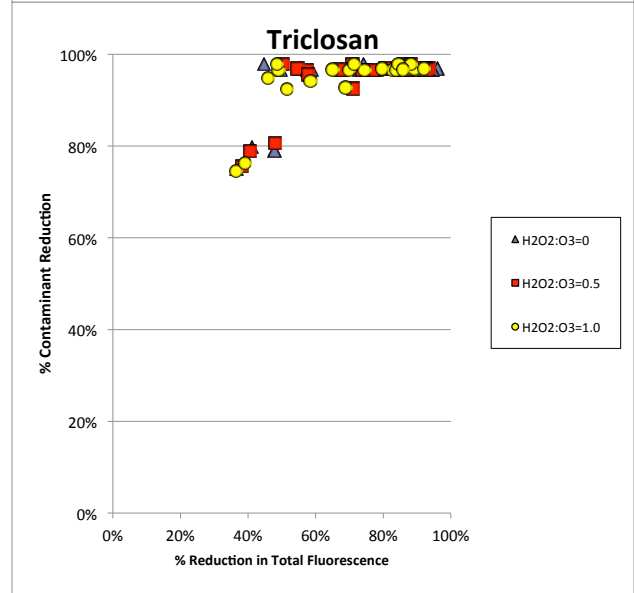
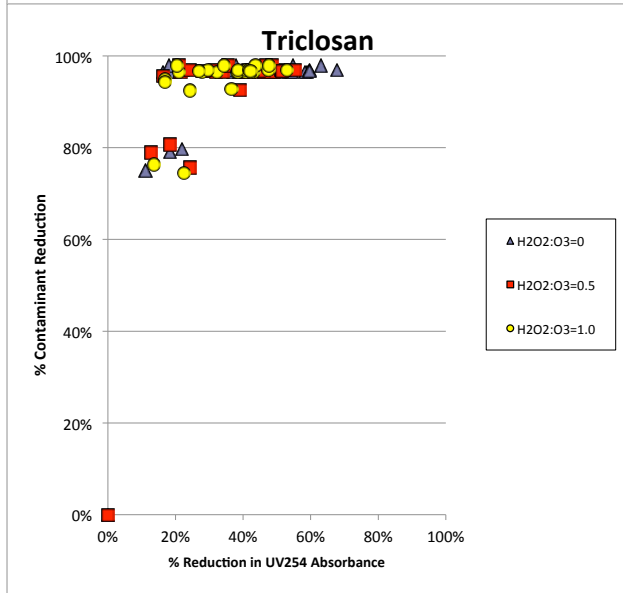
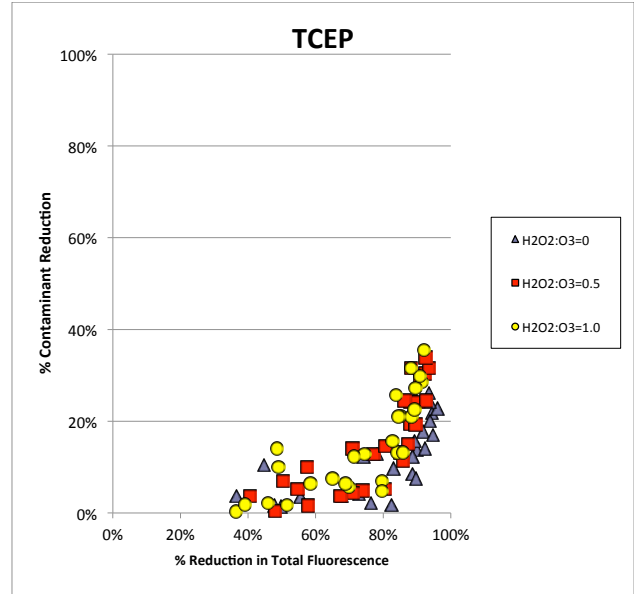
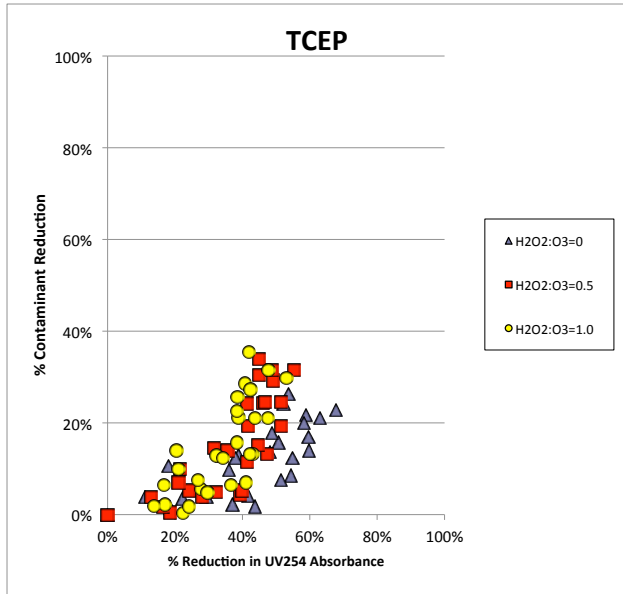
## Appendix 4 Comparison of H2O2 Doses Ozone and Ozone/H2O2



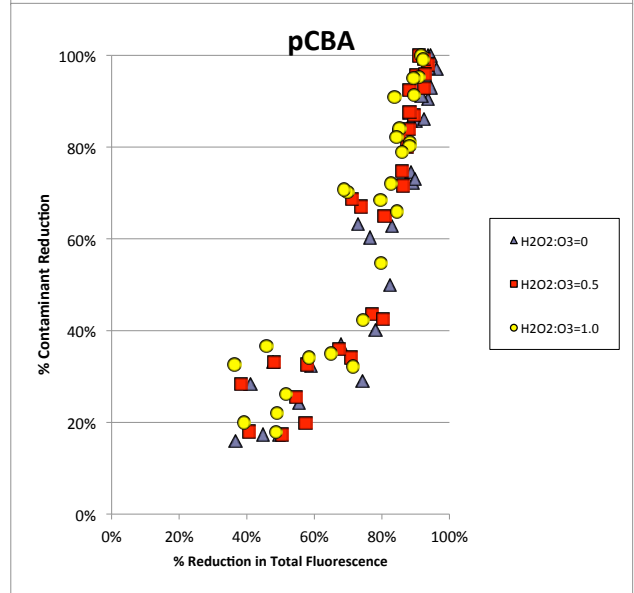
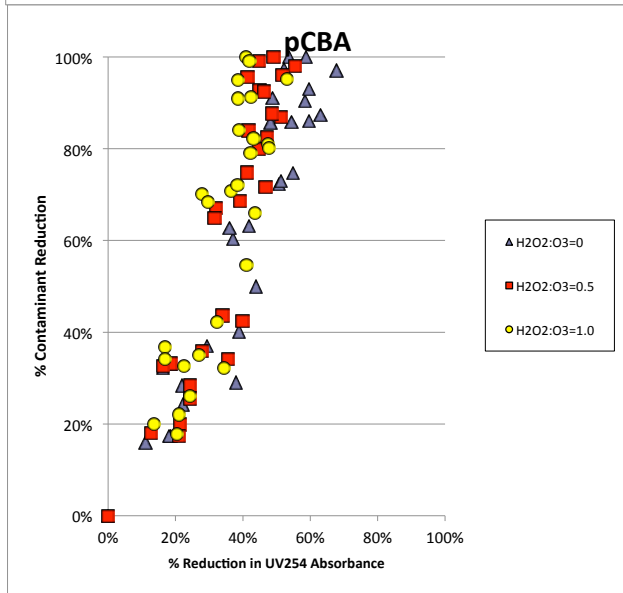
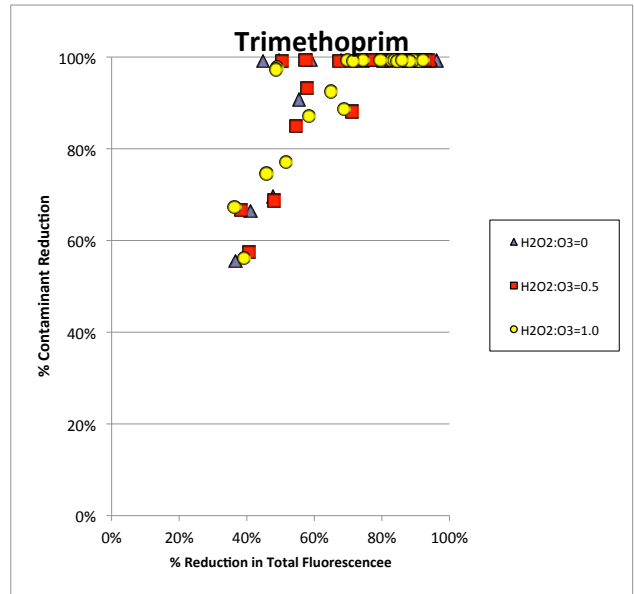
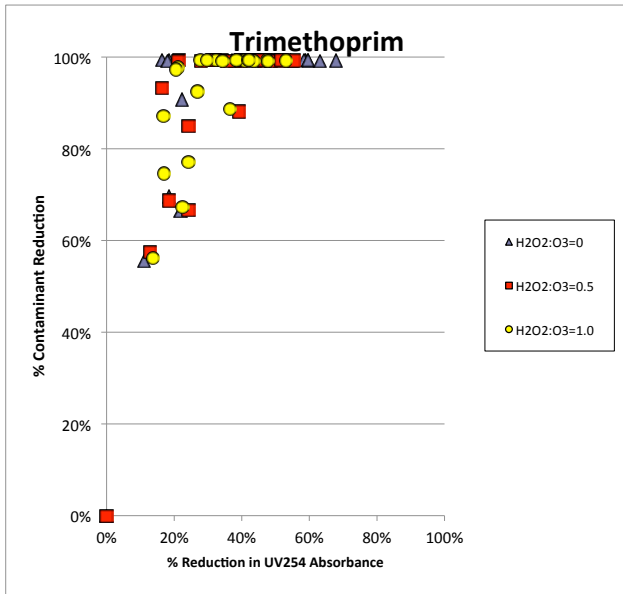
## Appendix 4 Comparison of H2O2 Doses Ozone and Ozone/H2O2



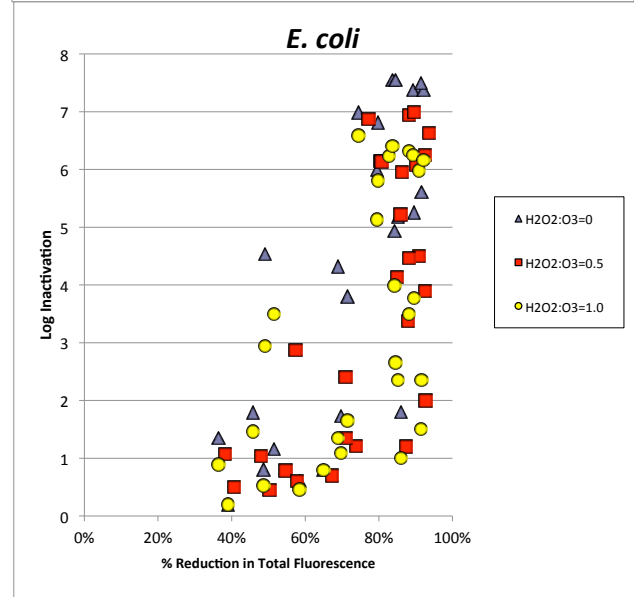
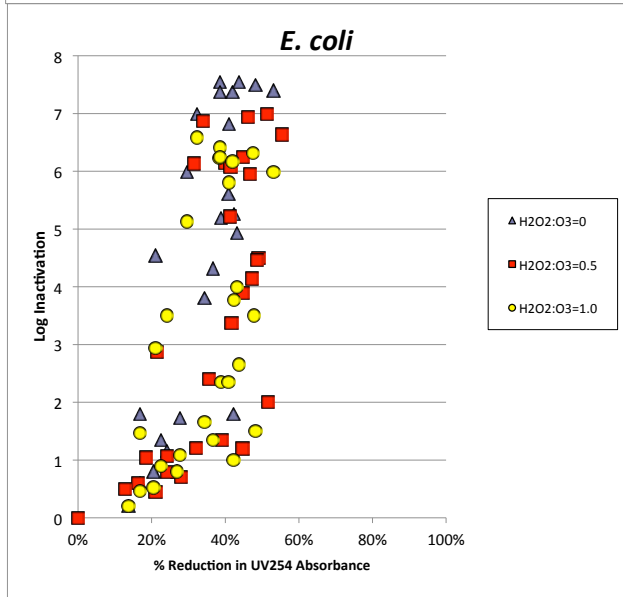
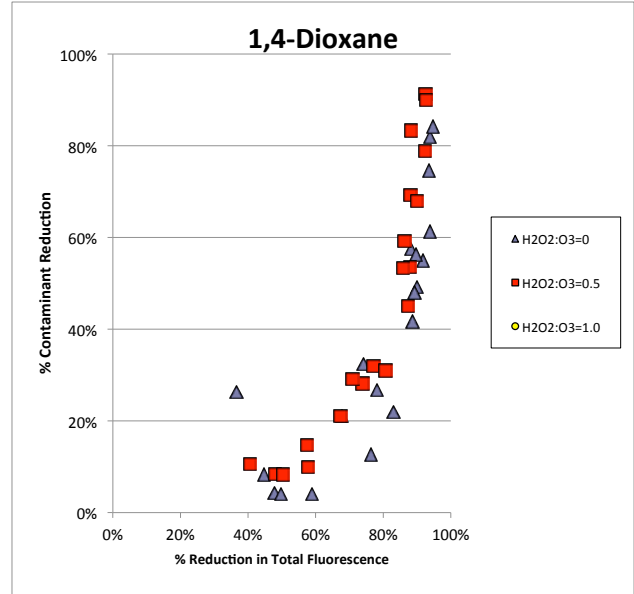
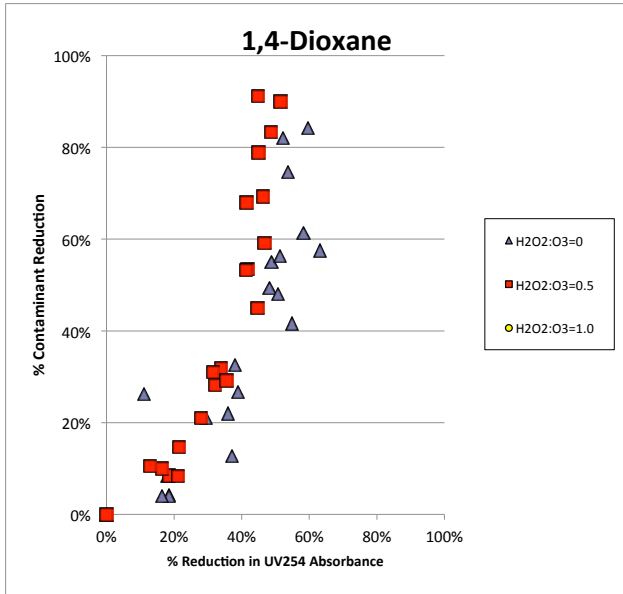
## Appendix 4 Comparison of H2O2 Doses Ozone and Ozone/H2O2



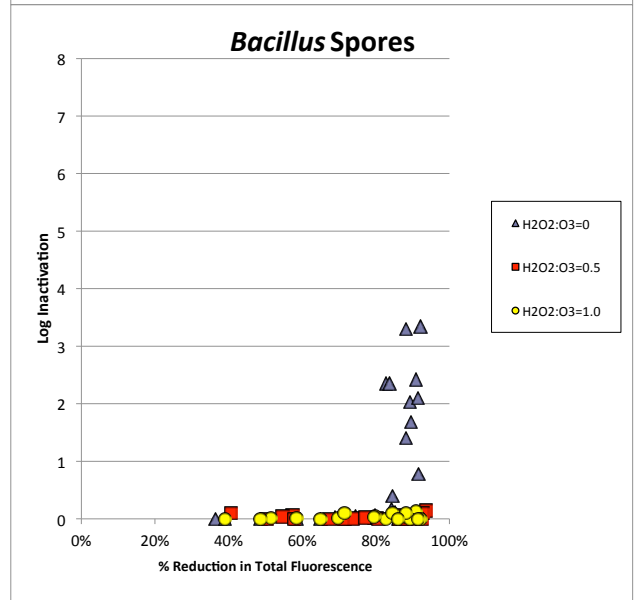
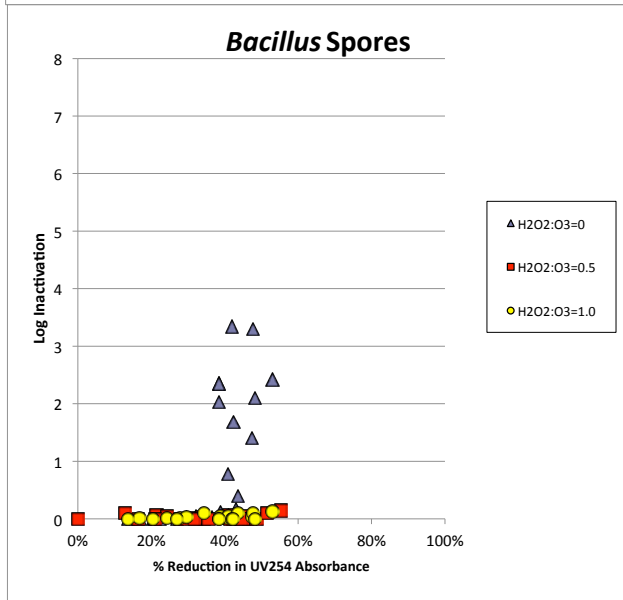
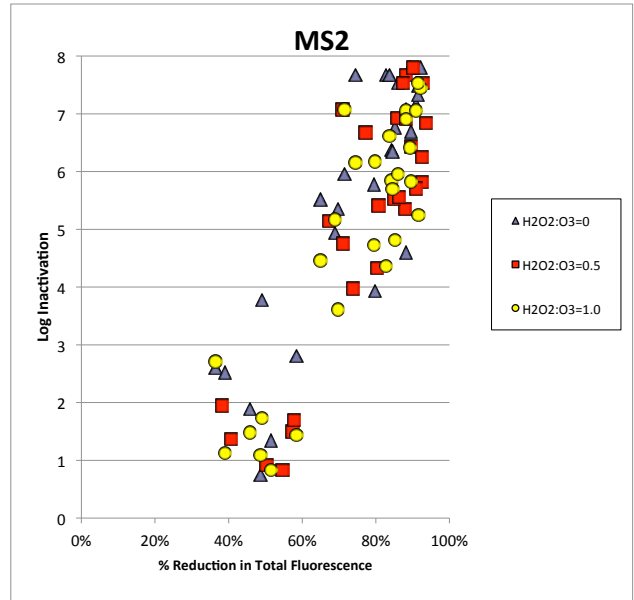
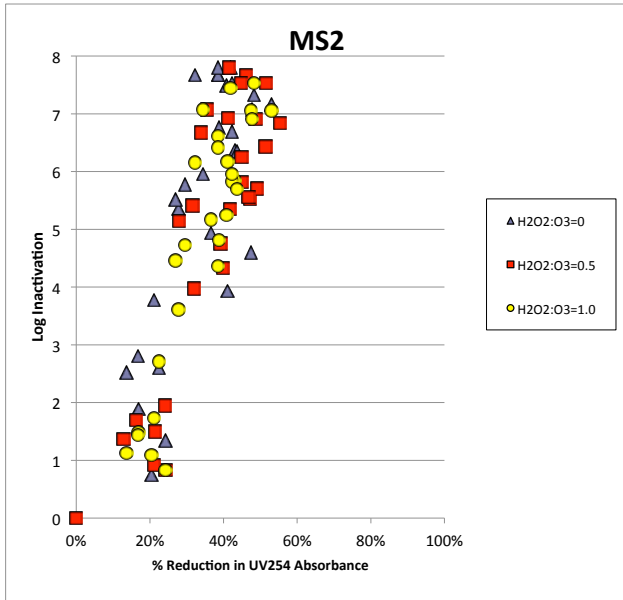
## Appendix 4 Comparison of H2O2 Doses Ozone and Ozone/H2O2



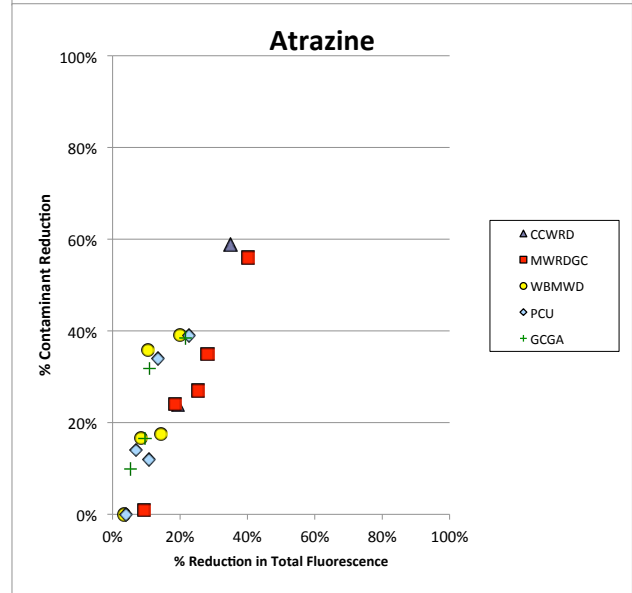
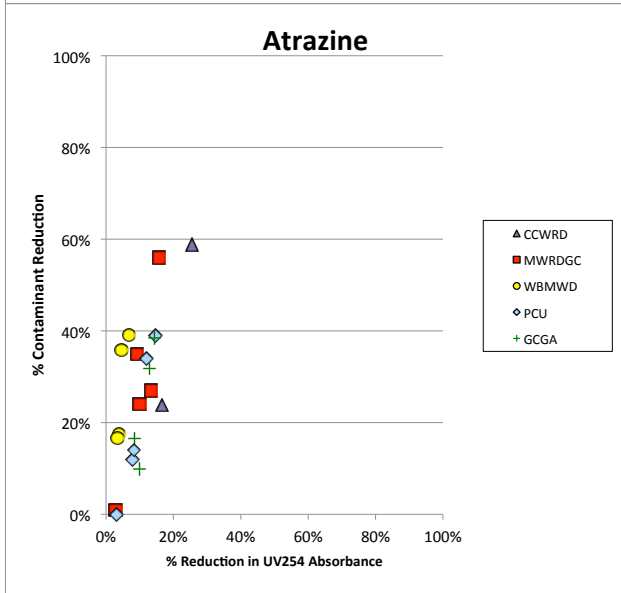
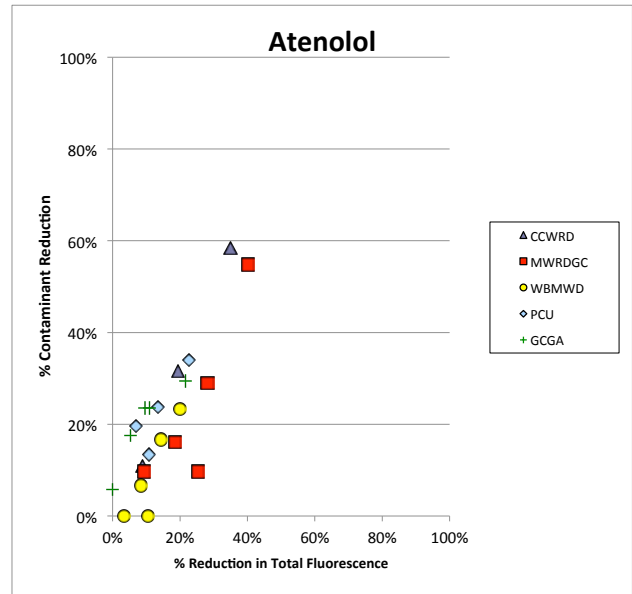
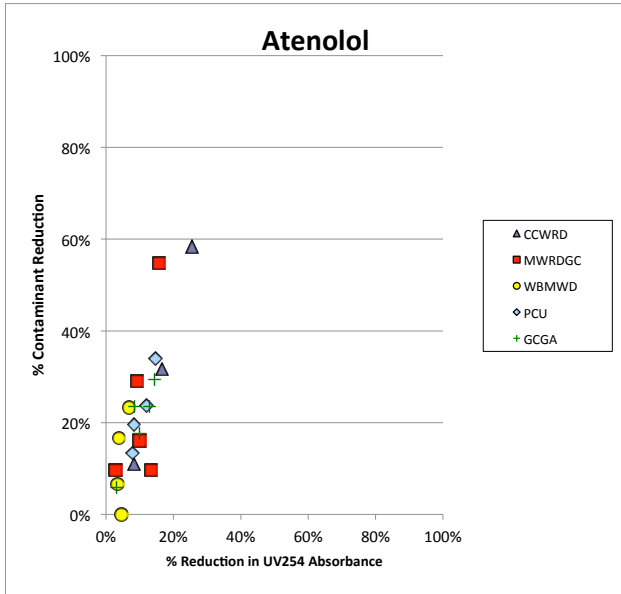
## Appendix 4 Comparison of H2O2 Doses Ozone and Ozone/H2O2



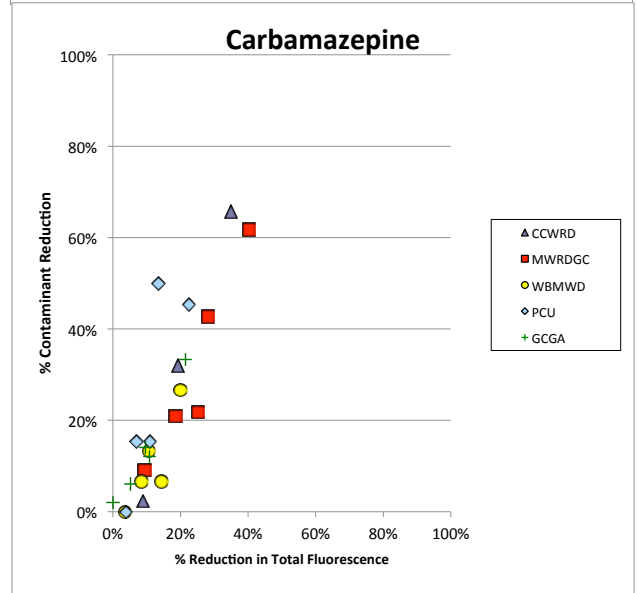
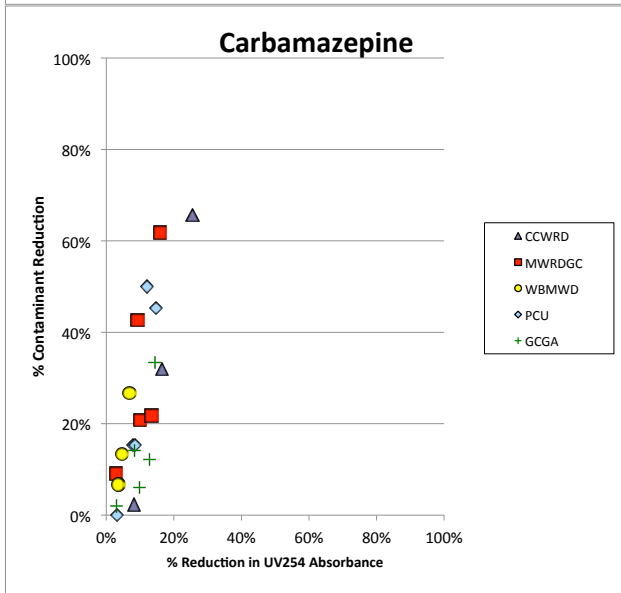
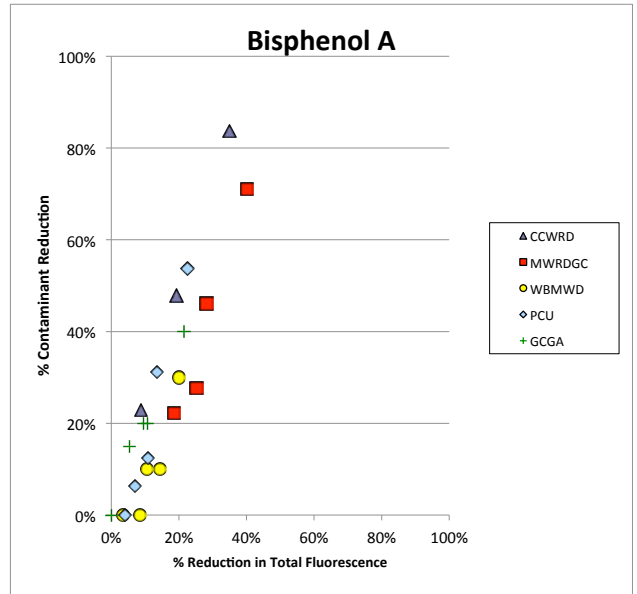
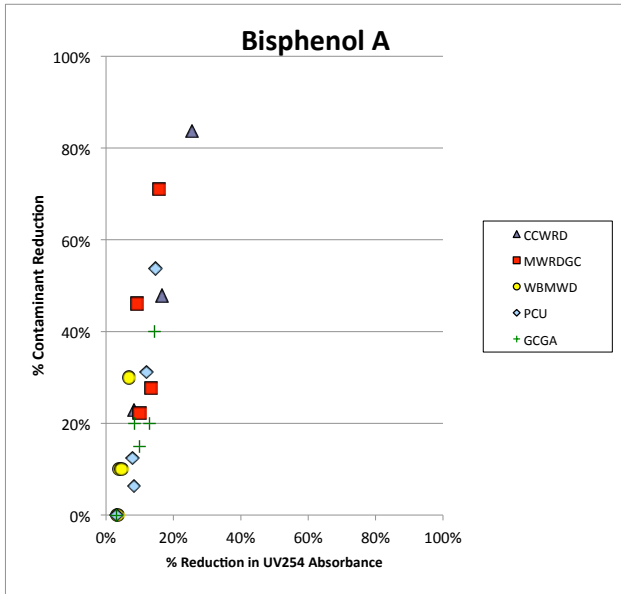
## Appendix 4 Comparison of H2O2 Doses Ozone and Ozone/H2O2



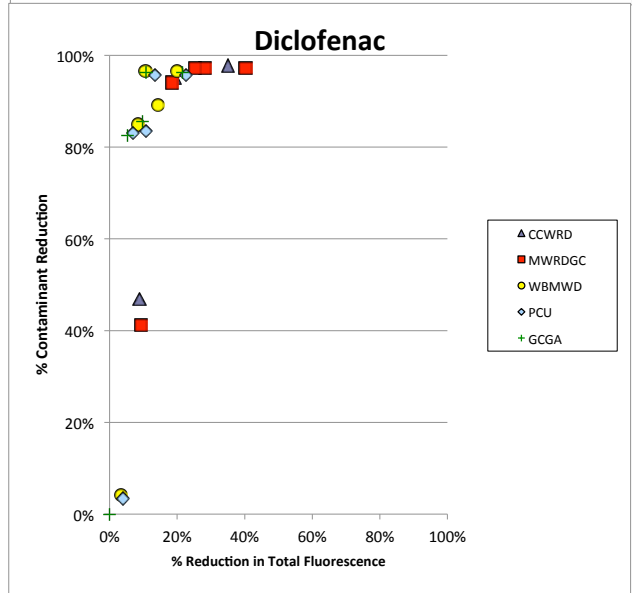
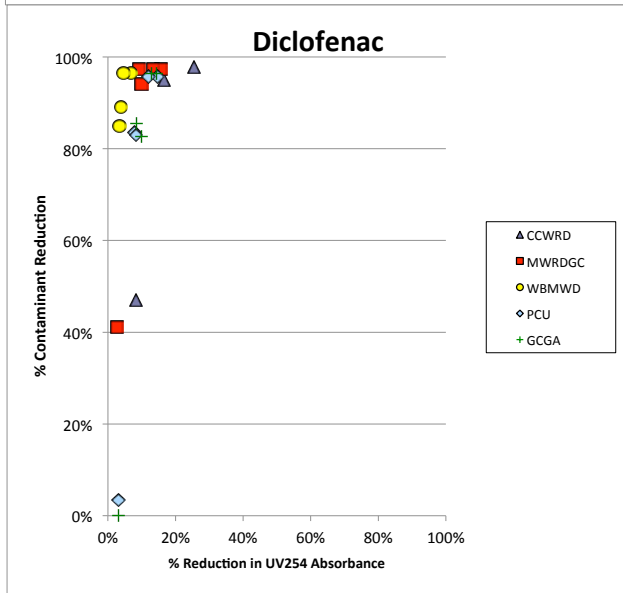
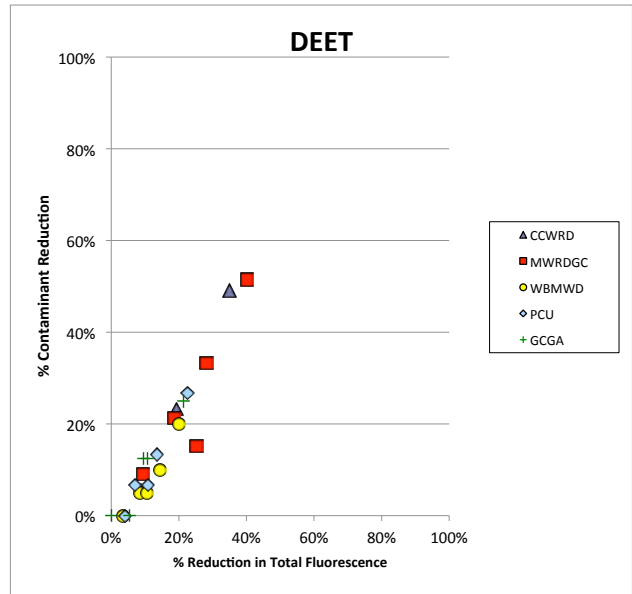
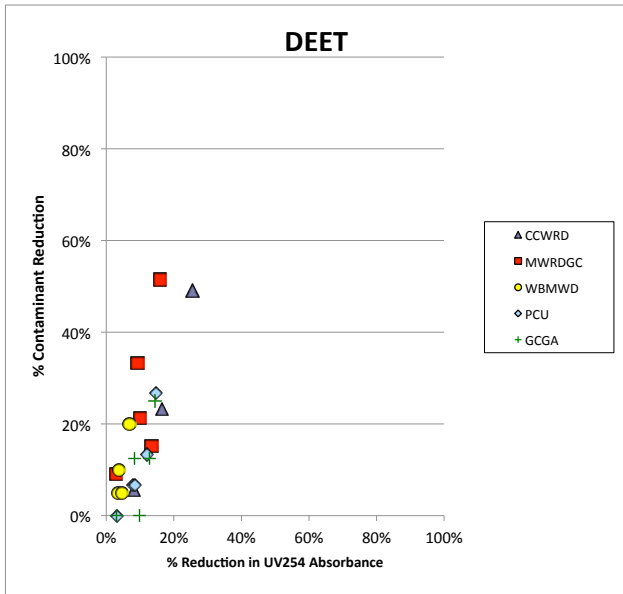
## Appendix 5 Comparison of Secondary Effluents UV/H2O2



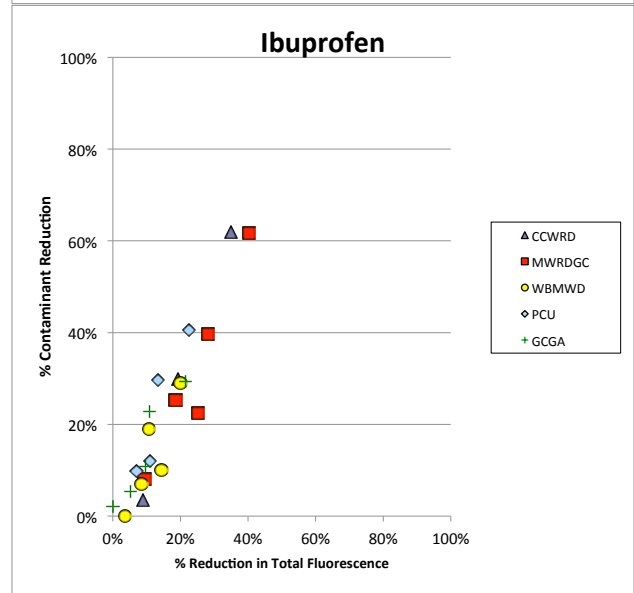
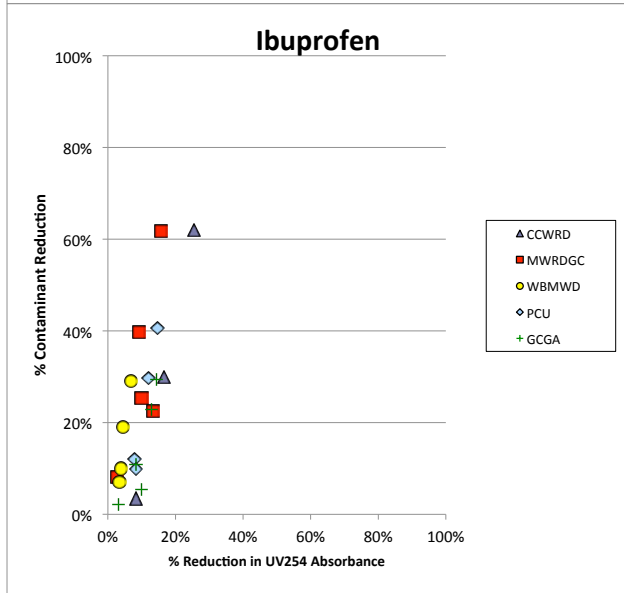
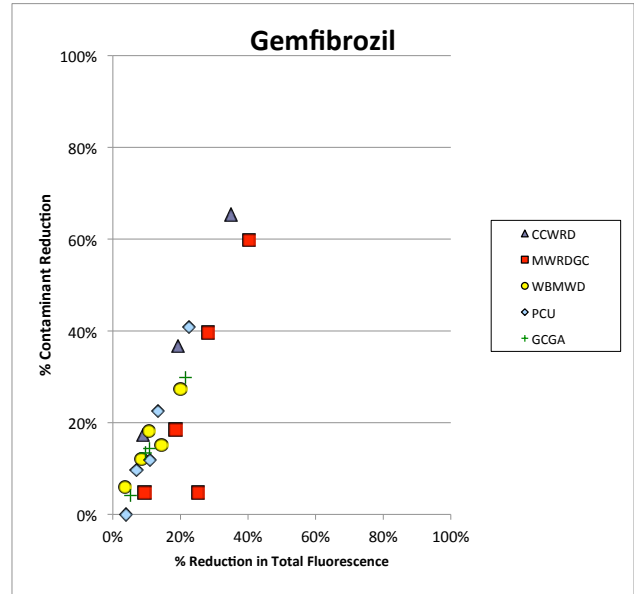
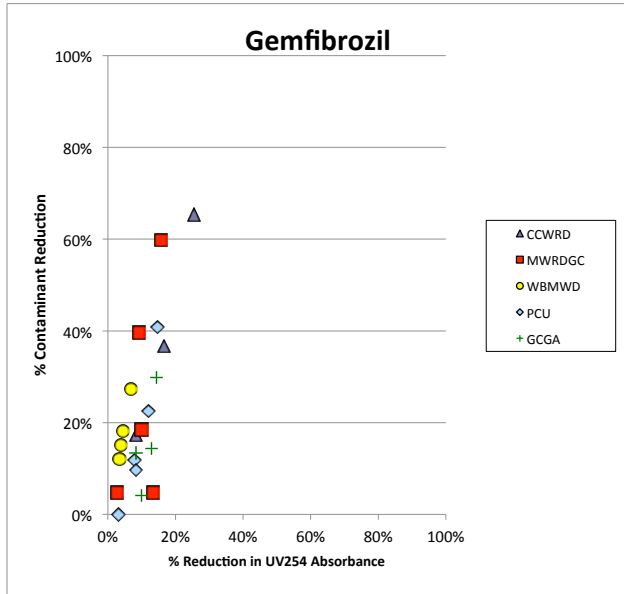
## Appendix 5 Comparison of Secondary Effluents UV/H2O2



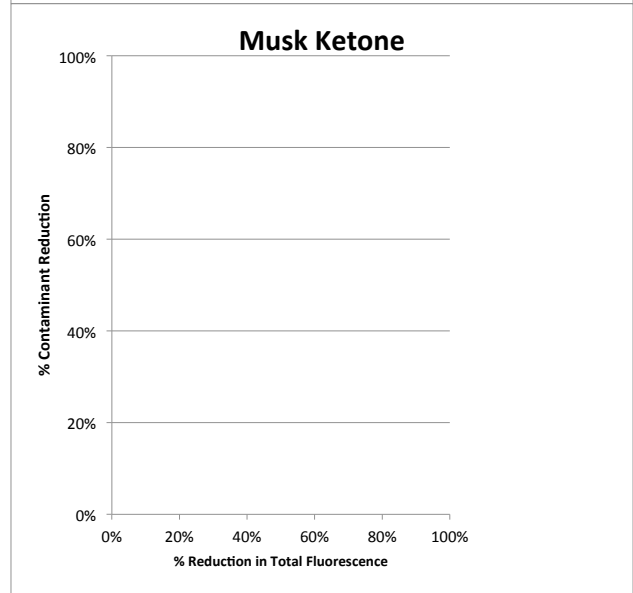
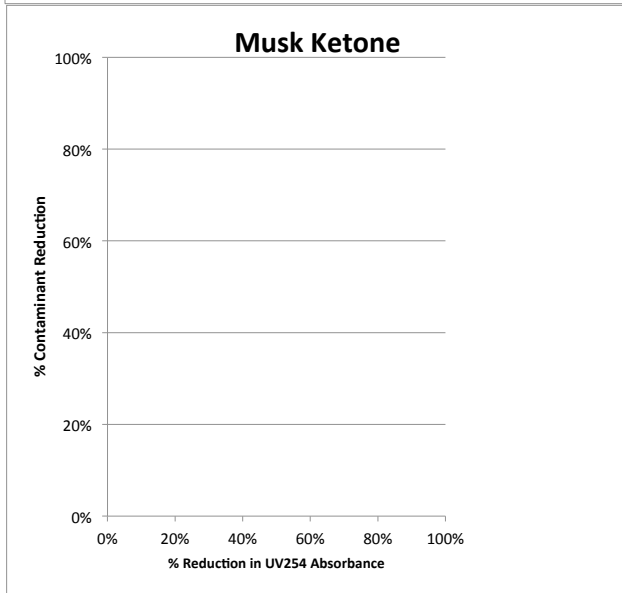
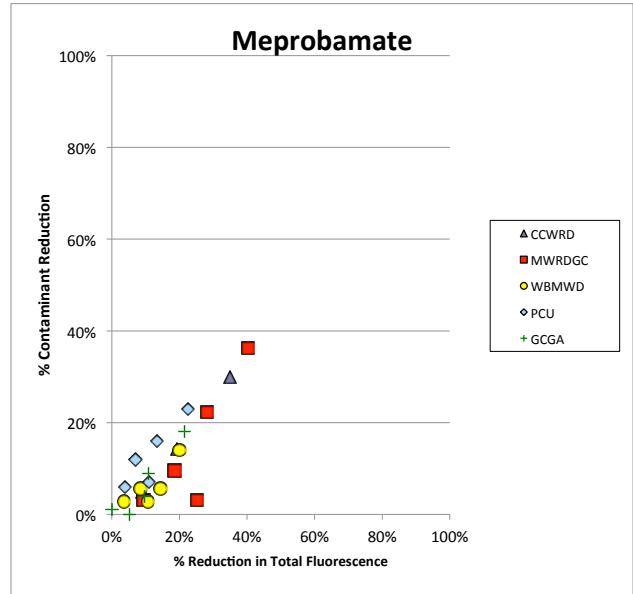
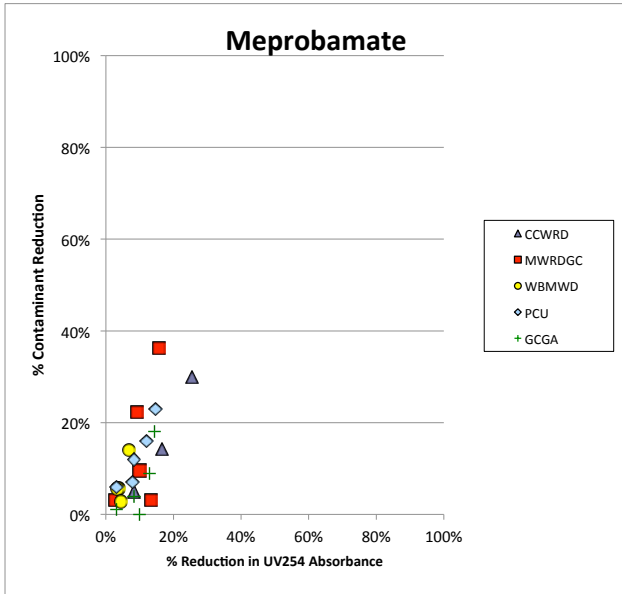
## Appendix 5 Comparison of Secondary Effluents UV/H2O2



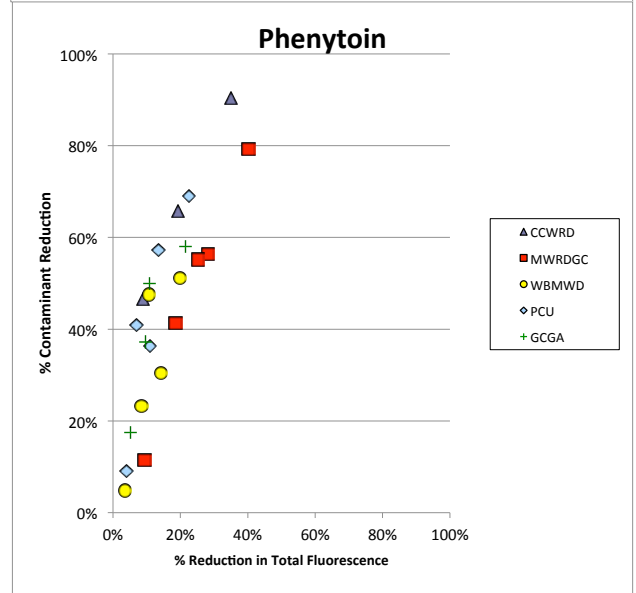
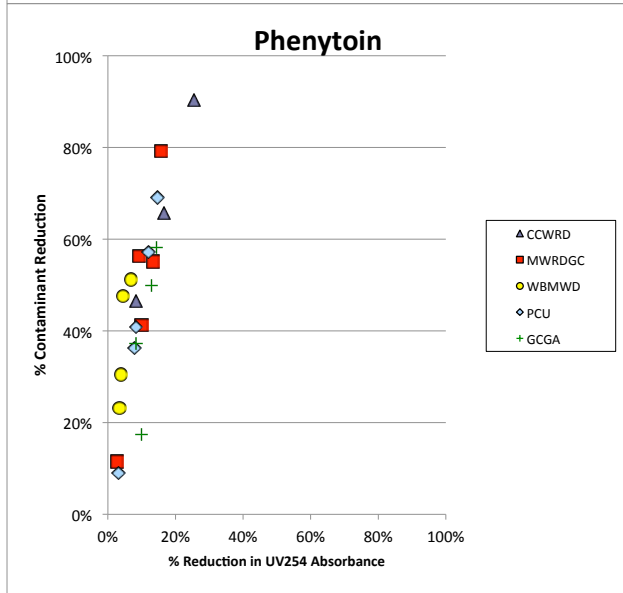
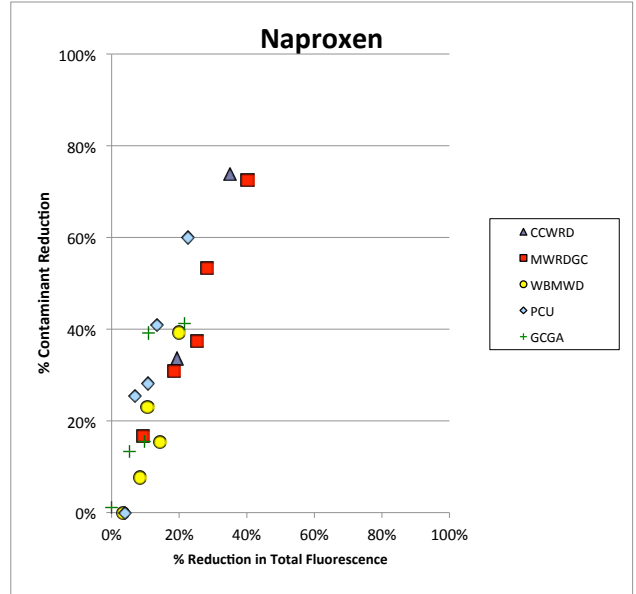
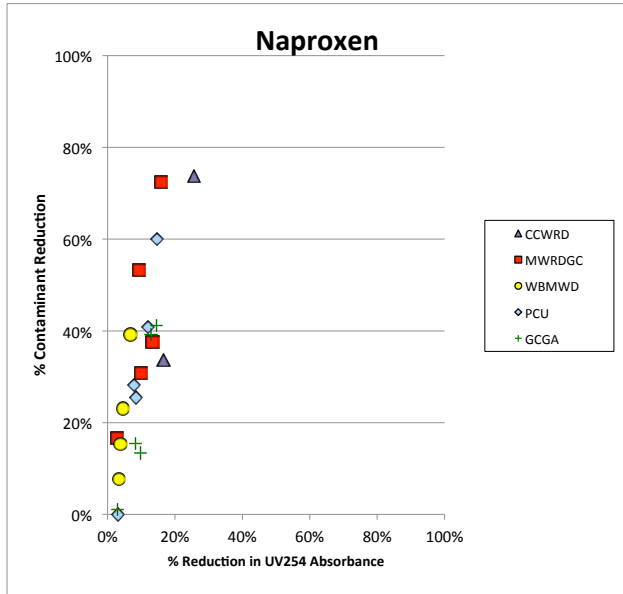
## Appendix 5 Comparison of Secondary Effluents UV/H<sub>2</sub>O<sub>2</sub>



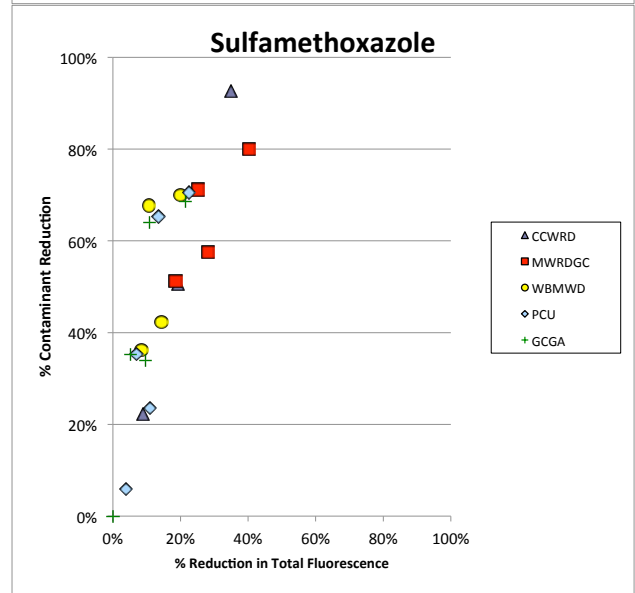
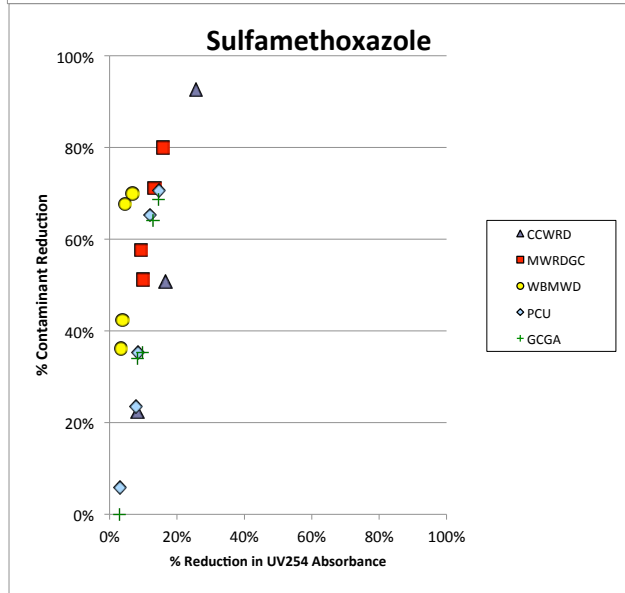
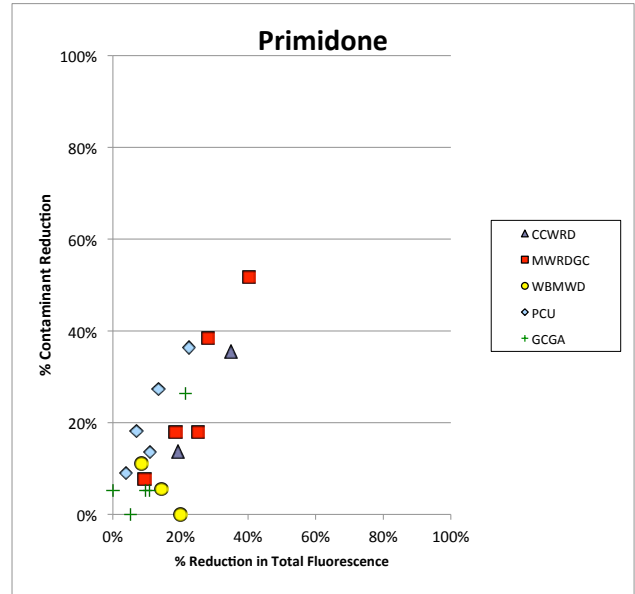
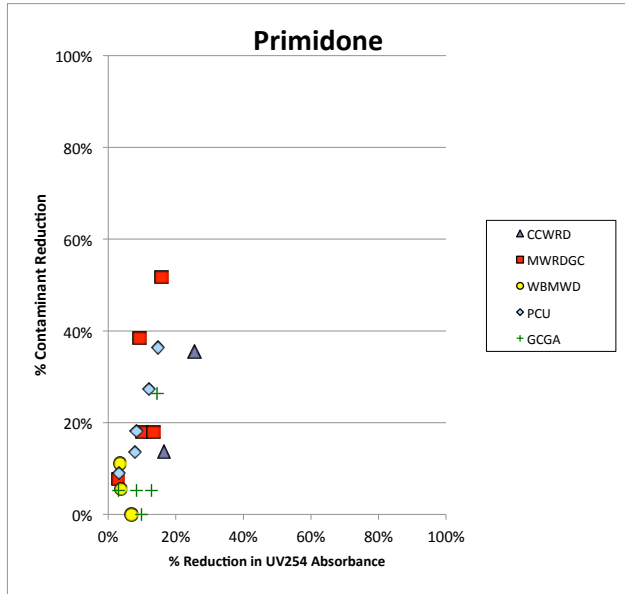
## Appendix 5 Comparison of Secondary Effluents UV/H<sub>2</sub>O<sub>2</sub>



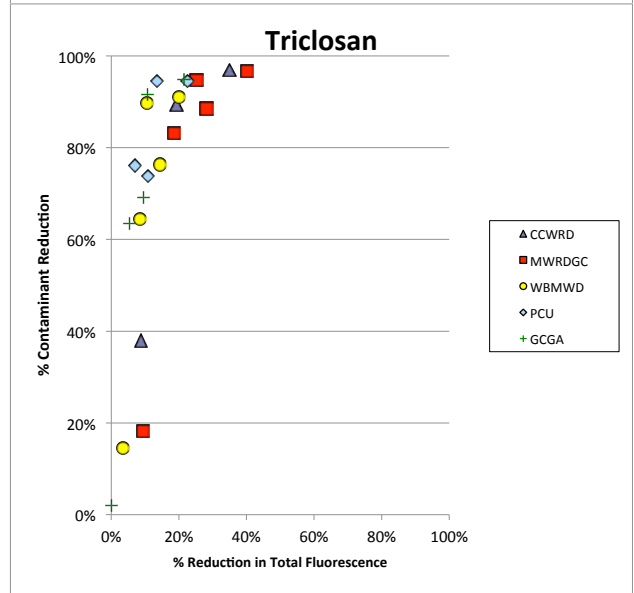
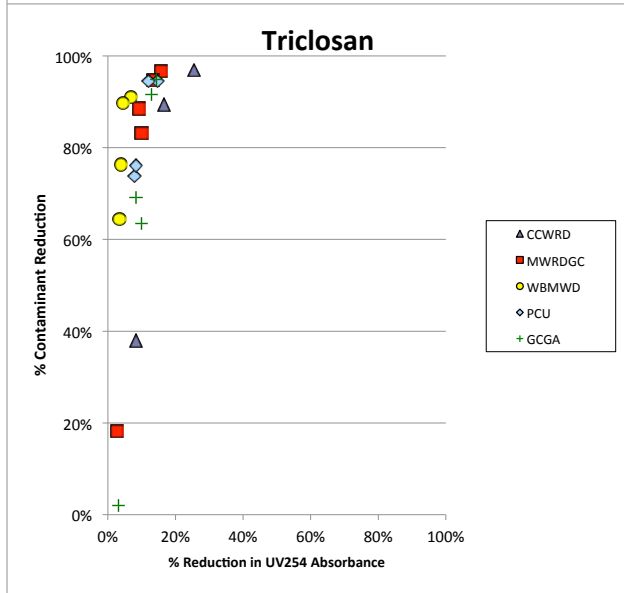
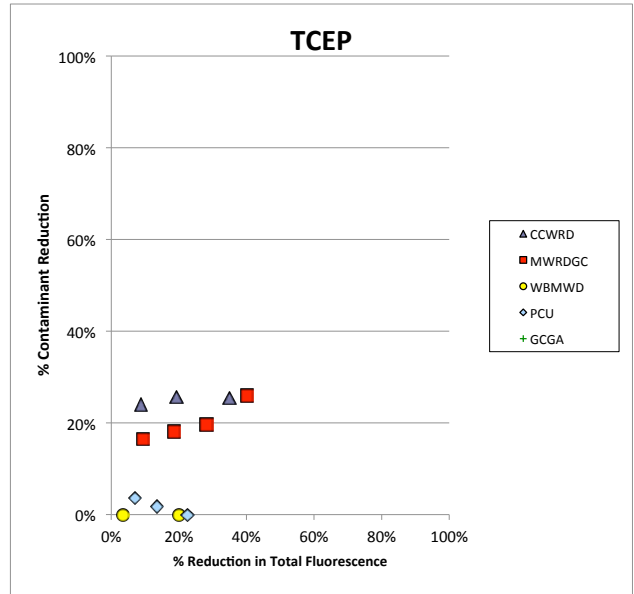
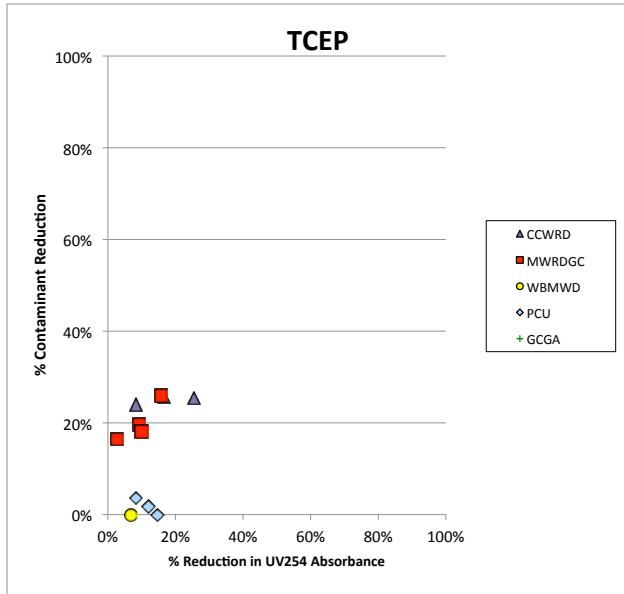
## Appendix 5 Comparison of Secondary Effluents UV/H2O2



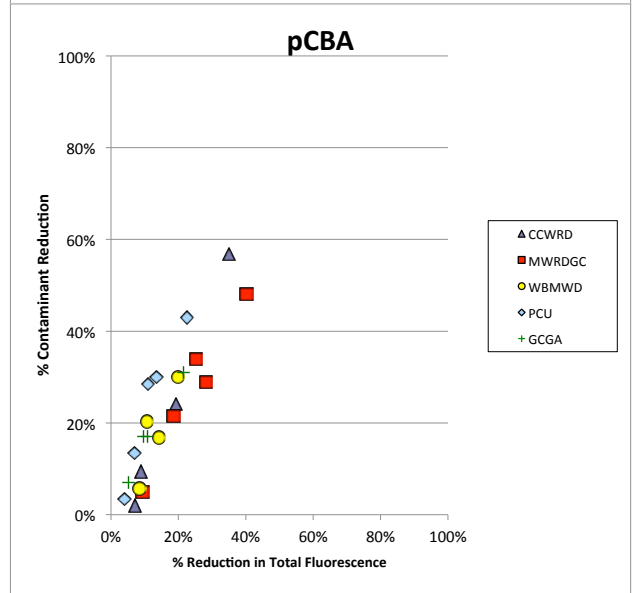
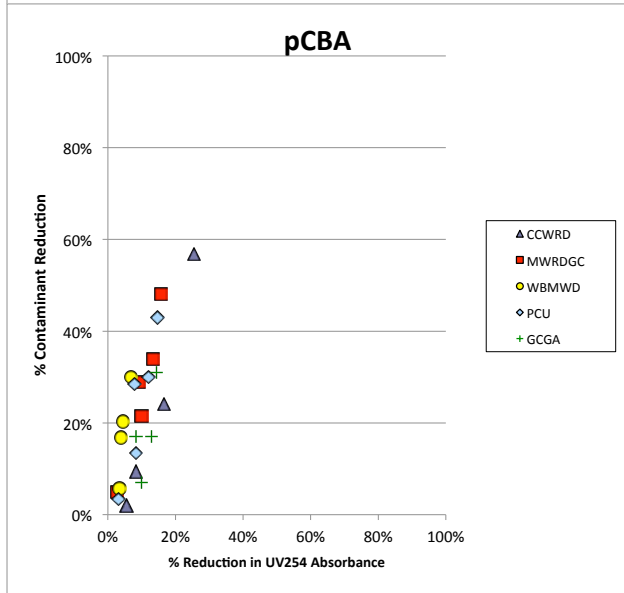
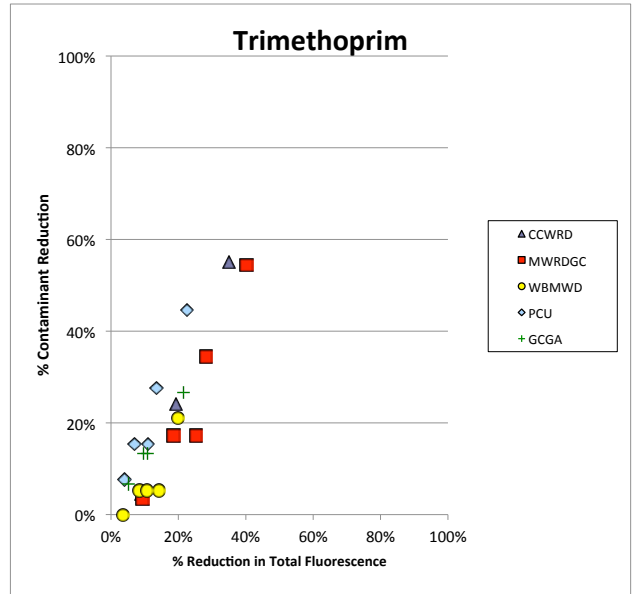
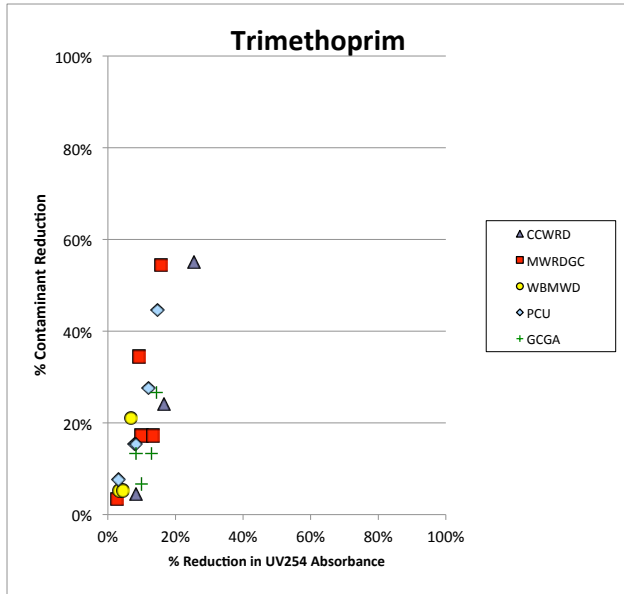
## Appendix 5 Comparison of Secondary Effluents UV/H<sub>2</sub>O<sub>2</sub>



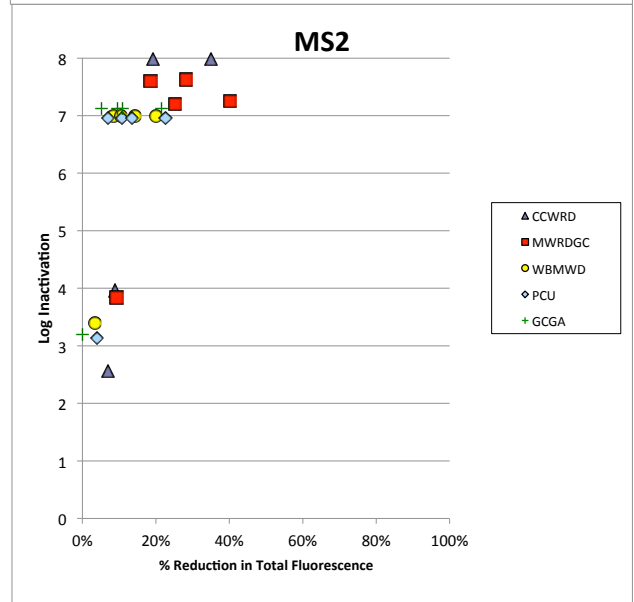
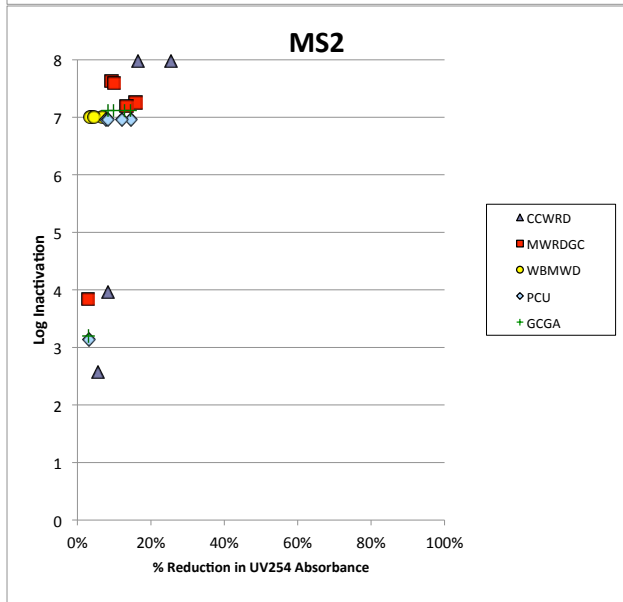
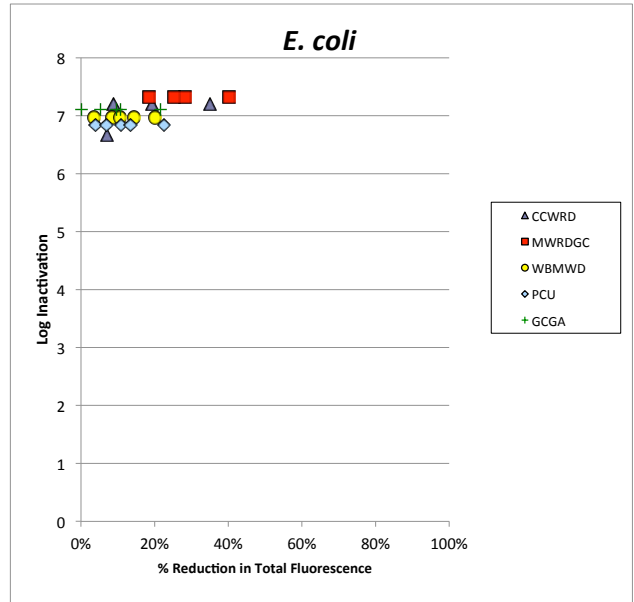
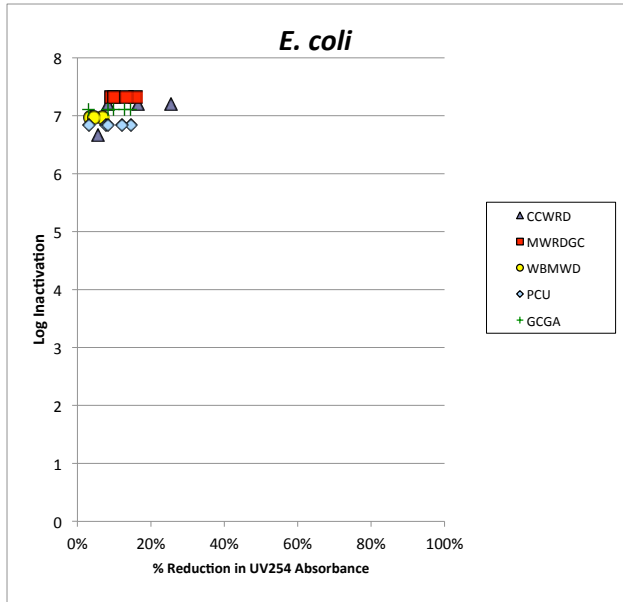
## Appendix 5 Comparison of Secondary Effluents UV/H2O2



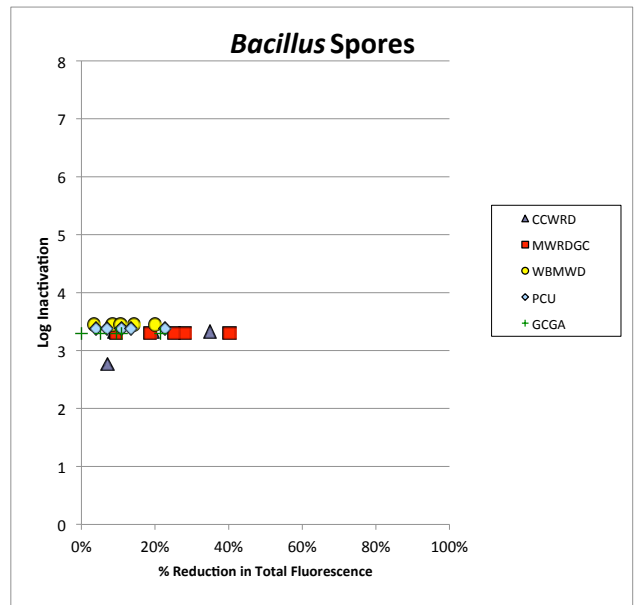
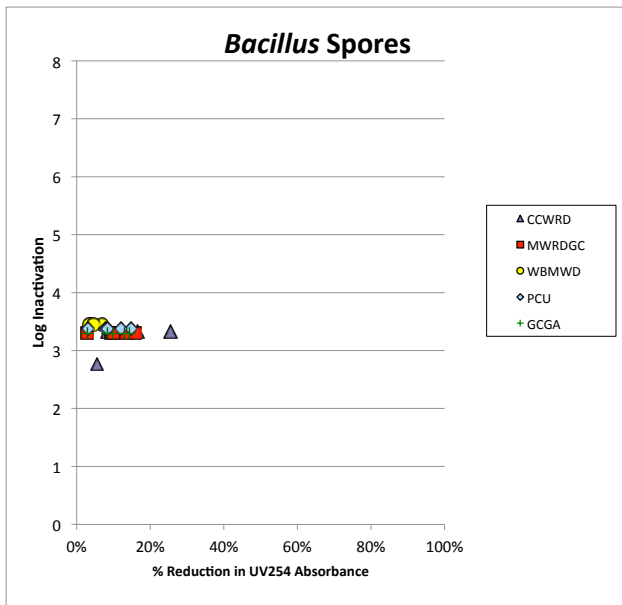
## Appendix 5 Comparison of Secondary Effluents UV/H2O2



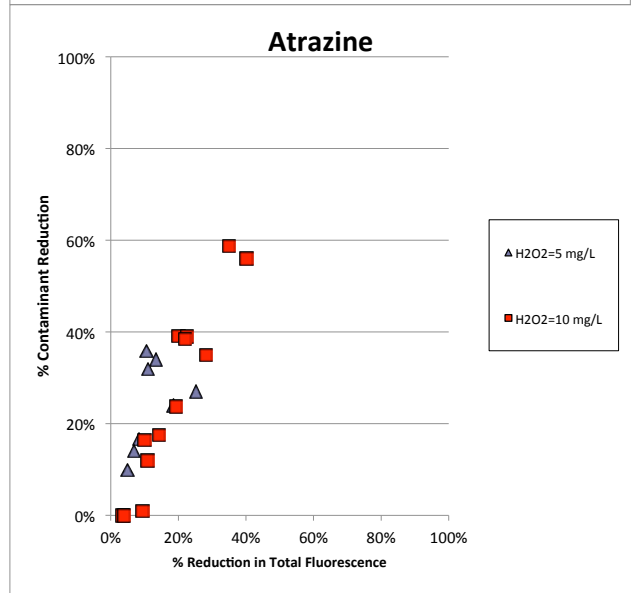
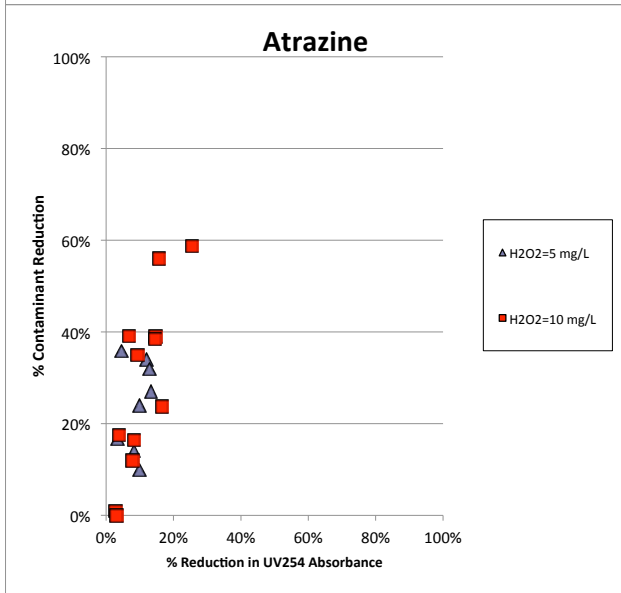
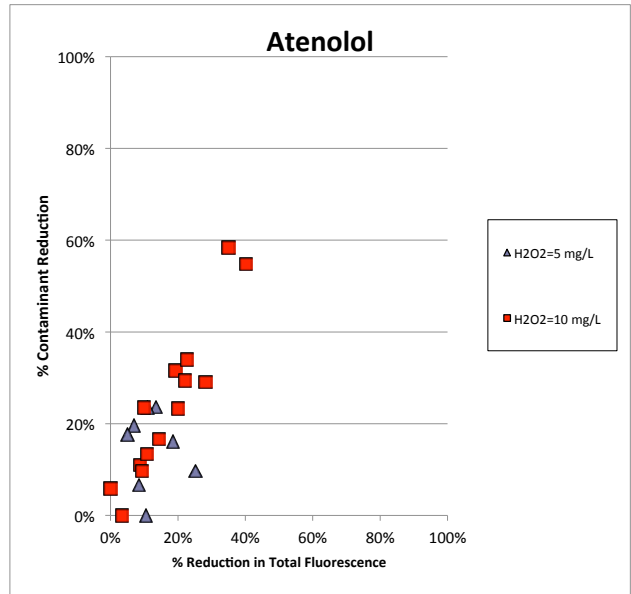
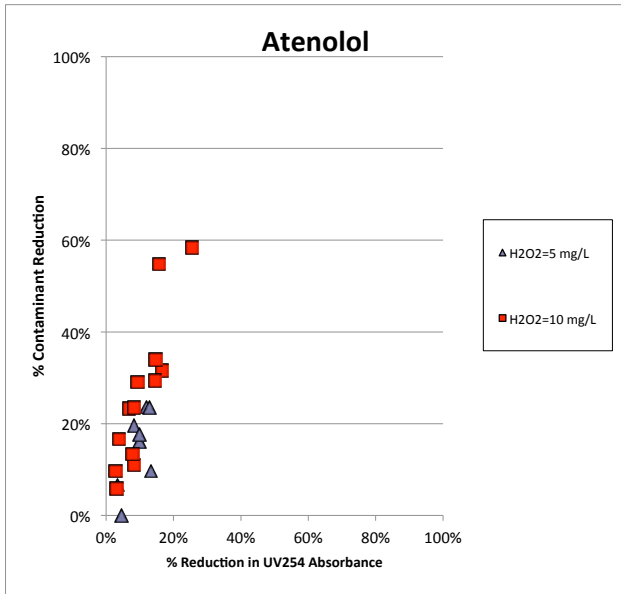
## Appendix 5 Comparison of Secondary Effluents UV/H2O2



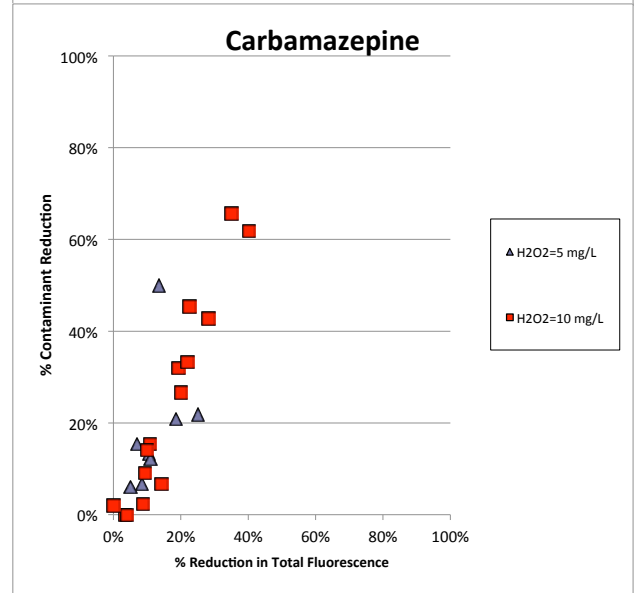
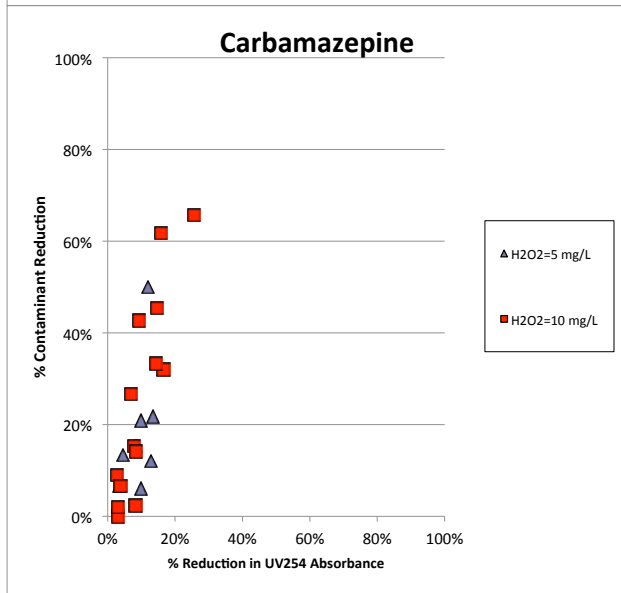
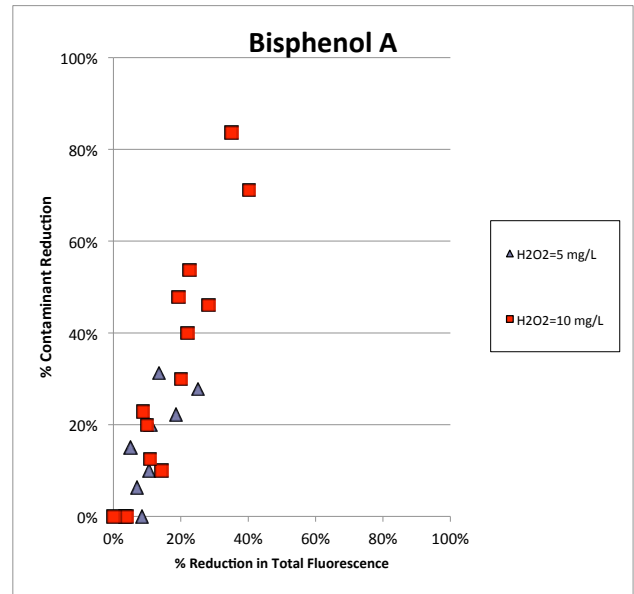
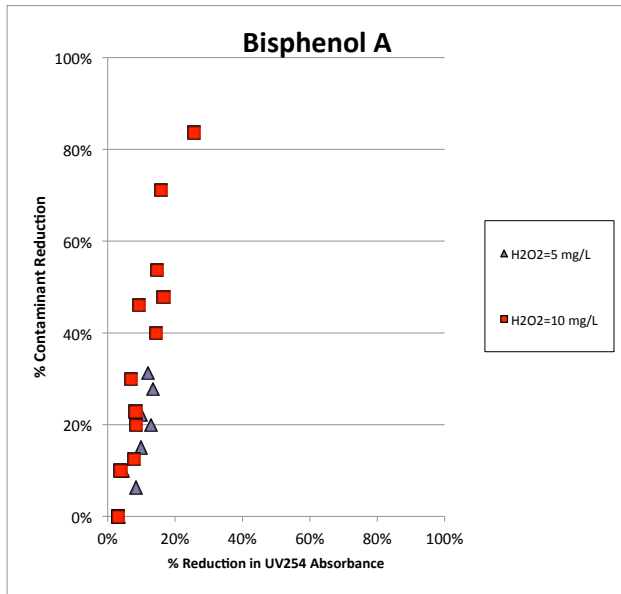
**Appendix 5**  
**Comparison of Secondary Effluents**  
**UV/H<sub>2</sub>O<sub>2</sub>**



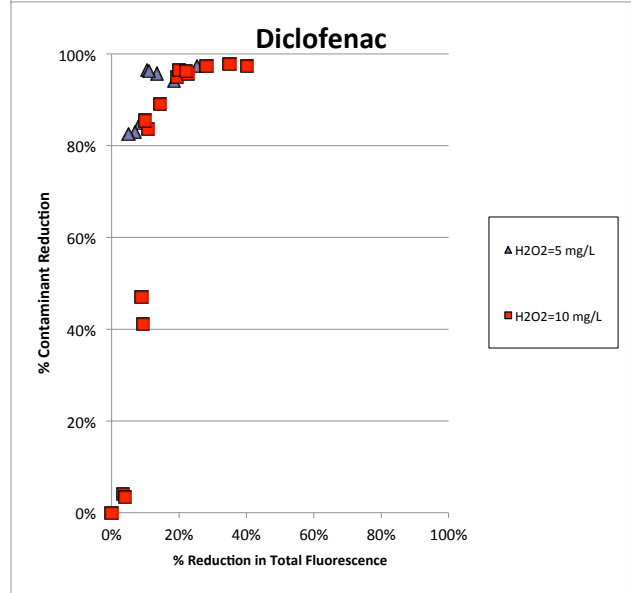
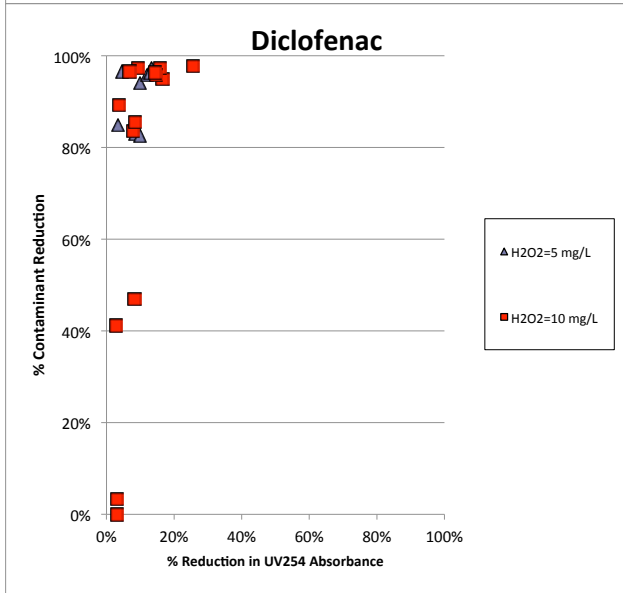
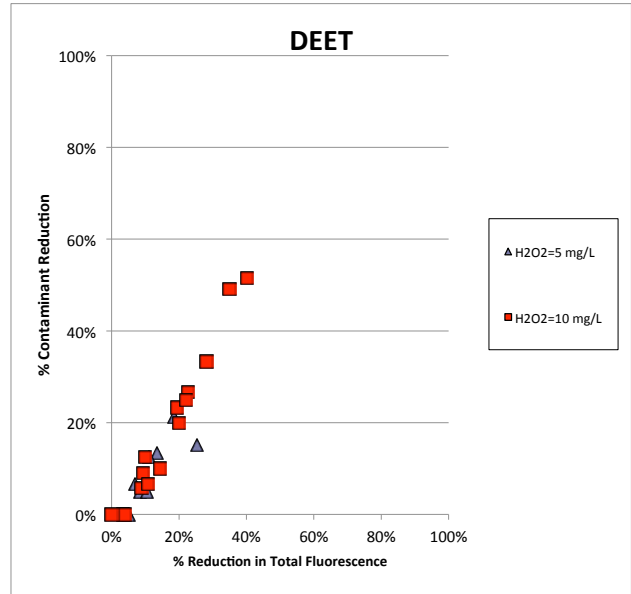
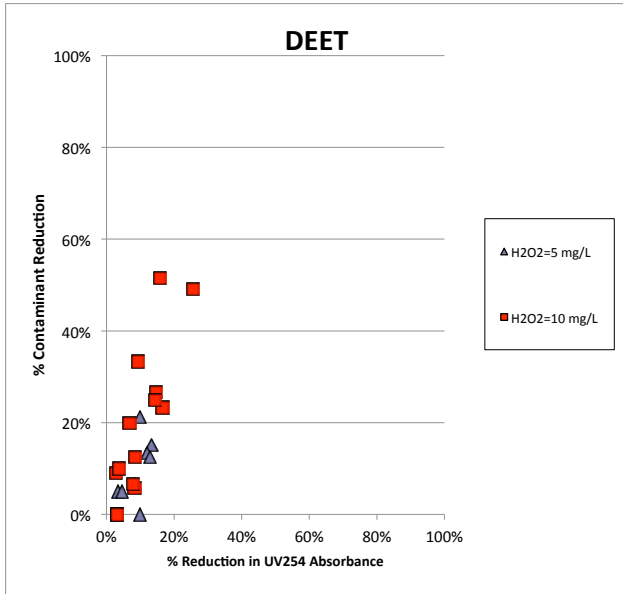
## Appendix 6 Comparison of H2O2 Doses UV/H2O2



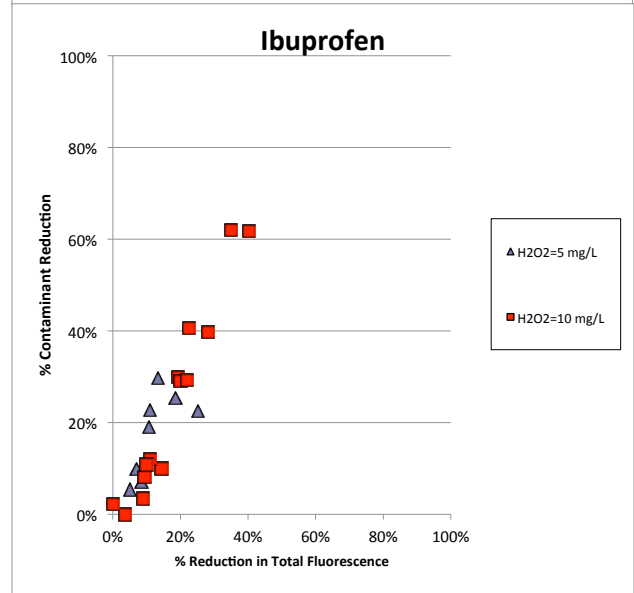
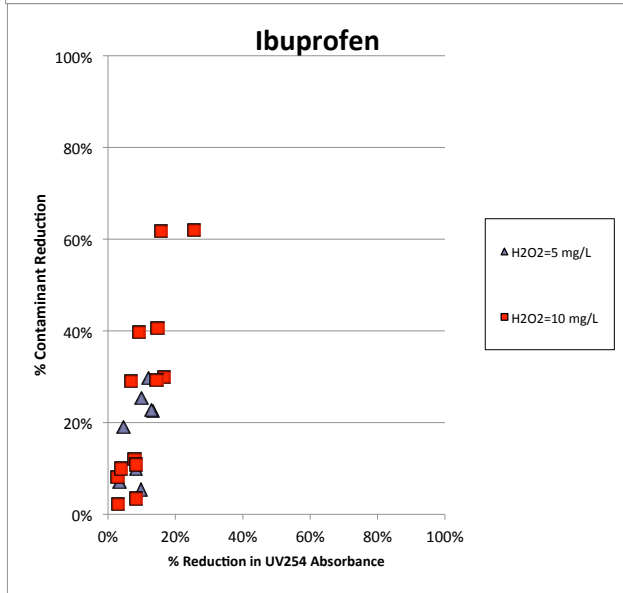
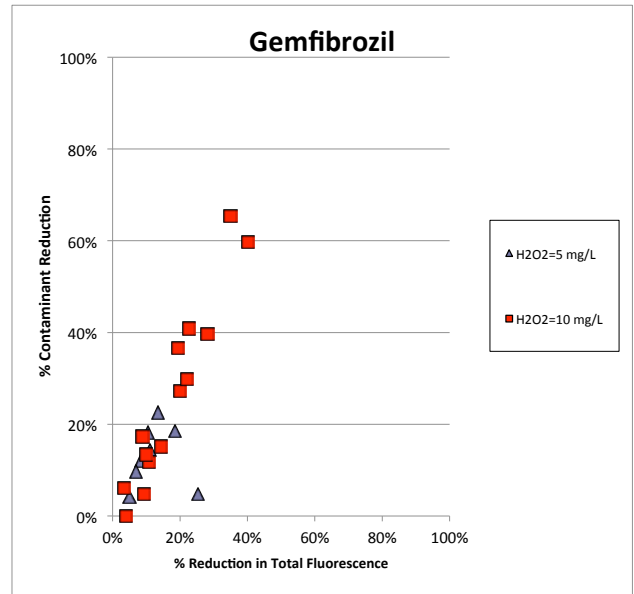
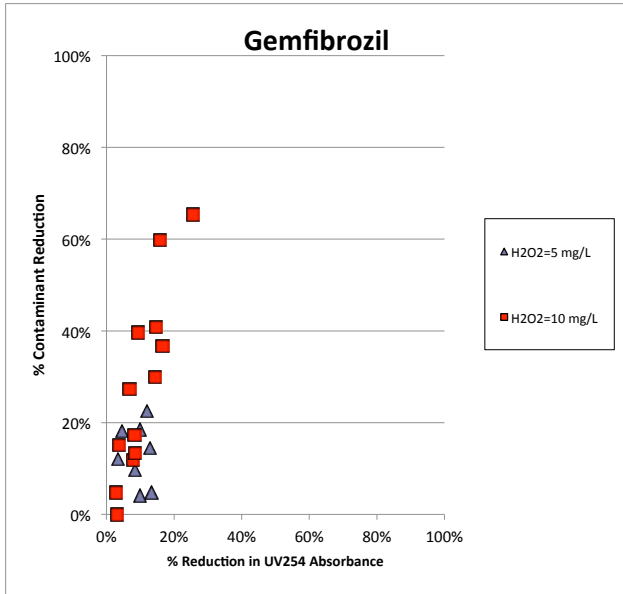
## Appendix 6 Comparison of H2O2 Doses UV/H2O2



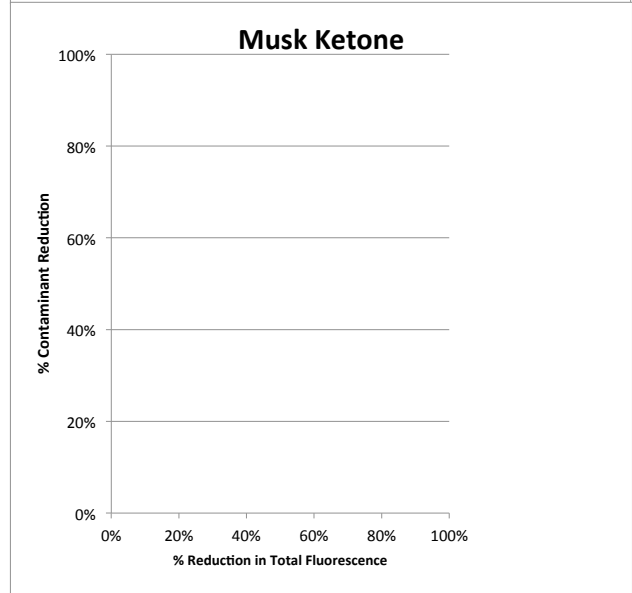
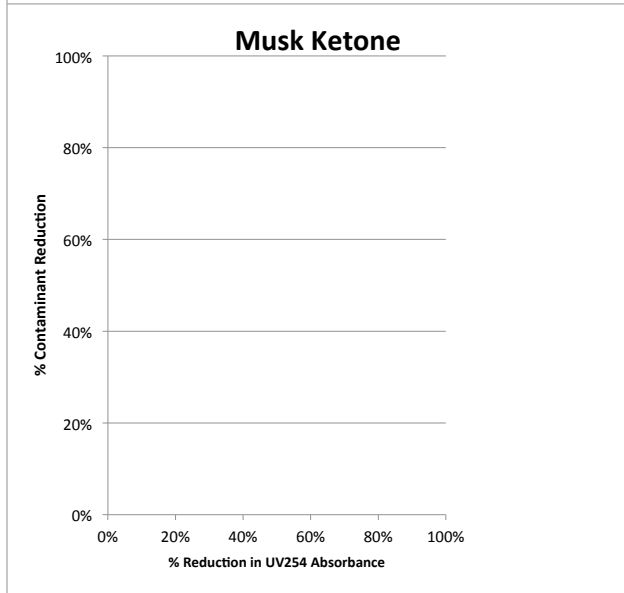
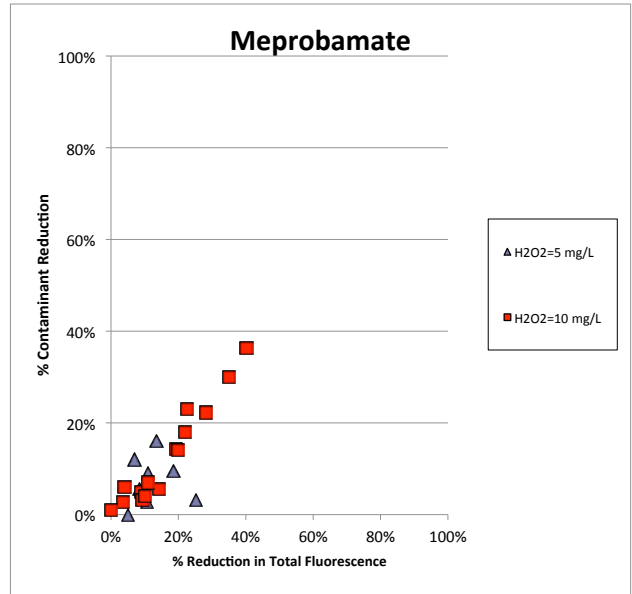
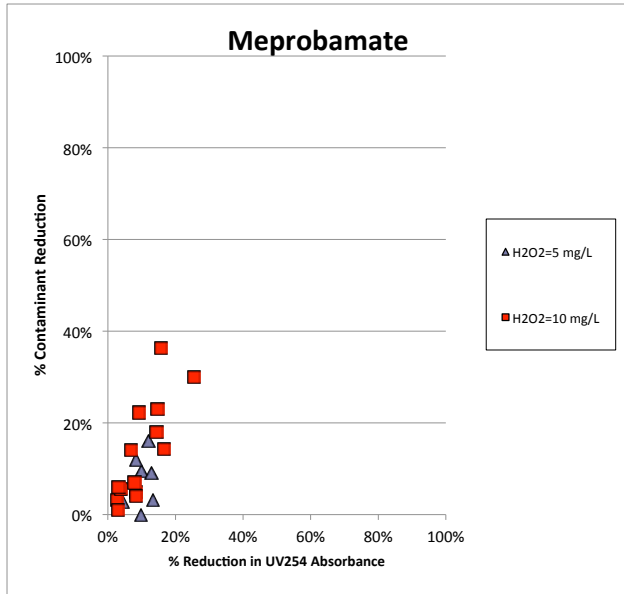
## Appendix 6 Comparison of H<sub>2</sub>O<sub>2</sub> Doses UV/H<sub>2</sub>O<sub>2</sub>



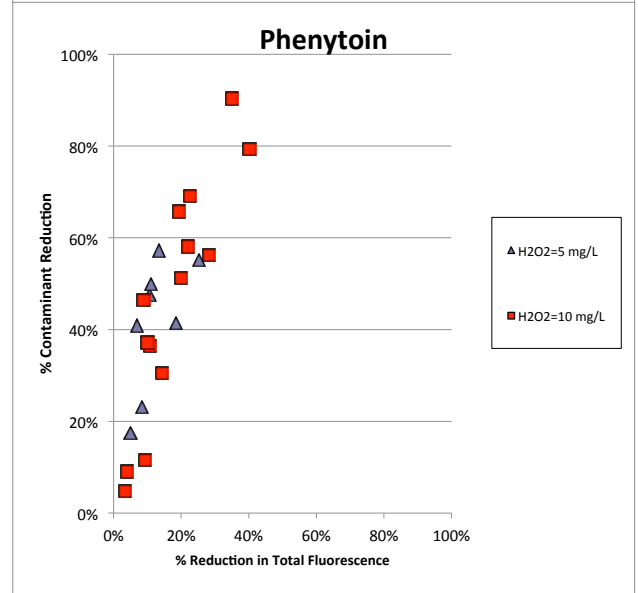
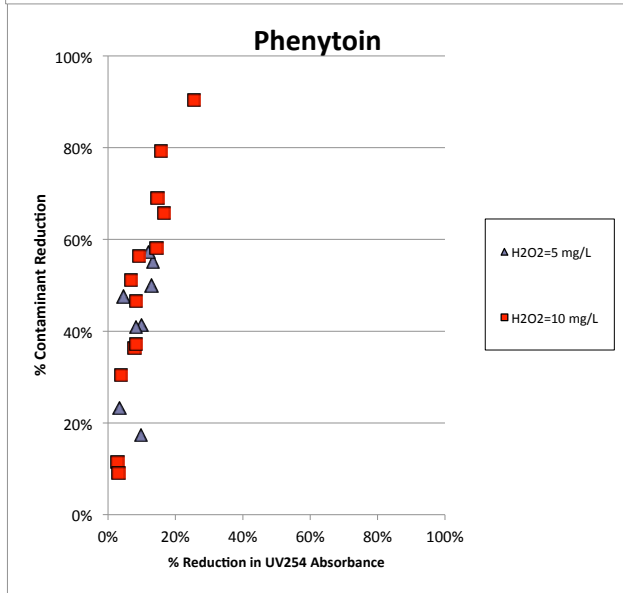
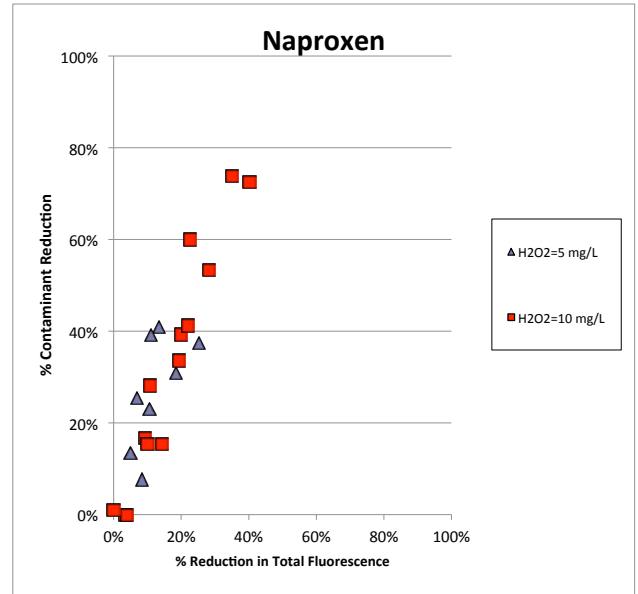
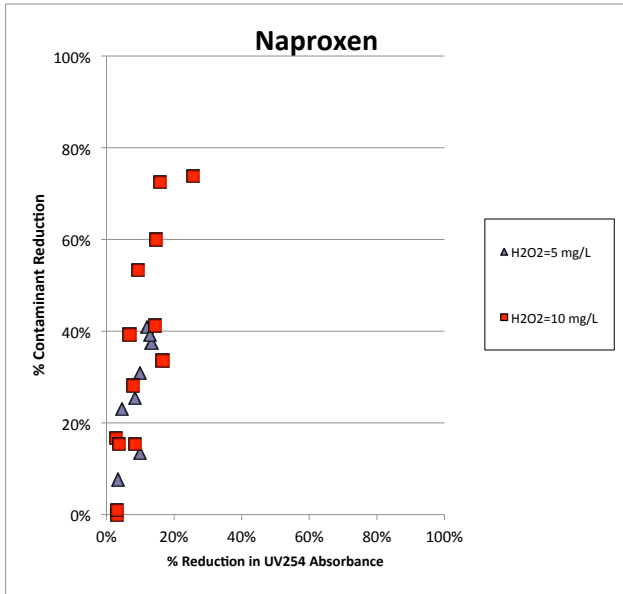
## Appendix 6 Comparison of H2O2 Doses UV/H2O2



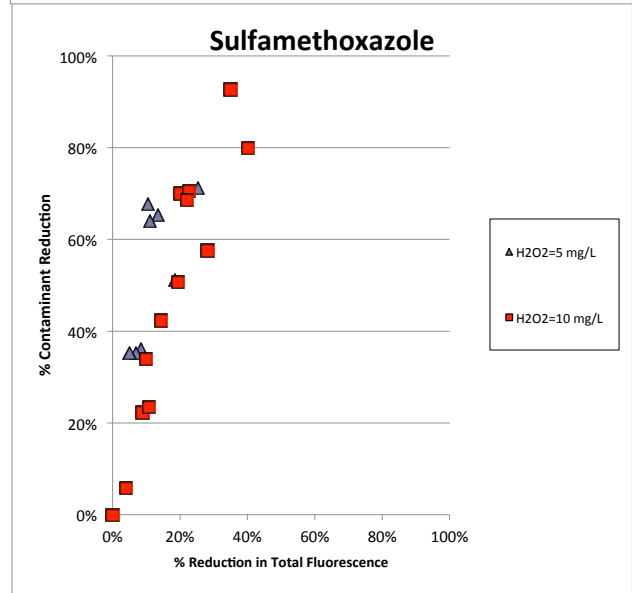
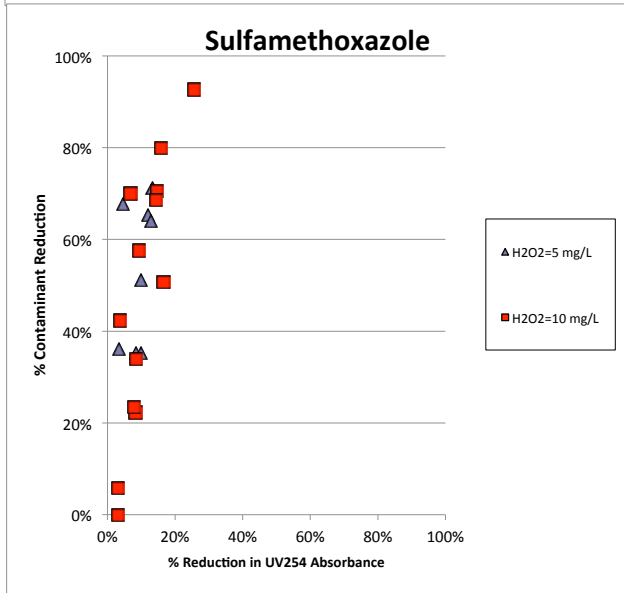
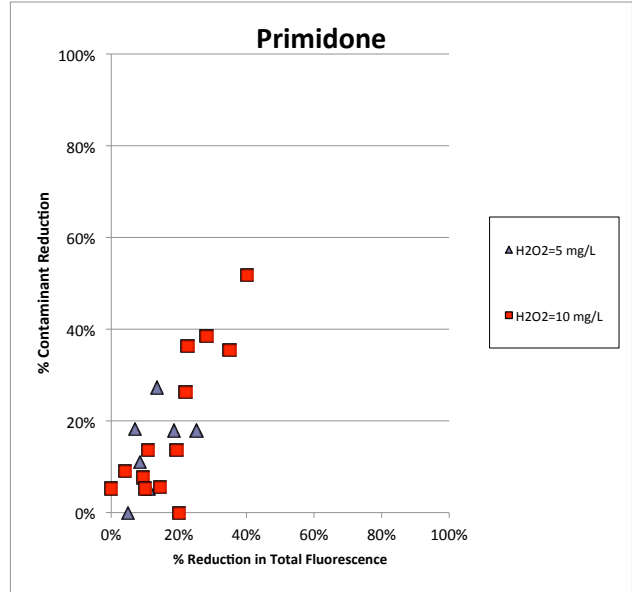
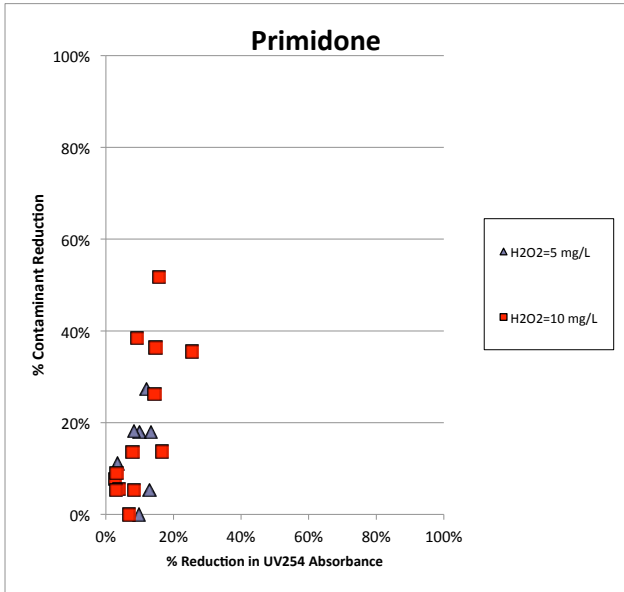
Appendix 6  
Comparison of H2O2 Doses  
UV/H2O2



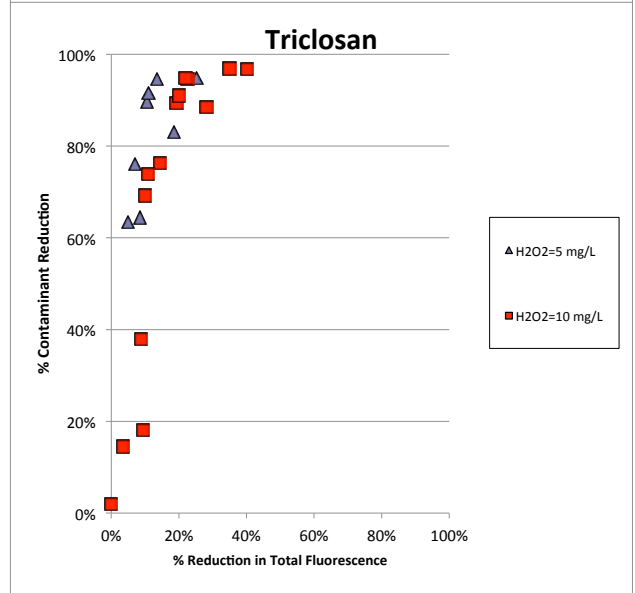
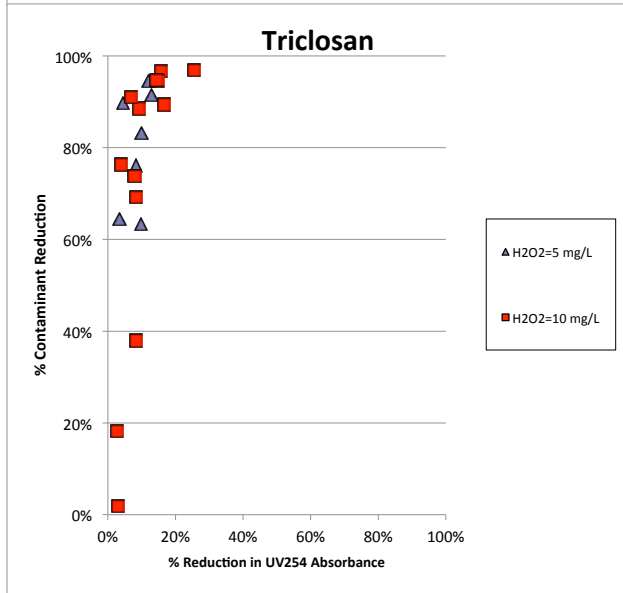
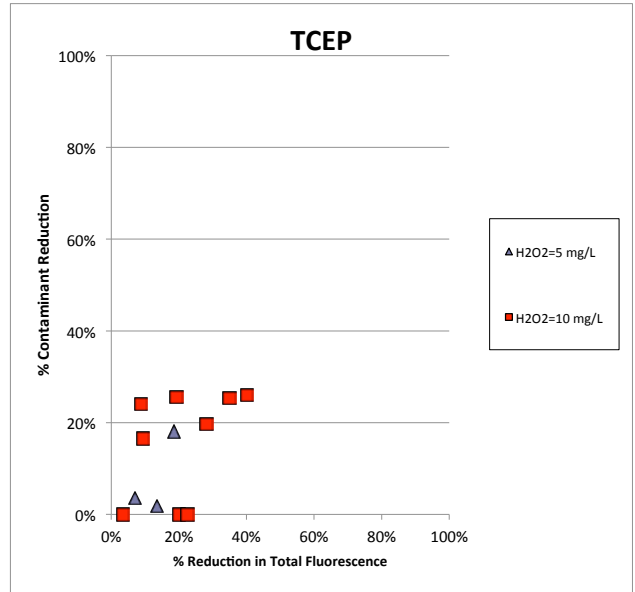
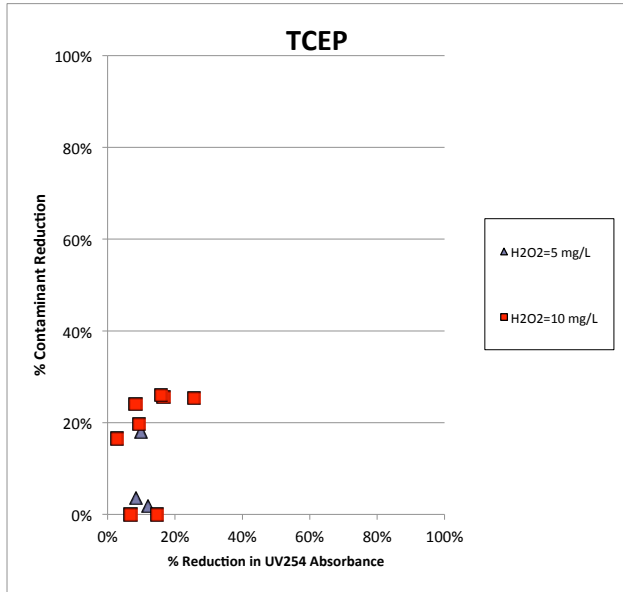
## Appendix 6 Comparison of H2O2 Doses UV/H2O2



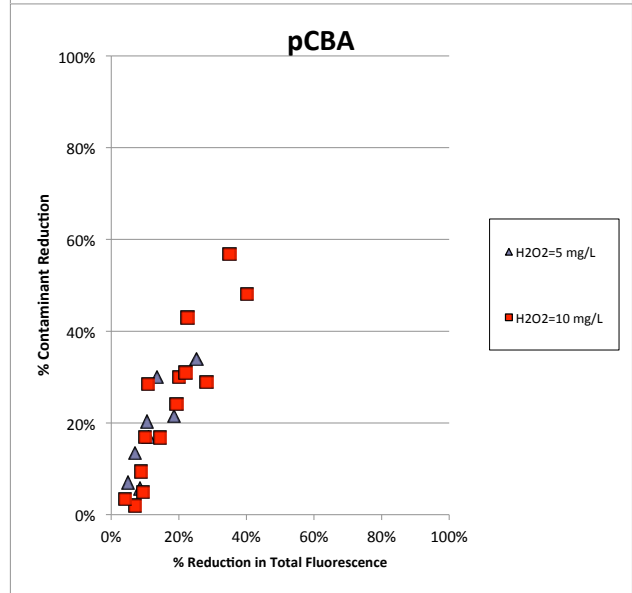
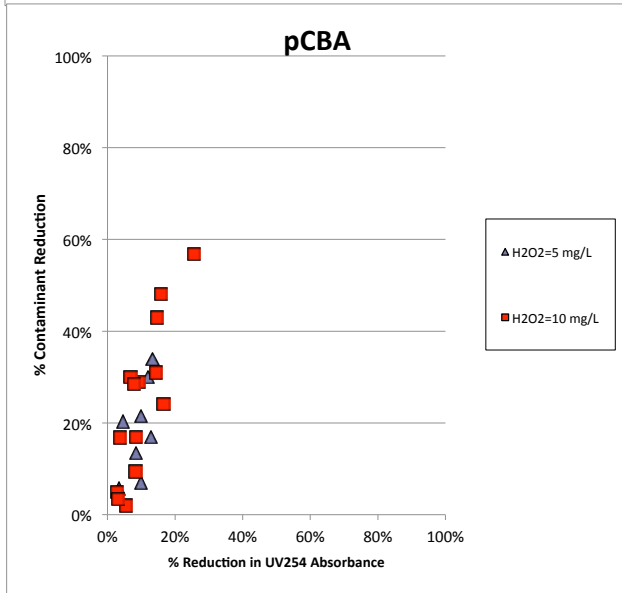
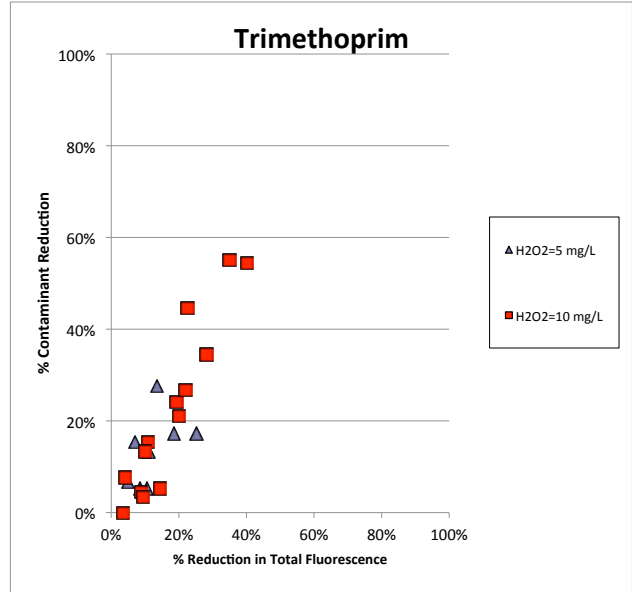
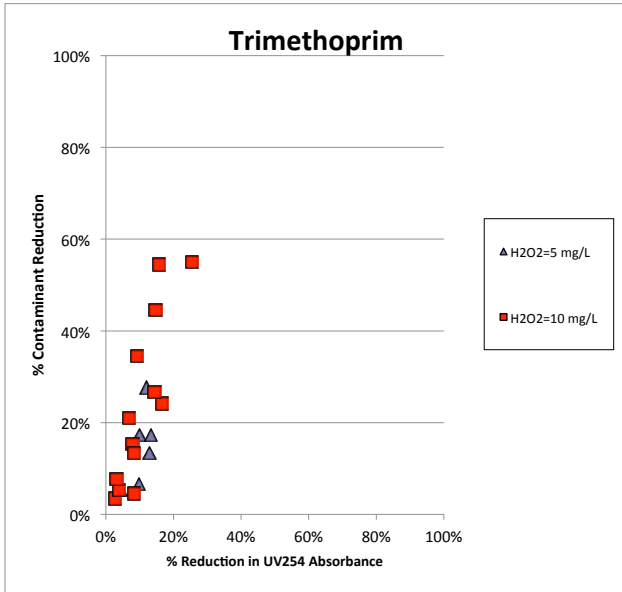
## Appendix 6 Comparison of H2O2 Doses UV/H2O2



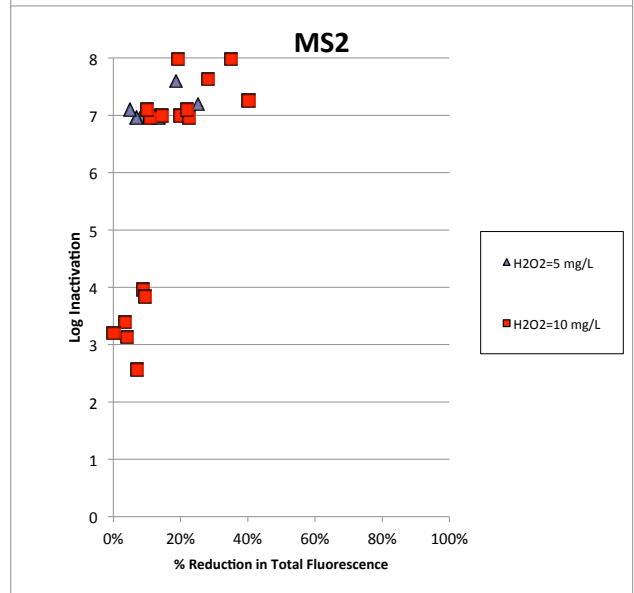
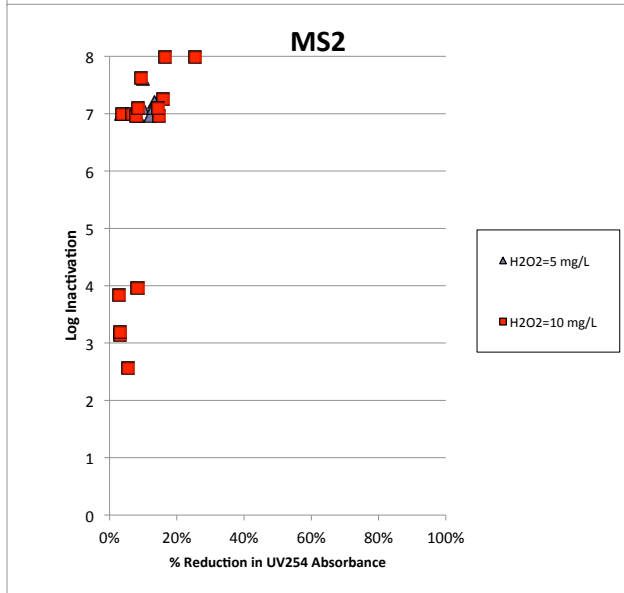
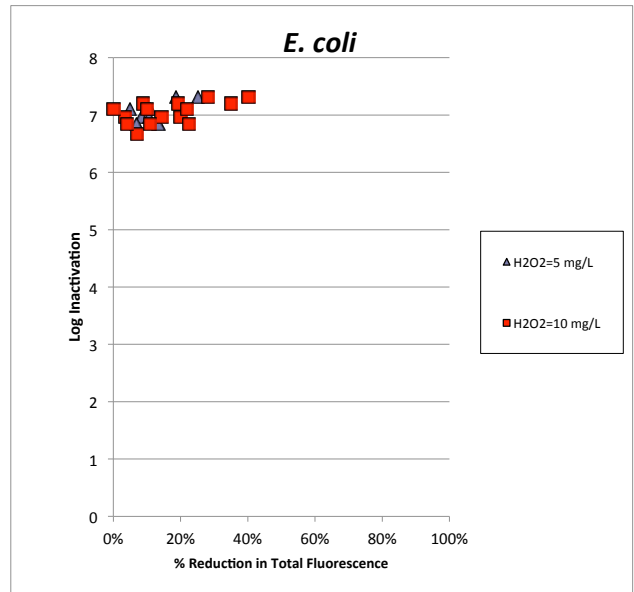
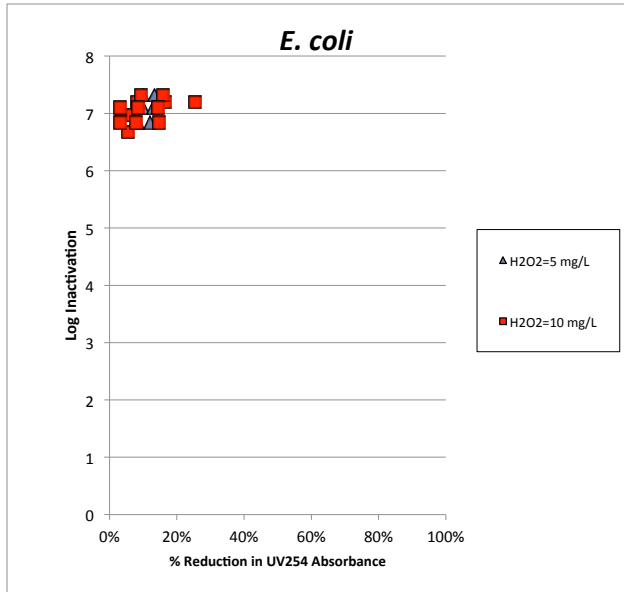
## Appendix 6 Comparison of H2O2 Doses UV/H2O2



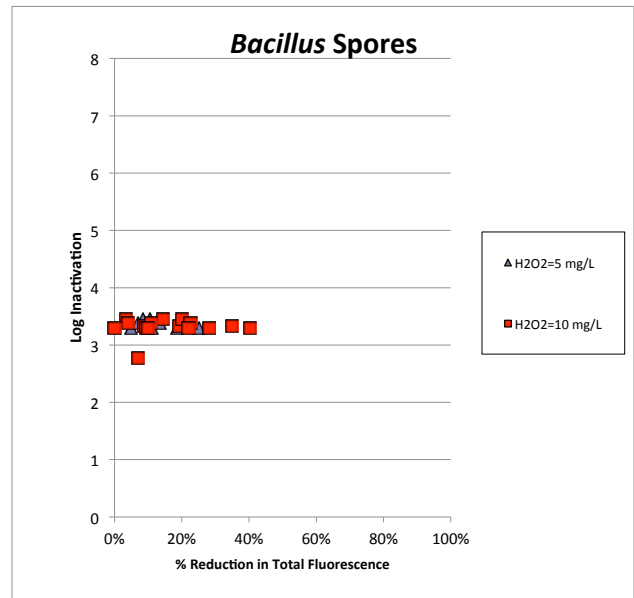
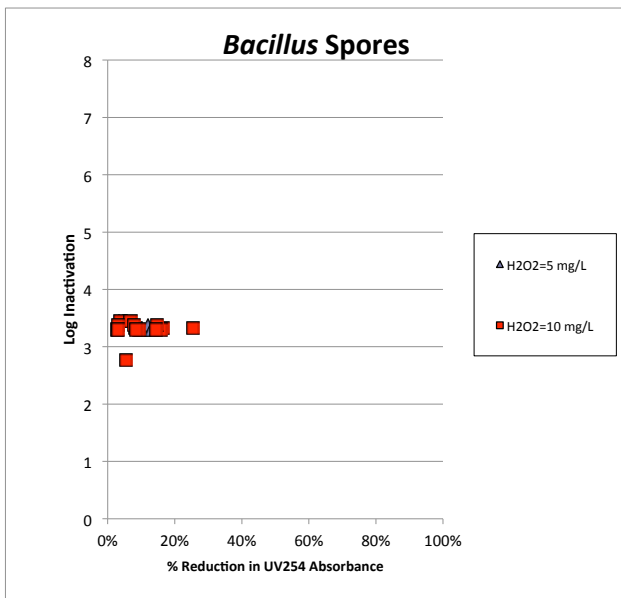
## Appendix 6 Comparison of H2O2 Doses UV/H2O2



# Appendix 6 Comparison of H2O2 Doses UV/H2O2



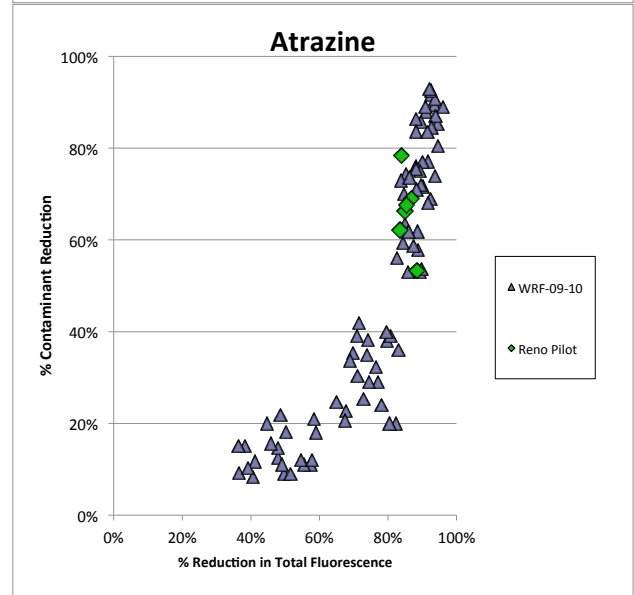
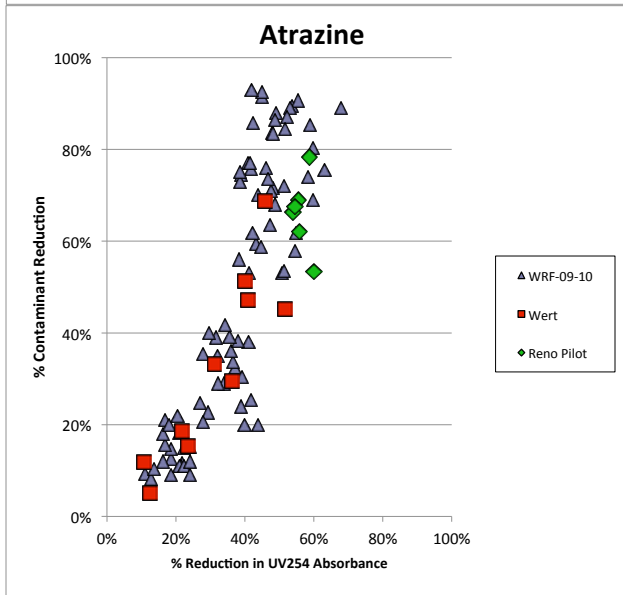
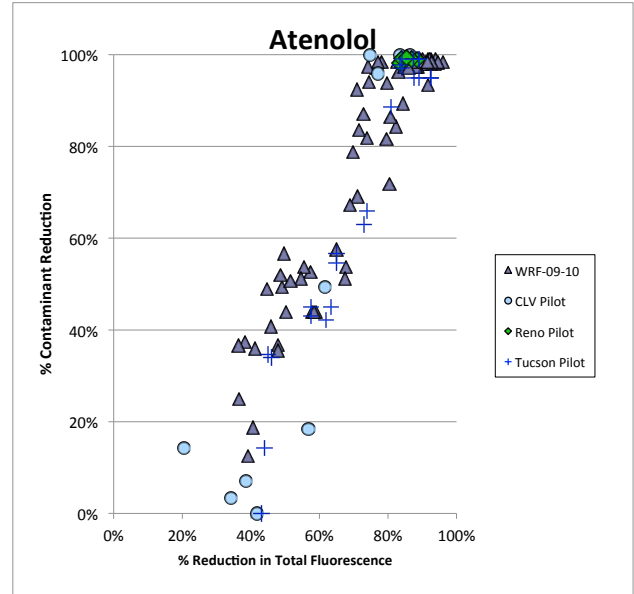
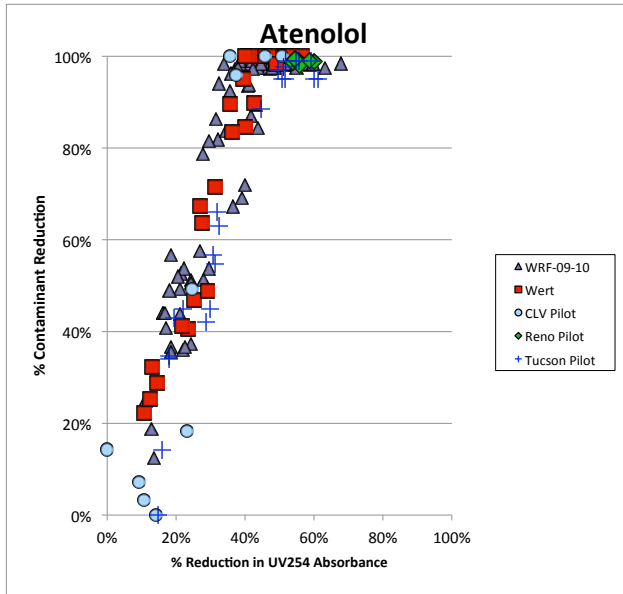
**Appendix 6**  
**Comparison of H<sub>2</sub>O<sub>2</sub> Doses**  
**UV/H<sub>2</sub>O<sub>2</sub>**



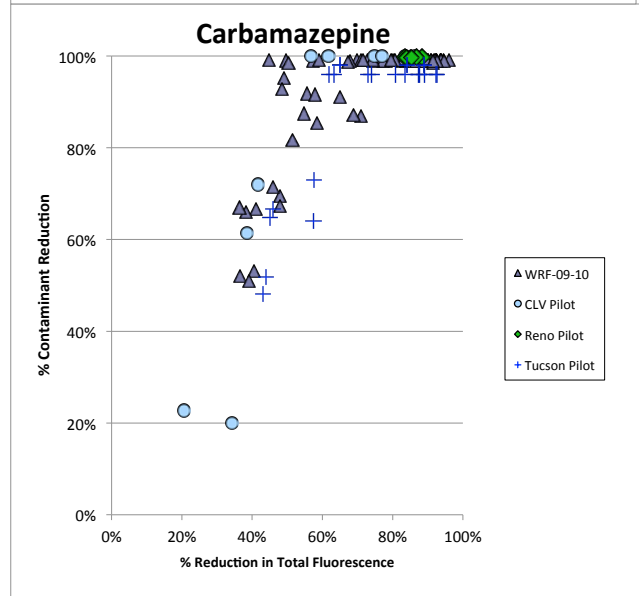
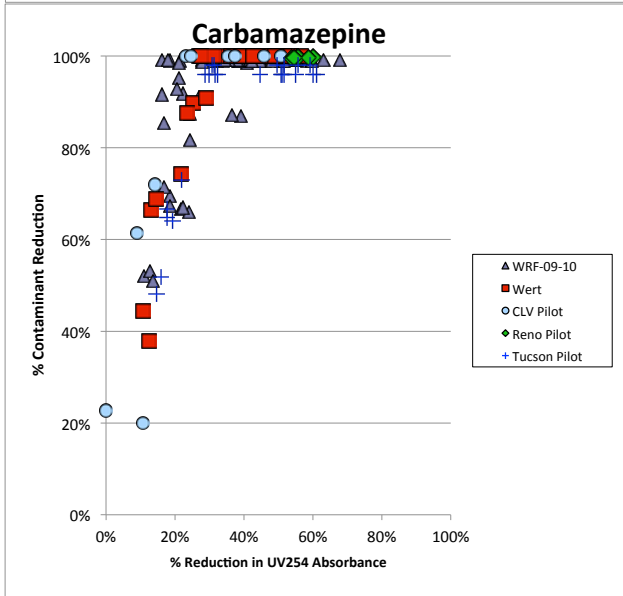
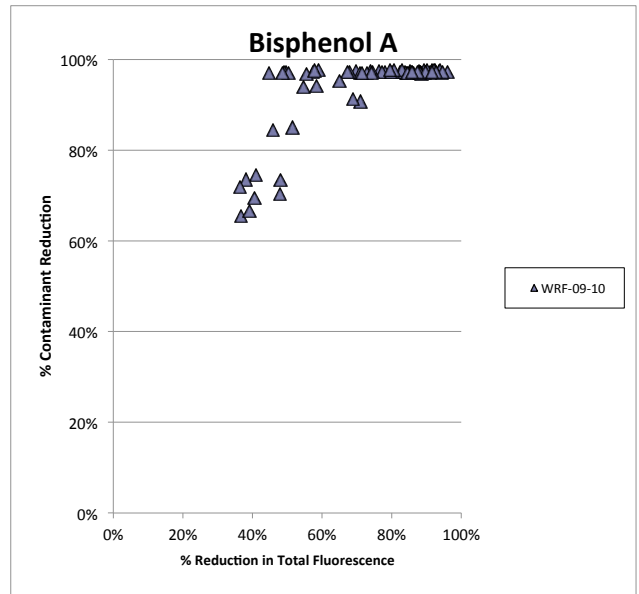
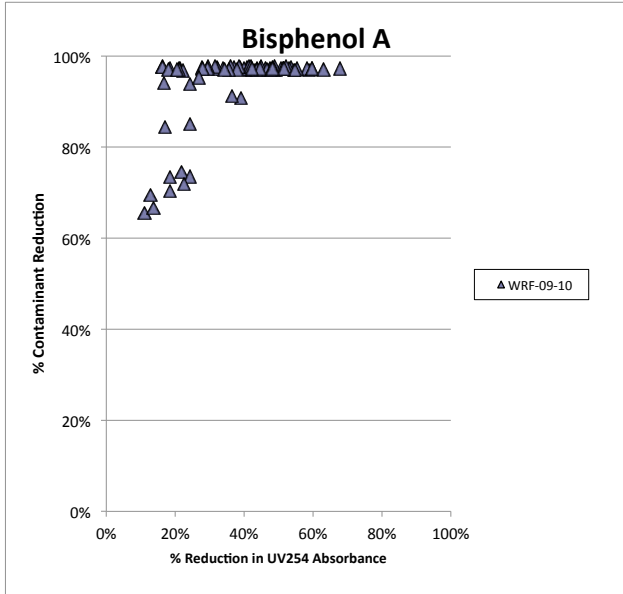
# Appendix 7

## Validation of Empirical Correlations

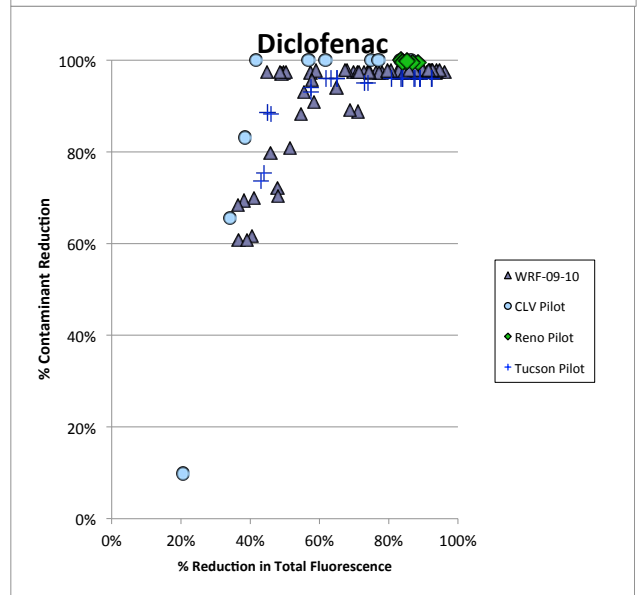
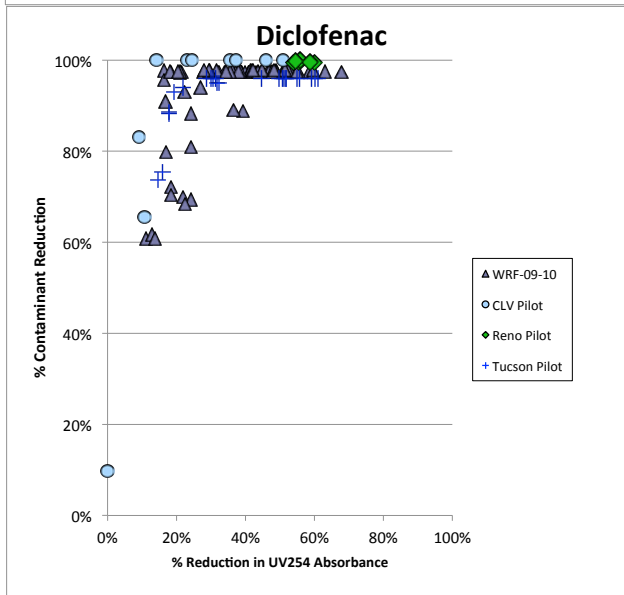
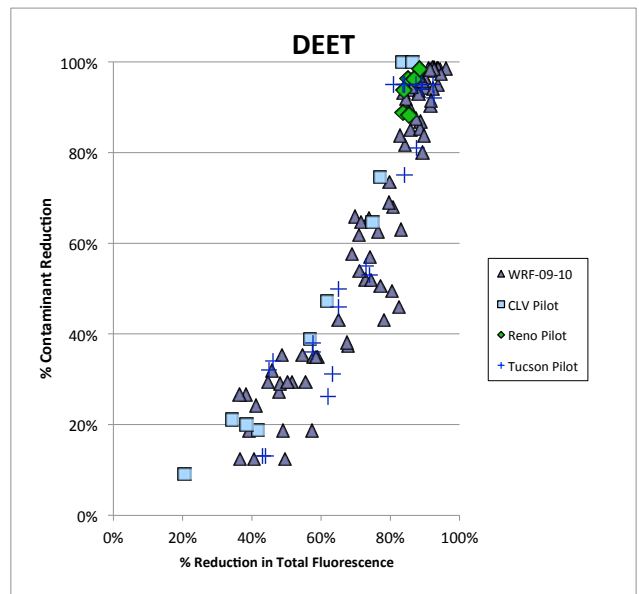
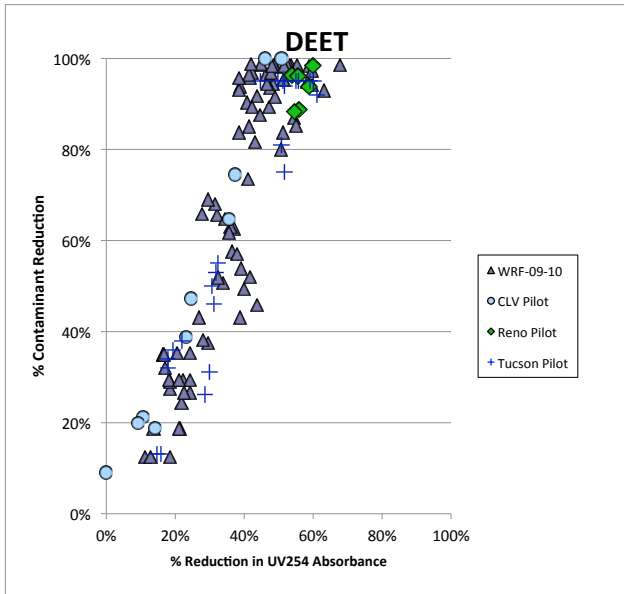
### Ozone and Ozone/H2O2



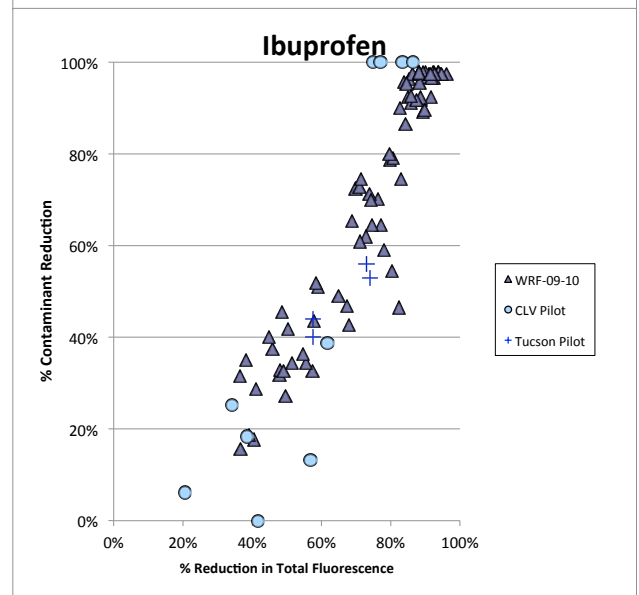
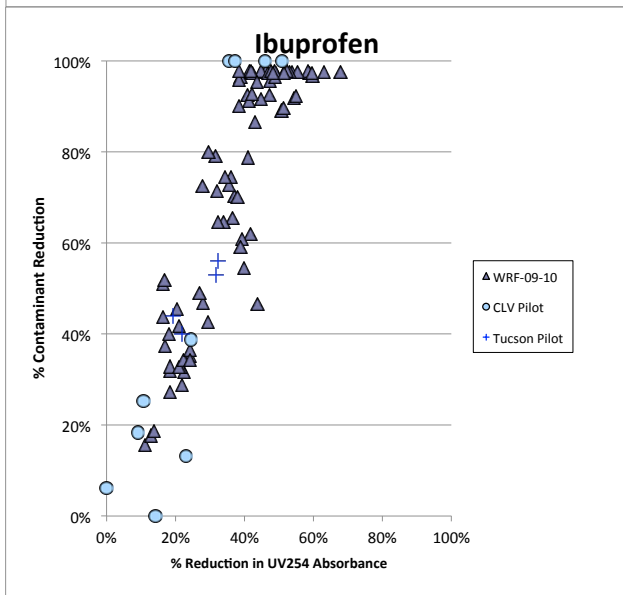
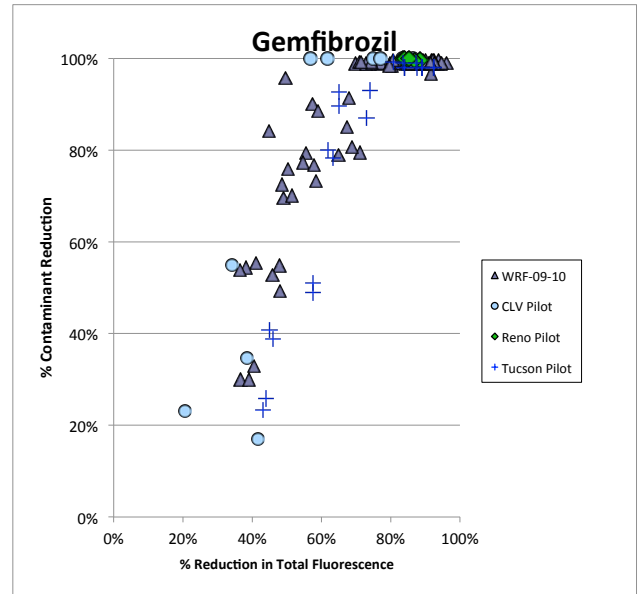
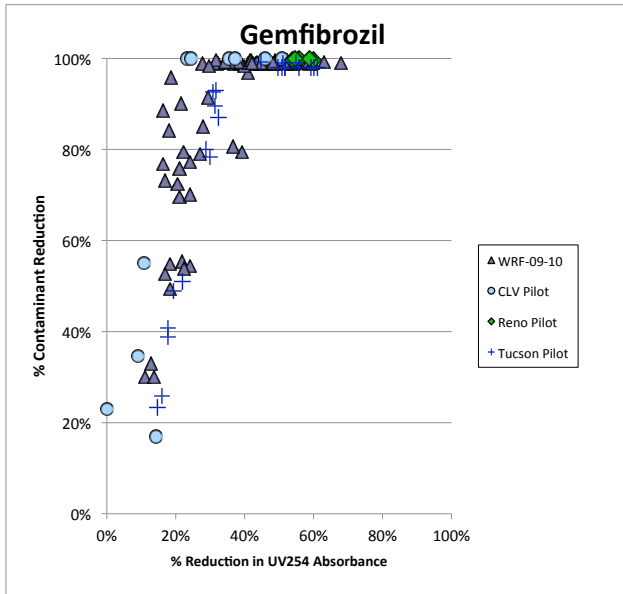
# Appendix 7 Validation of Empirical Correlations Ozone and Ozone/H2O2



# Appendix 7 Validation of Empirical Correlations Ozone and Ozone/H2O2



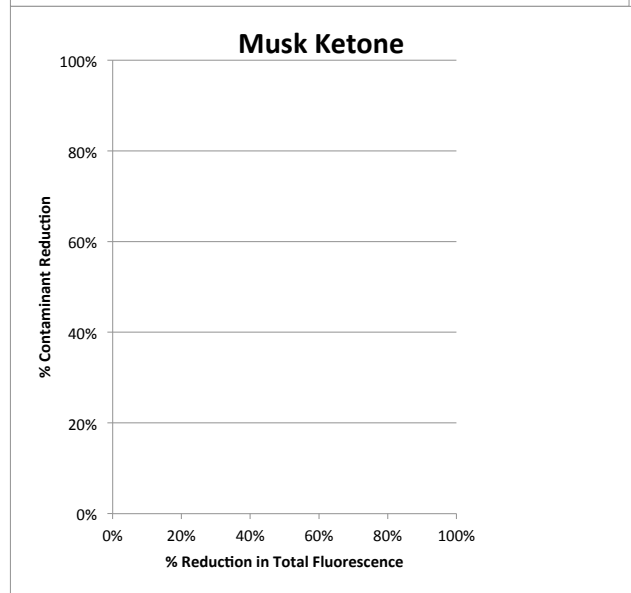
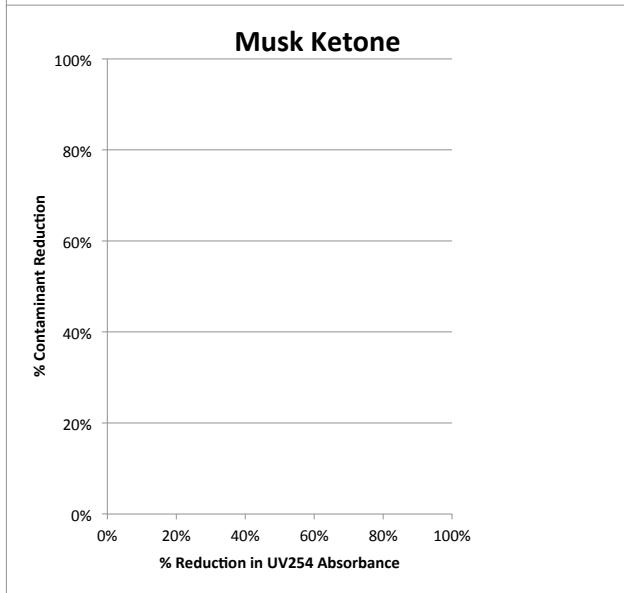
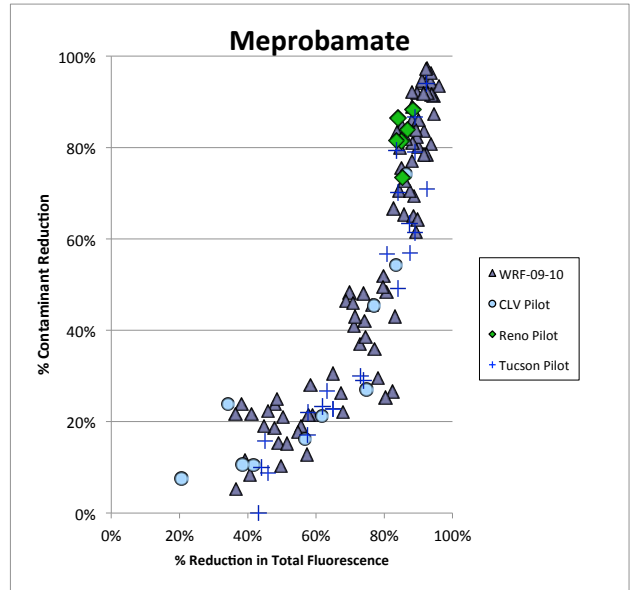
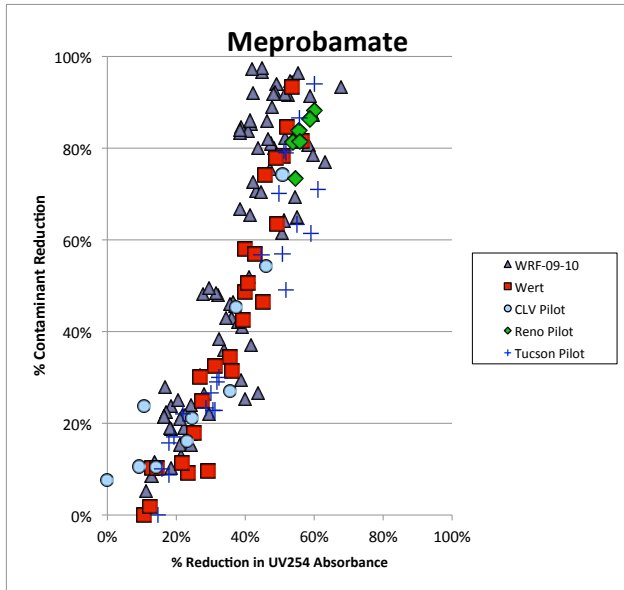
## Appendix 7 Validation of Empirical Correlations Ozone and Ozone/H2O2



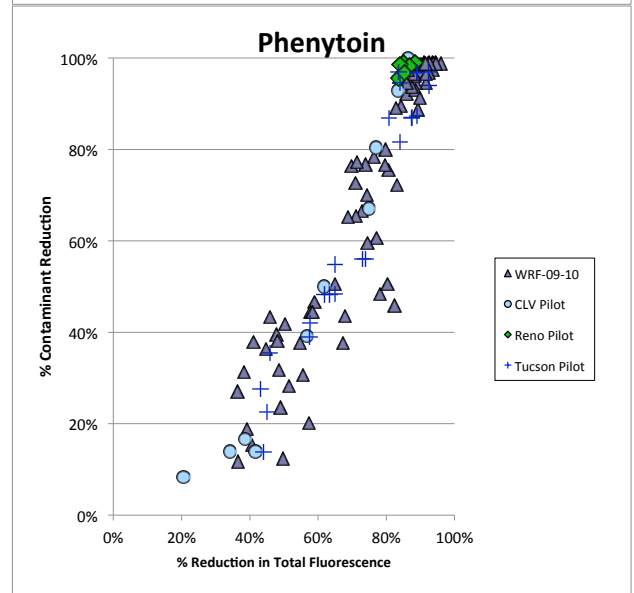
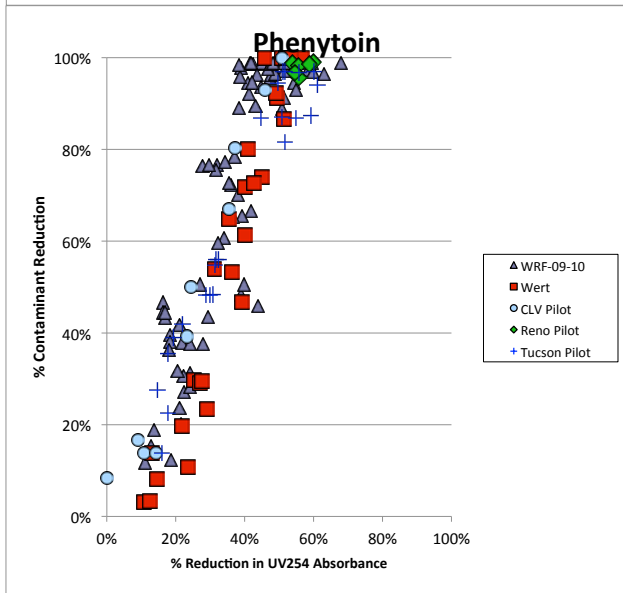
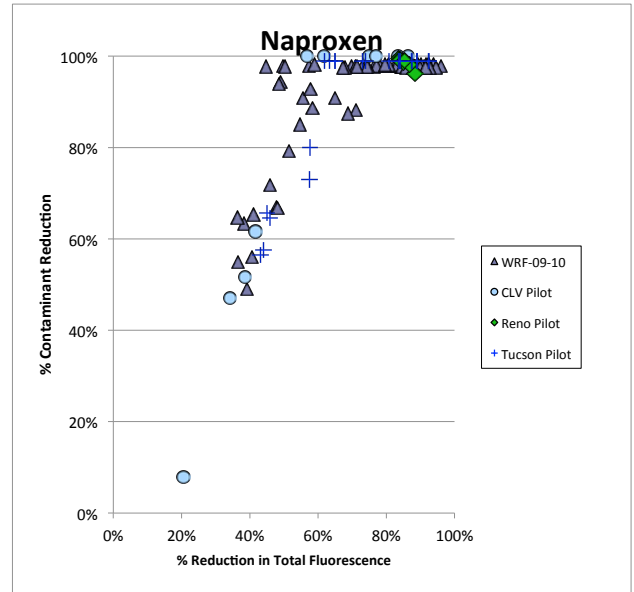
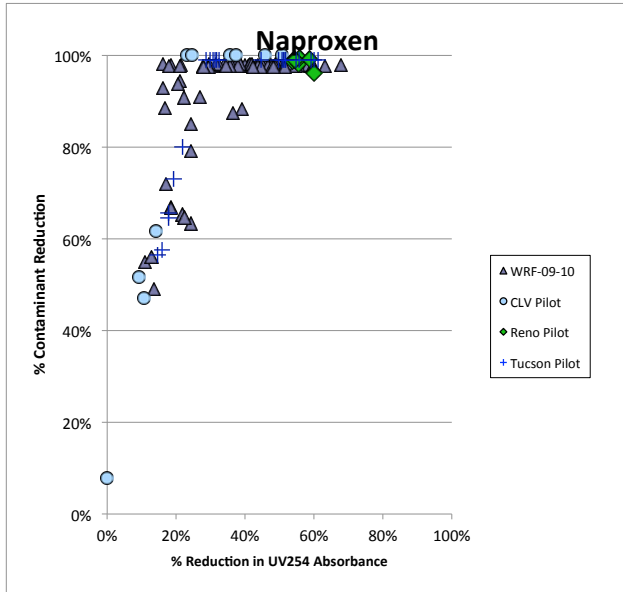
# Appendix 7

## Validation of Empirical Correlations

### Ozone and Ozone/H2O2



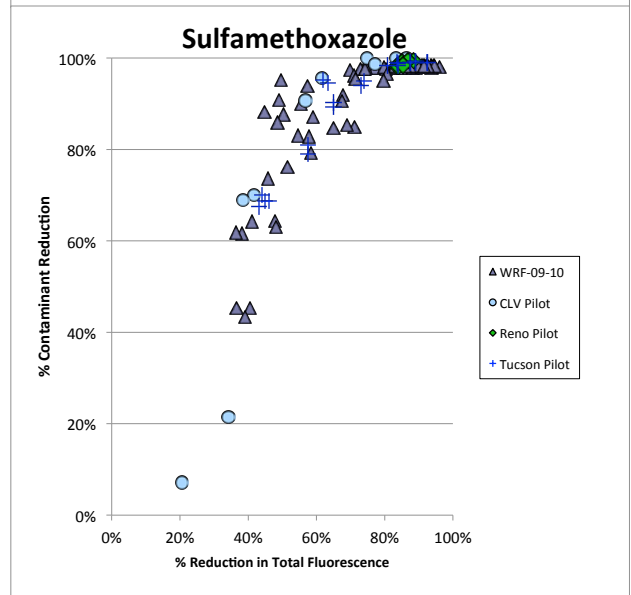
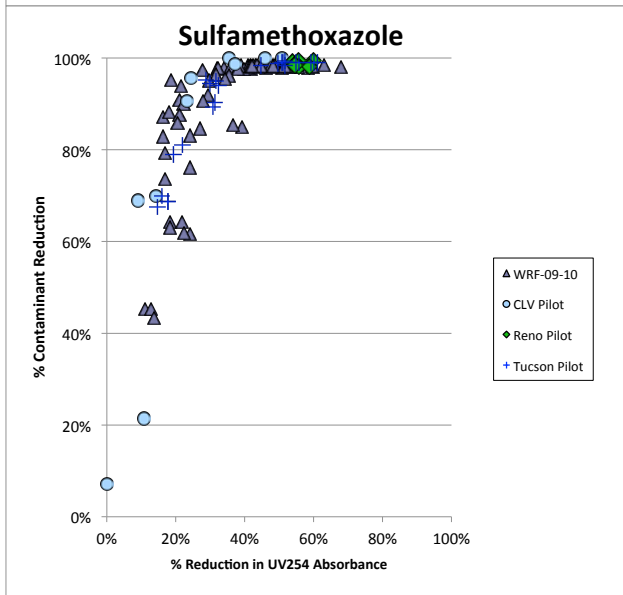
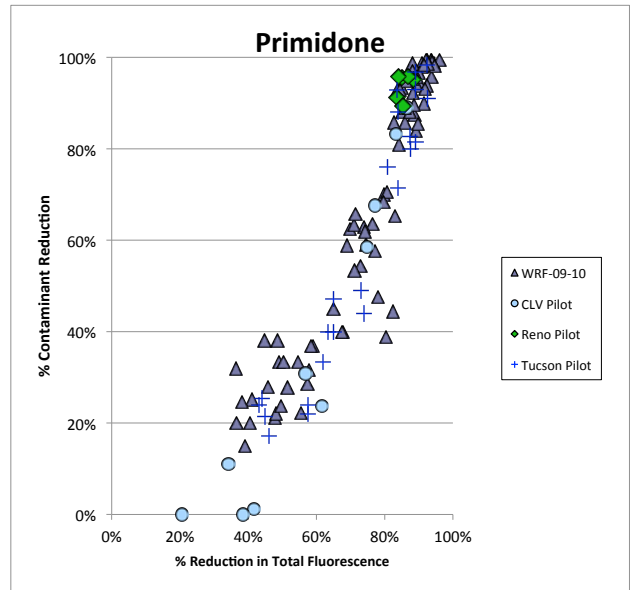
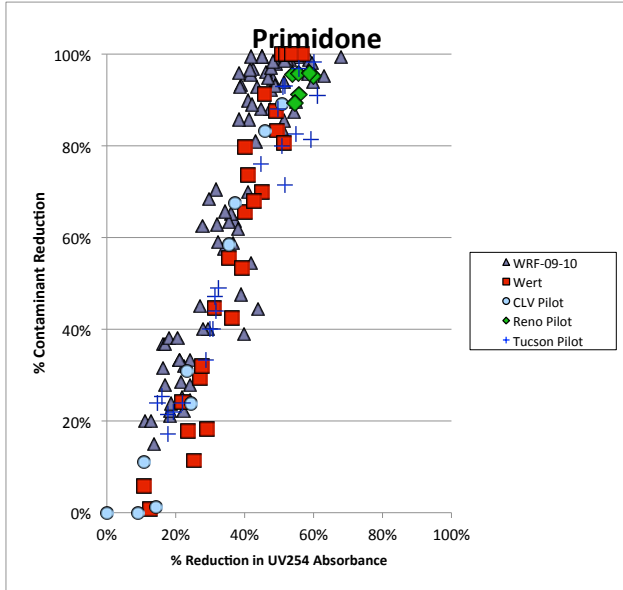
## Appendix 7 Validation of Empirical Correlations Ozone and Ozone/H2O2



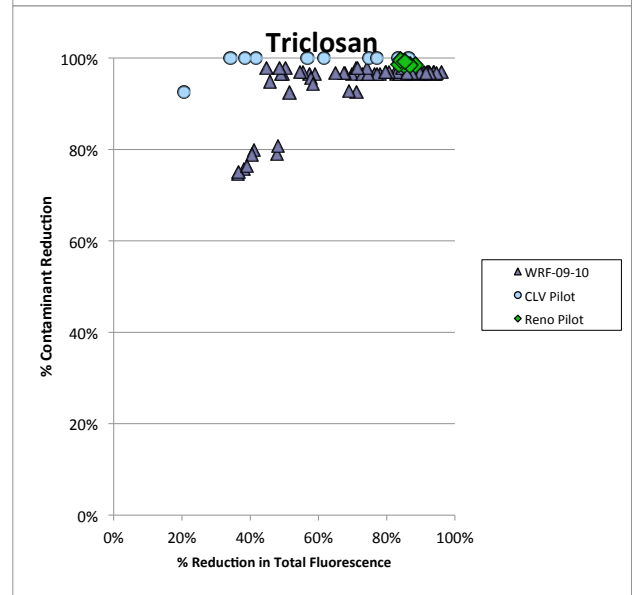
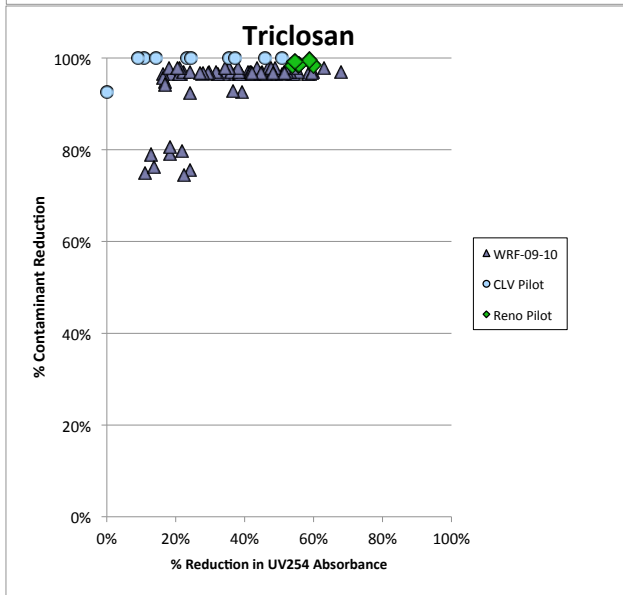
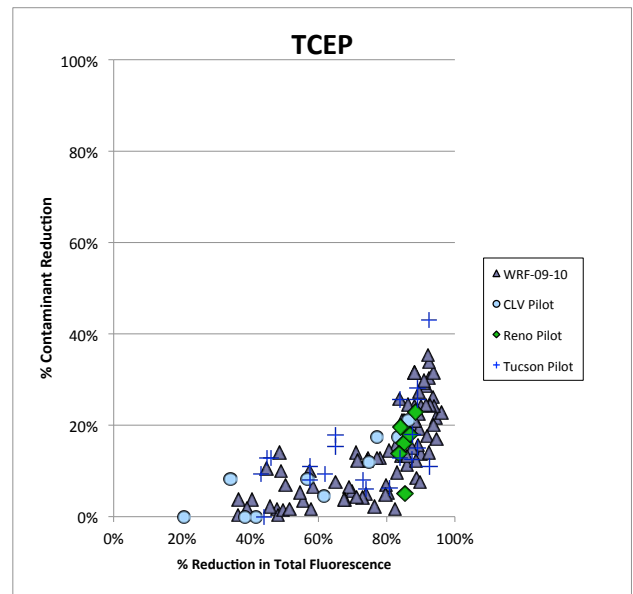
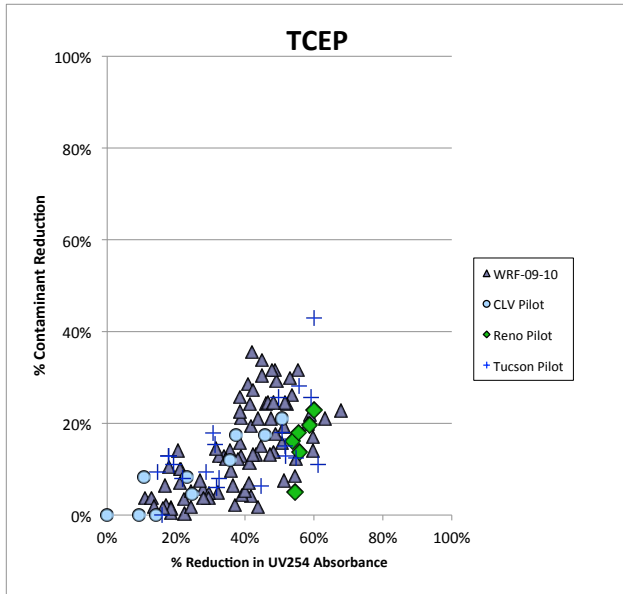
# Appendix 7

## Validation of Empirical Correlations

### Ozone and Ozone/H2O2



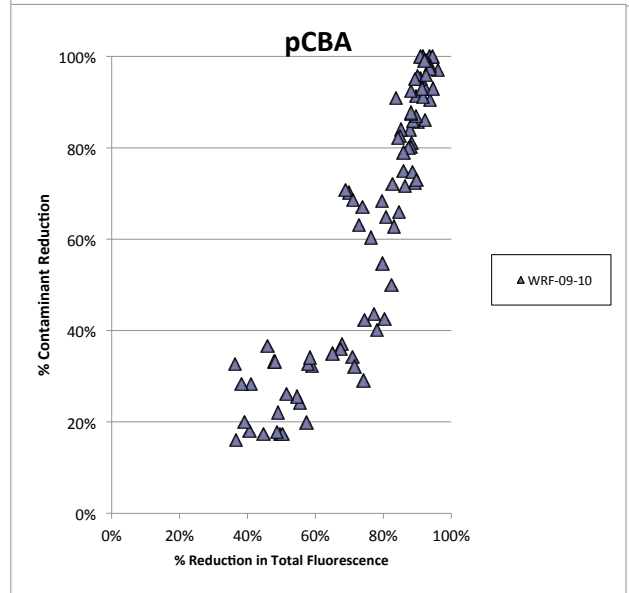
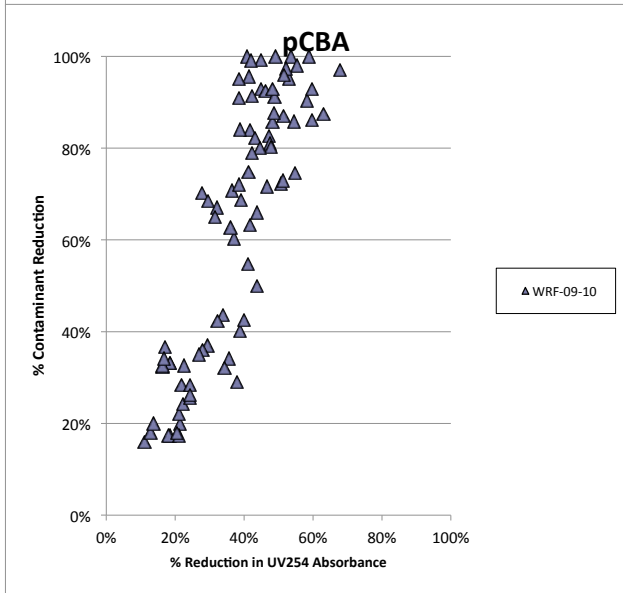
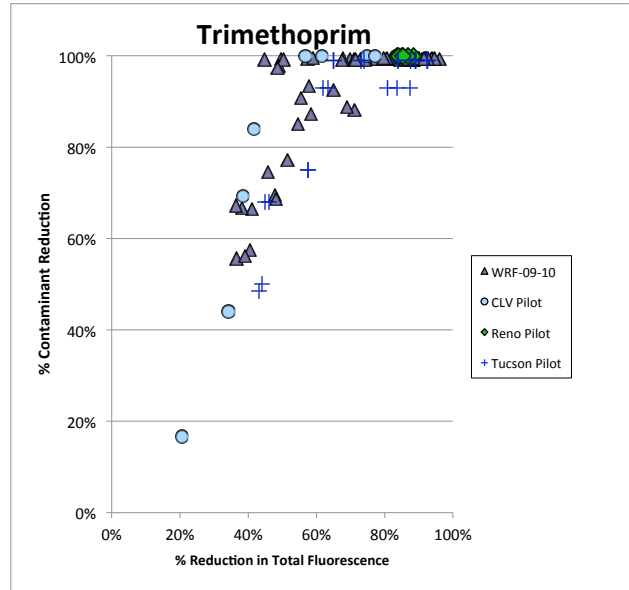
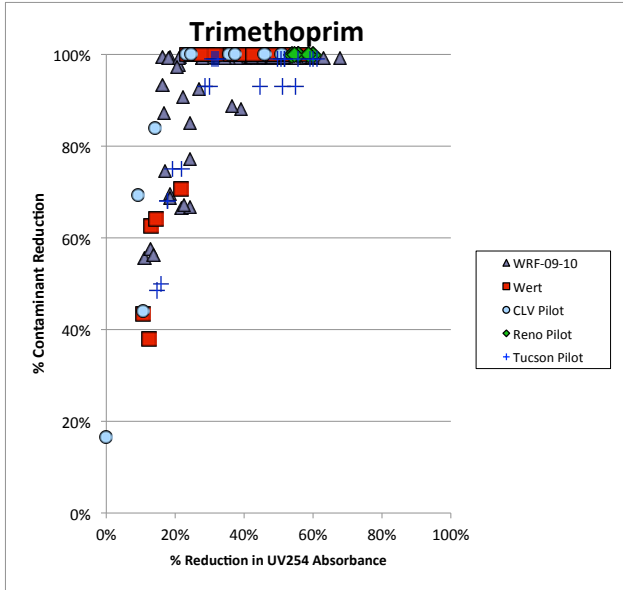
## Appendix 7 Validation of Empirical Correlations Ozone and Ozone/H2O2



# Appendix 7

## Validation of Empirical Correlations

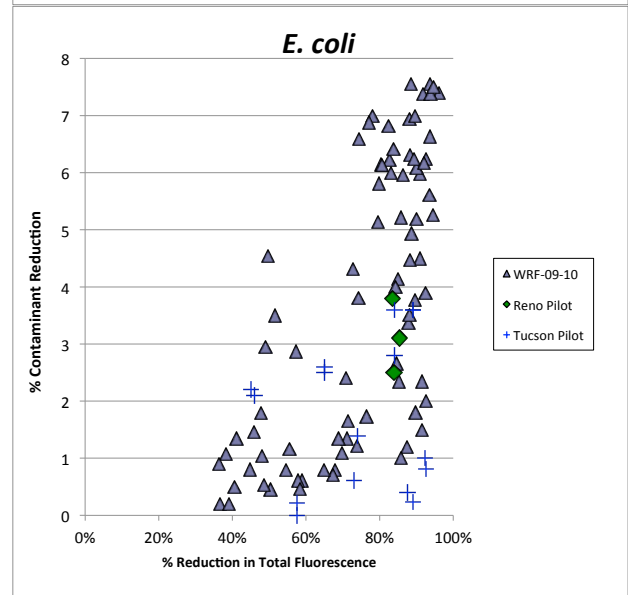
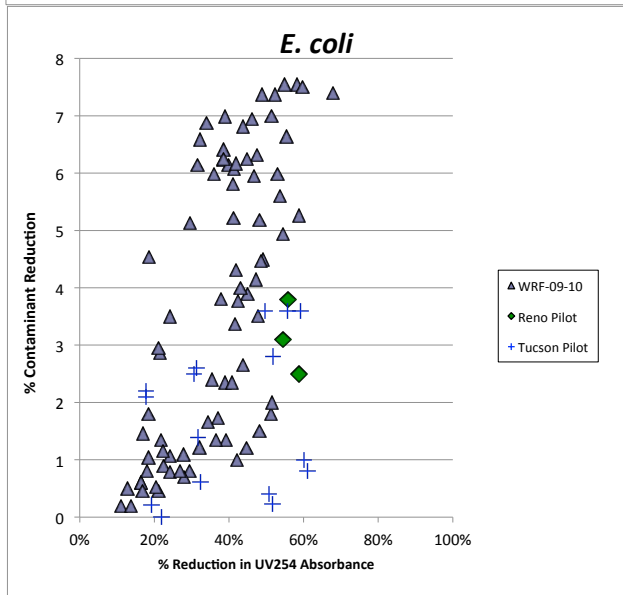
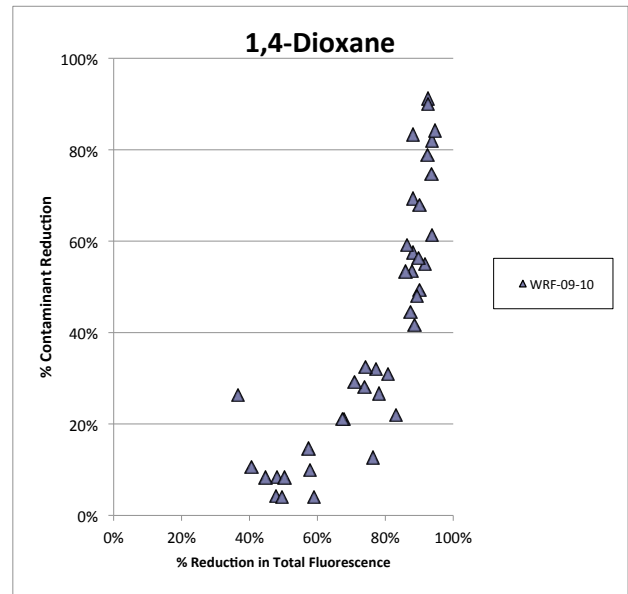
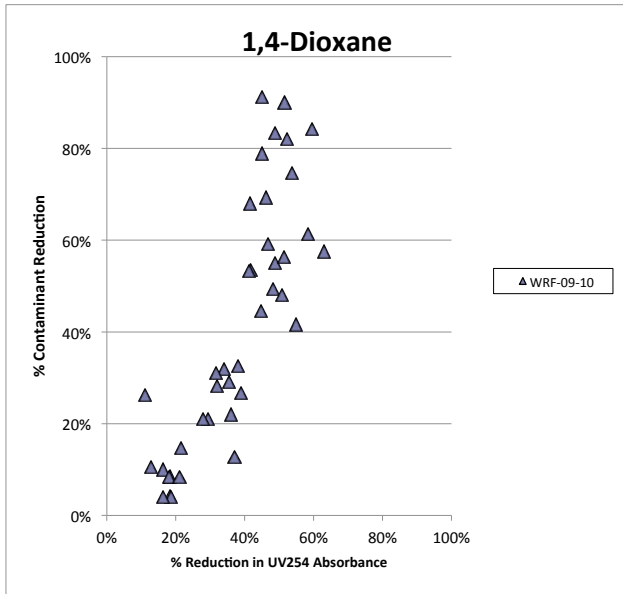
### Ozone and Ozone/H2O2



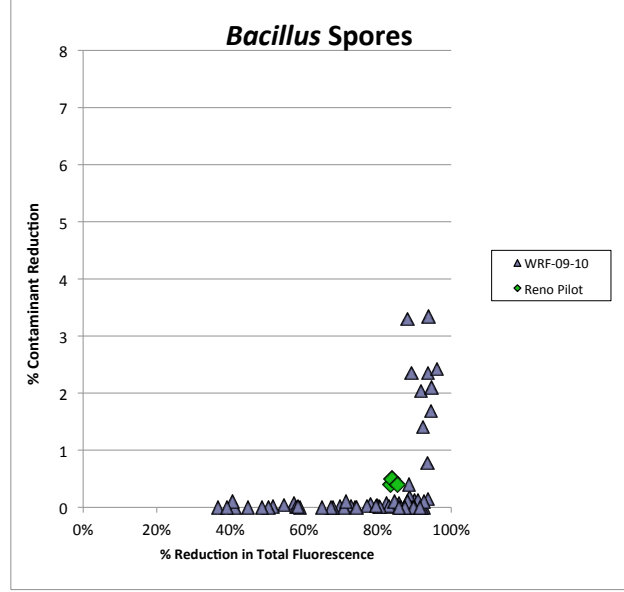
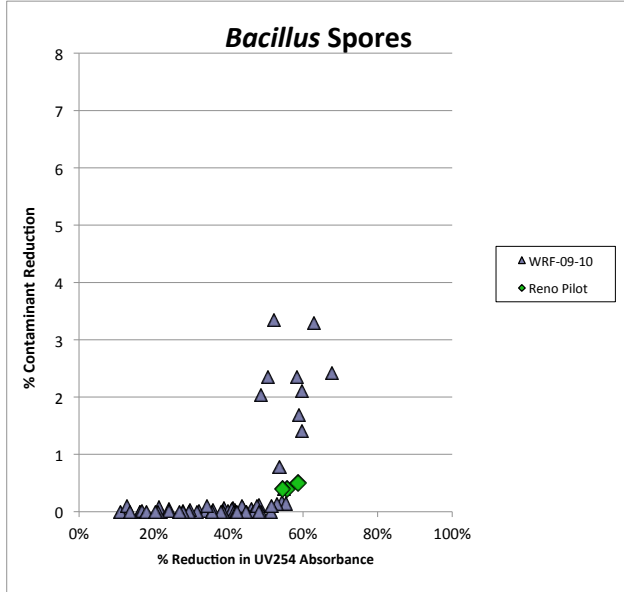
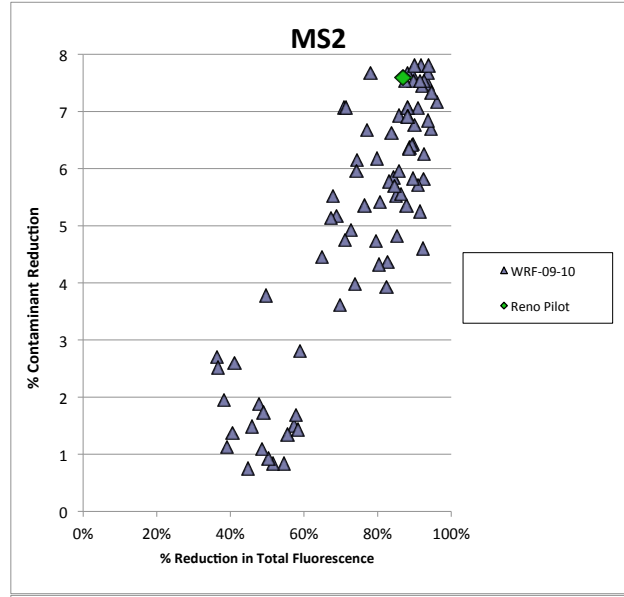
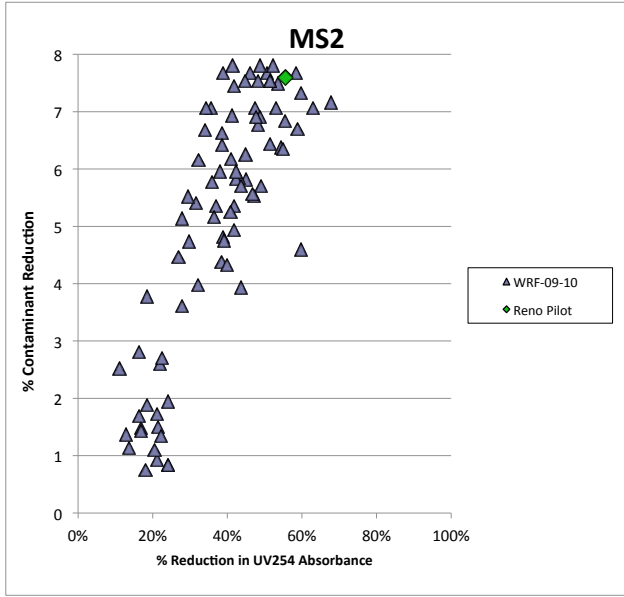
# Appendix 7

## Validation of Empirical Correlations

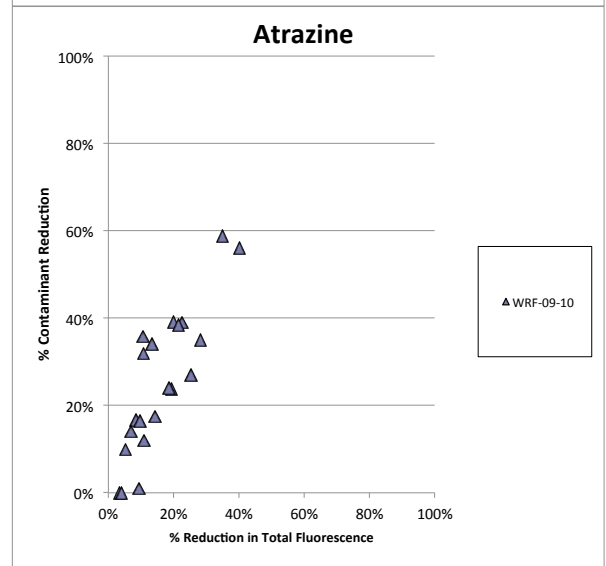
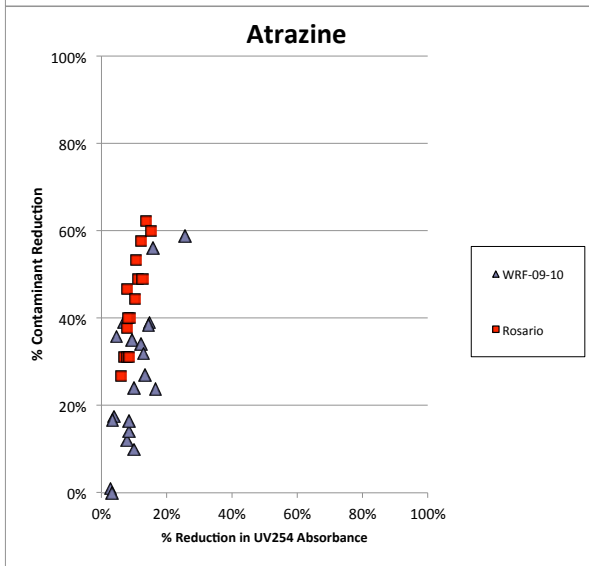
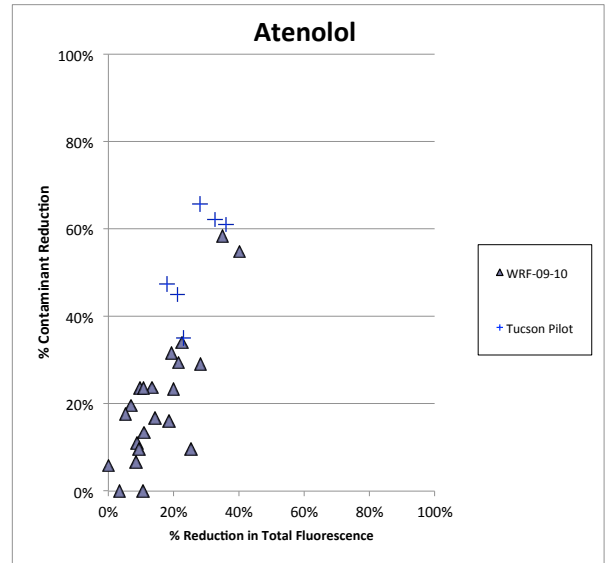
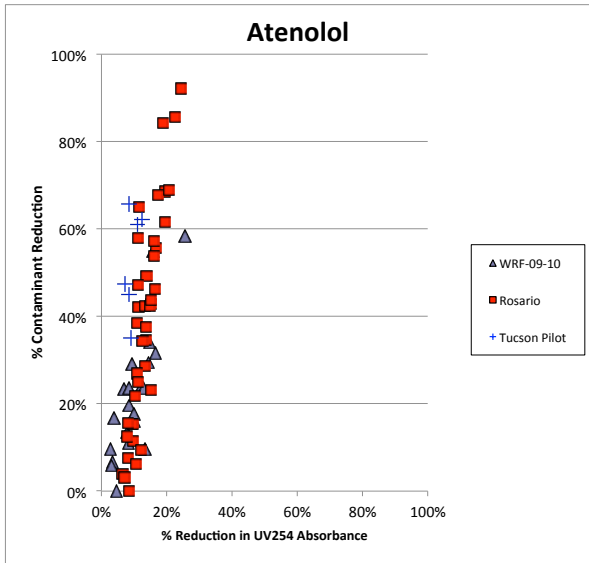
### Ozone and Ozone/H2O2



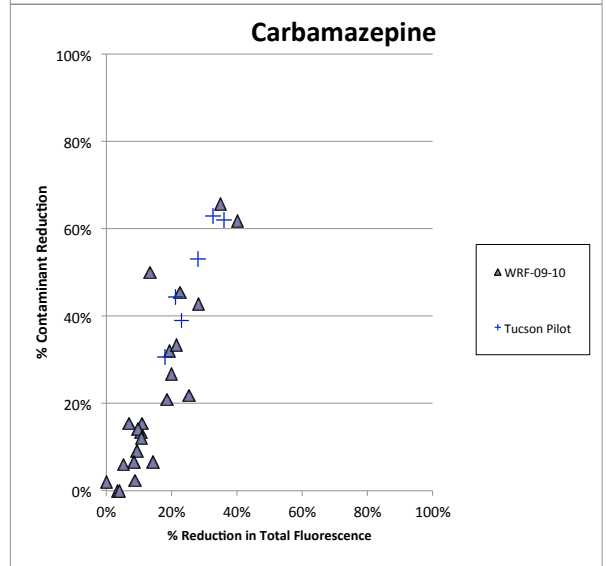
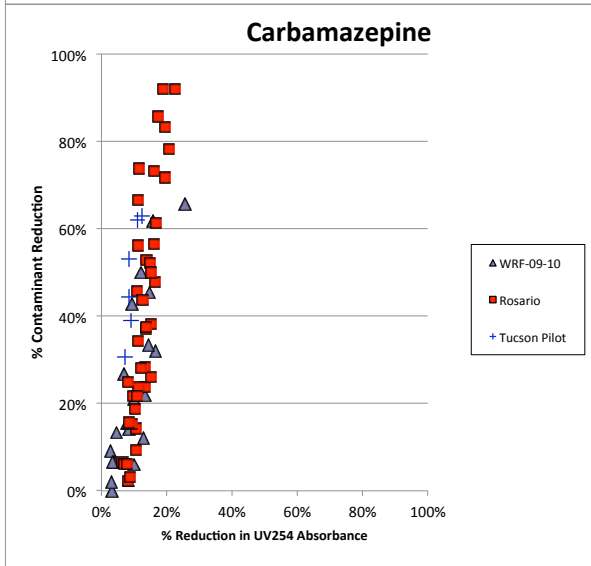
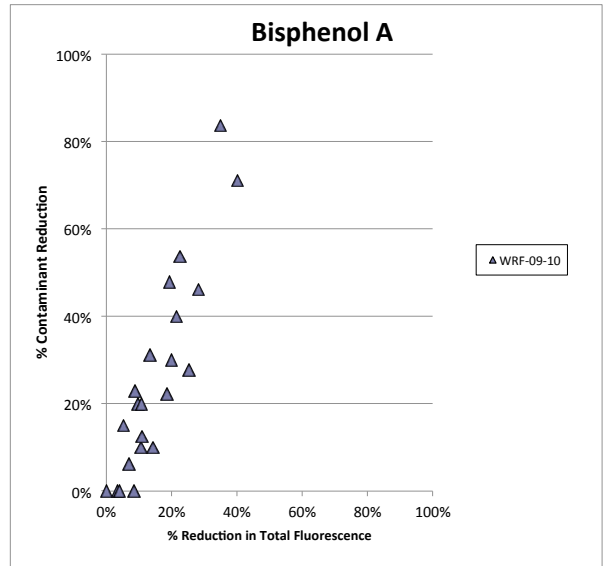
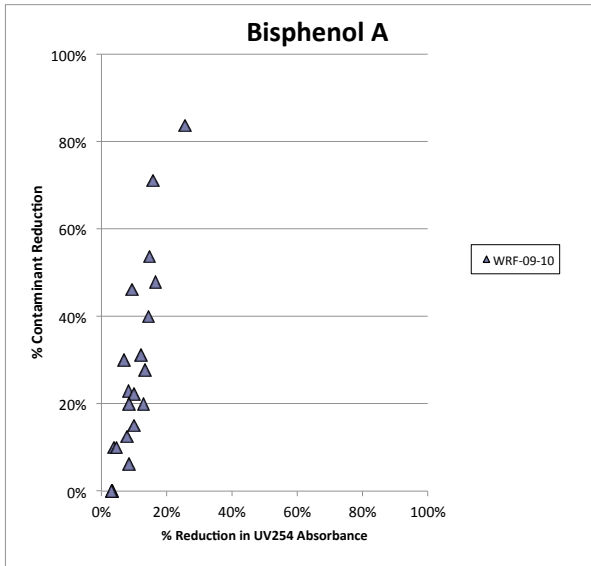
Appendix 7  
Validation of Empirical Correlations  
Ozone and Ozone/H2O2



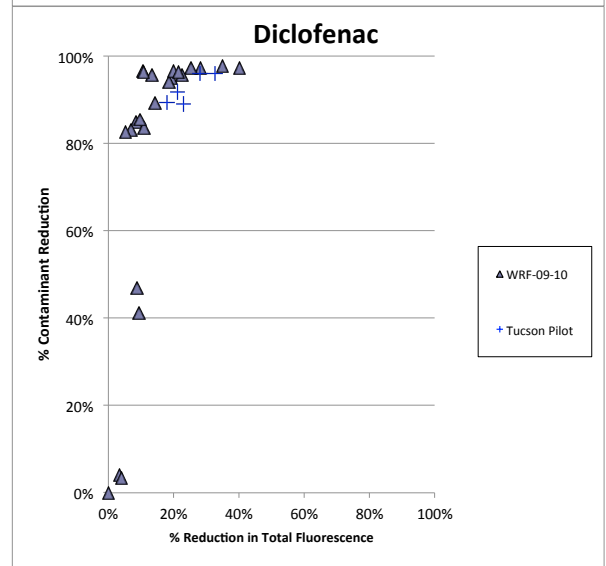
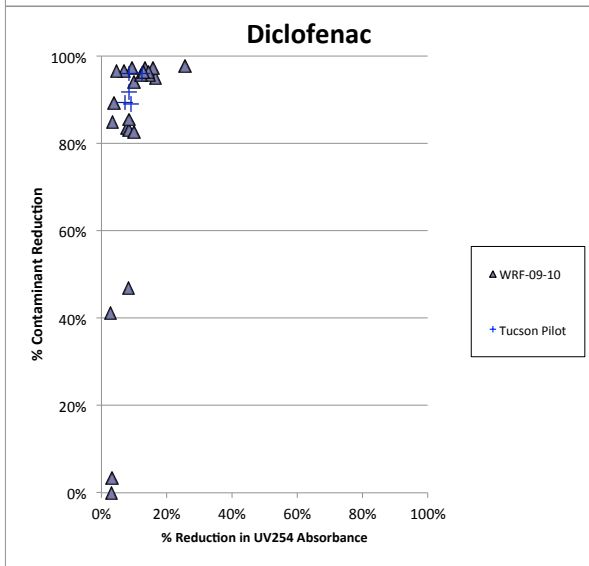
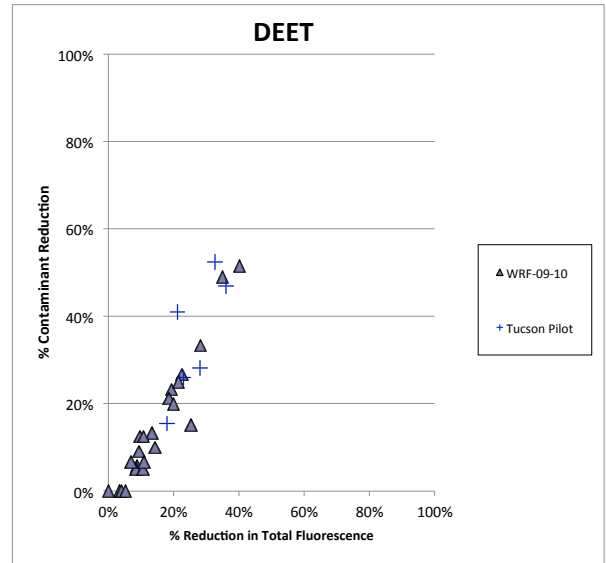
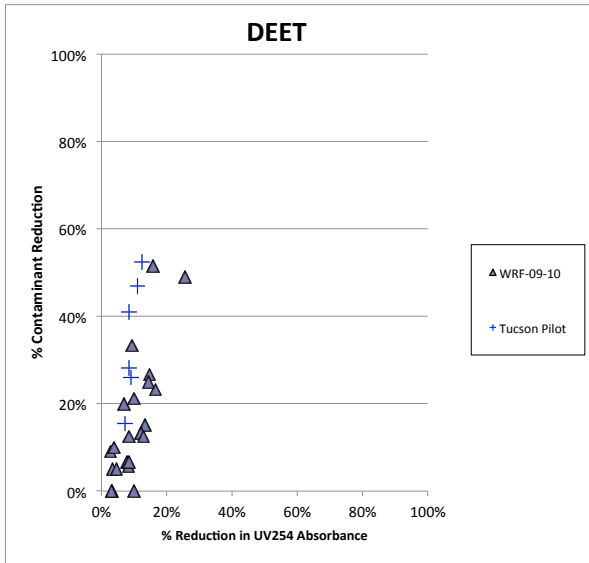
# Appendix 8 Validation of Empirical Correlations UV/H2O2



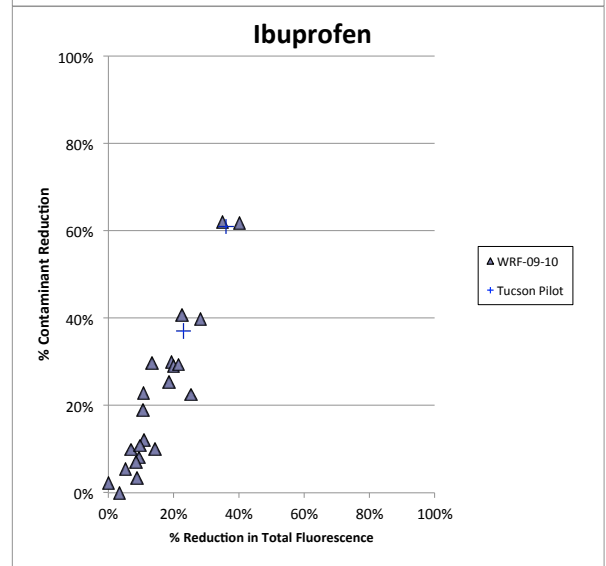
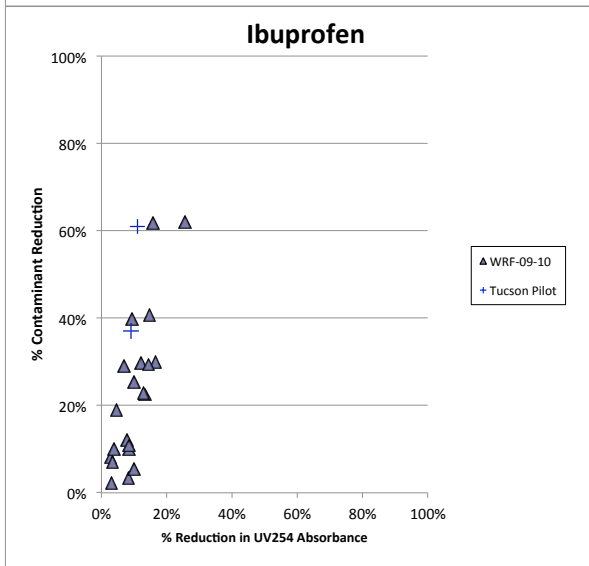
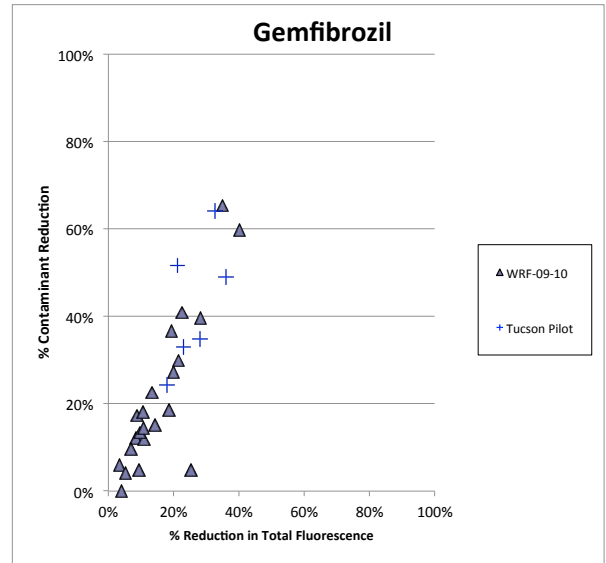
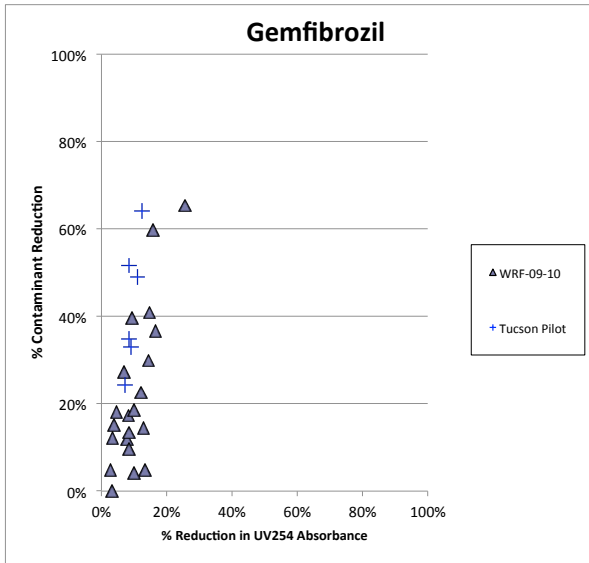
**Appendix 8**  
**Validation of Empirical Correlations**  
**UV/H2O2**



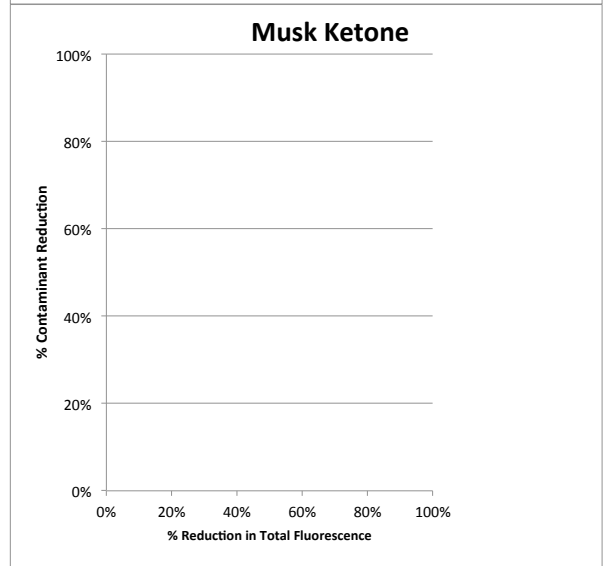
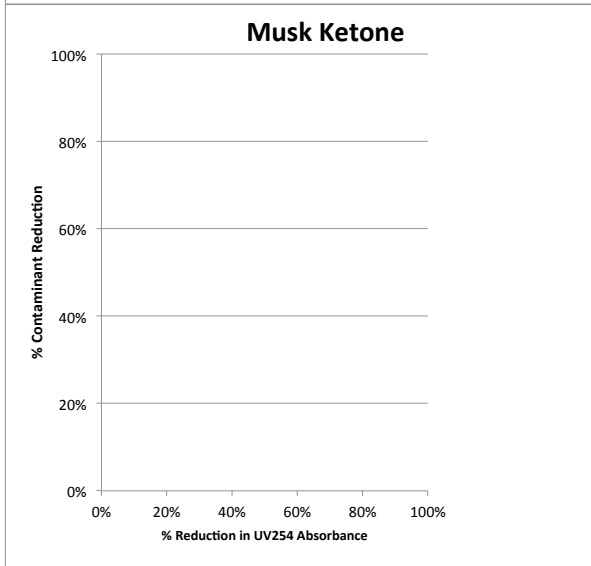
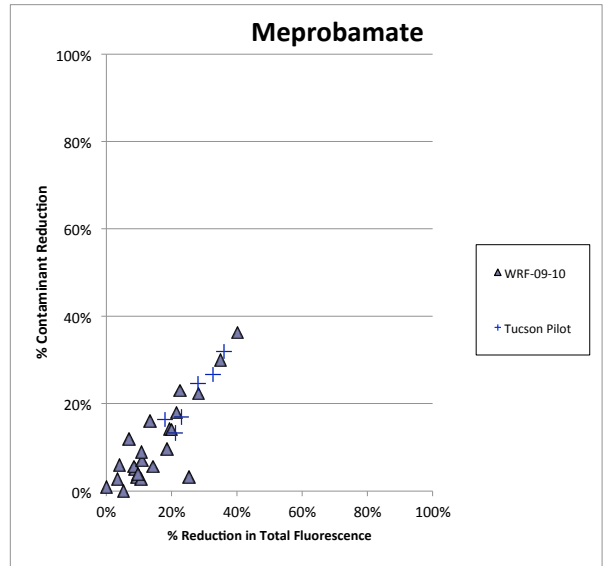
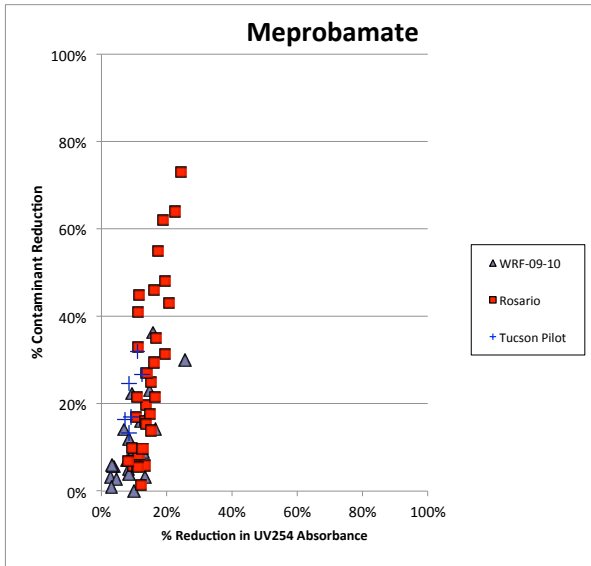
# Appendix 8 Validation of Empirical Correlations UV/H2O2



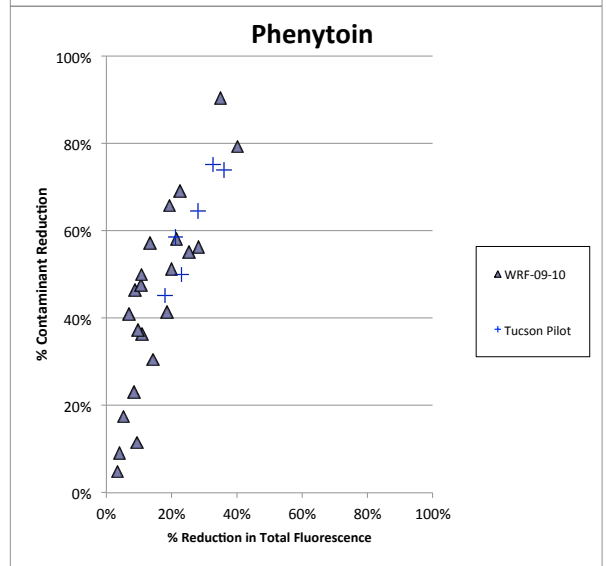
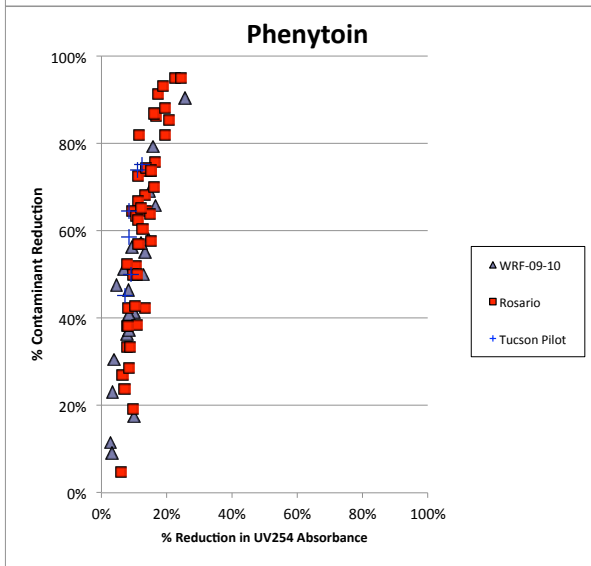
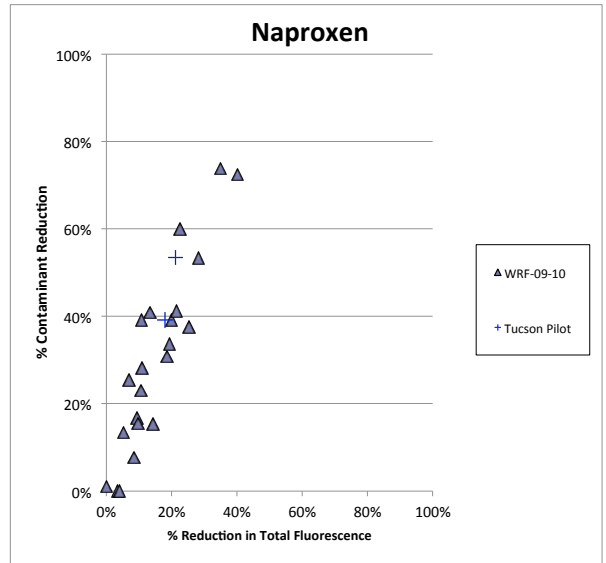
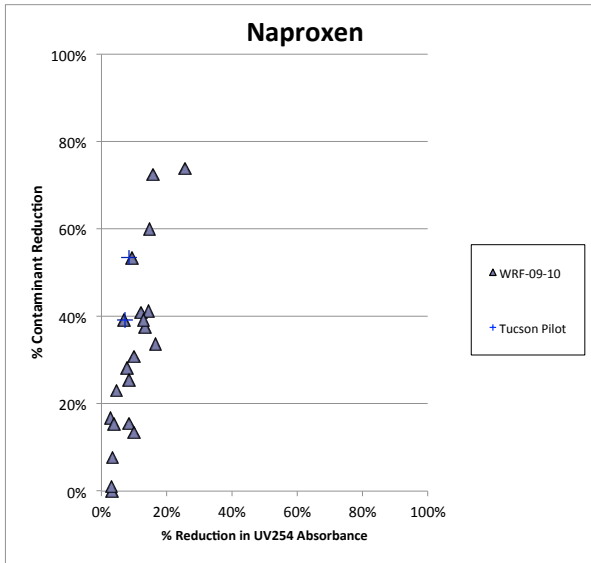
**Appendix 8**  
**Validation of Empirical Correlations**  
**UV/H2O2**



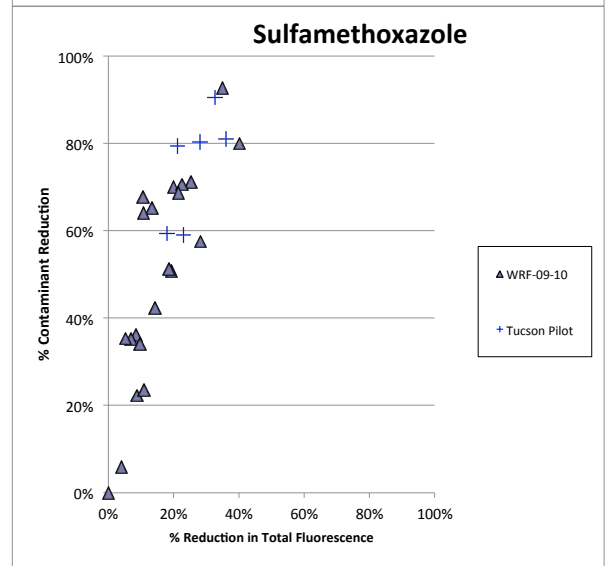
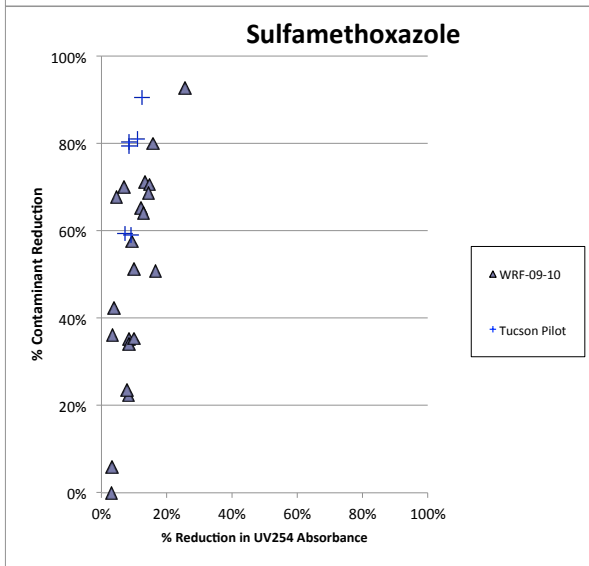
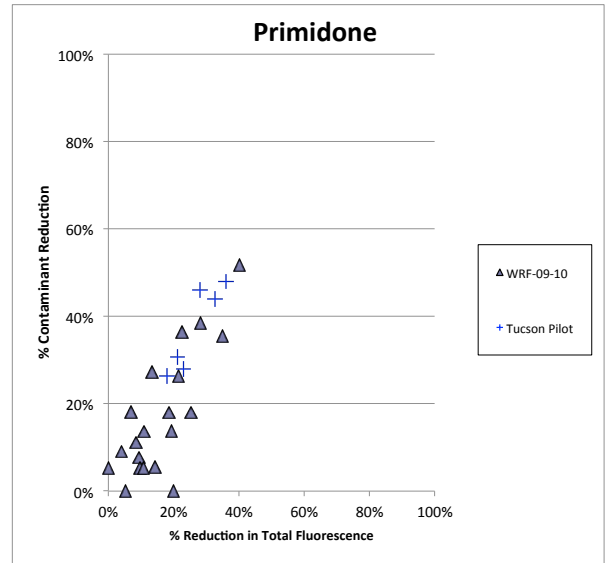
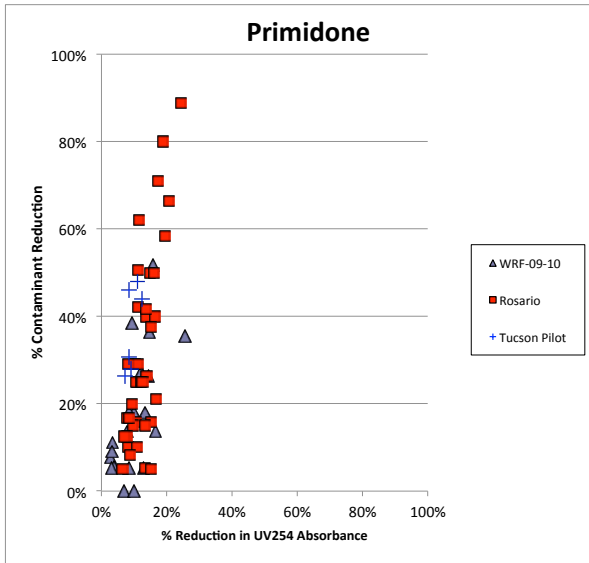
Appendix 8  
Validation of Empirical Correlations  
UV/H2O2



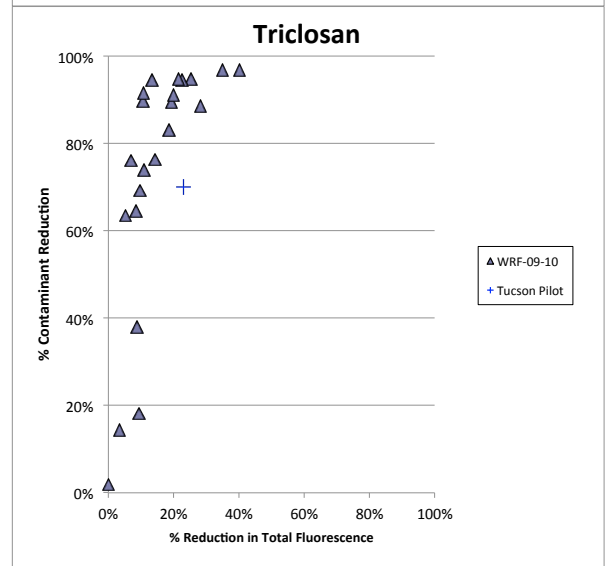
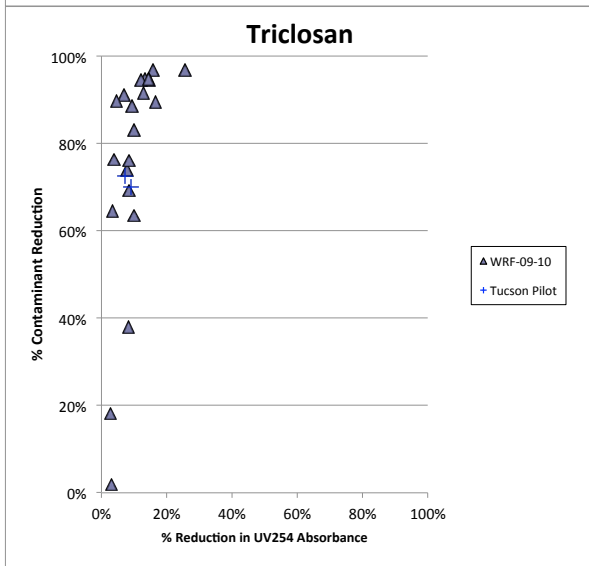
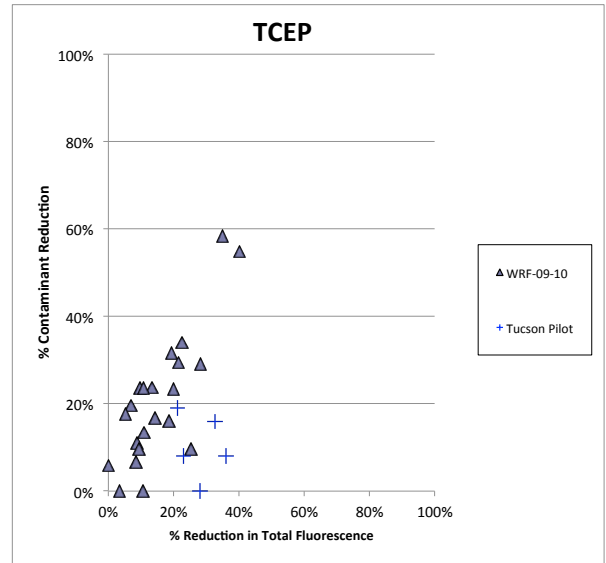
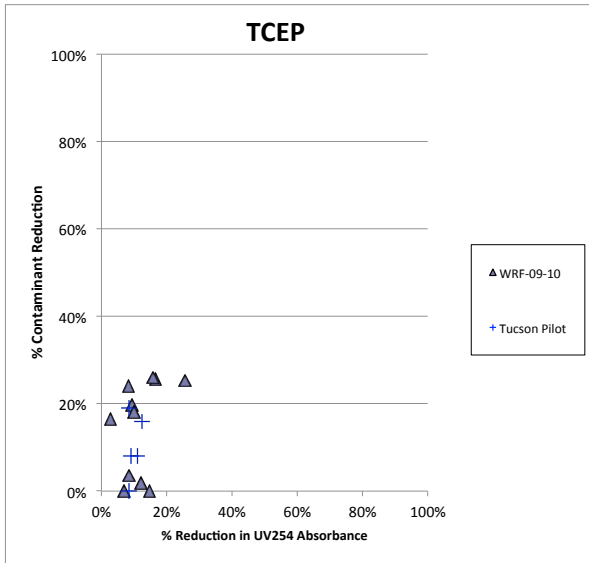
**Appendix 8**  
**Validation of Empirical Correlations**  
**UV/H2O2**



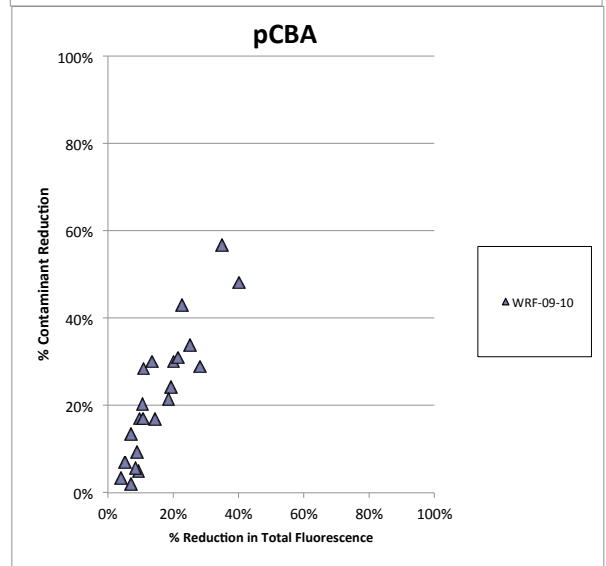
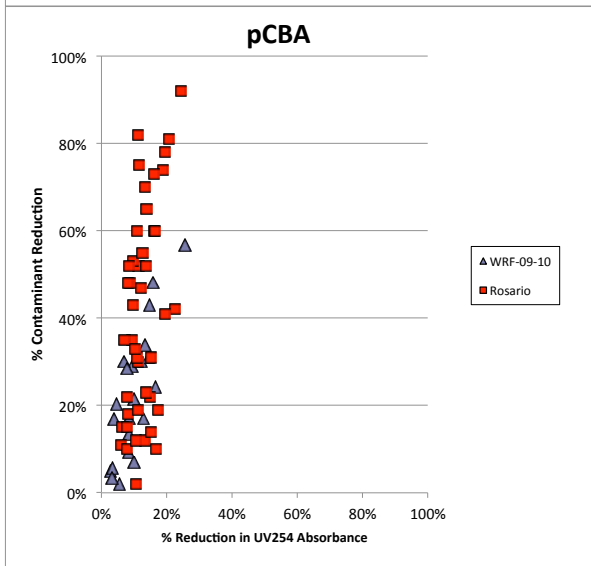
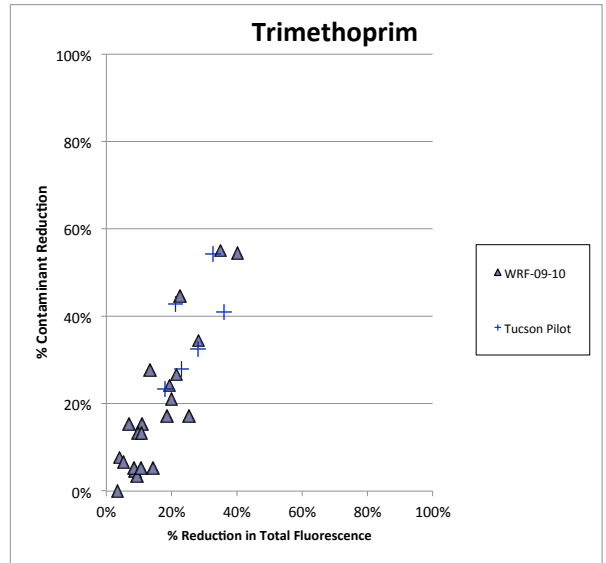
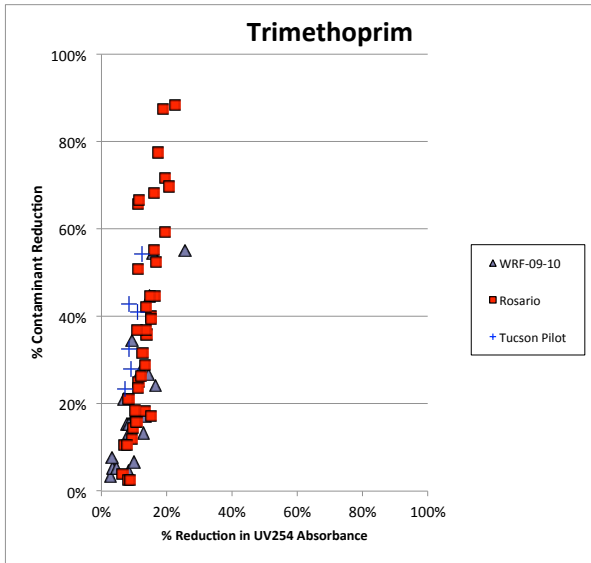
## Appendix 8 Validation of Empirical Correlations UV/H<sub>2</sub>O<sub>2</sub>



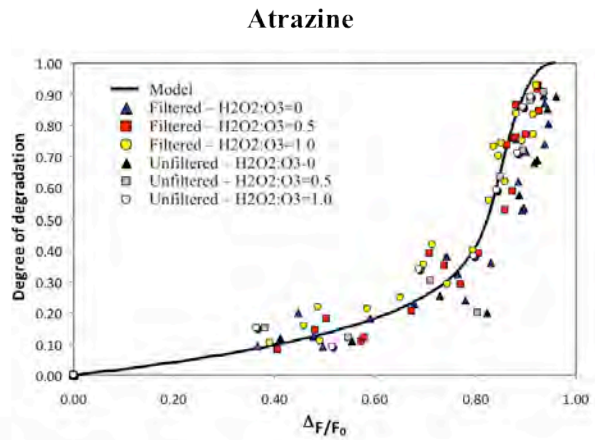
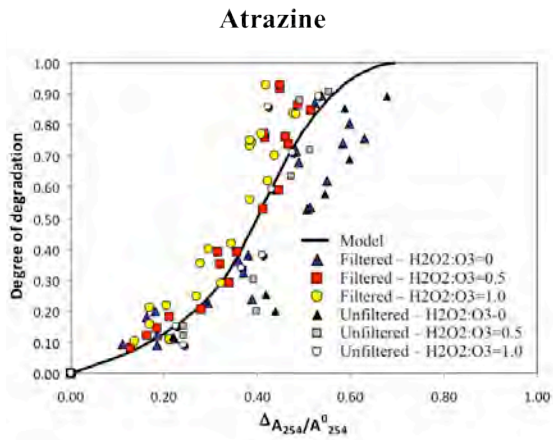
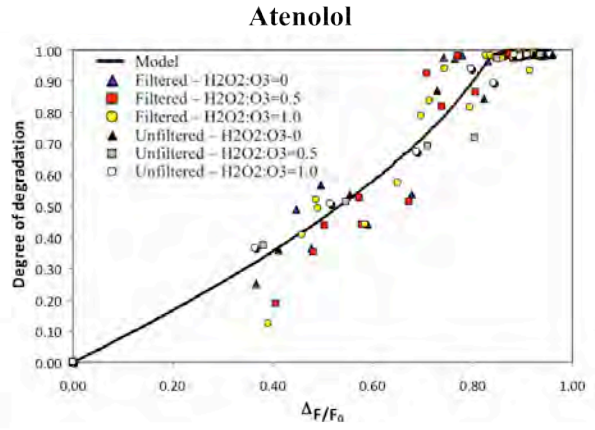
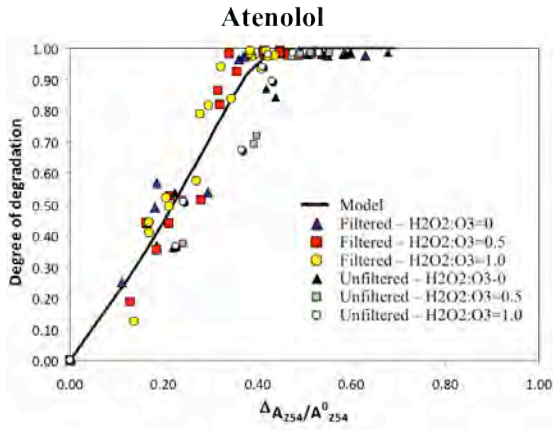
# Appendix 8 Validation of Empirical Correlations UV/H2O2



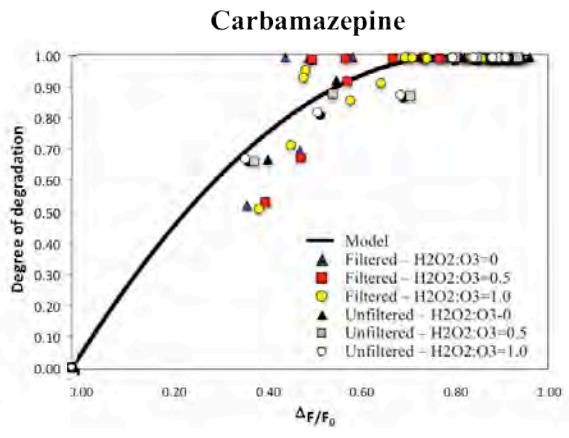
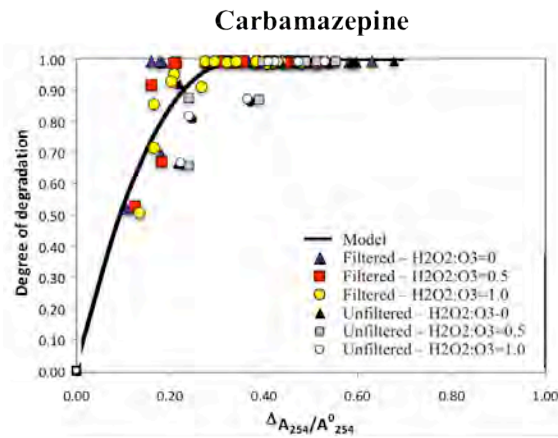
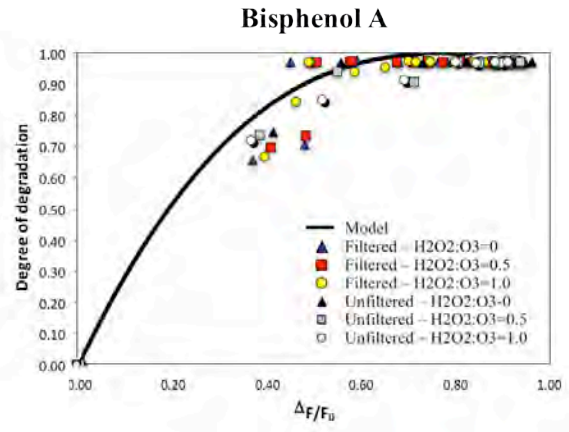
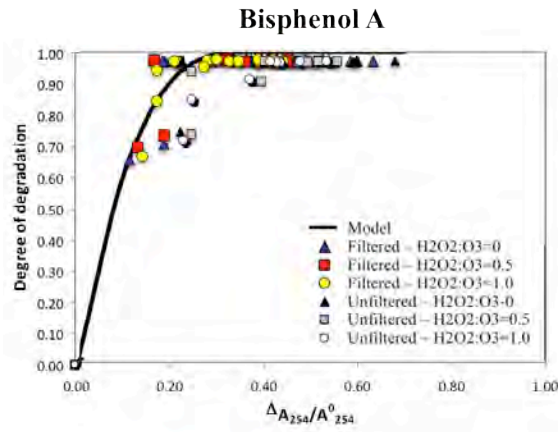
# Appendix 8 Validation of Empirical Correlations UV/H2O2



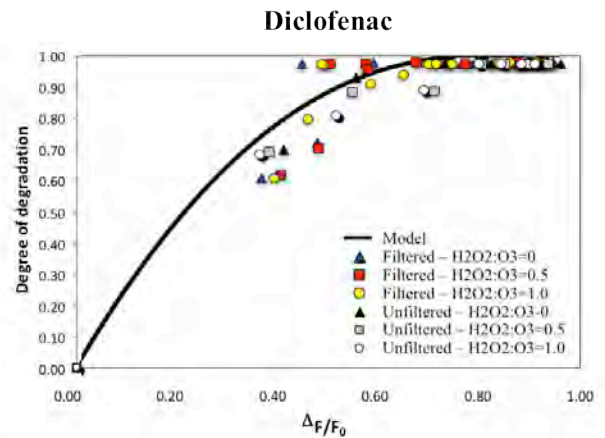
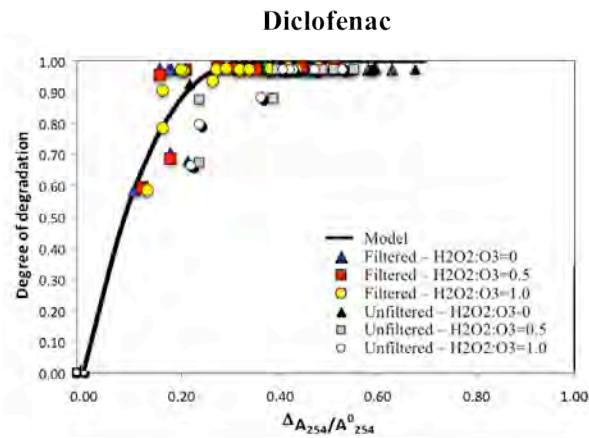
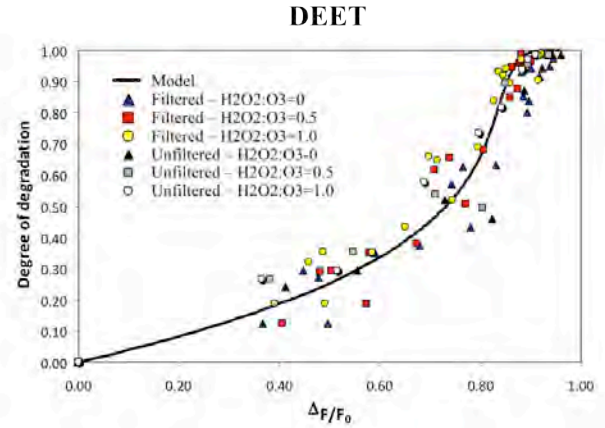
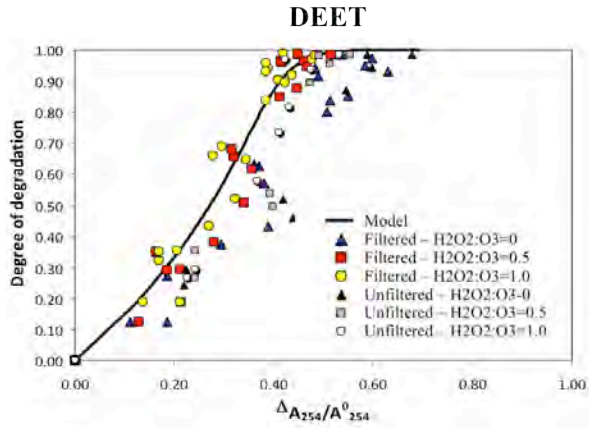
**Appendix 9**  
**Mechanistic Modeling**  
**Ozone and Ozone/H2O2 Correlations**



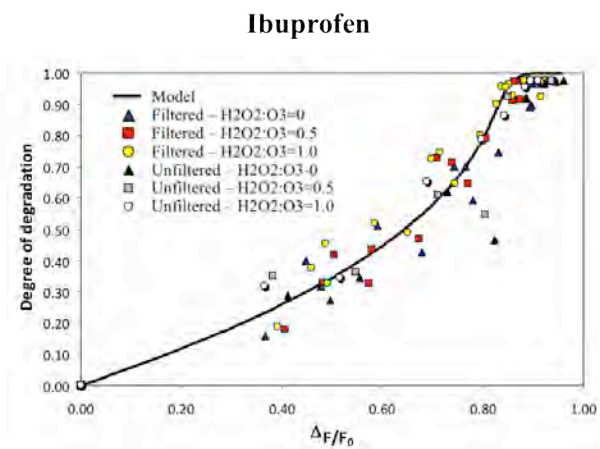
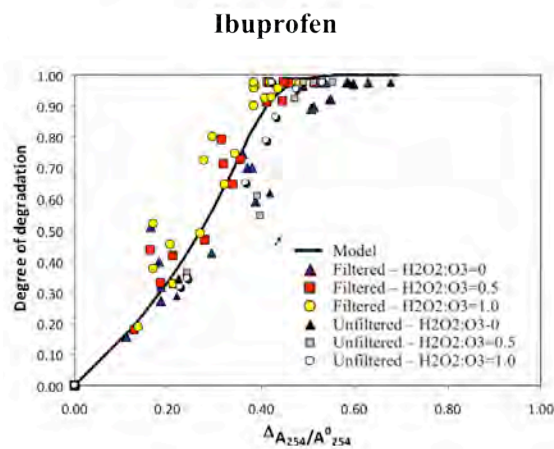
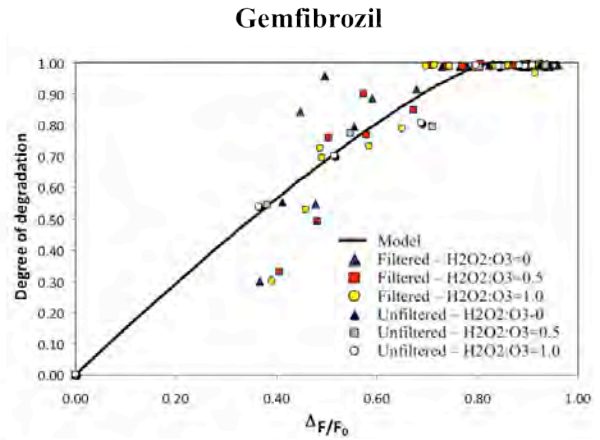
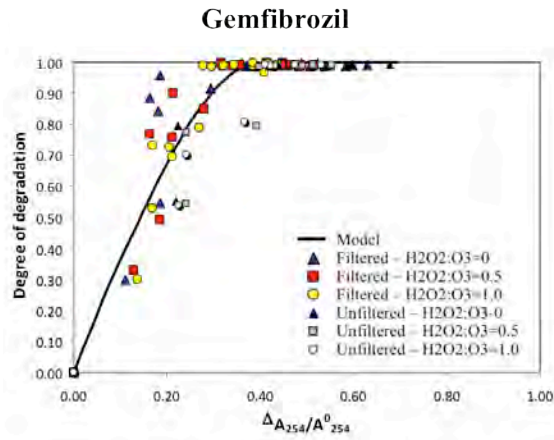
**Appendix 9**  
**Mechanistic Modeling**  
**Ozone and Ozone/H2O2 Correlations**



**Appendix 9**  
**Mechanistic Modeling**  
**Ozone and Ozone/H2O2 Correlations**

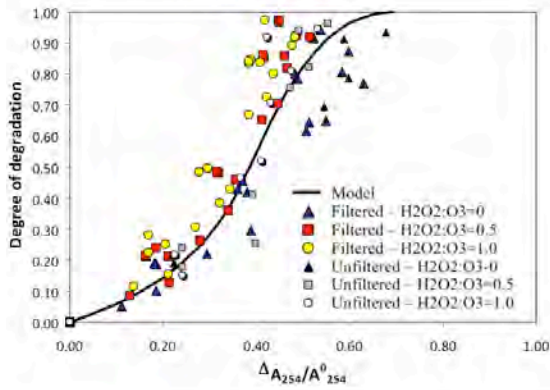


**Appendix 9**  
**Mechanistic Modeling**  
**Ozone and Ozone/H2O2 Correlations**

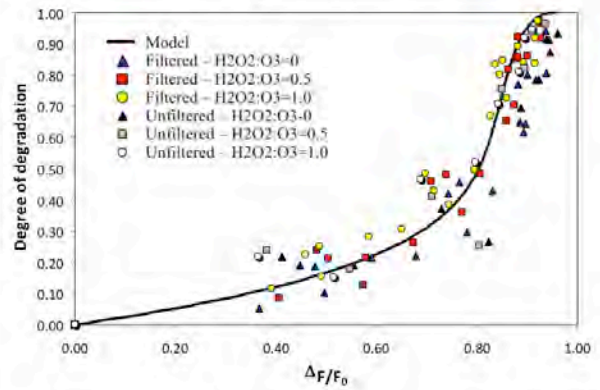


**Appendix 9**  
**Mechanistic Modeling**  
**Ozone and Ozone/H2O2 Correlations**

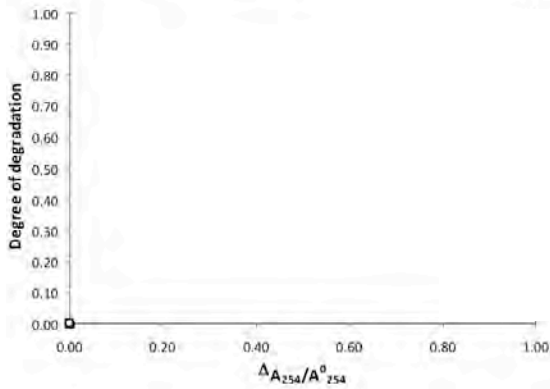
**Meprobamate**



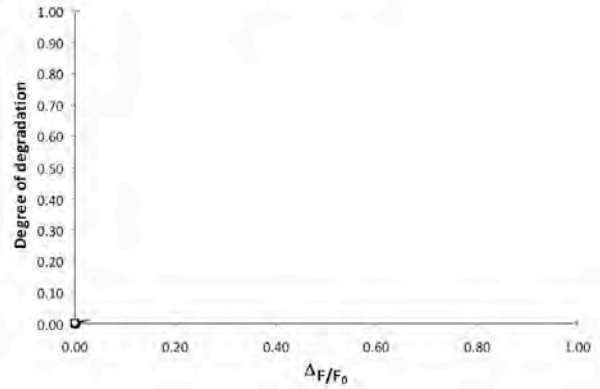
**Meprobamate**



**Musk Ketone**

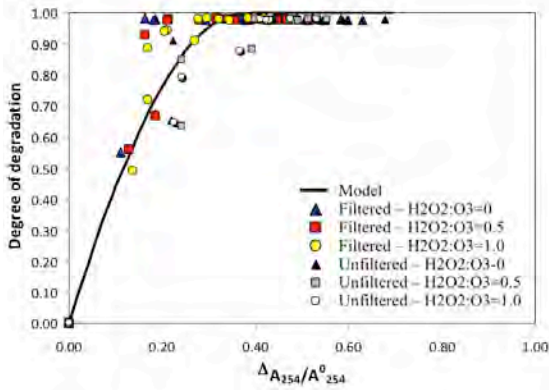


**Musk Ketone**

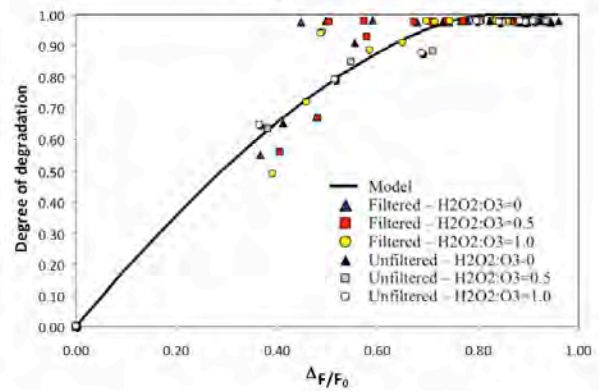


Appendix 9  
Mechanistic Modeling  
Ozone and Ozone/H2O2 Correlations

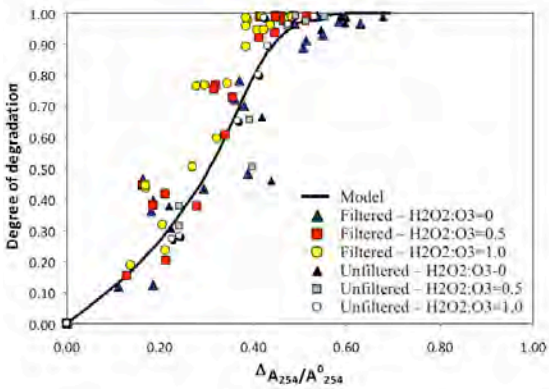
Naproxen



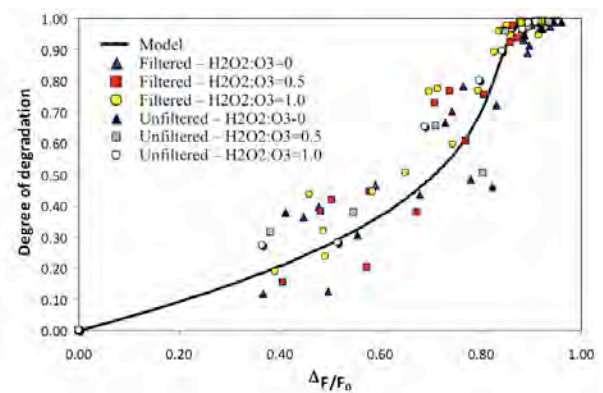
Naproxen



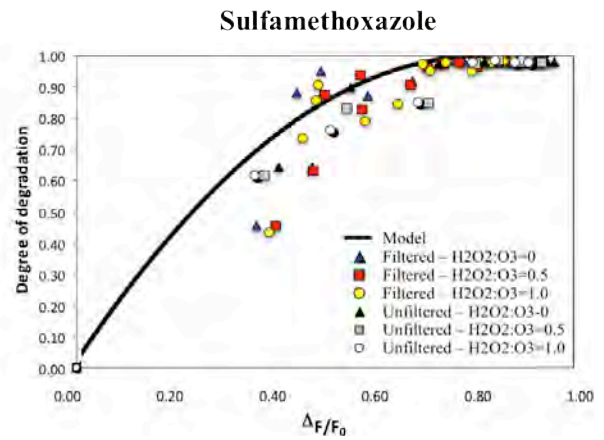
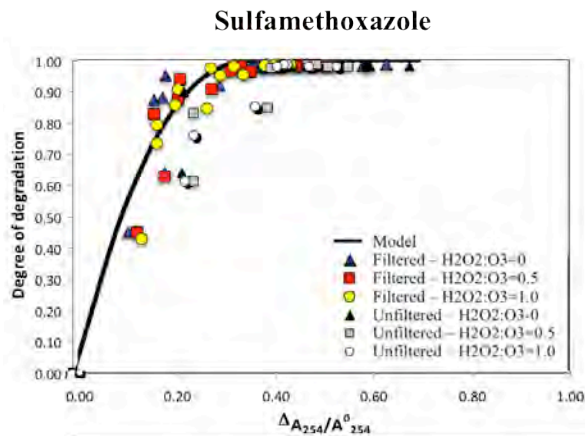
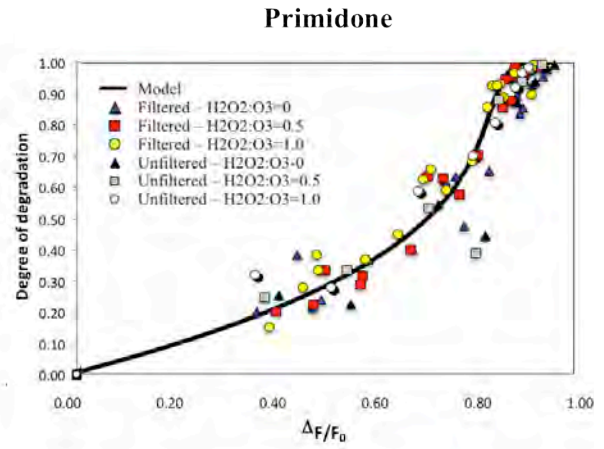
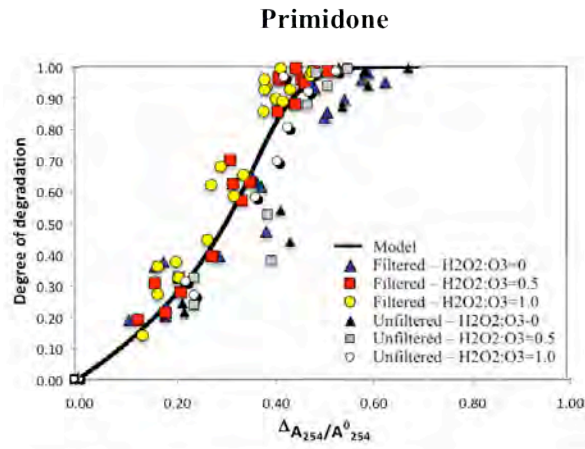
Phenytoin



Phenytoin

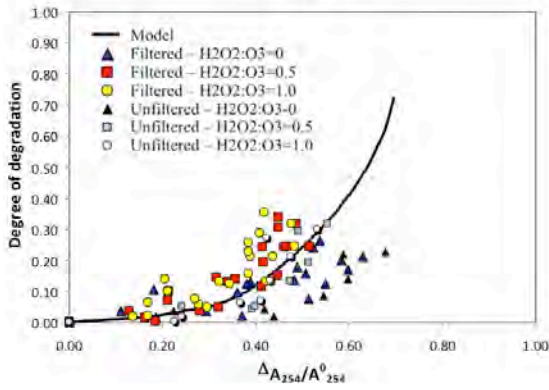


**Appendix 9**  
**Mechanistic Modeling**  
**Ozone and Ozone/H2O2 Correlations**

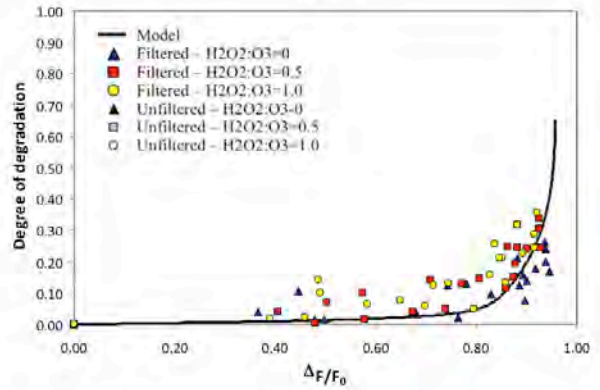


**Appendix 9**  
**Mechanistic Modeling**  
**Ozone and Ozone/H2O2 Correlations**

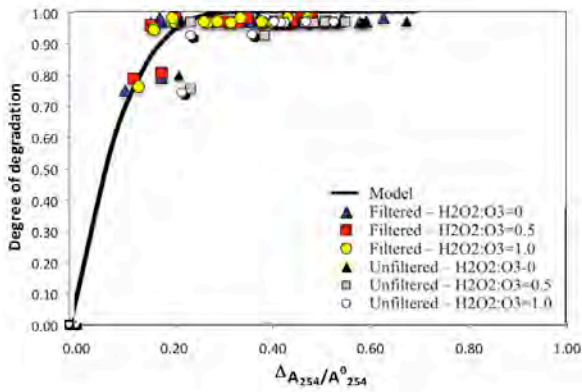
**TCEP**



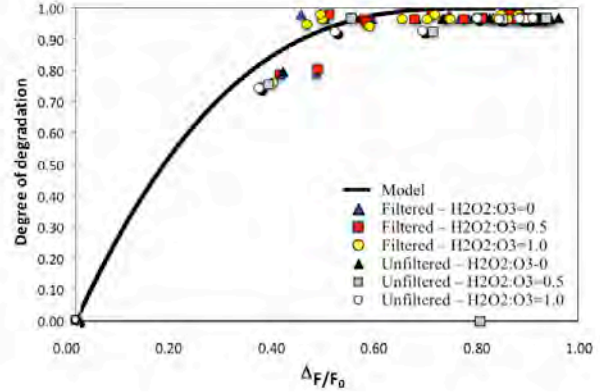
**TCEP**



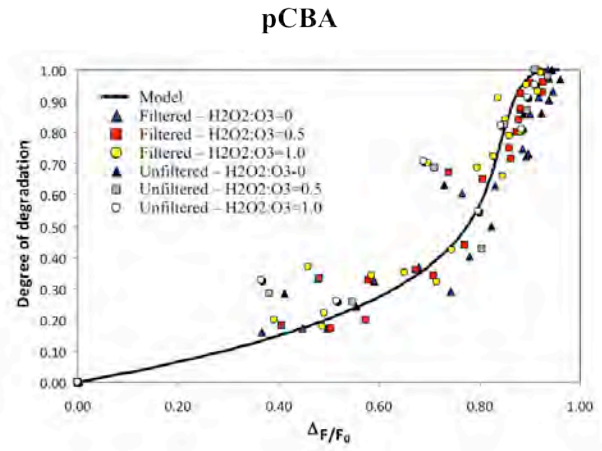
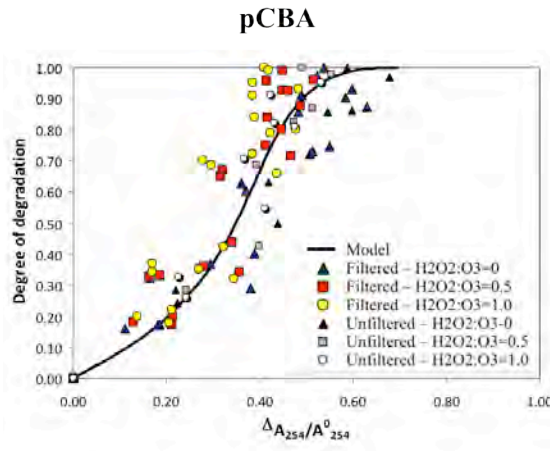
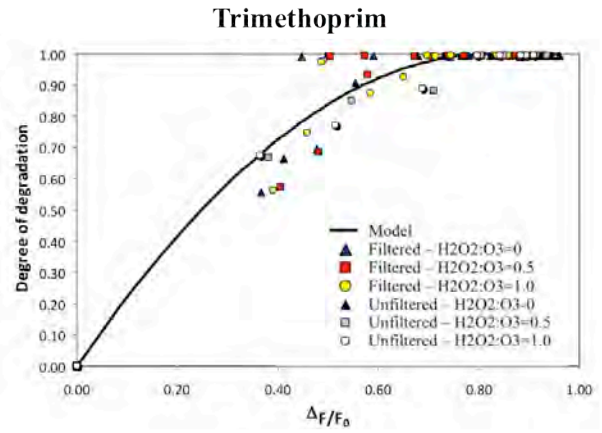
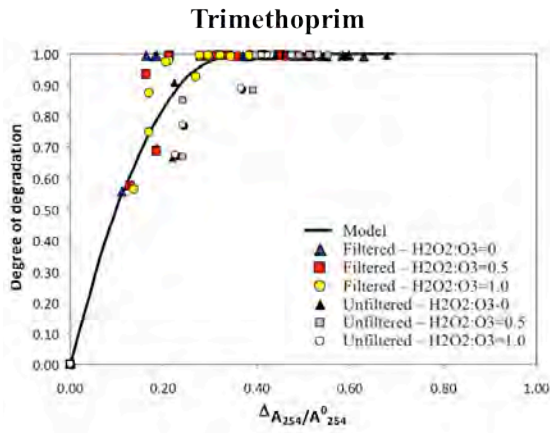
**Triclosan**



**Triclosan**

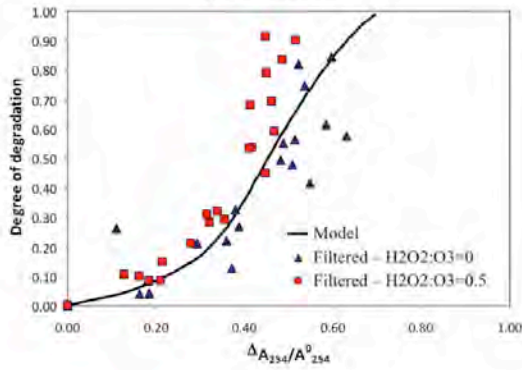


**Appendix 9**  
**Mechanistic Modeling**  
**Ozone and Ozone/H2O2 Correlations**

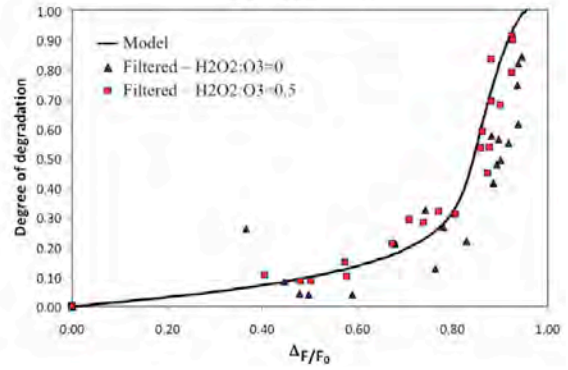


**Appendix 9**  
**Mechanistic Modeling**  
**Ozone and Ozone/H2O2 Correlations**

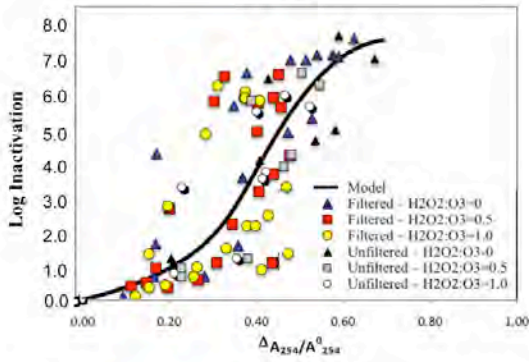
**1,4-Dioxane**



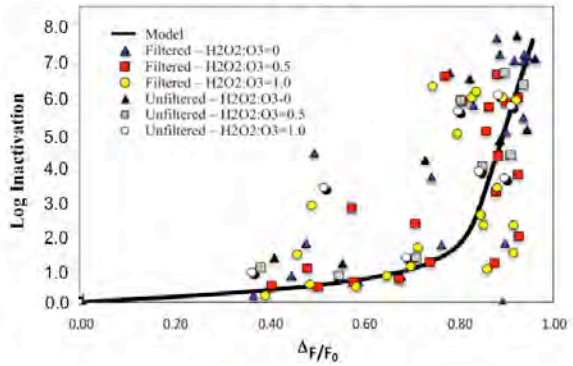
**1,4-Dioxane**



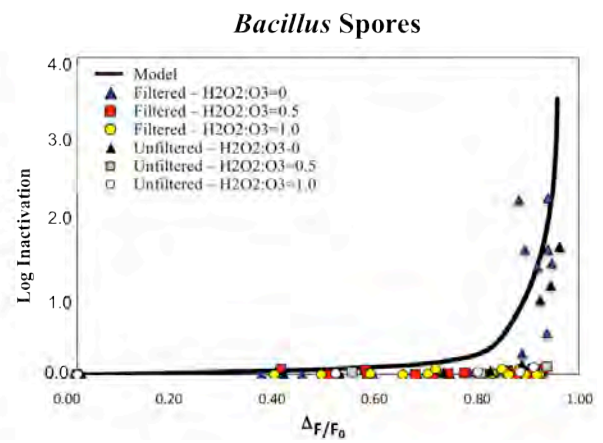
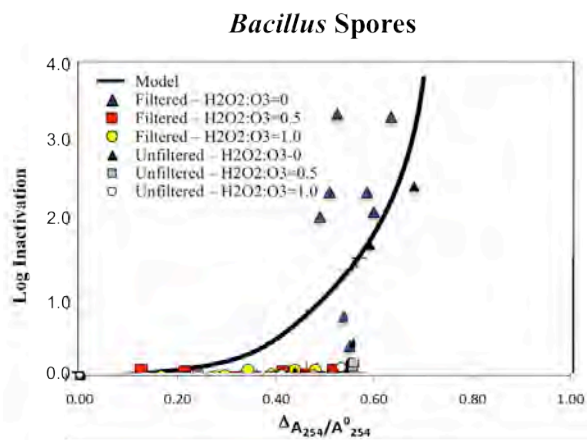
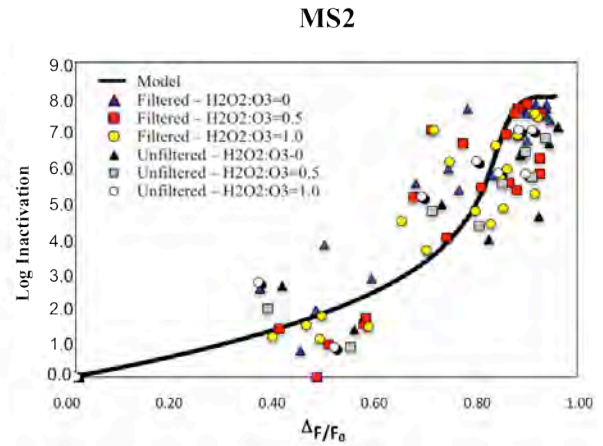
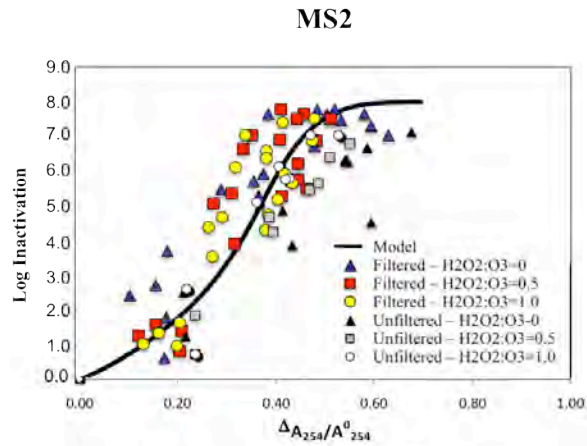
***E. coli***



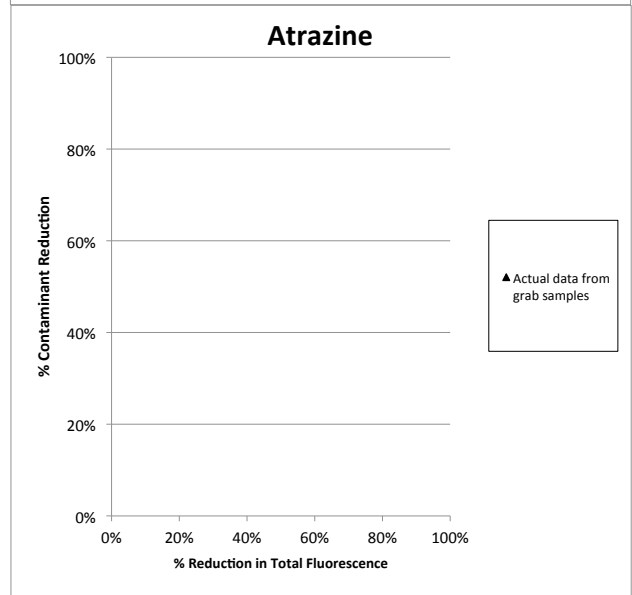
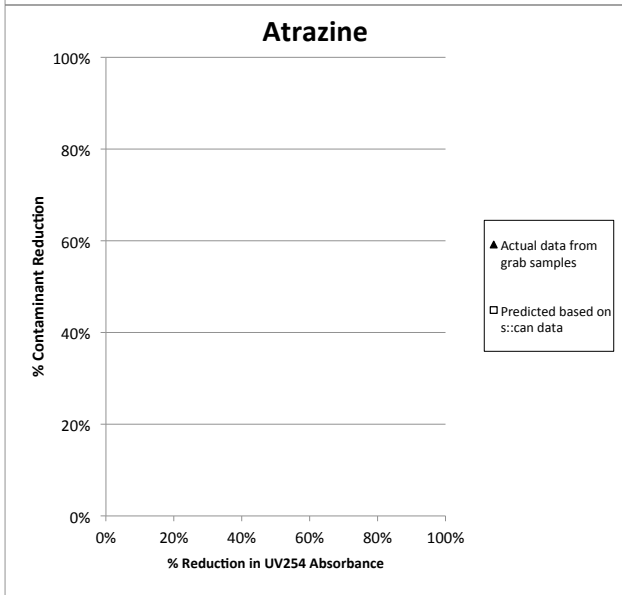
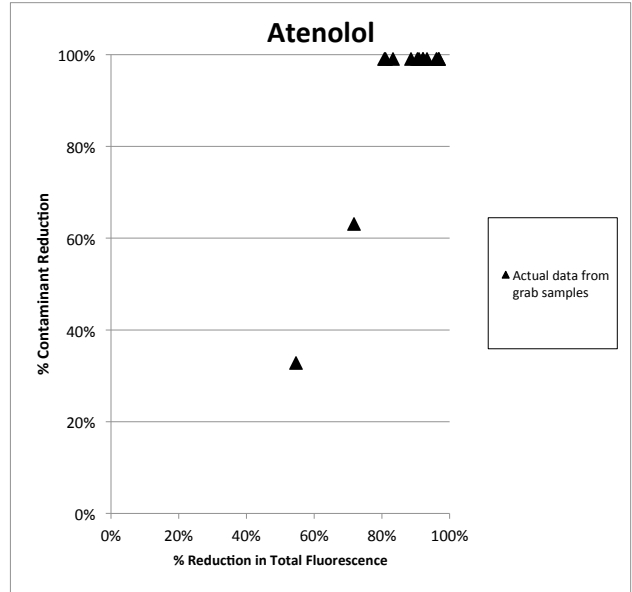
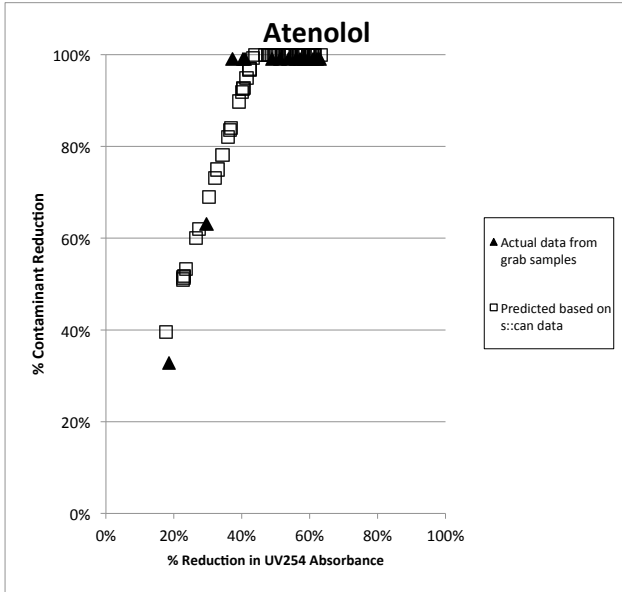
***E. coli***



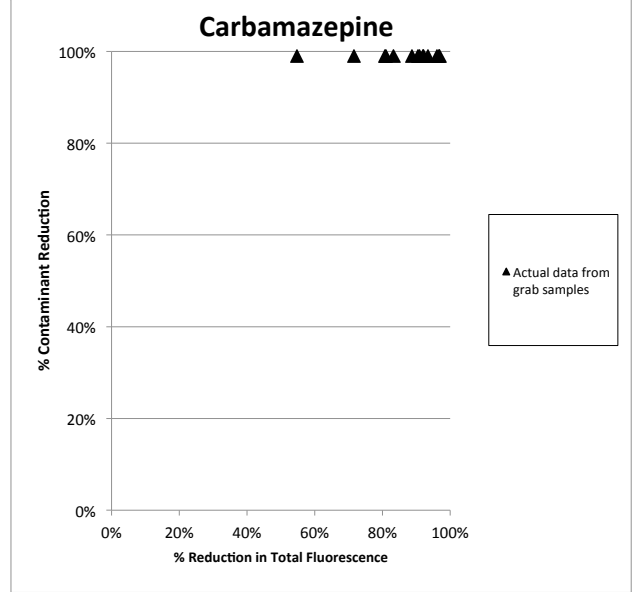
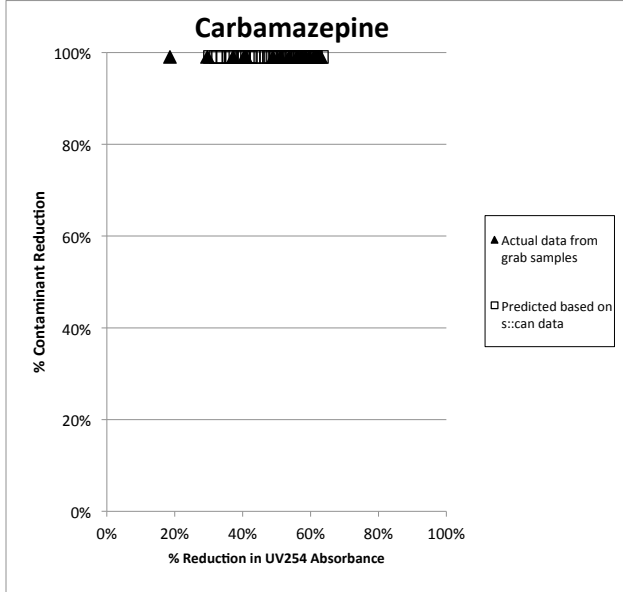
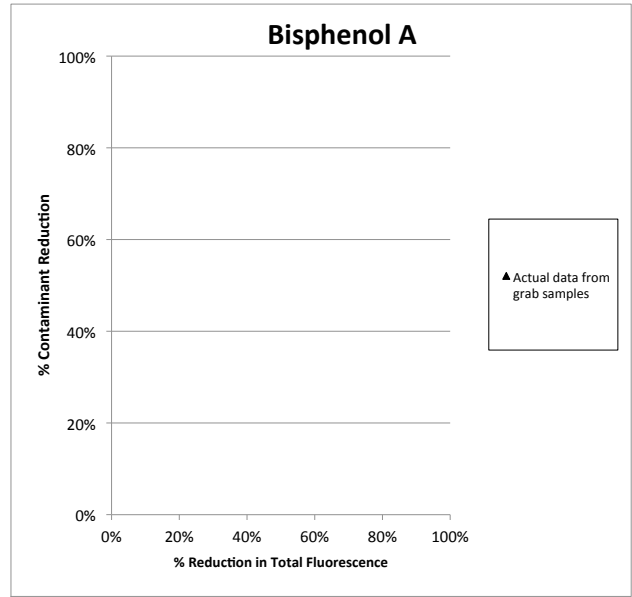
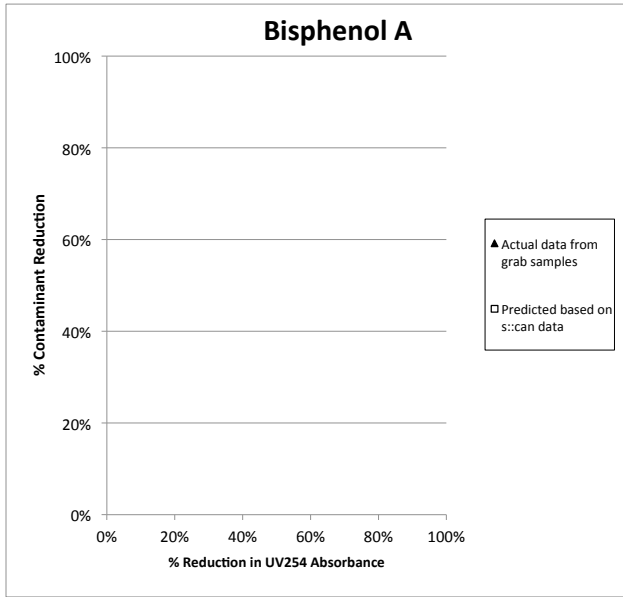
**Appendix 9**  
**Mechanistic Modeling**  
**Ozone and Ozone/H2O2 Correlations**



**Appendix 10**  
**CLV Pilot - Variable Dosing Experiment - s::can**  
**Ozone Correlations**



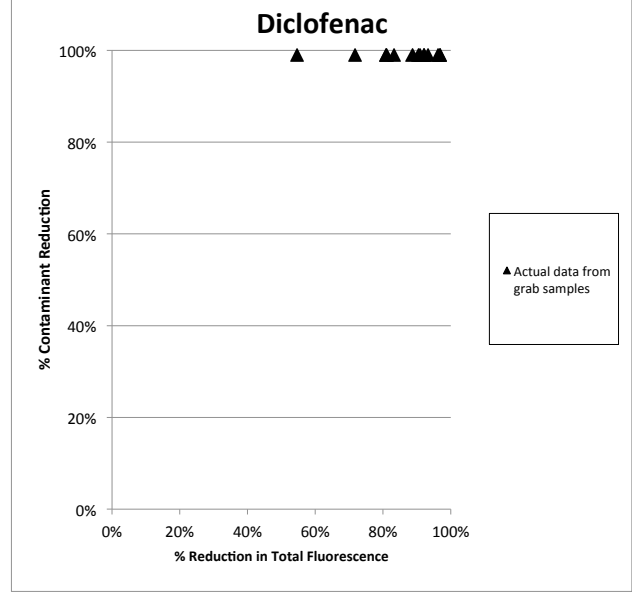
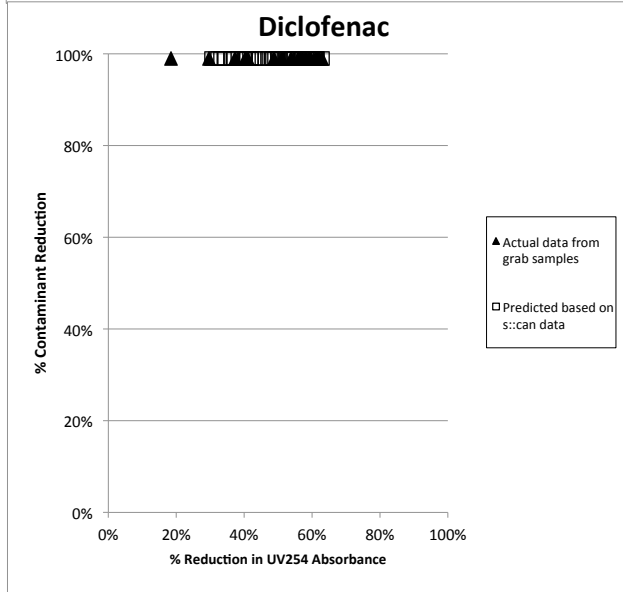
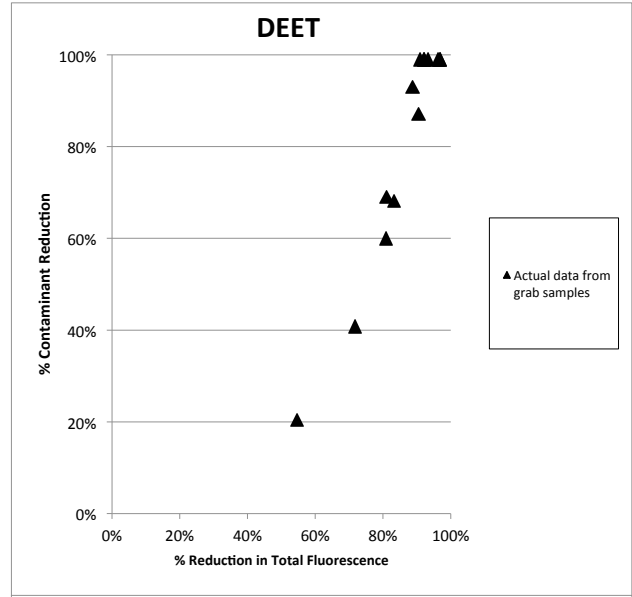
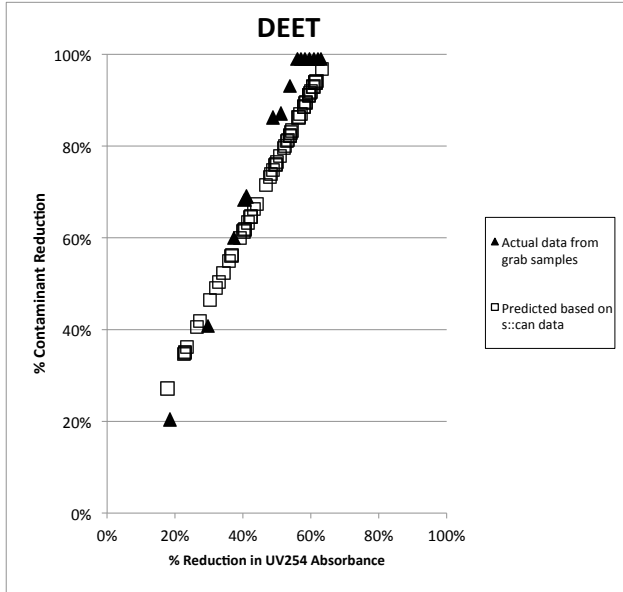
**Appendix 10**  
**CLV Pilot - Variable Dosing Experiment - s::can**  
**Ozone Correlations**



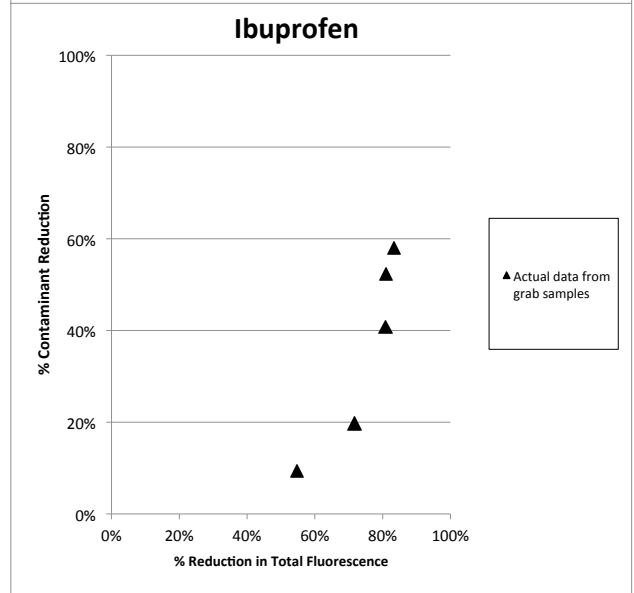
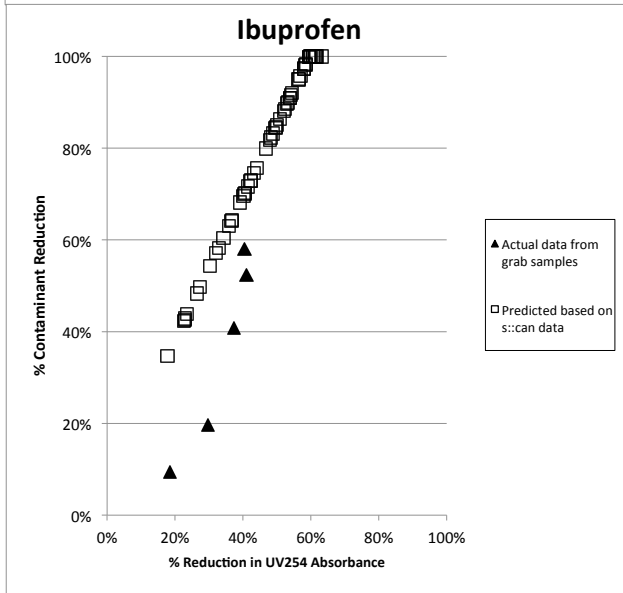
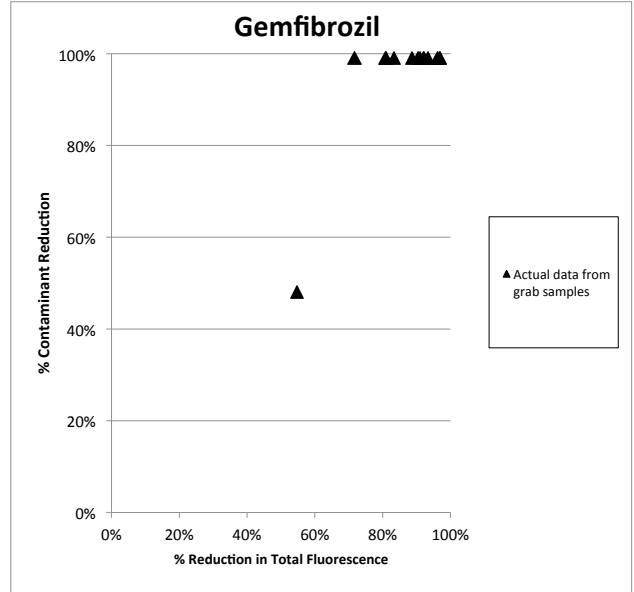
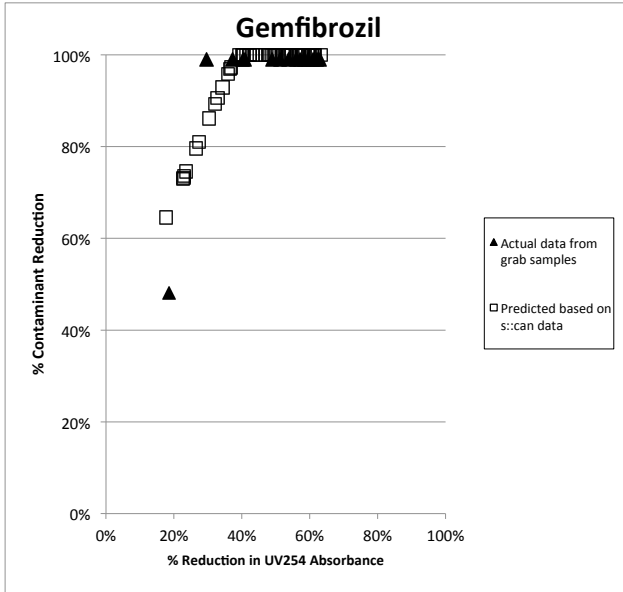
# Appendix 10

## CLV Pilot - Variable Dosing Experiment - s::can

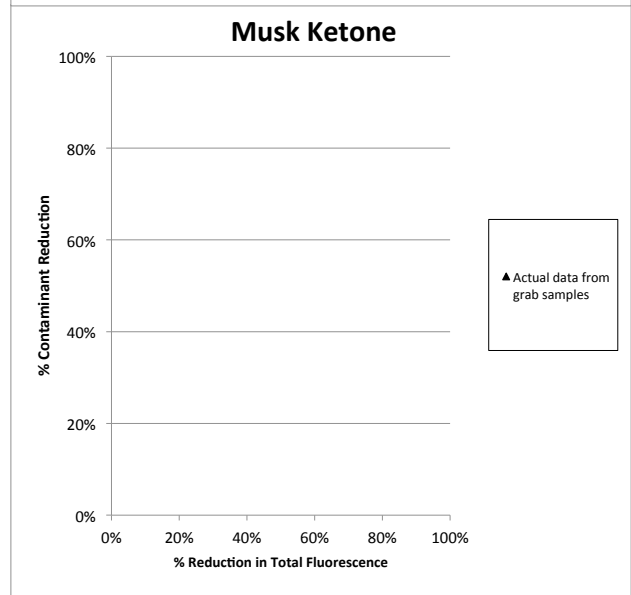
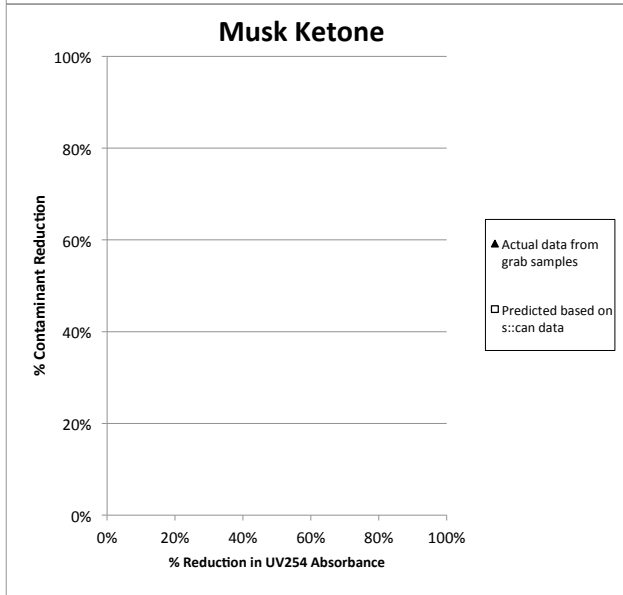
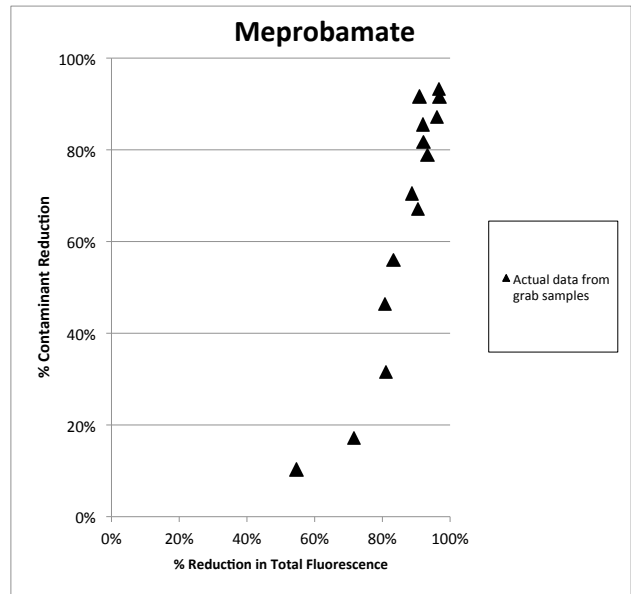
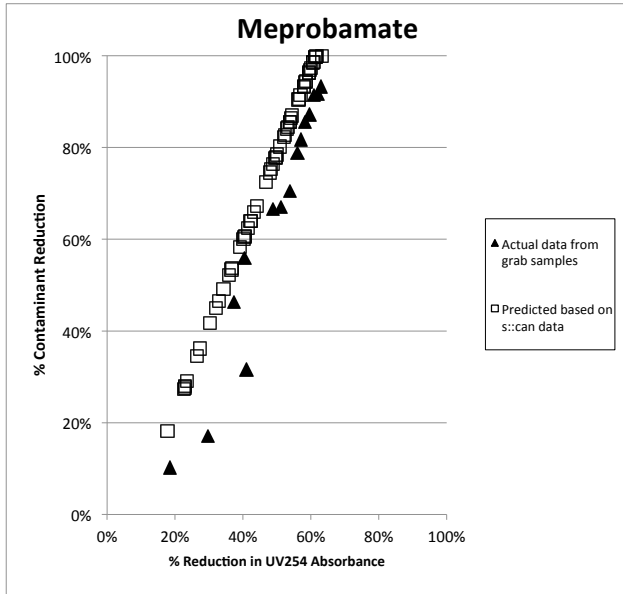
### Ozone Correlations



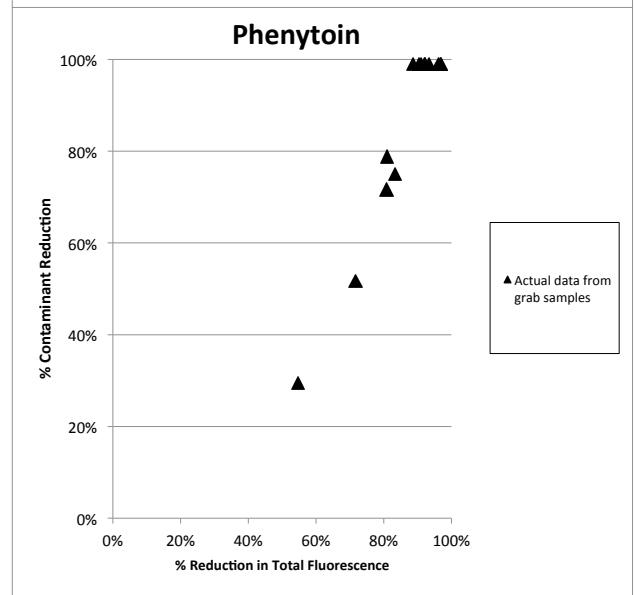
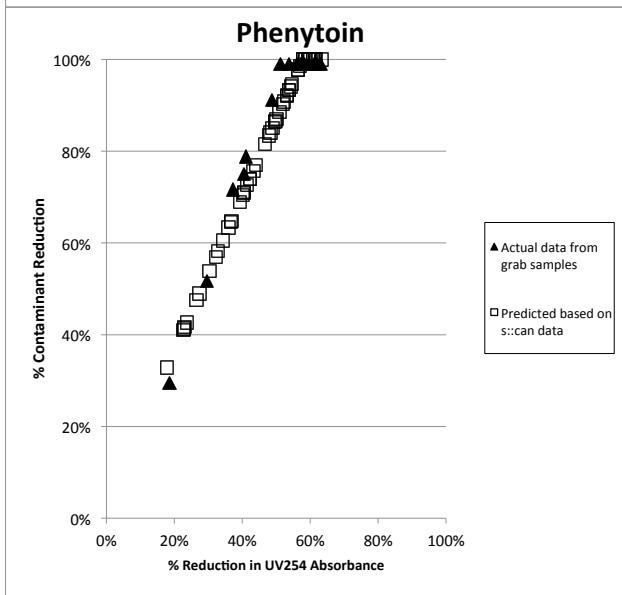
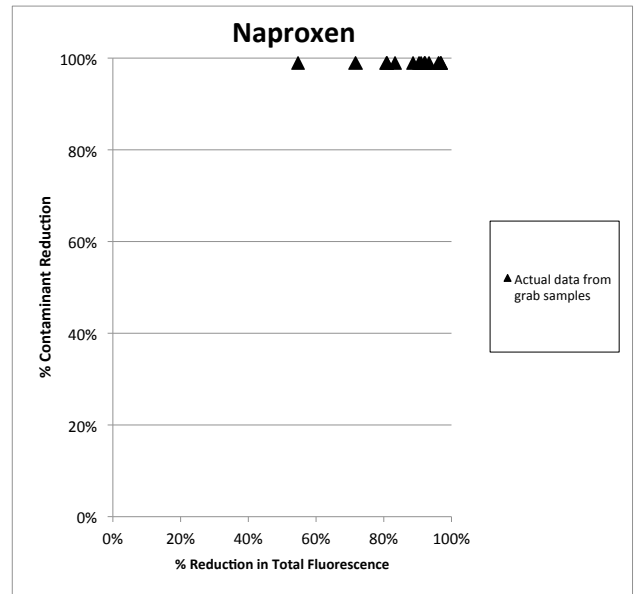
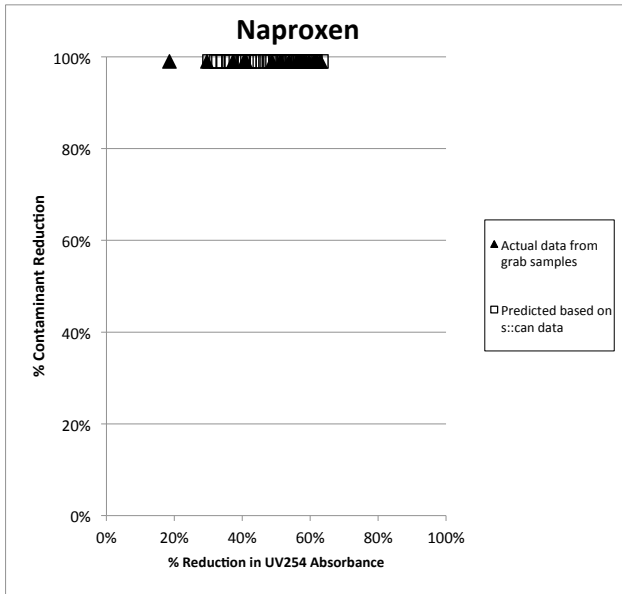
**Appendix 10**  
**CLV Pilot - Variable Dosing Experiment - s::can**  
**Ozone Correlations**



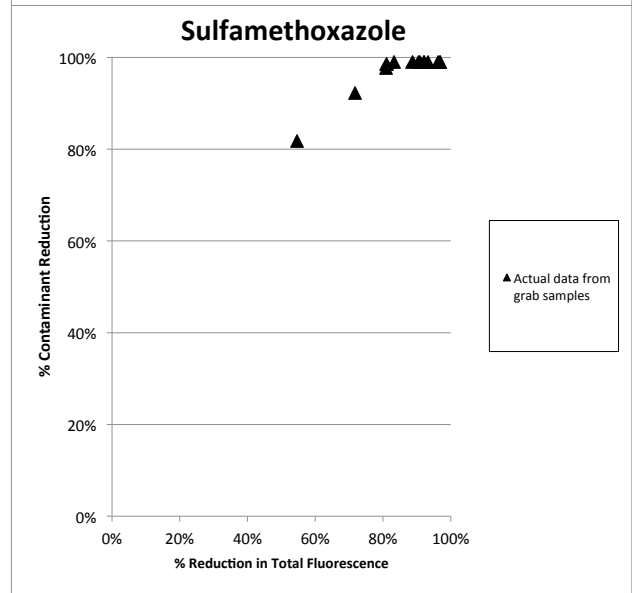
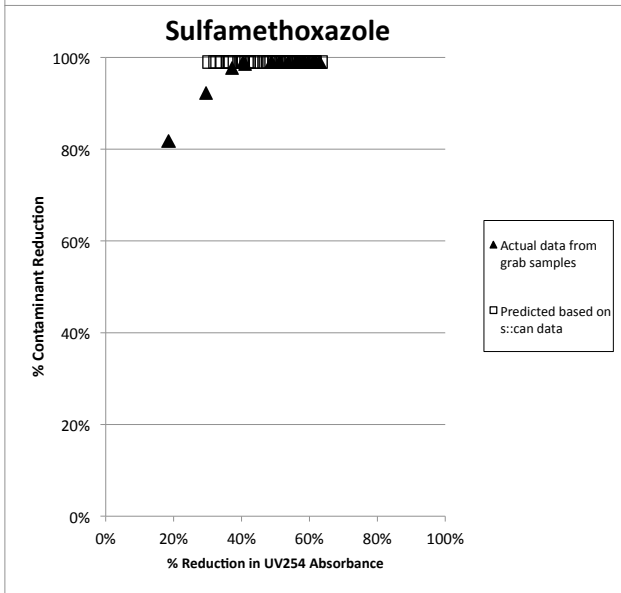
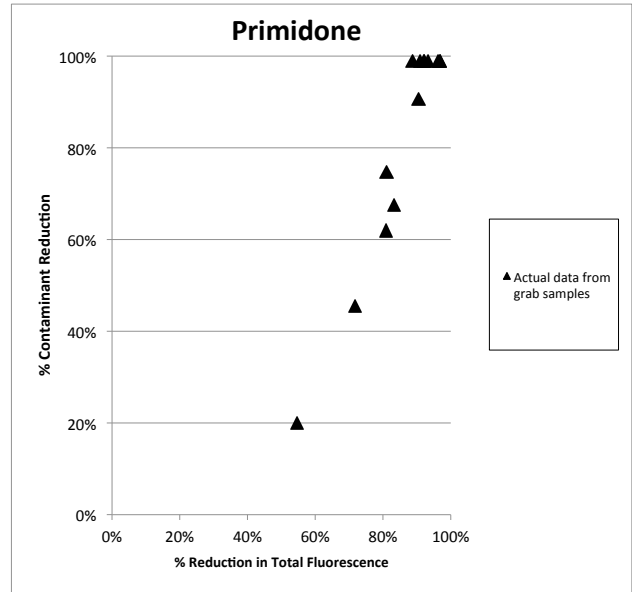
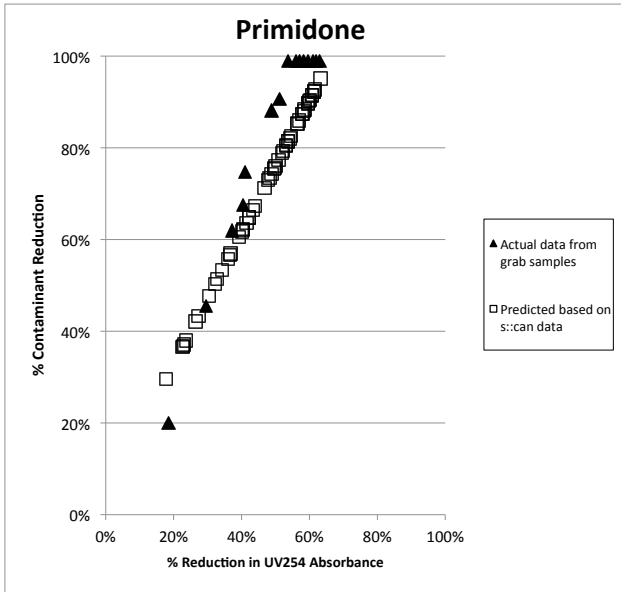
**Appendix 10**  
**CLV Pilot - Variable Dosing Experiment - s::can**  
**Ozone Correlations**



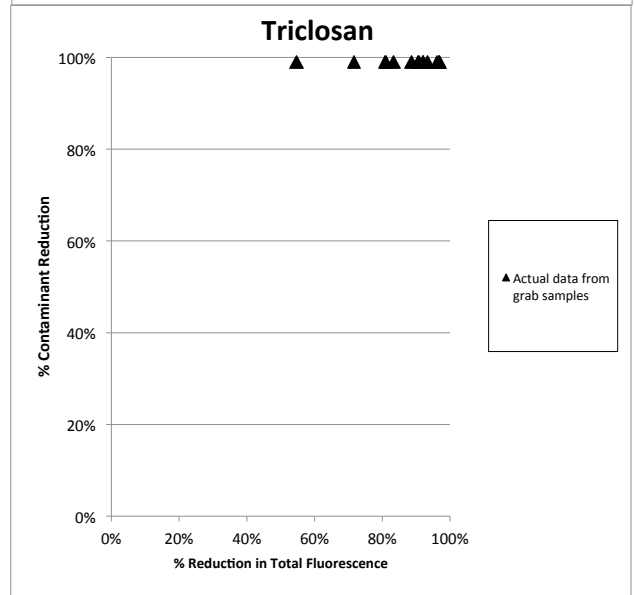
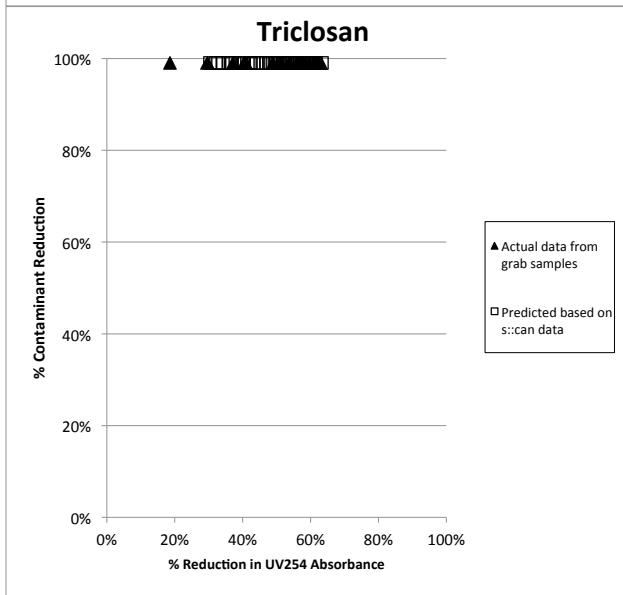
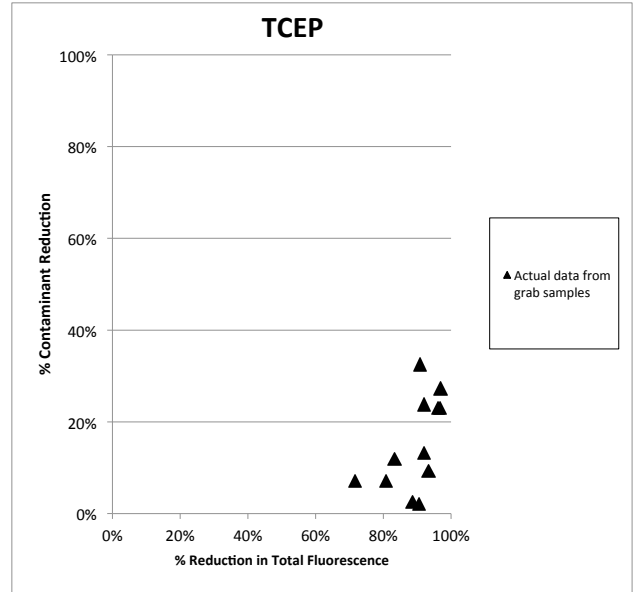
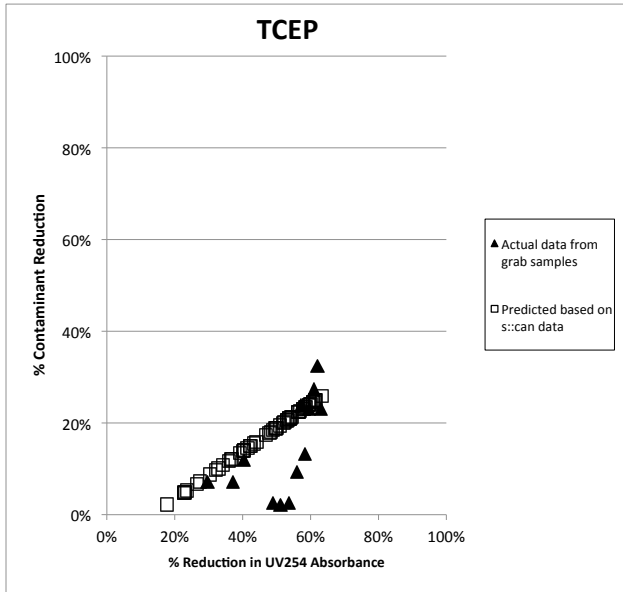
**Appendix 10**  
**CLV Pilot - Variable Dosing Experiment - s::can**  
**Ozone Correlations**



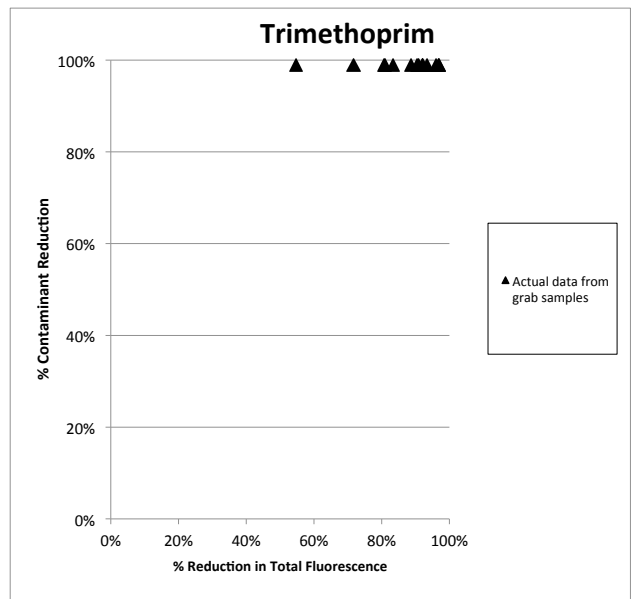
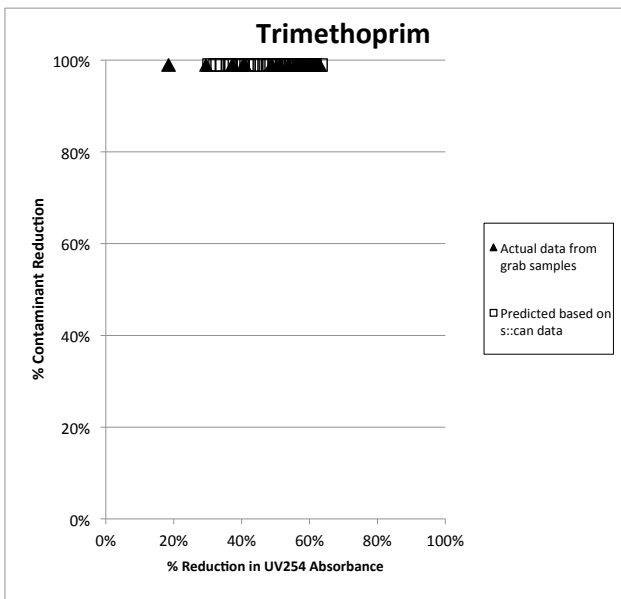
**Appendix 10**  
**CLV Pilot - Variable Dosing Experiment - s::can**  
**Ozone Correlations**



## Appendix 10 CLV Pilot - Variable Dosing Experiment - s::can Ozone Correlations



**Appendix 10**  
**CLV Pilot - Variable Dosing Experiment - s::can**  
**Ozone Correlations**







# *Advancing the Science of Water Reuse and Desalination*



**1199 North Fairfax Street, Suite 410**

**Alexandria, VA 22314 USA**

**(703) 548-0880**

**Fax (703) 548-5085**

**E-mail: [Foundation@WaterReuse.org](mailto:Foundation@WaterReuse.org)**

**[www.WaterReuse.org/Foundation](http://www.WaterReuse.org/Foundation)**